Etude de l'hétérogénéité clonale de tumeurs de patients atteints du cancer colorectal métastatique par l'analyse de l'ADN circulant au cours de leur prise en charge thérapeutique

Brice Pastor

THÈSE POUR OBTENIR LE GRADE DE DOCTEUR DE L'UNIVERSITÉ DE MONTPELLIER

En Biologie Santé

École doctorale
Sciences Chimiques et Biologiques pour la santé – CBS 2

Unité de recherche
Institut de Recherche en Cancérologie de Montpellier (IRCM) – INSERM U1194

Etude de l'hétérogénéité clonale de tumeurs de patients atteints du cancer colorectal métastatique par l'analyse de l'ADN circulant au cours de leur prise en charge thérapeutique

Présentée par Brice PASTOR
Le 9 mars 2022

Sous la direction de Alain THIERRY et Philippe BLACHE

Devant le jury composé de

Mme Valérie TALY, DR, Centre de Recherche des Cordeliers, Paris (Présidente du jury)	Rapporteure
Mr. Florent MOULIERE, Maitre de Conférences, Amsterdam University Medical Center, Amsterdam	Rapporteur
Mr. Thierry ANDRE, PU-PH, Hôpital Saint Antoine, Paris	Examinateur
Mr. Alain THIERRY, DR, Institut en Cancérologie de Montpellier, Montpellier	Directeur de thèse
Mr. Philippe BLACHE, DR, Institut en Cancérologie de Montpellier, Montpellier	Co-directeur de thèse
Mr. Didier TOUSCH, Maitre de Conférences, Université de Montpellier, Montpellier	Invité
Mr. Jérôme MOREAUX, Maitre de Conférences, Université de Montpellier, Montpellier	Invité

UNIVERSITÉ DE MONTPELLIER

Résumé :

Depuis sa découverte en 1948, l'analyse de l'ADN circulant (ADNcir) a démontré son potentiel clinique en oncologie.

Mon premier objectif de thèse a été d'étudier l'hétérogénéité clonale de tumeurs de patients atteints de cancer colorectal métastatique (CCRm) par l'analyse de l'ADNcir au cours de leur prise en charge thérapeutique. Seuls les patients ayant des tumeurs *RAS* non-mutées peuvent bénéficier des thérapies anti-EGFR. Avant traitement par anti-EGFR, l'analyse de l'ADNcir a montré la détection d'un plus grand nombre de mutations *RAS/BRAF* (76%, n=119) que l'analyse du tissu tumoral (55%, n=89) ainsi qu'une proportion élevée de mutations co-occurrentes (45%) chez les patients atteints de CCRm (étude *KPLEX2*). Nous avons montré que la médiane du délai entre la réception des échantillons et la communication des résultats était de 12 jours pour l'analyse du tissu tumoral (n=83; 3-273 jours) contre seulement de 2 jours pour l'analyse de l'ADNcir (n=121; 0-10 jours). Ces résultats indiquent que l'ADNcir pourrait remplacer l'analyse du tissu tumoral en pratique clinique.

Dans l'étude rétrospective *KPLEXR*, l'analyse longitudinale des patients atteints de CCRm traités par FOLFOX-dasatinib avec ou sans cetuximab a montré qu'à l'arrêt des traitements 98% des patients réfractaires aux traitements (n=42) sont mutés *RAS/BRAF*. Ce résultat démontre que les mutations *RAS/BRAF* induisent des résistances au traitement par anti-EGFR. L'analyse quantitative et longitudinale de l'ADNcir mime étroitement les changements des niveaux sanguins de l'ACE et l'évolution de la masse tumorale observée par CT-scan. De plus, 21% des mutations *RAS/BRAF* sont retrouvées avec des fréquences alléliques inférieures à 0.1% montrant la nécessité d'utiliser une méthode ultrasensible pour détecter les mutations ponctuelles avant et durant les traitements par anti-EGFR. Ces résultats indiquent le potentiel théranostique de l'ADNcir durant un traitement par anti-EGFR.

Les patients réfractaires à l'ensemble des thérapies standards peuvent être traités au regorafenib. Cependant, aujourd'hui aucun biomarqueur ne permet de prédire un bénéfice ou une résistance au regorafenib. C'est dans ce contexte qu'a été réalisé l'étude prospective *TEXCAN*. Nous avons montré que le statut muté *RAS/BRAF* des patients atteints de CCRm lourdement prétraités et réfractaires aux thérapies standards n'influe pas la survie de ces patients traités au régorafénib. Par contre, les resultats sugerent qu'il est possible d'identifier avant le traitement les patients qui auront un bénéfice clinique à cette molécule. En effet, nous avons pu établir des seuils de concentrations d'ADNcir total (26 ng/mL de plasma), d'ADNcir tumoral muté (2 ng/mL de plasma) et de fréquence allélique (6%) qui permettraient de prédire les patients qui auront une meilleure survie globale. L'ADNcir pourrait être un biomarqueur pour prédire les résistances ou les tolérances des tumeurs des patients au regorafenib.

Il est admis depuis longtemps que l'apoptose est le mécanisme de libération de l'ADNcir le plus pertinent puisque de nombreuses études ont montré que l'ADNcir a un profil de taille aux alentours de 150-180 bp. Le deuxième objectif de ma thèse a été d'évaluer l'association entre la formation des NETs (neutrophil extracellular traps) et la production des ADNcir chez les patients atteints de CCRm. Nous montrons qu'une fraction importante de l'ADNcir des patients CCRm proviendrait du phénomène de NETose. Ces travaux redéfinissent les paradigmes existants sur les mécanismes de libération de l'ADNcir. La dégradation des NETs pourrait expliquer la grande amplitude de la fréquence allélique dans le sang des patients atteints de CRCm. Cependant, il reste encore à révélerer l'ensemble des acteurs conduisant à la production des ADNcir par la dégradation des Nets *in vivo*.

Abstract:

Since its discovery in 1948, circulating DNA (cirDNA) analysis has demonstrated its clinical potential in oncology.

My first thesis objective was to study the clonal heterogeneity of tumors from metastatic colorectal cancer (mCRC) patients by cirDNA analysis during their therapeutic management. Only patients with non-mutant *RAS* tumors can benefit from anti-EGFR therapies. Prior to anti-EGFR therapy, cirDNA analysis showed the detection of higher *RAS/BRAF* mutations (76%, n=119) than tumor tissue analysis (55%, n=89) as well as a high proportion of co-occurring mutations (45%) in mCRC patients (*KPLEX2* study). We showed that the median data turn-around time was 12 days for tumor tissue analysis (n=83; 3-273 days) versus only 2 days for cirDNA analysis (n=121; 0-10 days). These results indicated that cirDNA could replace tumor tissue analysis in clinical practice.

In the retrospective *KPLEXR* study, longitudinal analysis of mCRC patients treated with FOLFOX-dasatinib with or without cetuximab showed that 98% of treatment-refractory patients (n=42) were *RAS/BRAF* mutant at the end of the treatment. This result suggested that *RAS/BRAF* mutations induce resistance to anti-EGFR therapy. Quantitative and longitudinal analysis of cirDNA closely mirrored variations in blood CEA levels and tumor mass as observed by CT-scan. Moreover, 21% of *RAS/BRAF* mutations were found with allelic frequencies lower than 0.1% revealing the need of the use of an ultrasensitive method to detect point mutations before and during anti-EGFR treatments. These results highlighted the theranostic potential of cirDNA during anti-EGFR therapy.

Refractory patient tumors to all standard therapies can be treated with regorafenib. However, there is currently no biomarker to predict benefit or resistance to regorafenib. Inthe prospective *TEXCAN* study we observed that the *RAS/BRAF* mutant status of heavily pretreated mCRC patients refractory to standard therapies does not influence the survival of these patients treated with regorafenib. On the other hand, we showed that it is possible to identify prior to treatment those patients who will benefit clinically from the drug. Indeed, we were able to establish thresholds for total cirDNA concentration (26 ng/mL plasma), mutant cirDNA concentration (2 ng/mL plasma) and allelic frequency (6%) that would predict which patients will have better overall survival. The cirDNA could be a biomarker for predicting patient tumor resistance or tolerance to regorafenib.

It has long been recognized that apoptosis is the most relevant mechanism of cirDNA release since many studies have shown that cirDNA has a size profile around 150-180 bp. The second objective of my thesis was to evaluate the association between NETs (neutrophil extracellular traps) formation and cirDNA production in mCRC patients. We show that a significant fraction of cirDNA in mCRC patients is derived from the NETosis mecanism. This work redefines existing paradigms on the mechanisms of cirDNA release. NET degradation and resultant cirDNA release could explain the large variation of allelic frequency in the blood of mCRC patients. However, the full set of enzymes leading to the production of cirDNA by the *in vivo* degradation of NETs remains to be demonstrated.

Remerciements :

A mes directeurs de thèse, ce fut un grand honneur de travailler sous votre direction. Je tiens à vous remercier pour votre disponibilité sans faille durant ces 3 années de thèse.

Monsieur Alain THIERRY, je vous remercie pour votre soutien durant ces 8 « longues » années passées ensemble. Tout a commencé à l'Université avec un projet basé sur l'analyse des ADN circulants dans le cadre du cancer du sein. Depuis ce jour, votre confiance envers moi n'a jamais faibli et je vous remercie pour cela. Je vous remercie pour vos conseils, votre encadrement et tous les heureux moments que nous avons passé ensemble au sein de l'institut et en dehors. J'espère que notre collaboration durera encore longtemps et que vous serez épanoui dans votre vie personnelle et scientifique.

Monsieur Philippe BLACHE, je te remercie pour ta confiance, ta simplicité et pour tes conseils. Au-delà de nos discussions scientifiques j'ai eu la chance de partager une autre passion que la science avec mon directeur de thèse, la pêche. Je te remercie pour ces discussions de pêche qui m'ont permis de prendre du recul dans les moments compliqués. Nous irons pécher en bateau cet été et je l'espère pour pêcher la daurade record.

A mes co-encadrants de thèse, je vous remercie pour votre aide et votre soutien.

Monsieur Thibault MAZARD, je tiens à te remercier pour la confiance que tu m'as porté durant de longues années. Je te remercie aussi pour m'avoir fait confiance lors des nombreux essais cliniques que nous avons menés ensemble. J'espère que l'essai PANIRINOX sera une réussite.

Monsieur Antoine ADENIS, je te remercie énormément pour ton aide et tes encouragements durant ma thèse. Tu n'es pas un co-encadrant officiel de ma thèse mais je te considère tout comme. Merci vivement pour m'avoir aidé à terminer dans de bonnes conditions l'essai ancillaire TEXCAN et de m'avoir associé à ton travail FOLFIRINOX-R.

A Marc YCHOU et Claude SARDET.

Monsieur Marc YCHOU, je ne sais pas comment vous remercier tellement vous avez contribué à ma réussite. Il est évident que sans votre soutien sans faille je n'aurais pas pu réaliser mes 4 années d'ingénieur et mon doctorat. Vous m'avez aidé humainement et financièrement en tant que : directeur de l'équipe de recherche, directeur du SIRIC Montpellier Cancer et enfin en tant directeur générale de l'ICM. Même si le côté financier n'est pas l'aspect le plus relevant pour des remerciements de thèse, je me dois de vous remercier pour cela car sans votre confiance je n'aurais pas pu réaliser me projets. Un immense MERCI !

Monsieur Claude SARDET, je vous remercie de m'avoir accueillie dans d'excellentes conditions au sein de l'IRCM. Je tiens également à vous remercier pour votre confiance tout au long de mon doctorat.

Aux membres de mon jury de thèse.

Madame Valérie TALY, je vous remercie vivement pour avoir accepté de juger mon travail de thèse en tant que rapporteure. Je vous remercie pour l'intérêt que vous portez à mon travail de thèse. C'est un honneur de vous vous compter parmi les rapporteurs de ce travail de thèse.

Monsieur Florent MOULIERE, je suis très heureux de te compter parmi mes rapporteurs de thèse. Tu as été présent lors mes premiers projets étudiants et pour mes premiers instants à l'IRCM. Je te remercie pour les conseils que tu m'as donnés avant mon doctorat et durant ma thèse lorsque nous nous sommes rencontrés à des congrès scientifiques. Je te souhaite le meilleur dans ta vie personnelle et professionnelle. C'est un honneur et un immense plaisir de t'avoir en tant que rapporteur pour juger mon travail de thèse.

Madame Céline GONGORA, je te remercie pour avoir accepté de juger mon travail de thèse en tant qu'examinatrice. Je te remercie pour ton aide et ta bonne humeur.

Monsieur Thierry ANDRE, vous me faites l'honneur d'être examinateur de ce travail de thèse. Je suis fier d'avoir travaillé avec vous lors de l'essai ancillaire TEXCAN et l'étude PaniCov. Cela a donné lieu à de belles publications dans Molecular Oncology et dans JAMA Network Open. Je suis honoré de travailler encore avec vous dans l'essai PANIRINOX, qui je l'espère sera une réussite.

Monsieur Didier TOUSH, je tiens à te remercier pour ton investissement sans faille depuis 2008. Tu auras été d'excellents conseils en tant que directeur de la licence BBB et du master DETC-BIO. Tu as toujours cru en moi à l'Université et tu as continué à m'aider pour mon inscription en doctorat. Enfin tu as accepté de m'épauler encore une fois durant ces trois années de thèse en tant que membre de mon jury de comité de thèse. Je ne sais pas comment te remercier pour tout ce que tu as fait pour moi mais j'espère pouvoir aider une personne à mon tour comme tu as pu le faire à mon égard. Je suis très heureux de t'inviter à composer mon jury de thèse.

Monsieur Jérôme MOREAUX, je te remercie pour ton aide durant ces trois années de doctorat en tant que membre de mon jury de comité de thèse. Ton expertise scientifique est connue de tous. Je tiens à te remercier pour ta simplicité, tes excellents conseils et la motivation que tu as pu me donner. Je suis très heureux de t'inviter à composer mon jury de thèse.

A mes Collègues et Amis

A mon sens on ne peut pas s'engager dans un doctorat si on est pas soutenu par des Collègues et des Amis.

Je tiens à remercier l'ensemble de mes Collègues pour leur bienveillance, leur écoute et bien évidement leur esprit de camaraderie qui est pour moi la plus importante des qualités. Certains d'entre eux sont devenus des Amis à part entière, je sais qu'ils se reconnaitront. Je tiens donc à remercier toutes les femmes de l'équipe anciennement nommée « Recherche intégrée pour une Médecine Personnalisée en Oncologie Digestive » et récemment baptisée « Biomarqueurs pour une Médecine de Précision » : Corinne, Evelyne, Caroline, Laurence, Rita, Zahra, Amaëlle, Cynthia, Ekaterina, Barbara, Safia, Laura, Audrey, Sonia, Florence, Alexia, Marie, Lucia et Camille. Je tiens à remercier très particulièrement Cynthia qui a toujours été présente pour moi et qui l'est encore aujourd'hui, *Ad Vitam Aeternam*. Je tiens à remercie tous les hommes qui ont composé ces deux équipes de recherches : Alain, Philippe, Marc, Thibault, Antoine, Alexandra, Jean-Daniel, Geoffroy, Nicolas, Simon, Benoit, Baptiste, Andrei et bien évidement Romain. Je suis conscient que j'ai pu oublier des personnes dans ces remerciements et j'en suis désolé pour cela.

Je tiens à remercier l'ensemble des mes Copains et Amis.

Je remercie mes Amis de longue date qui ont toujours été présent pour moi. Il n'y a rien à dire à ce sujet car ils savent déjà tout ce que je pense d'eux. Je ne les remercierais jamais assez, donc une nouvelle lois fois MERCI les Amis pour votre soutien intarissable, votre camaraderie indéfectible et votre amour sans fin. Bien conscient que ces quelques lignes soient fades comparé à notre Histoire, je vous donne rendez-vous au prochain apéro pour tous vous remercier individuellement et de vive voix.

Je vous laisse sur ces quelques mots de Joe qui ont bâti notre Histoire et que vous connaissez si bien :

« On allumait une cigarette et tout s'allumait
Et c'était la fête, le quatorze juillet
Il n'y avait jamais un copain de trop
Dans l'équipe à Jojo
Y avait moins de nuits sans guitare que de jours sans pain
On partageait tout et on n'avait rien
Qu'est-ce qu'on était fous, qu'est-ce qu'on s'en foutait
Qu'est-ce qu'on était bien »

L'équipe à Jojo, Joe Dassin.

A ma famille

Avant toute chose, sachez que ces quelques lignes ne reflètent pas l'immense bonheur que j'ai de vous avoir. Ces mots sont simples et brefs car il est difficile pour moi d'écrire davantage.

A mes parents, sans qui cela n'aurait pas été possible. Je vous remercie pour votre soutien inébranlable, votre courage et vos efforts qui m'ont porté dans la vie. Merci pour ce que vous êtes. Je vous aime.

A mes frères, qui m'ont toujours soutenu envers et contre tout. Vous êtes des modèles pour moi et je vous en remercie. Je vous aime.

A mes tontons et mes tatas, je vous remercie pour votre soutien et l'amour que vous me portez. Je vous aime.

A mes nièces, Mila et Arwen, je vous remercie pour votre joie de vivre, votre tendresse et vos sourires qui me remplissent de bonheur. Je vous aime.

A mes grand-mères, Irène et Lucette, vous avez été deux exemples pour moi. Je garderai toute ma vie l'immense bonheur et la joie que vous m'avez apporté. Votre vie a été exemplaire. Je ne vous oublierais jamais. Je vous aime.

A ma tante Nicole et à mon grand-père Louis. Vous avoir perdus durant mon doctorat a été l'épreuve la plus difficile de ma vie. Il suffisait que je repense à vous pour redresser la tête car votre courage me donne à chaque instant l'envie de poursuivre… Je vous aime

A toi Nicole et à toi Papi, cette thèse est pour vous !

Table des matières

Liste des abréviations :

5-FU: 5-fluoro-uracile

ACE: Antigène carcino-embryonaire

aCL: anti-cardiolipines

ADN: Acide désoxyribonucléique

ADNcir: ADN circulant

ADNmt: ADN mitochondrial

AFM: Microscopie à force atomique

AJCC: American Joint Committee on Cancer

ALAT: Alanine aminotransférase

AMM: Autorisation de mise sur le marché

APC: Adenomatus Polyposis Coli

aPL: anti-phospholipides

APS: Syndrome anti-phospholipides

ARN: Acide ribonucléique

ASAT: Aspartate aminotransférase

ASB: Allele specific blocker

ATP: Adénosine triphosphate

BEAMing: Beads, Emulsion, Amplification and Magnetics

BRAF: V-Raf murine sarcoma viral oncogene homolog B

CAD: Caspase-Activated Dnase

CAPOX: Capécitabine/oxaliplatine

CAPP-Seq: Cancer Personalized profiling by deep sequencing

CCR: Cancer colorectal

CCRm: Cancer colorectal métastatique

CHIP: Chimio-Hyperthermie Intra-Péritonéale

CNVs: Variations du nombre de copie

CRCDC: Centres de coordination régionaux des dépistages des cancers

CT: Chimiothérapies

ctDNA: ADNcir tumoral

CTLA-4: Cytotoxic T-lymphocyte Associated protein

CT-scan: Computerized Tomography

DAMP: Damage associated molecular pattern

ddPCR: digital droplet PCR

DII: DNA Integrity Index

DPNI: Dépistage prénatal non-invasif

DSP: libraries simple brin

ECOG: Eastern Cooperative Oncology Group

EGF: Epidermal growth factor

EGFR: Epidermal growth factor receptor

ERK: Extracellular signal-regulated kinase

FIT: Test immunologique fécal

FOLFIRI: Acide folinique/5-FU/irinotécan

FOLFIRINOX: Acide folinique/5-FU/irinotécan/oxaliplatine

FOLFOX: Leucovorine, 5-FU, oxaliplatine

HNPCC: Cancer colorectal héréditaire sans polypose

Inca: Institut national du cancer

Indels: Insertions/délétions

IRM: Imagerie à résonance magnétique

KRAS: Kirsten rat sarcoma viral oncogene homolog

LDH: Lactate déshydrogénase

MAPK: Mitogen Ativacted Protein Kinase

MLH1: MutL protein homolog 1

MMR: MisMatch Repair

MPO: Myelopéroxydase

MRD: Maladie résiduelle minimale

MSH2: MutS protein homolog 2

MSH6: MutS protein homolog 6

MSI: Instabilité micro-satellitaire

MSS: Stabilité micro-satellitaire

MYH: MutY homolog

NE: Neutrophile élastase

NETs: Neutrophil extracellular traps

NFS: Numération de la formule sanguine

NGS: Séquençage de nouvelle génération

NRAS: Neuroblastoma rat sarcoma viral oncogene homolog

NSCLC: Cancer du poumon non à petites cellules

OS: Survie globale

PAF: Polypose adénomateuse familiale

PAL: Phosphatase alcaline

Pb: Paires de bases

PCR: Réaction de polymérisation en chaine

PCRd: PCR digitale

PCRq: PCR quantitative

PD: Progressive Disease

PD-1: Programmed cell Death 1

PD-L1: Programmed cell Death Ligand 1

PFS: Survie sans progression

Pi3K: Phosphoinositide 3-kinase

PMS2: PMS1 Homolog 2

PRRs: Pattern recognition receptors

RC: Réponse complète

RCP: Réunions de concertation pluridisciplinaire

RCT: Radiochimiothérapies

RECIST: Response Evaluation Criteria in Solid Tumors

RP: Réponse partielle

RT: Radiothérapies

Safe-SeqS: Safe-Sequencing System

SD: Stable Disease

SLE: Lupus érythémateux systémique

SNVs: Single nucleotide variations

SSP: Libraries simple brin

Tam-seq: Tagged-Amplicon deep sequencing

TDM: Tomodensitométrie

TEP-scan: tomodensitométrie par émission de positions

TGFα: Transforming Growth Factor alpha

TK: Tyrosine-kinase

TKI: Inhibiteurs de tyrosine-kinase

TLR9: Toll-like receptor 9

Tm: Température de fusion

TME: Microenvironnement tumoral

TNM: Tumor Node Metastatis

TP53: Tumor protein 53

UID: Identifiant Unique

VEGF: Vascular Endothelial Growth Factor

VEGFR-1: Vascular Endothelial Growth Factor receptor 1

VEGFR-2: Vascular Endothelial Growth Factor receptor 2

WGS: Whole genome sequencing

WT: Wild Type

XELOX: Xeloda/oxaliplatine

Liste des figures :

Liste des tableaux :

Préambule

L'ADN circulant est un domaine très prometteur en oncologie, en effet son analyse permet d'obtenir la caractérisation moléculaire (génétique et épigénétique) des tumeurs d'un patient. L'ADN circulant peut-être analysé via une simple pise de sang à tout moment lors de la prise en charge d'un patient. De ce fait le potentiel clinique de l'analyse des ADN circulants offre des perspectives uniques afin de personnaliser la prise en charge des patients et notamment d'appréhender les résistances aux traitements anti-cancéreux. C'est dans cette dynamique de personnalisation des traitements que ma thèse s'est inscrite.

Objectifs de la thèse

L'objectif premier de ma thèse a été d'étudier l'hétérogénéité clonale des tumeurs de patients atteints de cancer colorectal métastatique par l'analyse de l'ADN circulant tumoral. Pour ce faire, mes travaux sont articulés autour d'essais cliniques déjà publiés ou qui sont toujours en encore en cours.

Dans un deuxième temps, j'ai mené des travaux ayant pour objectif principal de mettre en lumière une nouvelle source de la production des ADN circulants chez des patients atteints de cancer colorectal métastatique. L'hypothèse du laboratoire a été d'étudier l'association entre les pièges ADN extracellulaires produits par les neutrophiles et la production des ADN circulants.

Présentation du manuscrit

Ce manuscrit sera composé de deux parties : dans une première partie, une introduction sera faite sur le cancer colorectal, les ADN circulants et leur potentiel clinique en oncologie digestive. Dans une seconde partie, j'exposerai les résultats des travaux que j'ai réalisé avant l'inscription en doctorat et pendant ces trois années de préparation e ma thèse. Enfin cette partie sera clôturée par d'autres publications scientifiques dans lesquelles j'ai contribuer.

« On ne règle la matière qu'en lui obéissant »

Louis Vaissac

INTRODUCTION

I/ Modèle d'étude : Cancer colorectal

A/ Anatomie du côlon

Le cancer colorectal (CCR) affecte le côlon ou le rectum qui composent le gros intestin situé entre l'intestin grêle et l'anus. Le rôle majeur du gros intestin est la réabsorption de l'eau contenue dans les matières indigestes (non digérées par l'intestin grêle), il s'en suit la formation des selles. Le côlon se divise en quatre segments :

- Le côlon droit ou côlon ascendant commence après l'intestin grêle au niveau du caecum jusqu'à l'angle colique droit situé sous le foie.
- Le côlon transverse s'étend tout le long de la partie supérieur de l'abdomen et relie le côlon droit au côlon gauche.
- Le côlon gauche ou côlon descendant se prolonge jusqu'à la fosse iliaque gauche et relie le côlon sigmoïde.
- Le côlon sigmoïde est le dernier segment du côlon et se situe dans la cavité pelvienne avant de devenir le rectum.

B/ Epidémiologie

B.1 Les chiffres en France en 2018

Bien que nous soyons en 2022, les derniers chiffres officiels fournis par l'Institut National du cancer (Inca) sont datés de 2018[1]. Au cours de l'année 2018 en France le cancer colorectal se situe au troisième rang des cancers les plus fréquents (tous sexes confondus) avec plus de 43 000 nouveaux cas. Environ 17 000 personnes en sont décédées ce qui place le cancer colorectal comme la deuxième cause de décès par cancer chez l'homme et le troisième chez la femme en France. L'âge médian au diagnostic est de 71 ans chez l'homme et de 73 ans chez la femme tandis que l'âge médian au moment du décès et de 77 ans chez l'homme et de 81 ans chez la femme. Il est à noter, que dans 80% des cas, le cancer colorectal provient d'un lésion bégnine. La survie nette standardisée sur l'âge à 5 ans et de 63% et de 52% à 10 ans (tous sexes confondus). A noter que la survie nette correspond à la survie du patient qui serait observée si la seule cause de décès possible était le cancer[2,3].

B.2 Les chiffres dans le monde en 2018

Au niveau mondial, le cancer colorectal compte annuellement pour approximativement 10% des diagnostiques de cancer et 10% des morts par cancer[4]. Bien que son incidence et le taux de mortalité chez les femmes soit 25% inférieur que chez les hommes, il est le second cancer le plus diagnostiqué chez les femmes et le troisième chez les hommes dans le monde[5]. Les taux d'incidence et de mortalité diffèrent selon zones géographiques mais augmentent dans les pays les plus développés. Certaines prédictions indiquent que l'incidence du cancer colorectal va augmenter de 2.5 millions de nouveaux cas en 2035 dans le monde[4,6]. De nombreux facteurs de risque influent dans l'initiation tumorale des cancers du côlon et du rectum.

C/ Facteurs de risque

Il faut savoir qu'il existe trois risque de développer un cancer colorectal : moyen, élevé ou très élevé. Bien que l'âge augmente le risque de développer un cancer côlon puisque 9 personnes malades sur 10 ont plus de 50 ans, les facteurs de risques d'apparition d'un cancer colorectal sont variés. Dans ce contexte une personne âgée de moins de 50 ans à un risque faible d'être atteinte de cancer colorectal (5% des cas de cancers colorectaux) mais passé cet âge le risque devient « moyen ». De plus, il est à noter que les personnes ayant déjà été atteints par un cancer colorectal ont davantage de risque d'en développer un second et sont par conséquent des personnes à risque élevé et représentent 10 à 20% des cas[7,8]. Par extension, les personnes qui ont un ou plusieurs parents de premier degrés (mère, père, frères et sœurs) atteint de cancer colorectal ont un risque augmenté de développer un cancer colorectal. Les antécédents familiaux ne sont pas les seuls facteurs de risque du cancer colorectal. Les facteurs de risque héréditaires, environnementaux et comportementaux seront abordés dans cette partie.

C.1 Facteurs héréditaires

Dans le monde une analyse de plusieurs études révèle qu'approximativement 5% à 7% des patients atteints de cancer colorectal sont liés à un syndrome héréditaire[9]. Les syndromes héréditaires du cancer colorectal sont divisés en deux groupes : les syndromes de polypose (ex : la polypose adénomateuse familiale : PAF) et les syndromes non-polypose comme par

exemple le syndrome de Lynch. Les patients atteints de ces pathologies héréditaires sont dits à risque très élevé de développer un cancer colorectal.

Le syndrome de Lynch ou cancer colorectal héréditaire sans polypose (HNPCC) est la forme de cancer par hérédité la plus répandue. En France, environ 3% des cancers colorectaux seraient liés au syndrome de Lynch. Les personnes atteintes de ce syndrome sont classées à « très haut risque » et peuvent avoir jusqu'à 80% de risque de développer un cancer colorectal. Cette pathologie est causée généralement par des mutations sur 4 gènes codant pour des protéines appartenant au système de réparation de l'ADN ou système MMR (MisMatch Repair). Ces gènes sont le *MLH1* (*MutL protein homolog 1*), *MSH2* (*MutS protein homolog 2*), *MSH6* (*MutS protein homolog 6*) et *PMS2* (*PMS Homolog 2*)[10]. Ce syndrome expose à un risque cumulé de cancer colorectal de près de 50% à 70 ans, notamment pour les variants des gènes *MLH1* et *MSH2*.

Les personnes atteintes des syndromes de polypose sont rares mais sont plus facilement reconnaissables par les médecins au vu d'un grand nombre de polypes chez le patient. Par exemple, La polypose adénomateuse familiale est une maladie héréditaire principalement due à des mutations sur le gène *APC* (*Adenomatus Polyposis Coli*). Comme son nom l'indique ce syndrome est caractérisé par le développement de centaines, voire de milliers de polypes adénomateux au niveau de la muqueuse du côlon ou du rectum, parfois dès l'âge de 10-12 ans. On estime une éventuelle évolution en cancer de ces polypes adénomateux en 10-15 ans et survient avant l'âge de 40 ans. Certaines personnes atteintes de ce syndrome ont jusqu'à 100% de risque de développer un cancer colorectal. Il existe des formes atténuées de polypose dans lesquelles le gène *APC* n'est pas impliqué, dont par exemple le gène *MYH* (*mutY homolog*) ou d'autres gènes (5% des cas).

C.2 Facteurs environnementaux et comportementaux

Outre les facteurs de risque imputables aux antécédents familiaux et aux facteurs héréditaires, les facteurs liés au mode de vie augmentent considérablement le risque de développer un cancer colorectal[5] **(Figure 1)**.

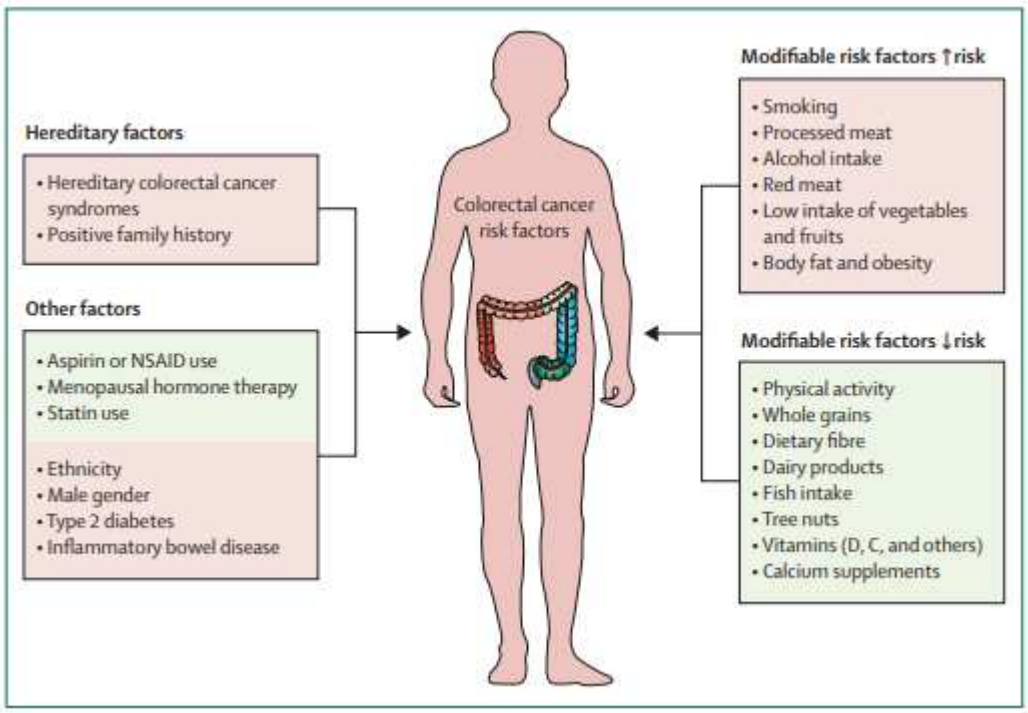

Figure 1: Liste des facteurs de risques du cancer colorectal Source : Dekker *et al,* 2019. Colorectal cancer[5](.

Il existe un grand nombre de facteurs de risque qui pourraient diminuer la mortalité par ce cancer. En France et dans le monde, le tabac est le premier d'entre eux[11] avec 5% et 10% de mortalité par cancer colorectal chez les femmes et les hommes, respectivement. Il a été démontré qu'un individu consommant 50 grammes d'alcool (environ 4 verres) par jour à un risque accru de mortalité qu'un non buveur[12]. De plus, le surpoids[13], la prise alimentaire de viande rouge[14] et la sédentarité sont des aussi facteurs favorisant le risque d'être atteint d'un cancer colorectal[5]. Au contraire, une activité physique journalière (environ 30 minutes), une alimentation riche en fibres, en fruits et légumes sont des facteurs protecteurs[5].

D/ Dépistage et Diagnostic

Souvent le cancer colorectal est asymptomatique et peut donc être diagnostiqué de façon fortuite et tardivement. Cependant, le diagnostic du cancer colorectal est réalisé lors d'une consultation face à des symptômes évocateurs. A noter, qu'une personne ayant des antécédents personnels et familiaux, des facteurs héréditaires connus (PAF, syndrome de lynch, etc.) doit faire l'objet d'une surveillance endoscopique spécifique et rapprochée dans le temps facilitant le dépistage et le diagnostic précoce de la maladie.

D.1 Dépistage

En complément de ce qui a été mentionné, en France le programme de dépistage organisé du cancer colorectal s'adresse aux femmes et aux hommes de 50 à 75 ans sans histoire familiale ni d'antécédents personnels de cancer colorectal ou d'adénomes et ne présentant pas de symptômes évocateur. Tous les deux ans, les centres de coordination régionaux des dépistages des cancers (CRCDC) invitent les personnes susmentionnées, si elles sont éligibles à se faire remettre un kit de dépistage. Le dépistage consiste à la recherche de sang (plus précisément le dosage de l'hémoglobine) occulte dans les selles. En France, le test immunologique fécal (FIT) a remplacé le test Gaïac (Hemocult). Le test FIT à l'avantage d'utiliser des anticorps spécifiques à la globine humaine et donc d'être spécifique d'un saignement colorectal. Ce test a aussi pour avantage d'avoir une méthode d'analyse immunologique quantitative automatisée permettant une interprétation fiable et reproductible. Bien que dans 96% des cas le résultat est négatif, cela n'exclue pas l'éventualité d'un cancer colorectal. Si la recherche de sang occulte dans les selles est positive, une coloscopie est prescrite chez un gastroentérologue. Cet examen permet de détecter la présence éventuelle d'un cancer ou de polypes jugés à risque (volumineux). A noter que la coloscopie détecte un polype dans moins de 50% des cas et un cancer dans 8% des cas.

D.2 Diagnostic

Le diagnostic peut être de façon fortuite, après lors d'une campagne de dépistage ou lors d'une consultation face à des symptômes évocateurs. C'est ce dernier cas que nous allons aborder ici.

Il est à noter que plus diagnostic tarde à être posé plus les symptômes sont nombreux et fréquents. De plus, les symptômes évocateurs d'un cancer colorectal sont multiples et ne sont pas spécifiques au cancer colorectal mais peuvent être causés par d'autres pathologie. Les symptômes les plus fréquents sont :

- L'apparition de douleurs abdominales liées à la contraction de l'intestin évoluant par crise de deux ou trois jours.
- Des troubles du transit intestinal (constipation brutale, diarrhée prolongée)
- La présence de sang dans les selles
- Une anémie
- Une occlusion intestinale

Suite à ces symptômes un examen clinique et un interrogatoire du patient permettent d'évaluer l'état du patient et de connaitre d'éventuels facteurs de risque. En premier lieu le toucher rectal permet de diagnostiquer un cancer du rectum s'il est situé approximativement à 8 cm de l'anus. Ensuite, la coloscopie est un examen dont l'objectif est de visualiser la muqueuse de la paroi intestinale et nécessite comme préalable particulier que le patient ne doit pas consommer de l'aspirine dans les dix jours avant la l'examen, qu'il doive signaler tout traitement par anticoagulant et qu'il doive adopter un régime sans résidus deux jours avant l'examen.

D.3 Examens radiologiques

Une fois le diagnostic établis, un bilan d'extension est indispensable afin d'établir l'étendue et l'agressivité de la tumeur. Un bilan d'imagerie par tomodensitométrie (TDM appelé scanner) ou par imagerie à résonance magnétique (IRM) sont les examens principalement utilisés pour explorer l'étendue du cancer des régions thoraco-abdomino-pelvienne. Ces techniques d'imagerie nécessitent l'absorption préalable d'un produit de contraste permettant de mieux visualiser les zones observées. Une IRM pelvienne ou une échographie endorectale est réalisée en cas du cancer du rectum. Aussi, en cas de suspicion de métastases hépatiques une échographie ou une IRM du foie peuvent être réalisés. Enfin, en cas de cancer métastatique et après injection de glucose radio-marqué, un TEP-scan (tomodensitométrie par émission de

positions) permet d'observer le métabolisme des cellules cancéreuses qui sont très consommatrice de glucose.

D.4 Examens biologiques

Le bilan d'extension comprend aussi des analyses biologiques qui sont réalisées pour rechercher et quantifier des marqueurs tumoraux et afin d'étudier le profil moléculaire de la tumeur. Il est effectué dans le même temps un bilan sanguin standard pour la surveillance des principales fonctions vitales. L'exploration de la fonction rénale (clairance créatine, créatininémie, urée plasmique) et l'exploration de la fonction hépatique (transaminases (ASAT, ALAT), bilirubine, PAL, LDH) seront effectuées. Aussi, un hémogramme sera réalisé pour connaitre la numération de la formule sanguine (NFS) et les plaquettes.

Le dosage de marqueurs tumoraux repose initialement sur la quantification de l'antigène carcino-embryonaire (ACE) qui est produit de façon physiologique dans l'organisme mais qui est produite en excès par les cellules cancéreuses. Un taux d'ACE anormalement élevé peut-être corrélé à la présence d'une tumeur mais en pratique il permet surtout l'évaluation initiale des cancers métastatiques. L'ACE sera utilisé tout au long de la prise en charge du patient car il est marqueurs pronostique dans les cas de cancer colorectal métastatique (Kanas, 2012). La connaissance du statut mutationnel des gènes *KRAS (Kirsten rat sarcoma viral oncogene homolog)* et *NRAS* (*neuroblastoma rat sarcoma viral oncogene homolog)* (*RAS*) des tumeurs est requis dans les traitement des cancers colorectaux métastatiques car il est prédictif de la réponse aux thérapies ciblées anti-EGFR (anti-Epidermal growth factor receptor) (Amado, 2008; Lièvre, 2006). Il sera aussi recherché le statut *MSI* (instabilité micro-satellitaire) des tumeurs.

E/ Stade (classification TNM)

Une fois que le diagnostic d'un cancer colorectal est établi, il est impératif de définir son stade et son grade. Pour cela une analyse histologique du tissu tumoral prélevé lors par biopsie lors de la coloscopie faite au diagnostic.

La classification histo-pronostique appelée classification TNM (Tumor Node Metastatis) et celle proposée par l'AJCC (American Joint Committee on Cancer) **(Tableau 1)**. Celle-ci est régulièrement mise à jour et la dernière édition est la TNM 8^{ième} édition qui est appliquée depuis 2017[15]. Celle-ci recommande l'examen d'au moins 12 ganglions régionaux pour établir le statut N de la classification TNM[15] et ce choix résulte d'un consensus au niveau international. Il faut savoir que quel que soit le stade, plus le nombre de ganglions analysés est grand, meilleur est le pronostic. Le stade tumoral est une macro-classifications de la classification TNM et regroupe souvent plusieurs TNM. Pour finir, cette classification des tumeurs a pour objectif de pronostiquer l'évolution de la maladie, adapter la prise en charge thérapeutique et de rendre homogène des groupes de malades en vue d'essai clinique.

A

Tis	carcinome *in situ*, tumeur intra-muqueuse envahissant la *lamina propria* (chorion) sans extension à travers la musculaire muqueuse à la sous-muqueuse
T1	tumeur envahissant la sous-muqueuse
T2	tumeur envahissant la musculeuse
T3	tumeur envahissant la sous-séreuse ou les tissus péri-coliques et péri-rectaux non péritonéalisés
T4	tumeur envahissant directement les autres organes ou structures et/ou perforant le péritoine viscéral T4a : tumeur perforant le péritoine viscéral * T4b : tumeur envahissant directement des autres organes ou structures de voisinage **
Nx	renseignements insuffisants pour classer les adénopathies régionales
N0	pas de métastase ganglionnaire régionale
N1	métastase dans 1 à 3 ganglions lymphatiques régionaux *** N1a : métastase dans 1 ganglion lymphatique régional N1b : métastases dans 2-3 ganglions lymphatiques régionaux N1c : nodule(s) (ou) dépôt(s) tumoral(aux) « satellites » dans la sous-séreuse, ou dans les tissus péri-coliques ou péri-rectaux non péritonéalisés, sans ganglion métastatique régional ****
N2	métastases ≥ 4 ganglions lymphatiques régionaux N2a : métastases dans 4-6 ganglions lymphatiques régionaux N2b : métastases dans ≥ 7 ganglions lymphatiques régionaux
M0	pas de métastase(s) à distance
M1	Métastase(s) à distance M1a : métastase(s) localisée(s) à un seul organe (foie, poumon, ovaire, ganglion(s) lymphatique(s) non régionaux) sans métastase péritonéale M1b : métastases atteignant plusieurs organes sans métastase péritonéale M1c : métastase(s) péritonéale(s) avec ou sans métastases d'autres organes

B

Stade 0	pTis N0 M0
Stade I	pT1-2 N0 M0
Stade IIA	pT3 N0 M0
Stade IIB	pT4a N0 M0
Stade IIC	pT4b N0 M0
Stade IIIA	pT1-T2 N1/N1c M0 et pT1 N2a M0
Stade IIIB	pT3-T4a N1N1c M0, pT2-T3 N2a M0, pT1-T2 N2b M0
Stade IIIC	pT4a N2a M0; p T3-T4a N2b M0; pT4b N1-N2 M0
Stade IVA	tout T, tout N, M1a
Stade IVB	tout T, tout N, M1b
Stade IVC	tout T, tout N, M1c

Tableau 1 : Classification TNM et par stade des tumeurs colorectales : Adapté de « Cancer du côlon non métastatique » Thésaurus National de Cancérologie Digestive, Mars 2021, [En ligne] [https://www.snfge.org/tncd et http://www.tncd.org][16]

F/ Prise en charge

La prise en charge des patients atteints de cancer colorectal est fonction du stade de la maladie. La complexité moléculaire des tumeurs ainsi que la multitude de localisations possibles rendent chaque cancer « unique ». Il sera alors conseillé pour chaque patient sur la base de l'avis rendu lors des réunions de concertation pluridisciplinaire (RCP) une prise en charge particulière ayant pour objectif d'améliorer la survie du patient que ce soit par la résection totale de la tumeur localisée, le traitement de la tumeur par radiothérapie ou encore l'administration de médicament anticancéreux et plus récemment l'utilisation de l'immunothérapie.

F.1 Chirurgie

La chirurgie est le traitement standard et de référence pour les stades précoces des cancers du côlon et du rectum.

F.1.1 Cancer du côlon

La chirurgie est le traitement de référence (recommandée) pour les patients atteints de cancer du côlon de stade I, II et III. Un traitement endoscopique est possible en cas de tumeur superficielle (résection d'un polype ou polypectomie) au stade 0. Au stade I**,** la chirurgie seule est recommandée et repose sur l'exérèse de la tumeur primitive (avec une marge distale et proximale sur le côlon sain d'au minimum 5 cm), des vaisseaux et du méso-côlon contenant les ganglions lymphatiques. Quel que soit le stade de la maladie, il existe différents types de résections en fonction de la localisation tumorale: hémicolectomie droite ou gauche, colectomie segmentaire ou gauche et la sigmoïdectomie de la charnière. Pour les patients atteints d'un cancer du côlon de stade II, le traitement principal est la chirurgie mais le patient peut bénéficier d'un traitement adjuvant par chimiothérapie ou d'une radiothérapie. Les traitements adjuvants conventionnels sont généralisés pour les patients en stade III.

La prise en charge des patients de stade IV est davantage sujette à discussion en RCP comprenant au moins un chirurgien et un radiologue expérimenté en pathologie hépatique. Il est notamment discuté du rapport bénéfice/risque de la chirurgie en fonction des critères d'opérabilité et de résécabilité (ou non-résécabilité) des tumeurs. La résection d'une tumeur primitive est prescrite que si l'exérèse complète de la tumeur est possible. Chez les patients de stade IV la présence de métastases est dite synchrone (25% des cas) si elles sont présentes

au moment du diagnostic du cancer (ou dans les 6 mois après le premier diagnostic) ou métachrone si elles sont observées 6 mois après le premier diagnostic. Généralement les métastases d'un cancer du côlon ou du rectum sont localisées au niveau hépatique et sont opérables dans 10 à 25% des cas. Le traitement chirurgical permet d'obtenir un taux de survie à 5 ans d'environ 30%. Les patients au stade IV de la maladie sont majoritairement traités par un protocole de chimiothérapie et/ou avec l'association d'une thérapie ciblées anti-EGFR. L'efficacité du protocole de chimiothérapie doit être évaluée tous les deux à trois mois puisqu'en cas de réponse le choix d'une chirurgie est rediscuté.

Les récidives du cancer du côlon sont bien souvent traitées comme pour un patient au stade IV de la maladie. Environ 80% des récidives ont lieu dans les 3 ans qui suivent le traitement curatif[17] dont 25% d'entre elles peuvent être traitées avec une intention curative[18]. Plusieurs examens sont à réaliser pour assurer une surveillance des patients en récidive. Un examen clinique et radiologique sont à réaliser tous les 3 mois pendant 3 ans puis tous les 6 mois pendant 2 ans, une coloscopie est faite 2 à 3 ans après l'intervention. Des analyses biologiques basées sur la recherche de l'ACE[19] est proposée chez les patient qui pourront supporter une ré-intervention ou une chimiothérapie.

F.1.2 Cancer du rectum

Comme pour les cancers du côlon la chirurgie est le traitement standard pour les patients atteints d'un cancer du rectum de stade 0. Pour les stades I et II d'un cancer du rectum la chirurgie est le traitement principal, il est préconisé de faire une résection de l'intestin plutôt qu'une exérèse transanale locale ou une microchirurgie endoscopique pour enlever une petite tumeur de bas grade car ces dernières engendrent un risque plus élevé de récidive. La chirurgie peut être accompagné d'une chimiothérapie ou d'une radiothérapie. A savoir que la qualité de l'exérèse chirurgicale est le facteur essentiel du pronostic. Avant chirurgie, la prise en charge des patients de stade II et III pour lesquels la tumeur est jugée opérable repose généralement sur l'instauration d'une radiothérapie voir une radiochimiothérapie néoadjuvante[20]. Pour les stades II et III (tumeur non opérable) une radiochimiothérapie est réalisée avant une réévaluation par imagerie afin d'envisager une exérèse dans le cas où cela est jugé possible en RCP. Enfin pour les stade IV, la prise ne charge des métastases est identique à celle du cancer de côlon.

F.2 Traitements conventionnels

F.2.1 Chimiothérapies

Le choix des différents protocoles de chimiothérapies (CT) proposées aux patients atteints d'un cancer colorectal sont discutés en RCP et tient compte : du stade de la tumeur et de ses caractéristiques, de l'état général du patient et des facteurs de comorbidités de celui-ci. L'oncologue prend aussi en considération le projet thérapeutique du patient. Les traitements de chimiothérapies sont prescrits dans le cadre de l'Autorisation de mise sur le marché (AMM) de molécules.

Elles associent principalement pour les stades non métastatiques le 5-fluoro-uracile (5-FU), l'oxaliplatine, l'irinotecan, capécitabine, la leucovorine (ou acide folinique) et la mitomycine C. Pour les stades II, si de mauvais facteurs pronostics comme un statut MSS (stabilité micro-satellitaire) ou un statut MSS/MSI indisponible, une lors d'une tumeur peu différenciée il peut être prescrit une CT adjuvante. A noter que la CT adjuvante n'est pas recommandée pour les stades 0 et I. Pour les stades III, il est prescrit une CT adjuvante par protocole de chimiothérapies de type FOLFOX4 (ou FOLFOX simplifié : leucovorine, 5-FU et oxaliplatine) **(Figure 2)** ou ses variantes modifiées comme le FOLFOX4s et le FOLFOX6, par XELOX (ou CAPOX : capécitabine et oxaliplatine) ou FOLFIRI (leucovorine, 5-FU et irinotecan) **(Figure 3)**. Ces protocoles de chimiothérapies sont souvent administrés pendant 6 mois et commence avant le 42^{ième} jour post-opératoire.

Enfin pour les stades IV (ou stade métastatique) les molécules de chiomithérapies sont identiques en y ajoutant le raltitrexed (TOMUDEX®) et l'uracile-tegafur. Le choix du traitement est décidé en RCP en fonction de l'opérabilité des métastases. De plus, à ce stade de la maladie ces protocoles de chimiothérapies sont associés à des thérapies ciblées anti-EGFR en fonction du statut *RAS* (*KRAS* et *NRAS*) de la tumeur ou à un anticorps anti-VEGF (Vascular Endothelial Growth Factor) inhibiteur de l'angiogenèse (voir partie F.3).

Plusieurs cas de figure existent :

- Métastases hépatiques et pulmonaires résécables : le plus souvent FOLFOX4s avec 6 cures préopératoires et 6 cures postopératoires[21].
- Métastases extra-hépatiques résécables : pour les carcinoses péritonéales, le recours à la CHIP (Chimio-Hyperthermie Intra-Péritonéale) après résection complète des lésions est indiqué lorsque la carcinose est isolée chez un patient en bon état général[22]. Elle utilise généralement le FOLFOX4 ou FOLFOX4s
- Métastases +/- résécables : Il est recommandé d'opérer dès que les métastases deviennent opérables sans attendre au-delà de 4 mois de CT et de respecter un délai de 4 à 6 semaines après la fin de la CT avant d'opérer. Pour les patients opérés, les associations sont nombreuses et entre autres :
    - 1ère ligne - *RAS* sauvage : FOLFOX4 + un anti-EGFR (Cetuximab ou Panitumumab)
    - 1ère ligne - *RAS* muté : FOLFOX4 + anti-angiogénique (Bevacizumab)
    - 2ième ligne - *RAS* sauvage : FOLFIRI + Cetuximab ou Panitumumab
- Métastases non résécables : Polychimiothérapie d'emblée pour faciliter une pause thérapeutique ou un allègement sous forme de mono chimiothérapie 5FU/Capécitabine en cas de contrôle de la maladie.

Tous traitements par chimiothérapies nécessitent un bilan clinique et biologique avant chaque cure afin d'adapter la prise en charge des patients. Il faut noter que les chimiothérapies entrainent des effets secondaires indésirables qui sont communs à toutes les chimiothérapies ou peuvent être dus à des molécules en particulier. On retrouve généralement des toxicités digestives (vomissements, nausées, diarrhée), hématologiques, cutanées, cardiaques et pulmonaires, et enfin des toxicités neurologiques.

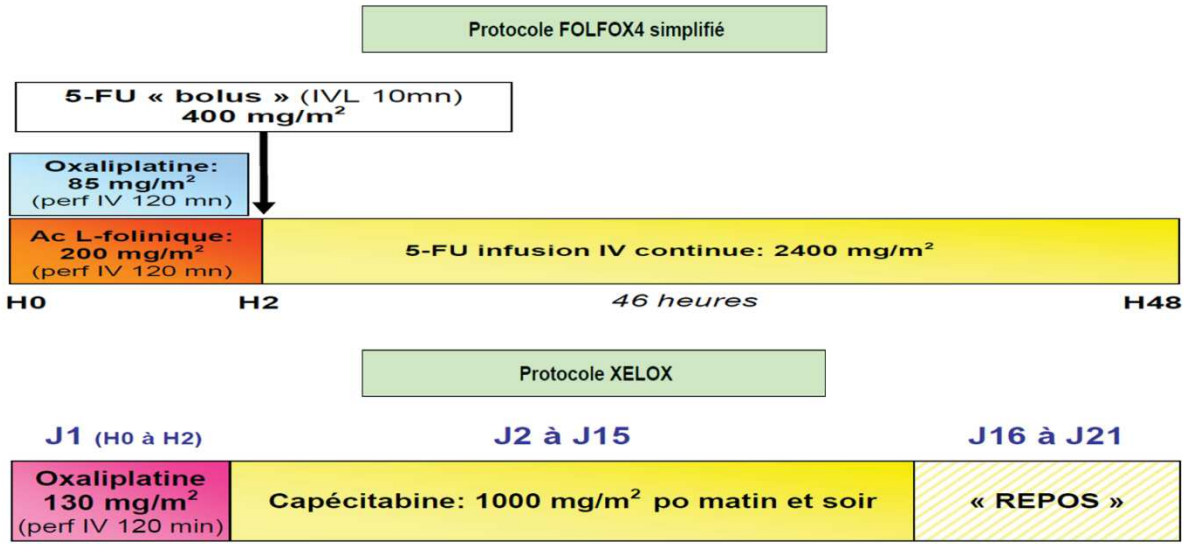

Figure 2: Protocoles d'administration FOLFOX4s et XELOX. *Source : Fédération Francophone de Cancérologie Digestive – Chimiothèque.*

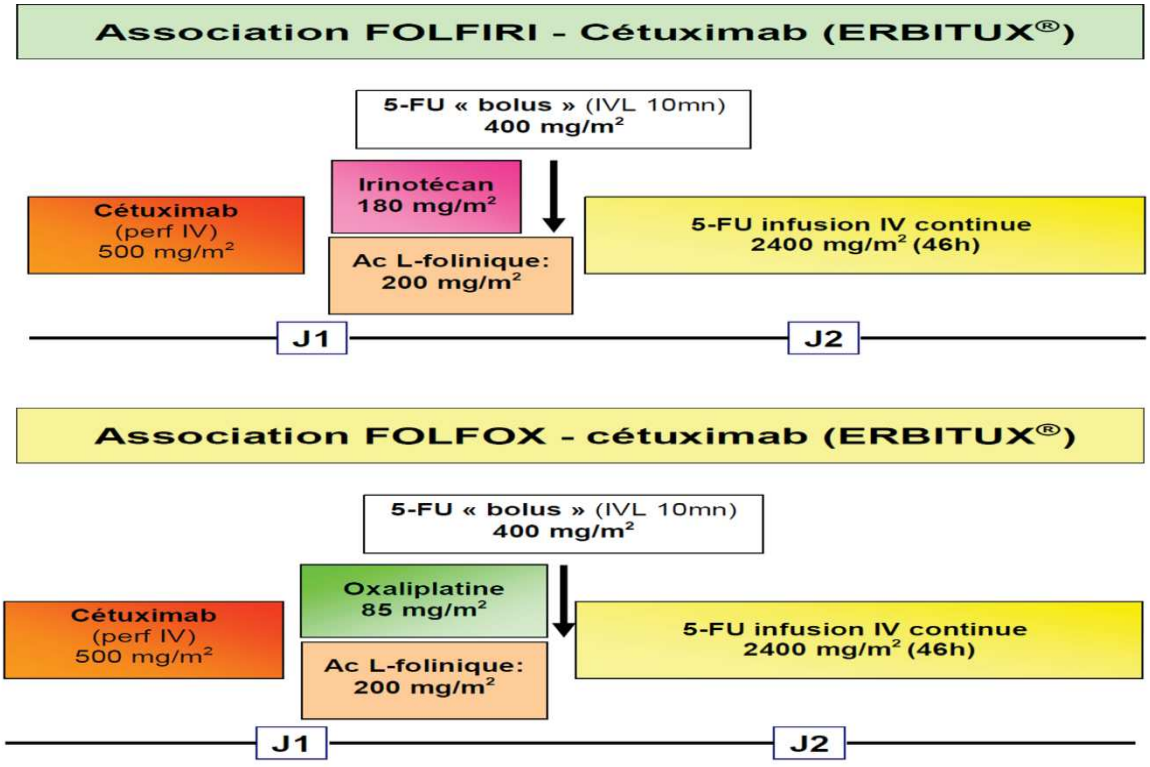

Figure 3: Protocoles d'administration des associations FOLFOX4 ou FOLFIRI + Anti-EGFR. *Source : Fédération Francophone de Cancérologie Digestive – Chimiothèque.*

F.2.2 Radiothérapies et radiochimiothérapies

Les radiothérapies (RT) et les radiochimiothérapies (RCT) sont préconisées comme thérapie néoadjuvante (voire adjuvantes) selon le stade de la maladie. Ces traitements peuvent être indiqués et réalisés de façon exclusive lorsqu'il y a une contre-indication à la réalisation d'une chirurgie. En terme de molécules il est indiqué d'utiliser du 5-FU (ou capécitabine)[23]. L'oxaliplatine est quant à lui à proscrire lorsqu'il est associé à la RT car il favorise les neutropénies[24]. Ces thérapies sont nécessaires lors d'une prise en charge du cancer du rectum. A noter que sauf exception (discutée en RCP) le recours à ces thérapies n'est pas indiqué aux stades 0 et I.

En cas de résécalibilté de la tumeur des stades II et III une RCT néoadjuvante est prescrite dans la majorité des cas pour une tumeur du moyen ou du bas rectum. Généralement il est préférable de réaliser des RT ou des RCT néoadjuvantes plutôt qu'adjuvantes en raison d'une meilleure efficacité et d'une faible toxicité[20,25]. En revanche, lorsque la tumeur n'est pas opérable pour les stades II et III une irradiation avec escalade de dose 50 à 60 Gy est indiquée car cela augmente la réponse tumorale et améliore le contrôle de la maladie[26]. Suite une nouvelle évaluation en RCP une exérèse de la tumeur peut être réalisable après une RT. Il n'existe pas de recommandations standards en termes de RT ou de RCT pour les stades IV. Cependant, une prise en charge sera effectuée en fonction du caractère symptomatique de la tumeur : à savoir une RT néoadjuvantes suivie d'une chirurgie peut être indiquées pour des tumeurs symptomatiques.

F.3 Thérapies ciblées

Les avancées de la biologie moléculaire ont pu mettre en évidence des voies de signalisation intracellulaire impliquée dans la prolifération et la survie cellulaire. De plus, la mise en évidence de mutations activatrices de ces voies de signalisation a permis l'établissement de thérapies dites ciblées qui à l'inverse des chimiothérapies standards vont essentiellement agir sur les cellules tumorales. Ces thérapies ciblées renforcent l'arsenal thérapeutique existant et améliorent la survie des patients tout en diminuant les effets secondaires. Il existe deux grands types de thérapies ciblées : (i) les inhibiteurs de tyrosine-kinase (TKI) qui sont des petites molécules qui interagissent avec le domaine tyrosine kinase de protéines intracellulaire les rendant inactives et (ii) les anticorps monoclonaux ciblant le domaine extracellulaire d'un

récepteur cellulaire (comme le récepteur au facteur de croissance épidermique, EGFR) ou bien visant un facteur soluble de croissance (comme le facteur de croissance de l'endothélium vasculaire, VEGF). Ces thérapies ciblées bloquent la transcription de gènes impliqués dans la prolifération et la survie cellulaire.

F.3.1 La voie de signalisation RAS/MAPK

La voie de signalisation RAS/MAPK (Mitogen Ativacted Protein Kinase) permet d'assurer la transduction intracellulaire d'un signal, depuis la stimulation des récepteurs membranaires de l'EGFR par la fixation d'un facteur de croissance (EGF, TGFα : Transforming Growth Factor, amphiréguline, épiréguline et autres…) jusqu'à la transcription des gènes impliqués dans l'angiogenèse, la prolifération, l'invasion, la migration et la survie cellulaire. Plus précisément, la fixation d'un ligand de l'EGFR à ce récepteur entraine sa dimérisation et son activation par phosphorylation au niveau du résidus tyrosine spécifiques situés sur son domaine intracellulaire appelé « domaine tyrosine kinase » **(Figure 4)**. L'activation de la voie de signalisation *RAS/MAPK* commence par l'activation de la protéine RAS qui elle-même par l'intermédiaire de phosphorisation successives va par la suite activée les protéines RAF, MEK puis ERK (Extracellular signal-regulated kinase). Cette dernière protéine est transloquée au niveau du noyau et va activer la transcription des gènes impliqués dans l'initiation du cycle cellulaire. La voie Pi3K/AKT (phosphoinositide 3-kinase/AKT) est une autre grande voie de signalisation intracellulaire activée soit par l'EGFR activé soit par la protéine RAS activée. Cette dernière voie de signalisation joue également un rôle important dans la prolifération et la survie cellulaire.

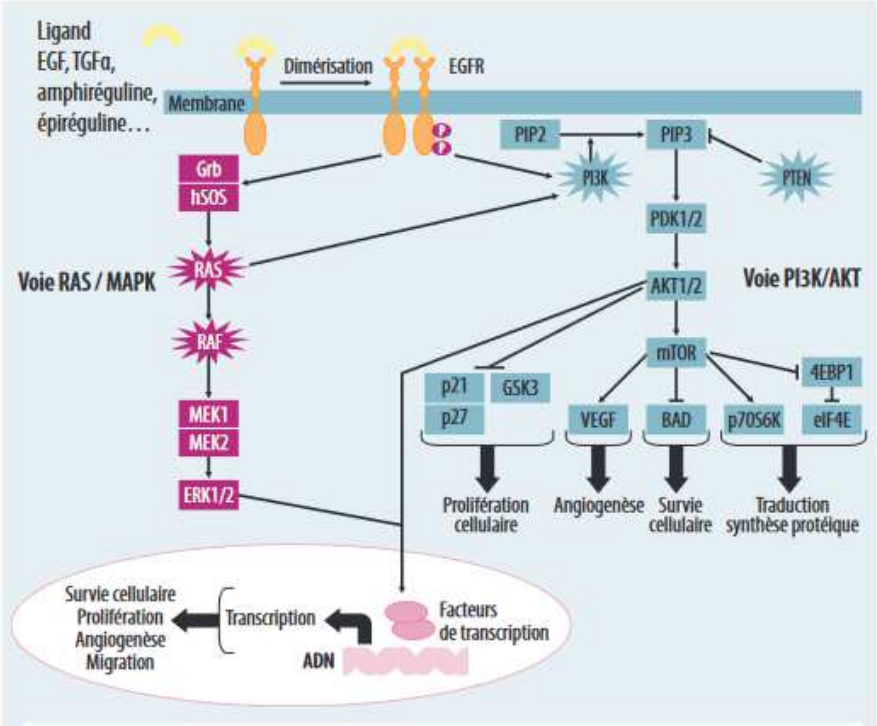

Figure 4: Activation de l'EGFR et des voies de signalisation intracellulaire en aval. Source : Lièvre *et al,* 2006. Mutations du gène *KRAS* et réponse aux anticorps anti-EGFR dans les cancers colorectaux : ce qu'il faut retenir[27].

F.3.2 Les anticorps monoclonaux anti-EGFR

Deux médicaments à base d'anticorps monoclonaux anti-EGFR ont reçus leur AMM au cours des années 2000, Le ERBITUX® (AMM, 2004) et le VECTIBIX® (AMM, 2006). Les molécules activent de ces deux médicaments sont le cetuximab (ERBITUX®) qui est une IgG1 chimérique et le panitumumab (VECTIBIX®) qui est une IgG2 recombinante totalement humaine (moins immunogène). Ces deux anticorps sont monoclonaux et cible le domaine extracellulaire de l'EGFR qui est surexprimé à la surface des cellules cancéreuses dans 30 à 80% épithéliaux dont les cancers colorectaux[27]. La fixation de ces anticorps va empêcher la dimérisation et l'activation de l'EGFR **(Figure 5)** ce qui va inhiber la survie, et la prolifération cellulaire. Ils sont tous deux prescrits chez les patients atteints de cancer colorectal métastatique (CCRm) ayant un statut *RAS* sauvage (ou non muté)[28–30] en association avec un protocole de chimiothérapie conventionnelle[31,32]. Ils peuvent aussi être donnés en monothérapie après un échec des protocoles de chimiothérapies conventionnelles. Les mutations recherchées sur les gènes *KRAS* et *NRAS* sont situées sur les exons 2,3 et 4. En première ligne de traitement les anti-EGFR

sont principalement prescrits avec un protocole FOLFOX. Pour les patients *RAS* sauvages ayants reçus en première ligne du 5-FU, il est préconisé en seconde ligne de traitement de prescrire le protocole FOLFIRI (leucovorine, 5-FU et irinotécan) associer à un anti-EGFR.

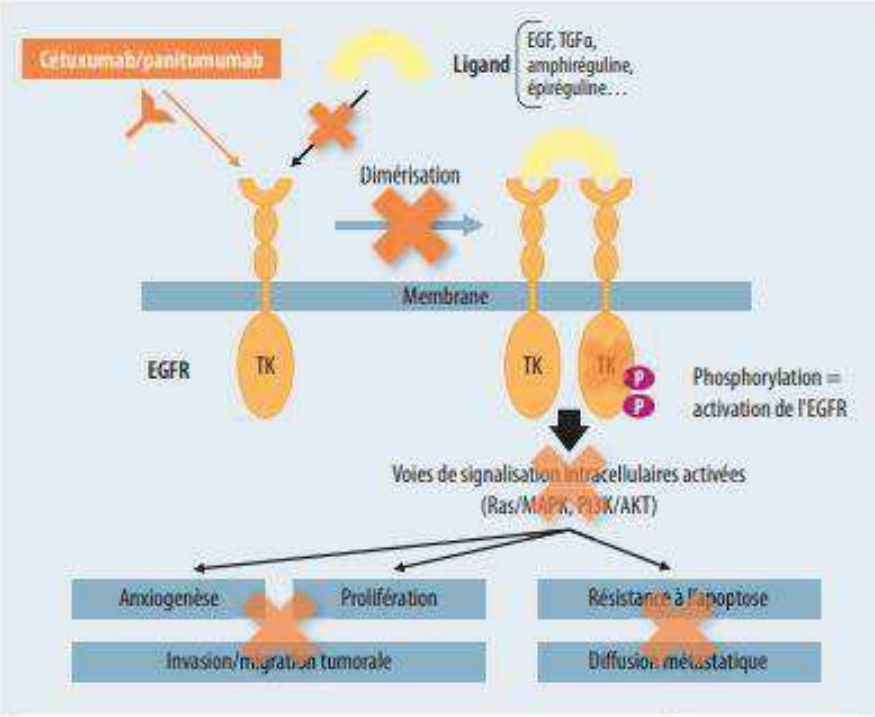

Figure 5: Mécanisme d'action des anti-EGFR. Source : Lièvre *et al,* 2006. Mutations du gène *KRAS* et réponse aux anticorps anti-EGFR dans les cancers colorectaux : ce qu'il faut retenir[27].

F.3.3 Le bevacizumab, anticorps monoclonal anti-VEGF

Le bevacizumab (AVASTIN®) est un anticorps monoclonal anti-VEGF. Il se lie au VEGF, facteur clé de l'angiogenèse, inhibant de ce fait la liaison du VEGF à ses récepteurs, Flt-1 (VEGFR-1) et KDR (VEGFR-2), à la surface des cellules endothéliales. La neutralisation de l'activité biologique angiogénique (anti-angiogénique) du VEGF limite la croissance tumorale en inhibant la formation de nouveaux vaisseaux tumoraux et en faisant régresser les vaisseaux tumoraux existants. Cette molécule complète la prise en charge des patients CCRm puisqu'elle est utilisée en présence de mutations *RAS* qui contre-indiquent l'utilisation des anti-EGFR. Le bevacizumab est utilisé en 1ère ligne en association à une CT à base de fluoropyrimidines[33].

En termes d'effets secondaires indésirables, les personnes traitées par bevacizumab sont potentiellement exposées à un risque de perforation intestinale et de fistule qui imposent

l'arrêt du traitement. Les effets indésirables les plus fréquemment observés chez les patients recevant le bevacizumab étaient : hypertension artérielle, fatigue ou asthénie, diarrhée, et douleur abdominale. Des troubles hématologiques de type neutropénie fébrile, leucopénie et thrombopénie sont aussi très fréquemment observés.

F.3.4 Le régorafénib

Le régorafénib (STIVARGA®) est un inhibiteur d'enzymes de type tyrosine-kinase (TK) intracellulaires ou liées à la membrane[34] **(Figure 6)** qui catalysent le transfert d'un groupement phosphate d'une molécule d'adénosine triphosphate (ATP) vers une protéine effectrice. ITK se fixent de manière compétitive au niveau des sites de liaisons de l'ATP et bloquent ainsi l'activation des tyrosines kinases, ce qui a pour effet de bloquer la voie de signalisation intracellulaire. Le régorafénib est autorisé pour les patients atteints de CCRm réfractaires aux thérapies standards. Ce médicament est un anti-angiogénique mais possède également des activités antiprolifératives moins connues[35]. Deux essais de phase III ont démontré un bénéfice en terme de survie globale pour le régorafénib par rapport au placebo chez les patients atteints de CCRm ayant progressé sous traitement standard, quel que soit leur statut *RAS*[36,37]. En termes d'effets secondaires indésirables et de toxicologie médicamenteuse, les événements indésirables les plus fréquemment observés dans l'étude ont été la fatigue, un syndrome « main-pied », anorexie, diarrhée, perte de poids, dysphonie, hypertension, rash cutané ou desquamation, stomatite, fièvre, hyperbilirubinémie, hémorragies et infections.

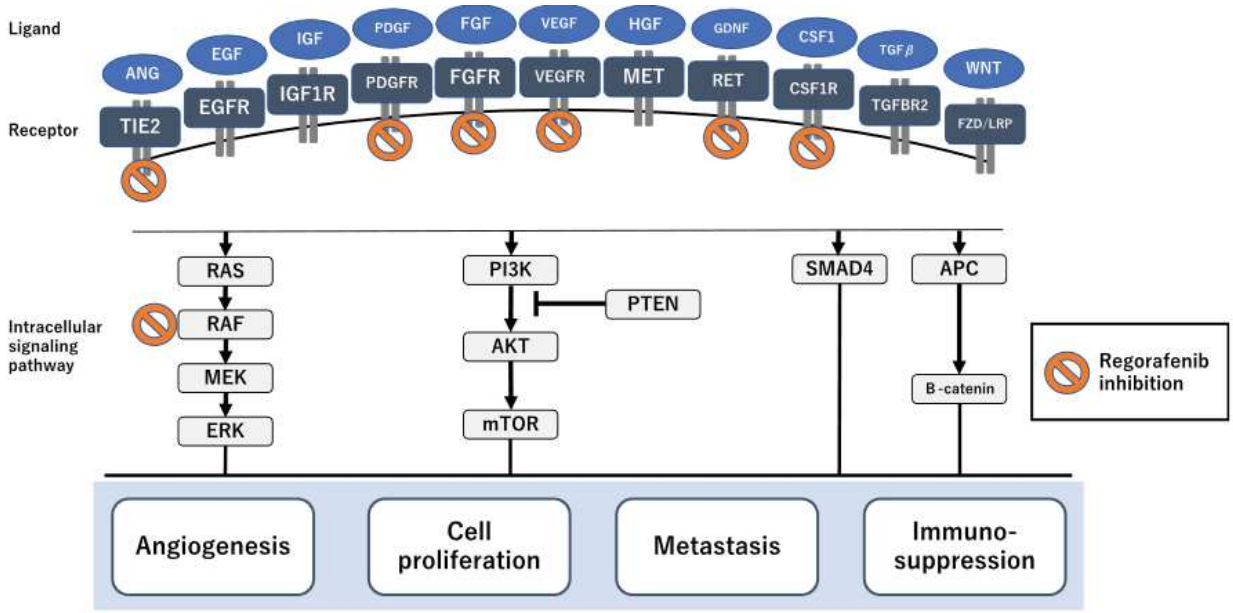

Figure 6: Mécanisme d'action du regorafenib. Source: Arai *et al,* 2019. Molecular insight of regorafenib treatment for colorectal cancer[34].

F.3.5 L'Immunothérapie anti PD-1

Il apparait que les patients atteints de cancer colorectal deviennent résistants aux chimiothérapies standards. Après l'utilisation de l'immunothérapie dans le traitement du mélanome, elle a été explorée dans différents types de cancers solides, dont le cancer colorectal. Le but de ses nouvelles thérapies est de restaurer ou de réactiver l'activité anti-tumorale en contournant les différents mécanismes d'échappement, dont les éléments clés sont appelés « point de contrôle » (CTLA-4, PD-1, PD-L1, et d'autres…). Le blocage de ces « points de contrôle » réactive le système immunitaire et permet de lutter efficacement contre les cellules tumorales. Le prembrolizumab (KEYTRUDA®) a reçu en 2017 l'autorisation par la FDA pour le traitement des tumeurs colorectales avec statut MSI (instabilité micro-satellitaire) après échec thérapeutique[38,39]. Le Nivolumab (OPDIVO®), a reçu l'AMM (autorisation de mise sur le marché) en 2018. L'association Nivolumab + Ipilimumab (Anti-CTLA-4) a donner de bon résultats avec un taux de réponse tumorale de 55% pour des patients atteints de cancers colorectaux[40].

G/ Evaluation de la réponse au traitement : critères RECIST 1.1

Actuellement l'appréciation de la réponse au traitement est basée sur l'évaluation de la réponse tumorale des différentes lésions par tomodensitométrie ou plus communément appelé CT-scan (Computerized Tomography ou scanner). Cette technique d'imagerie médicale est basée sur la mesure de l'absorption des rayons X par les tissus. Après traitement informatique une image 2D ou 3D est reconstituée afin de permettre de visualiser la tumeur au sein du tissu en différenciant les différentes densités du tissu.

Les critères RECIST pour Response Evaluation Criteria in Solid Tumors ont été publié pour la première fois en 2000[41] mais nous utilisons aujourd'hui la version RECIST 1.1 publié en 2009[42]. Ces critères sont basés sur l'évolution de la masse tumorale mesurée entre l'examen initial avant un traitement (dit baseline) et un examen de suivi pendant et à la fin du même traitement. Pour cela les critères RECIST définissent des lésions cibles et non cibles. Une lésion cible participe à l'évaluation tumorale et doit mesurer en pratique plus de 1 cm de diamètre ou plus de 1,5 cm de diamètre pour les ganglions. Cependant, toutes les lésions mesurables cibles ne sont pas dites cibles mais une sélection de cinq d'entre elles sera effectuée avant le traitement initial du patient. Deux lésions cibles (les plus grandes) maximum seront retenues par organes tandis que les autres lésions non cibles ne seront pas mesurées mais seront surveiller pendant la prise en charge du patient. La valeur qui est retenue pour l'évaluation (ou valeur utile) est la somme des diamètres, les plus grands pour les lésions non ganglionnaires et les petits diamètres pour les lésions ganglionnaires. On obtient une valeur unique de la somme qui servira d'une évaluation à l'autre pour faire les calculs de pourcentage de réponse ou de progression :

- **Lésions cibles :**
  - **Réponse complète (RC)** : disparition de toutes les lésions.
  - **Réponse partielle (RP)** : diminution de la somme des diamètres de 30% ou plus par rapport à l'examen initial.
  - **Progression (PD)** : augmentation de la somme des diamètres de 20% ou plus. L'apparition d'une nouvelle lésion est considérée comme une progression.
  - **Stabilisation (SD)** : la stabilisation est établie lorsqu'il n'y a ni RP ni PD.

- **Lésions non cibles :**
  - **Réponse complète (RC)** : disparition de toutes les lésions non cibles et normalisation des marqueurs tumoraux.
  - **Progression (PD)** : augmentation indiscutable de la taille des lésions ou apparition d'une nouvelle lésion.
  - **Stabilisation (SD)** : absence de disparition ou de progression des lésions non cibles et/ou persistance des marqueurs tumoraux au-dessus de la normale.

II/ Analyse moléculaire du tissu tumoral

L'analyse est moléculaire est réalisé au sein de plateformes de génétiques moléculaires (28 plateformes labélisées INCa en France).

Dans le contexte de la médecine personnalisée, l'orientation des traitements est basée sur l'analyse moléculaire du tissu tumoral ce qui est considéré comme étant le « gold standard » (ou technique de référence). L'analyse du tissu tumoral peut être réalisée sur une biopsie tissulaire ou par exérèse partielle/totale de la tumeur primitive ou d'une métastase appariée. Néanmoins, ce processus présente de nombreux inconvénients inhérents à la technique elle-même à savoir l'impact médico-économique, l'aspect éthique et technique. Effectivement, le coût de l'analyse du tissu tumoral est conséquent pour les organismes de santé puisqu'elle nécessite l'implication d'une multitude d'expertise de nombreux personnel de santé allant du chirurgien, au technicien en passant par l'anatomo-pathologiste. Aussi, le délai entre la réception du tissu tumoral et le rendu des résultats est d'environ 12 jours[43]. A cela s'ajoute que le prélèvement du tissu est très invasif et douloureux. Pour finir, le prélèvement est bien souvent de mauvaise qualité (préservé en paraffine ou congelé, le pourcentage de cellule tumorale des prélèvements peut être faible) ce qui ne permet pas son analyse. Aussi, les biopsies ne sont pas réalisables ou interprétables dans 15 à 20% des cas tous cancers confondus.

D'autres inconvénient biologiques liés aux caractéristiques intrinsèques des tumeurs sont à prendre à considération comme l'hétérogénéité clonale spatiale et temporelle.

III/ Hétérogénéité clonale des tumeurs

Lorsque que l'on étudie le cancer il faut prendre en considérations que celui-ci est une pathologie dynamique qui ne cesse d'évoluer dans le temps. L'évolution des tumeurs, qu'elle soit naturelle ou sous une pression thérapeutique implique l'apparition d'une importante diversité clonale. La diversité cellulaire des tumeurs (malignes, stromales non-malignes, immunitaires, etc) et l'hétérogénéité de ces sous-populations clonales tumorales peut conférer aux cellules une sensibilité ou une résistance aux traitements anticancéreux (radiothérapies, chimiothérapies, thérapies ciblées ainsi qu'à l'immunothérapie). De ce fait l'analyse du tissu tumoral qui est utilisée comme le « gold standard » afin de déterminer les caractéristiques moléculaires de la tumeur présente des biais biologiques liés à l'hétérogénéité clonale des tumeurs. Cette limite à l'analyse du tissu tumoral est majeure car elle conditionne directement le résultat de l'analyse moléculaire pouvant entrainer l'établissement d'un mauvais traitement.

La notion d'hétérogénéité clonale des tumeurs sera abordée dans cette partie, notamment en dissociant l'hétérogénéité spatiale de l'hétérogénéité temporelle des tumeurs.

A/ Altérations génétiques des tumeurs

On distingue deux types de aberrations génétiques en oncologie : les aberrations héréditaires et les aberrations somatiques. Les aberrations génétiques somatiques se caractérisent par des variations d'une seule base nucléotidique (SNVs), des délétions ou insertions d'une ou de plusieurs bases nucléotidiques qui se produisent dans toutes les cellules d'un organisme.

Les tumeurs accumulent des mutations au cours de leur croissance[44,45]. Bien que ces mutations surviennent au cours du temps, elles ne sont pas toutes responsables de la tumorigenèse. Majoritairement ces aberrations génétiques sont dites « passengers » et ne concèdent aucun bénéfice aux cellules cancéreuses alors que les variations génétiques dites « drivers » leur confèrent un avantage sélectif[45–49]. Ces dernières peuvent affecter des gènes suppresseurs de tumeur qui contrôlent la croissance et la division cellulaire comme les mutations du gène *TP53* (tumor protein 53) qui se produisent dans 50% de tous les cancers. On peut aussi noter le gène suppresseur de tumeurs *BRCA* (mutations BRCA1 et BRCA2) qui, lorsqu'il est muté augmente le risque d'une femme d'être atteinte du cancer du sein ou de

l'ovaire. La mutation BRCA2 augmente le risque d'apparition du cancer du sein, de la prostate et du pancréas. Les oncogènes sont des gènes qui lorsqu'ils sont mutés confèrent un gain de fonction incitant les cellules à se diviser et à croitre de façon désordonnée aboutissant à l'apparition de cancer. On peut retrouver dans ce cas les gènes *KRAS*, *EGFR*, *PIK3CA*. Ce sont les mutations de ces gènes que nous avons recherchées dans mon travail de thèse. Enfin les mutations des gènes de réparation de l'ADN (ou gènes du système MisMatch repair, MMR) qui entrainent un défaut dans la réparation de l'ADN se traduisant par la formation et la progression tumorale puisque le système MMR ne peut réparer les mutations apparues sur les gènes suppresseurs de tumeur et/ou sur les oncogènes. On peut citer dans cette famille de gènes, les gènes *MLH1*, *MLH2*, *MSH6* et *PMS2* qui lorsqu'ils sont mutés augmentent le risque d'apparition d'un cancer colorectal, notamment chez personnes atteintes du syndrome de Lynch. Chronologiquement les gènes de réparation de l'ADN sont mutés en premier entrainant des mutations sur les gènes suppresseurs de tumeurs et les oncogènes.

B/ L'hétérogénéité clonale des tumeurs

B.1 Hétérogénéité clonale intra-tumorale

L'hétérogénéité clonale intra-tumorale est caractérisée par une distribution non-uniforme des différentes sous-populations de clones tumoraux au sein d'une même lésion tumorale **(Figure 7)**. Cette hétérogénéité spatiale des clones tumoraux au sein d'une même lésion a été mise en évidence grâce au progrès de la génomique et aux nouvelles techniques de séquençage à haut débit[50]. La même année, les travaux de l'équipe de Charles Swanton ont évalué si une seule biopsie du tissu tumoral était suffisante pour identifier l'ensemble des altérations génétiques caractérisant une tumeur[51]. L'analyse par séquençage de l'exome entier des différentes biopsies a montré sans équivoque sur les carcinomes rénaux et leurs métastases que le prélèvement d'une seule biopsie ne permet pas d'identifier l'ensemble des altération génétiques d'une même lésion (que ce soit pour la tumeur primaire ou d'une métastase appariée) mais seulement qu'une fraction des clones tumoraux[51]. Ces travaux ont pu être confirmé par d'autres équipes de recherche et sur d'autres types de cancers[52–54]. Ces études conclues que l'analyse moléculaire réalisée à partir de deux biopsies distinctes d'une même lésion tumorales (tumeur primaire ou d'une métastase appariée) peut être discordante. Un résultat discordant peut entrainer par la suite l'initiation d'un mauvais traitement et

engendrer des effets secondaires sévères et une baisse de survie pour les patients. L'explication d'une telle hétérogénéité vient essentiellement de l'existence d'une évolution ramifiée des tumeurs solides ce qui [1–3]les rend extrêmement hétérogènes[49,55,56].

Il est a noté que des ADNcir portant des altérations épigénétiques (méthylations, acétylations et autres…) tumorales circulent dans le sang de patients atteints de tous types de cancers[57,58]. Ce manuscrit s'intéressera aux altérations génétiques plus qu'au altérations épigénétiques.

B.2 Hétérogénéité clonale inter-tumorale

Il est donc clairement établi dans la littérature qu'une même lésion tumorale est très hétérogène au niveau cellulaire et moléculaire **(Figure 7)**. Gerlinger et ses collègues ont montré pour la première fois en 2012 qu'une biopsie d'une tumeur primaire de carcinome rénal a un profil génétique différent de ses métastases appariés[51]. Ces observations pionnières ont pu être confirmées par d'autres équipes[59–61]. L'hétérogénéité clonale inter-tumorale s'ajoute à l'hétérogénéité intra-tumorale ce qui renforce les biais lors des analyses du tissu tumoral. Bien que l'hétérogénéité spatiale d'une tumeur ne soit pas un concept nouveau dans le développement d'un cancer[44,62], c'est à l'équipe de Charles Swanton que nous devons la primeur de l'établissement de l'hétérogénéité clonale intra- et inter-tumorale au niveau moléculaire. La connaissance de l'ensemble de la diversité clonale au sein d'un même organisme (individu) est indispensable puisque l'hétérogénéité intrinsèque aux tumeurs crée le réservoir de cellule à l'origine des phénomènes de chimiorésistance et plus récemment conduisant à des résistances aux thérapies ciblées.

Il faudrait par conséquent effectuer une multitude de biopsie au sein de la tumeur primitive et au sein de plusieurs métastases ce qui est irréalisable pour des raisons médico-économiques, éthiques et techniques. A cette complexité clonale des tumeurs s'ajoute le fait que l'hétérogénéité clonale des tumeurs est dynamique et évolue au cours du temps, notamment du fait des pressions sélectives dues aux différentes lignes de traitement successives. Il est évident qu'il est impossible d'effectuer des biopsies chez un patient à intervalle régulier durant sa prise en charge thérapeutique

C/ L'évolution temporelle

L'hétérogénéité clonale temporelle est définie par des changements dynamiques au cours du temps des sous-populations de clones tumoraux au sein d'une même ou de plusieurs lésions tumorales[44] **(Figure 7)**.

Des études sur des biopsies en série dans les cancers de l'œsophages afin de caractériser l'évolution des tumeurs ont démontré que la chimiothérapie peut modifier la composition moléculaire des tumeurs au fil du temps par des apparitions de mutations[63]. Une population clonale majoritaire peut disparaitre au cours du temps sous l'effet d'un traitement mais cela peut entrainer également la multiplication d'un ou de plusieurs clones jusque-là indétectable, sous la pression induite par le traitement. Le phénomène d'apparition de mutations dites *de novo* a pu être décrit[64,65]. Ces émergences de mutations *de novo* sont bien souvent associées à des mécanismes de résistance aux traitements et sont *in fine* la principale source d'échec thérapeutique comme notamment dans le traitement par anti-EGFR des patients atteints de CCRm[66–68]. Bien que les traitements non spécifiques tels que les chimiothérapies cytotoxiques exercent des pressions sélectives sur les cellules cancéreuses, l'usage des thérapies ciblées accentue considérablement ce phénomène de sélection. En effet, les observations les plus convaincantes concernant l'hétérogénéité temporelle ont été faites dans le contexte d'un traitement avec des thérapies ciblées et notamment celles à base d'anticorps monoclonaux ciblant le récepteur à l'EGF (Epidermal Growth Factor) comme le cetuximab (Erbitux®) ou le panitumumab (Vectibix®) où une résistance secondaire se développe chez quasiment tous les patients et peut être associée au développement de mutations secondaires *KRAS*, *NRAS*, *EGFR* ou *BRAF*[66–68].

L'hétérogénéité spatiale et temporelle des tumeurs sont les principales raisons pour lesquelles établir un traitement efficace reste compliqué et ce quel que soit le stade de la maladie. C'est le facteur incitatif pour effectuer une médicine personnalisée ou dite de précision. Seul l'analyse de l'ADN circulant (ADNcir) permet d'outrepasser les limites de l'hétérogénéité clonale.

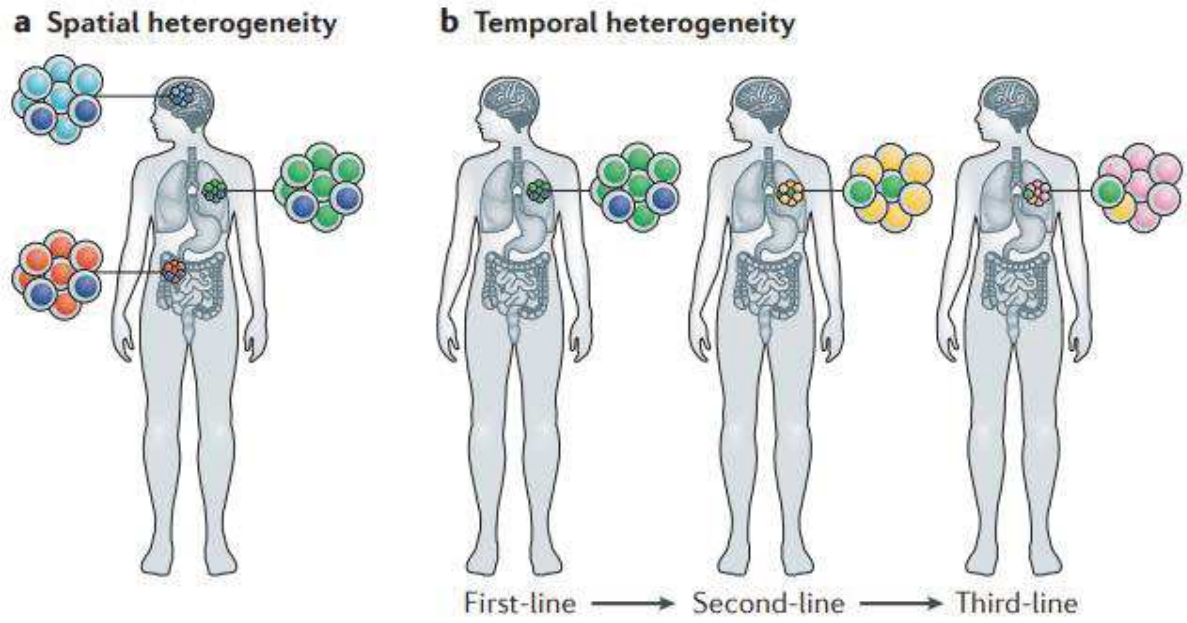

Figure 1 | **A conceptual framework for distinguishing between spatial and temporal intratumoural heterogeneity. a** | Spatial heterogeneity denotes an uneven distribution of cancer subclones across different regions of the primary tumour and/or metastatic sites. **b** | Temporal heterogeneity refers to variations in the molecular makeup of a single lesion over time, either as a result of natural progression of the tumour or as a result of exposure to selective pressures created by clinical interventions. Colours denote the presence of subclones with different genetic features.

Figure 7: Un cadre conceptuel pour distinguer l'hétérogénéité intra tumorale spatiale et temporelle. Source: Ibiayi Dagogo-Jack and Alice T. Shaw, 2017. Tumour heterogeneity and resistance to cancer therapies[69].

IV/ L'ADN circulant

A/ Historique et Généralités

L'ADN extracellulaire est composé d'ADN nucléaire et d'ADN mitochondrial libérés par les cellules de l'organisme. Ces ADN extracellulaires sont présents *in vivo* dans les fluides non circulants (urine, lait, ascites, salive, les fèces…) et *in vitro* dans le surnageant de culture cellulaires, d'organoïdes, voire même dans la culture d'embryon. Les ADN extracellulaires sont également présents *in vivo* dans les fluides biologiques circulants tels que le sang (ou ses dérivés comme le sérum et le plasma), le liquide céphalo rachidien et la lymphe, et constituent ainsi l'ADN extracellulaire circulant (ADNcir) **(Figure 8)**.

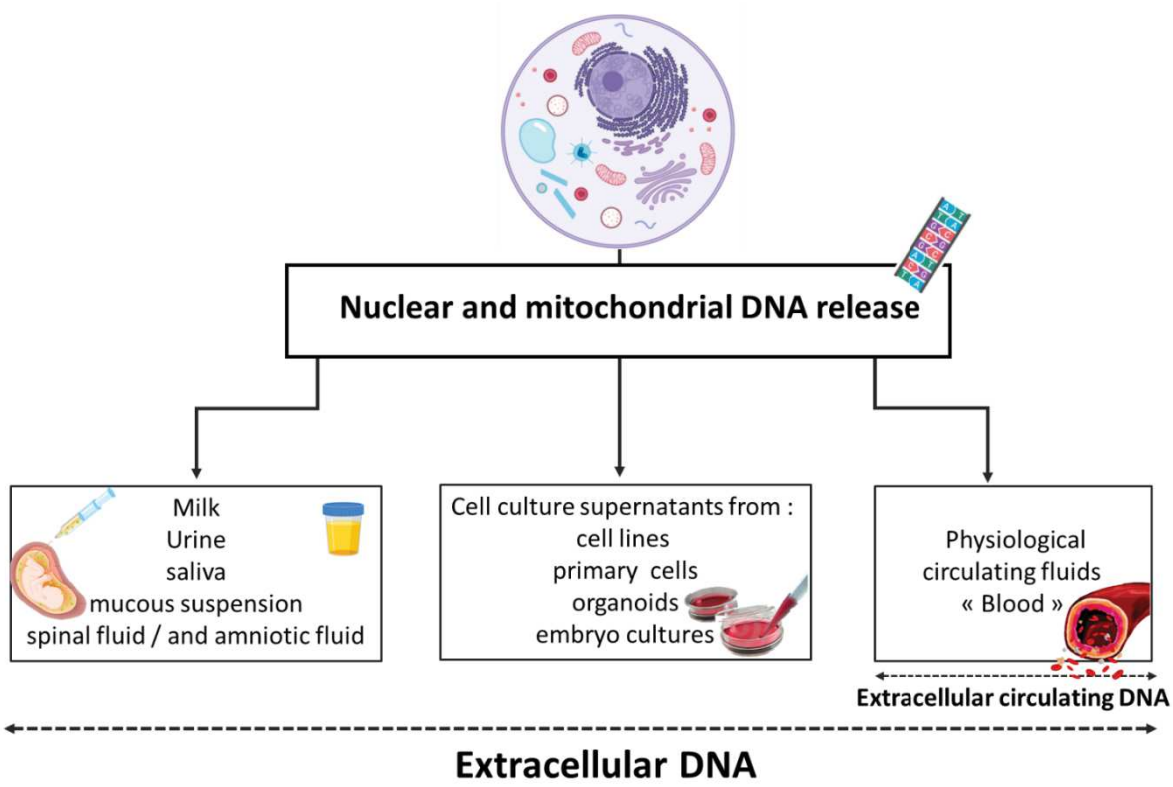

Figure 8: L'ADN extracellulaire

A.1 Cas du cancer

C'est en 1948 que les chercheurs français Mandel et Metais ont découvert pour la première fois la présence d'acides nucléiques (ADN et ARN) dans le sang de patients atteints de cancer mais aussi chez des individus sains[70]. Bien que cette découverte fût faite à la fin des années 1940, ce n'est bien que plusieurs décennies plus tard, dans les années 70 que des groupes de chercheurs se sont intéressés aux ADNcir **(Figure 9)**.

En 1977, Leon et ses collègues ont été les premiers à démontrer que la concentration des ADNcir était significativement plus élevée dans le sérum de patients atteints de cancer (poumons, sein, colorectal et autres…) que dans le sérum d'individus sains[71]. L'équipe de Stroun et Anker a mené la même année des travaux qui ont permis de mieux caractériser les ADNcir[72] et ont montré en 1989 qu'une fraction de l'ADNcir était d'origine tumorale car ils possédaient certaines altérations génétiques et épigénétiques spécifiques aux cellules de la tumeur d'origine[73]. En 1994, l'équipe de Vasioukhin a fait une découverte capitale en montrant la présence de mutations *NRAS* dans le sang de patients atteints de leucémie aigüe myeloïde et de syndrome myélodysplasique[74]. Ensuite, ce n'est qu'en 2005 que l'équipe de Diehl établit la première étude clinique portant sur la détection de mutations génétiques à partir de l'ADNcir chez des patients atteints de cancer colorectal[75]. Depuis ces découvertes majeures ont conduit à des recherches plus approfondies pour déterminer le potentiel des ADNcir, notamment comme biomarqueur en oncologie. Aussi, l'ensemble de ces travaux ont donné naissance au concept de biopsie liquide. Les avancées dans les techniques de biologie moléculaires ont permis de nombreuses découvertes pour sa validation clinique. A noter que la première validation clinique dans une étude prospective de l'analyse de l'ADNcir en oncologie a été réalisé au sein de notre laboratoire en 2014[76]. Dans cette étude notre équipe a déterminé en aveugle un taux de concordance sans précédent dans la détection des mutations *KRAS* et *BRAFV600E* entre l'analyse de l'ADNcir et l'analyse du tissu tumoral dans une large cohorte de patients atteints de cancer colorectal métastatique.

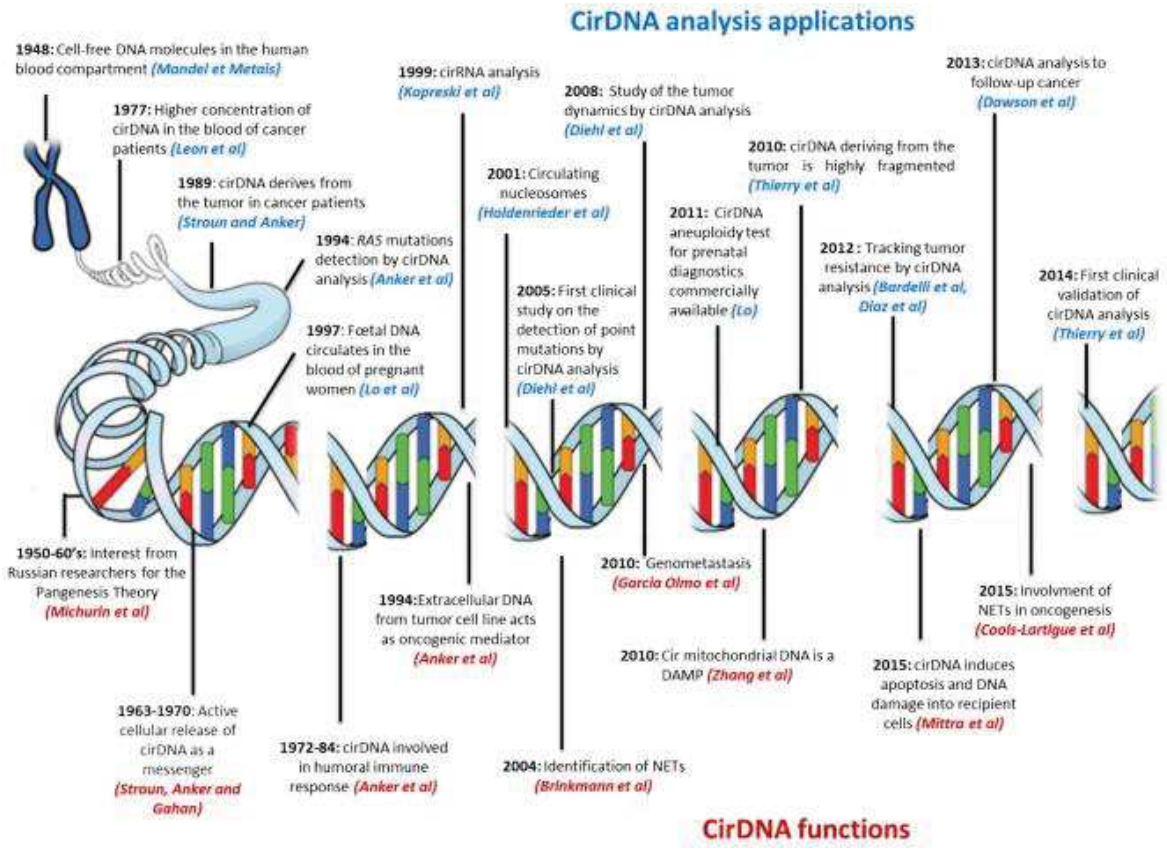

Figure 9: Chronologie des découvertes fondamentales sur les ADNcir. Source: Thierry *et al*, 2016. Origins, structures and functions of circulating DNA in oncology[77]

A.2 Autres domaines

Il est intéressant de noter que la présence d'ADNcir fœtale a été découvert dans le sang (plasma ou sérum) de femmes enceintes par l'équipe de Lo' en 1997[78]. Cette découverte a permis de nombreuses avancées dans le dépistage prénatal non-invasif (DPNI) de différentes pathologies comme la trisomie 21[79], la détermination du sexe fœtal et a permis le développement de méthodes non invasives dans le diagnostic prénatal[80].

Outre, l'oncologie et le diagnostic prénatal, l'analyse des ADNcir a été étudiée dans de nombreux domaines comme les maladies auto-immunes et notamment le lupus érythémateux systémique (SLE). Cette maladie se caractérise par la formation d'auto anticorps anti-ADN double brin et il a été montré que le taux d'ADN circulant chez les patients atteints de SLE était supérieur à ceux des individus sains[81] et que ce taux d'ADNcir pouvait augmenter chez des patients en progression[82]. L'étude des taux d'ADNcir permet de pronostiquer chez les patients atteints de sepsis[83] ou à l'issu d'un accident vasculaire

cérébrale[84]. L'ADNcir est aussi utilisé dans les rejets de greffes d'organes solides grâce à la détection de l'ADN de donneur dans le sang du receveur[85,86].

B/ Origines et Structures

L'ADNcir est présent sous la forme de fragments d'ADN associé à des protéines, à des structures vésiculaires (corps apoptotiques, exosomes ou des microparticules) et aux nucléosomes[77,87]. Les différentes structures des ADNcir retrouvées dans le sang sont dues à différentes origines et à différents mécanismes de libération de ces ADN vers le milieu extracellulaire. Il existe deux grands principes de libération des ADNcir dans le milieu extracellulaire : la mort cellulaire et la sécrétion active.

Bien que les origines, la caractérisation structurale ainsi que les mécanismes de la libération des ADNcir ne soient pas tous clairement connus, il sera discuté ici des connaissances publiées dans ce domaine.

B.1 Origines cellulaires

De nombreux travaux ont permis d'identifier certaines origines et structures des ADNcir[77,88]. Aujourd'hui, il est établi que les caractéristiques structurales (tailles et formes) des ADNcir peut être en lien avec leurs origines cellulaires et/ou avec leurs mécanismes de libération et de relargage des cellules vers la circulation sanguine[89,90]. Son origine intracellulaire peut être nucléaire ou mitochondriale.

Chez les patients atteints de cancer, les ADNcir peuvent provenir à la fois de cellules saines (non-malignes) et de cellules malignes. En effet, la quantification d'ADNcir chez des individus sains a révélé que les cellules saines (leucocytes, cellules musculaires…), circulantes ou non, libèrent leur ADN dans le sang[89]. De plus, de l'ADN tumorale est également présent dans le sang de patients cancéreux puisque des altérations génétiques sont portées par des ADNcir[71]. La tumeur est constituée à la fois de cellules malignes tumorales mais aussi de cellules associée au microenvironnement tumoral. Ce microenvironnement comporte les cellules stromales et des infiltrats de cellules immunitaires (principalement des lymphocytes) qui sont aussi une source d'ADNcir[77]. De ce fait, nous retrouvons dans le sang de patients cancéreux des ADNcir provenant de cellules saines (principalement immunitaires), de cellules malignes

issues de la tumeur et de cellules tumorales non-malignes provenant du microenvironnement **(Figure 10)**.

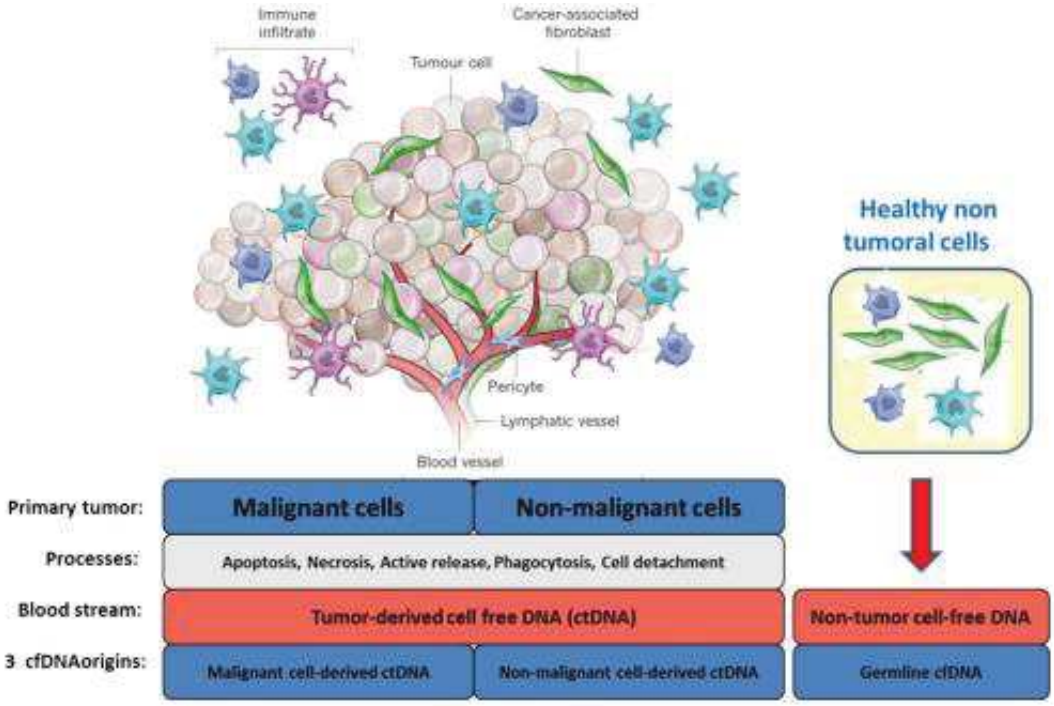

Figure 10: Origines cellulaires distinctes de l'ADN circulant trouvé dans le sang des patients atteints de cancer. Source: Thierry *et al*, 2016. Origins, structures and functions of circulating DNA in oncology[77].

B.2 La mort cellulaire

Les mécanismes de mort cellulaire sont dus à l'apoptose, à la nécrose, à la phagocytose ou encore à la NETose.

B.2.1 L'apoptose

Lorsque la question des mécanismes de libération de l'ADNcir est évoquée, la principale source abordée est le phénomène de mort cellulaire par apoptose ou mort cellulaire programmée. Ce mécanisme contrôlé d'élimination des cellules est impliqué dans le renouvellement des cellules, le maintien de l'homéostasie, l'embryogénèse ou encore la régression tumorale…[91]. L'apoptose est déclenché par des stimuli internes ou externes et peut donc être réalisé par deux voies cellulaires bien distinctes que sont : la voie extrinsèque et la voie intrinsèque médiée par des évènements mitochondriaux[92]. Il est clairement établi que ce processus de mort cellulaire (quel que soit la voie d'activation) provoque le clivage systématique de l'ADN nucléaire en mono-nucléosomes d'environ 166 paire de bases (bp), ou de multiples (poly-nucléosomes), à savoir en di-nucléosomes (environ 332bp) et en tri-nucléosomes (environ 498 pb)[93–96]. L'ADNcir plasmatique présente fréquemment une disposition en échelle (pattern ladder) en électrophorèse avec une large bande aux alentours de 160-180 bp, ce qui semble signifier un clivage apoptotique que ce soit chez des patients atteints de cancer[93] ou chez des patients atteint de lupus[97]. En étudiant le profil de taille des ADNcir par séquençage en librairie simple brin (SSP) et double brin (DSP) notre équipe a pu définir que la majorité des tailles des ADNcir était comprise entre 160-180 bp, que ce soit chez des individus sains ou chez des patients atteints de cancer colorectal métastatique[87]. Ces travaux confirment que le nucléosome est donc la principale structure sous laquelle se présente les ADNcir. A noter que le nucléosome est composé d'un octamère d'histones (2H2A, 2H2B, 2H3 et 2H4) autour duquel est enroulé l'ADN double brin (environ 147 bp), ce complexe protéique est associé à l'histone H1. Chaque nucléosome est lié à l'autre par de l'ADN double brin appelé : linker DNA (environ 20-90 bp).

Des corps apoptotiques peuvent être formés lors de la phase tardive de l'apoptose[98]. Ces structures mesurent entre 1 et 5 µm et contiennent de l'ADN dégradé lors du mécanisme d'apoptose.

B.2.2 La nécrose

La nécrose est un phénomène de mort cellulaire prématurée accidentelle qui se produit plus rapidement que l'apoptose et implique une perte du potentiel cellulaire de production de régénération énergétique[99,100]. Ce mécanisme de mort cellulaire survient généralement après des altérations sévères des conditions physiologiques comme par exemple l'ischémie, l'hypoxie, l'irradiation[101]. Ce phénomène s'accompagne d'un gonflement cellulaire intense, d'une rupture des organelles (mitochondrie incluses), d'une rupture de la membrane plasmique et génère des fragments d'ADN plus large d'environ 10 000 pb[93,94,96]. Bien que la nécrose soit accidentelle, il existe néanmoins d'autres formes de nécrose dite programmée : la nécroptose et pyroptose[102].

L'ADN mitochondriale (ADNmt) est libéré à la fois par l'apoptose et par la nécrose. Les mitochondries quant à elles peuvent être éliminées par mitophagie[103] entrainant aussi la libération d'ADN mitochondriaux dans le sang[104]. Il est à noter que notre équipe a été la première à mettre en évidence la présence de mitochondries viables dans le sang qui participerait en grande proportion à la concentration des ADNmt retrouvés dans le sang[105] . **Ces travaux auxquels j'ai contribué, seront discutés dans la partie « autres contributions ».**

B.2.3 La phagocytose

La phagocytose est très importante dans la libération des ADNcir puisqu'elle intervient dans la dégradation, entre autres, de cellules mortes ou mourantes. Il a été montré *in vitro*[106] et *in vivo*[107] que les macrophages jouent un rôle majeur dans la libération des ADNcir. Il peut arriver que les macrophages eux même n'arrivent pas à digérer l'ensemble des structures phagocytées ce qui peut causer leur mort et *in fine* conduire à la libération de leur propre ADN dans la circulation. En effet, les cellules nécrotiques, les corps apoptotiques ou les microviscules sont phagocytés entrainant des fragments d'ADN génomiques et mitochondriaux circulants dans le sang[108].

B.2.4 La NETose

La NETose est un phénomène propre aux neutrophiles qui se traduit par la formation et la libération de NETs (pour neutrophil extracellular traps) qui sont des structures de filet de chromatine modelé en réseau et décoré de protéines bactéricides comme la neutrophile élastase (NE) et la myolopéroxydase (MPO)[109,110]. Le rôle des NETs est de capturer, neutraliser et inactiver les pathogènes. Les neutrophiles peuvent être activés par différents *stimuli* (virus, bactéries) conduisant à deux voies distinctes de NETose : la NETose suicidaire (ou tardive) et la NETose vitale (ou rapide)[111] **(Figure 11)**.

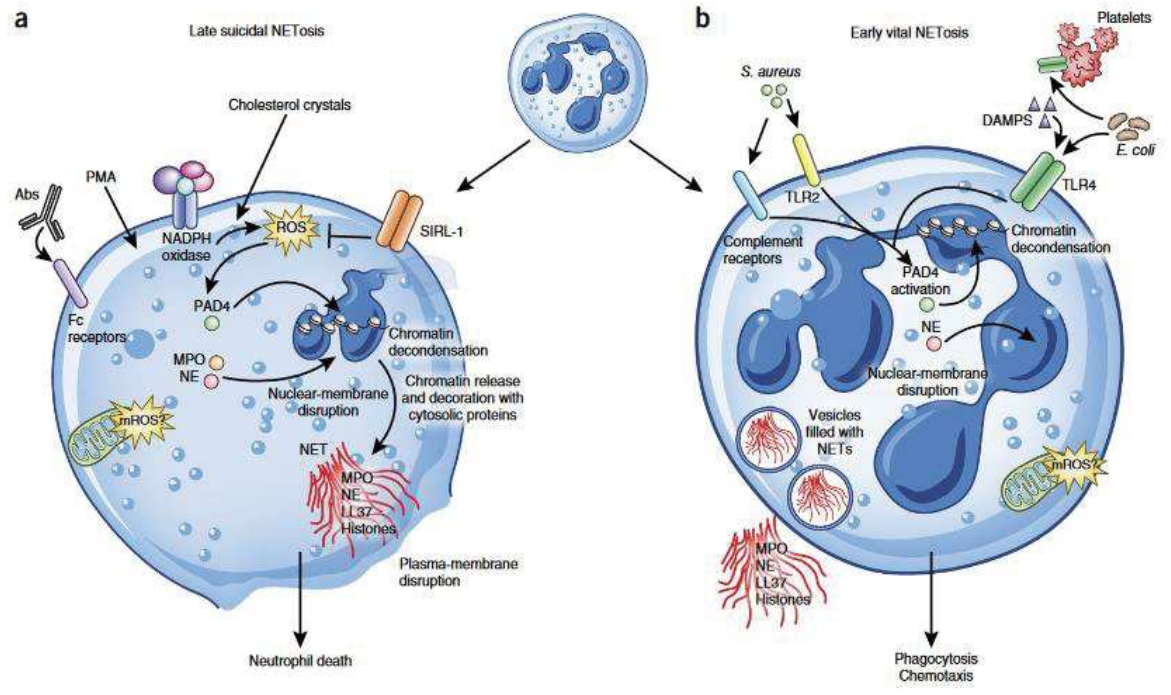

Figure 11: Aperçu de la NETose suicidaire (a) et de la NETose vitale (b). Source: Jorch *et al*, 2017. An emerging role for neutrophil extracellular traps in noninfectious disease[111]**.**

Le processus de NETose suicidaire est le plus fréquemment observé et se traduit par l'entrée de NE et de MPO dans le noyau cellulaire, d'une décondensation de la chromatine suivi d'une désintégration de l'enveloppe nucléaire et plasmique afin de libérer les NETs dans la circulation[112]. Par opposition, la NETose vitale vise à libérer les NETs rapidement dans la circulation sanguine, sans rupture des membranes et sans perte de fonction vitales pour les neutrophiles qui peuvent par la suite continuer leur rôle de phagocytose[113,114]. Enfin, des ADNmt peuvent être libérés via les NETs sans affecter la durée de vie des neutrophiles[115].

Bien que les NETs jouent un rôle clé dans la lutte contre les pathogènes et dans l'homéostasie, une production inappropriée et une exposition prolongée aux NETs pourrait être délétère pour les sujets atteints de cancer. Il a été démontré que les NETs pourrait enflammer les tissus et de ce fait créer des niches pré-métastatiques. Dans ce contexte, les NETs sont aussi impliqués dans la propagation du cancer en piégeant les cellules tumorales circulantes, facilitant ainsi le processus de métastase au niveau des sites pré-métastatiques[116]. Il est intéressant de noter que les NETs sont retrouvés dans les mêmes conditions pathologiques pour lesquelles des concentrations élevées d'ADNcir ont été rapportées comme le cancer[116], le sepsis[117], les maladies auto-immunes[118], les maladie thrombotiques[119] ou dans les maladies inflammatoires[120].

Ce phénomène de libération de l'ADN n'est pas restreint aux neutrophiles puisqu'il a été observé chez les éosinophiles et les mastocytes, ce qui regroupe tous ces phénomènes sous le terme «ETosis »[121]. Par opposition aux NETs les structures « extracellular traps » libérées par les éosinophiles ne contiennent que de l'ADNmt et cette production ne conduit pas à la mort de la cellule[122,123].

Les macrophages[124] et leur DNase I[108] participe à l'élimination des NETs mais néanmoins cette élimination reste incomplète. Ce qui suggère, soit qu'il existe d'autres mécanismes de dégradation des NETs soit que la dégradation incomplète des NETs entraine la libération de fragments d'ADN partiellement dégradé dans le sang. Les NETs seraient ainsi une source potentielle des ADNcir.

B.3 La sécrétion active

Les travaux mettant en évidence un mécanisme de sécrétion active remontent aux début des années 1970 avec les équipes de Rogers et de Stroun. Ces équipes ont montré que des lymphocytes humains[125,126] sécrètent de l'ADN double brin dans le milieu de culture. L'ADN est excrété des cellules vers le milieu extracellulaire par les exosomes ou des microvésicules **(Figure 12)**. Les exosomes sont des vésicules libérées par exocytose par différents types cellulaires, ils ont une taille d'environ 30 à 100 nm et contiennent des fragments d'ADN et d'ARN[127]. Les microvésicules ont quant à elles une taille entre 50 à 1000 nm et sont libérés dans l'espace extracellulaire par bourgeonnement et par fission de la membrane plasmique[128].

A noter que les exosomes ou les microparticules qui sont issus de cellules tumorales peuvent comporter du matériel oncogénique, ont une taille > 1 micron et sont appelés oncosomes[129].

Les mécanismes de sécrétions actives sont de plus en plus étudiés et remettent peu à peu en cause l'hypothèse selon laquelle l'apoptose est la source majeure de l'ADN circulant.

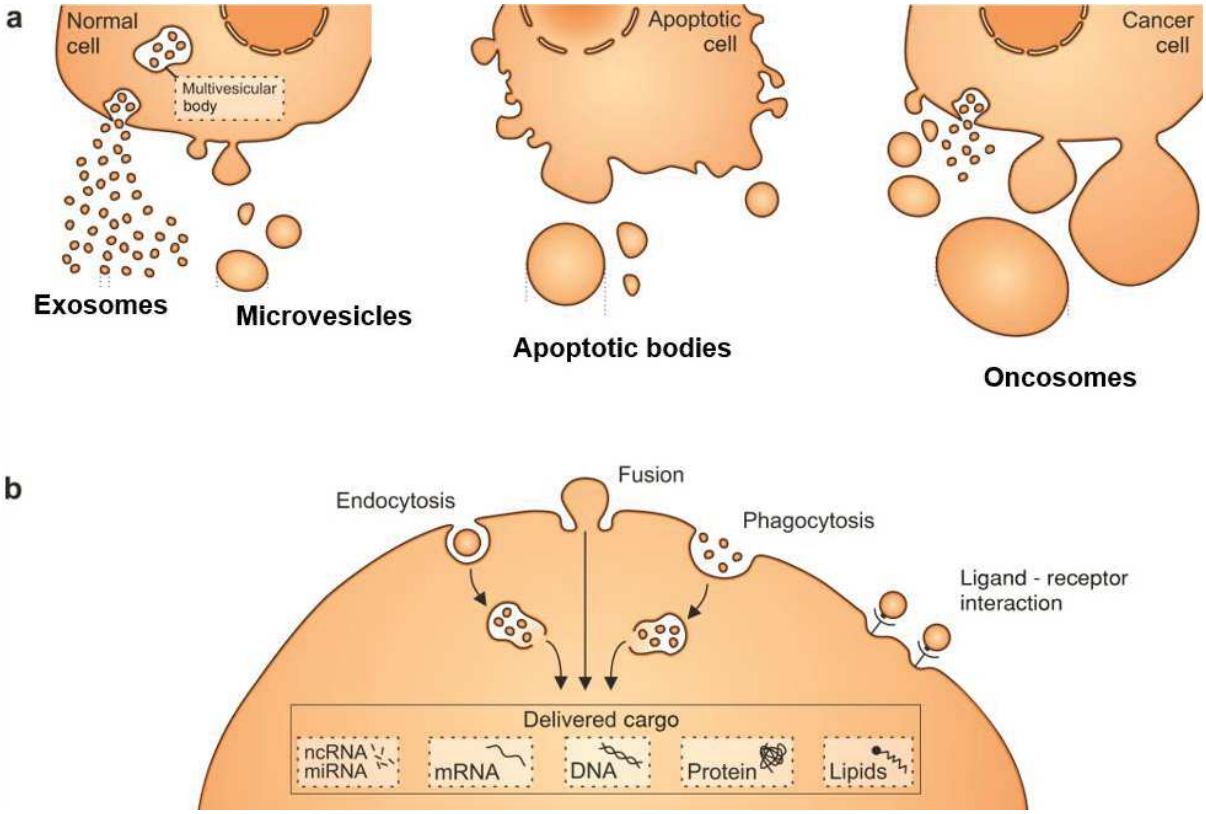

Figure 12: Les différents types de vésicules extracellulaires : Source : Zaborowski et al, 2015. Extracellular vesicules : Composition, Biological Rrelevance, and methods of study[130].

C/ Profil de taille et fragmentation de l'ADNcir

Comme discuté plus haut la grande majorité des ADNcir retrouvée chez les patients atteints de cancer ont une taille d'environ 160-180 pb, ce qui correspond à la taille de l'ADN enroulé autour d'un mono-nucléosome, caractérisé jusqu'alors comme étant la résultats d'un processus d'apoptose[99]. Cela dit, il est aussi retrouvé dans la circulation sanguine des ADNcir ayant une taille supérieure à 10 000 pb. Ceci suggère que ces ADNcir ne sont pas uniquement liés au phénomène d'apoptose mais sont également associé aux mécanismes de nécrose, voire même qu'ils sont associés à la dégradation de la chromatine libérée par des cellules sénéscentes[93].

Notre équipe a été l'une des premières à montrer que l'ADNcir muté était plus court que l'ADN sauvage[131–133]. L'équipe a démontré grâce à un modèle de souris xénogréffées avec des cellules cancéreuses humaines que l'ADNcir d'origine tumorale (humains) était plus court que l'ADNcir d'origine non-tumorale de la souris hôte[134] et cela a été confirmé en étudiant le profil de taille des ADNcir par PCRq (Réaction de polyméraisation en chaine quantitative) et par AFM (microscopie à force atomique)[131,132,135].

En 2017, underhill et ses collègues par séquençage ont montré un décalage entre la taille des ADNcir retrouvés chez des individus sains (167 pb) et celle des patients atteints de cancer (134-144 pb)[136]. Notre équipe montrent à la fois par une approche de PCRq et par séquençage en utilisant une librairie simple brin (SSP-S pour shallow Whole-genome sequencing of single-stranded DNA library) que la majorité des ADNcir retrouvés chez les patients atteints de cancer ont une taille qui correspond à l'empreinte nucléosomique, à savoir environ 166 bp[137]. De plus, des travaux récents menés par notre équipe par séquençage (shallow Whole genome sequencing, sWGS) et en utilisant des librairies simple brins et par PCRq, démontrent un décalage des tailles des ADNcir entre les individus sains et les patients cancéreux[87]. Nous observons aussi une periodicité de 10 pb dans la taille des ADNcir qui évoque un clivage enzymatique des ADN enroulés autour du mono-nucléosomes[87]. Enfin, la comparaison du profil de taille des ADNcir par sWGS chez des individus sains et atteints d'un cancer colorectal métastatique, en utilisant une librairie double brin montre que la proportion des ADNcir retrouvées est plus élevée pour les fragments compris entre 40 et 151 (Figure 13)[137] pb

Ces résultats valident que la taille des ADNcir chez les patients atteints de cancer est inférieure à 100-160 pb et que la taille des ADNcir permettrait de discriminer les ADNcir tumoraux et

non tumoraux. Ces travaux ouvrent le champ au dépistage du cancer par l'analyse de la fragmentation des ADNcir, maintenant appelé fragmentomic **(Figure 14)**. **J'ai pu participer à ce travail qui est discuté dans la partie « autres contributions ».**

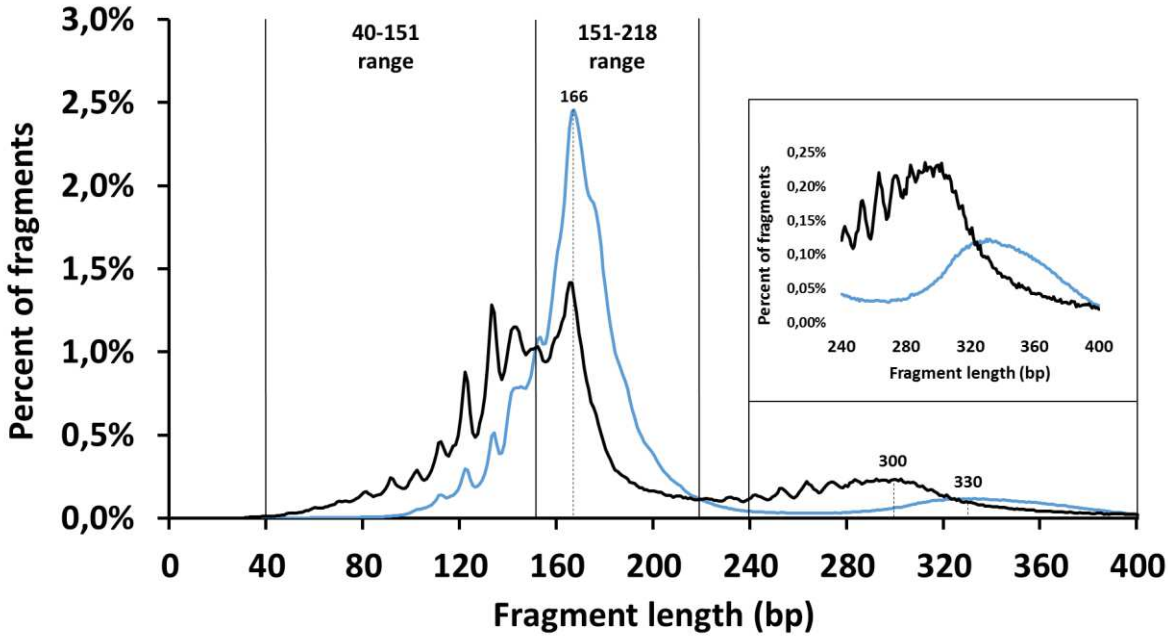

Figure 13: Comparaison du fragmentome d'un patient mCRC (ligne noire) et celui de la moyenne de 17 individus sains (ligne bleue) tel que déterminé par sWGS à partir d'une librairie double brin (DSP). Comparé à la moyenne des individus sains, le profil de taille des patients CCRm montre: un nombre accru de fragments compris entre 40 - 151 pb et 218 - 320, un nombre réduit de fragments compris 151 - 218 pb et 320 - 440 pb, une fréquence inférieure à la longueur de 166 pb, un pic correspondant au dinucléosome plus court (300 vs 330 pb), et un plateau entre 145 - 156 pb. Figure adaptée de Sanchez *et al*[137].

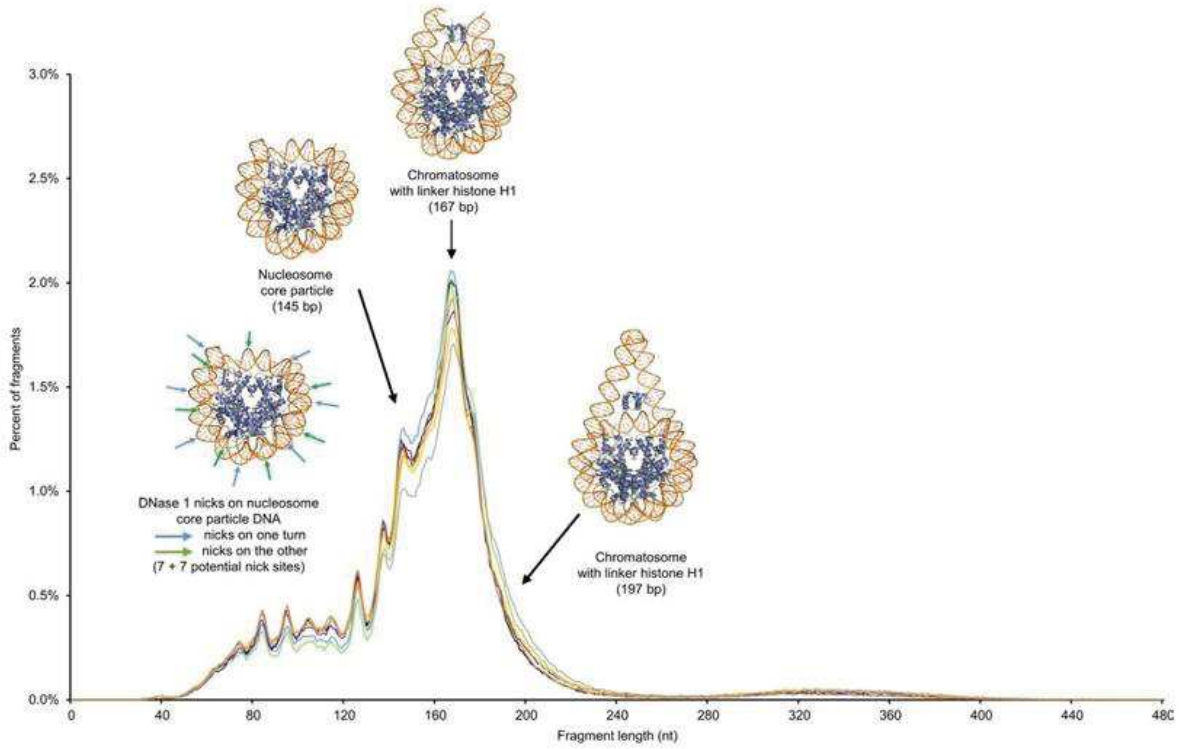

Figure 14: Représentation des différentes structures de l'ADN enroulé autour du nucleosome, du chromatosome et du chromatosome en fonction du profil de taille des fragments d'ADNcir. Source: Sanchez *et al*, 2021. Circulating nuclear DNA structural features, origins, and complete size profile revealed by fragmentomics[87].

D/ Aspects fonctionnels de l'ADN circulant

L'ADNcir est libéré dans la circulation sanguine via différents mécanismes de relargage, néanmoins cet ADNcir n'est pas seulement un déchet mais peuvent aussi jouer un rôle dans les conditions physiologiques ou mêmes pathologiques. Ils jouent un rôle actif dans le transfert horizontal de matériel génétique, déclencheurs du système immunitaire et enfin ils peuvent favoriser l'apparition de métastases dans le cancer.

D.1 Le transfert horizontal et la génométastase

Les premiers résultats montrant le rôle de l'ADNcir dans le transfert horizontal ont été découvert chez les végétaux. En oncologie, il a été démontré que l'ADNcir provenant de patients atteints de cancer pouvait entrer dans différents types cellulaires en culture et être transloqué dans les noyaux et ce très rapidement et générer l'apoptose[138]. Il a été démontré que les vésicules extracellulaires pouvaient aussi avoir un rôle dans le transfert horizontale affectant l'expression génique des cellules réceptrices[139,140]. Bendich et ses collègues ont observé pour la fois en 1965, que l'injection d'Adn tumoral dans le sang de souris était à l'origine d'un développement tumoral[141]. Ce phénomène a par la suite été validé par d'autres travaux et à donner lieu au terme de génométastase[142,143]. Enfin, comme discuté précédemment les NETs libérés par les neutrophiles peuvent contribuer à l'établissement de niches pré-métastatiques et ainsi favoriser la croissance tumorale[144,145]. Les NETs peuvent à la fois piéger des cellules circulantes tumorale ou de l'ADNcir tumoral et par la suite amener ces cellules ou ces ADN tumoraux sur des sites cibles pré-métastatiques.

D.2 Immunité et inflammation

L'ADNcir peut activer le système immunitaire et déclencher une réaction immunitaire. L'ADNcir mitochondriale joue un rôle particulier dans la réaction inflammatoire puisqu'il est par définition d'origine bactérienne est donc associé aux DAMP (damage associated molecular pattern)[146]. L'ADN mitochondriale peut se lier au récepteur TLR9 (toll-like receptor 9) des leucocytes par l'intermédiaire de motifs CpG hypométhylés entrainant une réaction inflammatoire[147]. L'ADNcir nucléaire quant à lui peut aussi stimuler le système immunitaire de par sa structure en double hélice ou les motifs particuliers de certaines séquences[148] qui sont reconnus par les récepteurs de forme PRRs (Pattern recognition receptors). L'activation du système immunitaire par les ADNcir peut être une conséquence d'un défaut de dégradation de ces ADN par les DNases. Ces ADNcir peuvent être aussi protégés des DNases sanguine par des vésicules extracellulaires. Dans ce contexte il a été demontré que les souris

déficientes en DNase étaient sensibles au développement de pathologies auto-immune[149]. Les patients atteints de SLE présentent une activité de la DNase 1 plus faible que les individus sains[150]. Enfin, les NETs peuvent aussi contribuer à la production d'anticorps anti-DNA.

E/ Conditions pré-analytiques

Les ADNcir à un fort potentiel biomédicales, ce qui en fait un biomarqueur très étudié en oncologie. Cependant, l'analyse de l'ADNcir n'est pas encore transposée en pratique clinique courante. De par ses origines cellulaires distinctes des ADNcir, son origine nucléaire ou mitochondrial, ses différents mécanismes de libération, l'analyse de l'ADNcir est un véritable challenge.

Bien que de nombreux travaux ont travailler sur l'optimisation des conditions pré-analytiques des ADNcir en oncologie[151], il n'y a pas de nos jours de protocoles accepté par l'ensemble des scientifiques, qui définirait les conditions optimales de prélèvement, d'analyse et de conservation des échantillons plasmatiques. Il existe toutefois des consensus sur une multitude de points mais des améliorations sont à apporter pour affiner l'analyse des ADNcir et conduire à l'établissement de procédures standardisées[152]. Une optimisation récente des procédures pré analytiques a pu être publiées dans ce domaine[88]. Notre équipe a depuis longtemps travaillée sur l'optimisation des conditions pré-analytiques des ADNcir en oncologie[153,154]. Nous avons par la suite continué à travailler sur les considérations pré-analytiques jusqu'à avoir publié le premier « guideline » qui établit précisément les conditions pré-analytiques des ADNcir en oncologie[155] **(Figure 15)**. Ce travail s'est basé sur les l'évaluation des paramètres influençant l'analyse des ADNcir chez les humains comme les aspects démographiques, pré-analytique et analytiques[153,154]. **J'ai notamment participé à la réalisation de ce travail[154] qui est discuté dans la partie « autres contributions » de ce manuscrit.**

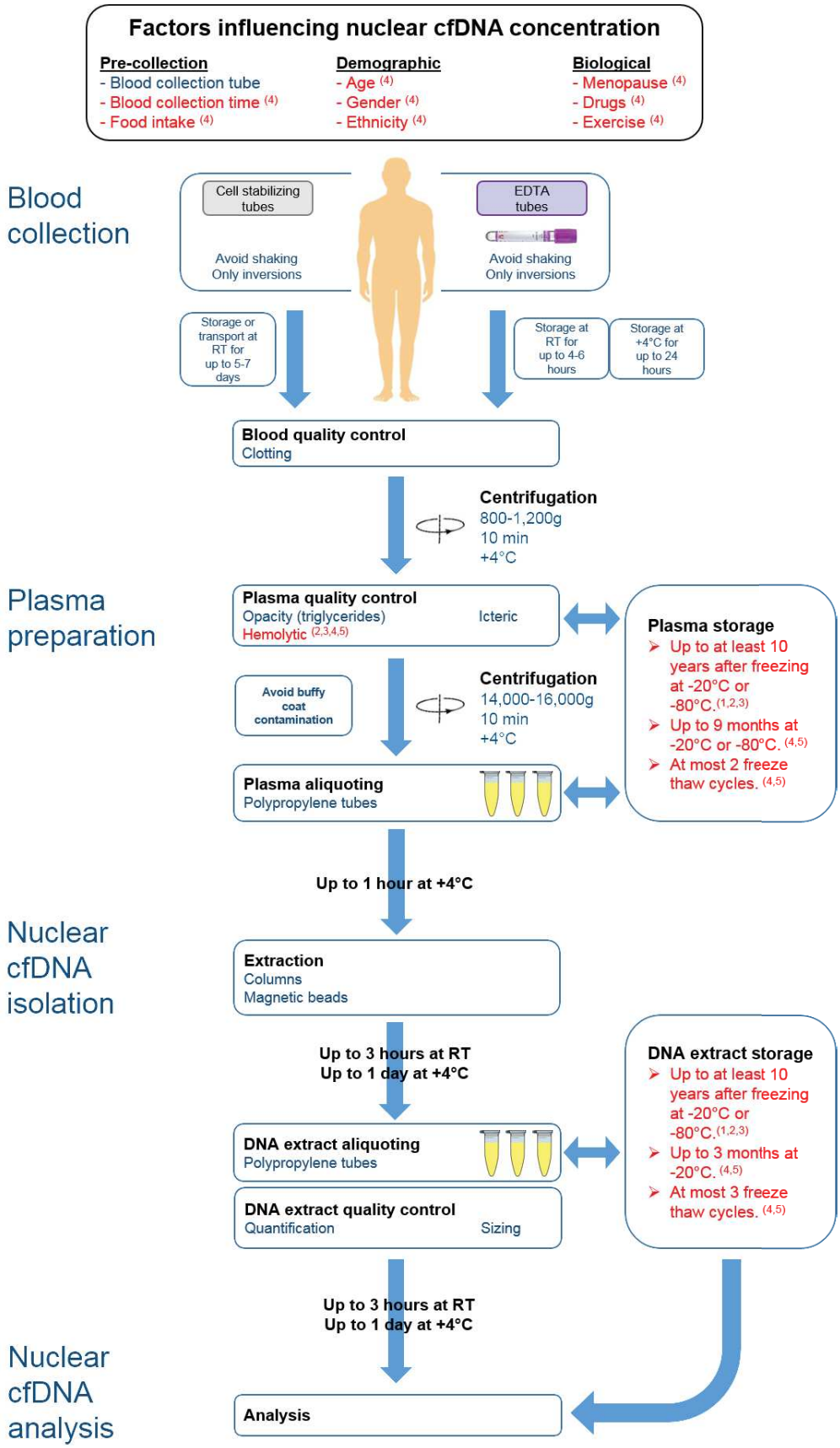

Figure 15: Guideline pour l'analyse de l'ADNcir nucléaire. *Source: Meddeb R. et al, 2019. Guidelines for the Preanalytical Conditions for Analyzing Circulating Cell-Free DNA*[155].

V/ Méthodes d'analyse de l'ADN circulant

Fondamentalement il existe deux grands principes pour la détection et la quantification des ADNcir: les méthodes basées sur le principe de la polymérisation en chaine par polymérase quantitative (PCRq) et les méthodes de séquençage à haut débit. Les méthodes basées sur le principe de PCRq sont dites ciblées puisqu'elles permettent de tester un nombre limité de mutations en une seule analyse alors que les méthodes de séquençage peuvent examiner soit l'ensemble du génome, soit l'ensemble des exons ou encore des panels de gènes pour les analyses les plus ciblées.

A/ Méthodes basées sur la polymérisation en chaine quantitative

La technique de polymérisation en chaine par polymérase quantitative est basée sur l'amplification d'une séquence ADN par hybridation d'amorces oligonucléotidiques spécifiques et complémentaires à la cible ADN. Outre la quantification de l'ADN, les méthodes de PCRq permettent aussi la détection de variation d'un seul nucléotide (SNP: single nucleotide variant) ainsi que la détection d'insertions ou de délétions nucléotidiques. Cette technique, très utilisée a l'avantage d'être rapide et peu couteuse. Bien que la PCRq classique à une sensibilité relativement faible pouvant détecter une mutation avec une fréquence allélique allant de 1 à 10%[156], de nombreuses équipes de recherches ont développé des méthodes ultrasensibles basées sur son principe. Ces nouvelles méthodes permettent l'analyse et la détection de d'évènements rares dans des milieux biologiques complexes comme le plasma ou le sérum.

La COLD-PCR ou la co-amplification à basse température de dénaturation basse permet d'amplifier préférentiellement une séquence mutée en contrôlant la température de dénaturation de l'ADN cible. Cette méthode à une sensibilité de détection de mutation approximativement de 0.1% (fréquence allélique)[157,158].

La PCR digitale (PCRd) est une technologie récente dont l'application première est de détecter et de quantifier les évènements rares dont les altérations génétiques de type SNP. Contrairement à de nombreuses méthode de PCRq qui analyse l'ADN d'un échantillon unique, la particularité de la PCRd est de partitionner un échantillon en une multitude (quelque milliers) de réaction de PCR en parallèle afin d'éliminer le bruit de fond[159,160]. La PCR digitale en gouttelettes (ddPCR) a été validée pour la détection des mutations *KRAS* dans le cancer colorectal métastatique[160,161] **(Figure 16)**. Dans cette méthodologie, les molécules cibles sont

séparées en un grand nombre de partitions de manière à ce que chaque partition reçoive un nombre de molécules (généralement compris entre 0 et 2) suivant une distribution de Poisson. Les mesures reposent sur le comptage du total des partitions (émulsions) positives contenant une ou plusieurs molécules cibles et des partitions négatives où aucune amplification n'est détectée. Cette partition permet la répartition et l'amplification des fragments d'ADN entre l'ensemble des réactions de PCR, ce qui signifie que le système est capable de diminuer le rapport ADN muté/ADN germinal, augmentant ainsi la sensibilité <0.1%[162,163]. Cette technique est donc adaptée à la recherche de mutations ponctuelles en oncologie[164]. Enfin, La PCR digitale peut fonctionner sur des puces en silicium (Quant studio 3D, Life technologies) ou dans des micro-gouttelettes (Bio-Rad Qx100, BioRad) (Figure X). Des recommandations sur cette technique ont été publié afin de bien utiliser cette méthode à des fins de recherche translationnelle[165].

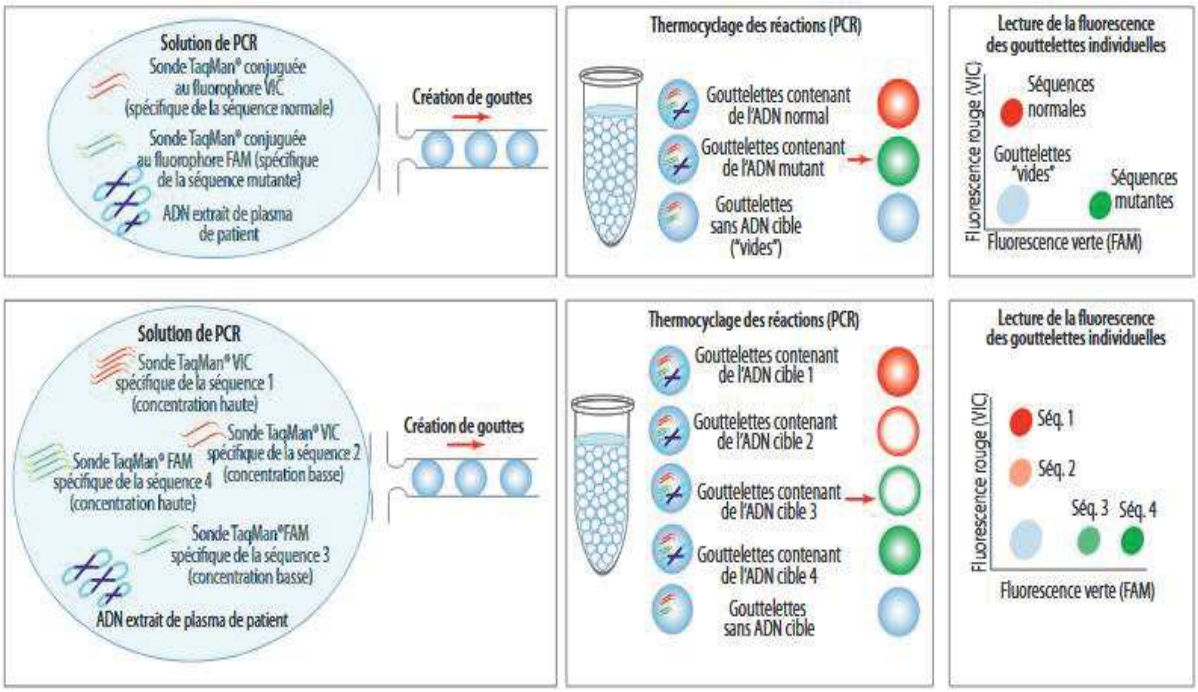

Figure 16: Les différentes étapes de la ddPCR. Source: Taly, V. *et al*, 2013. Multiplex picodroplet digital PCR to detect *KRAS* mutations in circulating DNA from the plasma of colorectal cancer patients[161].

La technologie BEAMing (Beads, Emulsion, Amplification and Magnetics) **(Figure 17)**, est basée sur une combinaison de PCR digitale en émulsion et de cytométrie en flux, utilisant des billes, une émulsion, une amplification et un magnétisme[166,167]. Les séquences d'ADN sont amplifiées

par PCR en émulsion, liées de manière covalente à des microbilles magnétiques par des interactions streptavidine-biotine ; les produits de PCR générés dans chaque gouttelette d'émulsion resteront physiquement fixés aux microbilles, ce qui permettra de les séparer et de les purifier facilement à l'aide d'un aimant, afin de déterminer la présence et le nombre de variations mutantes connues. La sensibilité de cette méthode est <0.01%[75,167]. Cette méthode est par conséquent appropriée pour détecter des mutations génétiques connues, même lorsque le nombre de copies est très faible. L'ADN de type sauvage ou mutant peut être facilement différencié par cytométrie en flux. Malheureusement, la technique de BEAMing est sophistiquée et complexe, ce qui limite la faisabilité et la reproductibilité de cette technologie en pratique clinique.

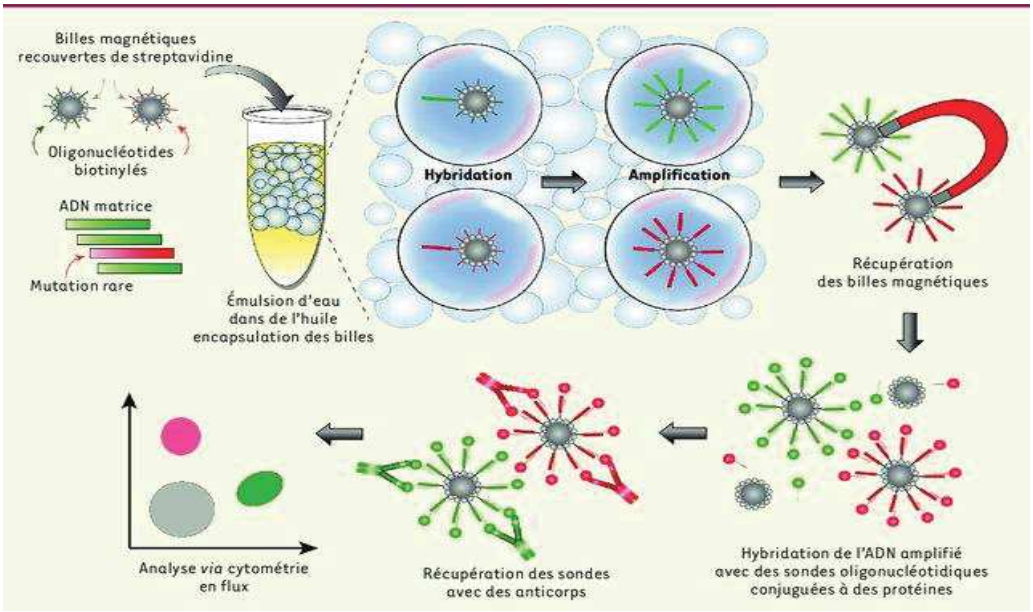

Figure 17: Les différentes étapes du BEAMing. *Source: Caen, O., et al, 2015. Digital PCR compartmentalization II. Contribution for the quantitative detection of circulating tumor DNA*[168].

Les méthodes basées sur le principe de PCRq semblent être adaptées à l'urgence théragnostique lorsqu'il est nécessaire d'avoir un test compagnon pour orienter rapidement le traitement ou pour modifier le traitement en cours de prise en charge thérapeutique. Ces techniques sont des approches ciblées avec une très grande sensibilité qui permettent la détection de mutations à de très faibles fractions alléliques. Bien qu'elles soient rapides et peu couteuses, elles permettent uniquement la détection de variants connus.

B/ Méthodes de séquençage à haut débit

Les méthodes de séquençage sont généralement moins sensibles et plus onéreuses que les techniques basées sur le principe de PCRq mais elles permettent d'analyser un large ensemble de gène et ont la capacité de détecter de altérations génétique autres que celles connues (ou hotspots)

Les méthodes de séquençage de nouvelle génération (ou méthodes NGS) peuvent détecter des variants à des fréquences alléliques entre 1 et 2% comparé au séquençage Sanger[169]. Le NGS peut être utilisé pour la détection d'un panel de gène précis afin d'étudier avec une sensibilité de détection élevée des mutations d'intérêt. Parmi ces méthodes de NGS ciblées nous retrouvons le *Tagged-Amplicon deep sequencing* (Tam-seq), *Safe-Sequencing System* (Safe-SeqS), *Cancer Personalized profiling by deep sequencing* (CAPP-Seq) et le Ion Torrent.

Le Tam-seq permet une détection de mutations aux alentours de 2%. Afin de contrôler les erreurs d'échantillonnage et la perte d'allèles, les amorces sont d'abord utilisées pour effectuer une préamplification afin d'amplifier l'ensemble de ADNcir. Ensuite, les matrices subissent une amplification individuelle pour être purifiées. Cette méthode combien donc deux étapes d'amplification par PCR. La version améliorée eTam-seq permet la détection d'un SNP avec une fréquence allélique inférieur à 0.25%[170]. Cette amélioration permet aussi de détecter les petite insertions/délétions (indels) ainsi que les variations du nombre de copie (CNVs).

Le Safe-SeqS quant à lui ajoute (i) des Identifiants Unique (UID) pour chacun des amplicon générés, (ii) l'amplification de chaque molécule matrice étiquetée de manière unique pour créer des familles d'UID, et (iii) réalise le séquençage redondant des produits d'amplification. Les fragments PCR ayant le même UID sont considérés comme mutants uniquement si ≥95% d'entre eux contiennent la même mutation. De cette façon le Safe-SeqS permet de réduire l'erreur de séquençage d'au moins 70 fois et permet une grande sensibilité de détection <0.1%[171].

Les techniques de séquençages sont moins sensibles que les techniques basées sur la PCRq mais elles permettent une approche plus complète et globale de l'information génétique nécessitant une plus grande fraction allélique tumorale[172] **(Figure 18)**.

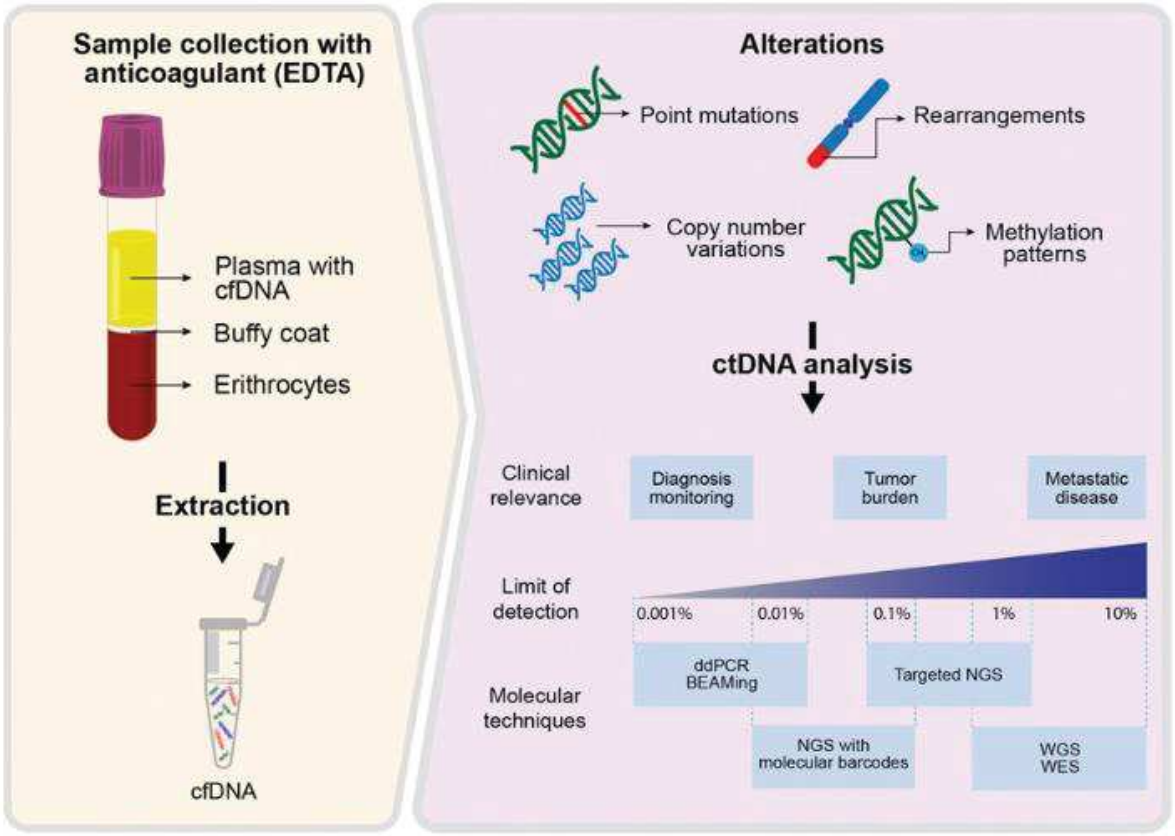

Figure 18: Les différentes méthodes de détection ont des limites de détection distinctes et de pertinence clinique. Source: De Oliveira *et al*, 2020. Current Perspectives on Circulating Tumor DNA, Precision Medicine, and Personalized Clinical Management of Cancer[172].

C/ La méthode IntPlex® : PCRq Allèle Spécifique Bloqueur

La méthode IntPlex® est une technique de PCRq allèle spécifique avec bloqueur (ASB, « allele specific blocker ») inventée et mise au point au sein de notre équipe[76] qui a permis la première validation clinique de l'analyse de l'ADNcir en oncologie pour la détection des mutations *KRAS/BRAF* chez des patients atteints de CCRm[76] **(Figure 19)**. Cette méthode de PCRq fait intervenir deux couples d'amorces qui vont amplifier deux séquences distinctes et qui sont séparées d'environ 250-300 pb. Le premier couple d'amorce va amplifier une séquence sauvage (Wild Type, WT) tandis que le second couple d'amorce va amplifier une séquence mutée grâce à une amorce spécifique qui ciblera la mutation sur le dernier nucléotide de son extrémité 3'. Les deux couples d'amorces vont générer des amplicons <100 bp afin de s'hybrider sur un maximum de fragments d'ADNcir. Il faut noter que l'équipe a pu démontrer à partir de plasma de patient CCRm qu'environ 80% des fragments d'ADNcir ont une taille inférieure à 100 pb. Les amorces utilisées ont une température de fusion basse (Tm), qui permet de s'hybrider spécifiquement aux cibles ADN. Un oligonucléotide bloqueur est utilisé pour s'hybrider sur la séquence sauvage à la position de la mutation ce qui diminue considérablement les amplifications non-spécifiques. L'oligonucléotide bloqueur qui a un Tm plus élevé que les amorces mutées va s'hybrider à l'ADN après les amorces mutées dans les cycles d'amplifications de PCR et en l'absence de mutation. Ce dernier possède un groupement phosphate à son extrimité 3' ce qui empêche sa polymérisation lorsqu'il est hybridé à sa cible ADN. Enfin l'utilisation d'un dernier couple d'amorce ciblant la totalité de la séquence d'environ 300 pb qui englobe les deux séquences précédemment évoquées permet d'apprécier la fragmentation de l'ADNcir grâce à un rapport appelé DNA Integrity Index (DII). Cette méthode permet de déterminer en un seul « run » de PCR cinq paramètres de l'analyse de l'ADNcir, quatre paramètres quantitatifs et un paramètre qualitatif. Le paramètre qualitatif est la présence ou non d'une mutation sur les gènes *KRAS* (codons 12, 13, 61, 117, 146), *NRAS* (codons 12, 13, 61) et *BRAF V600E*. Cette technique peut être adaptée pour toutes les mutations et pour tous types de cancer, elle a été adapté récemment pour les mutations des gènes *PIK3CA* et *EGFR*. Les paramètres quantitatifs sont : la concentration totale en ADNcir quantifiée grâce au couple d'amorce ciblant la séquence WT <100 pb, la concentration en ADNcir muté grâce au couple d'amorce a bas Tm ciblant la mutation, le calcul de la fréquence allélique mutée en faisant le rapport de ces deux premières concentrations et enfin elle permet d'établir le DII ou l'indice de fragmentation de l'ADNcir en faisant le rapport de la

concentration obtenue avec le couple d'amorces ciblant les séquences WT de 300 pb sur la concentration obtenue avec le couple d'amorces ciblant les séquences WT <100 pb.

Cette méthode à une sensibilité analytique de détection d'une copie d'ADNcir mutée avec une fréquence allélique de 0,0004% parmi les séquences WT. Dans des conditions cliniques la méthode IntPlex® a permis la détection d'une mutation ponctuelle avec une fréquence allélique allant jusqu'à 0,009%[173]. Nous avons montré que la méthode IntPlex® pouvait détecter un seul fragment d'ADNcir mutant selon la loi de Poisson[43]. Nous avons étudié cette loi de probabilité appliquée aux mutations présentes à un niveau très faible. Elle est exprimée comme le nombre d'événements observés dans le cas où les événements rares sont indépendants et aléatoires dans un espace/volume. Un extrait d'ADNcir mutant *KRAS G12V* a été dilué en série de 10 pg/µl à 0,1 pg/µl afin de détecter un fragment d'ADNcir mutant. Chaque dilution a été analysée selon la méthode Intplex dans dix puits (Figure 20). Nos résultats ont montré que la détection d'une mutation ponctuelle peut être effectuée avec précision selon une distribution de la loi de Poisson, démontrant la détection d'un seul fragment d'ADNc mutant. L'expérience a été réalisée en utilisant la plateforme LC480 de Roche ou la plateforme CFX de BioRad et n'a montré aucune différence (Figure 20).

L'avantage de cette technique est qu'elle est adaptable pour toutes les mutations, sur tous les gènes et pour tous les types de cancer. Récemment nous avons adaptés la technique IntPlex pour la détection et la quantification de certaines mutations des gènes *EGFR* et *PIK3CA* dans le cadre du cancer colorectal. La limite de cette technique est le fait qu'elle permet la recherche de mutations préalablement connues, à l'inverse du séquençage.

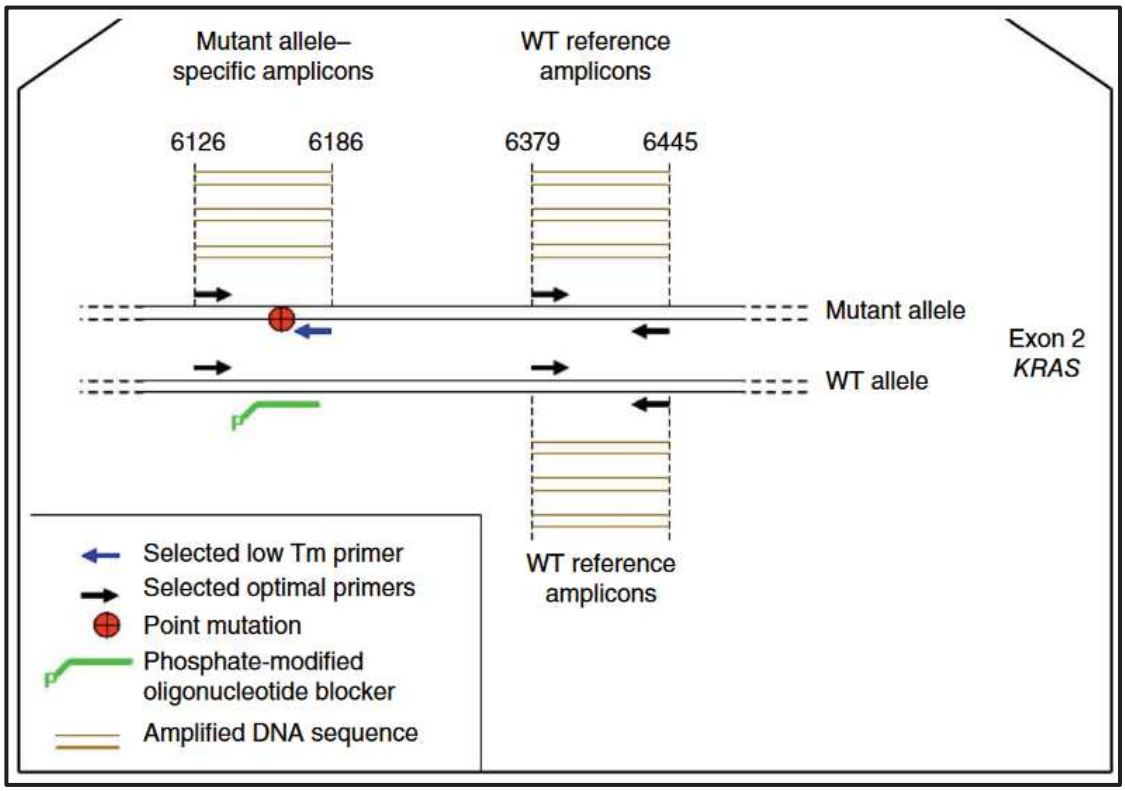

Figure 19: La technique Intplex®. *Source : Thierry, A. R. et al, 2014. Clinical validation of the detection of KRAS and BRAF mutations from circulating tumor DNA*[76].

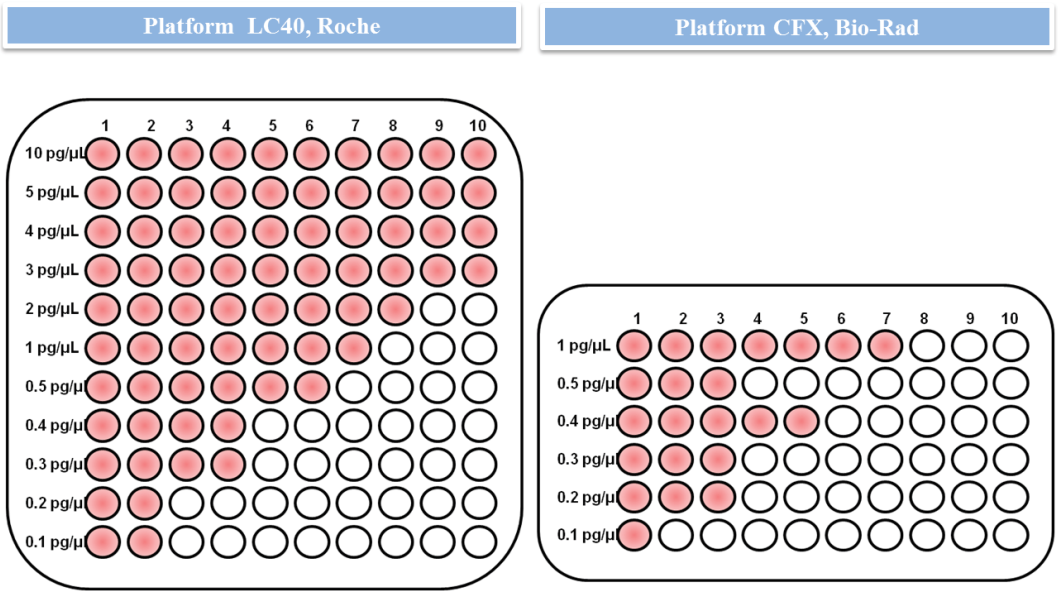

Figure 20 : Représentation schématique de la détection de mutation déterminée par l'analyse de l'ADNcir par la méthode Intplex selon la loi de Poisson avec la plate-forme LC480 (Roche) et la plate-forme CFX96 (BioRad). Les puits rouges sont positifs pour la mutation ; les puits blancs sont négatifs pour la mutation[43].

VI/ Potentiels cliniques de l'ADN circulant sur la prise thérapeutique des patient atteint de cancer colorectal

La validation du potentiel clinique des ADNcir (qu'il provienne de cellules saines ou cancéreuses) est un domaine majeur de recherche en oncologie. L'analyse de l'ADNcir permet de caractériser à faible coût différents types de cancers, à des stades précoces de façon non-invasive et par une simple prise de sang. En effet, l'ADNcir permettrait de mieux accompagner les patients durant leur prise en charge thérapeutique que ce soit pour (i) le dépistage de la maladie, son diagnostic, le pronostic, l'évaluation de la maladie résiduelle minimale (MRD pour minimal residual disease), la récurrence de la maladie et finalement dans la surveillance de la réponse aux traitements afin d'évaluer la résistance ou une sensibilité des tumeurs aux traitements[174]. L'ADN circulant fait l'objet de nombreux travaux de recherche en oncologie dont certains sont discutés dans une « review » écrite par notre équipe à la suite de l'organisation du 10ème congrès international sur les acides nucléiques circulants en oncologie « CNAPS »[175]. **J'ai par conséquent pu participer à (i) l'organisation de ce prestigieux congrès scientifique et à l'écriture de la review qui est discuté dans la partie « autres contributions » de ce manuscrit.**

Les différentes applications cliniques de l'analyse de l'ADNcir en oncologie seront développées dans cette partie.

A/ Le dépistage et le diagnostic précoce

Un dépistage précoce du cancer, avant l'apparition de signes clinique permettrait une prise en charge rapide des patients, a des stades plus précoces, augmenterait l'efficacité des traitements et par conséquent réduirait la mortalité liée au cancer.

Depuis la découverte que l'ADNcir est présent en quantités plus élevées dans le sang de patients atteints de différents types de cancer en comparaison avec des individus sains[71], de nombreuses études ont depuis confirmé cette observation[176]. La détection dans le sang d'altérations génétiques et épigénétiques spécifiques des tumeurs renforce le potentiel de l'ADNcir pour le dépistage du cancer. Pour exemple, dans le cas du cancer colorectal des études ont établis que le taux de détection du gène méthylé de la Septine 9 est significativement plus élevé chez les patients atteints de cancer colorectal comparé aux

individus sains, ce qui en fait un biomarqueur potentiel de ce cancer (Church, 2014). L'Epi proColon (Epigenomics AG, Corporation, Berlin, Allemagne) basé sur la détection dans le sang par PCR du gène de la Septine 9 méthylé, permet de distinguer les patients atteints de cancer colorectal des individus sains avec une sensibilité de 75-81% et une spécificité de 96-99%[177,178]. Chen et ses collègues ont montré dans une étude longitudinale récente, que l'analyse de la méthylation de l'ADNcir a permis de diagnostiquer un cancer chez 191 personnes (sur 605 testées) quatre années avant après la prise de sang[179]. Une revue récente publiée par l'équipe résume les différents tests de dépistage existant actuellment ainsi que ceux en cours de développement pour différents types de cancers[180] **(Tableau 2)**. L'ADNcir d'origine mitochondriale pourrait aussi permettre de discriminer des individus sains de patients atteints de cancers comme le montre les travaux de Tanos et ses collègues[181]. Pour finir, l'étude de la fragmentation des ADNcir ou « fragmentomics » permettait de discriminer des individus sains des patients atteints de cancers[87].

B/ Le pronostic

Bien que la concentration en ADNcir soit différente entre des individus sains et des patients atteints de cancer, cette concentration est aussi corrélée la taille de la tumeur et au stade tumoral[134,182]. La valeur pronostique de la concentration en ADNcir a pu être établis[183,183]. Notre équipe à étudier la survie globale (OS) des patients atteints de CCRm et a pu montrer que les patients ayant une concentration élevée en ADNcir total (>26 ng/mL de plasma) ont survie global amoindrie comparé aux patients ayant une concentration d'ADNcir plus faible (<26 ng/mL de plasma) (18,07 mois versus 28,5 mois)[184]. De plus, cette étude a montré par une analyse multivariée que la concentration en ADNcir total et le statut mutationnel *BRAFV600E* muté étaient des facteurs pronostiques puissants et indépendants[184]. Cette étude, montre aussi qu'une forte concentration en ADNcir muté et qu'un indice de fragmentation de l'ADNcir faible corrélaient avec une survie plus courte **(Figure 21)**. De nombreux travaux ont confirmé le potentiel pronostique de la concentration totale en ADNcir dans plusieurs types de cancers comme le cancer du poumon[185], le cancer de la prostate[186] et le cancer colorectal[187].

Catégorie		Test	Cancer	Sensibilité	Spécificité	AUC	Réf
Biomarqueurs et tests conventionnels utilisés		*CEA*	Colorectal	41-52 %	85-95 %	0,63-0,77	[11]
		CA19-9	Colorectal/ Pancréas	23 %	95 %	0,64	[11]
		FOBT	Colorectal	13-79 %	87-98 %	-	[12]
		FIT	Colorectal	79 %	94 %	-	[12]
		Cologuard (test d'ADN fécal)	Colorectal	41 %	94 %	-	[13]
		CA 15-3	Sein	55,6 %	98 %	-	[6]
		PHI (prostate health index)	Prostate	-	-	0,69-0,77	[54]
		PSA	Prostate	-	-	0,55	[7]
Biomarqueurs circulants en cours de développement	ADN circulant	*Epi ProColon* (détection du gène de la Septine 9 méthylé)	Colorectal	75-81 %	96-99 %	-	[23,24]
		7 promoteurs méthylés	Colorectal	91 %	73 %	0,85	[25]
		Volition (marqueurs de nucléosomes circulants)	Colorectal	75 %	86-90 %	0,97	[26]
			Poumon			0,88	[27]
		Concentration totale d'ADNcir nucléaire	Sein	78 %	83 %	0,91	[28]
			Ovaire	70 %	90 %	0,89	[29]
			Colorectal	-	-	0,91	[22]
		Détection du virus d'Epstein-Barr	Nasopharynx	97,1 %	98,6 %	-	[49]
		CancerSeek	Divers	30-99 %	99 %	0,91	[48]
	CTC	Numération	Poumon	30-78 %	88-100 %	0,60-0,86	[33,34,36]
	miARN circulants	Panel	Sein	83 %	41 %	0,67	[41]
			Poumon et mésothélium	73-75 %	54-79 %	-	[42]
	Autres	Combinaison de biomarqueurs protéiques circulants	Sein	-	-	0,70-0,99	[44]

Tableau 2: Récapitulatif des différents tests de dépistage du cancer et de leurs performances actuelles. *Source : Thierry, A. R. & Tanos, R, 2018. La biopsie liquide - Une voie possible pour le dépistage du cancer*[180].

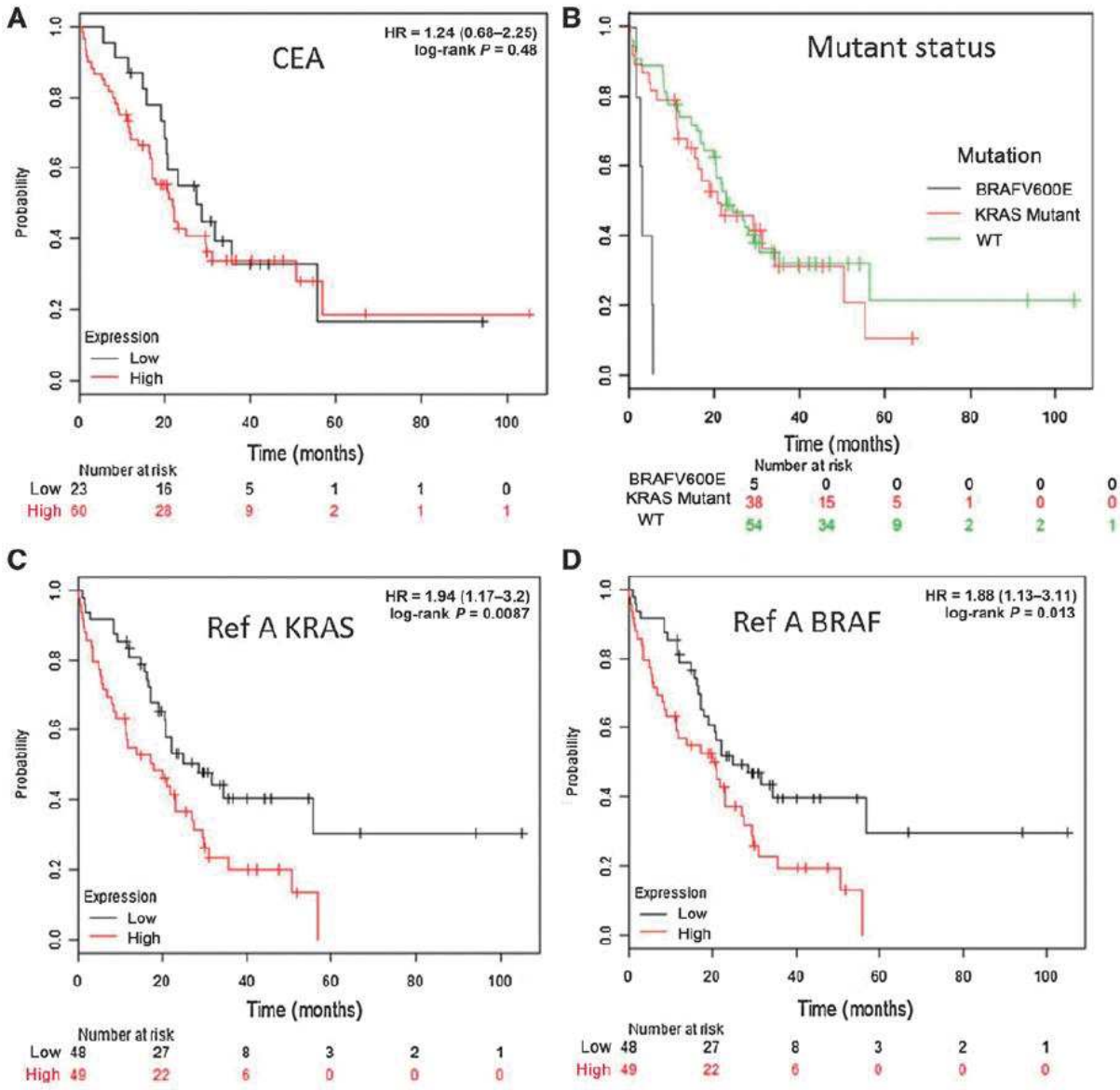

Figure 21: Analyse de la survie globale sur la cohorte entière. *Source: El Messaoudi, S. et al, 2016. Circulating DNA as a Strong Multimarker Prognostic Tool for Metastatic Colorectal Cancer Patient Management Care*[184].

C/ La maladie résiduelle minimale et récidive

La possibilité de pouvoir détecter une éventuelle maladie résiduelle minimale (MRD pour residual minimal disease) après une chirurgie est un enjeu capital dans la prise en charge des patients. En effet, environ 50 % des patients atteints de cancer colorectal localisé (stade II-III) et réséqué développeront des métastases[188]. L'ajout d'une chimiothérapie adjuvante après résection tumorale réduit considérablement le risque de rechute[189]. Le potentiel clinique du suivi de l'ADNcir pour détecter le MRD et stratifier les patients en fonction de leur risque de rechute est désormais bien établie dans les cas de cancer colorectal[190,191]. En 2016, Tie et ses collègues ont démontré dans un essai multicentrique et prospectif sur 230 patients atteints de cancer du côlon de stade II que de l'ADNcir tumoral après résection chirurgical était présent chez 79% des patients ayant rechutés[192]. Dans cette étude, la présence d'ADNcir tumoral a été détectée dans environ 8% (14/178) des patients après chirurgie. Aussi, Taieb et ses collègues ont déterminé la valeur pronostique et prédictive de L'ADNcir tumoral lors d'un traitement adjuvant. L'analyse multivariée a confirmé que la présence d'ADNcir après chirurgie était un marqueur pronostique indépendant de rechute[191]. Une autre étude montre que chez 125 patients atteints de cancer colorectal de stade I à III ayant subi une intervention chirurgicale à visée curative, que seulement 12% des patients n'ayant pas d'ADNcir tumoral détectable après résection (30 jours après la chirurgie) ont rechuté contre 70% pour les patients ayant un taux d'ADNcir tumoral détectable après chirurgie[193].

Nous terminons actuellement l'étude clinique DNAcirc : « Valeur diagnostique et pronostique de l'ADN circulant pour la surveillance des patients atteints de colorectal après un traitement curatif » (NCT02813928). Cette étude a pour objectif d'évaluer la valeur pronostique de l'analyse de l'ADNcir dans la détection précoce des récidives chez les patients traités pour un cancer colorectal de stade II ou III. **J'ai participé à l'analyse longitudinale des ADNcir des patients inclus lors de cette étude**. Les résultats de cette étude ne sont pas encore publiés et ils ne seront pas discutés dans ce manuscrit.

D/ Suivi des patients et surveillance de la résistance aux traitements

Comme discuté, les populations des clones cellulaires tumoraux évoluent avec le temps, de manière spontanée ou sous la pression sélective exercée par les différents traitements anti-cancéreux. L'évolution clonale des tumeurs peut engendrer des phénomènes de résistances acquises à certains traitements dont les thérapies ciblées anti-EGFR. Ce phénomène de résistance acquise aux traitements a été décrit dans plusieurs types de cancer comme le cancer de la prostate[194], du poumon[195], du sein[196] ou encore chez le patients atteints d'un mélanome[197]. Le suivi des patients au cours d'un traitement par l'analyse de l'ADNcir pourrait permettre d'anticiper les résistances secondaires aux traitements en détectant les mutations acquises impliquées dans la résistance thérapeutique. Dans le cas du cancer colorectal il a été démontré que l'émergence de mutations des gènes *RAS* engendrait des résistances secondaires aux traitements par anti-EGFR. Dans ce sens, la détection de ces sous clones tumoraux mutés durant le traitement pourrait permettre d'anticiper la progression radiologique[66,67,198]. Dans ce contexte de résistance aux traitements anti-EGFR, des études ont suggéré que des patients ayant des tumeurs préalablement *RAS* mutées tirent un bénéfice à être retraités par ces molécules si aucune mutations *RAS* n'est détectée après l'arrêt des anti-EGFR (on appelle cela le « rechallenge » de la molécule)[199–201]. C'est dans ce contexte de résistance aux traitements par anti-EGFR que nous avons réalisé l'étude rétrospective *KPLEXR*. **Les résultats de ce travail auquel j'ai contribué sont discutés dans la partie « Résultats » de ce manuscrit.**

Nous avons aussi mené une étude afin d'évaluer si l'analyse de l'ADNcir pouvait distinguer les répondeurs des non répondeurs avant un traitement par regorafenib. Les résultats de ce travail auquel j'ai contribué sont discutés dans la partie « Résultats » de ce manuscrit.

VII/ Objectifs de la thèse

Objectif n°1 : ***Mettre en évidence l'hétérogénéité et l'évolution clonale des tumeurs de patients atteints de cancer colorectal métastatique au cours de leur prise en charge thérapeutique***

A/ ***Détection des mutations RAS/BRAF chez des patients atteints de CCRm traités ou avant l'initiation d'un traitement par anticorps anti-EGFR***

Il est établi que seuls les patients atteints d'un CCRm ayant un statut *RAS* sauvage peuvent bénéficier d'un traitement par anticorps monoclonaux anti-EGFR (cetuximab ou panitumumab). Jusqu'à présent l'analyse moléculaire du tissu tumoral est la technique de référence pour étudier le statut *RAS* des tumeurs. Néanmoins, notre équipe a publiée en 2014 la première validation clinique de l'analyse de l'ADN circulant pour la détection des mutations *KRAS/BRAF* chez les patients atteints de cancer colorectal métastatique. Ces travaux ont montré une forte concordance de l'analyse de l'ADNcir avec l'analyse du tissu tumoral (96% pour les mutations de l'exon 2 de *KRAS* et 100% pour *BRAF V600E*)[76], ouvrant la voie à l'analyse des mutations *RAS* à partir de l'ADNcir.

Un des objectifs de ma thèse a été d'étudier le profil génétique des tumeurs de patients atteints de CCRm par l'analyse de l'ADNcir avant et durant une thérapie ciblée anti-EGFR. Le but est de confirmer l'utilité clinique de l'analyse de l'ADNcir que ce soit pour améliorer la stratification des patients CCRm avant un traitement par anti-EGFR, ou pour mettre en évidence des émergences de mutations secondaire *RAS/BRAF* entrainant la résistance des tumeurs aux traitement anti-EGFR.

Pour cela nous avons travaillé sur deux essais cliniques (KPLEX2 et KPLEXR) qui ont conduit à deux publication dans ce domaine :

« Clinical utility of circulating DNA analysis for rapid detection of actionable mutations to select metastatic colorectal patients for anti-EGFR treatment » **publié dans Annals of Oncology en 2017. Ce travail est détaillé dans la partie résultats "Article I".**

"Circulating DNA Demonstrates Convergent Evolution and Common Resistance Mechanisms during Treatment of Colorectal Cancer" publié dans Clinical Cancer research en 2017. **Ce travail est détaillé dans la partie résultats "Article II".**

B/ ***Détection des mutations RAS/BRAF chez des patients atteints de CCRm traités par régorafénib***

Il faut noter que les patients CRCm réfractaires aux traitements standards peuvent être traités avec des agents oraux tels que le trifluridine/tipiracil ou le regorafenib. Cependant, il n'existe actuellement aucun marqueur accepté permettant de prédire les bénéfices du régorafénib. Ces patients en dernière ligne de traitement et traités au régorafénib ont beaucoup d'effets secondaires. Il est donc crucial de distinguer les répondeurs des non répondeurs afin d'éviter l'acharnement thérapeutique et pouvoir ne traiter que les patients qui auront un bénéfice clinique.

Pour cela nous avons travaillé sur un essai clinique (TEXCAN) qui a conduit une publication dans ce domaine. Nous travaillons encore sur une étude clinique (FOLFIRINOX-R) dont le protocole clinique a pu être publié:

"Monitoring levels of circulating cell-free DNA in patients with metastatic colorectal cancer as a potential biomarker of responses to regorafenib treatment"publié dans Molecular Oncology en 2021. **Ce travail est détaillé dans la partie résultats "Article III".**

"FOLFIRINOX-R study design: a phase I/II trial of FOLFIRINOX plus regorafenib as first line therapy in patients with unresectable RAS-mutated metastatic colorectal cancer" publié dans BMC cancer en 2021. **Ce travail est détaillé dans la partie résultats "Article IV".**

Objectif n°2 : Etudier l'association entre la formation des neutrophils extracellular traps (NETs) avec la production des ADNcir chez les patients atteints de CCRm.

Les ADNcir tumoraux provenant des cellules malignes de la tumeur sont dilués par un relargage d'ADNcir provenant de cellules saines entrainant la diminution parfois drastique des fréquences alléliques tumorales. Les variations de la fréquence allélique rendent difficiles la détection des mutations *RAS/BRAF* chez des patients CRCm. Un défaut de détection d'une mutation peut entrainer des mauvais diagnostics et par conséquent donner lieu à de mauvais traitements.

Jusqu'à présent, Il est mentionné dans la littérature que l'ADN circulant est libéré via les mécanismes de nécrose, d'apoptose et par phénomènes de sécrétion active. Récemment il a été établi que les neutrophiles sont capables d'éliminer les agents pathogènes par le phénomène de NETose. Ce mécanisme consiste en une libération de pièges ADN extracellulaires sécrétés par des neutrophiles activés (NETs) qui sont composés d'un réseau de chromatine extracellulaire décorée de protéines cytosoliques et de granules bactéricides, telles que l'élastase des neutrophiles (NE) et la myéloperoxydase (MPO). De plus, les NETs sont retrouvés dans les mêmes conditions pathologiques pour lesquelles des concentrations élevées d'ADNcir ont été rapportées comme le cancer. Dans ce contexte, nous émettons l'hypothèse qu'une fraction de la production de l'ADNcir chez des patients atteints de cancer métastatique provient de la dégradation des NETs.

Le dernier objectif de ma thèse est donc d'évaluer l'association entre la formation de NETs avec la production des ADNcir totaux chez des patients atteints de CCRm.

Ces travaux ont conduit à la publication suivante :

"Association of Neutrophil Extracellular Traps with the production of circulating DNA in colorectal cancer patients" en cours de publication dans iScience, 2022. Ce travail est détaillé dans la partie résultats "Article V".

RESULTATS

1/ Hétérogénéité et évolution clonale des tumeurs de patients atteints de cancer colorectal métastatique au cours de leur prise en charge thérapeutique

A/ Détection des mutations *RAS/BRAF* chez des patients atteints de CCRm traités ou avant l'initiation d'un traitement par anticorps anti-EGFR

Article I*:* Utilité clinique de l'analyse de l'ADN circulant pour la détection rapide de mutations actionnables en vue de sélectionner les patients colorectaux métastatiques pour un traitement anti-EGFR (Etude *KPLEX2*)

A. R. Thierry, S. El Messaoudi, C. Mollevi, J. L. Raoul, R. Guimbaud, D. Pezet, P. Artru, E. Assenat, C. Borg, M. Mathonnet, C. De La Fouchardière, O. Bouche, C. Gavoille, C. Fiess, B. Auzemery, R. Meddeb, E. Lopez-Crapez, C. Sanchez, B. Pastor & M. Ychou

Rationnel: Les patients atteints de CRCm ne présentant pas de mutations sur les gènes *KRAS* et *NRAS* (*RAS*) peuvent être traités par thérapie ciblées anti-EGFR (cetuximab et panitumumab). Aujourd'hui, l'analyse moléculaire du tissu tumoral reste le « gold standard » pour les patients atteints de cancer colorectal. Cependant, ce « gold standard » est remis en question par l'arrivée de l'analyse de l'ADN tumoral circulant à partir d'une simple prise de sang. Après avoir réalisé la première validation clinique de l'ADN circulant plasmatique chez les patients atteints de cancer colorectal métastatique, nous avons ici évalué son utilité clinique dans le cadre d'une prise en charge standard.

Contribution: Dans ce projet j'ai des analyses de quantification des ADNcir totaux ainsi que la détection et la quantification des mutations *RAS/BRAF* chez les patients atteints de CCRm.

Introduction

La détection des mutations de *RAS* chez les patients atteints de CCRm est nécessaire afin de prédire la réponse aux anticorps monoclonaux anti-récepteur du facteur de croissance épidermique (EGFR)[27,202–207]. Aujourd'hui cette recherche de mutations est réalisée à partir de tissus tumoraux. Le prélèvement du tissu tumoral peut être effectué sur la tumeur primaire ou sur les métastases, qu'il soit effectué par une biopsie ou lors de d'une résection tumorale. Cependant, ce "gold standard" est remis en question par l'analyse de l'ADN circulant tumoral à partir d'échantillons de sang [77,184,208,209]. L'analyse de l'ADNcir constitue une approche prometteuse pour fournir une analyse moléculaire tumorale peu invasive des patients atteints de cancer [76,131,210–212]. L'utilisation des anticorps monoclonaux dirigés contre l'EGFR, comme le cetuximab et le panitumumab, dans le traitement du cancer colorectal métastatique (CCRm) est limitée aux patients de type *RAS* sauvage (ou wild type : WT)[27,203,206].

Alors que les approches de séquençage telle que le NGS permettent une couverture génétique élevée [213], l'approche ciblée telle que les techniques basées sur la Q-PCR (Beaming, dPCR ou Q-PCR améliorées) bénéficie d'une plus grande sensibilité pour détecter les mutations fréquentes déjà connues (hotspots). Nous avons démontré la première validation clinique de l'analyse de l'ADNcir en oncologie[76] en détectant les mutations ponctuelles de l'exon 2 du gène *KRAS* et de *BRAF V600E* chez des patients atteints de CRCm, et montré qu'un test sanguin pouvait remplacer l'analyse du tissu tumoral. Ici, nous avons élargis notre validation précédente de l'ADNcir[76] en comparant l'analyse de l'ADNcir avec l'analyse des tissus tumoraux dans une étude prospective, multicentrique et en aveugle. Il est a noté que nous avons apporté des différences significatives avec notre étude précédente qui sont: (i) l'analyse de l'ADNcir a été effectuée en flux tendu, ce qui permet une comparaison directe du délai d'exécution des données au cours de la pratique de routine standard ; (ii) le statut mutationnel à partir de l'analyse du plasma a été déterminé avec une sensibilité 50 fois plus élevée que dans notre étude antérieure ; (iii) la recherche des mutations a été étendue aux exons 3 et 4 des gènes *RAS* (*KRAS* et *NRAS*). Cette étude démontre l'utilité clinique de l'analyse de l'ADNcir dans le cas du cancer colorectal métastatique et ouvre la voie à de nouvelles perspectives.

ESMO GOOD SCIENCE BETTER MEDICINE BEST PRACTICE

Annals of Oncology 28: 2149–2159, 2017
doi:10.1093/annonc/mdx330
Published online 30 June 2017

ORIGINAL ARTICLE

Clinical utility of circulating DNA analysis for rapid detection of actionable mutations to select metastatic colorectal patients for anti-EGFR treatment

A. R. Thierry[1,2,3,4*], S. El Messaoudi[1,2,3,4†], C. Mollevi[1,2,3,4,5], J. L. Raoul[6], R. Guimbaud[7], D. Pezet[8], P. Artru[9], E. Assenat[10], C. Borg[11], M. Mathonnet[12], C. De La Fouchardière[13], O. Bouché[14], C. Gavoille[15], C. Fiess[16], B. Auzemery[1,2,3,4], R. Meddeb[1,2,3,4], E. Lopez-Crapez[1,2,3,4], C. Sanchez[1,2,3,4], B. Pastor[1,2,3,4] & M. Ychou[1,2,3,4,16]

[1]IRCM, Institute of Research in Oncology of Montpellier, Montpellier; [2]INSERM, U1194, Montpellier; [3]Department of Oncology, Montpellier University, Montpellier; [4]Regional Institute of Cancer of Montpellier, Montpellier; [5]Biometry Unit, Regional Institute of Cancer of Montpellier, Montpellier; [6]Department of Medical Oncology, Paoli Calmettes Institute, Marseille; [7]Department of Oncology, University Hospital Center of Toulouse – Hospital Rangueil-Purpan, Toulouse; [8]Digestive Oncology Unit, Department of Digestive Surgery, University Hospital Center of Clermont-Ferrand, UMR Inserm/Auvergne University U1071, Clermont-Ferrand; [9]Jean-Mermoz Private Hospital, Lyon; [10]CHRU Montpellier, St. Eloi Hospital, Montpellier; [11]CHRU Jean MINJOZ, Besançon; [12]Digestive Surgery Department, Clinical Investigation Centre, University Hospital Center of Limoges, INSERM 0801, Limoges; [13]Cancer Centre Léon Bérard, Lyon; [14]CHU Robert Debré, Reims; [15]Alexis Vautrin Oncology Institute of Lorraine, Nancy; [16]Digestive Oncology Department, Regional Institute of Cancer of Montpellier, Montpellier, France

*Correspondence to: Dr Alain R. Thierry, INSERM, U1194, IRCM, 208 rue des Apothicaires, 34298 Montpellier Cedex 5, France. Tel: +33-6-63-82-19-94; E-mail: alain.thierry@inserm.fr

†Present address: DiaDx SAS, Liquid Biopsy for Personalized Cancer Medicine, Montpellier, France.

Background: While tumor-tissue remains the 'gold standard' for genetic analysis in cancer patients, it is challenged with the advent of circulating cell-free tumor DNA (ctDNA) analysis from blood samples. Here, we broaden our previous study on the clinical validation of plasma DNA in metastatic colorectal cancer patients, by evaluating its clinical utility under standard management care.

Patients and methods: Concordance and data turnaround-time of ctDNA when compared with tumor-tissue analysis were studied in a real-time blinded prospective multicenter clinical study ($n = 140$ metastatic colorectal patients). Results are presented according to STARD criteria and were discussed in regard with clinical outcomes of patients.

Results: Much more mutations were found by ctDNA analysis: 59%, 11.8% and 14.4% of the patients were found *KRAS*, *NRAS* and *BRAF* mutant by ctDNA analysis instead of 44%, 8.8% and 7.2% by tumor-tissue analysis. Median tumor-tissue data turnaround-time was 16 days while 2 days for ctDNA analysis. Discordant samples analysis revealed that use of biopsy, long delay between tumor-tissue and blood collection and resection of the tumor at time of blood draw, tumor site, or type of tissue analyzed seem to affect concordance. Altogether, the clinical data with respect to the anti-epidermal growth factor receptor response (RAS status) and the prognosis (*BRAF* status) of those discordant patients do not appear contradictory to the mutational status as determined by plasma analysis. Lastly, we present the first distribution profile of the *RAS* and *BRAF* hotspot mutations as determined by ctDNA analysis ($n = 119$), revealing a high proportion of patients with multiple mutations (45% of the population and up to 5 mutations) and only 24% of WT scored patients for both genes. Mutation profile as determined from ctDNA analysis with using various detection thresholds highlights the importance of the test sensitivity.

Conclusion: Our study showed that ctDNA could replace tumor-tissue analysis, and also clinical utility of ctDNA analysis by considerably reducing data turnaround time.

Key words: circulating DNA, personalized medicine, colorectal cancer, diagnostic, clinical utility, mutation

Introduction

Mutation screening of *RAS* to predict response to anti-epidermal growth factor receptor (EGFR) monoclonal antibodies in metastatic colorectal cancer (mCRC) patients [1–7] is mandatory to maximize patient benefit. Currently, it is carried out from tumor-tissue. However, this 'gold-standard' is challenged with the advent of circulating cell-free tumor DNA (ctDNA) analysis from blood samples appearing as a 'liquid biopsy' approach [8–11]. ctDNA analysis constitutes a hopeful approach to provide a minimally invasive tumor molecular test for cancer patients [12–16]. In particular, ctDNA analysis is evaluated as a theragnostic test when the mutational status of specific gene is predictive of the therapeutic response. Sequencing- and targeted-based approaches are taken into consideration. While sequencing approaches such as NGS enable high gene coverage [17], targeted approach such as Q-PCR-based techniques (Beaming, dPCR or refined Q-PCR) beneficiates from higher sensitivity to detect previously known hotspot mutations. Based upon breakthrough information on ctDNA fragmentation and size [18, 19], we developed a Q-PCR-based-method (IntPlex®) which is the first multiplexed test for ctDNA. We demonstrated the first clinical validation of ctDNA analysis in oncology [16] by detecting *KRAS* exon 2 and *BRAF* V600E point mutations in mCRC patients, and showed that a blood test could replace tumor-section analysis.

Here, we broaden our previous validation of ctDNA [16] by comparing ctDNA analysis and tumor-tissue analysis in a prospective, multicenter and blinded study with significant differences with our previous study: (i) ctDNA analysis was just-in-time carried out allowing direct comparison of the data turnaround-time in the course of standard routine practice; (ii) the mutation status from plasma analysis was determined with a >50-fold higher sensitivity than in this earlier study; (iii) extended *RAS* hotspot mutations was tested. This study demonstrates clinical utility of ctDNA analysis and paves the way in considering it as next generation of companion diagnostics.

Materials and methods

Study design and participants

Kplex2 is a blinded multicenter prospective study ($n = 11$ clinical centers). A total 140 mCRC patients with requested *KRAS* mutational status for anti-EGFR therapeutic decision-making were enrolled. Patients were naive for anti-EGFR treatment. Full inclusion criteria and regulatory aspects are described in supplementary data, p. 2, available at *Annals of Oncology* online.

Masking

Clinical data and results of standard and index tests were collected prospectively by our Biostatistic Unit. Readers of the two tests were blinded to the results of the other test.

Mutation testing from tumor-tissue and plasma

Tumor-tissue analysis was carried out in each clinical center participating to the study in the context of the standard management care of mCRC patients considered for anti-EGFR treatment. According to our specific pre-analytical guideline for ctDNA analysis [20] (see supplementary data, pp. 2–9, available at *Annals of Oncology* online for more details). CtDNA analysis was just-in-time centrally carried out on one of the sites. ctDNA analysis was carried out from using 2 ml plasma for testing 28 different mutations testing. Mutation testing from plasma was carried out by using the IntPlex method applied as previously described [16] without any mutation sensitivity threshold so enabling a >50-fold higher sensitivity while keeping high analytical specificity and sensitivity due to the use of two negative and one positive control in each run and quality controls with regards to plasma pre-analytical conditions.

Outcomes

The outcomes consisted in (i) comparing the data turnaround time of tumor-tissue and plasma analysis, and (ii) studying concordance of the data obtained from both diagnostic approaches; the tumor-tissue analysis was regarded as the gold standard. The outcomes were carried out in blinded conditions where *KRAS* exon 2 and *BRAF* V600E mutation tests were made by both methods in 121 and 97 patients, respectively. The *RAS* extended mutation test as determined by ctDNA analysis was carried out in blinded conditions only for the patients scored WT for *KRAS* exon 2 and *BRAF* ($n = 50$) (see supplementary data, pp. 7–8, available at *Annals of Oncology* online).

Post hoc analysis

The study has two *post hoc* analyses. The first *post hoc* analysis consisted in examining the discordance and the factors potentially impacting it. The second *post hoc* analysis consisted of obtaining a direct mutation profiling when considering the actionable *RAS* and *BRAF* mutations carried out by both analytical approaches in a maximum of patients (see supplementary data, p. 9 for more detailed methodology, available at *Annals of Oncology* online).

Statistical analysis

The study has been designed with a false positive rate = 10%, a true positive rate = 85% and a ratio (percentage of patients with a negative test = non-mutated/percentage of patients with a positive test = mutated) = 60/40 = 1.5. Finally, 115 patients assessable (with determination of status by both methods) were required [22]. The diagnostic utility of the blood test was assessed using sensitivity, specificity, positive predictive value (PPV) and negative predictive value (NPV). Sensitivity reflects the diagnostic performance in detecting mutated patients, and specificity reflects the performance in detecting non-mutated patients. The PPV and NPV are the proportions of mutated (positive results) and WT predicted patients (negative results) that are really mutant (true positive result) and WT, respectively.

Results

Flow of participants

Results are presented according to STARD criteria (Figure 1; supplementary data, pp. 10–14, available at *Annals of Oncology* online). A total of 140 mCRC patients were enrolled from the 11 clinical centers (supplementary data, pp. 15–16, available at *Annals of Oncology* online). All plasma samples compliant for technical inclusion criteria were correctly analyzed (100% success rate). Finally, 121 mCRC participants were selected (Figure 1; supplementary data, p. 10, available at *Annals of Oncology* online). Baseline demographic, clinical characteristics and tumor-tissue analysis characteristics are presented in Table 1 (n = 121) (detailed supplementary data, pp. 13–18, available at *Annals of Oncology* online).

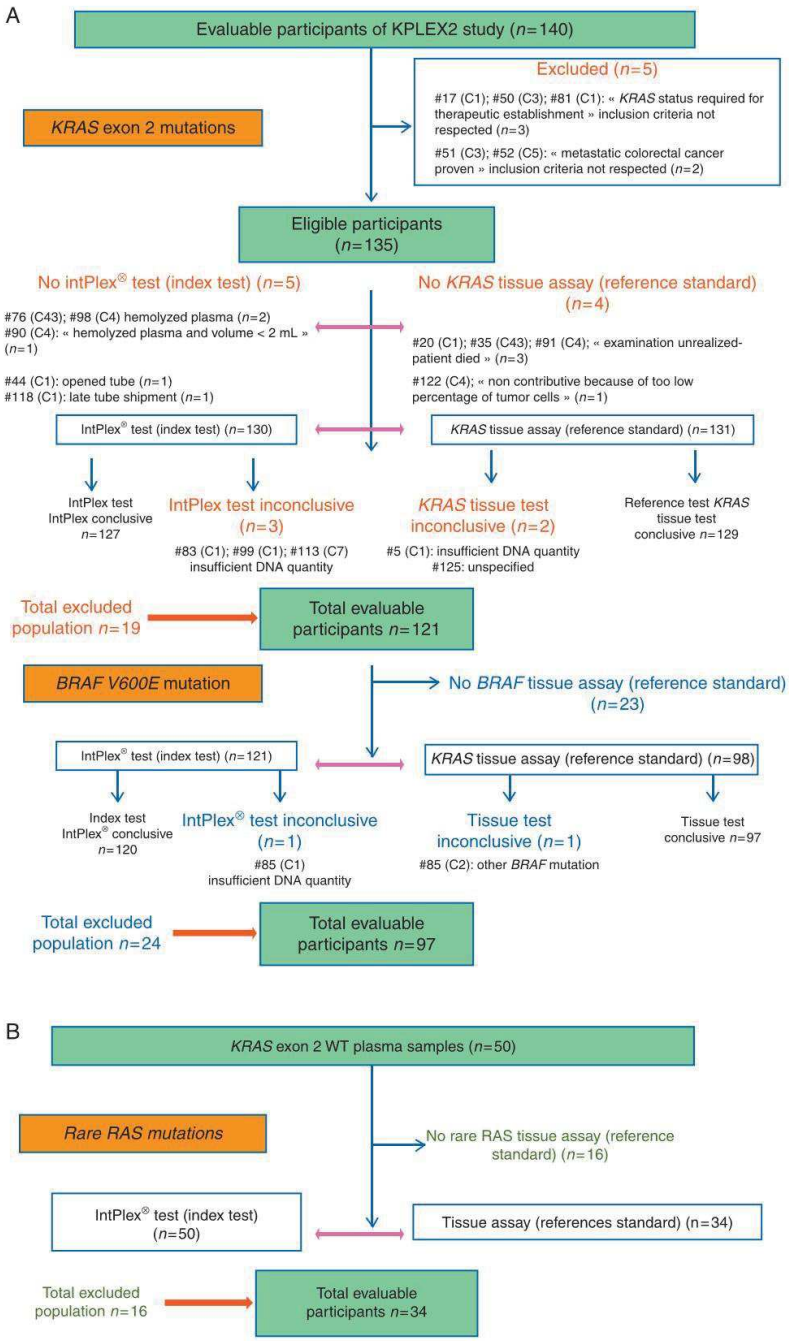

Figure 1. STARD flow diagram of participants to the study ($n = 140$). A, Blinded detection of *KRAS* exon 2 and *BRAF* V600E mutations. B, Blinded detection of rare *RAS* mutations (*KRAS* exon 3,4 and *NRAS* exon 2,3,4).

Table 1. Demographic, clinical data of patients at time of inclusion and characteristics of tumor-tissue analysis (n = 121)

	n=121	%
(A) Demographic data		
Gender		
Male	70	57.8
Female	51	42.1
Age (years)	66	[22; 91]
Clinical status of patients at time of inclusion		
Diagnosis		
Site of primary tumor		
Colon	63	52.1
Rectosigmoidian junction	28	23.1
Rectum	30	24.8
Histology		
Lieberkünian adenocarcinoma	114	94.2
Mucinous adenocarcinoma	7	5.8
Differentiation		
G1/Well differentiated	42	42.9
G2/Moderately differentiated	46	46.9
G3/Poorly differentiated	10	10.2
Missing Data	*23*	
Metastasis		
Metachronous	37	30.6
Synchronous	84	69.4
No of metastatic sites at time of blood sampling		
1	65	53.7
>1	56	46.3
Resection of primary tumor at time of blood sampling		
Y	59	48.8
N	62	51.2
Treatment before inclusion		
Chemotherapy		
Adjuvant	26	21.5
≥1[a]	33	27.3
Radiotherapy		
	22	18.2
(B) Tumor-tissue analysis characteristics (*n*=121)		
Collection		
Before metastatic diagnosis	45	39.5
After metastatic diagnosis	69	60.5
Missing data	*7*	
Collection		
Primary tumor	94	77.7
Metastasis	27	22.3
Brain	1	3.7
Colic	1	3.7
Hepatic	12	44.4
Hepatic and pulmonary	1	3.7
Peritoneal	3	11.1
Lymph nodes	3	11.1
Pulmonary	6	22.2
Nature of tumor piece analyzed		
Biopsy	61	50.4
Surgical specimen	60	49.6
% tumor cells within the sample		
<20%	3	2.8
[20%–50%]	44	41.5
>50%	59	55.7
Missing data	*15*	
Technology used		
Direct sequencing	14	11.6
HRM+ sequencing	30	24.8
Pyrosequencing	14	11.6
HRM+ pyrosequencing	28	23.1
RT-PCR	4	3.3
SNaPshot	15	12.4
Commercial kits	2	1.6
Other	14	11.6

[a]≥1: those patients received 1 or more previous lines of treatment. All the patients were naïve for anti-EGFR treatment.

Comparison of data turnaround time

The median delay between (i) inclusion and results communication was 18 days ($n = 121$; 4–288 days) for tumor-tissue analysis while 7 days ($n = 121$; 1–72 days) for plasma analysis; (ii) tissue sample reception by the hospital laboratory and communication of the results was 12 days ($n = 83$; 3–273 days) but only 2 days between the plasma sample reception by our laboratory and results communication ($n = 121$; 0–10 days) (Table 2).

Concordance study between ctDNA and tumor-tissue analysis

Evaluation of concordance was detected considering tumor-tissue analysis as the 'gold standard'.

KRAS exon 2 point mutations (n = *121*). Fifty-three mutant tumor-tissue samples (44%) and 71 mutant plasma samples (59%) were determined. Forty-five mutant samples (37%) and 42 WT samples (35%) were concordant. Eight WT plasma samples were found mutant by tumor-tissue analysis (7%). Conversely, 26 WT tumor-tissue samples were found mutant by plasma analysis (21.5%). Sensitivity, specificity, PPV and NPV were 85%, 62%, 63% and 84%, respectively (Table 2B; detailed data in supplementary Table S8, available at *Annals of Oncology* online).

BRAF V600E *point mutation.* Detection of the *BRAF* V600E point mutation was tested for 97 patients under routine standard management care and in 127 plasma samples. Concordance analysis was finally evaluated in 97 patients. Seven mutant tumor-tissue samples (7%) and 14 mutant plasma samples (14%) were determined. Four mutant samples and 80 WT samples were concordant. Three WT plasma samples were found mutant by tumor-tissue analysis. Inversely, 10 WT tumor-tissue samples were found mutant by plasma analysis. Sensitivity, specificity, PPV and NPV were 57%, 89%, 29% and 96%, respectively (Table 2B; detailed data in supplementary Table S8, available at *Annals of Oncology* online).

Table 2. Blinded comparison study between tumor-tissue and plasma ctDNA analysis: (A) data turnaround time (n = 121); (B) concordance study for the detection of KRAS exon two-point mutations (n = 121), *BRAF* V600E (n = 97), *KRAS* exon 3 and 4 (n = 34) and *NRAS* exon 2 and 3 (n = 34)

Comparison of data turnaround time between tumor-tissue and plasma ctDNA analysis (*n*=121)

Tumor-tissue analysis			**Plasma ctDNA analysis**		
	Median (days)	**Range [min; max]**		**Median (days)**	**Range [min; max]**
Time between tissue-drawing and prescription	33.5	[−87[a]; 2373]	Time between blood-drawing and sample shipment	1	[0; 7]
Missing	*1*				
Time between prescription and reception of tissue sample by the lab	4	[−10; 266]	Time between shipment and reception	1	[0; 5]
Missing	*39*				
Time between tissue sample reception by the lab and results communication	12	[3; 273]	Time between sample reception and results communication	2	[0; 10]
Missing	*38*				
Time between prescription and results communication	16	[3; 288]	Time between shipment and results communication	3	[1; 10]
Missing	*1*				
≤15 days	56	46.7%	≤15 days	121	0
>15 days	64	53.3%	>15 days	1	
≤1 month	99	83.2%	≤1 month	121	0
>1 month	20	16.8%	>1 month	1	
≤2 months	111	93.3%			
>2 months	8	6.7%			
Missing	*2*				
Time between inclusion and results communication	18	[4; 288]	Time between inclusion and results communication	7	[1; 72]
≤15 days	42	34.7%	≤15 days	98	81
>15 days	79	65.3%	>15 days	23	19
≤1 month	87	71.9%	≤1 month	112	92.6
>1 month	34	28.1%	>1 month	9	7.4
≤2 months	105	86.8%	≤2 months	120	99.2
>2 months	16	13.2%	>2 months	1	0.8

***KRAS* exon 2 (*n*=121)**

		Tumor-tissue analysis	
	Mutant	**WT**	
ctDNA analysis			
Mutant	45	26	71
WT	8	42	50
Total	*53*	*68*	*n=121*
Sensitivity (Se)			85%
Specificity (Sp)			62%
Global Accuracy (GC)			72%
Positive Predictive Value (PPV)			63%
Negative Predictive Value (NPV)			84%

***KRAS* exon 2/3 (*n*=34)**

		Tumor-tissue analysis	
	Mutant	**WT**	
ctDNA analysis			
Mutant	5	8	13
WT	1	20	21
total	*6*	*28*	*n=34*
Sensitivity (Se)			83%
Specificity (Sp)			71%
Global Accuracy (GC)			74%
Positive Predictive Value (PPV)			38%
Negative Predictive Value (NPV)			95%

***BRAF* V600E (*n*=97)**

		Tumor-tissue analysis	
	Mutant	**WT**	
ctDNA analysis			
Mutant	4	10	14
WT	3	80	83

***NRAS* exon 2/3 (*n*=34)**

		Tumor-tissue analysis	
	Mutant	**WT**	
ctDNA analysis			
Mutant	2	2	4
WT	1	29	30

Continued

Table 2. *Continued*

***BRAF* V600E (*n*=97)**				***NRAS* exon 2/3 (*n*=34)**			
		Tumor-tissue analysis				**Tumor-tissue analysis**	
	Mutant	**WT**			**Mutant**	**WT**	
Total	*7*	*90*	*n=97*	*total*	*3*	*31*	*n=34*
Sensitivity (Se)			57%	Sensitivity (Se)			67%
Specificity (Sp)			89%	Specificity (Sp)			94%
Global accuracy (GC)			87%	Global accuracy (GC)			92%
Positive predictive value (PPV)			29%	Positive predictive value (PPV)			50%
Negative predictive value (NPV)			96%	Negative predictive value (NPV)			97%

[a]Negative times indicate that tumor-tissue analysis was not made from original tumor specimen.
Prescription, prescription for RAS mutation testing; Inclusion, inclusion of a patient for the clinical study.

KRAS *exon 3/4 point mutations.* Of the 50 plasma samples tested for those mutations, only 34 matched tumor-tissue samples were also analyzed for those mutations. Six mutant tumor-tissue samples (18%) and 13 mutant plasma samples (38%) were determined. Five mutant samples and 20 WT samples were concordant. One mutant tumor-tissue sample was determined WT by plasma analysis. Inversely, eight mutant plasma samples were determined WT by tumor-tissue analysis. Sensitivity, specificity, PPV and NPV were 83%, 71%, 38% and 95%, respectively (Table 2B; detailed data in supplementary Table S8, available at *Annals of Oncology* online).

NRAS *point mutations (*n = *34).* On the 50 plasma samples tested for *NRAS* mutations, only 34 tumor-tissue samples were also analyzed for *NRAS* testing. Three mutant tumor-tissue samples (9%) and 4 mutant plasma samples (12%) were determined. Two mutant samples and 29 WT samples were concordant. One mutant tumor-tissue sample was determined WT by ctDNA analysis. Conversely, two mutant plasma samples were determined as WT by tumor-tissue analysis. Sensitivity, specificity, PPV and NPV were 67%, 94%, 50% and 97%, respectively (Table 2B; detailed data in supplementary Table S8, available at *Annals of Oncology* online).

Apparent false negative results ($n=13$, supplementary data and Table S13, available at *Annals of Oncology* online) might mostly be explained by (i) the large delay between collection of the surgical specimens and blood draw ($n=7$); (ii) by chemotreatment between biological source collection ($n=4$); (iii) by over-represented clones originating from under-represented clones at the time of tumor surgery or biopsy ($n=4$); and (iv) the limitation of the ctDNA analysis. Although the plasma assay contains rigorous quality controls theoretically impeding false positive data, we cannot rule out the presence of false positives. The concordance study as detailed by hotspot mutation is described in supplementary data, pp. 21–22, available at *Annals of Oncology* online (Supplemantary Table 3).

Quantitative multiparametric ctDNA analysis

As previously described [21], IntPlex allows quantitative analysis of ctDNA. In this study, the median mutant ctDNA concentration was 19 ng/ml of plasma (0.012–135 ng/ml) and the median mutation load or the mutant allele frequency was 1.1% ($n=99$; 0.003%–100%) (supplementary Table S9 and pp. 22–25, available at *Annals of Oncology* online).

Post hoc discordance analysis

We extensively examined most of the factors that could result in discordance between tumor-tissue and plasma analysis for determining the mutational status of the tested genes. In this *post hoc* analysis, technical factors such as either the use of biopsy versus surgical specimen or the cellularity of the analyzed tumor-tissue section as well as clinical factors such as the nature of the tumor piece analyzed (primary tumor or metastasis), cross conditions between tumor-tissue and plasma ctDNA analysis such as the time interval between tumor-tissue and blood collection, the presence of the primary tumor or the number of metastatic sites at the time of blood draw were assessed. Statistical analysis revealed that most of the discordant samples originate (i) from biopsy analysis (Fischer test; $P=0.31$, OR = 1.60); (ii) from archival tumor-tissue specimen ($P=0.4$; OR = 0.68); (iii) from a blood draw carried out in the absence of a primary tumor ($P=0.28$, OR = 0.62); and (iv) from rectal or rectosigmoid tumor-tissue analysis ($P=0.4$; OR = 1.50).

Examination of the factors potentially impacting sensitivity, specificity and concordance was made (described in supplementary data 'detailed discordance analysis' in pp. 27–35 and Tables 10 and 11, available at *Annals of Oncology* online). Discordant samples' analysis revealed that tumor site (colon versus rectum or rectosigmoid junction), type of tissue analyzed (biopsy versus surgical specimen), tissue derived from primary tumor or metastasis, time-lapse between tissue and blood collection, resection of the primary tumor or the metastasis used for tumor-tissue analysis at time of blood sampling as well as the number and the localization of metastatic sites at time of blood sampling seem to affect concordance. Note, no statistically significant differences were found between groups. Individual examination of discordant samples is described in supplementary Tables S11–S13, available at *Annals of Oncology* online.

Table 3. Follow-up clinical information and therapeutic responses from 16 to 28 months of survival period being scored WT by tissue and KRAS exon 2 mutant by plasma ctDNA analysis (n = 26) and patients scored WT by tissue and BRAFV600E by plasma ctDNA analysis (n = 10)

Summary of the therapeutic responses in patients scored *KRAS* exon 2 mutant by ctDNA analysis while scored WT for those mutations by tumor-tissue analysis (*n*=26)

Therapeutic response in non-anti-EGFR-treated patients				
Progressive disease	Stable disease	Partial response	Complete response	Total
3 (30%)	5 (50%)	2 (20%)	0	10
Therapeutic response in patients treated by chemotherapy in combination with an anti-EGFR				
Progressive disease	**Stable disease**	**Partial response**	**Complete response**	**Total**
5 (56%)	4 (44%)	0	0	9
Therapeutic response in neoadjuvant therapy and surgery-treated patients				
Progressive disease	**Stable disease**	**Partial response**	**Complete response**	**Total**
0	0	1 (100%)	0	1
Non-evaluable therapeutic response			**Too rapid progression for treatment**	
3			3	

Summary of the therapeutic responses in patients scored *BRA* FV600E mutant by ctDNA analysis while scored WT for those mutations by tumor-tissue analysis (*n*=10)

Therapeutic response in non-anti-EGFR-treated patients				
Progressive disease	Stable disease	Partial response	Complete response	Total
3 (30%)	5 (50%)	2 (20%)	0	10
Therapeutic response in patients treated by chemotherapy in combination with an anti-EGFR				
Progressive disease	**Stable disease**	**Partial response**	**Complete response**	**Total**
5 (56%)	4 (44%)	0	0	9
Therapeutic response in neoadjuvant therapy and surgery-treated patients				
Progressive disease	**Stable disease**	**Partial response**	**Complete Response**	**Total**
0	0	1 (100%)	0	1
Non-evaluable therapeutic response			**Too rapid progression for treatment**	
3			3	

SD, stable disease; PD, progressive disease; CR, complete response; PR, partial response.

Correlation with clinical outcome

Discordant samples scored KRAS *exon 2 mutant by ctDNA analysis while WT by tumor-tissue analysis* (n = *26).* We collected follow-up clinical information from 16 to 28 months of survival period. Only 9 of those 26 patients were treated with an anti-EGFR therapy (Table 3). Five of them showed progressive disease, four exhibited stable disease and there was no response in any patient. Mutant allele frequencies for those nine patients ranged from 0.005% to 8.8%. Five out of those nine patients exhibited mutant allele frequencies below 0.5%. Note, co-occurring *KRAS* and *BRAF* V600E mutations, as tested by the plasma assay, were found in two patients with progressive disease. Ten patients out of the 26 were treated by chemotherapy: 3, 5 and 2 patients showed progressive disease, stable disease and partial response, respectively (Table 3). Detailed therapeutic responses are described in supplementary Tables S14 and S15, and pp. 41–42, available at *Annals of Oncology* online.

Discordant samples scored BRAF V600E *mutant by ctDNA analysis while WT by tumor-tissue analysis* (n = *10).* Four of those patients received anti-EGFR therapy. One, one and two patients showed progressive disease, stable disease and partial responses, respectively. Five patients were treated by chemotherapy (1, 2 and 2 showing progressive disease, stable disease and partial response, respectively) (Table 3). Among those 10 patients, 4 patients died in <9 months and 1 in <25 months following mCRC diagnosis. Detailed therapeutic responses are described in supplementary Tables S14 and S15, and pp. 39–40, available at *Annals of Oncology* online.

Post hoc *mutation profiling.* Mutation profiling of *KRAS* exon 2, 3, 4; *BRAF* V600E and *NRAS* exon 2, 3 hotspots could be achieved in 119 plasma samples and matched with 86 matched tumor-tissue samples. Tumor-tissue analysis revealed that 39 samples harbored a single *RAS* mutation (45%), five samples were solely mutant for *BRAF* (6%) and 40 samples were WT for all mutations (47%). Two tumor-tissue samples harbored multiple *RAS* mutations (2%) (Figure 2).

When studying the tumor molecular profile by ctDNA analysis, 91 samples out of the 119 harbored at least one mutation (76% of the 119 mCRC cohort) while 28 samples harbored no mutation (24%). Thirty-five samples had single *RAS* mutations (29%) and three samples were solely mutant for *BRAF* V600E (2%). Note that no plasma sample was exclusively mutant for *NRAS.* We found that 53 samples were multiple mutants (45%) (Figure 2). The most prevalent combination of mutations was the concomitance of *KRAS* and *NRAS* point mutations since 24 samples harbored *KRAS* and *NRAS* point mutations (45% of the multiple mutant plasma cohort). Sixteen samples were multiple *KRAS* mutant (30%). Six samples were mutant for *KRAS* and *BRAF* (12%) and one sample was *BRAF* V600E and *NRAS* mutant (1%). Finally, we showed that six samples harbored co-occurring mutations in *KRAS, NRAS* and *BRAF* (11%) (Figure 2).

When using a sensitivity threshold of 0.5% mutant allele frequency, 36 samples were identified as single *RAS* mutant samples (30%), 9 samples as exclusively *BRAF* mutant (8%), 31 samples were determined multiple mutant (26%) and 43 samples were scored as WT (43%). Among those 31 multiple mutant samples,

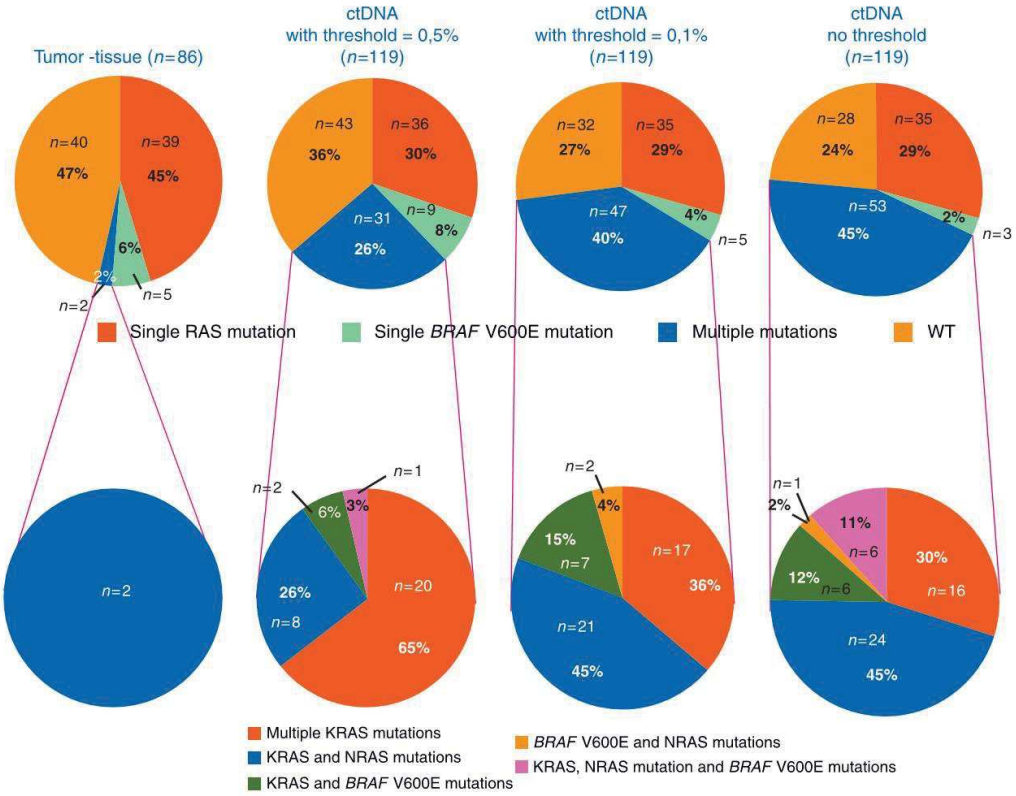

Figure 2. *Post hoc* mutation profiling of metastatic colorectal cancer patients for *RAS* and *BRAF* hotspot mutations. (A) *RAS* and *BRAF* distribution in mCRC patients as determined by tumor-tissue analysis ($n = 86$), ctDNA analysis with a threshold of mutant allele frequency of 0.5% ($n = 119$), ctDNA analysis with a threshold of mutant allele frequency of 0.1% ($n = 119$) and ctDNA analysis without any threshold ($n = 119$). (B) Multiple mutant as determined by tumor-tissue analysis ($n = 2$), ctDNA analysis with a threshold of mutant allele frequency of 0.5% ($n = 31$), ctDNA analysis with a threshold of mutant allele frequency of 0.1% ($n = 47$) and ctDNA analysis without any threshold ($n = 53$).

20 harbored multiple *KRAS* mutations (65%), 8 samples harbored mutations on *KRAS* and *NRAS* (26%); 2 samples were KRAS and *BRAF* mutant (6%) and 1 sample was scored mutant for *KRAS*, *NRAS* and *BRAF* (3%) (Figure 2).

When applying a sensitivity threshold of 0.1%, the proportions of single *RAS* mutant samples, single *BRAF* mutant samples, multiple mutant samples and WT samples were 29% ($n = 35$), 4% ($n = 5$), 40% ($n = 47$) and 27% ($n = 32$), respectively. Among the 47 multiple mutant samples, 17 were multiple *KRAS* mutant (36%), 21 were *KRAS* and *NRAS* mutant (45%), 7 were KRAS and *BRAF* mutant (15%) and 2 were mutant for KRAS, NRAS and *BRAF* ($n = 4\%$) (Figure 2).

Discussion

To confirm recent advances in the ctDNA field [8, 10, 13, 14, 23–25] and the first clinical validation of ctDNA in oncology [16], we carried out this prospective, multicenter, blinded study on 140 mCRC patients to better evaluating of ctDNA clinical utility. Our assay is not intended to compare the analytical performance of one method for plasma testing with that of one method for tissue testing, but rather to examine the value of plasma analysis versus tissue analysis under standard management care.

Data turnaround time

Data turnaround-time for ctDNA analysis was shorter and less variable than for tumor-tissue analysis. Tumor-tissue analysis delay could be detrimental for the patients who would not be selected for a potentially better treatment with anti-EGFR because of the late availability of the test results. Note, liquid biopsy testing was carried out in a centralized lab dedicated to this specific analysis, whereas tissue testing was carried out at participating institutions and it so might be affected by several, local organizational problems. Therefore, the different turnaround time might not reflect true differences in the time required to complete the two analyses.

Evaluation of concordance

Mutation profiles obtained from tumor-tissue analysis correspond to that obtained from PRIME [26] and FIRE [27] studies. Those observations were consistent with PRIME description with the exception that the PRIME study did not report any multiple

mutations as well as not reporting testing for *KRAS* exon 3, 4 and *NRAS* exon 2, 3 point mutations in *KRAS* exon 2 mutant samples [26] (supplementary Figure S4, available at *Annals of Oncology* online). However, in contrast to our previous report, it appears, to be moderately concordant with that obtained when using plasma analysis. Thus, in contrast with our previous work applying the same IntPlex® test and reporting very high accuracy with tumor-tissue analysis (96% for *KRAS* exon 2 mutations and 100% for *BRAF* V600E) [16], ctDNA mutation testing was made here without any sensitivity cutoff while a threshold of >0.5% (mutant to WT ctDNA ratio) was used in our previous report. Consequently, ctDNA mutation testing here is much more sensitive (>50-fold) with a sensitivity ranging from 0.001% to 0.005% depending upon the mutations. One must consider also the issue of the sensitivity level of the methods used for tumor-tissue analysis. Sanger, pyrosequencing, NGS or Q-PCR-based techniques show various sensitivity (10%, 2%–5%, 1% and 0.1%, respectively) resulting in analytical variability [28–30]. It is assumed that there is a reasonable concordance between results by the different methods, but one can debate about their absolute preciseness as several factors could interfere with their reliability. We carried out an extensive examination of the various factors which may lead to discordance between tumor-tissue and plasma analysis. The data revealed that either the use of a biopsy or absence of a primary-tumor in place at the time of blood draw or a long delay between tumor-tissue and blood collection mostly altered both specificity and sensitivity. As a consequence, a major limitation of tumor-tissue analysis is that sampling may not reflect tumor heterogeneity, especially in advanced cancers due to (i) intra-tumoral, (ii) inter-tumoral, and (iii) temporal heterogeneity [31–38]. In light of much recent evidence, it is now clear that there is a consistent level of discordance ranging from 3.6% to 17.5% [32] of the *RAS* mutational status between primary and paired metastasis.

ctDNA analytical method and the sensitivity issue

Our data on the clinical utility of ctDNA analysis rely on the use of the robustness and reliability of our analytical method. IntPlex® enables a single-copy detection of variant alleles down to an unprecedented sensitivity of ≥0.005% which is slightly higher to that of digital PCR and much higher than sequencing (0.1%–1%). Mutations with extremely low prevalence (0.005%) can be detected with very high sensitivity as experiments carried out under the Poisson law distribution unequivocally demonstrated that one mutated fragment can be reliably detected. Since there is no clear significance of low-prevalence *RAS* mutations in relation to the effectiveness of anti-EGFR therapy, one might also apply a sensitivity cutoff percentage filter [39–41].

When applying a sensitivity cutoff of 0.5% as used in our previous study, 15 out of 26 plasma samples identified as 'false positive' for *KRAS* exon 2 would be scored WT, greatly improving the assay specificity (84% instead of 62%). Alternatively, 11 mutant plasma samples concordant with tumor-tissue would be scored as negative (significantly decreasing the sensitivity, 64% instead of 85%). As a consequence, the need for a threshold of sensitivity as previously observed for tumor-tissue cannot be applied to plasma analysis. Sensitivity as termed for tumor-tissue analysis neither corresponds nor directly correlates with that determined from ctDNA. Sensitivity directly correlates with the number of malignant cells harboring the mutation from a macro- or micro-dissected region of a tissue section. This is not the case for ctDNA due to the significant circulating DNA release from the micro-environment cells occasionally resulting in high circulating DNA amounts as illustrated by the wide variation of the ctDNA mutation allelic frequency (0.003%–99%) [15, 21].

However, patients with a very low number of mutant cells within the tumor mass should theoretically benefit from first line anti-EGFR therapy and consequently, a sensitivity threshold when analyzing ctDNA might be used. While our assay in this study, without any threshold, scored 24% as WT mCRC patients, 27% and 36% would be scored WT when using a 0.1% and 0.5% detection cutoff, respectively. However, 9% and 2.5%, respectively, would appear as false negatives when compared with tumor-tissue, so illustrating the difficulty in applying a sensitivity threshold for ctDNA analysis. Stringent studies on the clinical response to anti-EGFR monotherapy regimen and use of a quantitative ctDNA detection method (such as IntPlex) might help in determining a reproducible threshold for treatment guidance [41].

Impact of our study on the demonstration of clinical utility of plasma DNA analysis

We explored the clinical outcome of patients being established WT by tumor-tissue analysis while mutant by plasma analysis and, consequently treated with anti-EGFR to address this issue. However, in addition to the low number of this set of patients, this examination is biased by the concomitant use of chemotherapy with anti-EGFR therapy. Altogether, the clinical data on those discordant patients do not appear contradictory to the mutational status as determined by plasma analysis. The moderate concordance found in this study (72%, 74% and 87% of accuracy for *KRAS* exon 2, *KRAS* exon 3, 4 and *BRAF* V600E, respectively) is due to higher mutation frequency found by plasma analysis. In comparison with tumor-tissue analysis, a blood test appears more cost-effective for genotyping-guided clinical care. In addition, rapid data turn-around time helps the oncologist to rapidly enroll mCRC patients that can benefit from anti-EGFR therapy. Long delays sometimes occurring only with tumor-tissue analysis preclude a significant group of patients to be treated by such an appropriate therapy. The limited number of anti-EGFR-treated patients precluded enough statistical power to initiate assessment of clinical utility in terms of concordance of ctDNA status from plasma with patient follow-up. However, there is here a clear demonstration that ctDNA provides strong evidence for a more rapid data turn-around time than tumor-tissue analysis, irrespective of the methods used. It is vital that the turnaround time is as short as possible to ensure that a treatment decision can be made quickly. Ideally this should be no more than seven working days, to ensure that all possible treatment options are available to a patient as soon as possible. ESMO consensus guidelines for the management of patients with mCRC [1] indicate that a fast initiation of targeted therapy as a first-line treatment is crucial for cancer patients as it increases overall survival rates. Thus, a timely detection of biomarkers is extremely important, reducing both patient anxiety while waiting for results and ensuring the best possible treatment. ESMO recommendation 4 stated that 'RAS testing should be carried out on all patients at the time of diagnosis of mCRC' and that RAS testing Turnaround time for RAS testing (expanded RAS analysis) should be ≤7 working days from the time of receipt of the specimen by

the testing laboratory to the time of issuing of the final report, for >90% of specimens [1]. Thus, this study constitutes an initial report demonstrating clinical utility with regards to the data turnaround time of using ctDNA analysis for testing *RAS* and *BRAF* mutational status in mCRC patients.

Conclusion

To date, there is no other report showing such an increase of mutation detection in comparison with tumor-tissue analysis and such a high proportion of co-occurring mutations. Therefore, mutation profiling based on ctDNA analysis may identify concomitant resistance mechanisms residing in separate metastases and within a tumor mass potentially enabling longitudinal assessment of the effect of therapies designed to overcome resistance. The liquid biopsy, by analyzing ctDNA especially, has important advantages over tissue biopsy in terms of more accurately detecting key mutations due to various issues mainly clonal intra- and inter-tumor heterogeneity [42], and dynamic genetic changes in the course of tumor growth and treatment over time [42–44].

In contrast, ctDNA analysis represents a wider genetic picture of the entire tumor mass and evaluates primary tumor and metastases with one sample so providing snapshot information of tumor dynamics in real-time. In the light of these issues, obtaining a higher mutation level as determined here with an ultrasensitive plasma test is common-sense. Ultrasensitive ctDNA analysis might otherwise result in further population selection of super-responders to anti-EGFR therapy. Lastly, we report here the first complete mutation profile with all actionable *RAS* and *BRAF* mutations in a large cohort of patients at time of mCRC diagnosis to guide anti-EGFR treatment decisions. By presenting the variation of this mutation profile with using various detection thresholds, our data illustrate the power of ctDNA analysis pointing out the importance of the test sensitivity in particular in adjusting the clinically relevant use of targeted agents. ctDNA provides a representation of the malignant disease as a whole and could be a reliable source of diagnostic DNA to replace the tumor-tissue. Plasma testing may be initially used when either a biopsy is insufficient for genotyping or cannot be obtained safely or when tumor-tissue is not available. Thus, this study represents one step closer to clinical routine implementation of ctDNA analysis to guide anti-EGFR treatment decision in mCRC.

Acknowledgements

The authors thank Jacques Collinge for statistics help. They are also grateful to Nathalie Nicolas, David Dupont, Brigitte Gillet, and Patrick Chalbos for collecting clinical data. They thank Frederic Bibeau, Thibault Mazard, Philippe Blache, Corinne Prevostel, and Celine Gongora for helpful discussion, Vanessa Guillaumon for help in supporting this work, and Peter Gahan for English editing.

Funding

ART is supported by INSERM (France). This study was partly supported by AMGEN (France) and by the SIRIC Montpellier Grant 'INCa-DGOS-Inserm 6045', France.

Disclosure

OB has received payment for consultancy work for Novartis, Bayer, Amgen, Roche, Merck Serono, Eli-Lilly and his institution has received grants from Roche and Pierre Fabre. MM has no conflict of interests, and her institution has received grants from Sanofi and Novartis. JLR has received payment for consultancy work for Bayer SP, BTG, Taiho, BMS, for payed lectures from Bayer SP, Merck Serono and received grants from Celgene. PA has received payment for consultancy work from Bayer, Amgen, Roche, Merck Serono, Lilly and Sanofi and support for travel to meetings paid by Roche and Merck Serono. CB has received payments for lectures from Roche and Sanofi, as well as research grants from Roche. DP received payment for consultancy work From SANOFI, Lilly and ROCHE and his institution received grant from AMGEN. ART received payment for consultancy work from DiaDx. All remaining authors have declared no conflicts of interest.

References

1. Van Cutsem E, Cervantes A, Adam R et al. ESMO consensus guidelines for the management of patients with metastatic colorectal cancer. Ann Oncol 2016; 27(8): 1386–1422.
2. Allegra CJ, Rumble RB, Schilsky RL. Extended RAS gene mutation testing in metastatic colorectal carcinoma to predict response to anti-epidermal growth factor receptor monoclonal antibody therapy: American Society of Clinical Oncology Provisional Clinical Opinion Update 2015 Summary. J Oncol Pract Am Soc Clin Oncol 2016; 12(2): 180–181.
3. De Roock W, Claes B, Bernasconi D et al. Effects of KRAS, BRAF, NRAS, and PIK3CA mutations on the efficacy of cetuximab plus chemotherapy in chemotherapy-refractory metastatic colorectal cancer: a retrospective consortium analysis. Lancet Oncol 2010; 11(8): 753–762.
4. Amado RG, Wolf M, Peeters M et al. Wild-type KRAS is required for panitumumab efficacy in patients with metastatic colorectal cancer. J Clin Oncol Off J Am Soc Clin Oncol 2008; 26(10): 1626–1634.
5. Van Cutsem E, Lenz H-J, Köhne C-H et al. Fluorouracil, leucovorin, and irinotecan plus cetuximab treatment and RAS mutations in colorectal cancer. J Clin Oncol 2015; 33(7): 692–700.
6. Lièvre A, Bachet J-B, Le Corre D et al. KRAS mutation status is predictive of response to cetuximab therapy in colorectal cancer. Cancer Res 2006; 66(8): 3992–3995.
7. Waring P, Tie J, Maru D, Karapetis CS. RAS mutations as predictive biomarkers in clinical management of metastatic colorectal cancer. Clin Colorectal Cancer 2016; 15(2): 95–103.
8. Thierry AR, El Messaoudi S, Gahan PB et al. Origins, structures, and functions of circulating DNA in oncology. Cancer Metastasis Rev 2016; 35: 347–376.
9. Schwarzenbach H, Hoon DSB, Pantel K. Cell-free nucleic acids as biomarkers in cancer patients. Nat Rev Cancer 2011; 11(6): 426–437.
10. Diaz LA, Bardelli A. Liquid biopsies: genotyping circulating tumor DNA. J Clin Oncol 2014; 32(6): 579–586.
11. El Messaoudi S, Mouliere F, Du Manoir S et al. Circulating DNA as a strong multimarker prognostic tool for metastatic colorectal cancer patient management care. Clin Cancer Res 2016; 22(12): 3067–3077.
12. Murtaza M, Dawson S-J, Tsui DWY et al. Non-invasive analysis of acquired resistance to cancer therapy by sequencing of plasma DNA. Nature 2013; 497(7447): 108–112.
13. Diehl F, Schmidt K, Choti MA et al. Circulating mutant DNA to assess tumor dynamics. Nat Med 2008; 14(9): 985–990.
14. Perkins G, Yap TA, Pope L et al. Multi-purpose utility of circulating plasma DNA testing in patients with advanced cancers. PLoS ONE 2012; 7(11): e47020.
15. Mouliere F, El Messaoudi S, Gongora C et al. Circulating cell-free DNA from colorectal cancer patients may reveal high KRAS or BRAF mutation load. Transl Oncol 2013; 6(3): 319–328.

16. Thierry AR, Mouliere F, El Messaoudi S et al. Clinical validation of the detection of KRAS and BRAF mutations from circulating tumor DNA. Nat Med 2014; 20(4): 430–435.
17. Fu Y, Jovelet C, Filleron T et al. Improving the performance of somatic mutation identification by recovering circulating tumor DNA mutations. Cancer Res 2016; 76: 5954–5961.
18. Thierry AR, Mouliere F, Gongora C et al. Origin and quantification of circulating DNA in mice with human colorectal cancer xenografts. Nucleic Acids Res 2010; 38(18): 6159–6175.
19. Mouliere F, Robert B, Arnau Peyrotte E et al. High fragmentation characterizes tumour-derived circulating DNA. PLoS One 2011; 6(9): e23418.
20. El Messaoudi S, Rolet F, Mouliere F, Thierry AR. Circulating cell free DNA: preanalytical considerations. Clin Chim Acta 2013; 424: 222–230.
21. Mouliere F, El Messaoudi S, Pang D et al. Multi-marker analysis of circulating cell-free DNA toward personalized medicine for colorectal cancer. Mol Oncol 2014; 8(5): 927–941.
22. Machin D, Campbell MJ, Tan S-B, Tan S-H (eds). Sample Size Tables for Clinical Studies. Hoboken, NJ: John Wiley & Sons, 2011.
23. Normanno N, Denis MG, Thress KS et al. Guide to detecting epidermal growth factor receptor (EGFR) mutations in ctDNA of patients with advanced non-small-cell lung cancer. Oncotarget 2017; 8: 12501–12516.
24. Bettegowda C, Sausen M, Leary RJ et al. Detection of circulating tumor DNA in early- and late-stage human malignancies. Sci Transl Med 2014; 6(224): 224ra24.
25. Tabernero J, Lenz H-J, Siena S et al. Analysis of circulating DNA and protein biomarkers to predict the clinical activity of regorafenib and assess prognosis in patients with metastatic colorectal cancer: a retrospective, exploratory analysis of the CORRECT trial. Lancet Oncol 2015; 16(8): 937–948.
26. Douillard JY, Siena S, Cassidy J et al. Final results from PRIME: randomized phase III study of panitumumab with FOLFOX4 for first-line treatment of metastatic colorectal cancer. Ann Oncol 2014; 25(7): 1346–1355.
27. Heinemann V, von Weikersthal LF, Decker T et al. FOLFIRI plus cetuximab versus FOLFIRI plus bevacizumab as first-line treatment for patients with metastatic colorectal cancer (FIRE-3): a randomised, open-label, phase 3 trial. Lancet Oncol 2014; 15(10): 1065–1075.
28. Westwood M, van Asselt T, Ramaekers B et al. KRAS mutation testing of tumours in adults with metastatic colorectal cancer: a systematic review and cost-effectiveness analysis. Health Technol Assess 2014; 18(62): 1–132.
29. Dudley J, Tseng L-H, Rooper L et al. Challenges posed to pathologists in the detection of KRAS mutations in colorectal cancers. Arch Pathol Lab Med 2015; 139(2): 211–218.
30. Lamy A, Blanchard F, Le Pessot F et al. Metastatic colorectal cancer KRAS genotyping in routine practice: results and pitfalls. Mod Pathol 2011; 24(8): 1090–1100.
31. Kim M-J, Lee HS, Kim JH et al. Different metastatic pattern according to the KRAS mutational status and site-specific discordance of KRAS status in patients with colorectal cancer. BMC Cancer 2012; 12: 347.
32. Lee KH, Kim JS, Lee CS, Kim JY. KRAS discordance between primary and recurrent tumors after radical resection of colorectal cancers. J Surg Oncol 2015; 111(8): 1059–1064.
33. Gerlinger M, Rowan AJ, Horswell S et al. Intratumor Heterogeneity and Branched Evolution Revealed by Multiregion Sequencing. N. Engl. J. Med 2012; 366(10): 883–892.
34. Vermaat JS, Nijman IJ, Koudijs MJ et al. Primary colorectal cancers and their subsequent hepatic metastases are genetically different: implications for selection of patients for targeted treatment. Clin Cancer Res 2012; 18(3): 688–699.
35. Knijn N, Mekenkamp LJM, Klomp M et al. KRAS mutation analysis: a comparison between primary tumours and matched liver metastases in 305 colorectal cancer patients. Br J Cancer 2011; 104(6): 1020–1026.
36. Cejas P, López-Gómez M, Aguayo C et al. Analysis of the concordance in the EGFR pathway status between primary tumors and related metastases of colorectal cancer patients: implications for cancer therapy. Curr Cancer Drug Targets 2012; 12(2): 124–131.
37. de Macedo MP, de Melo FM, Ribeiro J. d S et al. RAS mutations vary between lesions in synchronous primary colorectal cancer: testing only one lesion is not sufficient to guide anti-EGFR treatment decisions. Oncoscience 2015; 2(2): 125–130.
38. Kuo Y-B, Chen J-S, Fan C-W et al. Comparison of KRAS mutation analysis of primary tumors and matched circulating cell-free DNA in plasmas of patients with colorectal cancer. Clin Chim Acta 2014; 433: 284–289.
39. Laurent-Puig P, Pekin D, Normand C et al. Clinical relevance of KRAS-mutated subclones detected with picodroplet digital PCR in advanced colorectal cancer treated with anti-EGFR therapy. Clin Cancer Res 2015; 21(5): 1087–1097.
40. Tougeron D, Lecomte T, Pagès JC et al. Effect of low-frequency KRAS mutations on the response to anti-EGFR therapy in metastatic colorectal cancer. Ann Oncol 2013; 24(5): 1267–1273.
41. Thierry AR, Pastor B, Zhi-Qin CJ et al. Circulating DNA demonstrates convergent evolution and common resistance mechanisms during treatment of colorectal cancer. Clin Can Res 2017; doi: 10.1158/1078-0432.CCR-17-0232.
42. Sottoriva A, Kang H, Ma Z et al. A Big Bang model of human colorectal tumor growth. Nat Genet 2015; 47(3): 209–216.
43. Siravegna G, Mussolin B, Buscarino M et al. Clonal evolution and resistance to EGFR blockade in the blood of colorectal cancer patients. Nat Med 2015; 21(7): 827.
44. Diaz LA, Jr, Williams RT, Wu J et al. The molecular evolution of acquired resistance to targeted EGFR blockade in colorectal cancers. Nature 2012; 486(7404): 537–540.

Article II *:* L'ADN circulant démontre une évolution convergente et des mécanismes de résistance communs pendant le traitement du cancer colorectal (Etude *KPLEX R*)

Titre court: ADN circulant et évolution clonale sous thérapie ciblée

Alain R. Thierry, Brice Pastor, Zhi-Qin Jiang, Anastasia D. Katsiampoura, Christine Parseghian, Jonathan M. Loree, Michael J. Overman, Cynthia Sanchez, Safia El Messaoudi, Marc Ychou, and Scott Kopetz

Rationnel: Les patients atteints de CRCm ne présentant pas de mutations sur les gènes *KRAS* et *NRAS* (*RAS*) peuvent être traités par thérapie ciblées anti-EGFR. Cependant, l'émergence de mutations *RAS/BRAF* au cours du traitement chez des patients initialement sauvages entraine une résistance à ces thérapies. Dans ce contexte, l'analyse longitudinale de l'ADN circulant offre une occasion unique d'étudier l'évolution génomique des tumeurs pendant le traitement, et d'identifier l'émergence précoce de la résistance aux traitements anti-EGFR et de guider les décisions thérapeutiques ciblées.

Contribution: Dans ce projet j'ai réalisé les analyses de quantification des ADNcir totaux ainsi que la détection et la quantification des mutations *RAS/BRAF* chez les patients atteints de CCRm. J'ai participé à l'écriture du manuscrit.

Introduction

Comme discuté précédemment, l'utilisation des anticorps monoclonaux anti-EGFR, dans le traitement du CCRm est limitée aux patients de type *RAS* sauvage (WT). Il a été démontré que les mutations activatrices de *KRAS* et de *NRAS* (*RAS*) dans les exons 2,3 et 4 de ces gènes entraînent un manque de bénéfice clinique de la thérapie ciblant l'EGFR[29,214]. Bien que les thérapies ciblées soient une avancée majeure dans le traitement des patients atteints de CCRm, l'acquisition d'une résistance à ces traitements est observée dans un grand nombre de cas. Cette résistance peut se manifester par des mutations *de novo* ou par l'expansion d'une population sous-clonale de cellules présentant une résistance préexistante[215,216]. La détection de ces sous-clones résistants et le suivi des populations clonales au fil du temps sont difficiles et nécessitent le développement de tests sensibles et qui peuvent être réalisés tout au long du traitement. Malgré le fait que les progrès du séquençage de nouvelle génération (NGS) couplés à des biopsies pré et post-traitement puissent révéler une évolution clonale, ceci est difficile à mettre en place en pratique clinique et au cours d'une prise en charge thérapeutique. Les analyses sur biopsies ne permettent pas d'évaluer l'entièreté de l'hétérogénéité clonale des tumeurs car les biopsies sont par nature représentatives que d'un seul endroit de la tumeur[48,51,60].

De plus, une résistance secondaire se développe chez tous les patients et peut être associée au développement de mutations secondaires *KRAS*, *NRAS*, *EGFR* ou *BRAF*[204,209,217]. D'autres rapports ont confirmé l'utilisation des ADNcir pour la détection de mutation ponctuelles et soulignent son potentiel comme moyen puissant de suivre longitudinalement les patients atteints de cancer[28,218]. La détection précoce d'une résistance acquise peut permettre d'initier de nouvelles thérapies qui freineront l'expansion des sous-clones résistants qui entraîneraient la progression de la maladie. A l'inverse, il peut y avoir des populations clonales qui étaient résistantes aux thérapies antérieures et qui connaissent par la suite un événement d'extinction, rendant ainsi le patient sensible à la réutilisation d'une ligne de traitement et élargissant les options de traitement. Cette possibilité thérapeutique est une avancée dans la prise en charge des patients, on appelle cela le « Rechallenge » d'une molécule (Cremolini *et al*, JAMA oncology 2018).

L'ADN circulant permet de mieux saisir la complexité de l'hétérogénéité tumorale, tout en minimisant les risques pour le patient et les coûts associés[77,209]. En effet, des études ont montré que l'ADNcir peut être utilisé pour génotyper efficacement les tumeurs[182,219] et surveiller l'émergence de clones résistants au cours d'un traitement[66,210].

Dans ce contexte et afin d'évaluer les concentrations totales en ADNcir ainsi que la détection et la quantification des mutations *RAS/BRAF* nous avons utilisé la méthode Intplex. De par sa sensibilité la méthode IntPlex permets, la détermination simultanée de cinq paramètres : la concentration totale d'ADNcir, la présence d'une mutation ponctuelle, la concentration d'ADN mutant, les fréquences allèliques des ADNcir mutants et l'indice de fragmentation de l'ADNcir[135,184]. Nous avons évalué ces cinq paramètres dans le plasma de 42 patients atteints de CCRm traités dans le cadre d'un essai de phase Ib/II par le protocole de chimiothérapie FOLFOX couplé au dasatinib, avec ou sans cetuximab. Nous avons comparé nos résultats à ceux obtenus par l'analyse du tissu archivé, qui est encore actuellement considérée comme la norme pour la recherche des mutations. L'utilisation de collections sériées de plasma de certains patients a permis d'évaluer la dynamique clonale de mutations *RAS/BRAF* pendant le traitement. Les résultats obtenus sont comparés avec les critères d'imagerie RECIST et avec le niveau sanguin de l'antigène carcinoembryonnaire (ACE).

Published OnlineFirst April 11, 2017; DOI: 10.1158/1078-0432.CCR-17-0232

Cancer Therapy: Clinical

Clinical Cancer Research

Circulating DNA Demonstrates Convergent Evolution and Common Resistance Mechanisms during Treatment of Colorectal Cancer

Alain R. Thierry[1,2,3,4], Brice Pastor[1,2,3,4], Zhi-Qin Jiang[5], Anastasia D. Katsiampoura[5], Christine Parseghian[5], Jonathan M. Loree[5], Michael J. Overman[5], Cynthia Sanchez[1,2,3,4], Safia El Messaoudi[1,2,3,6], Marc Ychou[1,2,3,7], and Scott Kopetz[5]

Abstract

Purpose: Liquid biopsies allow the tracking of clonal dynamics and detection of mutations during treatment.

Experimental Design: We evaluated under blinded conditions the ability of cell-free DNA (cfDNA) to detect *RAS/BRAF* mutations in the plasma of 42 metastatic colorectal cancer patients treated on a phase Ib/II trial of FOLFOX and dasatinib, with or without cetuximab.

Results: Prior to treatment, sequencing of archival tissue detected mutations in 25 of 42 patients (60%), while the cfDNA assay detected mutations in 37 of 42 patients (88%). Our cfDNA assay detected mutations with allele frequencies as low as 0.01%. After exposure to treatment, 41 of 42 patients (98%) had a cfDNA-detected *RAS/BRAF* mutation. Of 21 patients followed with serial measurements who were *RAS/BRAF* mutant at baseline, 11 (52%) showed additional point mutation following treatment and 3 (14%) no longer had detectable levels of another mutant allele. Of *RAS/BRAF* wild-type tumors at baseline, 4 of 5 (80%) showed additional point mutations. cfDNA quantitative measurements from this study closely mirrored changes in CEA and CT scan results, highlighting the importance of obtaining quantitative data beyond the mere presence of a mutation.

Conclusions: Our findings demonstrate the development of new *RAS/BRAF* mutations in patients regardless of whether they had preexisting mutations in the pathway, demonstrating a convergent evolutionary pattern. *Clin Cancer Res; 23(16); 4578–91.* ©2017 AACR.

Introduction

Targeted therapies are rapidly being integrated into the treatment of patients with cancer. However, the acquisition of resistance to such treatments is observed in virtually all cases. This resistance may arise as *de novo* mutations or as the expansion of a subclonal population of cells with preexisting resistance (1, 2). Detecting these resistant subclones and monitoring clonal populations over time is difficult and requires the development of more sensitive assays that are also convenient and safe for patients to have serially performed. Although the advancement of next-generation sequencing (NGS) coupled with pre and posttreatment biopsies may provide snapshots of clonal evolution, they are often difficult to implement and do not provide a longitudinal assessment of heterogeneity (2–8).

Not only do these biopsies not provide the ability to frequently assess heterogeneity and follow changes, they are also hindered by the fact that biopsies are inherently of a single location, often the safest lesion to biopsy, and this may not represent the entire clonal population of a tumor (8–10).

The ability to comprehensively and longitudinally characterize the clonal architecture of a tumor will have profound treatment implications. Early detection of acquired resistance may allow initiation of new therapies that suppress the expansion of clones that would otherwise result in disease progression. In addition, there may be clonal populations that were resistant to previous therapies that subsequently experience an extinction event, thus rendering the patient sensitive to reuse of a previous line of therapy and expanding potential treatment options. "Liquid biopsies" or cell-free DNA (cfDNA) may better capture the complexity of tumor heterogeneity, while at the same time minimizing patient risks and associated costs (11, 12). Recent studies have shown that liquid biopsies can be used to effectively genotype tumors (13, 14) and monitor the emergence of resistant clones during the course of treatment (15–17).

Use of the EGFR-directed mAbs cetuximab and panitumumab in the treatment of metastatic colorectal cancer (mCRC) is limited to *RAS* wild-type (WT) patients (18–20). Activating *KRAS* and *NRAS* (*RAS*) mutations in exons 2, 3, and 4 of each gene have been shown to result in a lack of benefit from EGFR-targeted therapy (21, 22). Other genetic alterations associated with resistance to EGFR0directed therapy include *KRAS* amplification (4),

[1]IRCM, Institut de Recherche en Cancérologie de Montpellier, Montpellier, France. [2]INSERM, U1194, Montpellier, France. [3]Université de Montpellier, Montpellier, France. [4]Institut Régional du Cancer de Montpellier, Montpellier, France. [5]Department of Gastrointestinal Medical Oncology, The University of Texas MD Anderson Cancer Center, Houston, Texas. [6]DiaDx SAS, Montpellier, France. [7]Service de Chirurgie Digestive, Institut Régional du Cancer de Montpellier, Montpellier, France.

Note: Supplementary data for this article are available at Clinical Cancer Research Online (http://clincancerres.aacrjournals.org/).

Corresponding Author: Alain R. Thierry, IRCM U1194 Inserm, 208 rue des Apothicaires, Montpellier 34298, France. Phone: 336-63821994; E-mail: alain.thierry@inserm.fr

doi: 10.1158/1078-0432.CCR-17-0232

Published OnlineFirst April 11, 2017; DOI: 10.1158/1078-0432.CCR-17-0232

Translational Relevance

Cell-free circulating DNA (cfDNA) provides a liquid biopsy alternative to tissue biopsies for monitoring cancer genetic changes over time. In this study, we used a recently developed multimarker assay enabling a qualitative and a quantitative cfDNA analysis for tracking acquired resistance by studying the real-time clonal evolution of the tumor. cfDNA of refractory mCRC patients to anti-EGFR therapy may harbor mutations at very low frequency down to 0.01% before initiation or during treatment, revealing the need of a highly sensitive technique. cfDNA demonstrates convergent evolution and common resistance mechanisms during treatment of colorectal cancer. Serial analysis of cfDNA provides a unique opportunity to study the evolving genomic landscape of a cancer during therapy, and to identify the early emergence of treatment resistance and guide targeted therapeutic decisions.

activating *BRAF* mutations (4, 23), activating *PIK3CA* mutations, and *PTEN* loss (4, 24). Despite the knowledge of these mechanisms of resistance, there are still *RAS* WT patients without these other perturbations who display primary resistance to cetuximab/panitumumab (1, 19). In addition, secondary resistance develops in all patients and is associated with the development of secondary *KRAS, NRAS, EGFR* or *BRAF* mutations (11, 25, 26). This demonstrated the ability to detect additional mutation of these secondary *KRAS* and *NRAS* mutations in the blood of patients receiving anti-EGFR therapies using a liquid biopsy approach and showed that resistant clones could be detected months before radiographic progression. Further reports have confirmed this technique and highlight the potential of cfDNA as a powerful way to longitudinally follow cancer patients (27, 28). Diaz and colleagues (15) described a mathematical model to suggest variants that lead to resistance are present prior to initiation of therapy. Thus, we can speculate that the mutations corresponding to those emerging clones may have initially been below the limit of detection of the platform before treatment. As a result, we will below refer to the "detection of additional mutation" rather than "developed" or "emerging mutation."

In this study, we present IntPlex, a novel multimarker assay for the analysis of cfDNA and demonstrate its ability to sensitively detect the changing clonal dynamics of colorectal cancer. IntPlex is based on a refined allele-specific competitive blocker qPCR method specifically designed to improve quantification based on the structure and size of cfDNA (29–31). It enables simultaneous determination of five parameters: the total concentration of cfDNA, the presence of a point mutation, the mutant DNA concentration, the mutant allele fractions of cfDNA, and the cfDNA fragmentation index (32, 33). Using IntPlex, we evaluated cfDNA in the plasma of 42 mCRC patients treated on a phase Ib/II trial of FOLFOX and dasatinib with or without cetuximab and compared our findings with the results obtained from the archival tissue–based assay, currently considered the standard of care. The use of serial plasma collections from some of the patients on this trial allowed evaluation of the clonal dynamics of *RAS* and *BRAF* during therapy. Here, we present the evolutionary changes that occurred and compare our findings with standard clinical observation with radiographic imaging and carcinoembryonic antigen (CEA) of a select subset of patients.

Materials and Methods

Ethics statement, eligibility criteria, drug administration and study design, and treatment are described in Parseghian and colleagues (34).

Study design and treatment

We conducted a single-institution, open-label, investigator-initiated phase IB/II study in refractory mCRC patients treated with modified FOLFOX6, cetuximab, and dasatinib, with dasatinib dose escalation by cohort. This study is presented in a companion publication (34). The regimen consisted of cetuximab (400 mg/m^2 week 1 followed by weekly doses of 250 mg/m^2), oxaliplatin (85 mg/m^2 once every 2 weeks), bolus 5-fluorouracil (5-FU; 400 mg/m^2 once every 2 weeks), and leucovorin (400 mg/m^2 once every 2 weeks), followed by a 46-hour infusion of 5-FU (2,400 mg/m^2 once every 2 weeks). Dasatinib was dosed orally daily in cohorts of 100, 150, and 200 mg/day, administered without interruption. Dasatinib dose escalation was performed using a standard "3 + 3" design. Appropriate radiographic images were collected for all patients enrolled at baseline and at all postbaseline evaluations by the same radiological method, to assess response. All radiological tests that demonstrated tumor at baseline were repeated after every four cycles and at discontinuation of study treatment. For the phase II study, patients deemed to be *KRAS* codon 12/13 WT based on archival tissue received the MTD from the phase I study, while *KRAS* mutant patients received the same, without cetuximab.

Sample preparation

We retrospectively assessed archival tissue and plasma samples at baseline for mutational status, with repeat plasma samples occurring every four cycles prior to each restaging CT scan (2–6 hours after taking the daily dose of dasatinib). Investigators were blinded to the results of the clinical grade assay during the experiment. Plasma samples for cfDNA analysis were stored at −80°C and transferred between institutions on dry ice. The plasma isolation protocol we adapted from Chiu and colleagues (35) as well as handling and storage conditions were described previously (36). Briefly, plasma was first centrifuged at 1,600 × *g* at 4°C for 10 minutes, and supernatant was centrifuged at 16,000 × *g* at 4°C for 10 minutes. Supernatant was immediately used for DNA extraction and stored at −20°C. Total cfDNA was extracted from 1 mL of isolated plasma using the QIAamp DNA Mini Blood Kit (Qiagen) in accordance with the preanalytic guidelines we previously described (36) in an elution volume of 130 μL. DNA extracts were kept at −20°C until use or used immediately. In total, we analyzed 81 serial plasma samples from 46 mCRC patients (Supplementary Fig. S1).

Tumor tissue collection/storage/analysis

DNA was extracted from paraffin-embedded formalin-fixed tumor tissue. Genomic analysis samples were evaluated by using an NGS platform using the semiconductor-based ion PGM NGS platform with AmpliSeq Cancer HotSpot Panel v2 in 46 and 50 gene panels for the detection of frequently reported point mutations in human malignancies in Clinical Laboratory Improvement Amendments (CLIA)-certified molecular diagnostics laboratory.

IntPlex analysis of cfDNA

IntPlex analysis was performed as described previously (31, 32). Briefly, the qPCR assays were performed according the MIQE

Published OnlineFirst April 11, 2017; DOI: 10.1158/1078-0432.CCR-17-0232

guidelines. qPCR amplifications were carried out at least in duplicate in a 25 μL volume on a CFX96 instrument using the CFX manager software (Bio-Rad). Each PCR reaction was composed of 12.5 μL of IQ Supermix Sybr Green (Bio-Rad), 2.5 μL of free water (Qiagen) or specific oligoblocker, 2.5 μL of forward and reverse primers (0.3 pmol/mL), and 5 μL of template. Thermal cycling comprised three repeated steps: a hot-start activation step at 95°C for 3 minutes, followed by 40 cycles of denaturation–amplification at 95°C for 10 seconds, then 60°C for 30 seconds. Melting curves were investigated by increasing the temperature from 60°C to 90°C with a plate reading every 0.2°C. Standard curves were performed for each run with a genomic extract of the DiFi cell line at 1.8 pg/μL of DNA. Each PCR run was carried out with no template control and positive control for each primer set. Positive controls were extracted from cell lines bearing *KRAS/BRAF* or *NRAS* point mutations or we purchased synthetic DNA (Horizon dx). In each single run, negative and positive controls for each tested mutation were included and one standard curve was prepared. Validation of qPCR amplification was made by melt curve differentiation. ctDNA mutation testing was made here without any sensitivity cutoff, while a threshold of >0.5% (mutant to WT ctDNA ratio) was used in our previous report (31). Consequently, ctDNA mutation testing here is much more sensitive (up to 500-fold) with a sensitivity ranging from 0.001% to 0.005% depending upon the mutations. When point mutations were found in only one of the two replicates, the point mutation was confirmed in triplicate.

Design of patient's follow-up and detection of point mutations

Point mutations tested in this retrospective study with the IntPlex qPCR method are presented in the Supplementary Table S1. Total circulating cfDNA quantification was carried out on all serial plasma samples. However, for patients with *KRAS* c12/13, *NRAS*, or *BRAF V600E* point mutations at baseline, only these mutations were assessed for on-treatment samples. Final plasma samples at disease progression for all patients were assessed for all mutations in *KRAS* (exon 2, 3, 4), *NRAS* (exon 2, 3, 4), and *BRAF V600E*. In the case of a patient having no *KRAS/NRAS/BRAF* point mutation at baseline, we also assessed *KRAS* codons 61, 146 and *NRAS* point mutations in all on-treatment samples. *EGFR S492R* mutation testing was performed only on patients with prior cetuximab therapy (37, 38).

Results

Prior to initiation of therapy, 25 of 42 patients (59.5%) had detectable *KRAS 12/13*, *BRAFV600E*, or *NRAS* mutations in archival tumor tissue, and 37 of 42 patients (88%) were found to have mutations in cfDNA (Fig. 1A). Among the 25 patients with mutations in archival tissue, 24 (96%) also had mutations in cfDNA (Fig. 1B). Considering archival tumor sequencing as the "gold standard," the concordance between our cfDNA and tissue-based methodologies for *KRAS* exon2 testing was 71%, while the specificity and sensitivity of the cfDNA assay were 48% and 95%, respectively (Supplementary Table S2A). For *BRAFV600E* testing, the concordance between the two assays was 97%, while the specificity and sensitivity of the cfDNA was 97% and 100% respectively (Supplementary Table S2A), compared with the archival tissue-based assessment. As can be seen in Table 1, the two cohorts were well matched with no difference in age, gender, grade, presence of an intact primary, number of metastatic sites, or previous therapies. Fourteen patients in Cohort 2 had received prior anti-EGFR therapy, whereas only 1 patient in Cohort 1 had received prior anti-EGFR therapy.

Mutation analysis and cfDNA assay sensitivity

Cohort 1: Patients with previously documented RAS mutation and treated with FOLFOX plus dasatinib. Prior to treatment, 100% patients were found to have *KRAS* c*12/13* point mutations in archival tissue, while 20 of 21 (95%) patients had cfDNA mutations detected (Fig. 2A). No *BRAFV600E* mutations were detected at baseline in tissue or cfDNA. Compared with tissue-detected mutations, 4 of 19 patients (21%) had different *KRAS 12/13* point mutations noted in cfDNA, while 7 of 14 patients (50%) with concordant results had a second mutation detected in cfDNA (Fig. 1B). Of the 20 patients with cfDNA-detected mutations, 50% had a second concurrent mutation, while no patients with two concurrent mutations were detected in tissue (Fig. 2A).

Pretreatment (FOLFOX/dasatinib) and postprogression plasma was available for 11 of 21 patients (52%) who had completed between 4 and 8 cycles of therapy. New point mutations were found in 8 of 11 (73%) patients (Fig. 2B), 6 of whom had additional *KRAS* mutations, 1 of whom developed two new *KRAS* mutations, and 3 of whom developed new *BRAFV600E* mutations. There was 1 patient with a baseline *KRAS* G12C mutation that was no longer detected after four cycles of therapy. As all plasma were scored *KRAS* exon2/*BRAF* mutant at baseline or during treatment, no extended *RAS* mutation testing was performed in this cohort.

Cohort 2: Patients without a previously documented RAS mutation and treated with FOLFOX, dasatinib plus cetuximab. Eleven of 21 patients (52%) were *KRAS 12/13* mutant using our cfDNA analysis before treatment (Fig. 2A), while 3 patients (14%) were *BRAFV600E* mutant using the cfDNA analysis. Archival testing detected only 2 patients (10%) with *BRAFV600E* mutations (Fig. 2A). Concordance of *BRAFV600E* mutation results using archival tissue results as the "gold standard" was 95%, with specificity of 95% and sensitivity of 100% (Supplementary Table S2C). Extended *RAS* mutation testing was performed on cfDNA only in patients with WT *KRAS 12/13* and *BRAF*. No *KRAS* exon 3 or 4 mutations were noted in archival tissue, whereas 1 patient had a *KRAS Q61H* mutation by cfDNA testing prior to treatment. Two patients were *NRAS 61* mutant on tissue, while 3 were *NRAS 61* mutant in plasma (Fig. 2A). The same *NRAS* exon 61 mutation was detected from tumor tissue and plasma. Eight of 21 patients (38%) had concordant pretreatment results by archival tissue and cfDNA analysis. Conversely, 13 of 21 (62%) were scored mutant only using plasma cfDNA analysis: 11 were *KRAS 12/13* mutant, 1 was *KRAS Q61H* mutant, and another was *NRAS Q61R* mutant. In Cohort 2, 5 of 17 patients (29%) were found to have multiple concurrent *RAS* mutations by plasma analysis at baseline, while none had multiple mutations in the tissue -based assay (Fig. 2A). One patient was *KRAS 12/13* and *BRAFV600E* mutant before initiation of treatment.

Pretreatment and postprogression plasma was available for 15 of 21 patients who had completed between 4 and 16 cycles of FOLFOX, dasatinib plus cetuximab therapy. Plasma analysis showed new point mutations in 6 of 15 patients (40%), including detection of additional point mutations in patients who were WT extended *RAS/RAF* before treatment (Fig. 2B). Seven of 15 patients (47%) had no molecular change during treatment, including only 1 patient who remained *RAS/BRAF* WT during treatment and

Published OnlineFirst April 11, 2017; DOI: 10.1158/1078-0432.CCR-17-0232

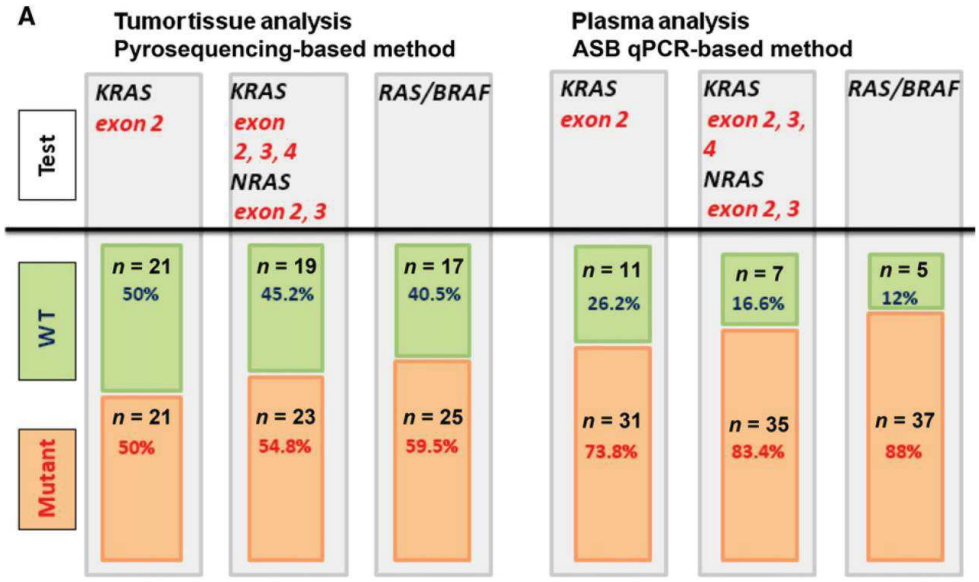

B

Cohort 1

Patient ID	Tissue-specific point mutation	Plasma-specific point mutation	Specific point mutation accuracy
#1	ND	*KRAS G13D and G12R*	–
#2	*KRAS G13D*	*KRAS G12C*	No
#3	*KRAS G12V*	*KRAS G12V*	Yes
#4	*KRAS G12V*	*KRAS G12V and G13D*	Yes
#5	*KRAS G12D*	*KRAS G12D*	Yes
#6	*KRAS G12A*	*KRAS G13D and G12D*	No
#7	*KRAS G12V*	*KRAS G12V and G13D*	Yes
#8	*KRAS G12A*	*KRAS G12A and G13D*	Yes
#9	ND	*KRAS G13D*	–
#10	*KRAS G13D*	*KRAS G13D*	Yes
#11	*KRAS G12S*	*KRAS G13D and G12S*	Yes
#12	*KRAS G12D*	*KRAS G13D and G12D*	Yes
#13	*KRAS G12V*	*KRAS G12V*	Yes
#14	*KRAS G12D*	*KRAS G12D*	Yes
#15	*KRAS G13D*	*KRAS G12A*	No
#16	*KRAS G12A*	*KRAS G13D, G12D and G12C*	No
#17	*KRAS G12D*	*KRAS G12D*	Yes
#18	*KRAS G12V*	*KRAS G12V and G13D*	Yes
#19	*KRAS G12C*	*WT*	No
#20	*KRAS G12D*	*KRAS G12D*	Yes
#21	*KRAS G13D*	*KRAS G13D and G12A*	Yes

Cohort 2

Patient ID	Tissue-specific point mutation	Plasma-specific point mutation	Specific point mutation accuracy
#22	*BRAF V600E*	*BRAF V600E*	Yes
#23	*WT*	*NRAS Q61R*	No
#24	*WT*	*KRAS G12R*	No
#25	*WT*	*WT*	Yes
#26	*WT*	*KRAS G12A*	No
#27	*WT*	*KRAS G12V and G12A*	No
#28	*WT*	*KRAS G12A*	No
#29	*WT*	*WT*	Yes
#30	*WT*	*KRAS G12D and G12R*	No
#31	*WT*	*KRAS G12A*	No
#32	*NRAS Q61R*	*NRAS Q61R*	Yes
#33	*BRAF V600E*	*BRAF V600E*	Yes
#34	*WT*	*KRAS G13D and BRAF V600E*	No
#35	*WT*	*KRAS G12R*	No
#36	*WT*	*KRAS G12A and G13D*	No
#37	*WT*	*WT*	Yes
#38	*NRAS Q61K*	*NRAS Q61K*	Yes
#39	*WT*	*WT*	Yes
#40	*WT*	*KRAS G12A*	No
#41	*WT*	*KRAS Q61H*	No
#42	*WT*	*KRAS G12V and G12A*	No

ND: scored positive but the mutation is nondetermined; WT: Wild type for mutations tested

Figure 1.

Comparison of mutational status of *RAS/BRAF* as determined by tumor tissue and plasma analysis at baseline ($n = 42$). **A,** Plasma analysis was carried out in Cohort 1 and 2 before initiation of treatments (baseline) accordingly with targeted genes. **B,** Comparison of the type of point mutation as determined by tumor tissue and plasma analysis before initiation of treatments and for Cohort 1 and 2. Extended *RAS* testing was only performed on plasma for patients who were *KRAS* exon 2 and *BRAFV600E* WT on all assays. ND, scored positive but the mutation is nondetermined; WT, wild type for mutations tested.

never developed a documented resistance mechanism in the *RAS/BRAF* pathway. In 2 of 15 patients (13%), the cfDNA point mutation detected at baseline was no longer detected during treatment. Compared with exon 2 *RAS* testing, extended *RAS* in plasma decreased the number of WT patients from 48% to 29% at baseline, and 43% to 19% upon completion of treatment (Fig. 2C). Our cfDNA assay reclassified even more patients to contain a mutation in the *RAS/BRAF* axis. Pretreatment, 19% of patients

Published OnlineFirst April 11, 2017; DOI: 10.1158/1078-0432.CCR-17-0232

Table 1. Patient's baseline clinicopathologic characteristics

	Cohorts *N (%)*		
	Cohorts 1 + 2	**Cohort 1**	**Cohort 2**
N	42	21 *(50)*	21 *(50)*
Age			
Median	58.5	58	59
Min–Max	26–74	26–74	33–70
Gender			
Male	27 *(64.3)*	15 *(35.7)*	12 *(28.6)*
Female	15 *(35.7)*	6 *(14.3)*	9 *(21.4)*
Grade of tumor			
Moderate	34 *(81)*	17 *(40.5)*	17 *(40.5)*
Moderate–poor	6 *(14)*	3 *(7)*	3 *(7)*
Missing data	2 *(4.8)*	1 *(2.4)*	1 *(2.4)*
Primary tumor in place			
Yes	21 *(50)*	8 *(19)*	13 *(31)*
No	20 *(47.6)*	13 *(31)*	7 *(16.6)*
Missing data	1 *(2.4)*	0	1 *(2.4)*
Delay between tumor tissue and blood collection			
<1 year	3 *(7)*	2 *(4.8)*	1 *(2.4)*
1–2 years	15 *(35.7)*	10 *(23.8)*	5 *(11.9)*
>2 years	24 *(57)*	9 *(21.7)*	15 *(35.7)*
No. of metastatic sites			
1	26 *(62)*	13 *(31)*	13 *(31)*
>1	15 *(36)*	8 *(19)*	7 *(17)*
Missing data	1 *(2.4)*	0	1 *(2.4)*
Previous chemotherapy			
Oxaliplatin	38 *(91)*	20 *(48)*	18 *(43)*
Irinotecan	33 *(78.6)*	16 *(38.1)*	17 *(40.5)*
Any	3 *(7.1)*	1 *(2.4)*	2 *(4.8)*
Previous targeted therapies			
Bevacizumab	33 *(78.6)*	19 *(45.3)*	14 *(33.3)*
Cetuximab	14 *(33.3)*	1 *(2.4)*	13 *(31)*
Panitumumab	2 *(4.8)*	0	2 *(4.8)*
Any	3 *(7.1)*	1 *(2.4)*	2 *(4.8)*

NOTE: FOLFOX/dasatinib treatment (Cohort 1) and FOLFOX/dasatinib/cetuximab treatment (Cohort 2).

were deemed to be extended *RAS* and *BRAF V600E* WT, whereas posttreatment, only 5% lacked a mutation. Three of 15 patients (20%) with single baseline *RAS* mutations developed novel concurrent *RAS* mutations by the time of disease progression.

Combined cohorts assay analysis

The median interval between tumor tissue and plasma collection was longer for Cohort 2 patients than for Cohort 1 (1,074 days and 699 days, respectively; $P = 0.038$; Supplementary Fig. S2A). Delay between tissue/plasma collection was statistically different between patients with concordant and discordant data [692 vs. 1,074 days, respectively ($P = 0.0163$; Supplementary Fig. S2B)]. The median time between tumor tissue collection and enrollment on the clinical trial was 845 days in both arms compared with less than one day for plasma collection.

Eighty percent of patients (4/5) who were *RAS/BRAF* WT on both tissue and cfDNA assay became *RAS* or *BRAF* mutant during or at the end of the therapy. Only one patient (2%) among the 42 examined in the two arms was WT for both *RAS/BRAF*. No detection of *EGFR S492R* was found either before or during anti-EGFR–targeted therapy in the plasma of this patient.

Impact of cetuximab rechallenge on mutational status

Among patients examined in Cohort 2, 13 patients had previously received cetuximab in a prior line of therapy. Of these patients, 9 of 13 (69%) had a *RAS* mutation noted and another 1 of 13 (8%) had a *BRAFV600E* mutation at baseline. Thus, 77% of rechallenged patients previously determined to be WT by archival tissue analysis were indeed mutant. Notably, 30% (3/10) of the rechallenged *RAS* mutant patients had multiple cooccurring *RAS* point mutations at baseline. All plasma samples originating from cetuximab-rechallenged patients ($n = 13$) were tested for the *EGFR S492R* point mutation. No patients carried *EGFR S492R* mutations before, during, or after FOLFOX, dasatinib plus cetuximab treatment.

Temporal trends in cfDNA concentration during therapy

Circulating WT KRAS/BRAF cfDNA concentration. The total concentration of WT cfDNA was determined by quantifying a WT sequence of both *KRAS* and *BRAF* genes and is shown in Table 2A and B, for Cohort 1 and 2, respectively. At baseline and as expected, data showed a linear positive relationship between the RefA values (ng/mL) of *KRAS* and *BRAF* WT sequences (Supplementary Fig. S3A) as previously observed (32). The *KRAS:BRAF* ratio was close to 1, both before and during treatment (Supplementary Fig. S3B). *KRAS* WT concentration did not statistically differ between cohorts ($P = 0.36$; Supplementary Fig. S4), and in most patients, *KRAS* WT concentration was higher at the end of treatment than at baseline (Fig. 3A and B). Of patients with serial measurements, 4 of 11 (36%) and 12 of 15 patients (80%) showed an increase of 50% (1.5-fold) above their baseline value at the end of FOLFOX plus dasatinib or FOLFOX, dasatinib plus cetuximab therapy, respectively (Fig. 3). No significant difference was seen in total concentration of WT cfDNA at baseline between patients whose treatment was stopped before cycle 4 and those treated with more than four cycles ($P = 0.76$; Supplementary Fig. S5).

Circulating mutant RAS/BRAF cfDNA concentration. Concentration of mutant cfDNA (Table 2A and B) did not differ at baseline when comparing Cohorts 1 and 2 ($P = 0.65$; Supplementary Fig. S6). No significant difference was observed in the baseline concentration of mutant cfDNA between patients whose treatment was stopped before the fourth cycle and patients who continued more than four cycles without progression ($P = 0.18$; Supplementary Fig. S7). In both cohorts combined, 7 of 46 point mutations (15.2%) found at baseline had concentrations higher than 1 ng/mL of plasma, 19 of 46 mutations (41.3%) had concentrations less than 0.1 ng/mL, and 4 of 46 (8.7%) were noted at 0.01 ng/mL (Table 2A and B).

Mutant allele frequency

The mutant allele frequency represents the proportion of detected alleles that are mutant for a particular point mutation. The distribution of mutant allele fraction (Table 2A and B) for both cohorts highly varied before and during treatment, ranging from 0.009% to 60% (Fig. 3C). Pretreatment, 65% (30/46) of detected mutations were below an allele frequency of 1%, including 45.68% (21/46) below 0.5% and 15% (7/46) below 0.1% (Table 2A and C). At baseline, mutant allele fraction varied from 0.009% to 31.83%. In patients with concordant results between archival tissue and cfDNA, 56% (10/18) had a mutant allele fraction >1%, 33% (6/18) were between 0.01% and 1%, and 11% (2/18) were <0.01% (Supplementary Table S3). One mutation was detectable but not quantifiable by our qPCR assay, as its allele fraction was <0.01%.

During treatment, 65% (31/48) of variants were found below 0.5% allele frequency, including 27% (13/48) below 0.1% (Table

Published OnlineFirst April 11, 2017; DOI: 10.1158/1078-0432.CCR-17-0232

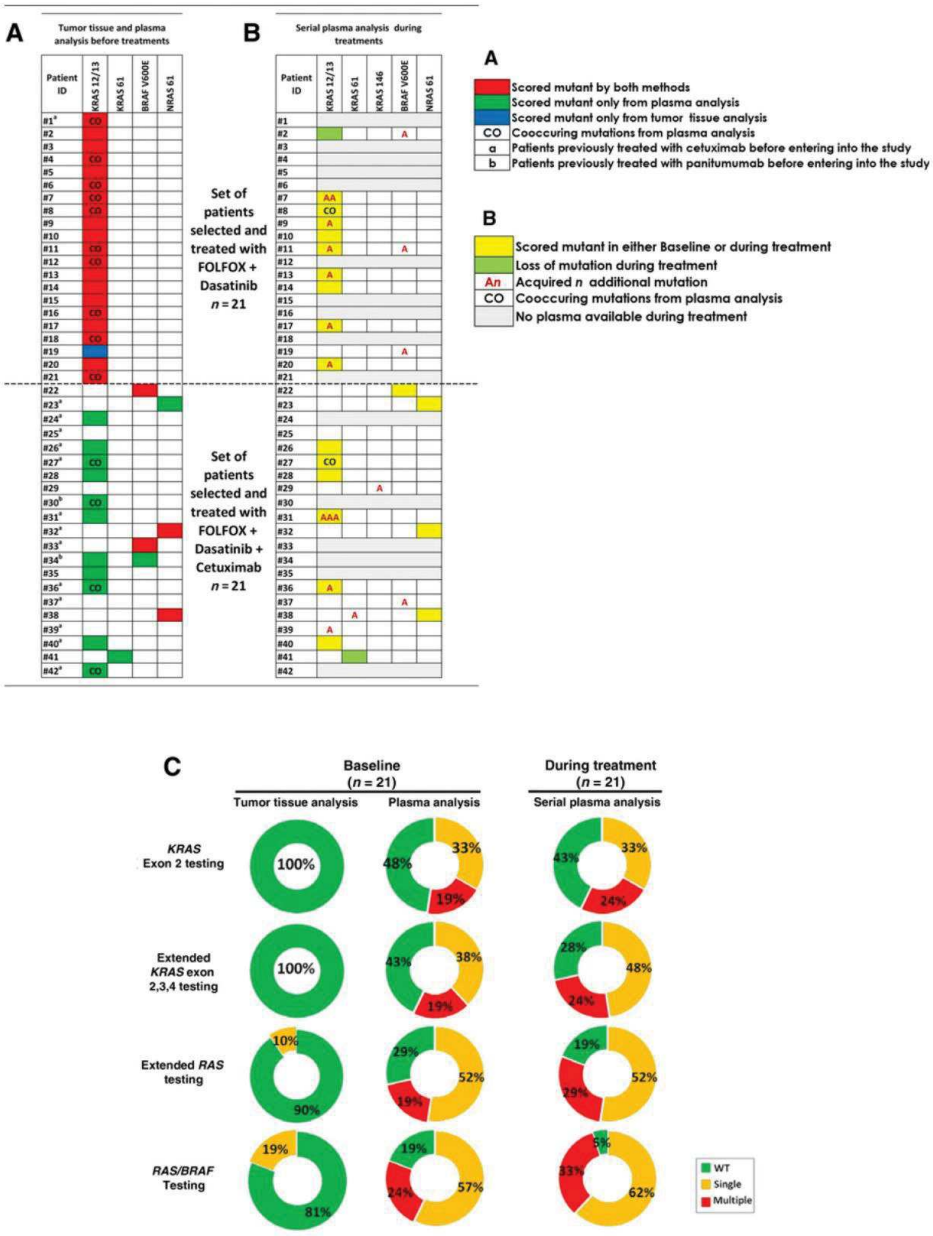

Figure 2.

RAS/BRAF mutational status. Comparison of *RAS/BRAF* mutational status as determined by tumor tissue and plasma analysis. **A,** Before initiation of treatment of cohorts 1 and 2 (baseline). **B,** Longitudinal plasma genotyping during treatment ($n = 26$). **C,** Distribution of mutational status from cfDNA analysis of cohort 2 patients before and after EGFR-directed therapy. Percentage of mutant patients as determined by tumor tissue analysis and plasma analysis before initiation and during FOLFOX/dasatinib + cetuximab treatment as determined by serial plasma analysis. Results are shown according the target genes. A*n*, acquired *n* additional mutation; CO, cooccurring mutations from plasma analysis; WT, wild type for mutations tested; single, one mutation was found in patient; multiple, at least two mutations were found in patient.

Published OnlineFirst April 11, 2017; DOI: 10.1158/1078-0432.CCR-17-0232

2A and B). We noted that 83% (15/18) of new point mutations during treatment occur with a mutant allele fraction less than 0.5% and 50% (9/18) and are first noted at fractions ≤0.1% (Supplementary Table S4). We observed no difference between mutant allele fraction at baseline between Cohorts 1 and 2 ($P = 0.77$; Supplementary Fig. S8).

Ability of cfDNA to monitor disease progression and track therapeutic resistance

We collected data on imaging CT scan and CEA biomarker in most of the patients from baseline to the end of the treatment and compared them with mutant cfDNA parameters, such as mA%, mA, or refA (Supplementary Table S5). To illustrate the clinical application of circulating cfDNA to track detection of additional mutant subclones and assess disease response/progression, we present 4 example patients. Patient #8 was treated with FOLFOX plus dasatinib, while patients #28, #31, and #36 were treated with FOLFOX, dasatinib plus cetuximab. Treatment of patients #8, #36, #28, and #31 was stopped at cycles 4, 8, 12, and 16, respectively (Fig. 4A and B). *RAS* WT and mutant allele concentration and mutant allele fraction were compared with standard clinical assessment with CT scan and CEA level. For all patients except #8, *RAS* WT concentration, *RAS*-mutant concentration, and mutant allele fraction closely matched laboratory and radiological indicators of disease status. For patient #36, cfDNA may have provided a signal of disease progression earlier than standard clinical assessments when a rising *KRAS* G12S clone was noted.

Interestingly, differential evolution of mutant subclones may be occurring in patients #31 and #36 (Fig. 4A and B), with some clones increasing in mutant allele frequency, while others decrease over time. In patient #36, there was detection of additional *KRAS* G12S–mutant subclone and a decrease of a *KRAS*

Table 2. Impact of treatment on total cfDNA and mutant *RAS/BRAF* cfDNA concentration and mutant *RAS/BRAF* allele frequency

A[a]

Cohort 1- *KRAS 12/13*–mutant patients by tumor tissue analysis										
	RefA *KRAS* (ng/mL of plasma) Time point treatment				mA (ng/mL of plasma) Time point treatment			mA% Time point treatment		
Patient ID	Baseline	Cycle 4	Cycle 8	Mutation	Baseline	Cycle 4	Cycle 8	Baseline	Cycle 4	Cycle 8
#1	11.35	—	—	*KRAS G12R*	0.84	—	—	7.42	—	—
—	—	—	—	*KRAS G13D*	0.15	—	—	1.28	—	—
#2	16.61	11.29	14.91	*KRAS G12C*	0.2	*ND*	*ND*	1.03	*ND*	*ND*
—	—	—	—	*BRAF V600E*	*ND*	*ND*	0.14	*ND*	*ND*	2.27
#3	13.18	—	—	*KRAS G12V*	0.08	—	—	0.62	—	—
#4	0.05	—	—	*KRAS G13D*	*NQ*	—	—	*NQ*	—	—
—	—	—	—	*KRAS G12V*	*NQ*	—	—	*NQ*	—	—
#5	29.84	—	—	*KRAS G12D*	1.27	—	—	4.27	—	—
#6	13.97	—	—	*KRAS G13D*	0.04	—	—	0.3	—	—
—	—	—	—	*KRAS G12D*	0.37	—	—	2.66	—	—
#7	37.97	52.19	—	*KRAS G13D*	0.06	0.07	—	0.15	0.13	—
—	—	—	—	*KRAS G12V*	3.76	4.59	—	9.9	8.8	—
—	—	—	—	*KRAS G12A*	*ND*	0.05	—	*ND*	0.09	—
—	—	—	—	*KRAS G12C*	*ND*	0.05	—	*ND*	0.09	—
#8	90.04	11.55	—	*KRAS G13D*	0.12	0.45	—	0.13	0.4	—
—	—	—	—	*KRAS G12A*	11.87	18.61	—	13.18	16.68	—
#9	6	37.13	—	*KRAS G13D*	0.036	0.14	—	0.6	0.24	—
—	—	—	—	*KRAS G12D*	*ND*	0.054	—	*ND*	0.15	—
#10	34.35	27.98	—	*KRAS G13D*	0.003	0.01	—	0.009	0.03	—
#11	51.31	54.36	—	*KRAS G12S*	16.33	32.77	—	31.83	60.28	—
—	—	—	—	*KRAS G13D*	0.1	0.01	—	0.2	0.02	—
—	—	—	—	*KRAS G12A*	*ND*	0.13	—	*ND*	0.24	—
—	—	—	—	*BRAF V600E*	*ND*	0.04	—	*ND*	0.07	—
#12	53.99	—	—	*KRAS G12D*	5.86	—	—	10.86	—	—
—	—	—	—	*KRAS G13D*	0.09	—	—	0.16	—	—
#13	13.46	17.95	—	*KRAS G12V*	0.73	1.11	—	5.44	6.17	—
—	—	—	—	*KRAS G13D*	*ND*	0.05	—	*ND*	0.3	—
#14	4.77	18.25	—	*KRAS G12D*	0.01	0.02	—	0.28	0.17	—
#15	32.53	—	—	*KRAS G12A*	0.03	—	—	0.09	—	—
#16	14.56	—	—	*KRAS G13D*	0.01	—	—	0.1	—	—
—	—	—	—	*KRAS G12D*	0.07	—	—	0.45	—	—
—	—	—	—	*KRAS G12C*	0.03	—	—	0.2	—	—
#17	22.61	33.2	—	*KRAS G12D*	0.97	0.54	—	4.3	1.63	—
—	—	—	—	*KRAS G12A*	*ND*	0.02	—	*ND*	0.05	—
#18	16.62	—	—	*KRAS G13D*	0.02	—	—	0.12	—	—
—	—	—	—	*KRAS G12V*	0.12	—	—	0.72	—	—
#19	2.46	6.89	—	*BRAF V600E*	*ND*	0.15	—	*ND*	3.96	—
#20	27.46	31.02	9.66	*KRAS G12D*	0.19	*ND*	0.02	0.67	*ND*	0.23
—	—	—	—	*KRAS G12A*	*ND*	0.08	0.02	*ND*	0.26	0.12
#21	17.48	—	—	*KRAS G12A*	0.03	—	—	0.19	—	—
—	—	—	—	*KRAS G13D*	0.01	—	—	0.08	—	—

[a]The total cfDNA concentration was determined by IntPlex as described in Materials and Methods, for each patient of Cohort 1 before initiation of treatment up to progression and at the end of treatment. Also, the concentration of mutant cfDNA and mutation loads was determined by IntPlex as described in Materials and Methods, for all point mutations found in each mutant patient of Cohort 1 before initiation of treatments up to the end of treatment.

(*Continued on the following page.*)

Published OnlineFirst April 11, 2017; DOI: 10.1158/1078-0432.CCR-17-0232

Table 2. *(Continued)*

B[b]

Cohort 2 - *KRAS 12/13* WT patients by tumor tissue analysis																
	RefA *KRAS* (ng/mL of plasma) Time point treatment						mA (ng/mL of plasma) Time point treatment					mA% Time point treatment				
Patient ID	Baseline	Cycle 4	Cycle 8	Cycle 12	Cycle 16	Mutation	Baseline	Cycle 4	Cycle 8	Cycle 12	Cycle 16	Baseline	Cycle 4	Cycle 8	Cycle 12	Cycle 16
#22	8.02	39.53	—	—	—	*BRAF V600E*	0.29	0.55	—	—	—	4.51	3.77	—	—	—
#23	7.7	22.79	—	—	—	*NRAS Q61R*	3	5.08	—	—	—	56	22.29	—	—	—
#24	11.81	—	—	—	—	*KRAS G12R*	0.09	—	—	—	—	0.72	—	—	—	—
#25	6.31	31.42	—	—	—	*WT*	*WT*	*WT*	—	—	—	*WT*	*WT*	—	—	—
#26	11.1	25.17	—	—	—	*KRAS G12A*	0.07	0.7	—	—	—	0.64	2.78	—	—	—
#27	12.12	13.34	21.25	—	—	*KRAS G12A*	0.28	0.05	*ND*	—	—	0.97	0.36	*ND*	—	—
—	—	—	—	—	—	*KRAS G12V*	0.06	0.02	*ND*	—	—	0.21	0.16	*ND*	—	—
#28	2.15	7.44	—	23.28	—	*KRAS G12A*	*NQ*	0.11	—	0.45	—	*NQ*	1.43	—	1.9	—
#29	14.92	33.35	—	—	—	*KRAS A146T*	*ND*	*NQ*	—	—	—	*ND*	*NQ*	—	—	—
#30	9.55	—	—	—	—	*KRAS G12R*	*NQ*	—	—	—	—	*NQ*	—	—	—	—
—	—	—	—	—	—	*KRAS G12D*	*NQ*	—	—	—	—	*NQ*	—	—	—	—
#31	116.29	26.27	45.01	47.45	350.48	*KRAS G12A*	0.052	0.03	0.015	0.17	0.16	0.04	0.11	0.03	0.45	0.04
—	—	—	—	—	—	*KRAS G13D*	*ND*	*ND*	*ND*	0.022	0.15	*ND*	*ND*	*ND*	0.05	0.03
—	—	—	—	—	—	*KRAS G12D*	*ND*	*ND*	*ND*	*ND*	0.088	*ND*	*ND*	*ND*	*ND*	0.01
—	—	—	—	—	—	*KRAS G12V*	*ND*	*ND*	*ND*	*ND*	0.47	*ND*	*ND*	*ND*	*ND*	0.11
#32	27.68	19.62	—	—	—	*NRAS Q61R*	0.46	0.43	—	—	—	0.76	3.4	—	—	—
#33	94.78	—	—	—	—	*BRAF V600E*	19.58	—	—	—	—	15.57	—	—	—	—
#34	110.14	—	—	—	—	*KRAS G13D*	0.03	—	—	—	—	0.03	—	—	—	—
—	—	—	—	—	—	*BRAF V600E*	0.23	—	—	—	—	0.16	—	—	—	—
#35	2.46	—	—	—	—	*KRAS G12R*	*NQ*	—	—	—	—	*NQ*	—	—	—	—
#36	69.44	41.26	191.3	—	—	*KRAS G12A*	0.03	0.26	0.06	—	—	0.05	0.26	0.03	—	—
—	—	—	—	—	—	*KRAS G13D*	0.16	3.41	4.57	—	—	0.22	8.27	2.39	—	—
—	—	—	—	—	—	*KRAS G12S*	*ND*	*ND*	0.05	—	—	*ND*	*ND*	0.02	—	—
#37	12.79	16.14	—	—	—	*BRAF V600E*	*ND*	0.15	—	—	—	*ND*	1.4	—	—	—
#38	5.43	9.19	—	—	—	*KRAS Q61H*	*ND*	*NQ*	—	—	—	*ND*	*NQ*	—	—	—
—	—	—	—	—	—	*NRAS Q61K*	0.85	3.94	—	—	—	18.87	18.74	—	—	—
#39	14	27.45	—	—	—	*KRAS G12A*	*ND*	0.04	—	—	—	*ND*	0.16	—	—	—
#40	8.17	13.49	—	—	—	*KRAS G12A*	0.05	0.04	—	—	—	0.58	0.28	—	—	—
#41	106.37	95.17	—	—	—	*KRAS Q61H*	*NQ*	*ND*	—	—	—	*NQ*	*ND*	—	—	—
#42	11.24	—	—	—	—	*KRAS G12A*	0.12	—	—	—	—	1.09	—	—	—	—
—	—	—	—	—	—	*KRAS G12V*	0.03	—	—	—	—	0.24	—	—	—	—

Abbreviations: ND, nondetected; NQ, scored positive but nonquantified; mA, concentration of mutant cfDNA (ng/mL of plasma); mA%, mutation load; RefA, concentration of total cfDNA (ng/mL of plasma); WT, wild type for mutations tested.

[b]The total cfDNA concentration was determined by IntPlex as described in Materials and Methods, for each patient of Cohort 2 before initiation of treatment up to progression and at the end of treatment. Also, the concentration of mutant cfDNA and mutation loads was determined by IntPlex as described in Materials and Methods, for all point mutations found in each mutant patient of Cohort 2 before initiation of treatment up to the end of treatment.

G12A subclone at cycle 8. Similarly in patient #31, there are *KRAS* G12A and G12V clones that have inverse dynamics noted.

Discussion

Although mAbs to EGFR improve mCRC patient survival, they are limited by primary and secondary resistance (39). Standard-of-care clinical biomarkers poorly track treatment resistance during early tumor progression. The selective pressure from targeted therapy combined with spatial and temporal clonal heterogeneity leads to a complex clinical challenge. Early detection of secondary resistance may impact clinical outcomes. Bertotti and colleagues (40) characterized secondary resistance to EGFR blockade in mCRC and observed that alterations in *KRAS, NRAS*, and *BRAF* were important mechanisms of resistance. With two recent reports showing the ability of cfDNA to detect secondary resistance to anti-EGFR therapies with using liquid biopsy (15, 17), this study further explored cfDNA and expanded upon work in the field by examining both the ability of cfDNA assays to assess for the presence of a mutation, and the ability of quantitative parameters associated with this assay, such as *RAS* WT concentration, *RAS* mutant concentration, and mutant allele fraction, to impact outcome.

cfDNA assay performance

Approximately half (52%) of the patients from Cohort 2 who initially tested WT for *KRAS* exon 2 mutations from archival tumor tissue analysis were actually noted to have *KRAS* exon 2 mutations in their plasma, and even more patients were found to have extended *RAS* or *BRAF* mutations. While concordance between tissue and plasma appeared better for *BRAFV600E* mutations, discordance for *KRAS* exon 2 mutations was notable. Concordance between cfDNA and archival tissue seems to be lower in patients who do not have their primary tumor *in situ* at the point of study entry as well in case of long delay between tumor tissue and blood collection (Supplementary Table S6). Our study suggests that cfDNA may be more sensitive than archival tumor tissue analysis in detecting mutations. We can speculate that discordance in 10 patients from Cohort 2 might result from the fact that blood was collected following prestudy targeted therapy, causing selection of mutant clones potentially detectable by plasma analysis at baseline before study treatment of Cohort 2. (Fig. 2A). We recently reported similar findings in another prospective and blinded study where we found a much higher proportion of mCRC patients with *RAS* or *BRAF* mutations using a cfDNA assay compared with tissue (76% instead of 55%; ref. 41). Various factors may explain this discordance. Tissue biopsies

Published OnlineFirst April 11, 2017; DOI: 10.1158/1078-0432.CCR-17-0232

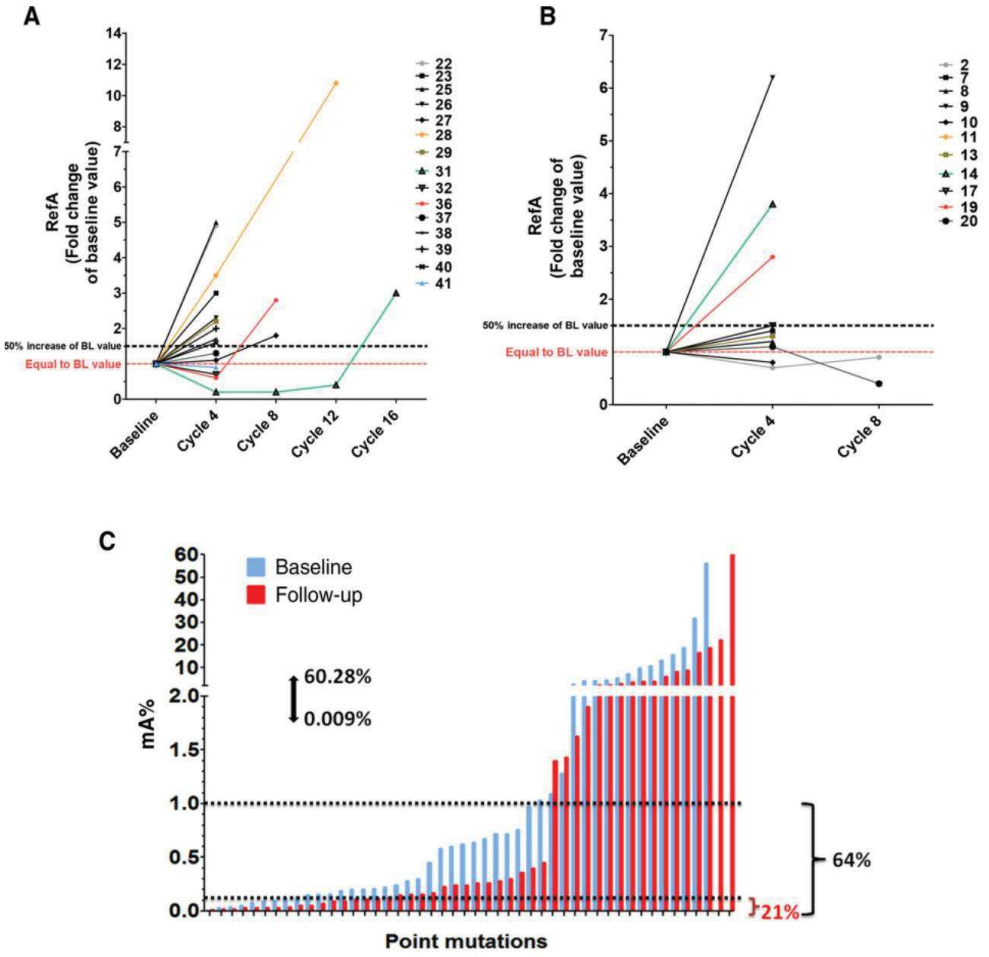

Figure 3.

Impact of treatment on the evolution of cfDNA concentration. **A** and **B,** RefA values during FOLFOX/dasatinib treatment (**A**; Cohort 1, $n = 11$), and during FOLFOX/dasatinib/cetuximab treatment (**B**; Cohort 2, $n = 15$). RefA are expressed in fold change of baseline value. **C,** cfDNA mutant allele frequency of each detected mutant samples. mA% was determined by IntPlex as described in Materials and Methods before (blue, baseline) and after treatment (red, follow-up) in both cohorts. mA% varies from 0.009% to 60.28%. Twenty-one percent and 64% of all samples showed a mutant allele frequency below 0.1% and 1% (dotted lines), respectively. RefA, concentration of total cfDNA (ng/mL of plasma); BL, baseline; mA%, cfDNA mutation load.

provide a static snapshot of the tumor at the time of tissue collection and do not necessarily represent the entire tumor genome due to tumor heterogeneity and clonal evolution (9, 10, 42). Temporal clonal evolution (43) may also impact concordance as we noted that time between collection of archival tissue and blood draw differed significantly between those with concordant and discordant results (692 vs. 1,074 respectively; $P = 0.016$; Supplementary Figs. S11 and S12). This suggests that therapeutic pressures and tumor evolution over time make archival tissue less reliable for determining the genotype of a tumor and highlights the advantage of real-time genotyping with cfDNA.

There are only a few other prospective studies examining the concordance of *RAS* mutation in tissue and cfDNA under blinded conditions (44–46).

Many other retrospective or small studies are available in the literature (45, 47). In these studies, specificity, sensitivity, and overall concordance in comparison with archival tissue were highly variable (55%–97%, 26%–92%, 64%–96%, respectively), likely due to assay characteristics coupled with time between

Published OnlineFirst April 11, 2017; DOI: 10.1158/1078-0432.CCR-17-0232

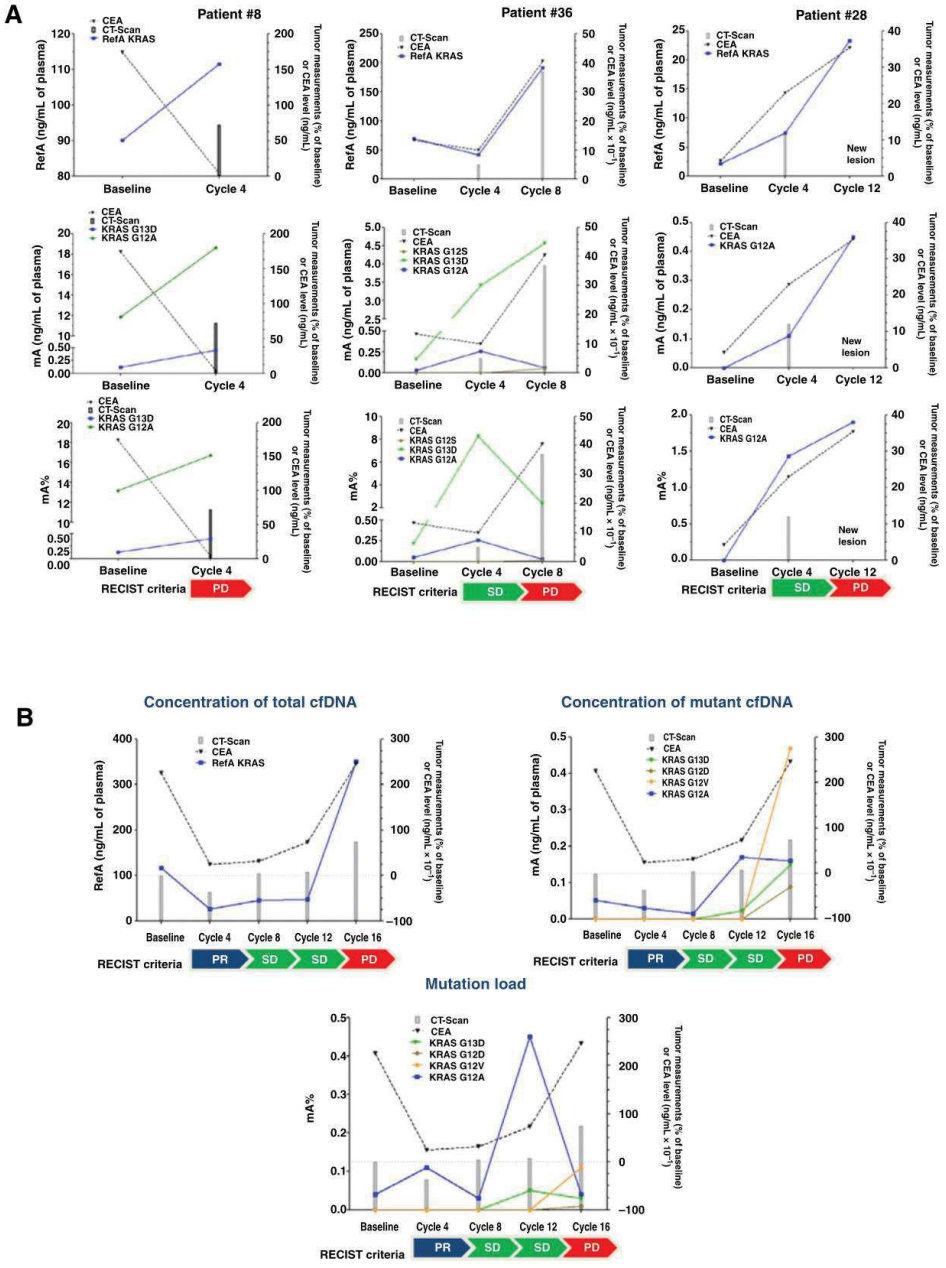

Figure 4.

Quantitative cfDNA analysis in the course of treatments in comparison with serum CEA and CT scan measurements. Patients #8, #28, #31, and #36 illustrate impact of treatment on those biomarkers. **A,** Patients #8, #28, and #36 are patients who responded to treatment with stable disease. **B,** Patient #31 was the single patient in both cohort showing initial response to therapy (cetuximab). CEA, carcinoembryonic antigen (expressed in ng/mL); CT scan, computed tomography scan (expressed as percentage change of baseline value); RefA, concentration of total cfDNA (ng/mL of plasma); mA, concentration of mutant cfDNA (ng/mL of plasma); mA%, mutation load; PR, partial response; SD, stable disease (RECIST criteria); PD, progressive disease (RECIST criteria).

Published OnlineFirst April 11, 2017; DOI: 10.1158/1078-0432.CCR-17-0232

tissue and plasma collection. When using an ultrasensitive method (48), such as employed in this study, another group noted a significant level of discordance (15%–25%), mainly associated with an increase in tumors classified as mutation positive by mutant cfDNA assessment. Our results are in agreement with Kuo and colleagues (49) who observed that 21% of patients who were WT by archival tissue were actually cfDNA positive for a *KRAS* mutation for an overall concordance of 79%. As detection of actionable mutations by plasma analysis is not limited by (i) intratumoral, (ii) intertumoral, and (iii) temporal clonal heterogeneity, in contrast to tumor tissue analysis, cfDNA testing has clear advantages that may lead to the earlier and more sensitive detection of mutations. Tumor tissue in now challenged as the gold standard in screening for actionable mutations in oncology.

Sensitivity is a crucial requirement for analyzing cfDNA due to the potentially low mutant allele frequency noted during sampling. To address this, we developed IntPlex, an allele-specific qPCR technique that uses several nested primer sets and takes into account the low fragment size of cfDNA (mean size of 100 bp) to optimize assay performance. IntPlex enables detection of variant alleles down to a sensitivity of 0.005% mutant to WT ratio that greatly surpasses conventional NGS-based methods (0.5%–2%; refs. 4, 50, 51). Spiking experiments showed clearly single-copy detection in highly diluted PCR mixture under Poisson law distribution (Supplementary Fig. S9). Using this technique, one mutant fragment may be detected among 10 billion cfDNA fragments providing a sensitivity level (0.005%, mutant/WT ratio) This targeted method is limited by the number of mutant fragments existing in the plasma, with a limit of 26 mutant cfDNA fragments/mL of plasma. Despite the fact that plasma for this study was stored frozen for more than 4 years (4–6 years of storage range) and the preanalytic conditions were not optimal, IntPlex was still able to detect mutations at very low frequencies and performed well. Note, no *KRAS* exon 2 and *BRAFV600E* mutation could be detected in 29 certified healthy volunteers in an ad hoc study of our previous report, regardless of the threshold of detection used (31).

There are some limitations to our assay. IntPlex enables the detection of only a restricted set of common mutations (i.e., known point mutations). Only 15 *KRAS*, 9 *NRAS*, and one *BRAF* mutations were tested in this study; however, these hotspot mutations represent more than 95%–99%, 92%–99% and 96%–97% of all mutations found in these three genes in colorectal patients, respectively.

Significance of low mutant allele frequency mutations

The impressive sensitivity of our assay and its ability to quantify mutations noted at as low as 0.01 ng/mL allowed the identification of many mutations with very small allelic fractions. The ability to confidently detect these low frequency mutations likely explains part of the discrepancy between the results from the initial clinical assay used for trial enrollment and our results. CLIA-certified laboratory often has a mutant allele fraction limit of detection of 5%. Positive results below this threshold are often suppressed from clinicians because a false positive result due to sequencing errors cannot be ruled out. We retrospectively sequenced archival tissue with a high-sensitivity assay to confirm mutations (Fig. 1B) and note significant discordance regardless of whether a clinical grade or high-sensitivity research-based platform is used (Fig. 1).

We observed subclones with very low allele frequency (down to 0.009%) either at baseline or during the course of the treatment (Supplementary Fig. S10). There were 30% of patients with a mutation at an allele frequency below 0.1% at baseline, and 20% of patients with a mutation noted below 0.1% during the course of the treatment. These rare subclones may exist before treatment but be undetectable by clinical grade assays and subsequently emerge under anti-EGFR treatment. Secondary *RAS* mutations have been previously shown to develop in up to 60% of tumors progressing during anti-EGFR therapy, and we noted that they could be found in all but 1 patient on this study; however, many of these mutations may have been present yet undetectable at baseline. Retrospective studies have suggested that many of these mutations may be detected in cfDNA prior to initiation of therapy (13), whereas other work using mathematic models of tumor kinetics and growth has shown that these mutations must be present prior to initiation of therapy (15).

As these low frequency mutations may result in treatment resistance, very sensitive methods to initially select patients for anti-EGFR therapies are needed. Tougeron and colleagues (52) recently demonstrated that low-prevalence *KRAS* mutations detected by an advanced pyrosequencing method in tumors previously defined as *KRAS* WT were associated with shorter PFS. Our data revealed that 52% (22/42) of patients had an allele fraction below 1%, 31% (13/42) were below 0.5%, and 19% (8/42) were below 0.1% (Supplementary Table S7). These low allelic values may not perfectly correlate to the allele frequency that would be detected in a tumor. Plasma analysis relies on the total number of cfDNA fragments shed into the blood stream from normal and tumor cells. In contrast, tumor tissue analysis relies on the number of malignant cells in a biopsy and may be enriched by pathologist selection of section with higher tumor content. As a consequence, the value used to estimate cfDNA sensitivity does not correspond directly to that of tumor tissue analysis, which precludes use of a universal sensitivity threshold for detection of mutations. We illustrated this by showing that in the 16% (4/25) of patients with cfDNA allele frequency below 0.5%, mutations could be readily detected in matched tumor tissue (Supplementary table S8; ref. 41).

Impact of therapy on clonal dynamics and development of additional *RAS* mutations

Following EGFR-directed therapy, we noted that 98% of patients had at least one mutation in *RAS* or *BRAF* that likely contributed to treatment resistance. More interestingly, of the 21 patients defined as *RAS/BRAF* mutant at baseline, 11 (50%) showed additional point mutation that was not present at baseline, while 3 (14%) lost previously detected mutations. There was even a single patient with a baseline *KRAS* G12A mutation that subsequently developed additional G12D, G12V, and G13D mutations after receiving 16 cycles of cetuximab-containing therapy. These findings demonstrate that even if a single clonal population with a resistance mechanism is present in a tumor, treatment pressures may drive the development of additional alternative resistance mechanisms in a pattern of convergent evolution. These multiple convergent mutations were noted to develop whether patients received FOLFOX plus dasatinib or FOLFOX, dasatinib plus cetuximab. Another important clonal dynamic that we noted was that some *RAS* mutations appeared to be more strongly associated with secondary mutation than

Published OnlineFirst April 11, 2017; DOI: 10.1158/1078-0432.CCR-17-0232

primary resistance. Our data show that *KRAS* codon 61 was expressed more frequently in acquired resistance mutations (5.5%) than in the general mCRC population (1%–4%; 2,51), suggesting that mutations at this codon might provide a selective growth advantage under cetuximab treatment. This was also observed for *KRAS* codon 146 mutations by Morelli and colleagues (48). Our findings also reinforce the importance of *BRAF* mutations as mechanisms of resistance, as we demonstrated that 4 of 42 patients (10%) had additional *BRAFV600E* mutations during therapy.

cfDNA to follow disease progression

cfDNA quantitative measurements from this study closely mirrored changes in CEA and CT scan results as evaluated in 18 and 16 patients in Cohort 1 and 2, respectively. We noted that both the qualitative detection of a mutation and quantitative information such as *RAS*-mutant and WT cfDNA concentrations and mutant allele fraction appeared to be useful in following disease course. The level of *RAS*/BRAF mutations expressed as the percentage of mutant cfDNA as well as ng/mL plasma of mutant cfDNA did not correlate with the treatment response, highlighting the necessity of detecting low level and low frequency mutations (Supplementary Table S9). The circulating WT cfDNA concentration appeared to closely approximate other clinical parameters, and it was not only the detection of a mutant cfDNA sample that was related to disease progression (Fig. 4B). The patient in Fig. 4B had an interesting molecular profile that demonstrated falling levels of *RAS* DNA, both WT and mutant during response to therapy. Subsequently, after 16 cycles of therapy, this patient had developed three additional *RAS* mutations beyond the baseline *KRAS* G12A mutation. Mutant allele frequency of the single baseline mutation was very low (0.04%), and the subsequent new clones all remained subclonal with allelic frequencies ranging from 0.01% to 0.11%, potentially explaining why the patient continued to respond for over several cycles. There was likely a large proportion of this tumor that lacked *RAS* mutations.

Siravegna and colleagues (53) elegantly demonstrated the utility of following cfDNA to measure *KRAS*-mutant subclones as a potential for reusing prior targeted therapies. Upon withdrawal of the selective pressure of anti-EGFR treatment, *KRAS*-mutant clones declined (53). These patients subsequently regained sensitivity to anti-EGFR therapy. In a similar manner, following the patient in Fig. 4B serially may allow continuation of therapy until a resistance clone becomes more dominant, highlighting the importance of obtaining quantitative data beyond the mere presence of a mutation (12, 54). If therapy had been stopped at the first incidence of a new resistance mutation, that patient would have switched therapy 2 months earlier than was required clinically.

Limitations

Although this study demonstrates the potential applications of highly sensitive cfDNA to follow tumor dynamics, it must be interpreted within the contexts of its limitations. The small sample size of our study makes it difficult to draw firm conclusions. Our assessment of mutation status was blinded and samples were prospectively collected, both features that add to the rigor of experimental design but do not obviate the need for larger trials for validation. We were also limited by the infrequent plasma samples that were available for cfDNA analysis, occurring at baseline and once every 4 cycles. Although our study does not provide evidence that cfDNA detects mutant clones and progression earlier than clinical assessment, this is likely due to the fact that we only assessed cfDNA once every four cycles.

An important finding in this study was the convergent evolution of clones with redundant resistance mechanisms in the *EGFR* pathway. We were only able to test three clinically relevant genes and did not test genes involved in EGFR downstream signaling pathways or the *mTOR* pathway. *PIK3CA* mutation, *PTEN* loss (55), *EGFR* mutations, as well as *MET* and *ERBB2* amplifications may predict a lack of response to anti-EGFR agents. Thus, it would be interesting to see whether there were redundant resistance pathways that also developed in these genes in addition to the multiple concurrent *KRAS* clones that were noted (40, 48). Because *EGFR S492R* has been described as an alternate mechanism of resistance, we did test the 13 plasma samples of patients who had previously received anti-EGFR therapy for *EGFR S492R* mutations at baseline; however, none of the 13 plasma samples were positive for this mutation.

Conclusions

With our assay, we were able to uncover the development of secondary resistance mutations in *RAS* and *BRAF* in all but one of 42 patients. A significant fraction of these mutations detected either before or in the course of treatment from plasma analysis harbors low mutant allele frequency in cfDNA. This shows the need of an ultrasensitive method to detect additional point mutation when tracking secondary resistance. Periodic liquid biopsies require a simple blood draw, and if optimized for clinical use would optimize patient safety and convenience. We note that not only was the qualitative presence of a mutant clone important, but the additional quantitative measurements of WT *KRAS* concentration, mutant *KRAS* concentration, and mutant allele fraction may be useful parameters to follow. We also noted that many patients experienced convergent evolution that resulted in redundant mutations that would provide multiple mechanisms of resistance to EGFR-directed therapy.

Disclosure of Potential Conflicts of Interest

No potential conflicts of interest were disclosed.

Authors' Contributions

Conception and design: A.R. Thierry
Development of methodology: A.R. Thierry, A.D. Katsiampoura
Acquisition of data (provided animals, acquired and managed patients, provided facilities, etc.): Z.-Q. Jiang, S. Kopetz
Analysis and interpretation of data (e.g., statistical analysis, biostatistics, computational analysis): A.R. Thierry, B. Pastor, Z.-Q. Jiang, A.D. Katsiampoura, J.M. Loree, M.J. Overman, S. El Messaoudi, M. Ychou
Writing, review, and/or revision of the manuscript: A.R. Thierry, B. Pastor, Z.-Q. Jiang, A.D. Katsiampoura, C. Parseghian, J.M. Loree, M.J. Overman, S. El Messaoudi, M. Ychou, S. Kopetz
Administrative, technical, or material support (i.e., reporting or organizing data, constructing databases): A.R. Thierry, B. Pastor, Z.-Q. Jiang, A.D. Katsiampoura, J.M. Loree, C. Sanchez
Study supervision: A.R. Thierry

Acknowledgments

The authors thank Thibault Mazard, Frederic Bibeau, Philippe Blache, Corinne Prevostel, Celine Gongora, and Evelyne Crapez for helpful discussion, Vanessa Guillaumon for help in supporting this work, Peter Gahan for editing

Published OnlineFirst April 11, 2017; DOI: 10.1158/1078-0432.CCR-17-0232

the manuscript, and Amaelle Otandault and Baptiste Auzemery for technical assistance.

Grant Support

This study was supported by the SIRIC Montpellier grant «INCa-DGOS-Inserm 6045» and BMS and Roche France. A.R. Thierry was supported by INSERM.

The costs of publication of this article were defrayed in part by the payment of page charges. This article must therefore be hereby marked *advertisement* in accordance with 18 U.S.C. Section 1734 solely to indicate this fact.

Received January 25, 2017; revised February 9, 2017; accepted April 6, 2017; published OnlineFirst April 11, 2017.

References

1. Fakih M. Biologic therapies in colorectal cancer: indications and contra-indications. Am Soc Clin Oncol Educ Book 2015;e197–206.
2. Li Z-Z, Wang F, Zhang Z-C, Wang F, Zhao Q, Zhang D-S, et al. Mutation profiling in chinese patients with metastatic colorectal cancer and its correlation with clinicopathological features and anti-EGFR treatment response. Oncotarget 2016;7:28356–68.
3. Blanco-Calvo M, Concha Á, Figueroa A, Garrido F, Valladares-Ayerbes M. Colorectal cancer classification and cell heterogeneity: a systems oncology approach. Int J Mol Sci 2015;16:13610–32.
4. Haley L, Tseng L-H, Zheng G, Dudley J, Anderson DA, Azad NS, et al. Performance characteristics of next-generation sequencing in clinical mutation detection of colorectal cancers. Mod Pathol 2015;28:1390–9.
5. Westwood M, van Asselt T, Ramaekers B, Whiting P, Joore M, Armstrong N, et al. KRAS mutation testing of tumours in adults with metastatic colorectal cancer: a systematic review and cost-effectiveness analysis. Health Technol Assess 2014;18:1–132.
6. Laurent-Puig P, Pekin D, Normand C, Kotsopoulos SK, Nizard P, Perez-Toralla K, et al. Clinical relevance of KRAS-mutated subclones detected with picodroplet digital PCR in advanced colorectal cancer treated with anti-EGFR therapy. Clin Cancer Res 2015;21:1087–97.
7. Ciardiello F, Normanno N, Maiello E, Martinelli E, Troiani T, Pisconti S, et al. Clinical activity of FOLFIRI plus cetuximab according to extended gene mutation status by next-generation sequencing: findings from the CAPRI-GOIM trial. Ann Oncol 2014;25:1756–61.
8. Caldas C. Cancer sequencing unravels clonal evolution. Nat Biotechnol 2012;30:408–10.
9. Gerlinger M, Rowan AJ, Horswell S, Larkin J, Endesfelder D, Gronroos E, et al. Intratumor heterogeneity and branched evolution revealed by multi-region sequencing. N Engl J Med 2012;366:883–92.
10. Swanton C. Intratumor heterogeneity: evolution through space and time. Cancer Res 2012;72:4875–82.
11. Diaz LA, Bardelli A. Liquid biopsies: genotyping circulating tumor DNA. J Clin Oncol 2014;32:579–86.
12. Thierry AR, El Messaoudi S, Gahan PB, Anker P, Stroun M. Origins, structures, and functions of circulating DNA in oncology. Cancer Metastasis Rev 2016;35:347–76.
13. Bettegowda C, Sausen M, Leary RJ, Kinde I, Wang Y, Agrawal N, et al. Detection of circulating tumor DNA in early- and late-stage human malignancies. Sci Transl Med 2014;6:224ra24.
14. Newman AM, Bratman SV, To J, Wynne JF, Eclov NCW, Modlin LA, et al. An ultrasensitive method for quantitating circulating tumor DNA with broad patient coverage. Nat Med 2014;20:548–54.
15. Diaz LA, Williams RT, Wu J, Kinde I, Hecht JR, Berlin J, et al. The molecular evolution of acquired resistance to targeted EGFR blockade in colorectal cancers. Nature 2012;486:537–40.
16. Murtaza M, Dawson S-J, Tsui DWY, Gale D, Forshew T, Piskorz AM, et al. Non-invasive analysis of acquired resistance to cancer therapy by sequencing of plasma DNA. Nature 2013;497:108–12.
17. Misale S, Yaeger R, Hobor S, Scala E, Janakiraman M, Liska D, et al. Emergence of KRAS mutations and acquired resistance to anti-EGFR therapy in colorectal cancer. Nature 2012;486:532–6.
18. Lièvre A, Bachet J-B, Le Corre D, Boige V, Landi B, Emile J-F, et al. KRAS mutation status is predictive of response to cetuximab therapy in colorectal cancer. Cancer Res 2006;66:3992–5.
19. Van Cutsem E, Lenz H-J, Köhne C-H, Heinemann V, Tejpar S, Melezínek I, et al. Fluorouracil, leucovorin, and irinotecan plus cetuximab treatment and RAS mutations in colorectal cancer. J Clin Oncol 2015;33:692–700.
20. Allegra CJ, Rumble RB, Hamilton SR, Mangu PB, Roach N, Hantel A, et al. Extended RAS gene mutation testing in metastatic colorectal carcinoma to predict response to anti-epidermal growth factor receptor monoclonal antibody therapy: American Society of Clinical Oncology Provisional Clinical Opinion Update 2015. J Clin Oncol 2016;34:179–85.
21. Sorich MJ, Wiese MD, Rowland A, Kichenadasse G, McKinnon RA, Karapetis CS. Extended RAS mutations and anti-EGFR monoclonal antibody survival benefit in metastatic colorectal cancer: a meta-analysis of randomized, controlled trials. Ann Oncol 2015;26:13–21.
22. Douillard JY, Siena S, Cassidy J, Tabernero J, Burkes R, Barugel M, et al. Final results from PRIME: randomized phase III study of panitumumab with FOLFOX4 for first-line treatment of metastatic colorectal cancer. Ann Oncol 2014;25:1346–55.
23. Boissière-Michot F, Lopez-Crapez E, Frugier H, Berthe M-L, Ho-Pun-Cheung A, Assenat E, et al. KRAS genotyping in rectal adenocarcinoma specimens with low tumor cellularity after neoadjuvant treatment. Mod Pathol 2012;25:731–9.
24. De Roock W, Claes B, Bernasconi D, De Schutter J, Biesmans B, Fountzilas G, et al. Effects of KRAS, BRAF, NRAS, and PIK3CA mutations on the efficacy of cetuximab plus chemotherapy in chemotherapy-refractory metastatic colorectal cancer: a retrospective consortium analysis. Lancet Oncol 2010;11:753–62.
25. Garcia-Murillas I, Schiavon G, Weigelt B, Ng C, Hrebien S, Cutts RJ, et al. Mutation tracking in circulating tumor DNA predicts relapse in early breast cancer. Sci Transl Med 2015;7:302ra133.
26. Reinert T, Schøler LV, Thomsen R, Tobiasen H, Vang S, Nordentoft I, et al. Analysis of circulating tumour DNA to monitor disease burden following colorectal cancer surgery. Gut 2016;65:625–34.
27. Douillard J-Y, Oliner KS, Siena S, Tabernero J, Burkes R, Barugel M, et al. Panitumumab-FOLFOX4 treatment and RAS mutations in colorectal cancer. N Engl J Med 2013;369:1023–34.
28. Kim M-J, Lee HS, Kim JH, Kim YJ, Kwon JH, Lee J-O, et al. Different metastatic pattern according to the KRAS mutational status and site-specific discordance of KRAS status in patients with colorectal cancer. BMC Cancer 2012;12:347.
29. Thierry AR, Mouliere F, Gongora C, Ollier J, Robert B, Ychou M, et al. Origin and quantification of circulating DNA in mice with human colorectal cancer xenografts. Nucleic Acids Res 2010;38:6159–75.
30. Mouliere F, Robert B, Arnau Peyrotte E, Del Rio M, Ychou M, Molina F, et al. High fragmentation characterizes tumour-derived circulating DNA. PLoS One 2011;6:e23418.
31. Thierry AR, Mouliere F, El Messaoudi S, Mollevi C, Lopez-Crapez E, Rolet F, et al. Clinical validation of the detection of KRAS and BRAF mutations from circulating tumor DNA. Nat Med 2014;20:430–5.
32. Mouliere F, El Messaoudi S, Pang D, Dritschilo A, Thierry AR. Multi-marker analysis of circulating cell-free DNA toward personalized medicine for colorectal cancer. Mol Oncol 2014;8:927–41.
33. El Messaoudi S, Mouliere F, Du Manoir S, Bascoul-Mollevi C, Gillet B, Nouaille M, et al. Circulating DNA as a strong multimarker prognostic tool for metastatic colorectal cancer patient management care. Clin Cancer Res 2016;22:3067–77.
34. Parseghian C, Parikh NU, Wu JY, Jiang Z-Q, Henderson LD, Tian F, et al. Dual Inhibition of EGFR and c-Src by cetuximab and dasatinib combined with FOLFOX chemotherapy in patients with metastatic colorectal cancer. Clin Cancer Res 2017 Mar 9. [Epub ahead of print].
35. Chiu RW, Poon LL, Lau TK, Leung TN, Wong EM, Lo YM. Effects of blood-processing protocols on fetal and total DNA quantification in maternal plasma. Clin Chem 2001;47:1607–13.
36. El Messaoudi S, Rolet F, Mouliere F, Thierry AR. Circulating cell free DNA: preanalytical considerations. Clin Chim Acta 2013;424:222–30.

Published OnlineFirst April 11, 2017; DOI: 10.1158/1078-0432.CCR-17-0232

37. Arena S, Bellosillo B, Siravegna G, Martínez A, Cañadas I, Lazzari L, et al. Emergence of multiple EGFR extracellular mutations during cetuximab treatment in colorectal cancer. Clin Cancer Res 2015;21:2157–66.
38. Esposito C, Rachiglio AM, La Porta ML, Sacco A, Roma C, Iannaccone A, et al. The S492R EGFR ectodomain mutation is never detected in KRAS wild-type colorectal carcinoma before exposure to EGFR monoclonal antibodies. Cancer Biol Ther 2013;14:1143–6.
39. Waring P, Tie J, Maru D, Karapetis CS. RAS mutations as predictive biomarkers in clinical management of metastatic colorectal cancer. Clin Colorectal Cancer 2016;15:95–103.
40. Bertotti A, Papp E, Jones S, Adleff V, Anagnostou V, Lupo B, et al. The genomic landscape of response to EGFR blockade in colorectal cancer. Nature 2015;526:263–7.
41. Thierry AR, Messaoudi SE, Mollevi C, Pastor B, Sanchez C, Raoul J-L, et al. Abstract 2632: clinical validation of circulating DNA analysis for the detection of point mutations and of the longitudinal metastatic colorectal patient follow up for detecting emergence of resistance to targeted therapy. Cancer Res 2016;76(14 Suppl):2632.
42. Ulz P, Auer M, Heitzer E. Detection of circulating tumor DNA in the blood of cancer patients: an important tool in cancer chemoprevention. Methods Mol Biol 2016;1379:45–68.
43. Uchi R, Takahashi Y, Niida A, Shimamura T, Hirata H, Sugimachi K, et al. Integrated multiregional analysis proposing a new model of colorectal cancer evolution. PLoS Genet 2016;12:e1005778.
44. Sasaki Y, Akasu T, Saito N, Kojima H, Matsuda K, Nakamori S, et al. Prognostic and predictive value of extended RAS mutation and mismatch repair status in stage III colorectal cancer. Cancer Sci 2016;107:1006–12.
45. Yen L-C, Yeh Y-S, Chen C-W, Wang H-M, Tsai H-L, Lu C-Y, et al. Detection of KRAS oncogene in peripheral blood as a predictor of the response to cetuximab plus chemotherapy in patients with metastatic colorectal cancer. Clin Cancer Res 2009;15:4508–13.
46. Spindler K-LG, Pallisgaard N, Appelt AL, Andersen RF, Schou JV, Nielsen D, et al. Clinical utility of KRAS status in circulating plasma DNA compared to archival tumour tissue from patients with metastatic colorectal cancer treated with anti-epidermal growth factor receptor therapy. Eur J Cancer 2015;51:2678–85.
47. Ryan BM, Lefort F, McManus R, Daly J, Keeling PWN, Weir DG, et al. A prospective study of circulating mutant KRAS2 in the serum of patients with colorectal neoplasia: strong prognostic indicator in postoperative follow up. Gut 2003;52:101–8.
48. Morelli MP, Overman MJ, Dasari A, Kazmi SMA, Mazard T, Vilar E, et al. Characterizing the patterns of clonal selection in circulating tumor DNA from patients with colorectal cancer refractory to anti-EGFR treatment. Ann Oncol 2015;26:731–6.
49. Kuo Y-B, Chen J-S, Fan C-W, Li Y-S, Chan E-C. Comparison of KRAS mutation analysis of primary tumors and matched circulating cell-free DNA in plasmas of patients with colorectal cancer. Clin Chim Acta 2014;433:284–9.
50. Altimari A, de Biase D, De Maglio G, Gruppioni E, Capizzi E, Degiovanni A, et al. 454 next generation-sequencing outperforms allele-specific PCR, Sanger sequencing, and pyrosequencing for routine KRAS mutation analysis of formalin-fixed, paraffin-embedded samples. OncoTargets Ther 2013;6:1057–64.
51. Gao J, Wu H, Wang L, Zhang H, Duan H, Lu J, et al. Validation of targeted next-generation sequencing for RAS mutation detection in FFPE colorectal cancer tissues: comparison with Sanger sequencing and ARMS-Scorpion real-time PCR. BMJ Open 2016;6:e009532.
52. Tougeron D, Lecomte T, Pagès JC, Villalva C, Collin C, Ferru A, et al. Effect of low-frequency KRAS mutations on the response to anti-EGFR therapy in metastatic colorectal cancer. Ann Oncol 2013;24:1267–73.
53. Siravegna G, Mussolin B, Buscarino M, Corti G, Cassingena A, Crisafulli G, et al. Clonal evolution and resistance to EGFR blockade in the blood of colorectal cancer patients. Nat Med 2015;21:827.
54. Perkins G, Yap TA, Pope L, Cassidy AM, Dukes JP, Riisnaes R, et al. Multi-purpose utility of circulating plasma DNA testing in patients with advanced cancers. PLoS One 2012;7:e47020.
55. Therkildsen C, Bergmann TK, Henrichsen-Schnack T, Ladelund S, Nilbert M. The predictive value of KRAS, NRAS, BRAF, PIK3CA and PTEN for anti-EGFR treatment in metastatic colorectal cancer: a systematic review and meta-analysis. Acta Oncol 2014;53:852–64.

Discussion

Ces deux études (*KPLEX2* et *KPLEXR*) ont été menée afin de confirmer les récentes avancées qui ont été faites dans le domaine des ADN circulants[43,173]. Aussi, dans un premier temps nous avons conduis une étude prospective, multicentrique et en aveugle sur 140 patients atteints de CCRm qui a pour objectif d'examiner la valeur de l'analyse de l'ADNcir plasmatique par rapport à l'analyse du tissu tumoral dans le cadre d'une prise en charge standard[43]. Il est a noté que cet essai se place dans un soucis d'une meilleure stratification des patients atteints CCRm avant l'initiation d'une thérapie ciblée anti-EGFR. Nous avons donc recherché les mutations *RAS/BRAF* dans le plasma de 140 patients atteints de CCRm avant l'initiation du traitement. La deuxième étude est réalisée sur 42 patients traités par FOLFOX, dasatinib avec ou sans cetuximab. L'analyse plasmatique longitudinal de ces patients permet d'établir des émergences de mutations *RAS/BRAF* pouvant entrainer une résistance secondaire aux anti-EGFR[173].

Pour les deux études présentées ici, nous avons réalisé l'analyse des mutations à partir de l'ADNcir sans seuil de sensibilité, alors qu'un seuil de > 0,5% pour la fréquence allélique avait été déterminé pour notre essai antérieur[76]. Cet essai antérieur a montré une forte concordance de l'analyse de l'ADNcir avec l'analyse du tissu tumoral pour la détection des mutations *RAS/BRAF* (96% pour les mutations de l'exon 2 de *KRAS* et 100% pour *BRAF V600E*)[76]. Par conséquent, le test de mutation de l'ADNcir présenté dans ces deux essais est significativement plus sensible (>50 fois) avec une sensibilité allant de 0,001% à 0,005% (fréquence allélique mutée) selon les mutations.

Dans chacune des deux études nous avons observés une baisse dans la concordance entre les analyses de l'ADNcir et les analyses réalisées sur tissu tumoral, et cela avant l'initiation du traitement. En considérant l'analyse sur le tissu tumoral comme le "gold standard", la concordance entre l'analyse de l'ADNcir et l'analyse du tissu pour le test *KRAS* exon 2 était de 72% et 71% dans nos essais publiés dans Annals of Oncology[43] et Clinical Cancer Research[173] respectivement.

Cela peut être expliqué par le fait que les techniques basées sur le Sanger, le pyroséquençage, le NGS ou la Q-PCR présentent des sensibilités différentes (10 %, 2 %-5 %, 1 % et 0,1 %, respectivement), ce qui entraîne une variabilité analytique[220,221]. De plus, nous avons procédé

à un examen approfondi des différents facteurs pouvant entraîner une discordance entre l'analyse des tissus tumoraux et celle du plasma. Nous avons montré que la médiane du délai entre la réception de l'échantillon de tissu et communication des résultats était de 12 jours contre seulement de 2 jours pour la réception du plasma et la communication des résultats. Nos données ont également révélé que l'utilisation d'une biopsie, l'absence de la tumeur primaire au moment de la prise de sang ou un long délai entre le prélèvement du tissu tumoral et la prise de sang altèrent principalement la spécificité et la sensibilité[43]. Par conséquent, l'une des principales limites de l'analyse des tissus tumoraux est que l'échantillonnage peut ne pas refléter l'hétérogénéité de la tumeur, en particulier dans les cancers avancés en raison (i) de l'hétérogénéité intra-tumorale, (ii) inter-tumorale et (iii) temporelle[51,59,218,220,222–225]. À la lumière de nombreuses études récentes, il est maintenant clair qu'il existe un niveau constant de discordance allant de 3,6 % à 17,5 %[223] du statut mutationnel *RAS* entre la tumeur primaire et la métastase appariée.

Les mutations dont la prévalence est extrêmement faible (0,005%) peuvent être détectées par la méthode IntPlex, car les expériences menées selon la distribution de la loi de Poisson ont démontré sans équivoque qu'un fragment muté peut être détecté de manière fiable[43]. Il faut noter qu'il n'y a pas de signification établis entre les mutations *RAS* à faible prévalence et l'efficacité de la thérapie anti-EGFR[173,226,227]. Par conséquent, la nécessité d'un seuil de sensibilité tel qu'observé précédemment pour les tissus tumoraux ne peut être appliqué à l'analyse du plasma. Il faut toutefois noter que la notion de sensibilité analytique entre l'analyse sur tissu et l'analyse de l'ADNcir est difficilement comparable. La sensibilité est directement liée au nombre de cellules malignes portant la mutation dans une région macro- ou micro-dissection d'une section de tissu. Ce n'est pas le cas pour l'ADNcir en raison de la libération importante d'ADN circulant par les cellules du micro-environnement ou par les cellules immunitaires circulantes, ce qui entraîne parfois des quantités élevées d'ADN circulant, comme l'illustre la grande variation de la fréquence allélique des mutations de l'ADNcir (0,003 %-99 %)[131,135].

Ce dernier point est critique et un véritable challenge lorsque l'on veut suivre l'évolution tumoral d'un patient traité aux anti-EGFR. La pression sélective exercée par les thérapies ciblées, associée à l'hétérogénéité clonale spatiale et temporelle, constitue un défi clinique complexe. La détection précoce de la résistance secondaire peut avoir un impact sur les

résultats cliniques comme l'a suggéré Bertotti et ses collègues[228] en caractérisant la résistance secondaire au blocage de l'EGFR dans le CCRm. Ils ont observé que les altérations de *KRAS*, *NRAS* et *BRAF* étaient des mécanismes importants de résistance[228]**.** Aussi, des travaux ont montré la capacité de l'ADNcir pour détecter la résistance secondaire aux thérapies anti-EGFR[66–68]. Nous avons pu établir que 64% de l'ensemble des mutations retrouvées avant traitement et au cours du traitement ont des fréquences alléliques inférieurs à 1% et 21% d'entre elles ont des fréquences alléliques inférieures à 0.1%[173]. Il est intéressant de noter que des sous-clones mutés émergents durant le traitement sont retrouvés avec des fréquences alléliques inférieurs à 0.1%[173].

Ces résultats renforcent le fait que l'analyse de l'ADNcir et notamment pour la stratification des patients en vue d'une thérapie anti-EGFR ou pour le suivi des patients sous thérapies ciblées ne peut se faire en utilisant un seuil de sensibilité. Cela montre la nécessité d'une méthode ultrasensible pour détecter les mutations ponctuelles. L'analyse de l'ADNcir nécessitent une simple prise de sang, qui peut être réalisée à tout moment d'une prise en charge thérapeutique du patient. Aussi, de par sa sensibilité l'ADNcir permettrait dans la routine clinique d'optimiser la prise en charge des patients atteints de CCRm.

Afin de pouvoir implémenter en pratique clinique l'analyse de l'ADNcir, il est nécessaire de réaliser une étude interventionnelle où l'analyse de l'ADNcir est utilisée pour déterminer le statut *RAS/BRAF* des patients atteinte de CCRm avant un traitement par anti-EGFR. C'est dans ce contexte qu'est menée l'étude PANIRINOX.

PANIRINOX : Etude randomisée de phase II comparant le Panitumumab + FOLFIRINOX versus Panitumumab + mFOLFOX6 chez des patients atteints de cancer colorectal métastatique ayant un statut *RAS/BRAF* non muté sélectionnés à partir de l'analyse de l'ADN circulant (NCT02980510).

Trial title: « Phase II randomized study comparing FOLFIRINOX + Panitumumab versus mFOLFOX6 + Panitumumab in metastatic colorectal cancer patients selected by RAS and B-RAF status from circulating DNA analysis **»**

Financement et Sponsors : Cette étude prospective, randomisée et interventionnelle est financée par AMGEN et sponsorisée par UNICANCER Recherche et Développement.

Originalités : Cette étude est le premier essai interventionnel où l'analyse de l'ADNcir est utilisée pour déterminer le statut *RAS/BRAF* des patients atteints de CCRm avant l'initiation d'une thérapie ciblée anti-EGFR. Aussi, un patient déterminé avec une mutation *RAS/BRAF* avec une fréquence allélique inférieur à 0.5% est déterminé comme non muté et peut être inclus dans l'essai. Ce seuil a été déterminé par AMGEN afin de réduire le nombre de faux positifs.

Promoteur et Coordinateurs : Le promoteur de cet essai est l'Institut régional du Cancer de Montpellier (ICM) et elle coordonnée par le Dr. Thibault MAZARD et le Dr. Alain THIERRY. Je suis responsable des analyses des ADNcir pour le screening des patients avant leur entrée dans l'étude et je serai en charge des analyses de suivi des patients au cours de leur traitement. L'inclusion des patients atteints de CCRm mobilise actuellement 29 centres de soins français.

Rationnel de l'étude : Le FOLFOX plus panitumumab est devenu un traitement standard depuis les résultats de l'étude PRIME[29]. Chez les patients avec un bon état de performance ECOG (Eastern Cooperative Oncology Group), les trithérapies cytotoxiques associées aux thérapies anti-EGFR atteignent une activité impressionnante (>70% de réponse objective) et permettent des métastasectomies secondaires R0 (taux de 28 à 35%) dans plusieurs études de phase II[229–231]. Néanmoins, la comparaison de l'association anti-EGFR avec un doublet de chimiothérapie versus un triplet chimiothérapie manque encore.

Pour déterminer le statut mutationnel *RAS/BRAF*, nous avons déjà démontré la validité clinique et l'utilité de l'analyse de l'ADN circulant (ADNcir) par la méthode IntPlex[43,76]. Dans une étude prospective multicentrique, rassemblant 106 patients atteints de mCRC avant

l'initiation d'un traitement anti-EGFR, l'analyse de l'ADNcir a montré un taux de concordance de 96 % pour les mutations de l'exon 2 du gène *KRAS* et de 100% pour la mutation *BRAFV600E*, par rapport à l'analyse du tissu tumoral[76]. Dans une autre étude clinique prospective multicentrique menée en aveugle et en flux tendu, incluant 140 patients atteints de CCRm, nous avons montré que l'analyse de l'ADNcir réduisait avantageusement le délai d'attente avant communication des résultats par rapport à l'analyse du tissu tumoral (délai médian = 2 jours contre 12 jours). Lorsqu'aucun seuil de détection de mutation n'est appliqué, l'analyse de l'ADNcir révèle également davantage de mutations détectée que l'analyse du tissu tumoral et de nombreuses mutations concomitantes, reflétant ainsi plus fidèlement l'hétérogénéité tumorale[43]. Comme indiqué par Van Cutsem il manque une étude interventionnelle « dans la vraie vie » démontrant l'avantage de l'analyse des ADNcir afin de finaliser l'évaluation dans un contexte théranostique et de promouvoir largement cette approche diagnostique en oncologie. Actuellement aucune étude interventionnelle n'a été mené pour sélectionner les patients en vue d'un traitement par anti-EGFR dans le cadre du cancer colorectal métastatique. Par conséquent nous avons choisi de sélectionner les patients ayant un statut mutationnel *RAS/BRAF* non muté à partir de l'analyse de l'ADNcir via la méthode IntPlex.

Objectifs de l'étude : L'objectif principal de l'essai est d'évaluer le taux de réponse complète au traitement associant FOLFIRINOX + panitumumab, et par conséquent nous évaluerons la disparition complète des métastases après 12 cycles de chimiothérapie. Un autre groupe recevant le traitement standard, mFOLFOX6 + panitumumab, sera utilisé comme groupe contrôle. Plusieurs objectifs secondaires seront investigués comme la survie globale (OS), la survie sans progression (PFS), le taux de résection secondaires ou encore la performance diagnostique de l'analyse de l'ADNcir par rapport à l'analyse du tissu tumoral.

Dans le cadre d'une étude ancillaire de cet essai, nous réalisons également un suivi par l'analyse des ADNcir des patients CCRm inclus et traités par anti-EGFR. Les échantillons de sang sont prélevés tous les 4 cycles de traitement. Cette étude est financée par la Ligue contre le Cancer et sera coordonnée par le Dr. Alain THIERRY et le Pr. Thierry ANDRE. L'objectif ancillaire est de détecter via l'analyse de l'ADNcir, l'émergence de mutations acquises *RAS, BRAF* et *PIK3CA* durant le traitement anti-EGFR et de corréler l'apparition de ces mutations avec l'OS et la PFS.

Principaux critères d'inclusion : Les patients âgés de 18 à 75 ans avec un ECOG PS entre 0 et 1, un adénocarcinome colorectal confirmé histologiquement, une maladie métastatique synchrone ou métachrone non traitée et jugée non résécable avec intention curative ; un statut tumoral *KRAS* (codons 12, 13, 61, 117, 146), *NRAS* (codons 12, 13, 61) et *BRAFV600E* non mité selon l'analyse plasmatique de l'ADNcir par la technologie Intplex ; une maladie mesurable selon RECIST version 1. 1 et des fonctions hématologiques, hépatiques et rénales adéquates pouvaient être incluses.

Principaux critères d'exclusion : Les patients ayant reçu un traitement adjuvant à l'oxaliplatine, un traitement antérieur pour une maladie métastatique, des métastases cérébrales, des antécédents d'hypersensibilité grave ou potentiellement mortelle aux substances actives ou à l'un des excipients administrés dans cette étude, une transplantation d'organe antérieure, le VIH ou d'autres syndromes d'immunodéficience, des médicaments/comorbidités concomitants pouvant empêcher le patient de recevoir le traitement de l'étude, des antécédents d'autres tumeurs malignes au cours des 5 dernières années et d'autres cancers concomitants sont exclus.

Design de l'étude : 209 patients non mutés *RAS/BRAF* seront randomisés 2:1 entre FOLFIRINOX-panitumumab (N=139) et mFOLFOX6-panitumumab (N=70) avec 12 cycles prévus dans chaque bras. Pour chaque bras, les patients sont stratifiés en fonction de l'étendue de la maladie (maladie non limitée ou limitée au foie) **(Figure 22)**.

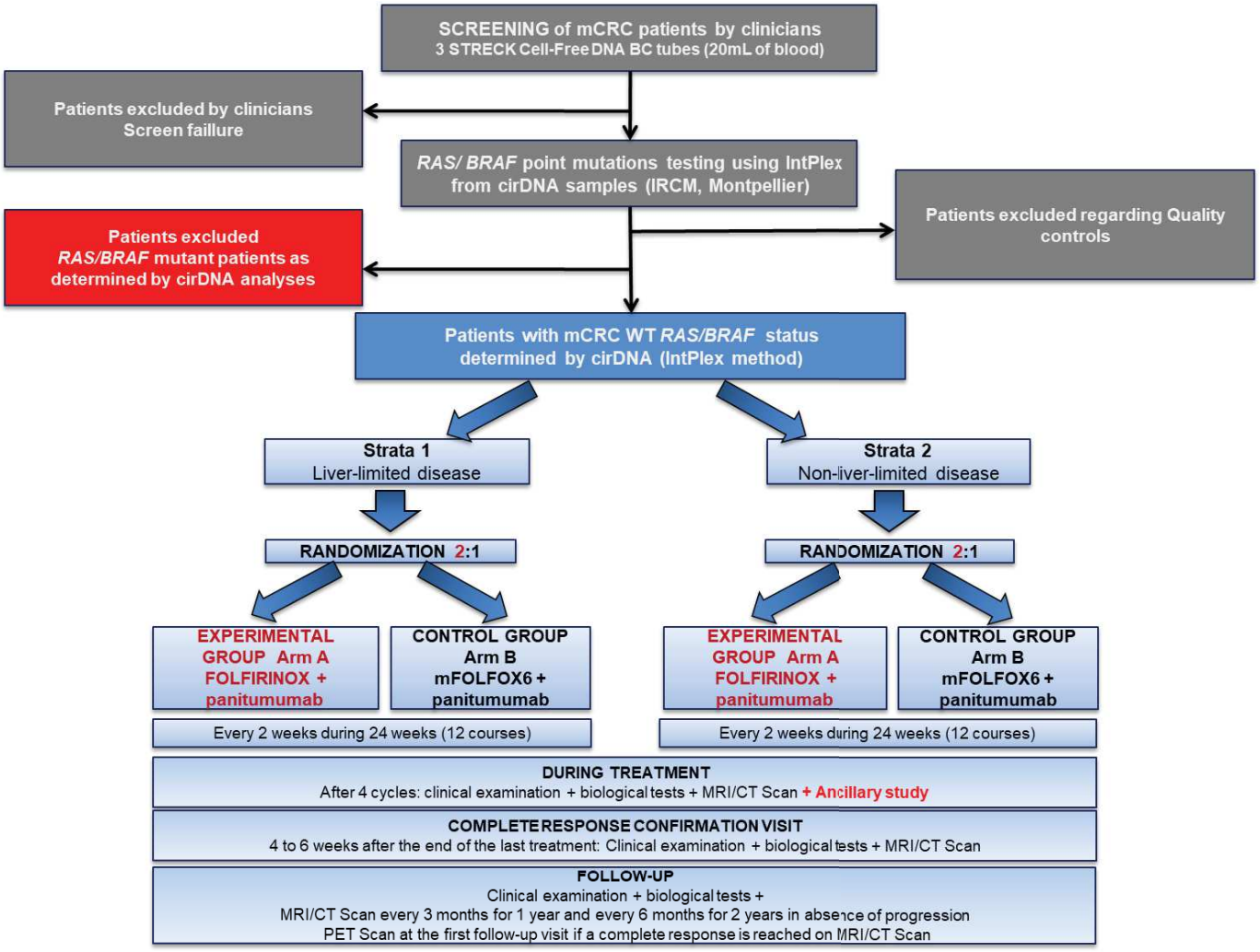

Figure 22 : Diagramme schématisant le design de l'essai PANIRINOX.

Matériels et Méthodes : Les patients atteints de CCRm sont enrôlés dans 29 centres de soins français après avoir signé un consentement éclairé. Le sang des patients atteints de CCRm est collecté dans trois tubes STRECK (Cell-Free DNA BCT®) et les tubes sont envoyés dans les 24 heures à température ambiante au laboratoire du Dr. Alain THIERRY (IRCM, Institut de Recherche en Cancérologie de Montpellier, U1194 INSERM). Les tubes de sang sont centrifugés 10 minutes à 1200 x g à 4°C et le surnageant de plasma est immédiatement centrifugé à 16 000 x g à 4°C pendant 10 minutes. L'ADNcir est extrait à partir de 1mL de plasma à l'aide du kit QIAamp DNA Mini Blood (Qiagen) dans un volume d'élution de 130µL. L'ADNcir est également extrait trois fois à partir de 1mL de plasma à l'aide de l'instrument Maxwell® RSC en utilisant le kit ccfDNA plasma (Promega Corporation) dans un volume

d'élution de 130µL. Les quatre extraits d'ADNcir sont conservés à -20°C jusqu'à leur utilisation ou utilisés immédiatement. Le plasma comme l'extrait d'ADN subit un stringent contrôle qualité conformément aux directives pré-analytiques que nous avons publiés. (Guidelines : El Messaoudi Clin Chem Acta, 2013 ; Meddeb, 2019). L'analyse de l'ADNcir est réalisée via la méthodologie IntPlex décrite dans le manuscrit (voir partie 5.C).

Les résultats de l'analyse des ADNcir sont rendus aux centres investigateurs et au sponsor UNICANCER dans les 5 jours après avoir reçu les prélèvements de sang au laboratoire (IRCM).

Contribution: Dans ce projet je suis le responsable des analyses des ADNcir. Mon rôle est de gérer la réception, le stockage et les analyses des échantillons de sang reçus. Je suis en charge du rendu des résultats, du reporting des résultats et de la gestion de la banque biologique de l'essai PANIRINOX (Plasmas/extraits ADNcir). Je gère sous la direction de AR Thierry les ressources humaines dédiées à ces analyses auxquelles participent 4 autres membres du laboratoire en fonction du nombre de plasmas reçus et des absences.

Résultats : L'étude est actuellement dans les dernier mois d'inclusion des patients. Au 31 janvier 2022, nous avons reçus 479 prélèvements de sang provenant de 462 patients atteints de CCRm. Il est possible que nous recevons deux prélèvements distincts pour un même patient dans le cas où le premier prélèvement n'est pas analysable car le contrôle qualité n'est pas satisfaisant (Hémolysé, ictérique, volume de plasma insuffisant, concentration en ADNcir inferieur à 3ng/mL de plasma, transport…). Actuellement, 177 patients sur 462 patients analysés par la méthode IntPlex ont été inclus dans l'essai PANIRINOX **(Figure 23)**. Nos analyses montrent que nous avons 38% de patients non mutés pour les mutations *RAS/BRAF*. Afin d'atteindre nos objectifs et posséder une puissance statistique conséquente, au moins 209 patients doivent être inclus dans l'essai. Nous sommes environ à 85% des inclusions nécessaires et nous pensons les terminer au cours de l'été 2022. Une fois les inclusions terminées nous commencerons à analyser le suivi des patients traités par anti-EGFR.

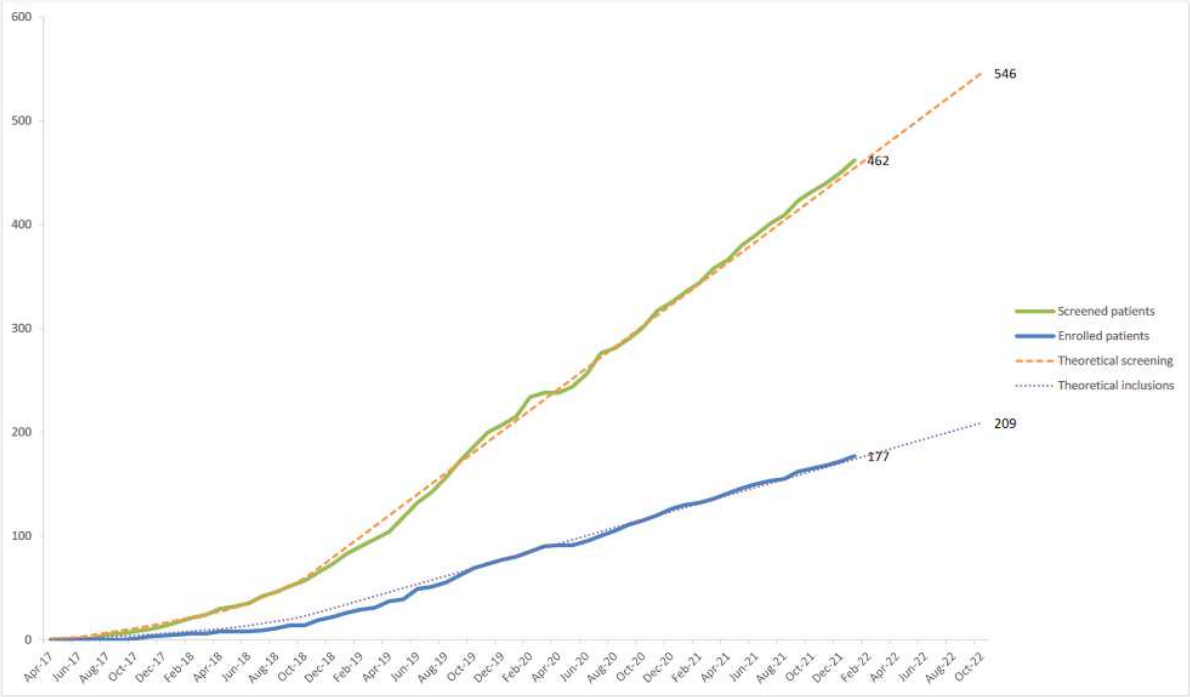

Figure 23 : Bilan global des inclusions de l'essai PANIRINOX.

Perspectives : Dans le cadre de l'analyse des ADNcir en oncologie, nous espérons que ce premier essai prospectif, multicentrique et interventionnel démontrera l'utilité clinique de son analyse pour l'orientation des traitements dans le cadre des cancers colorectaux métastatiques. Nous espérons que cet essai puisse permettre l'implémentation clinique de l'analyse de l'ADNcir pour la détection des mutations *RAS/BRAF* dans le cadre du cancer colorectal métastatique. Nous pensons également que cet essai ouvrira la voie à d'autres essais interventionnels incluant l'analyse des ADNcir dans différents types de cancers. Le suivi de ces patients CCRm via l'analyse des ADNcir permettra d'établir l'impact de la détection de l'émergence de mutations *RAS/BRAF/PIK3CA* dans la survie des patients et le rôle de ces mutations dans la résistance aux traitements anti-EGFR.

B/ Détection des mutations *RAS/BRAF* chez des patients atteints de CCRm traités par régorafénib

Article III*:* Surveillance des niveaux d'ADN circulant chez les patients atteints de cancer colorectal métastatique en tant que biomarqueur potentiel des réponses au traitement par régorafenib

Brice Pastor, Thierry Andre, Julie Henriques, Isabelle Trouilloud, Christophe Tournigand, Marine Jary, Thibault Mazard, Christophe Louvet, Simon Azan, Audrey Bauer, Benoit Roch, Cynthia Sanchez, Dewi Vernerey, Alain R. Thierry and Antoine Adenis

Rationnel: Cette étude fait partie intégrante de mon travail de thèse puisqu'il a pour objectif de prédire via l'analyse des ADNcir une résistance ou une sensibilité à un traitement anti-cancéreux. Actuellement, il n'existe aucun marqueur prédictif de la réponse au régorafénib qui est pourtant un médicament prescrit aux patients atteints de CCRm en échec thérapeutique face aux thérapies standards. Ces patients en dernière ligne de traitement et traités au régorafénib ont beaucoup d'effets secondaires liés à cette molécule. Il est donc crucial de distinguer les répondeurs des non répondeurs afin d'éviter l'acharnement thérapeutique et pouvoir ne traiter que les patients qui auront un bénéfice clinique.

Contribution: Dans ce projet j'ai réalisé les analyses de quantification des concentrations des ADNcir totaux ainsi que la détection et ka quantification des ADNcir mutés des patients atteints de CCRm. J'ai participé à l'écriture du manuscrit.

Introduction

Les patients atteints de CCRm sont traités, de manière concomitante ou séquentielle, avec différents agents cytotoxiques tels que les fluoropyrimidines, l'oxaliplatine et l'irinotécan, qui peuvent être associés à des anticorps monoclonaux dirigés contre le facteur de croissance vasculaire endothélial (VEGF) ou le récepteur du facteur de croissance épidermique (EGFR)[202]. Cette dernière combinaison est limitée aux patients présentant des tumeurs de type sauvage des gènes *KRAS* et *NRAS* (*RAS*). Enfin, les patients CRCm réfractaires à ces traitements standards, des agents oraux tels que le trifluridine/tipiracil ou le regorafenib peuvent être envisagés[202].

Le régorafénib est un inhibiteur de plusieurs tyrosines kinases qui montre *in vitro* et *in vivo* des activités anti-angiogéniques et cytotoxiques[35]. Il a été approuvé dans l'Union européenne pour les patients atteints de CCRm réfractaire aux thérapies standards sur la base de son activité par rapport au placebo et aux meilleurs soins de soutien dans les essais cliniques de phase III CORRECT et CONCUR[36,37]. Dans ces deux études, le régorafénib a démontré une amélioration significative de la survie globale (ou overall survival, OS) chez les patients atteints de CCRm qui avaient progressé après les traitements standard[36,37].

Cependant, la moitié des patients traités ont vu leur tumeur progresser deux mois après le début du traitement, ce qui les a exposés inutilement à des effets indésirables liés au regorafenib. Ce risque de toxicité pourrait être réduit en adoptant une stratégie d'escalade de dose pour optimiser le dosage du regorafenib mais avec une activité comparable[232]. Aussi, des études ont essayé de déterminer des marqueurs de non réponse au régorafenib. De manière intéressante, il a été observé une association entre un taux initial élevé d'ADNc et une réduction de la médiane réduite[233]. Par la suite, dans une étude rétrospective portant sur 654 patients atteints de CCRm qui ont reçu du régorafénib dans un programme d'utilisation compassionnelle, la survie globale était amoindri de manière indépendante par un mauvais status de performance ECOG (Eastern Cooperative Oncology Group), le court délai entre le diagnostic initial des métastases et le début du traitement par régorafénib, la faible dose initiale de régorafénib, un nombre de site métastatique >3, la présence de métastases hépatiques et la présence de mutations tissulaires du gène *KRAS*[234].

Cependant, il n'existe actuellement aucun marqueur largement accepté permettant de prédire les bénéfices du régorafénib. L'ADNcir est un biomarqueur plasmatique largement utilisé en oncologie[175], notamment pour détecter les mutations ponctuelles des gènes *RAS/BRAF* avant l'initiation des anticorps monoclonaux anti-EGFR chez les patients atteints de CRCm[43,76,182,235–237]. De plus, l'analyse longitudinale de l'ADNcir a été utilisée pour étudier l'hétérogénéité clonale temporelle et spatiale des tumeurs chez des patients atteints de mCRC au cours de traitements anti cancéreux[67,173,198,211,238,239].

L'essai de phase II TEXCAN (NCT02699073) visait à évaluer la réponse tumorale chez des patients réfractaires aux thérapies standards après 2 mois de traitement par regorafenib[240]. Nous avons participé à une des études ancillaires de l'essai TEXCAN. Dans cette étude translationelle et prospective, nous avons étudié l'activité clinique du régorafénib en analysant l'ADNcir chez 43 patients réfractaires aux thérapies standard. L'analyse longitudinale des plasmas par la méthode de Q-PCR IntPlex a été réalisé avant l'initiation du régorafénib en monothérapie, pendant le traitement et ce jusqu'à la fin du traitement. Les paramètres qualitatifs (détection des mutations *KRAS*, *NRAS, BRAV600E*) et quantitatifs (la concentration totale des ADNcir, la concentration des ADNcir mutés et la fraction allélique) ont été corrélé avec la survie globale et la survie sans progression des patients.

Molecular Oncology

FEBS PRESS

Monitoring levels of circulating cell-free DNA in patients with metastatic colorectal cancer as a potential biomarker of responses to regorafenib treatment

Brice Pastor[1], Thierry André[2,3], Julie Henriques[4], Isabelle Trouilloud[2,3], Christophe Tournigand[3,5], Marine Jary[3,6,7], Thibault Mazard[1,8], Christophe Louvet[3,9], Simon Azan[1], Audrey Bauer[1], Benoit Roch[1,10], Cynthia Sanchez[1], Dewi Vernerey[3,4], Alain R. Thierry[1,8] and Antoine Adenis[1,8]

1 Institut de Recherche en Cancérologie de Montpellier (IRCM), INSERM, Université de Montpellier, Montpellier Cancer Institute (ICM), France
2 Department of Medical Oncology, Saint-Antoine University Hospital, Sorbonne University, Paris, France
3 Oncology Multidisciplinary Research Group (GERCOR), Paris, France
4 Methodology and Quality of Life Unit in Oncology, Besançon University Hospital, France
5 Medical Oncology Service, Henri Mondor Hospital, AP-HP, Université Paris Est Créteil Créteil, France
6 INSERM, Etablissement Français du Sang Bourgogne Franche-Comté, UMR1098, Interactions Hôte-Greffon-Tumeur/Ingénierie Cellulaire et Génique, Bourgogne Franche-Comté University, Besançon, France
7 Department of Medical Oncology, Besançon University Hospital, France
8 Department of Medical Oncology, Montpellier Cancer Institute (ICM), France
9 Department of Medical Oncology, Institut Monsouris, Paris, France
10 Department of Thoracic Oncology, Montpellier University Hospital, Université de Montpellier, France

Keywords
circulating DNA; colorectal cancer; predictive biomarker; regorafenib; tumor response

Correspondence
A. Adenis, Department of Medical Oncology, Institut régional du Cancer de Montpellier, 208 avenue des Apothicaires, 34000, Montpellier, France
Fax: + 33 (0)4 67 61 30 62
Tel: + 33 4 67 61 47 01
E-mail: antoine.adenis@icm.unicancer.fr
A. R. Thierry, Institut de Recherche en Cancérologie de Montpellier, Inserm U1194, Campus Val d'Aurelle, 208 rue des Apothicaires, 34298 Montpellier Cedex 5, France
Tel: +33 6 63 82 19 94
E-mail: alain.thierry@inserm.fr

(Received 29 October 2020, revised 9 March 2021, accepted 20 April 2021, available online 22 June 2021)

doi:10.1002/1878-0261.12972

Circulating cell-free DNA (cfDNA) contains circulating tumor DNA (ctDNA), which can be obtained from serial liquid biopsies to enable tumor genome analysis throughout the course of treatment. We investigated cfDNA and mutant ctDNA as potential biomarkers to predict the best outcomes of regorafenib-treated metastatic colorectal cancer (mCRC) patients. We analyzed longitudinally collected plasma cfDNA of 43 mCRC patients prospectively enrolled in the phase II TEXCAN trial by IntPlex qPCR. Qualitative (*KRAS*, *NRAS*, $BRAF^{V600E}$ mutations) and quantitative (total cfDNA concentration, mutant ctDNA concentration, mutant ctDNA fraction) parameters were correlated with overall survival (OS) and progression-free survival (PFS). When examined as classes or continuous variables, the concentrations of total cfDNA, mutant ctDNA, and, partly, mutant ctDNA fraction prior to regorafenib treatment correlated with OS. Patients with baseline cfDNA > 26 ng·mL^{-1} had shorter OS than those with cfDNA value below this threshold (4.0 vs 6.9 months; log-rank $P = 0.0366$). Patients with baseline mutant ctDNA > 2 ng·mL^{-1} had shorter OS than those with mutant ctDNA below this threshold (log-rank $P = 0.0154$). We show that pretreatment cfDNA and mutant ctDNA levels may identify mCRC patients that may benefit from regorafenib treatment.

Abbreviations
95% CI, 95% confidence interval; C1, cycle 1; C2, cycle 2; cfDNA, circulating cell-free DNA; CRC, colorectal cancer; ctDNA, circulating tumor DNA; ECOG PS, Eastern Cooperative Oncology Group performance status; EGFR, epidermal growth factor receptor; EOT, end of treatment; HR, hazard ratio; IQR, interquartile range; mCRC, metastatic colorectal cancer; OS, overall survival; PFS, progression-free survival; RECIST, response evaluation criteria in solid tumors; WT, wild-type.

1. Introduction

Colorectal cancer (CRC) is a major cause of morbidity and mortality globally [1]. In 2018, there were nearly 2 million newly diagnosed patients and almost 880 792 deaths. Approximately 50% of patients develop metastasis, and most of them require palliative treatment. In that setting, patients with metastatic CRC (mCRC) are treated, concomitantly or sequentially, with different cytotoxic agents such as fluoropyrimidines, oxaliplatin, and irinotecan that may be combined with monoclonal antibodies against vascular endothelial growth factor or epidermal growth factor receptor (EGFR) [2]. The latter combination is restricted to patients with *KRAS* and *NRAS* (*RAS*) wild-type (WT) tumors. In otherwise standard therapies-refractory mCRC patients, oral agents such as trifluridine/tipiracil or regorafenib could be considered [2].

Regorafenib is a multityrosine kinase inhibitor that induces *in vitro* and *in vivo* anti-angiogenic and cytotoxic activities [3]. It was approved in the European Union for refractory mCRC based on the report of its activity versus placebo plus best supportive care in the CORRECT and CONCUR phase III clinical trials [4,5]. In these two studies, regorafenib demonstrated a significant improvement in overall survival (OS) in patients with mCRC who progressed on standard therapies [4,5]. However, half of the treated patients experienced tumor progression 2 months after starting treatment, which unnecessarily exposed them to treatment-related adverse events. That toxicity risk could be reduced by adopting a dose-escalation strategy for optimizing regorafenib dosing with comparable activity [6]. In an exploratory study of the pivotal CORRECT trial [4], Tabernero *et al.* (2015) showed a trend toward a better survival for patients treated with regorafenib who presented *KRAS* or *PIK3CA* WT genotypes, assessed using tissue DNA or circulating cell-free DNA (cfDNA). Interestingly, they also observed an association between high baseline cfDNA and reduced median OS [7]. Subsequently, in a retrospective study of 654 patients with mCRC who received regorafenib in a compassionate use program reported by Adenis *et al.* [8] OS was independently and unfavorably affected by poor performance status, short time from initial diagnosis of metastasis to the start of regorafenib treatment, low initial regorafenib dose, > 3 metastatic sites, the presence of the liver metastasis, and tissue *KRAS* mutations. However, there are currently no widely accepted criteria predicting benefits from regorafenib.

Circulating cell-free DNA is a plasma biomarker widely used in oncology [9], notably for detecting *RAS*/*BRAF* point mutations before the initiation of anti-EGFR agents in mCRC patients [10–15]. Moreover, longitudinally analysis of cfDNA was used to address the temporal and spatial clonal heterogeneity of mCRC patients [16–21].

Phase II TEXCAN trial aimed to evaluate tumor response in refractory, progressing mCRC patients after 2 months of treatment with regorafenib [22]. In the present study, we investigated the clinical activity of regorafenib in those patients according to analysis of circulating cfDNA.

2. Materials and method

2.1. Patients and study design

TEXCAN (NCT02699073) was a multicenter, prospective, open-label, single-arm phase II trial of patients with mCRC refractory to standard therapy. The study aimed to evaluate the 2-month tumor response to treatment with regorafenib (160 mg once daily for 3 weeks, followed by 1 week off therapy) using different measurement methods. Inclusion/exclusion criteria, study design, study objectives/endpoints, and clinical results have been previously reported [22]. Briefly, 55 patients (the intent-to-treat population) received at least one regorafenib tablet (1 tablet = 40 mg). According to response evaluation criteria in solid tumors (RECIST) 1.1, no partial and complete responses were observed. The best overall response observed was stable disease in 20/35 patients evaluable for the primary endpoint (i.e., a 2-month clinical response). The median OS was 5.3 months (95% confidence interval [CI]: 3.7–8.6). Unlike RECIST, other measurement methods, specifically Choi and modified Choi criteria, did not identify any survival benefit for mCRC patients [22].

The trial was submitted and approved by French regulatory authorities (Agence Nationale de Sécurité du Médicament et des Produits de Santé and the Comité de Protection des Personnes Ile de France VI [French Ethics Committee]; it complies with the Declaration of Helsinki and local regulations, and follows the standards of Good Clinical Practice (ICH-E6 R2). All patients provided a written informed consent. An exploratory analysis aimed (a) to determine whether a correlation exists between baseline cfDNA levels and survival outcomes, (b) to evaluate the dynamic of total cfDNA during treatment, and (c) to determine the *RAS*/*BRAF* mutational status in plasma samples, at baseline and at the end of treatment (EOT). Of 55 included patients, 12 were excluded because their

baseline samples failed to comply with our pre-analytical requirements ($n = 9$) [23,24] or lost during transportation ($n = 3$), leaving 43 eligible patients for cfDNA analysis (the cfDNA population; Fig. 1).

2.2. Sample preparation

Blood samples were collected between March 2016 and July 2017 in ethylenediaminetetraacetic acid tubes and centrifuged at 1200 ***g*** for 10 min at 4 °C, within 4 h after collection. Blood draws for cfDNA analysis were scheduled at baseline (before regorafenib therapy), during treatment (day 15 of cycles 1 and 2), and at the EOT. Plasma samples were immediately stored at 80 °C and transferred on dry ice from the recruiting institutions to our laboratory. Plasma was stored few months (4–24 months), and plasma was centrifuged at 16 000 ***g*** for 10 min at 4 °C. Total cfDNA was extracted from 1 mL of plasma using the QIAamp DNA Mini Blood Kit (Qiagen, Hilden, Germany) in accordance with the previously published pre-analytic guidelines [23,24] in an elution volume of 130 µL. DNA extracts were kept few days (1 to 3 days) at −20 °C until use if not used immediately. Circulating cfDNA was also extracted from 1 mL plasma (Maxwell® RSC Instrument) using the cfDNA Plasma Kit (Promega Corporation, Madison, WI, USA) in an elution volume of 130 µL. In total, 136 serial plasma samples from 43 patients were analyzed. We strictly followed the pre-analytical requirements to quantify cfDNA under the best conditions (plasma isolation, plasma storage at −80 °C; [23,24]). No significant variation of cfDNA concentration as determined by the WT sequence of the *KRAS* (67 bp length) was found upon storage at −80 °C [23–25] for up to 3 years. We performed analysis of all pre-analytical factors such as storage.

2.3. IntPlex® analysis of cfDNA

Analysis of cfDNA was done by IntPlex®, an allele-specific blocker quantitative PCR (ASB qPCR), which we previously described [10,21,26], according to the MIQE guidelines [27,28]. This IntPlex system specifically detect nuclear cfDNA. qPCR amplifications were carried out at least in two replicates in a total volume of 25 µL on a CFX96 instrument using the CFX manager software (Bio-Rad, Hercules, CA, USA). Each PCR was composed of 12.5 µL of IQ Supermix SYBR Green (Bio-Rad), 2.5 µL of DNase-free water (Qiagen) or specific oligoblocker, 2.5 µL of forward and reverse primers (0.3 pmol·mL^{-1}), and 5 µL of template. Thermal cycling comprised three repeated steps: a hot start activation step at 95 °C for 3 min, followed by 40 cycles of denaturation–amplification at 95 °C for 10 s, and then at 60 °C for 30 s. Melting curves were investigated by increasing the temperature from 60 to 90 °C with a plate reading every 0.2 °C. Standard curves were performed for each run with a genomic extract of the DiFi cell line at 1.8 ng·µL^{-1} of DNA. Each PCR run was carried out with no template control and positive control for each primer set. Positive controls were extracted from cell lines bearing *KRAS*/*BRAF* or *NRAS* point mutations, or synthetic DNA (Horizon dx). In each single run, negative and positive controls for each tested mutation were included and one standard curve was prepared. Validation of qPCR amplification was performed by melt curve differentiation.

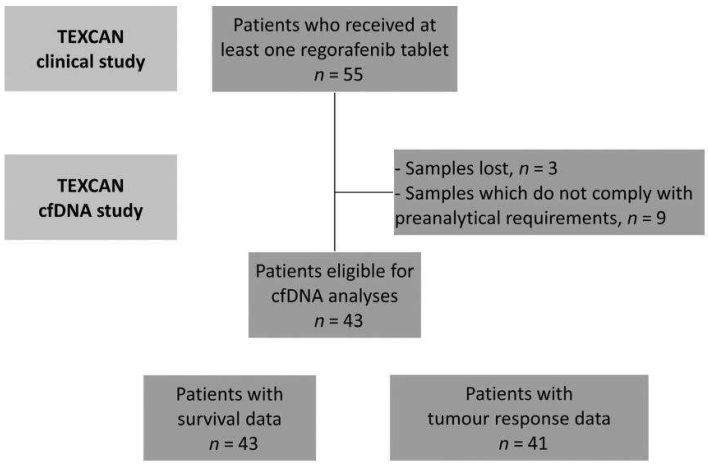

Fig. 1. Flowchart. 55 patients (the intent-to-treat population) received at least one regorafenib tablet. 43 out of 55 patients had survival data, and 41 out of 55 had tumor response data. Patients with survival and tumor response data had also circulating cell-free DNA data.

CfDNA mutation testing was done without any sensitivity cutoff. When point mutation was found in only one of the two replicates, it was confirmed in triplicate.

2.4. Design of cfDNA analyses

Changes in the total level of circulating cfDNA were analyzed in all serial plasma samples ($n = 136$). Quantification of cfDNA was obtained by amplifying a 67 bp length WT sequence of the *KRAS* gene. Pretreatment and after treatment plasma mutational analysis was performed (total number of plasma samples, $n = 70$). Point mutations analysis by IntPlex® ASB qPCR method included *KRAS* codons 12, 13, 61, 117, and 146, *NRAS* codons 12, 13, and 61, and $BRAF^{V600E}$. Detection and quantification of *KRAS*, *NRAS*, or *BRAF* point mutations were done by targeting a short specific mutant sequence (< 100 bp length). In this analysis, mutant ctDNA referred to all ctDNA point mutation-bearing sequences within one or more of the analyzed *RAS*/*BRAF* loci. Mutant ctDNA could be referred to as *RAS* mutant ctDNA where analysis focused solely on the quantification of *KRAS*- and *NRAS*-mutated ctDNA sequences. The mutation load corresponded to the proportion of mutant ctDNA fragments bearing a targeted mutation among all cfDNA fragments extracted from plasma. Likewise, the *RAS* mutation load was expressed as the proportion of *RAS* mutant ctDNA fragments bearing a targeted mutation in the *KRAS* and *NRAS* genes among all cfDNA fragments in a plasma extract.

2.5. Statistical analyses

Qualitative variables were described as percentages and quantitative variables as medians and interquartile ranges (IQR). Tumor response was defined according to RECIST 1.1 criteria. Progression-free survival (PFS) was measured from the start of treatment to the date of progression or death from any cause. OS was defined as the time between the start of the treatment to death from any cause. Patients alive were censored at the last date they were known to be alive. The survival curves for OS were estimated using the Kaplan–Meier method, described with median and 95% CI, and compared using the log-rank test. The associations between patient characteristics and outcomes were estimated using the Cox proportional hazard model, and hazard ratio (HR) was provided with their 95% CI. Proportional hazard assumptions were examined graphically by plotting the log minus log of survival. Restricted cubic spline methodology was used to estimate the association between continuous variables and OS in order to identify the best transformation to apply in Cox proportional hazard models and cutoff of interest. All analyses were performed using SAS version 9.4 (SAS Institute, Cary, NC, USA) and R software version 2.15.2 (R Development Core Team, Vienna, Austria; http://www.r-project.org). P values of < 0.05 were considered statistically significant, and all tests were two-sided. Due to the exploratory setting of the study, P values were not corrected for multiple tests.

3. Results

Patient and treatment characteristics are summarized in Table 1. In populations of patients with and without cfDNA measurements, clinical characteristics, treatments, and outcomes were similar. Of the 43 patients, 23 were male. The median age was 62.1 years. A total of 39 patients (90.7%) had their primary tumor located on the left side of the colon or rectum. All patients were refractory (or intolerant) to available standard cytotoxic agents. The majority of patients (97.7%) were previously treated with an anti-angiogenic agent (bevacizumab or aflibercept), while over 50% (22/43) received prior anti-EGFR monoclonal antibody (cetuximab or panitumumab) therapy. The available tumor genotyping data showed mutation of *KRAS* for 16/43, mutation of *NRAS* for 3/29, *NRAS* unknown status for 14/43, mutation of *BRAF* for 5/35, and *BRAF* unknown status for 8/43. Tumor genotyping data were obtained either from resections ($n = 27$) or biopsies ($n = 13$) of primary tumors ($n = 18$) or metastases ($n = 7$). Corresponding cfDNA genotypes are shown in Table S1. Median treatment duration was 8.29 weeks (IQR, 4.14–15.14). Median OS for all patients was 5.3 months (3.7–8.6). The actual regorafenib median dose of the prescribed dose was 82.5%. The median cfDNA concentration at baseline (the cfDNA population) was 21.18 $ng{\cdot}mL^{-1}$ (IQR, 7.81–62.80).

3.1. Relationship between circulating DNA markers and outcomes

Among patients evaluable for tumor response ($n = 41$), those with tumor control as the best response ($n = 33$) had a median baseline cfDNA concentration of 19.4 $ng{\cdot}mL^{-1}$ compared with 48.77 $ng{\cdot}mL^{-1}$ for those with tumor progression ($n = 8$; $P = 0.0784$; Fig. 2A). To assess the association between survival outcomes and total baseline cfDNA, we tested three different cutoff values. The 26 $ng{\cdot}mL^{-1}$ threshold was chosen

Table 1. Patient and treatment characteristics. ECOG PS, Eastern Cooperative Oncology Group performance status.

	TEXCAN population $N = 55$	Population without cfDNA analysis $n = 12$	Population with cfDNA analysis $n = 43$
Median age, years (IQR)	62.7 (52.6–68.9)	67.7 (59.7–70)	62.1 (50.5–68.3)
Gender			
Male	30 (55.5%)	7 (58.3%)	23 (53.5%)
Female	25 (45.5%)	5 (41.7%)	20 (46.5%)
ECOG PS			
0	17 (30.9%)	4 (33.3%)	13 (30.2%)
1	38 (69.1%)	8 (66.7%)	30 (69.8%)
Primary site of disease			
Right colon	6 (10.9%)	2 (16.6%)	4 (9.3%)
Left colon	49 (89.1%)	10 (83.4%)	39 (90.7%)
Archival tumor genotype status			
KRAS WT	34	7	27
KRAS mutant	21	5	16
NRAS WT	34	8	26
NRAS mutant	3	0	3
Missing	18	4	15
BRAF WT	37	7	30
BRAF mutant	6	1	5
Missing	12	4	8
Time from diagnosis of metastases < 18 months	12 (21.8%)	3 (25%)	9 (20.9%)
Previous anti-EGFR treatment	28 (50.9%)	6 (50%)	22 (54.1%)
Previous anti-angiogenic treatment	54 (98.2%)	12 (100%)	42 (97.7%)
Regorafenib treatment			
Treatment duration, weeks (IQR)	8.29 (4.14–16.29)	12.14 (4–21.79)	8.29 (4.14–15.14)
Actual dose / planned dose	84.5%	100%	82.5%
Median OS, months (95% CI)	5.32 (3.7–8.6)	3.9 (1.7–17.1)	5.3 (3.7–8.6)

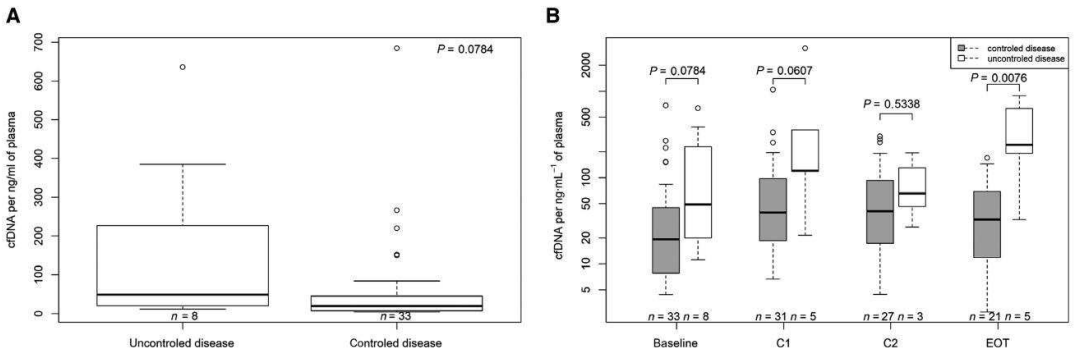

Fig. 2. Circulating cell-free DNA (cfDNA) and tumor response. (A) Baseline cfDNA and tumor control. (B) Dynamic changes in cfDNA concentrations throughout treatment duration. The boxplot shows medians with IQR (Q1–Q3), and whiskers represent the range within the 1.5 IQR. Test for comparison of median between groups is done by the Wilcoxon test. C1, cycle 1; C2, cycle 2; EOT, EOT.

based on our previous observation that mCRC patients with cfDNA concentration > 26 ng·mL^{-1} had a lower OS than those with a cfDNA concentration below this threshold [29]. Figure 3A shows that patients with baseline cfDNA level of > 26 ng·mL^{-1} had shorter OS than patients with higher cfDNA cut-off level (the median OS 4.0 vs 6.9 months, respectively; log-rank $P = 0.0366$). Similar findings were

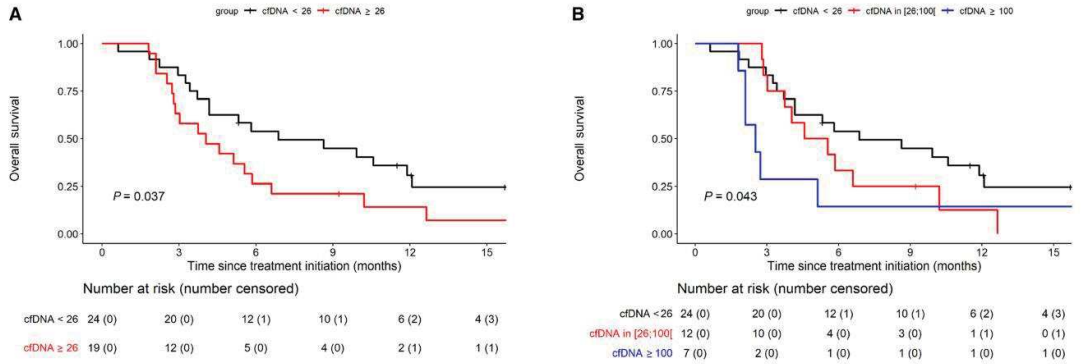

Fig. 3. OS according to the baseline circulating cell-free (cfDNA) concentrations. (A) Baseline cfDNA at 26 ng·mL^{-1} cutoff threshold. (B) Baseline cfDNA at 26, 26–110, and ≥ 100 ng·mL^{-1} cutoff thresholds. Survival curves are represented according to thresholds of the total cfDNA concentration (ng·mL^{-1} of plasma) determined at baseline. OS was estimated using the Kaplan–Meir method, described with median and 95% CI, and compared using the log-rank test.

observed with the 65 ng·mL^{-1} threshold (i.e., third IQR of the cfDNA concentration distributions of the analysis) and 100 ng·mL^{-1} threshold (Table 2, Fig. 3B). Interestingly, we found that the probability of being alive at 3 months (a key inclusion criteria in mCRC clinical trials) was 83.3% (95% CI: 66.61–92.14) and 28.6% (95% CI: 4.11–61.15) in patients with the cfDNA level of < 100 and ≥ 100, respectively.

Table 2. Univariate Cox regression analysis for survival according to baseline cfDNA.

	Baseline cfDNA (ng·mL^{-1})	*N* (events)	HR	95% CI	*P* value
OS	< 100	36 (29)	1		0.0355
	≥ 100	7 (7)	2.48	1.06–5.77	
	< 26	24 (18)	1		0.0407
	≥ 26	19 (18)	2.02	1.03–3.95	
	< 65	33 (26)	1		0.0458
	≥ 65	10 (10)	2.12	1.01–4.45	
	< 26	24 (18)	1		0.0534
	26–100	12 (11)	1.67	0.78–3.62	0.19
	≥ 100	7 (7)	2.93	1.20–7.17	0.0188
	Log	43(36)	1.26	1.01–1.56	0.0371
PFS	< 26	24 (22)	1		0.1947
	≥ 26	19 (19)	1.51	0.81–2.83	
	< 65	33 (31)	1		0.4507
	≥ 65	10 (10)	1.32	0.64–2.71	
	< 100	36 (4)	1		0.3683
	≥ 100	7 (7)	1.47	0.64–3.40	
	< 26	24 (22)	1		0.4115
	26–100	12 (12)	1.45	0.71–2.94	0.311
	≥ 100	7 (7)	1.66	0.69–4.00	0.2589
	log	43 (41)	1.2	0.97–1.49	0.0946

Given any association between OS and cfDNA concentrations in its continuous form, we evidenced a positive correlation between these two, the higher the baseline cfDNA concentration, the higher the risk of death (Fig. S1).

When assessing the *RAS* mutant ctDNA concentrations, we observed that mCRC patients with baseline *RAS* mutant ctDNA concentration of > 2 ng·mL^{-1} (the threshold established from the relationship between *RAS* mutant ctDNA concentrations and the risk of death using the restricted cubic spline regression analysis; data not shown) had shorter OS than those with below the threshold (log-rank $P = 0.0154$; Fig. 4). To a lesser extent, patients with a *RAS* mutation load of > 6% had shorter OS than the rest of patients (log-rank $P = 0.0200$; Fig. S2). No relationship was detected between PFS and any of the circulating DNA markers studied (Table 2).

3.2. Changes in cfDNA concentration during treatment

We did not observe any meaningful variation of cfDNA along treatment duration, but an early increase in total cfDNA concentration from baseline to day 15 of cycle 1 (paired analysis, Wilcoxon signed-rank test, $P = 0.0004$; Fig. S3). Moreover, patients without disease control had significantly higher cfDNA concentrations at the EOT than those who had stable disease as the best response ($P = 0.0076$; Fig. 2B). In fact, at baseline, on day 15 of cycle 1, on day 15 of cycle 2, and at EOT, patients with tumor control as best response had the following median cfDNA concentrations: 19.4, 39.29, 40.76, and 36.67 ng·mL^{-1}, respectively. Also, patients

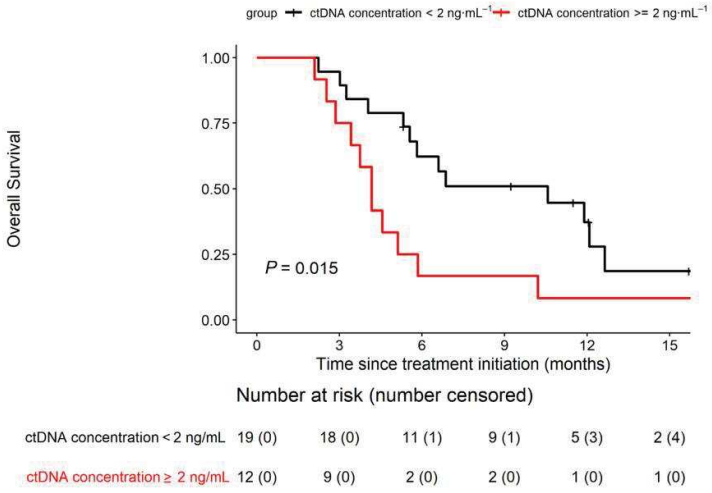

Fig. 4. OS according to ctDNA concentrations (threshold 2 ng·mL^{-1}) in patients with *RAS*-mutated tumors OS was estimated using the Kaplan–Meir method, described with median and 95% CI, and compared using the log-rank test.

who progressed had the following median cfDNA concentrations: 48.77, 119.73, 65.59, and 239.2, respectively (Fig. 2B).

3.3. Mutational analysis

At baseline, 33/43 patients (76.7%) showed *RAS*/*BRAF* mutations, of whom 30 had only *RAS* point mutations, two had $BRAF^{V600E}$ point mutations, and one had both *KRAS* and *BRAF* mutations (Table S1). At the EOT, mutation analysis of ctDNA of 27 patients showed *RAS* and/or *BRAF* mutations in 25 of theme (92.6%). Plasma analysis showed a high clonal heterogeneity of these patients' tumors with 10/33 and 12/25 mutated patients showing multiple concurrent *RAS*/*BRAF* mutations prior and after regorafenib treatment, respectively. Paired analysis revealed that for 23 patients whose ctDNA was mutated at baseline, ctDNA remained mutated at the EOT (including five patients with one or more newly point mutations detected during treatment that were not detectable at baseline). Two patients with WT tumors acquired mutations by the EOT (Table S1). Only for two patients, the *RAS*/*BRAF* status remained WT at the end of regorafenib treatment. Overall, we found that the mutational status changed from baseline to the EOT in 8/27 (29.6%). These changes did not translate into different outcomes from those identified at the baseline (data not shown). The *RAS*/*BRAF* mutation analysis performed on archival tumor tissue (gold standard) showed 13 false negatives and four false positives when compared to plasma analysis performed prior to the initiation of treatment (Table S1). The accuracy rate (*RAS*/*BRAF* mutant vs *RAS*/*BRAF* non-mutant patients) for the *RAS*/*BRAF* mutational status between the two assays was 60.5%, with a sensitivity of 83.3% and a specificity of 32%. These comparative values are similar to those previously reported [15], confirming the high sensitivity of the IntPlex detection test. The high number of false-negative samples can be due to several reasons: (a) the intra- and intertumoral heterogeneity of tumors, (b) the clonal evolution of tumors over time, which may be accentuated by the different types of treatment given to patients, or (c) the lack of analytical sensitivity of the sequencing techniques used on the tumor tissue.

4. Discussion

Here, we present the ancillary analysis of the phase II TEXCAN study population of regorafenib-treated mCRC patients. In this small, but prospective series, we found that the total cfDNA, *RAS* mutant ctDNA, and to a lesser extent the mutational load were correlated with OS, regardless of whether this relationship was studied as classes or as continuous variables. For example, patients with total baseline cfDNA $\geq$ 26 ng·mL^{-1} have double risk of death compared with those patients who have baseline cfDNA lower than 26 ng·mL^{-1}. Although pre-analytical requirements are becoming increasingly stringent with time [24], this threshold dichotomizes nicely the outcome of mCRC patients treated with regorafenib. This observation is similar to that of our earlier study [29]. Such inverse correlation between circulating DNA biomarkers and outcome in patients treated with regorafenib has also been reported

by others using different methods and various data sets [7,30–33]. We could not, however, define whether this relationship is driven by the regorafenib use due to the design of our trial, which lacks a control group of patients not treated with regorafenib. Conversely to what has been previously reported [31,34], we were unable to find a clear relationship between circulating DNA biomarkers and PFS. Similarly, although we did not identify any clear relationship between the total cfDNA level at baseline and disease control as the best response, a trend was observed. This could be explained by a weak impact of regorafenib on the tumor due to brevity of treatment duration related to adverse events and/or lack of the efficacy in this population of heavily pretreated patients for whom the best response is often tumor stabilization.

In line with other reports [30,31], we found the cfDNA level to be increased 2 weeks after regorafenib onset. It has been suggested that this may be related to the release of cfDNA into the bloodstream secondary to the toxic effects of regorafenib on normal tissues [30]. Vandeputte *et al.* in their study of 20 mCRC patients treated with regorafenib, suggested that cfDNA and mutant ctDNA evolve independently with different patterns of dynamics [30]. Although it is always difficult to do cross-studies comparison using different assays, conditions, and sets of patients, we hypothesize that this discrepancy could be related to the interstudy variability in the number of patients being sensitive to treatment (toxicity on normal tissues and/or an antitumor effect) to regorafenib.

As anticipated, we identified several mutational changes in circulating cfDNA (Table S1) within 8 weeks from the starting dose of regorafenib (i.e., the median duration of regorafenib treatment). Although these changes did not translate into different outcomes, their unprecedented rapid nature in our series is impressive. Based on this observation and of that from our previous report in a similar group of patients undergoing other experimental therapies [21], we suggest that these mutational changes are more likely related to the clinical characteristics of these heavily pretreated mCRC patients rather than to the regorafenib itself.

This study is exploratory and has some limitations, and the data should be interpreted carefully. Given the exploratory nature of this analysis, *P* values were not corrected for multiple testing. The sample size for this analysis was small could not counterbalance the lack of power due to the loss of 12 patients (22%) of the native TEXCAN population. Moreover, as regorafenib is more likely to be cytostatic than cytotoxic and as the treatment duration is very short, it would be unreasonable to expect meaningful tumor shrinkage with a sharp decrease in circulating DNA biomarkers in the setting of heavily pretreated mCRC patients.

5. Conclusion

In this ancillary study of the prospective TEXCAN phase II trial, we confirmed the potential benefit of cfDNA analysis prior to regorafenib treatment as a suitable method to identify mCRC patients more likely to have the best outcomes. Given our setting and inclusion of heavily pretreated mCRC patients, further investigation involving a larger validation cohort is needed to determine whether or not the 26 $ng{\cdot}mL^{-1}$ cutoff for cfDNA analysis is the most optimal to discriminate between patients with poor, good, and the best prognoses.

Acknowledgements

This study is supported by unrestricted research grants from the Fondation ARCAD (Aide et Recherche en Cancérologie Digestive) and Bayer Healthcare Pharmaceutical. Funders have no role in study design, management, analysis, or interpretation of data, nor do they have any role in the writing of the final report. The authors acknowledge the editorial assistance of Magdalena Benetkiewicz (Sc.D; GERCOR). This work was partially funded by the 'SIRIC Montpellier Cancer Grant INCa_Inserm_DGOS_12553'. ART is supported by the INSERM.

Conflict of interest

TA has served in a consulting/advisory role and/or received honoraria from Amgen, Bristol-Myers Squibb, Chugai, Clovis, Gritstone Oncology, Haliodx, MSD Oncology, Pierre Fabre, Roche/Ventana, Sanofi, Servier, and Tesaro/GSK, and has received travel, accommodation, and expenses from Roche/Genentech, MSD Oncology, and Bristol-Myers Squibb. MJ has received travel, accommodation, and expenses from Roche/Genentech, and Pfizer. DV has reported a consulting role for GERCOR, HalioDX, Incyte, OSE Immunotherapeutics, Janssen-Cilag, Pfizer, and CellProthera. CT has received travel expenses from Roche, Servier, Bayer, and BMS; has received research funding from Bayer; and has reported advisory board fees from Bayer, Roche, and Amgen. CL has reported a consulting/advisory role and receiving honoraria from MSD, Halozyme, Roche, Celgene, Amgen, and Servier, and has received travel accommodation from MSD and Roche. ART is a DiaDx stockholder. TM

has disclosed research funding from Roche and Amgen; has received honoraria from Amgen, Sanofi, Bristol-Myers Squibb, and Sandoz; has reported travel, accommodation, and expenses from Amgen and Merck. AA has reported a consulting/advisory role and/or receiving honoraria from Bristol-Myers Squibb, MSD Oncology, and Servier; and has received research funding from Bayer Pharmaceuticals. All remaining authors have declared no conflicts of interest.

Data Accessibility

The data are not available in a public database or repository. The data sets generated and analyzed in this study are available from the corresponding author on reasonable request.

Author contributions

ART and TA designed the study. BP and ART developed the methodology. BP, SA, AB, BR, and CS did the experiments under the supervision of ART. TA, IT, CT, MJ, TM, and CL contributed to the blood and clinical collections. JH and DV did the statistical analyses. AA and BP analyzed the data and prepared the manuscript. All of the authors (BP, TA, JH, IT, CT, MJ, TM, CL, SA, AB, BR, CS, DV, ART, and AA) discussed the results and approved the manuscript.

References

1 Ferlay J, Colombet M, Soerjomataram I, Mathers C, Parkin DM, Piñeros M, Znaor A & Bray F (2019) Estimating the global cancer incidence and mortality in 2018: GLOBOCAN sources and methods. *Int J. Cancer* **144**, 1941–1953.

2 Van Cutsem E, Cervantes A, Adam R, Sobrero A, Van Krieken JH, Aderka D, Aranda Aguilar E, Bardelli A, Benson A, Bodoky G *et al.* (2016) ESMO consensus guidelines for the management of patients with metastatic colorectal cancer. *Ann Oncol* **27**, 1386–1422.

3 Schmieder R, Hoffmann J, Becker M, Bhargava A, Müller T, Kahmann N, Ellinghaus P, Adams R, Rosenthal A, Thierauch K-H *et al.* (2014) Regorafenib (BAY 73–4506): antitumor and antimetastatic activities in preclinical models of colorectal cancer. *Int J Cancer* **135**, 1487–1496.

4 Grothey A, Van Cutsem E, Sobrero A, Siena S, Falcone A, Ychou M, Humblet Y, Bouché O, Mineur L, Barone C *et al.* (2013) Regorafenib monotherapy for previously treated metastatic colorectal cancer (CORRECT): an international, multicentre, randomised, placebo-controlled, phase 3 Trial. *Lancet* **381**, 303–312.

5 Li J, Qin S, Xu R, Yau TCC, Ma B, Pan H, Xu J, Bai Y, Chi Y, Wang L *et al.* (2015) Regorafenib plus best supportive care versus placebo plus best supportive care in asian patients with previously treated metastatic colorectal cancer (CONCUR): a randomised, double-blind, placebo-controlled, phase 3 trial. *Lancet Oncol* **16**, 619–629.

6 Bekaii-Saab TS, Ou F-S, Ahn DH, Boland PM, Ciombor KK, Heying EN, Dockter TJ, Jacobs NL, Pasche BC, Cleary JM *et al.* (2019) Regorafenib dose-optimisation in patients with refractory metastatic colorectal cancer (ReDOS): a randomised, multicentre, open-label, phase 2 study. *Lancet Oncol* **20**, 1070–1082.

7 Tabernero J, Lenz H-J, Siena S, Sobrero A, Falcone A, Ychou M, Humblet Y, Bouché O, Mineur L, Barone C *et al.* (2015) Analysis of circulating DNA and protein biomarkers to predict the clinical activity of regorafenib and assess prognosis in patients with metastatic colorectal cancer: a retrospective, exploratory analysis of the CORRECT trial. *Lancet Oncol* **16**, 937–948.

8 Adenis A, de la Fouchardiere C, Paule B, Burtin P, Tougeron D, Wallet J, Dourthe L-M, Etienne P-L, Mineur L, Clisant S *et al.* (2016) Survival, safety, and prognostic factors for outcome with regorafenib in patients with metastatic colorectal cancer refractory to standard therapies: results from a multicenter study (REBECCA) nested within a compassionate use program. *BMC Cancer* **16**, 412.

9 Otandault A, Anker P, Al Amir Dache Z, Guillaumon V, Meddeb R, Pastor B, Pisareva E, Sanchez C, Tanos R, Tousch G *et al.* (2019) Recent advances in circulating nucleic acids in oncology. *Ann Oncol* **30**, 374–384.

10 Thierry AR, Mouliere F, El Messaoudi S, Mollevi C, Lopez-Crapez E, Rolet F, Gillet B, Gongora C, Dechelotte P, Robert B *et al.* (2014) Clinical validation of the detection of KRAS and BRAF mutations from circulating tumor DNA. *Nat Med* **20**, 430–435.

11 Bettegowda C, Sausen M, Leary RJ, Kinde I, Wang Y, Agrawal N, Bartlett BR, Wang H, Luber B, Alani RM *et al.* (2014). Detection of circulating tumor DNA in early- and late-stage human malignancies. *Sci Transl Med* **6**, 224ra24.

12 Vitiello PP, De Falco V, Giunta EF, Ciardiello D, Cardone C, Vitale P, Zanaletti N, Borrelli C, Poliero L, Terminiello M *et al.* (2019) Clinical practice use of liquid biopsy to identify RAS/BRAF mutations in patients with metastatic colorectal cancer (MCRC): a single institution experience. *Cancers* **11**, 1504.

13 Yao J, Zang W, Ge Y, Weygant N, Yu P, Li L, Rao G, Jiang Z, Yan R, He L *et al.* (2018) RAS/BRAF circulating tumor DNA mutations as a predictor of response to first-line chemotherapy in metastatic

colorectal cancer patients. *Can J Gastroenterol Hepatol* **2018**, 4248971.
14 van Helden EJ, Angus L, der Houven M-V, van Oordt CW, Heideman DAM, Boon E, van Es SC, Radema SA, van Herpen CML, de Groot DJA *et al.* (2019) RAS and BRAF mutations in cell-free DNA are predictive for outcome of Cetuximab monotherapy in patients with tissue-tested RAS wild-type advanced colorectal cancer. *Mol Oncol* **13**, 2361–2374.
15 Thierry AR, El Messaoudi S, Mollevi C, Raoul JL, Guimbaud R, Pezet D, Artru P, Assenat E, Borg C, Mathonnet M *et al.* (2017) Clinical utility of circulating DNA analysis for rapid detection of actionable mutations to select metastatic colorectal patients for anti-EGFR treatment. *Ann Oncol* **28**, 2149–2159.
16 Diehl F, Schmidt K, Choti MA, Romans K, Goodman S, Li M, Thornton K, Agrawal N, Sokoll L, Szabo SA *et al.* (2008) Circulating mutant DNA to assess tumor dynamics. *Nat Med* **14**, 985–990.
17 Misale S, Yaeger R, Hobor S, Scala E, Janakiraman M, Liska D, Valtorta E, Schiavo R, Buscarino M, Siravegna G *et al.* (2012) Emergence of KRAS mutations and acquired resistance to anti-EGFR therapy in colorectal cancer. *Nature* **486**, 532–536.
18 Siravegna G, Mussolin B, Buscarino M, Corti G, Cassingena A, Crisafulli G, Ponzetti A, Cremolini C, Amatu A, Lauricella C *et al.* (2015) Clonal evolution and resistance to EGFR blockade in the blood of colorectal cancer patients. *Nat Med* **21**, 827.
19 Danese E, Minicozzi AM, Benati M, Montagnana M, Paviati E, Salvagno GL, Lima-Oliveira G, Gusella M, Pasini F, Lippi G *et al.* (2015) Comparison of genetic and epigenetic alterations of primary tumors and matched plasma samples in patients with colorectal cancer. *PLoS One* **10**, e0126417.
20 Gao J, Wang H, Zang W, Li B, Rao G, Li L, Yu Y, Li Z, Dong B, Lu Z *et al.* (2017) Circulating tumor DNA functions as an alternative for tissue to overcome tumor heterogeneity in advanced gastric cancer. *Cancer Sci* **108**, 1881–1887.
21 Thierry AR, Pastor B, Jiang Z-Q, Katsiampoura AD, Parseghian C, Loree JM, Overman MJ, Sanchez C, Messaoudi SE, Ychou M *et al.* (2017) Circulating DNA demonstrates convergent evolution and common resistance mechanisms during treatment of colorectal cancer. *Clin Cancer Res* **23**, 4578–4591.
22 Lucidarme O, Wagner M, Gillard P, Kim S, Bachet J-B, Rousseau B, Mazard T, Louvet C, Chibaudel B, Cohen R *et al.* (2019) "RECIST and CHOI criteria in the evaluation of tumor response in patients with metastatic colorectal cancer treated with regorafenib, a prospective multicenter study. *Cancer Imaging* **19**, 85.
23 El Messaoudi S, Rolet F, Mouliere F & Thierry AR (2013) Circulating cell free DNA: preanalytical considerations. *Clin Chim Acta Int J Clin Chem* **424**, 222–230.
24 Meddeb R, Pisareva E & Thierry AR (2019) Guidelines for the preanalytical conditions for analyzing circulating cell-Free DNA. *Clin Chem* **65**, 623–633.
25 Tanos R, Tosato G, Otandault A, Al Amir Dache Z, Pique Lasorsa L, Tousch G, El Messaoudi S, Meddeb R, Diab Assaf M, Ychou M *et al.* (2020) Machine learning-assisted evaluation of circulating DNA quantitative analysis for cancer screening. *Adv Sci* **7**, 2000486.
26 Mouliere F, El Messaoudi S, Pang D, Dritschilo A & Thierry AR (2014) Multi-marker analysis of circulating cell-free DNA toward personalized medicine for colorectal cancer. *Mol Oncol* **8**, 927–941.
27 Bustin SA (2010) Why the need for QPCR publication guidelines?–The case for MIQE. *Methods San Diego Calif* **50**, 217–226.
28 Bustin SA, Benes V, Garson JA, Hellemans J, Huggett J, Kubista M, Mueller R, Nolan T, Pfaffl MW, Shipley GL *et al.* (2009) The MIQE guidelines: minimum information for publication of quantitative real-time PCR experiments. *Clin Chem* **55**, 611–622.
29 El Messaoudi S, Mouliere F, Du Manoir S, Bascoul-Mollevi C, Gillet B, Nouaille M, Fiess C, Crapez E, Bibeau F, Theillet C *et al.* (2016) Circulating DNA as a strong multimarker prognostic tool for metastatic colorectal cancer patient management care. *Clin Cancer Res* **22**, 3067–3077.
30 Vandeputte C, Kehagias P, El Housni H, Ameye L, Laes J-F, Desmedt C, Sotiriou C, Deleporte A, Puleo F, Geboes K *et al.* (2018) Circulating tumor DNA in early response assessment and monitoring of advanced colorectal cancer treated with a multi-kinase inhibitor. *Oncotarget* **9**, 17756–17769.
31 Amatu A, Schirripa M, Tosi F, Lonardi S, Bencardino K, Bonazzina E, Palmeri L, Patanè DA, Pizzutilo EG, Mussolin B *et al.* (2019) High circulating methylated DNA is a negative predictive and prognostic marker in metastatic colorectal cancer patients treated with regorafenib. *Front. Oncol* **9**, 622.
32 Khan K, Rata M, Cunningham D, Koh D-M, Tunariu N, Hahne JC, Vlachogiannis G, Hedayat S, Marchetti S, Lampis A *et al.* (2018) Functional imaging and circulating biomarkers of response to regorafenib in treatment-refractory metastatic colorectal cancer patients in a prospective phase II study. *Gut* **67**, 1484–1492.
33 Jensen LH, Olesen R, Petersen LN, Boysen AK, Andersen RF, Lindebjerg J, Nottelmann L, Thomsen CEB, Havelund BM, Jakobsen A *et al.* (2019) NPY gene methylation as a universal, longitudinal plasma marker for evaluating the clinical benefit from last-line treatment with regorafenib in metastatic colorectal cancer. *Cancers* **11**, 1649.
34 Wong ALA, Lim JSJ, Sinha A, Gopinathan A, Lim R, Tan C-S, Soh T, Venkatesh S, Titin C, Sapari NS *et al.* (2015) Tumour pharmacodynamics and circulating cell

free DNA in patients with refractory colorectal carcinoma treated with regorafenib. *J Transl Med* **13**, 57.

Supporting information

Additional supporting information may be found online in the Supporting Information section at the end of the article.

Fig. S1. Risk of death according to baseline cfDNA concentrations. The dotted lines represents the 95% confidence interval for the risk of death according to cfDNA concentration at baseline (continuous line).

Fig. S2. Overall survival according to mutation load (threshold 6%).

Fig. S3. Changes of cfDNA concentrations during treatment. Serial concentration of circulating cfDNA ($ng{\cdot}mL^{-1}$ of plasma) was determined using the IntPlex ASB qPCR method targeting a 67 bp-length wild-type sequence of the *KRAS* gene. A significant increase of cfDNA concentrations from baseline to day 15 of cycle 1 was observed; test for comparison of cfDNA medians between baseline and cycle 1 with paired data (Wilcoxon signed rank test, $P = 0.0004$). EOT, End Of Treatment.

Table S1. Tumor genotyping analysis. Comparison of *KRAS*, *BRAF*, and *NRAS* genotypes in archival tissues and blood samples taken prior and at the end of regorafenib treatment.

Article IV: Conception de l'étude FOLFIRINOX-R : un essai de phase I/II sur le FOLFIRINOX associé au regorafenib en première ligne de traitement chez des patients atteints de cancer colorectal métastatique RAS muté non résécable

Antoine Adenis, Thibault Mazard, Julien Fraisse, Patrick Chalbos, Brice Pastor, Ludovic Evesque, Francois Ghiringhelli, Caroline Mollevi, Stéphanie Delaine and Marc Ychou

Rationnel: Le triplet de chimiothérapie FOLFOXIRI associé à l'anticorps anti-VEGF (bevacizumab) est une option chez certains patients atteints de CCRm. Dans ce contexte, le cancer colorectal métastatique muté *RAS* ne bénéficie pas du même traitement que le cancer CCRm de type *RAS* sauvage. En plus de ses propriétés anti-angiogéniques, le régorafénib possède également des activités anti-prolifératives, quel que soit le statut *RAS*. Le présent essai vise à étudier l'innocuité et l'efficacité du régorafénib en association avec le protocole FOLFIRINOX chez les patients atteints d'un cancer colorectal métastatique muté *RAS*.

Contribution: Dans ce projet j'ai uniquement participé à la relecture du manuscrit. Je suis en charge des analyses des mutations afin d'intégrer ou non les patients dans cette étude qui est toujours en cours.

Introduction

Bien que certains patients CCRm présentant des métastases hépatiques (ou pulmonaires) soient techniquement opérables et peuvent de ce fait être guéris par la chirurgie uniquement, la plupart des patients auront besoin d'un traitement systémique palliatif car leurs métastases sont jugées non opérables[202]. Selon les directives de la Société européenne d'oncologie médicale (ESMO), la chimiothérapie de première ligne pour le cancer colorectal métastatique (CCRm) fait généralement appel à un doublet de chimiothérapie (bi-CT) de 5-fluorouracile, d'acide folinique et d'oxaliplatine (FOLFOX) ou d'irinotécan (FOLFIRI)[202]. Cependant, Falcone *et al* ont rapporté des taux de réponse plus élevés et de meilleurs taux de survie avec l'utilisation d'un triplet de chimiothérapie (tri-CT) combinant 5-fluorouracil, acide folinique, oxaliplatine et irinotécan (FOLFOXIRI) par rapport au bi-CT[241]. De même, il a été rapporté des résultats favorables chez des patients présentant des métastases hépatiques non opérables d'origine colorectale, avec les trois mêmes médicaments mais en utilisant un schéma posologique différent, à savoir le schéma FOLFIRINOX[242]. Il est également admis que l'ajout de thérapies ciblées telles que les anti-VEGF ou d'anticorps monoclonaux anti-EGFR au bi-CT ou au tri-CT est bénéfique chez les patients présentant un état général acceptable lorsque la réduction de la tumeur est un objectif majeur pour permettre une chirurgie de conversion[202]. Les mutations *RAS* sont identifiées dans environ 60 % des tumeurs du cancer colorectal métastatique et sont connues comme des indicateurs prédictifs négatifs de l'efficacité du traitement par anti-EGFR dans le cancer colorectal métastatique[243].

Il est intéressant de noter que le mauvais pronostic lié aux mutations *RAS* a été observé dans différents régimes de traitement (sous-groupes de patients traités à l'irinotécan et à l'oxaliplatine, ainsi que chez les patients traités ou non au bevacizumab)[243]. Des différences de survie similaires en fonction du statut *RAS* ont également été observées dans les essais cliniques portant sur les avantages du tri-CT par rapport au bi-CT. Le consortium TRIBE a rapporté que le (tri-CT) (FOLFOXIRI) associé au bevacizumab offrait une PFS et une OS significativement plus longues que le bi-CT avec FOLFIRI plus bevacizumab[244,245]. Aussi, en examinant la survie en fonction du statut *RAS*, Cremolini *et al* ont rapporté que médiane de l'OS était meilleure dans le sous-groupe *RAS* muté que dans le sous-groupe *RAS*-sauvage[245]. Malgré cela, il est indispensable d'améliorer la prise en charge des patients atteints de CCRm avec une tumeur *RAS* mutée.

Le régorafénib est une petite molécule inhibitrice de multiples kinases, qu'elles soient intracellulaires ou liées à la membrane[35], autorisée pour les patients atteint de CRCm réfractaires aux thérapies standards. Outre ses propriétés anti-angiogéniques bien connues, le régorafénib possède également des activités antiprolifératives moins connues dans des lignées cellulaires humaines de cancer du côlon[35]. Deux essais de phase III ont démontré un bénéfice en termes de survie globale (OS) pour le régorafénib par rapport au placebo chez les patients atteints de CCRm ayant progressé sous traitement standard, quel que soit leur statut *RAS*[36,37,246]. Cependant, la moitié des patients qui ont reçu du régorafénib dans ce contexte ont progressé deux mois après le début du traitement[36,246] et ont alors été exposés inutilement à des effets indésirables. Comme discuté précédemment, il n'existe pas de biomarqueur pleinement accepté capable de prédire le bénéfice du régorafénib. Deux essais de phase II ont également étudié le profil de sécurité et d'efficacité du régorafénib lorsqu'il est associé à une chimiothérapie chez des patients atteints de cancer colorectal métastatique[246,247]. L'étude de Schultheis *et al* visait à déterminer si l'ajout du régorafénib à FOLFOX ou FOLFIRI pouvait être réalisable en tant que traitement de première ou de deuxième ligne du cancer colorectal métastatique[246]. Le régorafénib a montré une tolérance acceptable en association avec la chimiothérapie.

L'étude de Sanoff *et al* a été conçue pour montrer si l'ajout du régorafenib à FOLFIRI améliore la PFS (par rapport à un groupe placebo-FOLFIRI) lorsqu'il est administré en traitement de seconde ligne à des patients précédemment traités par un régime à base d'oxaliplatine et de fluoropyrimidine[247]. L'étude a démontré que l'ajout de regorafenib au FOLFIRI prolonge la PFS par rapport au FOLFIRI seul avec un Hazard Ratio (HR) de 0,72. En examinant la réponse tumorale, les auteurs ont constaté que le regorafenib (associé à la chimiothérapie) a fourni plus de réponses partielles que la chimiothérapie plus le placebo (35% contre 19%, p = 0,045). La tolérance était acceptable, avec une faible augmentation de la toxicité par rapport au régime de chimiothérapie de contrôle[247]. L'essai FOLFIRINOX-R vise à étudier l'innocuité, la tolérance et l'efficacité du régorafénib en l'association avec le protocole de tri-CT FOLFIRINOX chez les patients atteints CCRm *RAS* muté.

Adenis et al. BMC Cancer (2021) 21:564
https://doi.org/10.1186/s12885-021-08312-7

BMC Cancer

STUDY PROTOCOL Open Access

FOLFIRINOX-R study design: a phase I/II trial of FOLFIRINOX plus regorafenib as first line therapy in patients with unresectable RAS-mutated metastatic colorectal cancer

Antoine Adenis[1,2,3*], Thibault Mazard[1,2], Julien Fraisse[4], Patrick Chalbos[5], Brice Pastor[1,6], Ludovic Evesque[7], Francois Ghiringhelli[8], Caroline Mollevi[1,4], Stéphanie Delaine[5] and Marc Ychou[1,2]

Abstract

Background: The chemotherapy triplet FOLFOXIRI combined to the anti-VEGF antibody bevacizumab is an option in selected patients with metastatic colorectal cancer. In this setting, RAS-mutated metastatic colorectal cancer do not benefit the same from treatment than RAS-wildtype metastatic colorectal cancer do. Together with its antiangiogenic properties, the tyrosine-kinase inhibitor regorafenib has also anti-proliferative activities whatever the RAS status is. The present trial aims at studying the safety and the efficacy of regorafenib in combination with FOLFIRINOX – a chemotherapy triplet using a different dosing schedule than FOLFOXIRI - in patients with *RAS*-mutated metastatic colorectal cancer.

Methods: FOLFIRINOX-R is a prospective, multicentric, non-randomised, dose-finding phase 1–2 trial. The primary endpoints are the determination of the maximum tolerated dose, the recommended phase 2 dose, and the proportion of patients achieving disease control at 48-weeks. Phase 1 follows a 3 + 3 design (12 to 24 patients to be included). Sixty nine patients will be necessary in phase 2, including 5% non-evaluable ones, with the following assumptions, one-stage Fleming design, $\alpha = 5\%$, $\beta = 20\%$, $p0 = 35\%$ and $p1 = 50\%$. Key eligibility criteria include Eastern Cooperative Oncology Group Performance Status of ≤1 and RAS-mutated metastatic colorectal cancer not amenable to surgery with curative intent and not previously treated for metastatic disease. FOLFIRINOX (oxaliplatin 85 mg/m^2, folinic acid 400 mg/m^2, irinotecan 150–180 mg/m^2, 5-fluorouracil: 400 mg/m^2 then 2400 mg/m^2 over 46 h) is administered every 14 days. Regorafenib (80 to 160 mg, as per dose-level) is administered orally, once daily on days 4 to 10 of each cycle.

Discussion: FOLFIRINOX-R is the first phase I/II study to evaluate the safety and efficacy of regorafenib in combination with FOLFIRINOX as frontline therapy for patients with RAS-mutated metastatic colorectal cancer.

Trial registration: EudraCT: 2018-003541-42; ClinicalTrials.gov: NCT03828799.

Keywords: Colorectal cancer, Chemotherapy triplet, Regorafenib, Phase 1–2 trial

* Correspondence: antoine.adenis@icm.unicancer.fr
[1]IRCM, Inserm, Université Montpellier, ICM, Montpellier, France
[2]Department of Medical Oncology, Montpellier Cancer Institute (ICM), Montpellier, France
Full list of author information is available at the end of the article

Background

Metastatic colorectal cancer

Colorectal cancer (CRC) is a major cause of morbidity and mortality globally [1]. More than 50% of patients will develop metastatic disease, and while some patients with technically resectable liver (or lung) metastases could be cured with surgery only, most of the patients will require palliative systemic therapy as their metastases are found unresectable [2]. As per European Society for Medical Oncology guidelines, frontline chemotherapy for metastatic CRC (mCRC) commonly involves the doublet (2-CTx) regimens of 5-fluorouracil, folinic acid, and either oxaliplatin (FOLFOX) or irinotecan (FOLFIRI) [2]. However, Falcone et al. [3] reported higher response rates and better survival rates with the use of a chemotherapy triplet (3-CTx) that combined 5-fluorouracil, folinic acid, oxaliplatin and irinotecan (FOLFOXIRI) over 2-CTx. Similarly, our group reported favorable outcomes in patients with unresectable liver metastases from colorectal origin, with the same three drugs but using a different dosing schedule, i.e. the FOLFIRINOX regimen [4]. It is also accepted that the addition of targeted therapies such as bevacizumab (a monoclonal antibody which binds circulating vascular endothelial growth factor-A) or as monoclonal antibodies (cetuximab, panitumumab) directed to epidermal growth factor receptor to 2-CTx or 3-CTx it is beneficial in fit patients when tumor shrinkage is a major objective to allow conversion surgery [2].

RAS mutations are identified in about 60% of mCRC tumors and are known as negative predictors of efficacy for anti-epidermal growth factor receptor therapy in mCRC [5]. *RAS* status also carries distinct prognostic information, as reported in a series of 1239 mCRC patients who have been treated with 2-CTx in five randomized trials [5]. Interestingly, the poor prognosis related to *RAS* mutations was observed across different treatment regimens (subgroups of irinotecan- and oxaliplatin-treated patients as well as in bevacizumab- and non-bevacizumab-treated patients). Median progression-free survival (PFS) and overall survival (OS) were 10.3 vs. 9.5 months and 26.9 vs. 21.1 months in *RAS*-wild type (and *BRAF*-wild type) and *RAS*-mutated tumors, respectively [5]. Similar survival differences by *RAS* status were also observed in clinical trials which addressed the benefit of 3-CTx over 2-CTx. The TRIBE consortium reported that 3-CTx (FOLFOXIRI) combined with bevacizumab provided a significantly longer PFS and OS than did 2-CTx with FOLFIRI plus bevacizumab [6, 7]. Actually, when looking at survival by *RAS* status, Cremolini et al. [7] reported that median OS was 37.1 months (95%CI, 29.7–42.7) in the *RAS*- and *BRAF*-wild-type subgroup compared with 25.6 months (95%CI, 22.4–28.6) in the *RAS*-mutated subgroup (HR 1.49, 95%CI, 1.11–1·99). For sure, we need to increase the treatment benefit in this setting of RAS-mutated mCRC.

Regorafenib

Regorafenib is a small-molecule inhibitor of multiple membrane-bound and intracellular kinases such as *RET, VEGFR-1, − 2, − 3, c-KIT, PDGFR, FGFR1, TIE2, DDR1, Trk2A, Eph2A, SAPK2, PTK5, Abl, CSF1R, RAF-1, BRAF*, and *BRAF V600E* [8] which is approved for refractory mCRC. Beyond its well-known antiangiogenic properties, regorafenib has also less-known anti-proliferative activities in human colon cancer cell lines [8]. Interestingly, regorafenib potently inhibits growth of patient-derived CRC xenografts alone and in combination with irinotecan [8–10]. Two phase III trials demonstrated an overall survival benefit for regorafenib (160 mg orally, once daily for the first 21 days of each 28-day cycles) over placebo in patients with mCRC who progressed on standard therapies, whatever the *RAS* status was [11, 12]. However, half of the patients who received regorafenib in that setting progressed 2 months after the onset of treatment [11, 12] and were then possibly unnecessary exposed to adverse events (AEs). Unfortunately, there is no fully accepted biomarker able to predict regorafenib benefit. Two phase II trials also studied the safety and efficacy profile of regorafenib when combined to chemotherapy in patients with mCRC [13, 14]. The study from Schultheis et al. [13] was designed to explore whether the addition of regorafenib to FOLFOX or FOLFIRI could be feasible as first- or second-line treatment of mCRC. Forty-five patients were treated every 2 weeks with 5-fluorouracil 400 mg/m^2 bolus then 2400 mg/m^2 over 46 h, folinic acid 400 mg/m^2, and either oxaliplatin 85 mg/m^2 or irinotecan 180 mg/m^2. On days 4 to 10, patients received regorafenib 160 mg orally once daily. Regorafenib showed acceptable tolerability in combination with chemotherapy. The most frequent grade 3–4 AEs were: neutropenia (45%), Hand-Foot Skin Reaction (15%), diarrhea (10%), and hypophosphatemia (12%). The study from Sanoff et al. [14] was designed to show whether the addition of regorafenib to FOLFIRI (same regimen than in the Schultheis trial [13]) improves PFS (over a placebo-FOLFIRI arm) when given as second-line treatment for patients previously treated with oxaliplatin and fluoropyrimidine-based regimen. The study met its primary endpoint, demonstrating that the addition of regorafenib to FOLFIRI prolongs PFS compared to FOLFIRI alone with a HR of 0.72. When looking at tumor response, the authors found that regorafenib (combined to chemotherapy) provided more partial responses than chemotherapy plus placebo (35% vs. 19%, $p = 0.045$). Tolerability was acceptable, with little increase in toxicity compared to the control chemotherapy regimen [14]. Based on these encouraging

results, it could be worth studying the combination of 3-CTx to regorafenib, with the ultimate objective of providing a more efficacious alternative to a selected population of eligible patients.

Aim of the study

The present FOLFIRINOX-R trial aims at studying the safety, tolerability and efficacy of regorafenib in combination with FOLFIRINOX in patients with *RAS*-mutated mCRC.

Methods and design

Study design and treatment

FOLFIRINOX-R trial is a standard 3 + 3 design for dose escalation/de-escalation followed by a phase II trial when the recommended phase II dose (RP2D) is determined. It is designed as a single-arm, prospective, non-randomized, open label, multicenter, dose-finding phase I/II trial. It aims at determining the maximum tolerated dose (MTD) and the RP2D of the combination of regorafenib and FOLFIRINOX in the phase I-part of the trial. It aims too at evaluating the efficacy of the treatment in the phase II - part of the trial.

FOLFIRINOX is administered as per standard procedures every 14 days (1 cycle = 14 days) as follows, oxaliplatin 85 mg/m^2 on day 1, IV infusion over 2 h, immediately followed by folinic acid 400 mg/m^2 or calcium levofolinate 200 mg/m^2 given as a 2-h IV infusion, with the addition of irinotecan 150–180 mg/m^2 as per dose-level given as a 90-min intravenous infusion through a Y-connector immediately followed by 5-fluorouracil: 400 mg/m^2 IV bolus then 2400 mg/m^2 over 46 h continuous infusion. Primary prophylactic G-CSF is delivered from Day-7 to Day-12. Regorafenib is administered orally at a dose of 80 to 160 mg, as per dose-level, once daily on days 4 to 10 of each cycle (see Fig. 1 for an overview of the study design).

The pre-defined dose levels are the following, step − 1 (0 to 6 patients to be treated): irinotecan 150 mg/m^2 plus regorafenib 80 mg/m^2; step 1 (3 to 6 patients to be treated): irinotecan 150 mg/m^2 plus regorafenib 120 mg/m^2; step 2 (3 to 6 patients to be treated): irinotecan 180 mg/m^2 plus regorafenib 120 mg/m^2; step 3 (3 to 6 patients to be treated): irinotecan 180 mg/m^2 plus regorafenib 160 mg/m^2.

Twelve cycles of FOLFIRINOX have to be delivered consecutively or not. Indeed, treatment can be temporarily stopped to perform surgical resection or regional procedures (radiofrequency, cryoablation, radiation therapy) if the disease becomes accessible to them but if it happens, before the end of the 12 planned cycles, the treatment has to be resumed within 4 to 8 weeks after the loco-regional procedure completion in order to reach a total number of 12 cycles delivered. Regorafenib dosing is 80 to 160 mg/m^2 according to each level of dose, by mouth daily on days 4 to 10 of each 14 days cycle, according with the regorafenib schedule reported by Schultheis et al. [13]. Regorafenib is continued until tumor progression or unacceptable toxicity, even after 12 cycles of FOLFIRINOX. Clinical evaluation will be made at each cycle. The following biologic assessments are performed before each cycle: RBC, hemoglobin, hematocrit, platelet count, WBC, coagulation panel (Prothrombin time, Partial Thromboplastin Time), electrolyte panel (sodium, potassium, chloride, magnesium, calcium, bicarbonates, phosphate), chemistry panel (albumin, lipase, glucose, serum creatinine, MDRD clearance, uric acid, urea, protein total), hepatic panel (AST, ALT, direct and indirect bilirubin, alkaline phosphatase, gammaglutamyl transpeptidase, lactate dehydrogenase), urine analysis (PH, protein, glucose, bilirubin, ketones, blood cells and leukocytes). TSH is performed every 6 weeks. The following biologic assessments is performed on day 8 of cycle 1, 2, 3: RBC, hemoglobin, hematocrit, platelet count and WBC (including differential neutrophil, lymphocyte, monocyte, basophil and eosinophil counts), chemistry panel (albumin, total protein, lipase, glucose, serum creatinine, MDRD clearance, uric acid and Urea), liver function panel (AST, ALT, direct and indirect bilirubin, gammaglutamyl transpeptidase, lactate dehydrogenase). Blood pressure is monitored every other week for the three first cycles of study treatment. Clinical, morphological imaging (RECIST criteria, v1.1) and biological (CEA and CA19.9) tumor assessment are done every 8 weeks. Prespecified dose adjustments (dose modifications and/or dose delay) for regorafenib or FOLFIRINOX could be made to manage adverse events.

Recruitment is currently active in three cancer centers (Dijon, Montpellier, and Nice) in France. Written informed consent is obtained from each patient before any screening and inclusion procedure. Patients remain on study until one of the following condition applies, study withdrawal, discontinuation of treatment or death.

Study objectives and endpoints

The primary objective of the phase 1 – part of the study is to determine the MTD and the RP2D of the combination of regorafenib and FOLFIRINOX. DLT is defined as the occurrence of one or more of the following toxicities during the three first cycles of treatment:

- Unplanned interruption > 7 days of regorafenib due to drug-related toxicity
- Grade (gr.) ≥ 3 (CTCAE v5) non-hematologic toxicity, except: gr. 3 nausea, gr. 3 vomiting, gr. 3 diarrhea, and gr. ≥ 3 lipase elevation without signs of pancreatitis,

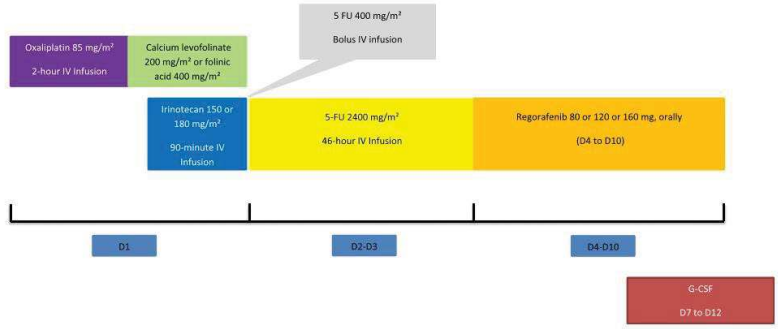

Fig. 1 Treatment design

- Gr. ≥ 2 posterior reversible encephalopathy syndrome,
- Gr. ≥ 2 retinopathy,
- Any of the following liver-specific DLTs: gr. ≥ 3 bilirubin increase, gr. ≥ 3 AST and/or ALT increase, or AST and/or ALT increase > 3 x UNL with concurrent bilirubin increase (> 2 x UNL)
- Gr. 4 neutropenia lasting > 3 days,
- Gr. ≥3 febrile neutropenia (ANC < 1000/mm3 with fever ≥38.5 °C),
- Gr. 4 anemia,
- Platelets < 25,000 /mm3 or platelets < 50,000 /mm3 with bleeding,
- INR or PTT elevation of Gr. ≥ 3 with bleeding,
- Gr. ≥ 3 hemorrhage/bleeding events.

The primary objective of the Phase 2 – part of the study is to evaluate the efficacy, with the 48-week disease-control rate assessment. The latter is defined as the rate of non-progressing patients (after central review) at 48-week post-initiation of therapy, in all treated patients.

The secondary endpoints of the phase 2 – part of the project include safety (according to NCI-CTC v5 scale), overall response rate (according to RECIST v1.1), duration of response, 8-week response rate, deepness of response, disease-control rate, resectability (R0/R1) rate among patients with liver-only metastases, progression-free survival, progression-free survival since maintenance therapy onset with regorafenib, and the overall survival.

Statistical design

A minimum of 12 and a maximum of 24 patients will be included in the phase I – part of the study, with a minimum of 3 and a maximum of 6 patients per dose level. Six patients will be included at the RP2D. It would be necessary to include 65 evaluable patients (actually 69 patients, including 5% non-evaluable patients) in the phase II-part of the trial with the following assumptions, one-stage Fleming design, $\alpha = 5\%$, $\beta = 20\%$, p0 (the probability of maximal inefficiency) = 35% and p1 (the probability of minimal efficiency) = 50%. FOLFIRINOX-R will be considered sufficiently effective (rejection of the null hypothesis) if at least 29 successes occur (defined as a 48-week disease control) out of 65 evaluable patients, the success rate (48-weeks disease control rate) being significantly greater than 35%. FOLFIRINOX-R will be considered insufficiently effective (rejection of the alternative hypothesis) in case of 28 or less successes out of 65 evaluable patients, the success rate (48-weeks disease control rate) being significantly lower than 50%. Overall, a maximum of 87 patients (18 patients for phase I + 69 patients for phase II, including 6 patients treated at the RP2D during the phase I) will be included.

Study procedures

Enrollment into FOLFIRINOX-R will be performed in two stages (a molecular testing then a full testing if appropriate) (Fig. 2) with two separate inform-consent forms. Only patients with the following characteristics, histological or cytological documented metastatic colorectal cancer not amenable to surgical resection with curative intent, no prior therapy for metastatic disease, measurable disease, aged 18 or older, with an Eastern Cooperative Oncology Group performance status ≤1 and a life expectancy of at least 3 months, will undergo the molecular testing which includes a circulating cell-free DNA (ccfDNA) *RAS*-mutation detection, a serum uracil assessment, and an assessment of the polymorphisms of UGT1A*28.

Study population

The patients identified with all the conditions or characteristics listed Table 1 could be included in the study, whereas those identified with at least one condition or characteristic listed Table 2 could not be included.

Table 2 Exclusion criteria

- Previous cancer within 5 years prior to study inclusion except for curatively treated cervical cancer in-situ, non-melanoma skin cancer and superficial bladder tumors (Ta, Tis and T1)
- Diagnostic of metastases within 6 months after the termination of adjuvant chemotherapy.
- Previous treatment for metastatic disease.
- Active cardiac disease including any of the following: congestive heart failure (class 2 NYHA), new-onset angina (begun within the last 3 months), previous myocardial infarction (within the last 6 months), cardiac arrhythmias requiring anti-arrhythmic therapy (beta-blockers or digoxin are permitted).
- ECG with a QT/QTc interval higher than 450 ms for men and higher than 470 ms for women.
- Uncontrolled hypertension, i.e.,: systolic blood pressure > 140 mmHg or diastolic pressure > 90 mmHg despite optimal medical management
- Arterial or venous thrombotic or embolic events such as cerebrovascular accident, deep vein thrombosis or pulmonary embolism within 6 months before the start of treatment.
- Major surgical procedure, open biopsy, or significant traumatic injury within 28 days prior to first dose of treatment. Non-healing wound, ulcer, or bone fracture. History of gastrointestinal fistula or perforation.
- Persistent NCI-CTCAE v5 gr.3 proteinuria, i.e.: urinary protein ≥3.5 g/24 h)
- Peripheral neuropathy > gr.1
- Ongoing infection > gr.2. Live attenuated vaccines are prohibited 10 days before the treatment, during the treatment and 3 months after the treatment
- Known history of human immunodeficiency virus (HIV) infection and/or chronic hepatitis B or C infection.
- Seizure disorder requiring medication.
- Symptomatic metastatic brain or meningeal tumors.
- Evidence or history of any bleeding diathesis, irrespective of severity. Any hemorrhage or bleeding event ≥ gr.3 within 4 weeks prior to the start of study medication.
- History of organ allograft.
- Dehydration ≥ gr.1.
- Substance abuse, medical, psychological, or social conditions that may interfere with the patient's participation in the study or evaluation of the study results.
- Known hypersensitivity to any of the study drugs, study drug classes, or any constituent of the products.
- Interstitial lung disease with ongoing signs and symptoms.
- Concomitant intakes of St. John's Wort.
- Inability to swallow oral medication or any malabsorption condition.
- Pregnant or breast-feeding subjects.
- Participation in another clinical study with an investigational product during the last 30 days before inclusion. Any condition that, in the opinion of the investigator, would interfere with the evaluation of study treatment or interpretation of patient safety or study results
- Patients who might be interconnected with or dependent on the sponsor site or the investigator.
- Legal incapacity or limited legal capacity.

worth studying the combination of 3-CTx to regorafenib in *RAS*-mutant mCRC patients. On that line, we expect that this FOLFIRINOX-regorafenib combination will be able to challenge the FOLFIRINOX-bevacizumab regimen in primarily unresectable mCRC patients with *RAS*-mutant tumors.

We preferentially used FOLFIRINOX as backbone 3-CTx rather than FOLFOXIRI which was investigated by the GONO group [6] because we have a pioneered and long-lasting experience with FOLFIRINOX, both in the metastatic and in the adjuvant setting in colorectal and pancreatic cancer [4, 16–18]. The key difference between FOLFIRINOX and FOLFOXIRI relies on irinotecan and fluorouracil dosing (FOLFIRINOX: irinotecan 150 mg/m^2, fluorouracil 2400 mg/m^2 as a continuous infusion plus bolus fluorouracil 400 mg/m^2; FOLFOXIRI: irinotecan 165 mg/m^2, fluorouracil 3200 mg/m^2 as a continuous infusion without any bolus of fluorouracil). As there is no evidence that FOLFIRINOX is different from FOLFOXIRI, we use the 3-CTx regimen we are confident with, i.e.: the FOLFIRINOX regimen. We used regorafenib continuation beyond the scheduled interruption of chemotherapy after 12 cycles. For patients who achieved disease control after 4 cycles of chemotherapy (most of the time 2-CTx with or without bevacizumab), the most common maintenance strategies are the following: maintenance with fluoropyrimidine or with fluoropyrimidine plus bevacizumab or observation [19]. Less is known for patients achieving disease control with 12 cycles of 3-CTx plus bevacizumab. In this clinical trial, the regorafenib use is all the more relevant for maintenance therapy that it provides (as opposed to bevacizumab monotherapy) an already demonstrated antitumour activity in mCRC [11, 12].

Conclusion

The FOLFIRINOX-R study is the first phase I/II study to evaluate the safety and efficacy of regorafenib in combination with FOLFIRINOX as initial therapy for patients with primarily unresectable mCRC, which are found *RAS*-mutated on plasmatic ccfDNA assessment. Our objective is to demonstrate that this FOLFIRINOX-regorafenib combination provides enough clinical benefit to be tested in a controlled study in a selected patient population.

Abbreviations

CRC: Colorectal cancer; mCRC: Metastatic colorectal cancer; 2-CTx: Chemotherapy doublet; 3-CTx: Chemotherapy triplet; PFS: Progression-free survival; OS: Overall survival; ccfDNA: Circulating cell-free DNA

Acknowledgements

Not Applicable.

Authors' contributions

AA, TM, CBM, and MY designed the clinical study and will contribute to data interpretation. AA, TM, LE and FG contributed to the drafting of the manuscript. PC contributed to the trial set-up. PC and SD are responsible for data collection and for administrative support. BP does the circulating cell-free DNA analyses. JF and CBM designed the statistical part of the study and will contribute to statistical analysis. All authors contributed to the revision of the manuscript and approved it for submission.

Funding

This on-going study is supported by an unrestricted research grant from Bayer Healthcare Pharmaceutical, which also provided regorafenib. The funder has no role in study design, management, analysis and interpretation of data as well as no role in the writing of the final report.

Availability of data and materials
Data sharing is not applicable to this article as no datasets were generated or analysed up to now for the current study.

Declarations

Ethics approval and consent to participate
The study was approved by French regulatory authorities (Agence nationale de sécurité du médicament et des produits de santé) on Jan 24th 2019, received a favorable opinion by the "Comité de Protection des Personnes EST III" (Dec 6th, 2018) and complies with the Helsinki declaration and French laws and regulations, and follows the International Conference on Harmonisation E6 (R2) Guideline for Good Clinical Practice. Written informed consent will be obtained from each patient before any screening and inclusion procedure. The trial results, even inconclusive, will be submitted in a peer-reviewed journal. Trial registration numbers are the following: EudraCT number: 2018–003541-42; ClinicalTrials.gov number: NCT03828799.

Consent for publication
Not Applicable.

Competing interests
The authors declare that they have no competing interests.

Author details
[1]IRCM, Inserm, Université Montpellier, ICM, Montpellier, France. [2]Department of Medical Oncology, Montpellier Cancer Institute (ICM), Montpellier, France. [3]Department of Gastrointestinal Oncology, Institut Régional du Cancer de Montpellier, 208 Avenue des Apothicaires, 34000 Montpellier, France. [4]Biometrics Unit, Montpellier Cancer Institute (ICM), Montpellier, France. [5]Department of Clinical Research, Montpellier Cancer Institute (ICM), University of Montpellier, Montpellier, France. [6]IRCM, Inserm U1194, Montpellier, France. [7]Department of Medical Oncology, Centre Antoine Lacassagne, Nice, France. [8]Department of Medical Oncology, Georges François Leclerc, Dijon, France.

Received: 10 August 2020 Accepted: 6 May 2021
Published online: 17 May 2021

References

1. Bray F, Colombet M, Mery L, Piñeros M, Znaor A, Zanetti R, Ferlay J, editors. Cancer Incidence in Five Continents, Vol. XI. IARC Scientific Publication No. 166. Lyon: International Agency for Research on Cancer; 2020. Available from: https://publications.iarc.fr/597.
2. Van Cutsem E, Cervantes A, Adam R, et al. ESMO consensus guidelines for the management of patients with metastatic colorectal cancer. Ann Oncol. 2016;27(8):1386–422. https://doi.org/10.1093/annonc/mdw235.
3. Falcone A, Ricci S, Brunetti I, Pfanner E, Allegrini G, Barbara C, et al. Phase III trial of infusional fluorouracil, leucovorin, oxaliplatin, and irinotecan (FOLFOXIRI) compared with infusional fluorouracil, leucovorin, and irinotecan (FOLFIRI) as first-line treatment for metastatic colorectal cancer. J Clin Oncol. 2007;25(13):1670–6. https://doi.org/10.1200/JCO.2006.09.0928.
4. Ychou M, Rivoire M, Thezenas S, Quenet F, Delpero JR, Rebischung C, et al. A randomized phase II trial of three intensified chemotherapy regimens in first-line treatment of colorectal cancer patients with initially unresectable or not optimally resectable liver metastases. The METHEP trial. Ann Surg Oncol. 2013;20(13):4289–97. https://doi.org/10.1245/s10434-013-3217-x.
5. Modest DP, Ricard I, Heinemann V, Hegewisch-Becker S, Schmiegel W, Porschen R, et al. Outcome according to KRAS-, NRAS- and BRAF-mutation as well as KRAS mutation variants: pooled analysis of five randomized trials in metastatic colorectal cancer by the AIO colorectal cancer study group. Ann Oncol. 2016;27(9):1746–17. https://doi.org/10.1093/annonc/mdw261.
6. Loupakis F, Cremolini C, Masi G, Lonardi S, Zagonel V, Salvatore L, et al. Initial therapy with FOLFOXIRI and bevacizumab for metastatic colorectal cancer. N Engl J Med. 2014;371(17):1609–18. https://doi.org/10.1056/NEJMoa1403108.
7. Cremolini C, Loupakis F, Antoniotti C, Lupi C, Sensi E, Lonardi S, et al. FOLFOXIRI plus bevacizumab versus FOLFIRI plus bevacizumab as first-line treatment of patients with metastatic colorectal cancer: updated overall survival and molecular subgroup analyses of the open-label, phase 3 TRIBE study. Lancet Oncol. 2015;16(13):1306–15. https://doi.org/10.1016/S1470-2045(15)00122-9.
8. Schmieder R, Hoffmann J, Becker M, Bhargava A, Müller T, Kahmann N, et al. Regorafenib (BAY 73-4506): antitumor and antimetastatic activities in preclinical models of colorectal cancer. Int J Cancer. 2014;135(6):1487–96. https://doi.org/10.1002/ijc.28669.
9. Mross K, Frost A, Steinbild S, Hedbom S, Büchert M, Fasol U, et al. Phase I dose-escalation study of regorafenib (BAY 73 4506), an inhibitor of oncogenic, angiogenic, and stromal kinases, in patients with advanced solid tumors. Clin Cancer Res. 2012;18(9):2658–67. https://doi.org/10.1158/1078-0432.CCR-11-1900.
10. Jeong W, Doroshow JH, Kummar S. US FDA approved oral kinase inhibitors for the treatment of malignancies. Curr Probl Cancer. 2013;37(3):110–44. https://doi.org/10.1016/j.currproblcancer.2013.06.001.
11. Grothey A, Van Cutsem E, Sobrero A, et al. Regorafenib monotherapy for previously treated metastatic colorectal cancer (CORRECT): an international, multicentre, randomised, placebo controlled, phase 3 trial. Lancet. 2013;381(9863):303–12. https://doi.org/10.1016/S0140-6736(12)61900-X.
12. Li J, Qin S, Xu R, Yau TC, Ma B, Pan H, et al. Regorafenib plus best supportive care versus placebo plus best supportive care in Asian patients with previously treated metastatic colorectal cancer (CONCUR): a randomised, double-blind, placebo-controlled, phase 3 trial. Lancet Oncol. 2015;16(6):619–29. https://doi.org/10.1016/S1470-2045(15)70156-7.
13. Schultheis B, Folprecht G, Kuhlmann J, Ehrenberg R, Hacker UT, Köhne CH, et al. Regorafenib in combination with FOLFOX or FOLFIRI as first- or second-line treatment of colorectal cancer: results of a multicenter phase Ib study. Ann Oncol. 2013;24(6):1560–7. https://doi.org/10.1093/annonc/mdt056.
14. Sanoff HK, Goldberg RM, Ivanova A, O'Reilly S, Kasbari SS, Kim RD, et al. Multicenter, randomized, double-blind phase 2 trial of FOLFIRI with regorafenib or placebo as second-line therapy for metastatic colorectal cancer. Cancer. 2018;124(15):3118–26. https://doi.org/10.1002/cncr.31552.
15. Tabernero J, Lenz HJ, Siena S, Sobrero A, Falcone A, Ychou M, et al. Analysis of circulating DNA and protein biomarkers to predict the clinical activity of regorafenib and assess prognosis in patients with metastatic colorectal cancer: a retrospective, exploratory analysis of the CORRECT trial. Lancet Oncol. 2015;16(8):937–48. https://doi.org/10.1016/S1470-2045(15)00138-2.
16. Ychou M, Viret F, Kramar A, Desseigne F, Mitry E, Guimbaud R, et al. Tritherapy with fluorouracil/leucovorin, irinotecan and oxaliplatin (FOLFIRINOX): a phase II study in colorectal cancer patients with non-resectable liver metastases. Cancer Chemother Pharmacol. 2008;62(2):195–201. https://doi.org/10.1007/s00280-007-0588-3.
17. Conroy T, Desseigne F, Ychou M, Bouché O, Guimbaud R, Bécouarn Y, et al. FOLFIRINOX versus gemcitabine for metastatic pancreatic cancer. N Engl J Med. 2011;364(19):1817–25. https://doi.org/10.1056/NEJMoa1011923.
18. Conroy T, Hammel P, Hebbar M, Ben Abdelghani M, Wei AC, Raoul JL, et al. FOLFIRINOX or gemcitabine as adjuvant therapy for pancreatic cancer. N Engl J Med. 2018;379(25):2395–406. https://doi.org/10.1056/NEJMoa1809775.
19. Sonbol MB, Mountjoy LJ, Firwana B, Liu AJ, Almader-Douglas D, Mody K, et al. The role of maintenance strategies in metastatic colorectal cancer: a systematic review and network meta-analysis of randomized clinical trials. JAMA Oncol. 2020;6(3):e194489. https://doi.org/10.1001/jamaoncol.2019.4489.

Publisher's Note

Discussion

Dans l'étude ancillaire et prospective de l'essai TEXCAN les données montrent que la concentration totale en ADNcir, la concentration des ADNcir tumoraux *RAS*-mutés ainsi que la fréquence allélique des ADNcir *RAS*-mutés était corrélé à la survie globale des patients CCRm traités au régorafénib. En revanche, nous n'avons pas pu établir de corrélations entre ces paramètres et la survie sans progression. Cela peut être expliqué par le peu d'effet du régorafénib sur la tumeur dans un temps aussi court (environ 2 mois). Nous pensons aussi que dans cette population de patients CRCm lourdement prétraités, la meilleure des réponses espérée est la stabilisation tumorale.

Avant l'initiation du traitement, les résultats suggèrent que les patients ayant une concentration totale en ADNcir supérieure à 26 ng/mL de plasma ont un risque de décès doublé comparé aux patients qui ont des concentrations inférieures à ce seuil. Nous avons pu déjà observer ce résultat dans une étude similaire menée par l'équipe[184]. Aussi, les données montrent que la concentration totale en ADNcir augmente deux semaines après l'initiation du traitement au régorafénib. Ce résultat a pu être décri par d'autres études[248,249] et les auteurs suggèrent que cette augmentation rapide été dues à un relargage d'ADNcir dans la circulation sanguine suite aux effets toxiques du régorafénib sur les cellules des tissus sains[248].

Nous avons montré que les patients ayant une concentration en ADNcir *RAS*-muté inférieure à 2ng/mL de plasma avant l'initiation du traitement par régorafénib avaient une meilleure survie globale que les patients ayant une concentration d'ADNcir *RAS*-mutés supérieure à ce seuil. De plus, comme attendu, nous avons identifié plusieurs changements mutationnels dans les 8 semaines suivant la dose initiale de régorafénib (c'est-à-dire la durée médiane du traitement par régorafénib). Bien que ces changements ne se soient pas traduits par des résultats différents, leur nature rapide sans précédent dans notre série est impressionnante. A notre connaissance ces résultats sont les premiers publiés sur le sujet. Sur la base de cette observation et de celle de notre précédent rapport sur un groupe similaire de patients soumis à d'autres thérapies expérimentales[173], nous suggérons que ces changements mutationnels sont plus probablement liés aux caractéristiques cliniques de ces patients atteints de cancer colorectal métastatique fortement prétraité plutôt qu'au régorafénib lui-même.

Notre étude est exploratoire et comporte certaines limites et par conséquent les données doivent être interprétées avec prudence. Étant donné la nature exploratoire de cette analyse, les valeurs P n'ont pas été corrigées pour les tests multiples. La taille réduite de l'échantillon pour cette analyse n'a pas pu contrebalancer le manque de puissance dû à la perte de 12 patients (22%) de la population native de TEXCAN. De plus, étant donné que le régorafénib est plus susceptible d'être cytostatique que cytotoxique et que la durée du traitement est très courte, il serait déraisonnable de s'attendre à une réduction significative de la tumeur accompagnée d'une forte diminution des biomarqueurs de l'ADN circulant chez les patients atteints de cancer colorectal métastatique fortement prétraité.

Pour conclure, dans l'essai TEXCAN nous confirmons le bénéfice potentiel de l'analyse de l'ADNcir avant le traitement par regorafenib comme méthode appropriée pour identifier les patients atteints de CRCm plus susceptibles d'avoir les meilleurs résultats. Compte tenu de notre contexte et de l'inclusion de patients atteints de cancer colorectal métastatique fortement prétraité, des recherches supplémentaires impliquant une cohorte de validation plus importante sont nécessaires pour déterminer si le seuil de 26 ng/mL pour l'analyse de l'ADNcir est le plus optimal pour distinguer les patients ayant un mauvais ou un meilleur pronostic.

Pour aller plus loin, l'étude FOLFIRINOX-R^{250} que nous menons est actuellement la première étude de phase I/II visant à évaluer l'innocuité et l'efficacité du régorafénib en association avec FOLFIRINOX comme traitement initial chez les patients atteints CCRm principalement non opérable et dont l'anlayse de l'ADNcir plasmatique révèle une mutation *RAS*. Notre objectif est de démontrer que cette association FOLFIRINOX-régorafenib apporte un bénéfice clinique suffisant pour être testée dans une étude contrôlée dans une population de patients sélectionnés. Un suivi de ces patients par l'analyse longitudinale de l'ADNcir lors du traitement serait une opportunité supplémentaire afin d'établir de potentiels biomarqueurs de sensibilité ou de résistance au régorafenib.

2/ Origine des ADN circulant chez les patients atteints de cancer colorectal métastatique

Article V: Association entre de la formation de pièges extracellulaires des neutrophiles avec la production d'ADN circulant chez les patients atteints d'un cancer colorectal métastatique. (Étude PaniNet)

Brice Pastor, Jean-Daniel Abraham, Ekaterina Pisareva, Cynthia Sanchez, Andrei Kudriavstev, Rita Tanos, Alexia Mirandola, Lucia Mihalovičová, Veronique Pezzella, Antoine Adeni[4], Marc Ychou, Thibault Mazard and Alain R. Thierry

Accepté dans iScience le 30 janvier 2022

Rationnel: Cette étude fait partie intégrante de mon travail de thèse puisqu'il a pour objectif de mettre en lumière une nouvelle source potentielle des ADNcir en oncologie. Cette nouvelle source des ADNcir pourrait expliquer les grandes variations de fréquence allélique retrouvée chez les patients atteints de CRCm, même si ces patients ont des caractéristiques cliniques « identiques » et des masses tumorales « similaires ». En effet, les ADNcir tumoraux sont dilués par un relargage d'ADNcir provenant de cellules saines entrainant la diminution parfois drastique des fréquences alléliques tumorales. Les variations de fréquence allélique sont cruciales dans tous mes travaux basés sur la détection des mutations *RAS/BRAF* chez des patients CRCm car elle peut entrainer des mauvais diagnostics et par conséquent donner lieu à de mauvais traitements.

Contribution: J'ai réalisé les analyses de quantification des ADNcir, de NE et de MPO chez les patients atteints de CCRm (patients screenés lors de l'esai PANIRINOX) et chez les individus sains. J'ai aussi réalisé les analyses de corrélation ainsi que les statistiques. Enfin j'ai participé à l'écriture du manuscrit.

Introduction

L'analyse de l'ADNcir est un domaine très prometteur en oncologie et l'intérêt qu'on lui prête ne cesse d'être grandissant ces dernières années. Notamment pour les cliniciens-oncologues pour lesquels de nombreuses études ont démontré son potentiel afin d'orienter et d'assurer la prise en charge des patients, et ce quel que soit le stade de la maladie. Bien qu'un grandissant de travaux ait été mené pour mieux caractériser les origines et les structures des ADNcir, les connaissances reste incomplètes à ce sujet[77].

Jusqu'à présent, Il est mentionné dans la littérature que l'ADN circulant est libéré via les mécanismes de nécrose[93,251], d'apoptose[95,251]et par phénomènes de sécrétion active[94,125]. Aussi, chez les patients cancéreux la proportion des ADNcir issus des différentes origines cellulaires comme les cellules malignes, les cellules non-malignes, les cellules du microenvironnement tumoral (TME) ou encore les cellules immunitaires n'a pas été clairement établi.

Les neutrophiles sont les cellules immunitaires innées les plus abondantes dans la circulation sanguine, et offrent une première ligne de défense immunitaire contre les bactéries, les virus et les parasites. L'élimination de ces agents pathogènes par les neutrophiles fait intervenir quatre mécanismes distincts: la phagocytose, la dégranulation, la production de cytokines et la NETose[109,110]. Cette dernière consiste en une libération de pièges ADN extracellulaires sécrétés par des neutrophiles activés (NETs) qui sont composés d'un réseau de chromatine extracellulaire décorée de protéines cytosoliques et de granules bactéricides, telles que l'élastase des neutrophiles (NE) et la myéloperoxydase (MPO)[252]. Il est intéressant de noter que les NETs sont retrouvés dans les mêmes conditions pathologiques pour lesquelles des concentrations élevées d'ADNcir ont été rapportées: exemples[77,114].

De plus, outre la contribution des NETs à la survenue de thromboses[253], les anti-phospholipides (aPL) tels que les anti-cardiolipines (aCL) ont été associés à la thrombose dans diverses maladies, en particulier dans les maladies chroniques[254,255]. Bien que le processus thrombophilique ou l'association directe de l'aPL ne soit pas clair, il a été suggéré que des niveaux élevés du d'aPL dans le plasma pourrait déclencher une thrombose chez les patients cancéreux[256,257]. Aussi, il semblerait que les cadiolipines via leurs chaines carbonées ont une conformation structurale similaire à celle des ADN. Nous pensons donc qu'une réaction

croisée entre les autoanticorps anti-DNA contre les cardiolipines et les anti-aCL contre les ADNcir peut se faire dans le plasma de patients atteints de cancer. L'accumulation de NETs pourrait exacerber ce phénomène de cross-réactivité et pourrait se traduire par l'apparition de thrombose.

Dans ce contexte, nous émettons l'hypothèse qu'une fraction de la production de l'ADNcir chez des patients atteints de cancer métastatique provient de la dégradation des NETs. Parallèlement aux niveaux de marqueurs de NETs et à ceux de l'ADNcir, nous avons déterminé les niveaux d'aCL afin d'étudier leur association. Pour ce faire, nous avons exploité les données et les échantillons de plasma des patients screenés dans le cadre de l'essai clinique PANIRINOX de l'UCGI 28 (NCT02980510).

L'examen concomitant des biomarqueurs protéiques des NETs (NE et MPO) avec la quantification de l'ADNcir sont évalués chez 219 patients atteints de CRCm au moment du diagnostic du cancer métastatique. La corrélation respective de ces composés biologiques circulants est comparée à une cohorte témoin constituée d'individus sains (N=114).

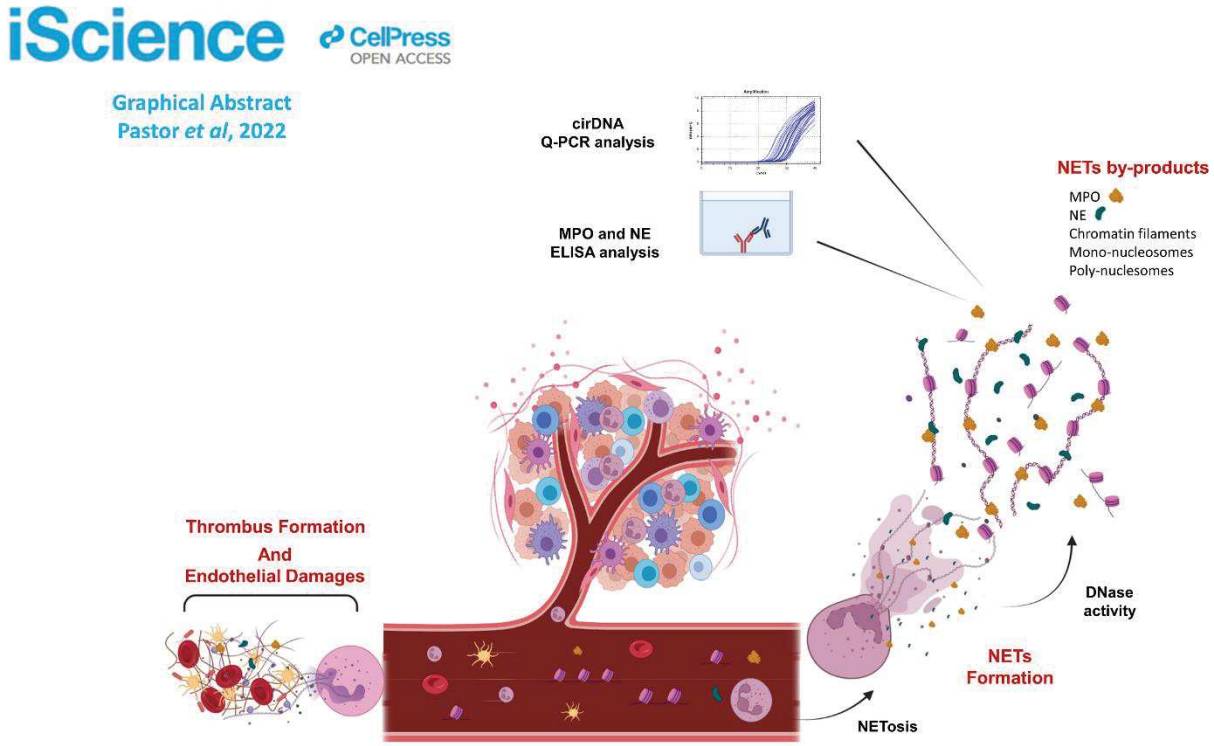

Association of Neutrophil Extracellular Traps with the production of circulating DNA in colorectal cancer patients

Running title: Neutrophil Extracellular Traps and cirDNA concentrations in mCRC patients

Brice Pastor[1,5], Jean-Daniel Abraham[1,5], Ekaterina Pisareva[1], Cynthia Sanchez[1], Andrei Kudriavstev[1], Rita Tanos[1], Alexia Mirandola[1], Lucia Mihalovičová[1,2], Veronique Pezzella[3], Antoine Adenis[1,4], Marc Ychou[1,4], Thibault Mazard[1,4] and Alain R. Thierry[1,4,6]*

1. *IRCM, Institut de Recherche en Cancérologie de Montpellier, INSERM U1194, Université de Montpellier, Institut régional du Cancer de Montpellier, Montpellier, F-34298, France*

2. *Institute of Molecular Biomedicine, Faculty of Medicine, Comenius University, Sasinkova 4, 811 08, Bratislava, Slovakia*

3. *UNICANCER, Paris, France*

4. *Department of Medical Oncology, Montpellier Cancer Institute (ICM), Montpellier, France*

5. These authors contributed equally

6. Lead contact

* Corresponding author: Alain R. Thierry, alain.thierry@inserm.fr
IRCM, Institut de Recherche en Cancérologie de Montpellier, INSERM U1194, Université de Montpellier, Institut régional du Cancer de Montpellier, Montpellier, F-34298, France.
Tel: +33 663 821994

Keywords: colorectal cancer, circulating DNA, neutrophil extracellular traps, extracellular traps, neutrophil elastase, myeloperoxidase,

SUMMARY

We postulate that a significant part of circulating DNA (cirDNA) originates in the degradation of neutrophil extracellular traps (NETs). In this study, we examined the plasma level of two markers of NETs (myeloperoxidase (MPO) and neutrophil elastase (NE)), as well as cirDNA levels in 219 patients with a metastatic colorectal cancer (mCRC), and in 114 healthy individuals (HI). We found that in mCRC patients the content of these analytes was (i) highly correlated, and (ii) all statistically different ($P<0.0001$) than in HI ($N=114$). These three NETs markers may readily distinguish between mCRC patients from HI, (0.88, 0.86, 0.84 and 0.95 AUC values for NE, MPO, cirDNA and NE+MPO+cirDNA, respectively). Concomitant analysis of anti-phospholipid (anti-cardiolipin), NE, MPO, and cirDNA plasma concentrations in mCRC patients might have value for thrombosis prevention, and suggested that NETosis may be a critical factor in the immunological response/phenomena linked to tumor progression.

INTRODUCTION

Circulating cell-free DNA (cirDNA) is one of the fastest growing and most promising areas in oncology in recent years. CirDNA is defined as extracellular DNA occurring in blood (Bronkhorst et al., 2021). Studies have indicated the great potential of cirDNA for "liquid biopsies" in oncology (Diaz and Bardelli, 2014; Heitzer et al., 2020; Thierry et al., 2016; Wan et al., 2017) and for non-invasive prenatal testing (Dennis Lo and Poon, 2003).
While cirDNA analysis is routinely implemented in cancer theranostics, for example for the detection of *EGFR* mutations in lung cancer, it also has significant appeal to researchers and clinicians in many other areas of cancer management care, including the detection of minimal residual disease (Benešová et al., 2019; Parikh et al., 2021; Tie et al., 2016), treatment monitoring (Sefrioui et al., 2021; Thierry et al., 2017), cancer recurrence surveillance (Parikh et al., 2021; Sefrioui et al., 2021), and even cancer screening (Cohen et al., 2018; Cristiano et al., 2019; Sanchez et al., 2021; Tanos et al., 2020). That said, cirDNA's biological features and potential functions remain poorly known. Its analytic performance, however, has been greatly improved by critical discoveries regarding its structure/topology (Chandrananda et al., 2015; Jiang et al., 2015; Mouliere et al., 2011) and its origin (nuclear vs mitochondrial (Al Amir Dache et al., 2020; Meddeb, Dache, et al., 2019). Recent advances in knowledge acquired through fragmentomics by cirDNA size profile analysis (Chandrananda et al., 2015; Sanchez et al., 2018, 2021; Serpas et al., 2019), methylation (Jensen et al., 2019; Lehmann-Werman et al., 2016; Moss et al., 2018) and nucleosome positioning (Snyder et al., 2016) may contribute to higher capacities in diagnostics or early cancer detection(Cohen et al., 2018; Cristiano et al., 2019; Tanos et al., 2020). Up to now, the impact of malignant cells, tumor microenvironment (TME) and germinal origin on cirDNA release in cancer patients has not been clearly established. We hypothesize that a significant fraction of cirDNA production derives from the degradation of neutrophil extracellular traps (NETs).

Neutrophils are the most abundant innate immune cells, and offer a first line of immune defense against bacteria, viruses, parasites, yeast and fungi (Urban et al., 2006; Waisberg et al., 2014; Yipp et al., 2012). The elimination of pathogens by neutrophils involves four distinct mechanisms: phagocytosis, degranulation, cytokines production and NETosis (Brinkmann, 2018). The latter consists of a release of Neutrophil Extracellular Traps (NETs) which are an extracellular web-like chromatin decorated with cytosolic and bactericidal granules proteins, such as neutrophil elastase (NE) and myeloperoxidase (MPO) (Metzler et al., 2014). While extracellular traps (ETs) formation is prominent in neutrophils, several other types of innate or adaptive immune cells reportedly release (following strong activation signals) chromatin and granular proteins (MPO, NE,…) into the extracellular space, thus forming ETs: macrophages, eosinophils, basophils, mast cells and lymphocytes (Daniel et al., 2019). NETosis is one of the phenomena by which extracellular DNA may be released into the bloodstream by cell death and active secretion (Al-Khafaji et al., 2016; Papayannopoulos, 2018; Yousefi et al., 2019).

Over the past dozen years, numerous studies have elucidated the role of circulating neutrophils, circulating NETs and circulating NETs by-product in cancer. It has been demonstrated that various cancer types such as breast, lung or colorectal cancer exhibit an increase in circulating neutrophil numbers(Gentles et al., 2015; Templeton et al., 2014). There is currently an exponential growth in the literature reporting the emerging role of NETs in tumor progression and metastasis (Erpenbeck and Schön, 2017; Kos and de Visser, 2021; Munir et al., 2021; Nolan and Malanchi, 2020; Yang et al., 2020). CRC is one of the malignant diseases which shows the greatest involvement of NETs in tumor

progression and metastasis (Kos and de Visser, 2021; Nolan & Malanchi, 2020). It appears that, by sequestering circulating tumor cells in NETs, neutrophils fertilize the pre-metastasis niche. Furthermore, cancers predispose neutrophils to release extracellular DNA traps, which contribute to cancer-associated thrombosis (Wolach et al., 2018).

Interestingly, NETs are found in the same pathological conditions in which high concentrations of cirDNA have been reported, such as autoimmune diseases (Hakkim et al., 2010), inflammatory diseases (Kaplan and Radic, 2012), sepsis (Luo et al., 2014), thrombotic illnesses (Fuchs et al., 2012) and cancer (Daniel et al., 2019; Thierry et al., 2021; Thierry and Roch, 2020). In the case of cancer patients, we postulate that higher concentrations of circulating neutrophils and their longer lifespan (activated in cancers) could increase the formation of NETs and NETs by-products. These could play a crucial role in cirDNA production, notably in the degradation of the web-like chromatin derived from NETs in blood. In addition to NET's contribution to the occurrence of thrombosis (Wolach et al., 2018), anti-PL such as aCL were associated with thrombosis in various diseases, in particular with chronic diseases (Abdel-Wahab et al., 2020; Leal Rato et al., 2021). While aPL thrombophilic process or direct association is unclear, it has been suggested that aPL plasma high level may trigger thrombosis in cancer patients (Gómez-Puerta et al., 2006; Islam, 2020). Thus, concurrent with NET markers and cirDNA, we determined aCL levels in order to investigate their association.

To explore our hypothesis, we will exploit data and plasma samples from patients screened within the UCGI 28 PANIRINOX clinical trial (NCT02980510), which uses cirDNA analysis to determine their *RAS* and *BRAF* status. This ongoing clinical study is the first interventional study to use cirDNA as a companion test for selecting mCRC patients towards anti-EGFR targeted therapy. Concurrent examination of the conventional NET protein biomarkers (NE and MPO) with the quantification of cirDNA of nuclear and mitochondrial origin are assessed in a large number of mCRC patients at diagnosis (N=219). The respective correlation of these circulating biological compounds will be compared with a control cohort constituted of healthy individuals (N=114).

RESULTS

Concentrations of NETs markers and cirDNA are higher in mCRC patients than in healthy individuals.

The formation of neutrophil extracellular traps was assessed in plasma samples from 219 mCRC patients and 114 healthy individuals (Table 1), as estimated by the concentration of NE and MPO. The concentrations of NE and MPO are significantly higher in mCRC patients than in healthy Individuals (Figure 1) ($p<0.0001$), with respective median concentrations of 12.90 ng/mL and 11.91 ng/mL in HI and 34.70 ng/mL and 38.90 ng/mL in mCRC patients. The concentration of cirDNA is significantly higher in mCRC patients than in HI, with median concentrations of 18.36 ng/mL versus 5.76 ng/mL, respectively **(Figure 1)** ($p<0.0001$). Data revealed the presence of NETs by-products (NE and MPO) in healthy individuals, and their increased presence in mCRC patients.

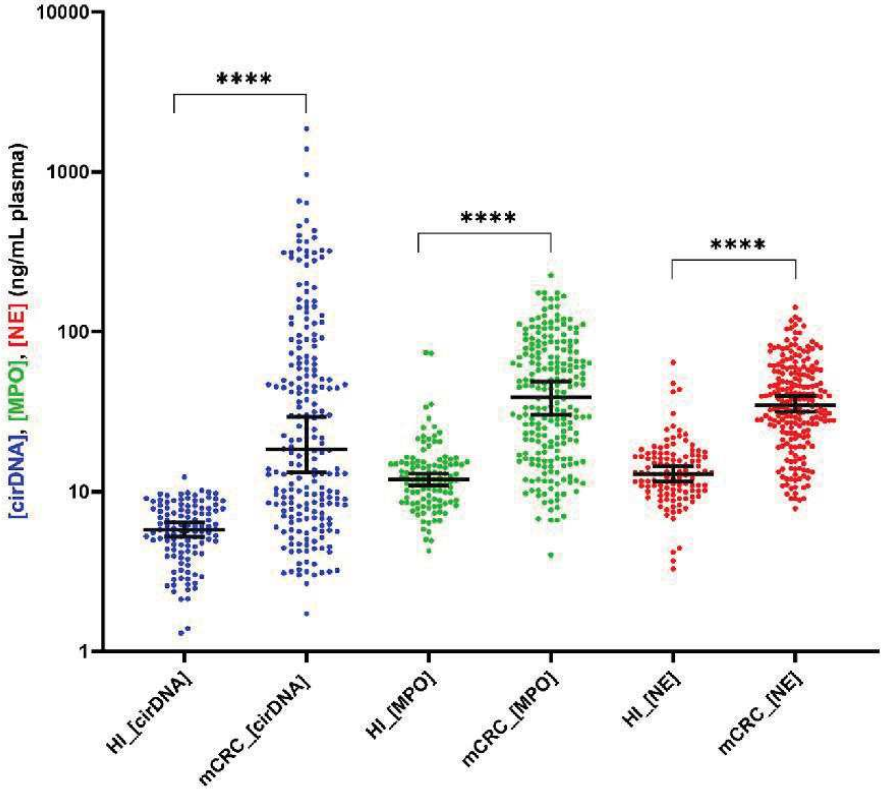

Figure 1: Comparison of cirDNA, MPO and NE concentrations (ng/mL of plasma) in mCRC patients (mCRC) (n=219) and healthy individuals (HI) (n=114). Lines represent median with 95% CI. Mann-Whitney test was performed to compare values for cirDNA, MPO and NE in mCRC patient and in HI (****$p< 0.0001$). A probability of less than 0.05 was considered statistically significant; ****$p< 0.0001$. Each dot represents the values of a single patient or a single healthy individual. CirDNA: circulating cell-free DNA; MPO: myeloperoxidase; NE: neutrophil elastase

Table 1: Patient characteristic

Table 1: Patient characteristics		
Characteristic	**mCRC patients**	**Healthy Individuals (HI)**
N	219	114
Age, y		
Median (range)	61 (37-77)	41 (19-69)
Missing data	96	
Sex		
Male (%)	73 (58,9)	59 (51,8)
Female (%)	51 (41,1)	55 (48,2)
missing data	95	
Location of primary tumour		
Right colon (%)	34 (27,9)	
Left colon (%)	88 (72,1)	
Missing data	97	
Primary tumor in place		
Yes (%)	96 (78)	
No (%)	27 (22)	
Missing data	96	
Number of metastatic sites		
Median (range)	2 (1-4)	
1 (%)	51 (44,3)	
>1 (%)	64 (55,6)	
Missing data	104	
Limited liver disease		
Yes (%)	45 (36,3)	
No (%)	79 (63,7)	
Missing data	95	
Leucocytes cell count (G/L)		
Median (range)	8 (3,93-27,33)	
Missing data	104	
LDH level (U/L)		
Median (range)	315,5 (148-4502)	
Missing data	123	
CEA level (ng/mL)		
Median (range)	41,7 (0,70-14034)	
Missing data	107	
Platelet count (G/L)		
Median (range)	314 (116-849)	
Missing data	152	
Creatinine clearance (mL/min) CKD		
Median (range)	93,5 (44-120)	
Missing data	155	

CEA: carcinoembryonic antigen; LDH: Lactate dehydrogenase; mCRC: metastatic colorectal cancer

Concentrations of cirDNA and neutrophil extracellular traps markers in mCRC patients are associated.

We used a Spearman correlation test to assess the association between cirDNA concentrations and NETs markers. First, data show a significantly positive association between NE and MPO in both mCRC patients (n=219) and HI (n=114), r=0.79 (p<0.0001) and r=0.37 (p<0.0001), respectively **(Figure 2)**. This positive correlation between NE and MPO shows that NETs are generated in mCRC patients as well as in healthy individuals. In mCRC patients, data revealed a significantly positive associations between both MPO and cirDNA concentrations and NE and cirDNA concentrations, r=0.59 (p<0.0001) and r=0.38 (p<0.0001), respectively **(Figure 2A)**. No or poor association between MPO, NE and cirDNA concentrations was found in HI (**Figure 2B)**. As observed in our previous work, cirDNA concentrations as determined by targeting *KRAS* and *BRAF* wild type sequences showed a very high correlation, r=0.97 (p<0.0001) (Figure S1), confirming earlier observation when validating a *KRAS* sequence-based Q-PCR system, and using a *BRAF* sequence-based Q-PCR system as quality control.

To evaluate the influence of strong concentration of cirDNA in mCRC patients on the correlation between NETs markers and cirDNA concentrations, we dichotomized the mCRC population into subgroups based on their cirDNA concentrations, and compared their NE and MPO values with those of healthy individuals (Figure S2). Given that the median cirDNA concentrations is about 6 ng/mL in HI **(Figure 1)**, we first compared mCRC patients with cirDNA concentrations below 6 ng/mL to match with cirDNA values of HI. Then, we also dichotomized mCRC patients into subgroups of cirDNA concentrations over 6 ng/mL. Data reveals that for cirDNA concentrations close to 6 ng/mL, the MPO concentrations are significantly higher in mCRC patients than in healthy individuals, with median concentrations of 17.76 ng/mL and 11.91 ng/mL (p<0.0001), respectively (Figure S2A). Similar observations were made for NE concentrations, with median concentrations of 28.18 ng/mL and 12.90 ng/mL (p<0.001) in mCRC patients and HI respectively (Figure S2B).

In the same way, data shows that in mCRC patients, the higher the concentrations of NETs markers, the higher the cirDNA concentration (Figure S2).

To evaluate whether cirDNA production derives partly from NETs in cancer patients, we dichotomized the mCRC patients and the HI cohort by their MPO and NE median values, and then compared the cirDNA concentrations with the concentrations of NETs markers (Figure S3). For mCRC patients, we observed a significant increase of cirDNA values in patients with MPO and NE concentrations higher than the medians values, as compared to patients with cirDNA concentrations under the median values, 38.9 ng/mL and 34.7 ng/mL (p<0.0001), respectively (Figure S3A and S3C). Alternatively, when we dichotomized healthy individuals by their MPO median value (11.91 ng/mL), we did not observe a significant variation of cirDNA concentrations between the two groups of HI (Figure S3B). When the HI cohort was dichotomized by the NE median value (12.90 ng/mL), a slightly significant increase of cirDNA concentrations in HI with NE concentrations higher than the median value as compared to HI with NE concentrations below the median value was observed (Figure S3D).

A

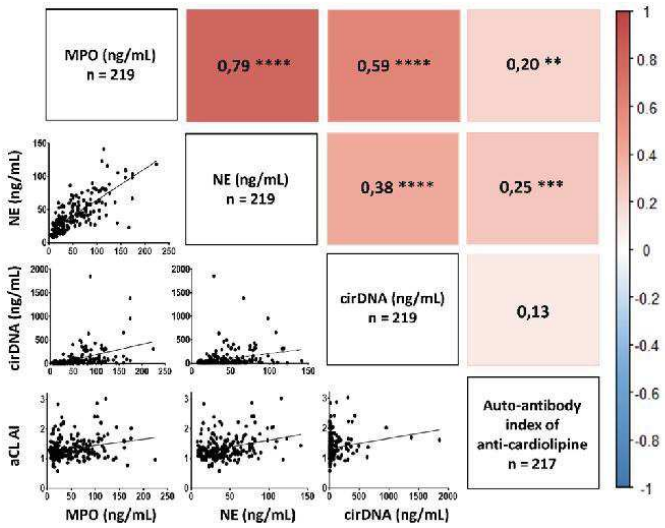

B

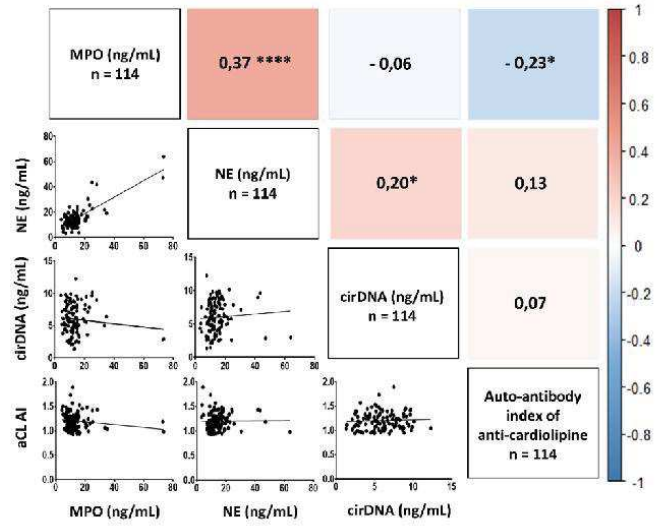

Figure 2: Correlation matrix of cirDNA, MPO and NE concentrations (ng/mL plasma) and the anti-cardiolipin autoantibody index (aCL AI) in mCRC patients (n=219) (A) and in healthy individuals (n=114) (B). Heatmap manifests the strength of relationship by Spearman's correlation analysis (red: positive correlation; blue: negative correlation). A probability of less than 0.05 was considered statistically significant;** p< 0.01; ***p< 0.001. CirDNA: circulating cell-free DNA; MPO: myeloperoxidase; NE: neutrophil elastase; aCL AI: anti-cardiolipin autoantibody index.

Association between NE, MPO and cirDNA concentrations and neutrophil and lymphocyte cell counts.

To confirm that NETs markers concentrations and cirDNA concentrations are generated by neutrophils, we interrogated the association between these markers and neutrophil and lymphocyte cell counts in mCRC patients. Data revealed a very significant association between NE, MPO and cirDNA concentrations and leucocyte cell counts, with r=0.51, r=0.54 and r=0.48 (p<0.0001), respectively **(Figure 3)**. Interestingly, there was a significant association between neutrophil cell counts, the absence of surgery on the primary tumor, and the number of metastatic sites (threshold >1) (Figure 4A). Similarly, we found the same results between the leucocytes cell count and the absence of surgery on the primary tumor, and the number of metastatic sites (threshold >1) (Figure S4). Nevertheless, we did not find any association between lymphocyte cell counts and those clinical characteristics (Figure 4B). Similarly, a very significant association was observed between cirDNA, MPO, and NE concentrations and neutrophil cell counts, with r=0.49, r=0.62 and r=0.54 (p<0.0001), respectively **(Figure 4C, Figure 4D and Figure 4E)**. Conversely, we did not find any association between lymphocyte cell counts and cirDNA, MPO, and NE concentrations in this cohort **(Figure 4F, 4G and 4H)**. The neutrophil to lymphocyte Ratio (NLR) is significantly associated with cirDNA, MPO and NE concentrations in mCRC patients **(Figure 4I, Figure 4J and Figure 4K)**.

Association with other clinical and biological factors.

In mCRC patients, we observed a positive correlation between the NETs markers and NLR, the lactate dehydrogenase level (LDH, U/L), the carcinoembryonic antigen level (CEA, ng/mL), the corrected calcemia level (mmol/L), the platelet count (G/L), and the total bilirubin level (µmol/L) **(Figure 3)**. We observed a negative correlation with the haemoglobin level (g/dL) with NETs markers **(Figure 3)**. Note, MPO is the marker that correlated most with such others factors. In contrast, in mCRC patients poor or no association was detected between NETs markers and the DNA integrity index (DII), age, the number of metastatic sites, and the creatinine clearance (mL/min, CKD) (Figure 3). CirDNA, MPO and NE globally correlate the same way with respect to those factors.

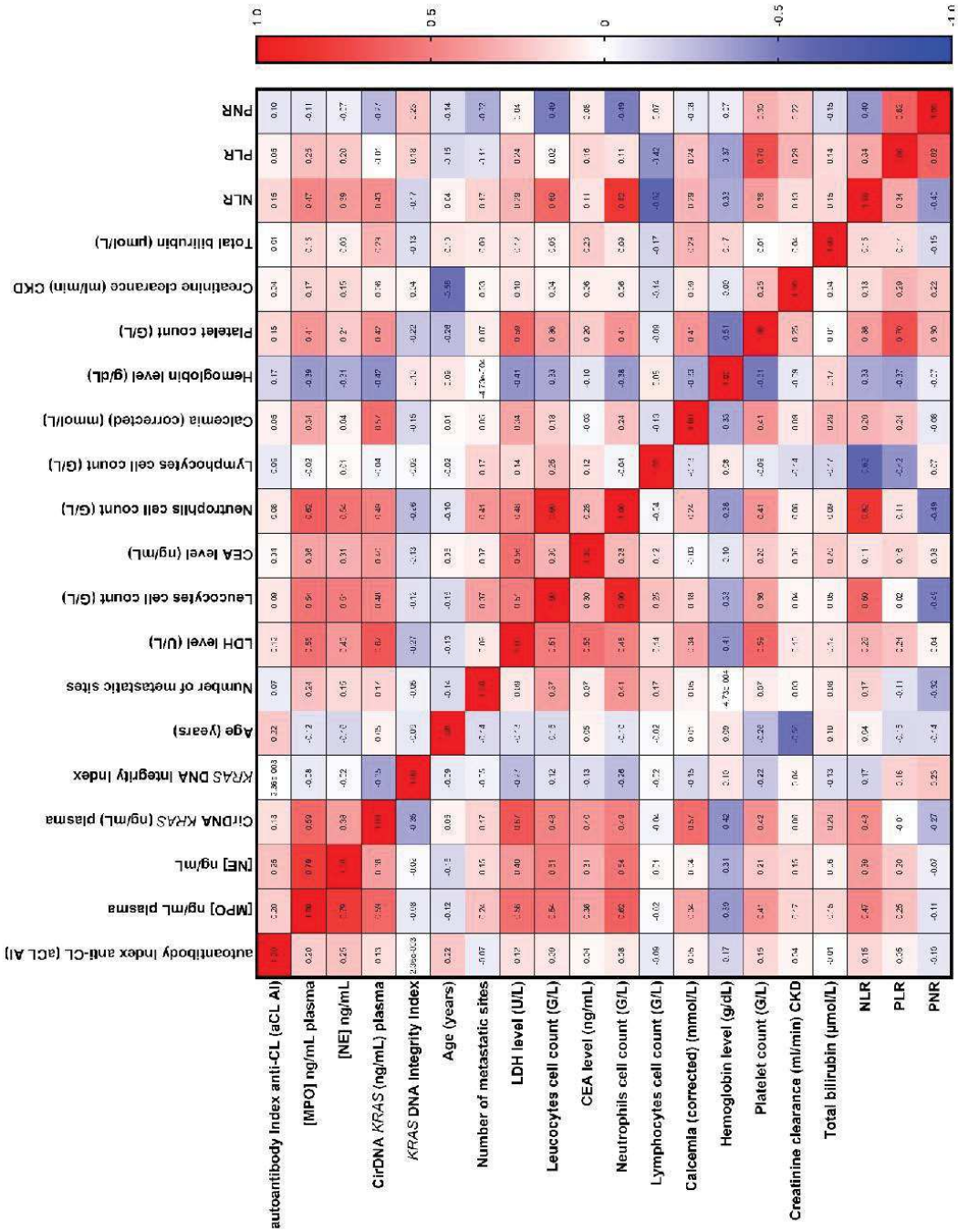

Figure 3: Correlation matrix of cirDNA, MPO and NE concentrations (ng/mL plasma) with numerous clinical and biological features in mCRC patient (n=219). Heatmap manifests the strength of relationship by Spearman's correlation analysis (red: positive correlation; blue: negative correlation). CirDNA: circulating cell-free DNA; MPO: myeloperoxidase; NE: neutrophil elastase; aCL AI: anti-cardiolipin autoantibody index; CEA: carcinoembryonic antigen; LDH: Lactate dehydrogenase; NLR: the neutrophil to lymphocyte Ratio; PLR: the platelet to lymphocytes Ratio; PNR: the platelet to neutrophil Ratio.

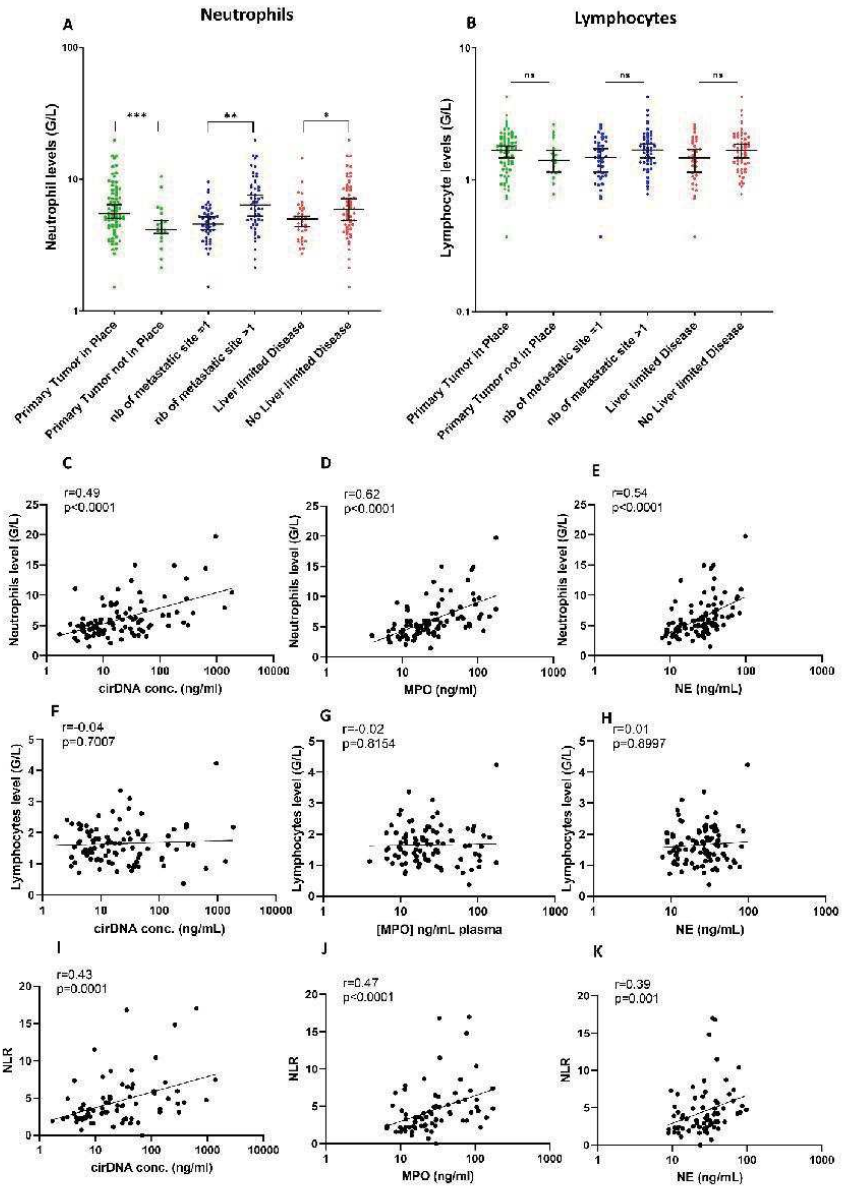

Figure 4: Comparison of neutrophils and lymphocytes cell count (G/L) with clinical features and association of neutrophils cell count (G/L) and the neutrophil to lymphocyte ration (NLR) with cirDNA, MPO and NE concentrations (ng/mL of plasma) in mCRC patients (n=219). Lines represent median with 95% CI. Mann-Whitney test was performed to compare (A) neutrophils cell count (G/L) with clinical features, (B) lymphocytes cell count (G/L) with clinical features. Association between (C) neutrophils cell count (G/L) and cirDNA concentrations (ng/mL), (D) neutrophils cell count (G/L) and MPO concentrations (ng/mL), (E) neutrophils cell count (G/L) and NE concentrations (ng/mL), (F) lymphocytes cell count (G/L) and cirDNA concentrations (ng/mL), (G) lymphocytes cell count (G/L) and MPO concentrations (ng/mL), (H) lymphocytes cell count (G/L) and NE concentrations (ng/mL) (I) the NLR and cirDNA concentration (ng/mL), (J) the NLR and MPO concentration (ng/mL), and (K) the NLR and NE concentration (ng/mL). Each dot represents the values of a single patient. A probability of less than 0.05 was considered statistically significant. CirDNA: circulating cell-free DNA; MPO: myeloperoxidase; NE: neutrophil elastase; NLR: the neutrophil to lymphocyte Ratio.

Anti-cardiolipin autoantibody detection, and its association between NE, MPO and cirDNA concentrations in mCRC patients.

First, the anti-cardiolipin autoantibody index (aCL AI) is significantly higher in mCRC patients than in HI, with mean concentrations of 0.389 [95%CI, 0.308-0.470] and 0.091 [95% CI, 0.064 - 0.117], respectively (p<0.0001) **(Figure 5)**. A statistically significant association was observed between the anti-cardiolipin autoantibody index with MPO, NE (r=0.20, p<0.01; and r=0.25, p<0.001) respectively; while a slight, non-statistically significant association with cirDNA concentrations was observed in mCRC patients, (r=0.13) **(Figure 2A)**. Conversely, we did not observe any correlation between these anti-cardiolipin autoantibodies index and circulating NETs markers in HI (Figure 2B).

There are 50.7% of mCRC patients (110/217) showing an aCL AI value over the mean 95% CI value of the healthy subjects and 62.2% of mCRC patients (135/217) showing an aCL AI value over the median value of HI. Medians are 0.125 [95% CI, 0.041 - 0.204] and 0.000 [0.000 – 0.049] for mCRC patients and healthy individuals respectively (p<0.0001). Moreover, there are 40.6% of mCRC patients (88/217) showing an aCL AI value over 0.281 which represents the 90% higher aCL AI value of the healthy subjects.

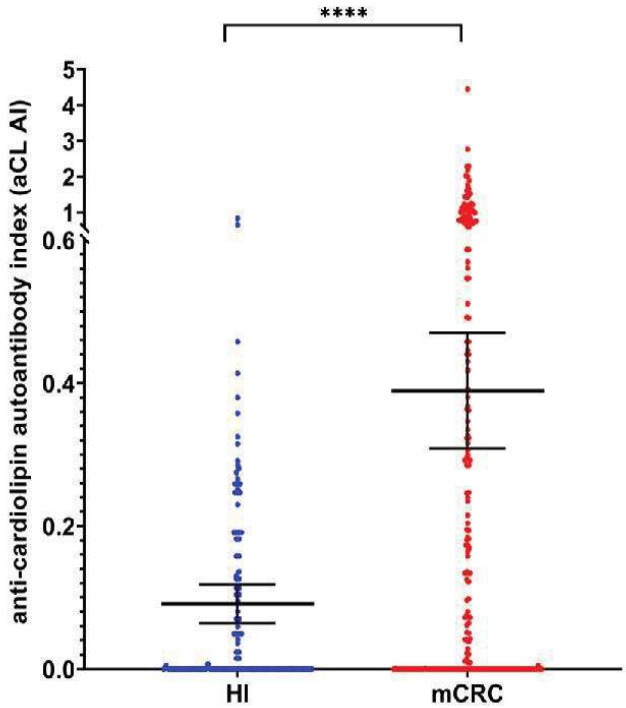

Figure 5: Comparison of the anti-cardiolipin autoantibody index (aCL AI) in mCRC patients (mCRC) (n=217) and healthy individuals (HI) (n=114). The long horizontal bars indicate the mean, the shorter bars represent the 95% Confidential Interval (95% CI). Each dot indicate the aCL AI of a single patient or a single HI. The Student *t*-test was performed to compare means of aCL AI values in mCRC patients and in HI. A probability of less than 0.05 was considered statistically significant; ***p< 0.001.

CirDNA, MPO and NE concentrations could be used to distinguish mCRC patients from the healthy individuals.

To explore whether cirDNA, MPO and NE concentrations could be used to distinguish mCRC patients from the healthy individuals, we interrogated the receiver operating characteristics (ROC) curve analysis for the concentrations of the aforementioned NETs markers. The ROC curves showed an AUC (area under curve) of 0.84 (0.7938–0.8770, 95% CI; confidence interval), 0.86 (0.8213-0.9000, 95% CI) and 0.88 (0.8435-0.9182, 95% CI) for cirDNA, MPO and NE concentrations, respectively (Figure 6A, 6B and 6C). When the three NETs marker concentrations were combined (cirDNA, MPO and NE), the AUC of the ROC curve increased to 0.95 (0.9283-0.9759, 95% CI) (Figure 6D). The concentrations of the combination of these three markers are significantly higher in mCRC patients than in healthy individuals ($p<0.0001$), with respective median concentrations of 29.96 ng/mL in HI and 99.40 ng/mL in mCRC patients. Similar observations were made when we combined MPO and NE concentrations, producing a new total AUC of the ROC curve of 0.94 (0.9137-0.9676) (Figure S5).

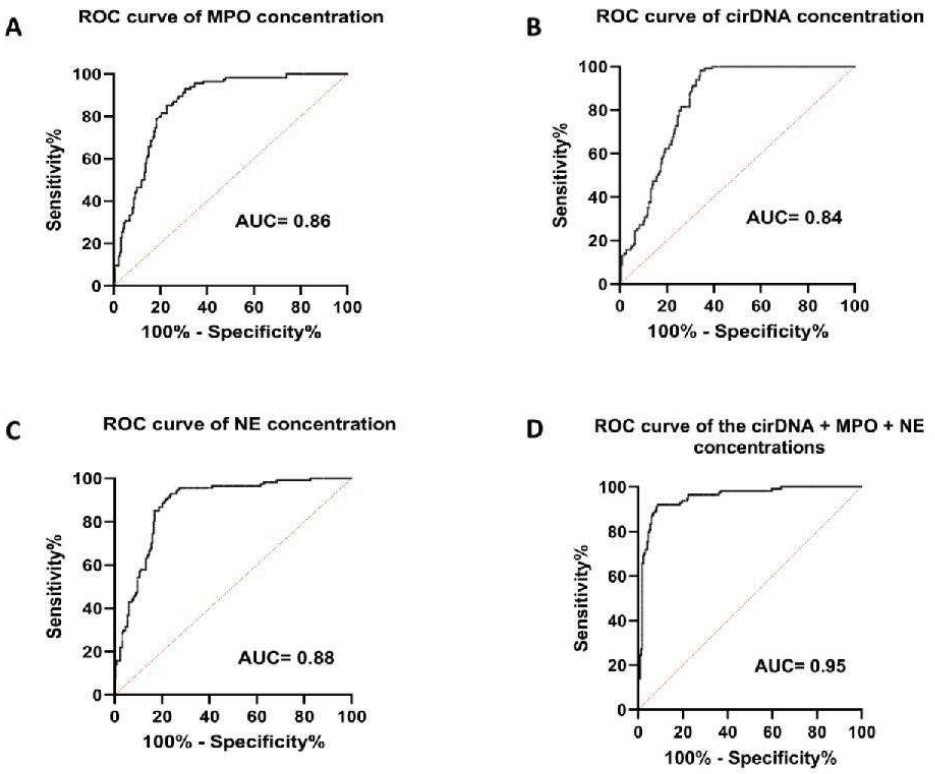

Figure 6: ROC curves for the cirDNA concentration, the MPO concentration and the NE concentration between healthy individuals and mCRC patients. ROC curve of (A) the cirDNA concentration (ng/mL), (B) the MPO concentration (ng/mL), (C) the NE concentration (ng/mL) and (D) the addition of three analyte concentrations (cirDNA, MPO and NE). ROC: receiver operating characteristics; AUC, area under curve; cirDNA: circulating cell-free DNA; MPO: myeloperoxidase; NE: neutrophil elastase.

DISCUSSION

For more than two decades, it was postulated that cirDNA originates from cell death (Rostami et al., 2020), in particular from apoptosis and necrosis. This conclusion was based on the results of non-sophisticated methods such as electrophoresis, which revealed a strong 150-180 bp electrophoretic band (and weak bands of multiples thereof) (Jahr et al., 2001), highlighting the presence of DNA principally in mononucleosomes, and to a lesser extent in di- or tri-nucleosomes, which is the hallmark of apoptotic DNA cleavage. In addition, necrosis is thought to lead to fragments of high cirDNA fragment size (>10,000 bp) (Jahr et al., 2001; Thierry et al., 2016). Recently, Rostami et al (Rostami et al., 2020) provided well-argued evidence that cirDNA release is modulated through a combination of apoptotic and senescent triggers and inhibitors. However, we postulate that short-sized nucleosomal structures could also result from the progressive nuclease degradation of longer cirDNA originating from necrosis, phagocytosis, microparticle-containing DNA, or active release from leucocytes, in particular NETosis. Indeed, chromatin fragments, oligo-nucleosomes and nucleosomes can be liberated from the degradation process of NETs, and can contribute to the pool of cirDNA and histones. The prominence accorded to apoptosis as the main mechanism of release, therefore, may have to be reconsidered. Paunel-Görgülü et al have demonstrated that cirDNA amplify NETosis in an intracellular TLR9-independent manner, and one can speculate that an excess of cirDNA might have a positive feed-back loop on NETs formation (Paunel-Görgülü et al., 2017).

Several studies report that tumors release cell-free DNA into the blood stream in quantities proportional to their mass, especially in the case of metastatic colorectal cancer (Bhangu et al., 2017; Thierry, Pastor, et al., 2017; Wang et al., 2018; Wei et al., 2019; Xu et al., 2020). We may assume that cirDNA content depends upon the release of three cells of origin in a cancer patient: (i) germline cells, according to cirDNA release in healthy individuals (2 to 7 ng/mL (Meddeb, Dache, et al., 2019; Thierry et al., 2016)); (ii) tumor malignant cells; (iii) tumor microenvironment (stroma; endothelial and immunological cells) (Papayannopoulos, 2018). The release of wild type DNA deriving from non-malignant cells may depend upon the quantity and the heterogeneity of the tumor microenvironment, as well as other sources, such as the lymphocytic cells. This might explain the high variation in the mutation allele's frequency (MAF), as determined by cirDNA analysis. We previously found that MAF varied from 0.03% to 78% in a cohort of mCRC patients (Mouliere et al., 2013). Thus MAF is not directly related to tumor aggressiveness (Thierry, El Messaoudi, et al., 2017), and should not be compared with MAF determined within tumor tissue.

Our data revealed that (i), the concentrations of cirDNA and NETs markers (NE, MPO) are higher in mCRC patient than in HI; (ii), an association exists between cirDNA concentrations and NETs markers concentrations in an mCRC cohort, and (iii), cirDNA, NE and MPO concentrations correlate with leucocyte and neutrophil cell counts. A causal link can only be shown if the inhibition of NET formation (i.e. by the addition of DNase I) could lead to a decrease in the amount of cirDNA produced. Although correlation does not mean causation, we speculate that a significant cirDNA fraction derives from NETs formation, which itself is generated by active circulating neutrophils and/or by neutrophils infiltrating the tumor microenvironment. It is likely that NET chromatin filaments are rapidly and dynamically degraded by the very active plasma nucleases, which results in the release of chromatin fragments of high molecular size decreasing down to low molecular size DNA that is associated with mononucleosome/chromatosome chromatin unit (that appeared as the most prominent and the most stabilizing cirDNA structure in blood (Sanchez et al., 2018, 2021; Serpas et al., 2019; Waisberg et al.,

2014)). Since MPO and NE are among the most important NET granule constituents, their contents highly correlated in HI and mCRC plasma. Both enzymes are otherwise physiologically independent.
In contrast, an increase in cirDNA concentrations is significantly associated with an increase in NETs conventional markers (NE and MPO) in mCRC patients, while no such association was observed in healthy individuals. Remarkably, mCRC patient plasma with cirDNA concentrations close to the median of HI (6 ng/mL) showed higher concentrations of NE and MPO than HI. Thus, we may assume that cirDNA found in mCRC conditions derives from NETs in a manner unrelated to cirDNA concentrations. Confirming the above observations, ROC experiments revealed that the quantification of NE, MPO and cirDNA shows a high diagnostic performance. The determination of an optimal test which would combine all NET markers using machine learning assistance is ongoing in our team.
It should be noted that leucocyte and neutrophil cell counts (but not lymphocyte cell count) increased in patients with a primary tumor in place and in patients with two or more metastatic sites. This might suggest that leucocytes and neutrophils - and by extension NETs - are directly implicated in tumor growth or cancer dissemination, as previously suggested (Daniel et al., 2019; Kos and de Visser, 2021; Nolan and Malanchi, 2020; Yang et al., 2020).
Assuming that cirDNA are indirect NETs markers, and are a marker of tumor mass in mCRC, our study suggests the association of increased circulation of NETs markers and disease severity. We may speculate that cirDNA and NETs by-products are markers of the inflammation associated with solid tumors, and more globally with inflammatory diseases. It is possible, therefore, that cirDNA concentrations associated with others NETs circulating markers could provide significant information about cancer severity, cancer prognosis or treatment guidance, which could constitute a significant advance in cancer along with the advent of immunotherapy and the growing knowledge of tumor immunology.
An association of anti-cardiolipin autoantibodies (aCL) with circulating NETs markers was observed in a significant part of mCRC patients, but not in HI. ACL is part of the anti-phospholipid antibody family (aPL) characteristic of the anti-phospholipid syndrome (Syrigos et al., 1998; Wichmann et al., 2020), an immune-mediated disorder resulting in pregnancy morbidity and arterial or venous thrombotic events. While aPL is present in 1-5 % of the general population, APS prevalence is 40-50/100,000 subjects (Leal Rato et al., 2021). However, this prevalence can increase to 50% among elderly patients with chronic diseases (Abdel-Wahab et al., 2020; Leal Rato et al., 2021). Several works report higher aPL levels in various haematological and solid tumors (Gómez-Puerta et al., 2006; Islam, 2020), with the percentage of aPL positive cancer patients varying from 5% to 70%. Since the risk of thrombosis is 4 to 60-fold higher in cancer patients than in the general population, it has been suggested that an elevated level of aPL might trigger thrombosis in cancer patients. A meta-analysis revealed that patients with gastrointestinal, genitourinary and lung cancer are at a higher risk of developing aPL (Gómez-Puerta et al., 2006). While the appearance of aPL such as aCL could be as an essential step in the prevention of thrombosis, the direct or indirect implication of aPL in the thrombophilic process remains unclear. It is clear, however, that neutrophils and NETs contribute to APS pathophysiology (Tambralli et al., 2020).
It should also be noted that exacerbated NET formation has been linked to anti-phospholipid syndrome (APS) in numerous auto-immune and non-auto-immune pathologies (such as lupus) which showed elevated levels of aCL (Thierry and Roch, 2020). The clear statistical difference between healthy and mCRC subject study cohorts revealed that a majority or a significant fraction of mCRC patients at diagnosis showed an auto-production of aCL at a low, moderate and high level.

In conclusion, our work shows for the first time that a correlation exists between NET markers (MPO and NE) and cirDNA in mCRC patients, suggesting that cirDNA might appear as a marker of NETs. In addition, this finding redefines existing paradigms of cirDNA release mechanisms, and could suggest that a significant fraction of the cirDNA quantity derives from NETs in cancer patients with mCRC.Moreover, we revealed that concomitant analyses of NETs markers (NE, MPO) and cirDNA also enables the differentiation of mCRC patients from healthy individuals. This warrants the evaluation of NET by-products analysis in cancer diagnosis, in particular for thrombosis prevention, for patient follow-up, in guiding immunotherapy, or eventually as a means of devising an improved liquid biopsy cancer screening test. Our study is the first to show the close association of aPL with NET markers and cirDNA in cancer patients, suggesting that the examination of these markers might be useful in preventing thrombosis in cancer patients. Lastly, our observations contribute to the understanding of the imbalance which cancer can cause between the immunological system and haemostasis. This deepened understanding may prove useful in improving long term cancer survival rates.

Limitation of the study

Although we showed a positive correlation between cirDNA levels and the levels of NETs markers (NE and MPO), these results should be confirmed on another larger validation cohort. In addition, this study was conducted on mCRC patients at initial diagnosis, and it would have been interesting to examine this correlation in locally advanced disease, in the course of post-surgery treatment, as well as in other malignancies. Moreover, none of the patients had neutropenia at the time of initial diagnosis, however the influence of neutropenia at initial diagnosis and during chemotherapy treatment should be evaluated in another study. While we found that the impact of number of neutrophils on the correlation between cirDNA levels with MPO levels is negligible supporting the main observation of this study, the influence of neutrophils numbers during chemotherapy treatment should be evaluated in another studies. Finally, a thorough mechanistic study of NETs degradation in blood (as well as in plasma and serum) of cancer patients and healthy individuals needs to be conducted to confirm the causality between NETs formation and cirDNA production in cancer patients. Our team is actively working on this last topic.

Author contributions

ART and BP designed the study. BP and ART developed the methodology. BP, CS, AK, EP, and AM did the experiments under the supervision of ART. BP did the statistical analyses. BP and ART analyzed the data and prepared the manuscript. All of the authors (BP, JDA, EP, CS, AK, RT, AM, LM, VP, AA, MY, TM and ART discussed the results and approved the manuscript.

Acknowledgments

The PANIRINOX study is funded by AMGEN. B. Pastor was partially supported by SIRIC Montpellier Cancer Grant INCa_Inserm_DGOS_12553, and AR Thierry by INSERM. PANIRINOX study is sponsored by R&D Unicancer. The sponsor had a role in the collection, management, analysis, and interpretation of the data; preparation, review, or approval of the manuscript; and decision to submit the manuscript for publication. The funder had no role in the design and conduct of this present study; collection, management, analysis, and interpretation of the data; preparation, review, or approval of the manuscript; and decision to submit the manuscript for publication. We thank our patients and their families for their trust; all the participating physicians and supporting staff; Datacenter Unicancer members (Institut Regional du Cancer de Montpellier) and Marie Bergeaud (R&D Unicancer). The authors thank the excellent technical assistance of C. Sanchez and A. Kudriavtsev (IRCM, Institut de Recherche en Cancérologie de Montpellier, INSERM U1194, Université de Montpellier, Institut régional du Cancer de Montpellier, Montpellier, F-34134298, France) and Cormac Mc Carthy (Mc Carthy Consultant, Montpellier) for English editing (financial compensation). We thank also all CRA and clinical co-investigators, Marie Bergeaud (Unicancer, Paris). We are grateful to K. Billings and Streck corp. for providing the cell-free DNA blood collection tubes. We thank all the patients and healthy donors who participated in this study. We also thank the clinical investigators of the centers who participated in this study.

Declaration of Interest

TM reported receiving grants from Amgen SAS; nonfinancial support from Servier and MSD; and personal fees from Merck Serono, Bristol Myers Squibb, Sanofi Genzyme, AAA, Sandoz, and Bayer outside the submitted work. AA has reported a consulting/advisory role and/or receiving honoraria from Bristol-Myers Squibb, MSD Oncology, and Servier; and has received research funding from Bayer Pharmaceuticals. ART is a DiaDx stockholder. BP, JDA, EP, CS, AK, LM, RT, VP, MY and AM declare no competing interests.

STAR METHOD

Key resource table

Resource availability

Lead contact

Further information and requests for resources and reagents should be directed to and will be fulfilled by the lead contact, Alain R. Thierry (alain.thierry@inserm.fr).

Materials availability

This study did not generate newly generated materials or new unique reagents.

Data and code availability

• All data reported in this paper will be shared by the lead contact upon request

• This paper does not report original code.

• Additional information required to reanalyze the data reported in this paper is available from the lead contact upon request.

Experimental model and subject details

Data recorded during this trial are subject to a computerized treatment at the Unicancer Central Data Center in Montpellier in compliance with the "Loi Informatique et Libertés n° 78-17, 6 January 1978 modified". The collection of biological samples implemented within the framework of the trial was declared to ANSM in the same time that the request of Clinical Trial Authorization. After the trial, and in case of storage, the storage of the collection of biological samples will be notified to the Minister of Research (and submitted to the CPP to notice if change of purpose of Research)"

Human subjects

In this study, we included 219 mCRC patients (51 females (41.1%) and 73 males (28.9%) (Table 1) from the screening procedure of the ongoing UCGI 28 PANIRINOX study (NCT02980510/EudraCT n°2016-001490-33). We investigated the correlation of MPO concentrations, NE concentrations and the nuclear cell-free DNA (cirDNA) concentrations to demonstrate that a very significant fraction of cirDNA derives from the degradation of neutrophil extracellular traps (NETs). PANIRINOX is the first interventional study to use cirDNA as a companion test for selecting mCRC patients towards anti-EGFR targeted therapy by the IntPlex® method. Briefly: eligible patients were recruited in the PANIRINOX screening procedures at diagnosis; patients accepted for inclusion were male or female, aged between 18 and 75 years old, with a ECOG performance status 0 or 1, a histologically confirmed colo-rectal adenocarcinoma, an untreated synchronous or metachronous metastatic disease deemed unresectable with curative intent; a *KRAS* (codons 12, 13, 61, 117, 146), *NRAS* (codons 12, 13, 61) and *BRAFV600E* wild type (WT) tumor status according to plasma analysis of cirDNA by Intplex technology;

STAR METHOD

Key resource table

Resource availability

Lead contact

Further information and requests for resources and reagents should be directed to and will be fulfilled by the lead contact, Alain R. Thierry (alain.thierry@inserm.fr).

Materials availability

This study did not generate newly generated materials or new unique reagents.

Data and code availability

• All data reported in this paper will be shared by the lead contact upon request

• This paper does not report original code.

• Additional information required to reanalyze the data reported in this paper is available from the lead contact upon request.

Experimental model and subject details

Data recorded during this trial are subject to a computerized treatment at the Unicancer Central Data Center in Montpellier in compliance with the "Loi Informatique et Libertés n° 78-17, 6 January 1978 modified". The collection of biological samples implemented within the framework of the trial was declared to ANSM in the same time that the request of Clinical Trial Authorization. After the trial, and in case of storage, the storage of the collection of biological samples will be notified to the Minister of Research (and submitted to the CPP to notice if change of purpose of Research)"

Human subjects

In this study, we included 219 mCRC patients (51 females (41.1%) and 73 males (28.9%) (Table 1) from the screening procedure of the ongoing UCGI 28 PANIRINOX study (NCT02980510/EudraCT n°2016-001490-33). We investigated the correlation of MPO concentrations, NE concentrations and the nuclear cell-free DNA (cirDNA) concentrations to demonstrate that a very significant fraction of cirDNA derives from the degradation of neutrophil extracellular traps (NETs). PANIRINOX is the first interventional study to use cirDNA as a companion test for selecting mCRC patients towards anti-EGFR targeted therapy by the IntPlex® method. Briefly: eligible patients were recruited in the PANIRINOX screening procedures at diagnosis; patients accepted for inclusion were male or female, aged between 18 and 75 years old, with a ECOG performance status 0 or 1, a histologically confirmed colo-rectal adenocarcinoma, an untreated synchronous or metachronous metastatic disease deemed unresectable with curative intent; a *KRAS* (codons 12, 13, 61, 117, 146), *NRAS* (codons 12, 13, 61) and *BRAFV600E* wild type (WT) tumor status according to plasma analysis of cirDNA by Intplex technology;

validated (Thierry, El Messaoudi, et al., 2017; Thierry et al., 2014), and showed unprecedented specificity and sensitivity, to the point of permitting the detection of a single DNA fragment molecule under Poisson Law distribution (Thierry, El Messaoudi, et al., 2017). An intra-and inter-experimental reproducibility study shows a 19% and 24% coefficient of variation (Mouliere et al., 2013, 2014) when jointly taking into consideration plasma preparation, cirDNA extraction and Q-PCR measurement.

Myeloperoxidase and Neutrophil Elastase assay

MPO and NE concentrations were measured using enzyme-linked immunosorbent assay (ELISA) according to the manufacturer's standard protocol (Duoset R&D Systems, DY008, DY3174, and DY9167-05). Briefly, captured antibodies were diluted at the working concentrations in the Reagent Diluent (RD) provided on ancillary reagent kits (DY008) and coated overnight at room temperature (RT) on 96-well microplates with 100µL per wells. Then, captured antibodies were removed from the microplate, and wells were washed three times with 300µL of Wash Buffer (WB). Microplates were blocked at RT for 2 hours by adding 300µL of RD to each well. RD were removed from the microplates, and wells were washed three times with 300µL of WB. Then, 100µL of negative controls, standards and plasma samples (diluted 1/10) were added to the appropriate wells for one hour at RT. Samples, controls and standards were removed from the microplates, and wells were washed three times with 300µL of WB. Detection antibodies were diluted at the working concentrations in the RD, and then added by 100µL per well, for one hour at RT. Detection antibodies were removed from the microplates, and wells were washed three times with 300µL of WB. Then, 100µL of Streptavidin-HRP was added to each well and microplates were incubated at RT for 30 minutes. Repeat wash three times. Finally, 100µL per well of substrate solution was added and incubated for 15 minutes, and the Optical Density (O.D) of each well was read immediately at 450nm with the PHERAstar FS instrument using the PHERAstar control software.

Anti-cardiolipin autoantibody Index calculation

The antibody index of total human autoantibodies against cardiolipin (IgG, IgM and IgA) was measured using direct ELISA according to the manufacturer's standard protocol (Boster, EK7027). Briefly, 100µL of negative controls, positive controls, calibrator and diluted plasma samples (1/21) was dispensed into cardiolipin-coated wells and incubated for 30 minutes at RT. Samples, controls and calibrator were removed from the microplates and the wells were washed three times with 300µL of WB. Then, 100µL of enzyme conjugate was added in each well for 20 minutes at RT. The washing step was repeated. 100µL of TMB substrate was dispensed into wells for 10 minutes. Finally, 100µL of stop solution was added to each well and O.D was immediately read at 450nm with the PHERAstar FS instrument using the PHERAstar control software. The cut-off value of each plate was calculated as follows: Calibrator O.D x Calibrator Factor (CF) of the kit. The aCL AI is calculated by dividing the O.D value of each sample by cut-off value.

In order to globally evaluate the difference between HI and mCRC subjects, we compared the quantitative data (aCL AI) rather the qualitative data that can be inferred from a positivity threshold determined from a calibrator. In case of the Boster kit, the calibrator corresponds to a diagnosed APLS

patient known to have very high level of aCL, and it is consequently not appropriate for studying cancer or pregnancy follow up.

The marketed kits use internal standards whose value has been defined in relation to sera commonly called "Harris standards". There is a low concordance between the batches of standards: this results in disparities between the kits, depending on whether they have been standardized with a particular batch of Harris standard (the aCL may have varying rates 2 to 3 times, depending on the kit). As with all ELISA techniques, determining the positivity threshold is delicate. Antibody levels in healthy populations are not distributed normally and vary with the source of the antigen used (calibration with each change of antigen lot). Note, a negative result for anti-cardiolipins IgG or IgM indicates that this type of antibody was not present or was present in a too low amount in the blood sample being tested.

In our assay, three negative controls are analyzed in each plate: (1), the blank (no test sample); (2), the kit negative control; and (3), a plasma of a healthy individual. We defined an arbitrary unit of aCL concentration (Anticardiolipin autoantibody index, aCL AI) taking in consideration plate to plate variation and standard batch level: (OD - 1.35xnegative control) / blank. The OD median of healthy individuals is 1.35-fold higher than the kit negative control, irrespective of the plate. The plasma of the healthy individual plasma control is useful as a quality control to check the kit negative control level, and routinely showed an 1.1-fold (+/- 10%) increase as compared to the kit negative control.

Weak or moderately positive results are sometimes observed temporarily in older healthy people without symptoms following infection or following medication. These results are most often of little clinical significance, but should be interpreted in light of other clinical information. This explains the low and moderate aCL AI we found in a small fraction of healthy individuals. Quantification of results is important, since there is a correlation between the rate of aCL (in particular IgG) and the risk of thrombosis. In view of this, low to moderate aCL levels are taken into consideration in contexts of repeated spontaneous miscarriages (Abdel-Wahab et al., 2020).

Quantification and statistical analysis

The Mann-Whitney U test was used for non-parametric data and the Student t-test was used for parametric data. Correlation analysis was performed using the Spearman test (Graph Pad Prism 8.3.1 software). A probability of less than 0.05 was considered to be statistically significant; *p<0.05, **p<0.01; ***p< 0.001; ****p< 0.0001.

Additional Resources

PANIRINOX clinical trial: NCT02980510

https://clinicaltrials.gov/ct2/show/NCT02980510?term=PANIRINOX&draw=2&rank=1

REFERENCES

Abdel-Wahab, N., Tayar, J. H., Fa'ak, F., Sharma, G., Lopez-Olivo, M. A., Yousif, A., Shagroni, T., Al-Hawamdeh, S., Rojas-Hernandez, C. M., & Suarez-Almazor, M. E. (2020). Systematic review of observational studies reporting antiphospholipid antibodies in patients with solid tumors. *Blood Advances*, *4*(8), 1746–1755. https://doi.org/10.1182/bloodadvances.2020001557

Al Amir Dache, Z., Otandault, A., Tanos, R., Pastor, B., Meddeb, R., Sanchez, C., Arena, G., Lasorsa, L., Bennett, A., Grange, T., El Messaoudi, S., Mazard, T., Prevostel, C., & Thierry, A. R. (2020). Blood contains circulating cell-free respiratory competent mitochondria. *FASEB Journal: Official Publication of the Federation of American Societies for Experimental Biology*. https://doi.org/10.1096/fj.201901917RR

Al-Khafaji, A. B., Tohme, S., Yazdani, H. O., Miller, D., Huang, H., & Tsung, A. (2016). Superoxide induces Neutrophil Extracellular Trap Formation in a TLR-4 and NOX-Dependent Mechanism. *Molecular Medicine*, *22*(1), 621–631. https://doi.org/10.2119/molmed.2016.00054

Benešová, L., Hálková, T., Ptáčková, R., Semyakina, A., Menclová, K., Pudil, J., Ryska, M., Levý, M., Šimša, J., Pazdírek, F., Hoch, J., Blaha, M., & Minárik, M. (2019). Significance of postoperative follow-up of patients with metastatic colorectal cancer using circulating tumor DNA. *World Journal of Gastroenterology*, *25*(48), 6939–6948. https://doi.org/10.3748/wjg.v25.i48.6939

Bhangu, J. S., Taghizadeh, H., Braunschmid, T., Bachleitner-Hofmann, T., & Mannhalter, C. (2017). Circulating cell-free DNA in plasma of colorectal cancer patients—A potential biomarker for tumor burden. *Surgical Oncology*, *26*(4), 395–401. https://doi.org/10.1016/j.suronc.2017.08.001

Brinkmann, V. (2018). Neutrophil Extracellular Traps in the Second Decade. *Journal of Innate Immunity*, *10*(5–6), 414–421. https://doi.org/10.1159/000489829

Bronkhorst, A. J., Ungerer, V., Diehl, F., Anker, P., Dor, Y., Fleischhacker, M., Gahan, P. B., Hui, L., Holdenrieder, S., & Thierry, A. R. (2021). Towards systematic nomenclature for cell-free DNA. *Human Genetics*, *140*(4), 565–578. https://doi.org/10.1007/s00439-020-02227-2

Bustin, S. A. (2010). Why the need for qPCR publication guidelines?—The case for MIQE. *Methods (San Diego, Calif.)*, *50*(4), 217–226. https://doi.org/10.1016/j.ymeth.2009.12.006

Bustin, S. A., Benes, V., Garson, J. A., Hellemans, J., Huggett, J., Kubista, M., Mueller, R., Nolan, T., Pfaffl, M. W., Shipley, G. L., Vandesompele, J., & Wittwer, C. T. (2009). The MIQE Guidelines: Minimum Information for Publication of Quantitative Real-Time PCR Experiments. *Clinical Chemistry*, *55*(4), 611–622. https://doi.org/10.1373/clinchem.2008.112797

Chandrananda, D., Thorne, N. P., & Bahlo, M. (2015). High-resolution characterization of sequence signatures due to non-random cleavage of cell-free DNA. *BMC Medical Genomics*, *8*, 29. https://doi.org/10.1186/s12920-015-0107-z

Cohen, J. D., Li, L., Wang, Y., Thoburn, C., Afsari, B., Danilova, L., Douville, C., Javed, A. A., Wong, F., Mattox, A., Hruban, R. H., Wolfgang, C. L., Goggins, M. G., Molin, M. D., Wang, T.-L., Roden, R., Klein, A. P., Ptak, J., Dobbyn, L., … Papadopoulos, N. (2018). Detection and localization of surgically resectable cancers with a multi-analyte blood test. *Science*, *359*(6378), 926–930. https://doi.org/10.1126/science.aar3247

Cristiano, S., Leal, A., Phallen, J., Fiksel, J., Adleff, V., Bruhm, D. C., Jensen, S. Ø., Medina, J. E., Hruban, C., White, J. R., Palsgrove, D. N., Niknafs, N., Anagnostou, V., Forde, P., Naidoo, J., Marrone, K., Brahmer, J., Woodward, B. D., Husain, H., … Velculescu, V. E. (2019). Genome-wide cell-

free DNA fragmentation in patients with cancer. *Nature*, *570*(7761), 385. https://doi.org/10.1038/s41586-019-1272-6

Daniel, C., Leppkes, M., Muñoz, L. E., Schley, G., Schett, G., & Herrmann, M. (2019). Extracellular DNA traps in inflammation, injury and healing. *Nature Reviews Nephrology*, *15*(9), 559–575. https://doi.org/10.1038/s41581-019-0163-2

Dennis Lo, Y., & Poon, L. L. (2003). The ins and outs of fetal DNA in maternal plasma. *The Lancet*, *361*(9353), 193–194. https://doi.org/10.1016/S0140-6736(03)12319-7

Diaz, L. A., & Bardelli, A. (2014). Liquid biopsies: Genotyping circulating tumor DNA. *Journal of Clinical Oncology: Official Journal of the American Society of Clinical Oncology*, *32*(6), 579–586. https://doi.org/10.1200/JCO.2012.45.2011

El Messaoudi, S., Rolet, F., Mouliere, F., & Thierry, A. R. (2013). Circulating cell free DNA: Preanalytical considerations. *Clinica Chimica Acta; International Journal of Clinical Chemistry*, *424*, 222–230. https://doi.org/10.1016/j.cca.2013.05.022

Erpenbeck, L., & Schön, M. P. (2017). Neutrophil extracellular traps: Protagonists of cancer progression? *Oncogene*, *36*(18), 2483–2490. https://doi.org/10.1038/onc.2016.406

Fuchs, T. A., Kremer Hovinga, J. A., Schatzberg, D., Wagner, D. D., & Lämmle, B. (2012). Circulating DNA and myeloperoxidase indicate disease activity in patients with thrombotic microangiopathies. *Blood*, *120*(6), 1157–1164. https://doi.org/10.1182/blood-2012-02-412197

Gentles, A. J., Newman, A. M., Liu, C. L., Bratman, S. V., Feng, W., Kim, D., Nair, V. S., Xu, Y., Khuong, A., Hoang, C. D., Diehn, M., West, R. B., Plevritis, S. K., & Alizadeh, A. A. (2015). The prognostic landscape of genes and infiltrating immune cells across human cancers. *Nature Medicine*, *21*(8), 938–945. https://doi.org/10.1038/nm.3909

Gómez-Puerta, J. A., Cervera, R., Espinosa, G., Aguiló, S., Bucciarelli, S., Ramos-Casals, M., Ingelmo, M., Asherson, R. A., & Font, J. (2006). Antiphospholipid Antibodies Associated with Malignancies: Clinical and Pathological Characteristics of 120 Patients. *Seminars in Arthritis and Rheumatism*, *35*(5), 322–332. https://doi.org/10.1016/j.semarthrit.2005.07.003

Hakkim, A., Furnrohr, B. G., Amann, K., Laube, B., Abed, U. A., Brinkmann, V., Herrmann, M., Voll, R. E., & Zychlinsky, A. (2010). Impairment of neutrophil extracellular trap degradation is associated with lupus nephritis. *Proceedings of the National Academy of Sciences*, *107*(21), 9813–9818. https://doi.org/10.1073/pnas.0909927107

Heitzer, E., Auinger, L., & Speicher, M. R. (2020). Cell-Free DNA and Apoptosis: How Dead Cells Inform About the Living. *Trends in Molecular Medicine*, *26*(5), 519–528. https://doi.org/10.1016/j.molmed.2020.01.012

Islam, Md. A. (2020). Antiphospholipid antibodies and antiphospholipid syndrome in cancer: Uninvited guests in troubled times. *Seminars in Cancer Biology*, *64*, 108–113. https://doi.org/10.1016/j.semcancer.2019.07.019

Jahr, S., Hentze, H., Englisch, S., Hardt, D., Fackelmayer, F. O., Hesch, R.-D., & Knippers, R. (2001). DNA Fragments in the Blood Plasma of Cancer Patients: Quantitations and Evidence for Their Origin from Apoptotic and Necrotic Cells. *Cancer Research*, *61*(4), 1659–1665.

Jensen, S. Ø., Øgaard, N., Ørntoft, M.-B. W., Rasmussen, M. H., Bramsen, J. B., Kristensen, H., Mouritzen, P., Madsen, M. R., Madsen, A. H., Sunesen, K. G., Iversen, L. H., Laurberg, S., Christensen, I. J., Nielsen, H. J., & Andersen, C. L. (2019). Novel DNA methylation biomarkers show high sensitivity and specificity for blood-based detection of colorectal cancer—A

free DNA fragmentation in patients with cancer. *Nature*, *570*(7761), 385. https://doi.org/10.1038/s41586-019-1272-6

Daniel, C., Leppkes, M., Muñoz, L. E., Schley, G., Schett, G., & Herrmann, M. (2019). Extracellular DNA traps in inflammation, injury and healing. *Nature Reviews Nephrology*, *15*(9), 559–575. https://doi.org/10.1038/s41581-019-0163-2

Dennis Lo, Y., & Poon, L. L. (2003). The ins and outs of fetal DNA in maternal plasma. *The Lancet*, *361*(9353), 193–194. https://doi.org/10.1016/S0140-6736(03)12319-7

Diaz, L. A., & Bardelli, A. (2014). Liquid biopsies: Genotyping circulating tumor DNA. *Journal of Clinical Oncology: Official Journal of the American Society of Clinical Oncology*, *32*(6), 579–586. https://doi.org/10.1200/JCO.2012.45.2011

El Messaoudi, S., Rolet, F., Mouliere, F., & Thierry, A. R. (2013). Circulating cell free DNA: Preanalytical considerations. *Clinica Chimica Acta; International Journal of Clinical Chemistry*, *424*, 222–230. https://doi.org/10.1016/j.cca.2013.05.022

Erpenbeck, L., & Schön, M. P. (2017). Neutrophil extracellular traps: Protagonists of cancer progression? *Oncogene*, *36*(18), 2483–2490. https://doi.org/10.1038/onc.2016.406

Fuchs, T. A., Kremer Hovinga, J. A., Schatzberg, D., Wagner, D. D., & Lämmle, B. (2012). Circulating DNA and myeloperoxidase indicate disease activity in patients with thrombotic microangiopathies. *Blood*, *120*(6), 1157–1164. https://doi.org/10.1182/blood-2012-02-412197

Gentles, A. J., Newman, A. M., Liu, C. L., Bratman, S. V., Feng, W., Kim, D., Nair, V. S., Xu, Y., Khuong, A., Hoang, C. D., Diehn, M., West, R. B., Plevritis, S. K., & Alizadeh, A. A. (2015). The prognostic landscape of genes and infiltrating immune cells across human cancers. *Nature Medicine*, *21*(8), 938–945. https://doi.org/10.1038/nm.3909

Gómez-Puerta, J. A., Cervera, R., Espinosa, G., Aguiló, S., Bucciarelli, S., Ramos-Casals, M., Ingelmo, M., Asherson, R. A., & Font, J. (2006). Antiphospholipid Antibodies Associated with Malignancies: Clinical and Pathological Characteristics of 120 Patients. *Seminars in Arthritis and Rheumatism*, *35*(5), 322–332. https://doi.org/10.1016/j.semarthrit.2005.07.003

Hakkim, A., Furnrohr, B. G., Amann, K., Laube, B., Abed, U. A., Brinkmann, V., Herrmann, M., Voll, R. E., & Zychlinsky, A. (2010). Impairment of neutrophil extracellular trap degradation is associated with lupus nephritis. *Proceedings of the National Academy of Sciences*, *107*(21), 9813–9818. https://doi.org/10.1073/pnas.0909927107

Heitzer, E., Auinger, L., & Speicher, M. R. (2020). Cell-Free DNA and Apoptosis: How Dead Cells Inform About the Living. *Trends in Molecular Medicine*, *26*(5), 519–528. https://doi.org/10.1016/j.molmed.2020.01.012

Islam, Md. A. (2020). Antiphospholipid antibodies and antiphospholipid syndrome in cancer: Uninvited guests in troubled times. *Seminars in Cancer Biology*, *64*, 108–113. https://doi.org/10.1016/j.semcancer.2019.07.019

Jahr, S., Hentze, H., Englisch, S., Hardt, D., Fackelmayer, F. O., Hesch, R.-D., & Knippers, R. (2001). DNA Fragments in the Blood Plasma of Cancer Patients: Quantitations and Evidence for Their Origin from Apoptotic and Necrotic Cells. *Cancer Research*, *61*(4), 1659–1665.

Jensen, S. Ø., Øgaard, N., Ørntoft, M.-B. W., Rasmussen, M. H., Bramsen, J. B., Kristensen, H., Mouritzen, P., Madsen, M. R., Madsen, A. H., Sunesen, K. G., Iversen, L. H., Laurberg, S., Christensen, I. J., Nielsen, H. J., & Andersen, C. L. (2019). Novel DNA methylation biomarkers show high sensitivity and specificity for blood-based detection of colorectal cancer—A

Mouliere, F., El Messaoudi, S., Pang, D., Dritschilo, A., & Thierry, A. R. (2014). Multi-marker analysis of circulating cell-free DNA toward personalized medicine for colorectal cancer. *Molecular Oncology*, *8*(5), 927–941. https://doi.org/10.1016/j.molonc.2014.02.005

Mouliere, F., Robert, B., Arnau Peyrotte, E., Del Rio, M., Ychou, M., Molina, F., Gongora, C., & Thierry, A. R. (2011). High fragmentation characterizes tumour-derived circulating DNA. *PloS One*, *6*(9), e23418. https://doi.org/10.1371/journal.pone.0023418

Munir, H., Jones, J. O., Janowitz, T., Hoffmann, M., Euler, M., Martins, C. P., Welsh, S. J., & Shields, J. D. (2021). Stromal-driven and Amyloid β-dependent induction of neutrophil extracellular traps modulates tumor growth. *Nature Communications*, *12*(1), 683. https://doi.org/10.1038/s41467-021-20982-2

Nolan, E., & Malanchi, I. (2020). Neutrophil 'safety net' causes cancer cells to metastasize and proliferate. *Nature*, *583*(7814), 32–33. https://doi.org/10.1038/d41586-020-01672-3

Papayannopoulos, V. (2018). Neutrophil extracellular traps in immunity and disease. *Nature Reviews. Immunology*, *18*(2), 134–147. https://doi.org/10.1038/nri.2017.105

Parikh, A. R., Van Seventer, E. E., Siravegna, G., Hartwig, A. V., Jaimovich, A., He, Y., Kanter, K., Fish, M. G., Fosbenner, K. D., Miao, B., Phillips, S., Carmichael, J. H., Sharma, N., Jarnagin, J., Baiev, I., Shah, Y. S., Fetter, I. J., Shahzade, H. A., Allen, J. N., … Corcoran, R. B. (2021). Minimal Residual Disease Detection using a Plasma-only Circulating Tumor DNA Assay in Patients with Colorectal Cancer. *Clinical Cancer Research*, 1078-0432.CCR-21–0410. https://doi.org/10.1158/1078-0432.CCR-21-0410

Paunel-Görgülü, A., Wacker, M., El Aita, M., Hassan, S., Schlachtenberger, G., Deppe, A., Choi, Y.-H., Kuhn, E., Mehler, T. O., & Wahlers, T. (2017). CfDNA correlates with endothelial damage after cardiac surgery with prolonged cardiopulmonary bypass and amplifies NETosis in an intracellular TLR9-independent manner. *Scientific Reports*, *7*(1), 17421. https://doi.org/10.1038/s41598-017-17561-1

Rostami, A., Lambie, M., Yu, C. W., Stambolic, V., Waldron, J. N., & Bratman, S. V. (2020). Senescence, Necrosis, and Apoptosis Govern Circulating Cell-free DNA Release Kinetics. *Cell Reports*, *31*(13), 107830. https://doi.org/10.1016/j.celrep.2020.107830

Sanchez, C., Roch, B., Mazard, T., Blache, P., Dache, Z. A. A., Pastor, B., Pisareva, E., Tanos, R., & Thierry, A. R. (2021). Circulating nuclear DNA structural features, origins, and complete size profile revealed by fragmentomics. *JCI Insight*, *6*(7), e144561. https://doi.org/10.1172/jci.insight.144561

Sanchez, C., Snyder, M. W., Tanos, R., Shendure, J., & Thierry, A. R. (2018). New insights into structural features and optimal detection of circulating tumor DNA determined by single-strand DNA analysis. *NPJ Genomic Medicine*, *3*, 31. https://doi.org/10.1038/s41525-018-0069-0

Sefrioui, D., Beaussire, L., Gillibert, A., Blanchard, F., Toure, E., Bazille, C., Perdrix, A., Ziegler, F., Gangloff, A., Hassine, M., Elie, C., Bignon, A.-L., Parzy, A., Gomez, P., Thill, C., Clatot, F., Sabourin, J.-C., Frebourg, T., Benichou, J., … Di Fiore, F. (2021). CEA, CA19-9, circulating DNA and circulating tumour cell kinetics in patients treated for metastatic colorectal cancer (mCRC). *British Journal of Cancer*. https://doi.org/10.1038/s41416-021-01431-9

Serpas, L., Chan, R. W. Y., Jiang, P., Ni, M., Sun, K., Rashidfarrokhi, A., Soni, C., Sisirak, V., Lee, W.-S., Cheng, S. H., Peng, W., Chan, K. C. A., Chiu, R. W. K., Reizis, B., & Lo, Y. M. D. (2019). Dnase1l3 deletion causes aberrations in length and end-motif frequencies in plasma DNA. *Proceedings*

of the National Academy of Sciences of the United States of America, *116*(2), 641–649. https://doi.org/10.1073/pnas.1815031116

Snyder, M. W., Kircher, M., Hill, A. J., Daza, R. M., & Shendure, J. (2016). Cell-free DNA comprises an in vivo nucleosome footprint that informs its tissues-of-origin. *Cell*, *164*(0), 57. https://doi.org/10.1016/j.cell.2015.11.050

Syrigos, K. N., Charalampopoulos, A., Konstantoulakis, M. M., Karayiannakis, A., Tsibloulis, V., & Peveretos, P. (1998). Autoantibodies against Cardiolipin in the Serum of Patients with Colorectal Adenocarcinoma:Their Prognostic Significance. *European Surgical Research*, *30*(1), 55–60. https://doi.org/10.1159/000008558

Tambralli, A., Gockman, K., & Knight, J. S. (2020). NETs in APS: Current Knowledge and Future Perspectives. *Current Rheumatology Reports*, *22*(10), 67. https://doi.org/10.1007/s11926-020-00936-1

Tanos, R., Tosato, G., Otandault, A., Al Amir Dache, Z., Pique Lasorsa, L., Tousch, G., El Messaoudi, S., Meddeb, R., Diab Assaf, M., Ychou, M., Du Manoir, S., Pezet, D., Gagnière, J., Colombo, P.-E., Jacot, W., Assénat, E., Dupuy, M., Adenis, A., Mazard, T., … Thierry, A. R. (2020). Machine Learning-Assisted Evaluation of Circulating DNA Quantitative Analysis for Cancer Screening. *Advanced Science (Weinheim, Baden-Wurttemberg, Germany)*, *7*(18), 2000486. https://doi.org/10.1002/advs.202000486

Templeton, A. J., McNamara, M. G., Šeruga, B., Vera-Badillo, F. E., Aneja, P., Ocaña, A., Leibowitz-Amit, R., Sonpavde, G., Knox, J. J., Tran, B., Tannock, I. F., & Amir, E. (2014). Prognostic Role of Neutrophil-to-Lymphocyte Ratio in Solid Tumors: A Systematic Review and Meta-Analysis. *JNCI: Journal of the National Cancer Institute*, *106*(6). https://doi.org/10.1093/jnci/dju124

Thierry, A. R., El Messaoudi, S., Gahan, P. B., Anker, P., & Stroun, M. (2016). Origins, structures, and functions of circulating DNA in oncology. *Cancer Metastasis Reviews*, *35*(3), 347–376. https://doi.org/10.1007/s10555-016-9629-x

Thierry, A. R., El Messaoudi, S., Mollevi, C., Raoul, J. L., Guimbaud, R., Pezet, D., Artru, P., Assenat, E., Borg, C., Mathonnet, M., De La Fouchardière, C., Bouché, O., Gavoille, C., Fiess, C., Auzemery, B., Meddeb, R., Lopez-Crapez, E., Sanchez, C., Pastor, B., & Ychou, M. (2017). Clinical utility of circulating DNA analysis for rapid detection of actionable mutations to select metastatic colorectal patients for anti-EGFR treatment. *Annals of Oncology: Official Journal of the European Society for Medical Oncology*, *28*(9), 2149–2159. https://doi.org/10.1093/annonc/mdx330

Thierry, A. R., Mouliere, F., El Messaoudi, S., Mollevi, C., Lopez-Crapez, E., Rolet, F., Gillet, B., Gongora, C., Dechelotte, P., Robert, B., Del Rio, M., Lamy, P.-J., Bibeau, F., Nouaille, M., Loriot, V., Jarrousse, A.-S., Molina, F., Mathonnet, M., Pezet, D., & Ychou, M. (2014). Clinical validation of the detection of KRAS and BRAF mutations from circulating tumor DNA. *Nature Medicine*, *20*(4), 430–435. https://doi.org/10.1038/nm.3511

Thierry, A. R., Pastor, B., Abraham, J.-D., Pisareva, E., & Mazard, T. (2021). Abstract P11: The elevated level of the main markers of neutrophil extracellular traps in metastatic colorectal cancer plasma highlights the enhanced risk of severe forms of COVID-19 in cancer patients. *Clinical Cancer Research*, *27*(6 Supplement), P11–P11. https://doi.org/10.1158/1557-3265.COVID-19-21-P11

Thierry, A. R., Pastor, B., Jiang, Z.-Q., Katsiampoura, A. D., Parseghian, C., Loree, J. M., Overman, M. J., Sanchez, C., Messaoudi, S. E., Ychou, M., & Kopetz, S. (2017). Circulating DNA Demonstrates Convergent Evolution and Common Resistance Mechanisms during Treatment of Colorectal

Cancer. *Clinical Cancer Research: An Official Journal of the American Association for Cancer Research*, *23*(16), 4578–4591. https://doi.org/10.1158/1078-0432.CCR-17-0232

Thierry, A. R., & Roch, B. (2020). Neutrophil Extracellular Traps and By-Products Play a Key Role in COVID-19: Pathogenesis, Risk Factors, and Therapy. *Journal of Clinical Medicine*, *9*(9), 2942. https://doi.org/10.3390/jcm9092942

Tie, J., Wang, Y., Tomasetti, C., Li, L., Springer, S., Kinde, I., Silliman, N., Tacey, M., Wong, H.-L., Christie, M., Kosmider, S., Skinner, I., Wong, R., Steel, M., Tran, B., Desai, J., Jones, I., Haydon, A., Hayes, T., … Gibbs, P. (2016). Circulating tumor DNA analysis detects minimal residual disease and predicts recurrence in patients with stage II colon cancer. *Science Translational Medicine*, *8*(346), 346ra92. https://doi.org/10.1126/scitranslmed.aaf6219

Urban, C. F., Lourido, S., & Zychlinsky, A. (2006). How do microbes evade neutrophil killing? *Cellular Microbiology*, *8*(11), 1687–1696. https://doi.org/10.1111/j.1462-5822.2006.00792.x

Waisberg, M., Molina-Cruz, A., Mizurini, D. M., Gera, N., Sousa, B. C., Ma, D., Leal, A. C., Gomes, T., Kotsyfakis, M., Ribeiro, J. M. C., Lukszo, J., Reiter, K., Porcella, S. F., Oliveira, C. J., Monteiro, R. Q., Barillas-Mury, C., Pierce, S. K., & Francischetti, I. M. B. (2014). Plasmodium falciparum Infection Induces Expression of a Mosquito Salivary Protein (Agaphelin) That Targets Neutrophil Function and Inhibits Thrombosis without Impairing Hemostasis. *PLoS Pathogens*, *10*(9), e1004338. https://doi.org/10.1371/journal.ppat.1004338

Wan, J. C. M., Massie, C., Garcia-Corbacho, J., Mouliere, F., Brenton, J. D., Caldas, C., Pacey, S., Baird, R., & Rosenfeld, N. (2017). Liquid biopsies come of age: Towards implementation of circulating tumour DNA. *Nature Reviews Cancer*, *17*(4), 223–238. https://doi.org/10.1038/nrc.2017.7

Wang, X., Wang, L., Su, Y., Yue, Z., Xing, T., Zhao, W., Zhao, Q., Duan, C., Huang, C., Zhang, D., Jin, M., Cheng, X., Chen, S., Liu, Y., & Ma, X. (2018). Plasma cell-free DNA quantification is highly correlated to tumor burden in children with neuroblastoma. *Cancer Medicine*, *7*(7), 3022–3030. https://doi.org/10.1002/cam4.1586

Wei, T., Zhang, Q., Li, X., Su, W., Li, G., Ma, T., Gao, S., Lou, J., Que, R., Zheng, L., Bai, X., & Liang, T. (2019). Monitoring Tumor Burden in Response to FOLFIRINOX Chemotherapy Via Profiling Circulating Cell-Free DNA in Pancreatic Cancer. *Molecular Cancer Therapeutics*, *18*(1), 196–203. https://doi.org/10.1158/1535-7163.MCT-17-1298

Wichmann, D., Sperhake, J.-P., Lütgehetmann, M., Steurer, S., Edler, C., Heinemann, A., Heinrich, F., Mushumba, H., Kniep, I., Schröder, A. S., Burdelski, C., de Heer, G., Nierhaus, A., Frings, D., Pfefferle, S., Becker, H., Bredereke-Wiedling, H., de Weerth, A., Paschen, H.-R., … Kluge, S. (2020). Autopsy Findings and Venous Thromboembolism in Patients With COVID-19: A Prospective Cohort Study. *Annals of Internal Medicine*, *173*(4), 268–277. https://doi.org/10.7326/M20-2003

Wolach, O., Sellar, R. S., Martinod, K., Cherpokova, D., McConkey, M., Chappell, R. J., Silver, A. J., Adams, D., Castellano, C. A., Schneider, R. K., Padera, R. F., DeAngelo, D. J., Wadleigh, M., Steensma, D. P., Galinsky, I., Stone, R. M., Genovese, G., McCarroll, S. A., Iliadou, B., … Ebert, B. L. (2018). Increased neutrophil extracellular trap formation promotes thrombosis in myeloproliferative neoplasms. *Science Translational Medicine*, *10*(436), eaan8292. https://doi.org/10.1126/scitranslmed.aan8292

Xu, X., Yu, Y., Shen, M., Liu, M., Wu, S., Liang, L., Huang, F., Zhang, C., Guo, W., & Liu, T. (2020). Role of circulating free DNA in evaluating clinical tumor burden and predicting survival in Chinese

metastatic colorectal cancer patients. *BMC Cancer*, *20*(1), 1006. https://doi.org/10.1186/s12885-020-07516-7

Yang, L., Liu, Q., Zhang, X., Liu, X., Zhou, B., Chen, J., Huang, D., Li, J., Li, H., Chen, F., Liu, J., Xing, Y., Chen, X., Su, S., & Song, E. (2020). DNA of neutrophil extracellular traps promotes cancer metastasis via CCDC25. *Nature*, *583*(7814), 133–138. https://doi.org/10.1038/s41586-020-2394-6

Yipp, B. G., Petri, B., Salina, D., Jenne, C. N., Scott, B. N. V., Zbytnuik, L. D., Pittman, K., Asaduzzaman, M., Wu, K., Meijndert, H. C., Malawista, S. E., de Boisfleury Chevance, A., Zhang, K., Conly, J., & Kubes, P. (2012). Infection-induced NETosis is a dynamic process involving neutrophil multitasking in vivo. *Nature Medicine*, *18*(9), 1386–1393. https://doi.org/10.1038/nm.2847

Yousefi, S., Stojkov, D., Germic, N., Simon, D., Wang, X., Benarafa, C., & Simon, H.-U. (2019). Untangling "NETosis" from NETs. *European Journal of Immunology*, *49*(2), 221–227. https://doi.org/10.1002/eji.201747053

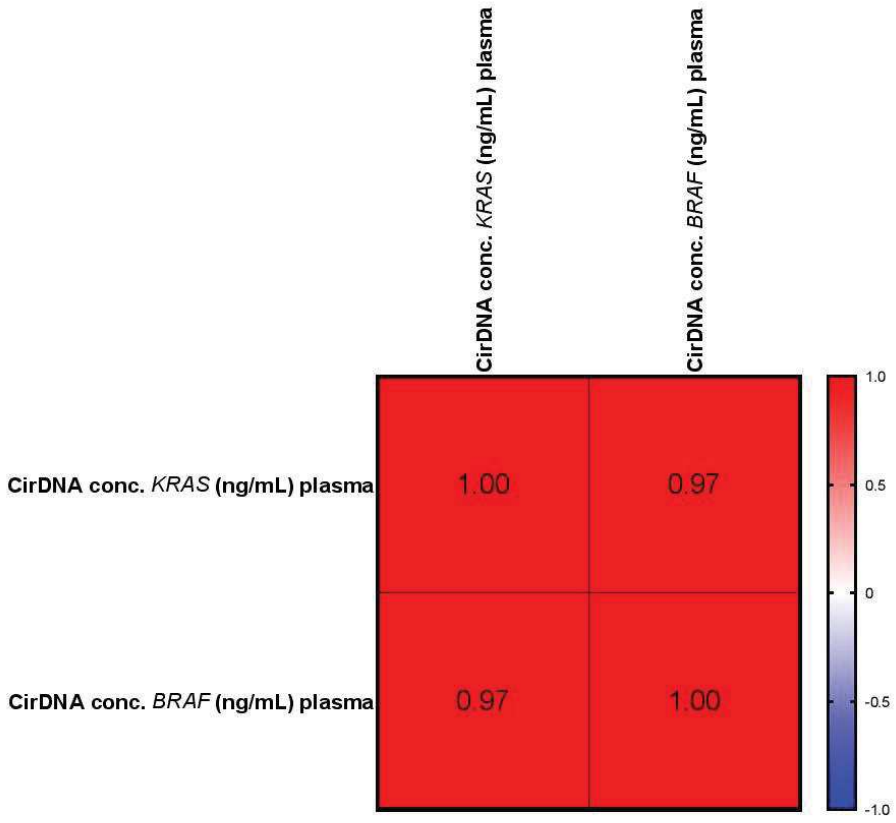

Figure S1: Correlation matrix of cirDNA concentrations (ng/mL of plasma) based on the *KRAS* and *BRAF* genes amplification in mCRC patient (n=219), Related to Figure 3. Heatmap manifests the strength of relationship by Spearman's correlation analysis (red: positive correlation; blue: negative correlation). CirDNA: circulating cell-free DNA.

A

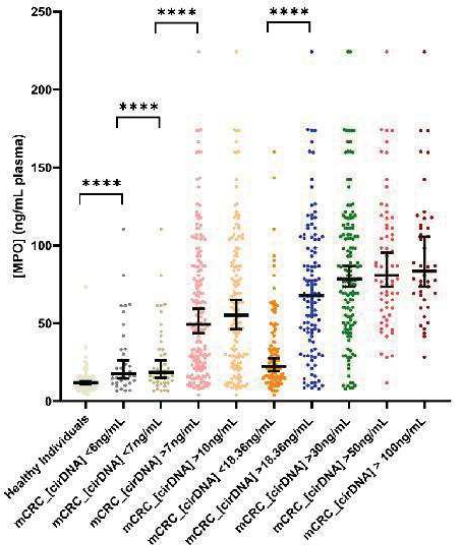

B

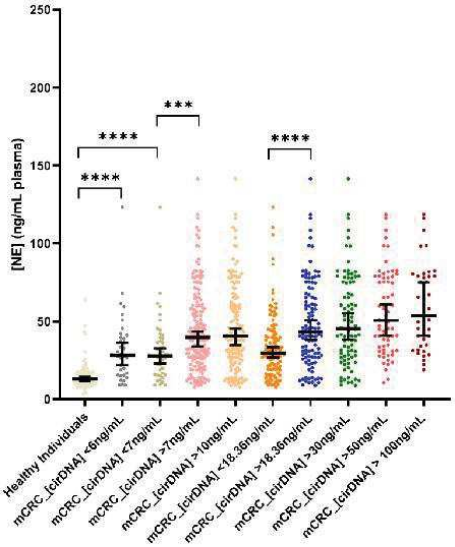

Figure S2: Comparison of MPO and NE concentrations (ng/mL of plasma) in heathy individuals (n=114) and in mCRC patients (mCRC) (n=219), Related to Figure 2. Lines represent median with 95% CI. Mann-Whitney test was performed to compare values for MPO (A) and NE (B) in HI and subgroups of mCRC patients based on their cirDNA concentrations (median value = 18.36 ng/mL). Each dot represents the values of a single patient or a single healthy individual. A probability of less than 0.05 was considered statistically significant; ***p< 0.001; ****p< 0.0001. CirDNA: circulating cell-free DNA; MPO: myeloperoxidase; NE: neutrophil elastase.

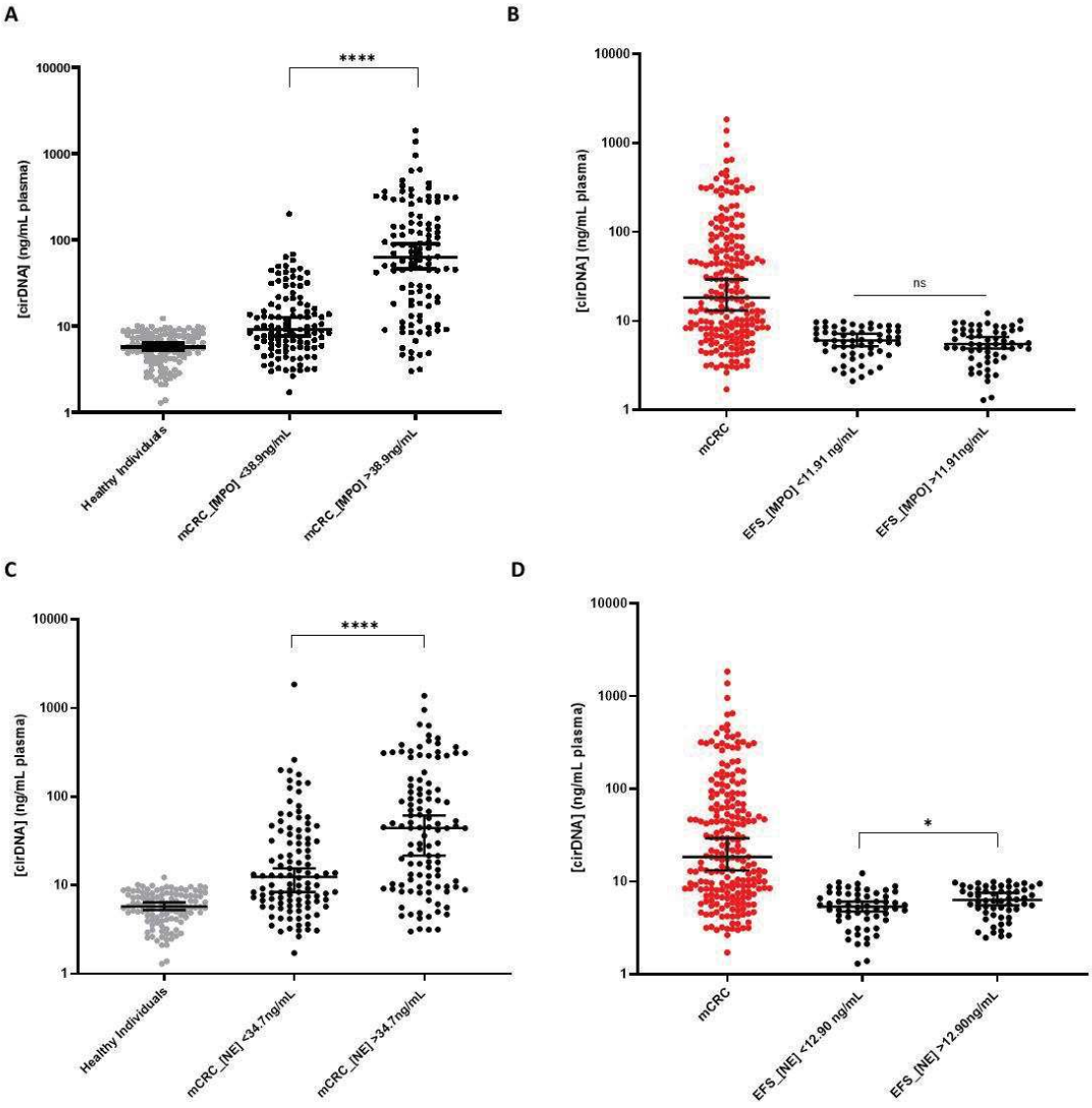

Figure S3: Comparison of cirDNA concentrations (ng/mL of plasma) in heathy individuals (n=114) and in mCRC patients (mCRC) (n=219), Related to Figure 1. Lines represent median with 95% CI. Mann-Whitney test was performed to compare values for (A) cirDNA concentrations in mCRC patients with MPO concentrations below and above the median (38.9 ng/mL), (B) cirDNA concentrations in healthy individuals with MPO concentrations below and above the median (11.91 ng/mL), (C) cirDNA concentrations in mCRC patients with NE concentrations below and above the median (34.7 ng/mL), (D) cirDNA concentrations in healthy individuals with NE concentrations below and above the median (12.90 ng/mL). Each dot represents the values of a single patient or a single healthy individual. A probability of less than 0.05 was considered statistically significant; *p<0.05, ****p< 0.0001. CirDNA: circulating cell-free DNA; MPO: myeloperoxidase; NE: neutrophil elastase.

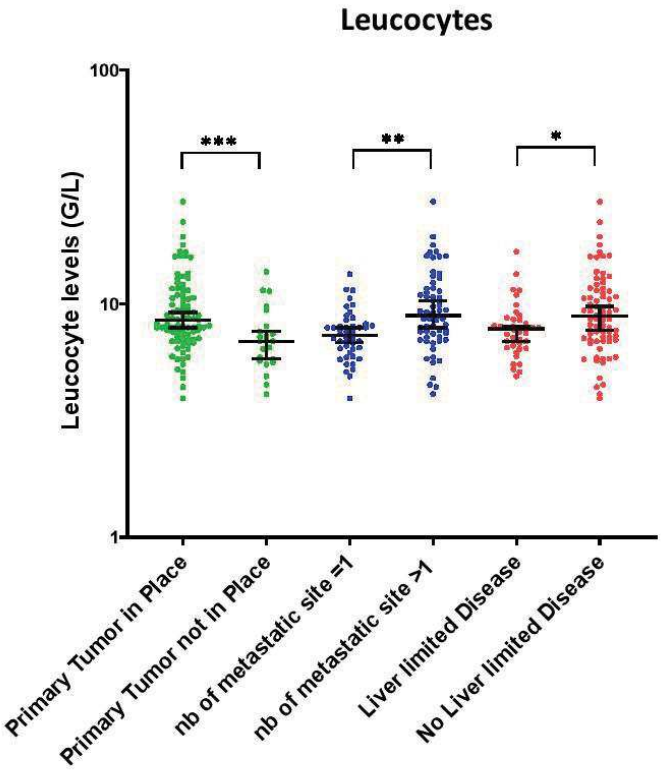

Figure S4: Comparison of leucocytes cell count (G/L) with clinical features in mCRC patients (n=219), Related to Figure 6. Lines represent median with 95% CI. Mann-Whitney test was performed to compare values for leucocytes cell count (G/L) versus different groups of clinical features. Each dot represents the values of a single patient. A probability of less than 0.05 was considered statistically significant; *p<0.05, **p<0.01; ***p< 0.001.

Figure S5

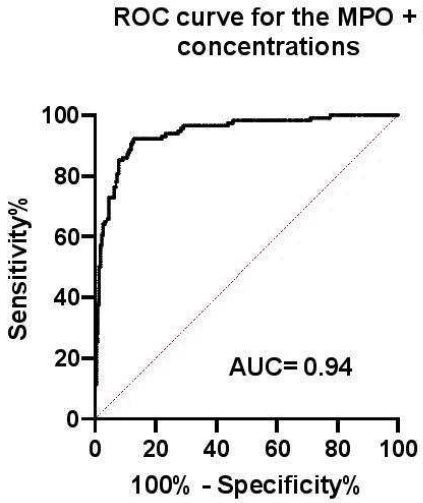

Figure S5: ROC curves for the MPO concentration and the NE concentration between healthy individuals and mCRC patients, Related to Figure 4. ROC curve of the addition of the MPO and NE concentrations. ROC: receiver operating characteristics; AUC, area under curve; MPO: myeloperoxidase; NE: neutrophil elastase.

Discussion

Les mécanismes de libération des ADNcir par morts cellulaires sont étudiés depuis plus d'une vingtaine d'années en particulier quand on parle d'apoptose, de nécrose ou de sénescence des cellules[251]. Il a longtemps été établis que l'apoptose était l'un des mécanismes de relargage des ADNcir le plus pertinent. En effet, de nombreuses études ont montré par électrophorèse que l'ADNcir a un profil de taille aux alentours de 150-180 bp (et des multiples de cette taille), comme le montre l'étude de Jahr et ses collègues[93]. Ces travaux montrent que la taille des ADNcir correspond aux tailles des ADN enroulés au sein d'un mono-nucléosome, ou dans les di-tri-nucléosomes, qui sont des signes distinctifs d'un clivage apoptotique de l'ADN. Au contraire, il est établi que le mécanisme de nécrose entraine la formation de longs fragments d'ADN allant jusqu'à des tailles >10 000 bp[77,93]. Il faut aussi prendre en considération que les ADNcir proviennent de mécanisme de sécrétion active excrétant des vésicules extracellulaires comme les exosomes, les oncosomes, les corps apoptotiques ou les microvésicules où toutes comportent de l'ADN. Les tailles d'ADN retrouvées au sein de ces vésicules extracellulaires dépendent du type de vésicules et peuvent aller de plusieurs millions de paires de bases (pb) pour les oncosomes[258] à 100 pb ou 2.5 Kpb pour les exosomes[259]. Tous les ADN relâchés par ces mécanismes sont une source des ADNcir et sont clivés par les DNases retrouvées dans le sang.

La NETose est l'un des phénomènes par lequel l'ADN extracellulaire peut être libéré dans la circulation sanguine par mort cellulaire et par sécrétion active[113–115,260]. De ce fait, cela pourrait remettre en question la prééminence accordée à l'apoptose comme principal mécanisme de libération de l'ADN circulant. Nous résultats révèlent que les concentrations en ADNcir, de NE et de MPO sont significativement plus élevées chez les patients atteints de CCRm que chez les individus sains. Nous montrons aussi une forte association positive entre les niveaux d'ADNcir et les concentrations des marqueurs des NETs (NE+MPO) chez les patients CCRm. A noter, qu'une augmentation des concentrations d'ADNcir est significativement associée à une augmentation des marqueurs des NETS (NE et MPO) chez les patients atteints de mCRC, alors qu'aucune association de ce type n'a été observée chez les individus sains. Remarquablement, les patients mCRC qui ont des concentrations d'ADNcir proches de la médiane des individus sains (6 ng/mL) ont montré des concentrations de NE et MPO plus élevées que les individus sains. Enfin, les concentrations en ADNcir, NE et MPO chez

les patients CCRm corrèlent avec le nombre de leucocytes et de neutrophiles circulants. Bien que la corrélation ne signifie pas la causalité, ces résultats combinés laissent penser que la formation des NETs chez les patients CCRm sont à la l'origine de la production d'une certaine proportion des ADNcir. Dans ce sens, des fragments de chromatine, des oligo-nucléosomes et des nucléosomes peuvent être libérés lors du processus de dégradation des NETs par des protéases, nucléases ou par des cellules immunitaires, pouvant contribuer au « pool » d'ADNcir et d'histones.

Les analyses ROC ont révélé que la quantification de la NE, de la MPO et de l'ADNcir présente une performance diagnostique élevée pour discriminer les individus sains des patients atteints de CCRm. Dans ce contexte, la détermination d'un test optimal qui combinerait tous les marqueurs des NETs en utilisant l'apprentissage automatique (ou machine learning) est en cours dans notre équipe.

Plusieurs études rapportent que les tumeurs libèrent de l'ADN dans la circulation sanguine en quantités indirectement proportionnelles à leur masse, notamment dans le cas du cancer colorectal métastatique[43,261–264]. Aussi, nous supposons que la quantité de l'ADNcir dépend de la libération de trois grandes origines cellulaires chez un patient cancéreux: (i) des cellules somatiques, au vu la libération d'ADNcir chez les individus sains[77,105,154]; (ii) des cellules malignes de la tumeur; (iii) du microenvironnement tumoral (stroma; cellules endothéliales et immunologiques)[114]. Toutes ces origines cellulaires et tous les mécanismes précités de relargages de l'ADN contribuent au « pool » des ADNcir retrouvés dans la circulation sanguine. De ce fait, les ADNcir tumoraux se retrouvent dilués dans une abondance d'ADNcir provenant de cellules non-tumorales. Nous avons précédemment constaté que la fréquence allélique variait de 0,03% à 78% dans une cohorte de patients atteints de mCRC[131]. La fréquence allélique n'est donc pas directement liée à l'agressivité de la tumeur[43], et ne doit pas être comparée à celle déterminée à partir du tissu tumoral.

Pour la première fois, une association entre des auto-anticorps anti-cardiolipine (aCL) avec les marqueurs circulants des NETs a été observée chez une partie significative des patients mCRC, mais pas chez les individus sains. L'aCL fait partie de la famille des anticorps anti-phospholipides (aPL) caractéristiques du syndrome des anti-phospholipides (APS)[265,266]. Alors que l'aPL est présente chez 1-5 % de la population générale, la prévalence dans les cas APS est de 40-50/100 000 sujets[255]. Cependant, cette prévalence peut augmenter jusqu'à 50% chez

les patients âgés atteints de maladies chroniques[254,255]. Plusieurs travaux rapportent des taux d'aPL plus élevés dans diverses tumeurs hématologiques et solides[256,257], le pourcentage de patients cancéreux positifs à l'aPL varie de 5% à 70%. Le risque de thrombose étant 4 à 60 fois plus élevé chez les patients cancéreux que dans la population générale, il a été suggéré qu'un taux élevé d'aPL pourrait déclencher une thrombose chez les patients cancéreux. Une méta-analyse a révélé que les patients atteints de cancers gastro-intestinaux, génito-urinaires et pulmonaires présentent un risque plus élevé de développer une aPL[256]. Alors que l'apparition d'aPL comme l'aCL pourrait être une étape essentielle dans la prévention de la thrombose, l'implication directe ou indirecte des aPL dans le processus thrombophilique reste peu claire. Cependant, Il est établi que les neutrophiles et les NETs contribuent à la physiopathologie APS[267]. Il convient également de noter que la formation exacerbée de NETs a été liée à l'APS dans de nombreuses pathologies auto-immunes et non-auto-immunes (comme le lupus) qui ont montré des niveaux élevés d'aCL[268]. La différence statistique nette entre les individus sains et les patients atteints de CCRm a révélé qu'une fraction significative des patients présentait une autoproduction d'aCL à des niveaux faibles, modérés et élevés.

Pour conclure, ces travaux redéfinissent les paradigmes existants sur les mécanismes de libération de l'ADNcir et pourrait suggérer qu'une fraction significative de la quantité des ADNcir proviendrait des NETs chez les patients atteints de CCRm. Ce travail est en lien étroit avec les détections de mutations chez les patients CCRm puisque la dégradation des NETs pourraient expliquer que nous retrouvons une grande amplitude de la fréquence allélique dans le sang des patients atteints de CRCm. Cependant, il reste encore à démontrer l'ensemble des acteurs conduisant à la production des ADNcir par la dégradation des Nets *in vivo*. C'est un domaine dans lequel notre équipe de recherche travaille activement.

DISCUSSION GENERALE

La grande majorité de mes travaux de recherche s'est focalisée sur la détection et la quantification des ADN circulants chez des patients atteints de cancer colorectal métastatique. Effectivement un des grands enjeux actuels en oncologie est d'apporter aux patients une médecine personnalisée ou une médecine dite « de précision » afin d'optimiser pour chaque patient une prise en charge basée sur les caractéristiques moléculaires leur tumeur. Ceci devient possible notamment grâce aux avancées majeures de la biologie moléculaire, ce qui a permis de mieux comprendre les différents mécanismes mis en jeu au niveau des cellules tumorales et ainsi, d'identifier de nouvelles cibles thérapeutiques. La meilleure compréhension moléculaire des tumeurs et l'avènement des thérapies ciblées en oncologie ont accentué l'importance de l'individualisation des traitements. La découverte de nouvelles molécules anticancéreuses a permis d'améliorer la survie des patients atteints de CCRm. En effet, la survie globale médiane des patients n'a cessé d'augmenter chez les patients CCRm depuis la fin du XXème siècle, passant d'environ 8-12 mois à environ 30 mois aujourd'hui[202]. Parmi les possibilités thérapeutiques, l'association des thérapies ciblées à la chimiothérapie a contribuée à l'amélioration de la survie[202]. Cependant, l'accès à ces nouvelles molécules à action ciblée nécessite la caractérisation génétique de la tumeur primaire et des métastases associées puisque certaines altérations génétiques peuvent entrainer des résistances aux traitements, notamment dans le cas des thérapies ciblées anti-EGFR chez les patients atteints de CCRm.

De nos jours, l'analyse moléculaire des tumeurs de patients atteints de cancer colorectal est réalisée à partir du tissu tumoral. Ce processus nécessite une analyse longue et couteuse qui est réalisée par des anatomopathologistes ainsi que par l'intervention de spécialistes afin de pratiquer un acte chirurgical qui reste douloureux et invasif pour les patients. La pièce tumorale à analyser est prélevée lors d'une biopsie de la tumeur primaire et/ou d'une métastase. Cependant, l'analyse du tissu tumoral ne permet pas d'apprécier l'ensemble de l'hétérogénéité clonale intra- et inter-tumorale des tumeurs[51]. Aussi, l'aspect très invasif de cette technique, ne permet pas de réaliser une biopsie tout au long d'une prise en charge d'un patient. Les limites de l'analyse du tissu tumoral ont contraint les scientifiques à trouver une nouvelle source d'ADN tumoral qui serait non invasive et qui serait le miroir de l'hétérogénéité clonale de l'ensemble des sites tumoraux d'un patient.

L'analyse de l'ADN circulant permet d'apprécier l'hétérogénéité clonale intra- et inter-tumorale

Dans ce contexte, l'ADN circulant permet d'outrepasser les limites de l'analyse moléculaire du tissu tumoral[182,198,269]. En effet, l'ADNcir est analysé via une simple prise de sang ce qui en fait une méthode peu invasive[131,210–212]. De plus, les cellules malignes de la tumeur primaire et de chaque métastase peuvent libérer leurs ADN dans la circulation générale entrainant un « pool » d'ADNcir tumoral circulant (ctDNA) portant l'ensemble des altérations génétiques et épigénétiques des tumeurs[71]. Cette découverte a permis de mettre en exergue le potentiel biomédical de l'analyse des ADNcir en oncologie notamment pour le dépistage, le diagnostic, le pronostic, mais aussi pour l'adaptation thérapeutique (ou théranostique), la détection de l'émergence de mutations entrainant des résistances aux traitements et le suivi des patients atteints de tous types de cancers. L'engouement autour de la « biopsie liquide » a permis l'optimisation sans précèdent des méthodes d'analyse de l'ADNcir. Comme discuté dans ce manuscrit, il y a deux grands concepts de méthode pour analyser les ADNcir : les techniques basées sur la PCR quantitative (PCRq) et les méthodes de séquençage à haut débit. Bien qu'il y ait eu des progrès considérables ces dernières années pour accentuer la sensibilité des méthodes de séquençage à haut débit, celle-ci peuvent détecter difficilement une mutation avec une fréquence allélique <1% (Tam-Seq ou Safe-Seq)[270]. En revanche, les techniques de PCRq améliorées comme la digitale droplet PCR (ddPCR), le BEAMing, ou la méthode IntPlex[135] ont des sensibilités pouvant détecter des mutations avec une fréquence allélique <0.1% et dans certain cas <0.01%.

Durant mon travail de thèse j'ai participé à plusieurs projets qui ont eu pour objectif de (i) valider un grand nombre de potentiels cliniques de l'ADNcir en oncologie, et plus précisément dans la prise en charge des patients atteint de cancer colorectal métastatique, puis de (i) mieux connaitre les origines et les structures des ADNcir. Ma thèse est largement articulée autour de la recherche translationnelle et particulièrement sur la détection des mutations des gènes *KRAS*, *NRAS* et *BRAF* dans le plasma de patients CCRm. En parallèle, j'ai également effectué de recherche fondamentale portant sur les origines des ADNcir plasmatiques.

Détermination du statut *RAS/BRAF* via l'analyse de l'ADNcir chez des patients atteints de CCRm avant l'initiation d'une thérapie ciblée anti-EGFR

Le premier objectif de thèse a été d'étudier l'hétérogénéité clonale de tumeurs de patients atteints de cancer colorectal métastatique par l'analyse de l'ADN circulant au cours de leur prise en charge thérapeutique. Ce travail a commencé après la première validation clinique de l'analyse de l'ADNcir tumoral pour la détection des mutations *KRAS* et *BRAF* en oncologie, réalisée par notre équipe en 2014[76]. Cette étude a été engagé suite à la démonstration que seuls les patients CCRm avec un statut *KRAS* c12/13 et *BRAFV600E* sauvage avait un bénéfice clinique lors d'un traitement à base d'anticorps dirigés contre l'EGFR[27,204]. Dans ce travail l'équipe a montré pour la première fois un niveau de concordance inégalé du statut mutationnel *KRAS/BRAF* entre l'analyse du tissu tumoral et l'analyse de l'ADNcir chez 95 patients atteints de CCRm, avec 96% et 100% de concordance pour les mutations de l'exon 2 du gène *KRAS* (c12/13) et pour la mutation *BRAF V600E*, respectivement. D'autre travaux ont montré que l'analyse de l'ADNcir pouvait remplacer l'analyse du tissu tumoral pour rechercher ces mutations avant l'initiation d'une thérapie ciblée anti-EGFR[182,235–237]. L'étude Prime a démontré l'impact des mutations de l'exon 3 et 4 du gène *KRAS* ainsi que certaines mutations des exons 2,3 et 4 du gène *NRAS* sur la résistance aux traitement anti-EGFR chez des patients CCRm[28,29]. Bien qu'il existe d'autres aberrations moléculaires induisant la résistance des tumeurs à ces thérapies ciblées, il n'est obligatoire que de rechercher l'ensemble des mutations *RAS* des exons 2, 3 et 4 avant d'initier un traitement par anti-EGFR pour les patients CCRm. La raison est que ceux sont les altérations génétiques les plus fréquentes donnant lieu à ces résistances. La mutation *BRAFV600E* est recherchée couramment lors des analyses moléculaires car elle est indicative d'un mauvais pronostic pour les patients atteints de cancer colorectal[271]. Aussi, l'essai FIRE-4.5 conclu à une meilleur PFS chez les patients CCRm traités par tri-chimiothérapie (tri-CT) plus bevacizumab comparé à une tri-CT plus cetuximab. L'ensemble de ces travaux nous ont poussé à réaliser l'étude de l'utilité clinique de l'ADNcir pour la détection rapide des mutations des exons 2, 3 et 4 des gènes *KRAS* et *NRAS* et la mutation *BRAFV600E* en vue d'une sélection des patients atteints de CCRm pour un traitement anti-EGFR. J'ai contribué à cette étude nommée KPLEX2 dont les résultats sont discutés dans ce manuscrit. Cette étude fait suite à l'étude de validation clinique des ADNcir en oncologie[76] en y a joutant une dimension médico-économique. De plus, aucun seuil de sensibilité pour la détection des mutations a été effectué, ce qui la différencie significativement de notre étude

antérieur[76]. Tout d'abord notre étude a montré que la médiane du délai entre la réception de l'échantillon de tissu par le laboratoire de l'hôpital et la communication des résultats était de 12 jours (n=83 ; 3-273 jours) mais était seulement de 2 jours entre la réception de l'échantillon de plasma par notre laboratoire et la communication des résultats (n=121 ; 0-10 jours). Cette étude montre la rapidité de l'analyse de l'ADNcir via une prise de sang et renforce l'impact de cette analyse dans la prise en charge rapide des patients et notamment pour des stades avancés de la maladie. Un sondage (7 centres impliqués) sur la pratique réelle de la « biopsie liquide » pour le dépistage de la mutation T790M du gène *EGFR* (cobas® EGFR Mutation Test v2) chez les patients atteints de cancer du poumon non à petites cellules (NSCLC) montre que l'analyse de l'ADNcir est réalisée en 24 heures[272]. Ce résultat confirme qu'en pratique clinique l'analyse de l'ADNcir est possible et apporte une rapidité de prise en charge des patients. Même si ces validations constituent une avancée notable en vue d'une transposition en pratique clinique de routine, il reste actuellement beaucoup de problématiques à résoudre qui sont autant de freins à cette transposition. De nos jours, le test plasmatique peut être utilisé lorsqu'une biopsie tissulaire est insuffisante pour la détection de la mutation *EGFR T790M* chez les patients atteints de NSCLC ou si elle ne peut être obtenue en toute sécurité, voire si le tissu tumoral n'est pas disponible. Il faut prendre en considération que les biopsies tissulaires ne sont pas réalisables ou ne sont pas interprétables dans environ 15 à 20% des cas tous cancers confondus. Enfin, notre étude a aussi montré une augmentation sans précédent du nombre de détection des mutations *RAS/BRAF* par rapport à l'analyse du tissu tumoral et une proportion très élevée de mutations co-occurrentes. Effectivement, 76% des patients ont été déterminé comme muté *RAS/BRAF* par l'analyse de l'ADNcir contre 55% des patients lors de l'analyse du tissu tumoral. Des forts taux de discordance entre l'analyse du tissu tumoral et l'analyse de l'ADNcir pour la détermination moléculaire *RAS/BRAF* des tumeurs ont déjà été démontré[223]. Ceci est principalement dû au fait que l'analyse de l'ADNcir tumoral permet l'analyse de l'ensemble des clones tumoraux de la tumeur primaire et des métastases avec un seul échantillon, fournissant ainsi des informations instantanées sur la dynamique tumorale en temps réel, ce que le tissu ne permet pas. Le second point important et non des moindres est l'ultra-sensibilité des méthodes d'analyses de l'ADNcir, notamment celle que nous utilisons, la méthode de Q-PCR « Allele Specific Blocker » (ASB) IntPlex. Cette méthode à une sensibilité analytique de détection des mutations allant de 0,001% à 0,005% de fréquence allélique suivant les mutations testées[76]. D'autres méthodes d'analyses de l'ADNcir à partir du

plasma, comme la ddPCR ou le BEAMing ont des niveaux de sensibilité de détection de mutations équivalents[162,163]. La biopsie liquide surmonte donc l'hétérogénéité clonale intra- et inter-tumorale[273] et présente des avantages importants par rapport à la biopsie tissulaire. Par conséquent, le profilage des mutations basé sur l'analyse de l'ADNcir tumoral peut identifier des mécanismes de résistance concomitants résidant dans des métastases distinctes et au sein d'une lésion tumorale, permettant potentiellement une évaluation longitudinale de l'émergence de mutations ponctuelles pouvant induire des résistances aux thérapies anti-EGFR chez les patients atteints de CCRm[66,68,198].

Suivi du statut *RAS/BRAF* via l'analyse de l'ADNcir chez des patients atteints de CCRm traités aux anti-EGFR

C'est dans ce contexte que nous avons réalisé l'étude rétrospective intitulée KPLEX R[173] dont les résultats sont présentés dans ce manuscrit. Dans cet essai clinique de phase IB/II nous avons rétrospectivement évalué l'analyse de l'ADNcir dans le plasma de 42 patients atteints de CCRm réfractaires aux thérapies standards et traités avec du FOLFOX-dasatinib avec ou sans cetuximab. Seuls les patients n'ayant pas de mutations sur le gène *KRAS* (codons 12/13, n=21) déterminés par l'analyse du tissu tumoral lors de la phase IB ont été traité avec du cetuximab. L'analyse longitudinale des plasmas de certains patients de cet essai a permis d'évaluer la dynamique clonale de *RAS*/*BRAF* pendant le traitement et de comparer nos résultats avec les critères radiographiques RECIST ainsi qu'avec les dosages sanguins de l'ACE. Approximativement 52% des patients initialement déterminé non mutés par l'analyse du tissu tumoral présentent au moins une mutation *RAS/BRAF* lors de l'analyse de l'ADNcir. Nous montrons aussi dans cette étude que 64% des mutations retrouvées via l'analyse de l'ADNcir ont une fréquence allélique inférieure à 1% et que 21% d'entre elles sont retrouvées avec une fréquence allélique inférieure à 0.1%. Avant traitement, 25/42 patients (60%) été déterminé muté *RAS/BRAF* par l'analyse du tissu tumoral alors que 37/42 (88%) sont déterminés mutés par analyse de l'ADNcir. De plus, l'analyse de l'ADNcir a montré que 11/21 patients (52.4%) traités au cetuximab, ont été déterminé muté sur les codons 12/13 du gène *KRAS* alors qu'ils ont été déterminés non mutés pour ce « hotspot » par l'analyse tissulaire réalisé par pyroséquençage. Cette divergence de concordance du statut mutationnel peut s'expliquer par l'hétérogénéité clonale intra- et inter-tumorale, le manque de sensibilité de la méthode d'analyse par pyroséquencages (5%-10% de fréquence allélique lors de cette étude), un long délai entre le prélèvement de la pièce tumoral et la collection du sang, et pour finir par le fait

que la tumeur primaire peut ne pas être présente lors de la prise de sang. Ces premiers résultats démontrent le potentiel de l'ADNcir tumoral et ils valident le fait que son analyse est plus performante que celle du tissu tumoral pour la sélection des patients atteints de CCRm en vue d'un traitement anti-EGFR. De plus, l'évolution clonale temporelle des tumeurs est un véritable challenge dans la prise en charge des patients. Cette hétérogénéité temporelle est amplifiée par la pression thérapeutique et notamment chez les patients traités par anti-EGFR. En effet, la détection précoce de l'émergence de mutation au cours du traitement peut avoir un impact sur les résultats cliniques comme l'a suggéré Bertotti et ses collègues en caractérisant la résistance secondaire au blocage de l'EGFR dans le CCRm[228]. Dans ce contexte, nous avons réalisé une analyse longitudinale des plasmas de 18 patients afin d'observer la détection de mutations qui n'ont pas été détectées avant l'initiation des traitements. Nous avons observé que 83% (15/18) des mutations ponctuelles nouvellement déterminées par l'analyse de l'ADNcir pendant le traitement ont une fraction allélique inférieure à 0,5% et que 50% (9/18) d'entre elles apparaissent pour la première fois à des fractions alléliques inferieurs à 0,1%. A noter que dans cette étude nous avons pu détecter une mutation ponctuelle avec une fréquence allélique de 0.009%. Il est difficile d'affirmer que ces mutations nouvellement observées sont des « émergences pures » car ces mutations pouvaient être présentes avant l'initiation des traitements mais que la sensibilité de notre méthode ne permettait pas de les détecter plus tôt. Sur ce sujet, des études rétrospectives ont suggéré que certaine de ces mutations peuvent être détectées via l'analyse l'ADNcir avant le début du traitement[182]. D'autre travaux en utilisant des modèles mathématiques sur la cinétique de la croissance tumorale ont montré que ces mutations doivent être présentes avant le début du traitement[66]. Les données de l'analyse de l'ADNcir obtenues dans le cadre de cette étude reflètent étroitement les changements dynamiques des concentrations plasmatique de l'ACE ainsi que les mesures tumorales réalisées par CT-scan (changements en % de la mesure tumorale réalisée avant l'initiation des traitements), évalués chez 34 patients. Nous avons noté que la détection qualitative d'une mutation et les informations quantitatives telles que les concentrations d'ADNcir tumoral *RAS*-mutant, les concentrations d'ADNcir total et la fraction d'allèle mutant semble être utiles pour suivre l'évolution de la maladie. Finalement, lors de cette étude nous montrons que tous les patients sauf un présentent au moins une mutation *RAS/BRAF* que ce soit avant le traitement ou acquise (ou sélectionnée) durant les traitements et qu'une fraction significative de ces mutations présente une faible fréquence

d'allélique mutée. Nous avons également constaté que de nombreux patients ont connu une évolution moléculaire convergente malgré qu'ils aient été traités par des thérapies différentes (avec ou sans cetuximab), ce qui a donné lieu à des mutations redondantes qui fourniraient des mécanismes multiples de résistance au traitement dirigé contre l'EGFR. L'analyse longitudinale de l'ADNcir nécessite une simple prise de sang et permettrait donc l'optimisation et l'orientation des traitements des patients atteints de CCRm qui pourraient bénéficier d'un traitement approprié avant l'apparition clinique d'une résistance secondaire. Siravegna et ses collègues[198] ont investigué l'utilité du suivi de l'ADNcir pour mesurer les sous-clones mutés sur le gène *KRAS* comme un biomarqueur potentiel pour réutiliser des thérapies ciblées antérieures. Ils ont démontré que lors d'un arrêt de la pression sélective du traitement anti-EGFR, les fréquences alléliques des clones mutants *KRAS* avaient diminué et que ces patients sont ensuite redevenus sensibles au traitement anti-EGFR[198].

Suivi par l'analyse de l'ADNcir de patients atteints de CCRm réfractaires aux thérapies standards et traités par régorafénib en dernière ligne de traitement

Bien que "rechallenger" (ou retraiter) les patients avec une thérapie ciblée anti-EGFR soit une perspective de choix dans l'option thérapeutique des patients atteints de CCRm réfractaires aux thérapies standards, cela n'est pas encore le cas en pratique clinique courante[198,274]. Actuellement, ces patients réfractaires peuvent être traités en dernière ligne, soit avec du régorafénib soit avec du trifluridine/tipiracil. Comme présenté dans ce manuscrit, le régorafénib est un inhibiteur de multityrosine kinase qui induit des activités anti-angiogéniques et cytotoxiques que ce soit dans des expériences *in vitro* et *in vivo*[35]. Il a été autorisé dans l'union européenne pour le traitement des patients CCRm réfractaires aux thérapies standards sur la base de son activité anti-tumorale par rapport au placebo et aux meilleurs soins de soutien montrés dans les essais cliniques de phase III CORRECT et CONCUR[36,37]. Depuis cette approbation de nombreux travaux ont cherché un marqueur ou biomarqueur de réponse et/ou de non réponse clinique à cette molécule. En effet, la moitié des patients traités au régorafénib connaissent une progression tumorale deux mois après le début du traitement, ce qui les a exposés inutilement à des effets indésirables liés au traitement. Ce risque de toxicité pourrait être réduit par l'adoption d'une stratégie d'escalade des doses pour optimiser la posologie du régorafénib avec une activité comparable[232]. L'étude TEXCAN (NCT02699073) a confirmé sur 35 patients qu'une maladie stable (SD) à deux mois évaluée par les critères RECIST 1.1 représentait un bénéfice clinique chez les patients CCRm

traité au régorafénib. Ils ont aussi montré que les critères de Choi (ou mChoi) n'apportaient pas d'informations utiles sur l'efficacité du régorafenib chez ces patients[240]. D'autres travaux ont été mené pour rechercher si l'analyse de l'ADNcir pouvait prédire les patients répondeurs ou les non répondeurs au régorafénib. Dans une étude exploratoire de l'essai CORRECT[36], Tabernero *et al*, ont montré une tendance à une meilleure survie pour les patients traités par régorafénib qui présentaient des génotypes sauvages pour les gènes *KRAS/PIK3CA*, évalués soit à partir de l'ADN tissulaire, soit à partir de l'ADNcir. Il est intéressant de noter qu'ils ont également observé avant l'initiation du traitement une association entre de forts niveaux d'ADNcir et une réduction de la durée médiane de survie[233]. Cependant, malgré tous ces travaux, il n'existe pas encore de marqueur ou biomarqueur de réponse clinique ou de non réponse à cette molécule.

Afin de répondre à cette question nous avons participé à une des études ancillaires de l'essai TEXCAN dont les résultats sont présentés dans ce manuscrit[275]. Dans cette étude prospective, nous avons étudié l'activité clinique du régorafénib chez des patients CCRm réfractaires aux thérapies standards via l'analyse de l'ADNcir. Nous avons pu constater que la concentration en ADNcir total, la concentration en ADNcir *RAS* muté, et dans une moindre mesure, la fréquence allélique étaient inversement corrélés à l'OS. Cette relation a été observée qu'elle soit étudiée sous forme de classes ou de variables continues. Ces résultats ont pu être mis en exergue par plusieurs groupes[233,248,249,276]. A l'instar des travaux publiés sur le sujet, l'avantage de notre étude est que nous avons pu établir des seuils de concentrations d'ADNcir total (26 ng/mL de plasma), d'ADNcir tumoral muté (2 ng/mL de plasma) et de fréquence allélique (6%) qui permettraient de prédire les patients qui auront une meilleure survie globale. Pour exemple, nous avons montré que les patients ayant une concentration d'ADNcir total >26 ng/mL de plasma avant le traitement ont un risque de mort doublé comparé à ceux avec une concentration inférieure à ce seuil. De façon très intéressante, nous montrons dans cette étude qu'avant l'initiation du traitement, les patients qui ont une concentration en ADNcir total >100 ng/mL de plasma ont une probabilité d'être vivant à 3 mois de seulement 30% contre 80% pour les patients en deçà de ce seuil. Ces résultats sont en droite ligne avec ceux obtenus dans deux travaux antérieurs de l'équipe[184,277]. Aussi, nous confirmons qu'il y a une rapide augmentation de la concentration totale en ADNcir entre le début du traitement et le 14ième jours de traitement[248]. Nous supposons que cela est dû au relargage massif d'ADNcir

de cellules saines suite aux effets toxiques du regorafenib sur les tissus sains. La deuxième nouveauté et que nous sommes en capacité de montrer une évolution clonale *RAS/BRAF* dans cette petite cohorte de patients et cela malgré la courte durée du traitement. Nous montrons pour la première fois sur cette population de patients traités au régorafénib que l'évolution clonale *RAS/BRAF* des patients au cours du traitement n'influe ni l'OS, ni la PFS des patients. A l'inverse d'autres travaux, aucune relation n'a été établi dans notre étude entre l'analyse de l'ADNcir et la PFS[249,278]. Cependant, étant donné que le régorafénib est plus susceptible d'être cytostatique que cytotoxique et que la durée du traitement est très courte, il est difficile de s'attendre à une réduction significative de la tumeur et qu'elle soit accompagnée d'une forte diminution des biomarqueurs de l'ADNcir chez des patients fortement prétraités. Notre étude est exploratoire et les résultats doivent être interprétés prudemment puisqu'ils sont réalisés sur une cohorte à faible effectif. C'est dans ce contexte que nous avons proposé dans BMC cancer un protocole clinique visant à traiter les patients CCRm avec le régorafénib plus précocement afin d'avoir une durée de traitement significativement plus importante[250]. Le protocole clinique de cet essai auquel j'ai contribué, est discuté dans ce manuscrit[250].

Nous avons donc initié l'essai FOLFINOX-R qui est une étude de phase I/II, prospective, multicentrique et non randomisée pour évaluer l'innocuité et l'efficacité du régorafénib en association avec le FOLFIRINOX lors d'un traitement de première ligne des patients atteints de CCRm ayant un statut *RAS* muté déterminé à partir de l'ADNcir[250]. Il sera réalisé une analyse longitudinale des plasmas prélevés avant le traitement, tous les deux cycles de traitement et à l'arrêt du traitement. Nous surveillerons les variations des paramètres de l'ADNcir pour vérifier l'efficacité ou la résistance au traitement. Nous prévoyons également d'examiner, sur des échantillons de tissus colorectaux, l'activité et l'expression de certaines kinases ciblées par le régorafénib. Notre objectif premier est de démontrer que cette association FOLFIRINOX-régorafénib apporte un bénéfice clinique suffisant pour être testée dans une étude contrôlée et dans une population de patients sélectionnés.

Stratification des patients atteints de CCRm en vue d'un traitement par anti-EGFR lors du premier essai interventionnel où l'analyse de l'ADNcir détermine le statut *RAS/BRAF* sauvage des patients

En parallèle de tous ces projets, nous réalisons l'essai UCGI 28 PANIRINOX (NCT02980510), qui est une étude de phase II randomisée, prospective et multicentrique visant à comparer le traitement FOLFIRINOX-panitumumab avec le traitement mFOLFOX6-panitumumab chez des patients CCRm pour lesquels le statut *RAS/BRAF* sauvages a été déterminé via l'analyse de l'ADNcir. PANIRINOX est la première étude mondiale interventionnelle à utiliser l'ADNcir comme test compagnon afin de sélectionner des patients CCRm en vue d'une thérapie ciblée anti-EGFR. L'objectif primaire de cet essai est d'évaluer le taux de réponse complète des patients traités par FOLFIRINOX-panitumumab. Cette étude est la suite logique à tous nos travaux impliquant la détection des mutations *RAS/BRAF* par l'analyse de l'ADNcir[43,76,173]. De plus, c'est l'étude interventionnelle qui manque à la démonstration complète de l'utilité de clinique de l'ADNcir.Nous voulons par cet essai démontrer que l'ADNcir peut remplacer l'analyse moléculaire *RAS/BRAF* du tissu tumoral et par conséquent montrer que cela est réalisable en pratique clinique courante puisque l'étude est menée en flux tendu. Nous confronterons les résultats de l'analyse mutationnelle *RAS/BRAF* obtenus à partir du tissu tumoral et à partir de l'ADNcir. Actuellement, 174 patients sur 209 requis sont inclus dans cette étude, soit près de 85% des inclusions sont déjà réalisées (454 patients analysés). De plus, un essai ancillaire de PANIRINOX est en cours et consiste au suivi des patients inclus dans l'étude. L'analyse longitudinale des plasmas des patients via l'analyse de l'ADNcir aura pour objectif de détecter l'émergence de mutations *RAS/BRAF/PIK3CA* et de corréler l'apparition de ces mutations avec l'OS et la PFS. Ce travail établira l'impact des mutations acquises survenues durant le traitement et la résistance aux anti-EGFR. Dans ce sens, nous pensons que ce travail confirmera de précédents travaux dans le domaine[66–68,198,274]. Il faut noter que l'essai PANIRINOX a une particularité singulière puisque nous estimons qu'un patient *RAS/BRAF* muté ayant une fréquence allélique inférieur à 0.5% est considéré comme étant *RAS/BRAF* sauvage. Ce seuil a été choisi pour déterminer, pour la première fois dans un essai prospectif, si une faible fréquence allélique *RAS/BRAF* mutée au départ d'un traitement anti-EGFR en première ligne chez des patients CCRm adresse réellement une résistance aux traitements. Il n'existe aucune étude qui a défini une valeur seuil décisionnelle pour l'administration d'un traitement, bien que cela serait potentiellement indicatif dans le cas des traitements aux anti-

EGFR. Si tel est le cas nous pourrons établir aussi la dynamique des clones mutés chez des patients naïfs de traitements au cours du traitement et évaluer le temps d'apparition d'une résistance clinique. Enfin, cet essai renseignera sur la possibilité d'arrêter le traitement avant une manifestation de résistance clinique.

Il sera possible par la suite de retraiter aux anti-EGFR, lors d'une deuxième ou troisième ligne de traitement les patients qui n'auront aucune émergence acquise de mutations à la fin de cette étude comme le suggère de nombreux essais[279]. Pour la première fois dans une étude prospective (essai CRICKET), Cremolini et ses collègues ont montré qu'un « rechallenge » des patients *RAS*/*BRAF* mutés avec du cetuximab plus irinotecan est une alternative de choix pour remplacer le traitement en troisième ligne par trifluridine/tipiracil ou par régorafénib des patients CCRm réfractaires[199].

Etude d'une nouvelle origine potentielle des ADNcir chez des patients atteints de CCRm : Les NETs

Le deuxième volet de ma thèse a été de mieux comprendre les origines des ADNcir chez les patients atteints de CCRm. Parmi l'ensemble des mécanismes de relargage des ADNcir dans la circulation, il a longtemps été établis que l'apoptose était le plus pertinent. Ce postulat est dû au fait que de nombreuses études ont montré que l'ADNcir a un profil de taille aux alentours de 150-180 bp (et des multiples de cette taille). Jahr et ses collègues ont montré que la taille des ADNcir correspond aux tailles des ADN enroulés au sein d'un mono-nucléosome, ou dans les di-tri-nucléosomes, qui sont des signes distinctifs d'un clivage apoptotique de l'ADN[93]. Le mécanisme de nécrose quant à lui entraine la formation de longs fragments d'ADN allant jusqu'à des tailles >10 000 bp[77,93]. Il faut aussi prendre en considération que les ADNcir proviennent de mécanisme de sécrétion active excrétant des vésicules extracellulaires comme les exosomes, les oncosomes, les corps apoptotiques ou les microvésicules où toutes comportent de l'ADN. Tous les ADN libérés par ces mécanismes sont une source des ADNcir et sont en partie clivés par les DNases présentes en grande quantités dans le sang. L'équipe a réalisé l'étude PaniNet (discuté dans ce manuscrit) pour tenter de remettre en question la prééminence accordée à l'apoptose comme principal mécanisme de libération de l'ADN circulant.

Nous nous sommes intéressés à la NETose qui est un des phénomènes par lequel l'ADN extracellulaire peut être libéré dans la circulation sanguine par mort cellulaire et par sécrétion

active[113,115,260]. Cette dernière consiste en une libération de pièges ADN extracellulaires sécrétés par des neutrophiles activés (NETs) qui sont composés d'un réseau de chromatine extracellulaire décorée de protéines cytosoliques et de granules bactéricides, telles que l'élastase des neutrophiles (NE) et la myéloperoxydase (MPO)[252]. Remarquablement, les NETs sont retrouvés dans les mêmes conditions pathologiques pour lesquelles des concentrations élevées d'ADNcir ont été rapportées[77,114].

Nos résultats confirment que les concentrations totales en ADNcir sont significativement plus élevées chez les patients atteints de CCRm que chez les individus sains. Ce résultat pris indépendamment pourrait laisser penser que l'augmentation de cette concentration est due au relargage massif des ADNcir par la tumeur elle-même. Cependant nous montrons aussi que les niveaux de NE et de MPO sont significativement plus élevées chez les patients atteints de CCRm que chez les individus sains. Cela indique donc une présence accrue de NETs ou de produits de NETs chez les patients cancéreux. Ce résultat suggère que l'augmentation de la concentration des ADNcir pourrait donc dériver en partie des NETs et par extension proviendrait des neutrophiles circulants ou des neutrophiles infiltrés au sein de la tumeur des patients. Dans ce sens, nous montrons une forte association positive entre les niveaux d'ADNcir et les concentrations des marqueurs des NETs (NE+MPO) chez les patients CCRm. A noter, qu'une augmentation des concentrations d'ADNcir est significativement associée à une augmentation des marqueurs des NETS (NE et MPO) chez les patients atteints de mCRC, alors qu'aucune association de ce type n'a été observée chez les individus sains. Remarquablement, les patients mCRC qui ont des concentrations d'ADNcir proches de la médiane des individus sains (6 ng/mL) ont montré des concentrations de NE et MPO plus élevées que les individus sains. Aussi, nous montrons que les concentrations en ADNcir, NE et MPO chez les patients CCRm corrèlent avec le nombre de leucocytes et de neutrophiles circulants. Cela tend à confirmer l'idée que dans cet essai les ADNcir dérivent des NETs via leur dégradation par des cellules phagocytaires ou par des DNases présentent dans le sang. A ce sujet, il convient de noter que le nombre de leucocytes et de neutrophiles circulants (mais pas le nombre de lymphocytes) est significativement plus élevé chez les patients ayant une tumeur primaire en place et chez les patients ayant deux sites métastatiques ou plus. Cela pourrait suggérer que les leucocytes et les neutrophiles, et par extension les NETs sont directement impliqués dans

la croissance tumorale ou la dissémination du cancer, comme cela a été suggéré dans des travaux antérieurs[280–283].

Les macrophages et plus précisément la DNase 1 de ceux-ci participent à l'élimination des NETs, ce mécanisme est incomplet et conduit à la libération de fragments d'ADN partiellement dégradés dans la circulation sanguine[108,124]. Mizuta et ses collègues ont montré dans des expériences *in vivo* et *in vitro* que la DNase activée par la caspase (Caspase-Activated DNase, CAD) et la DNase1L3 (ou DNase γ) sont capables de dégrader l'ADN lié aux protéines et à la chromatine dans des unités mono, di, tri-nucléosomes[284]. Cette équipe a également montré que la DNase1L3 était capable d'initier la dégradation des structures de type NETs, contrairement à la Dnase1 et à la CAD[284]. De plus, Jimenez-Alcazar *et al* ont rapporté que la DNase1L3 et la DNase 1 dégradent ensemble les NETs *in vitro*[285]. L'équipe de Dennis Lo' montre également l'implication de la DNase1L3 dans la dégradation de l'ADN circulant extracellulaire en montrant que la délétion de la Dnase1L3 chez la souris entraîne des aberrations de longueur et des fréquences des motifs terminaux dans l'ADNcir plasmatique[286]. On peut donc raisonnablement penser que les réseaux de chromatine des NETs sont rapidement et dynamiquement dégradés très activement par les nucléases plasmatiques, ce qui entraîne la libération de fragments de chromatine de taille moléculaire élevée diminuant jusqu'à des structures d'ADN de faibles tailles moléculaires qui sont associées au mononucléosome/chromatosome, qui est apparue comme la structure d'ADNcir la plus importante et la plus stable dans le sang[87,137,286,287]. Dans ce sens, des fragments de chromatine, des oligo-nucléosomes et des nucléosomes peuvent être libérés lors du processus de dégradation des NETs par des protéases, nucléases ou par des cellules immunitaires, pouvant contribuer au « pool » d'ADNcir et d'histones. Pour aller plus, loin Paunel-Görgülü et ses collègues ont démontré que les ADNcir amplifient la NETose d'une manière intracellulaire indépendante de la voie d'activation du TLR9 (Toll-like receptor 9), et par conséquent nous pouvons spéculer qu'un excès d'ADNcir pourrait activer une boucle de rétroaction positive sur la formation de NETs[288]. Cependant, il reste encore à rechercher l'ensemble des acteurs conduisant à la production des ADNcir par la dégradation des NETs *in vivo*. C'est un domaine dans lequel notre équipe travaille activement.

Nous montrons pour la première fois chez une partie significative des patients mCRC, qu'une association positive existe entre les auto-anticorps anti-cardiolipine (aCL) et les marqueurs

circulants des NETs. Cette association n'est pas observée chez les individus sains. Les données montrent qu'une majorité de patients atteints de CCRm présentait une autoproduction d'aCL à des niveaux faibles, modérés et élevés. L'aCL fait partie de la famille des anti-phospholipides (aPL) caractéristiques du syndrome des anti-phospholipides (APS)[265,266]. Alors que l'aPL est présente chez 1-5 % de la population générale, la prévalence dans les cas APS est de 40-50/100 000 sujets[255]. Plusieurs travaux rapportent des taux d'aPL plus élevés dans diverses tumeurs hématologiques et solides[256,257], le pourcentage de patients cancéreux positifs à l'aPL varie de 5% à 70%. Le risque de thrombose étant 4 à 60 fois plus élevé chez les patients cancéreux que dans la population générale, il a été suggéré qu'un taux élevé d'aPL pourrait déclencher une thrombose chez les patients cancéreux. Alors que l'apparition d'aPL comme l'aCL pourrait être une étape essentielle dans la prévention de la thrombose, l'implication directe ou indirecte des aPL dans le processus thrombophilique reste peu claire. Cependant, Il est évident que les neutrophiles et les NETs contribuent à la physiopathologie APS[267]. Il convient également de noter que la formation exacerbée de NETs a été liée à l'APS dans de nombreuses pathologies auto-immunes et non-auto-immunes qui ont montré des niveaux élevés d'aCL[268].

Ces travaux redéfinissent le paradigme existant sur les mécanismes de libération de l'ADNcir et pourrait suggérer qu'une fraction significative de la quantité des ADNcir proviendrait des NETs chez les patients atteints de CCRm. Une étude approfondie sur les mécanismes de dégradation des NETs dans le sang de patients cancéreux et d'individus sains est en cours de publication par notre équipe. Aussi, nous avons révélé que les analyses combinées des marqueurs des NETs et de l'ADNcir permettent également de différencier les patients atteints de CCRm des individus sains. Enfin, notre étude est la première à montrer l'association étroite de l'aPL avec les marqueurs NETs et le cirDNA chez les patients cancéreux, suggérant que l'examen de ces marqueurs serait utile pour prévenir les thromboses.

L'ensemble des mes travaux de thèse de science sont liés puisque la détection de mutations chez les patients CCRm peut être drastiquement amoindrie chez les patients ayant une exacerbation de production de NETs. En effet, la dégradation des NETs pourrait expliquer que nous retrouvons une grande amplitude de la fréquence allélique dans le sang de ces patients. L'ensemble des travaux présentés ici renforce l'intérêt de travailler avec une méthode de détection des mutations ultrasensible lorsque l'on travaille sur les ADNcir et notamment pour la détection de mutations ponctuelles avec un objectif théranostique.

CONCLUSION GENERALE

L'ADNcir est largement utilisé en recherche dans le domaine de l'oncologie, en effet il permet d'établir le dépistage, le pronostic, de mettre en évidence la maladie résiduelle minimale et l'apparition de la récurrence, la stratification des patients avant l'initiation de thérapie ciblée et enfin la surveillance des patients sous thérapie pour mettre évidence des résistances aux traitements. Bien que son potentiel clinique soit de plus en plus avéré, l'analyse de l'ADNcir n'est pas encore utilisée en routine. Une des raisons à cela est le manque d'harmonisation des étapes de pré-analytique et analytique pour l'analyse des ADNcir. Dans ce sens notre équipe a largement travaillé sur les origines et les structures des ADNcir que ce soit chez des individus sains ou des patients atteints de cancer[154,155]. Ces données ont contribué à établir des conditions pré-analytiques et analytiques à respecter et ont par la suite permis l'établissement du premier « guideline » pour l'analyse des ADNcir en oncologie[155]. La deuxième raison est certainement le fait qu'il faut des méthodes d'analyses robustes, rapides, sensibles et peu couteuses afin de pouvoir les transposer en routine clinique. Ces dernières années de nombreuses équipes ont montré qu'une multitude de technique ont l'ensemble de ses caractéristiques dont notre méthode IntPlex[135,289].

Ma thèse s'est principalement intéressée à la détection de mutations ponctuelles *RAS/BRAF* dans le plasma de patients atteints de CCRm. L'objectif a été de montrer que l'analyse de l'ADNcir via la méthode IntPlex permet de déterminer le statut mutationnel *RAS/BRAF* avant l'initiation d'un traitement anti-EGFR et de pouvoir suivre l'émergence de ces mutations au cours de traitement. Pour ce faire, nous montrons à travers l'ensemble des publications discutées dans ce manuscrit qu'il est nécessaire d'avoir une sensibilité analytique pouvant détecter des mutations à une fréquence allélique inférieur à 0.01%. Bien que le potentiel théranostique de l'ADNcir soit démontré dans des études prospectives et rétrospectives il manque des essais interventionnels afin de valider la valeur clinique des ADNcir. L'essai multicentrique et prospectif PANIRINOX est le premier essai interventionnel où l'analyse de l'ADNcir conditionne l'initiation d'un traitement par anticorps anti-EGFR chez des patients CCRm ayant un statut *RAS/BRAF* sauvages. Nous espérons que cet essai ouvrira la voie à l'implémentation des analyses des ADNcir comme test compagnon pour orienter un traitement anti-EGFR chez les patients atteints de CCRm. Grâce au suivi des patients via l'analyse de l'ADNcir, cet essai établira pour la première fois dans un essai prospectif si un

seuil de sensibilité pour la détection des mutations *RAS/BRAF* est nécessaire pour prévenir les patients non-répondeurs à ces thérapies ciblées.

Bien que nous avons vu que les patients réfractaires aux thérapies ciblées anti-EGFR puissent être « rechallengés » avec ces thérapies ciblées, il faut savoir que cette pratique n'est pas appliquée en pratique clinique. Ces patients CCRm sont donc traités en dernière ligne avec du régorafénib sans que nous puissions déterminer quels sont les patients qui répondront à cette molécule. Dans l'essai ancillaire TEXCAN, nous avons montré que le statut muté *RAS/BRAF* des patients atteints de CCRm lourdement prétraités et réfractaires aux thérapies standards n'influe pas la survie de ces patients traité au régorafénib en troisième ligne. Par contre, nous montrons dans cet essai qu'il est possible d'identifier avant le traitement les patients qui n'auront pas de bénéfice clinique. En effet, nous avons pu établir des seuils de concentrations d'ADNcir total (26 ng/mL de plasma), d'ADNcir tumoral muté (2 ng/mL de plasma) et de fréquence allélique (6%) qui permettraient de prédire les patients qui auront une meilleure survie globale. Afin de précisé nos résultats, nous avons initié l'essai FOLFINOX-R qui est une étude de phase I/II, prospective, multicentrique et non randomisée pour évaluer l'innocuité et l'efficacité du régorafénib en association avec le FOLFIRINOX lors d'un traitement de première ligne des patients atteints de CCRm ayant un statut *RAS* muté déterminé à partir de l'ADNcir[250].

Pour finir, il a longtemps été établis que l'apoptose était le mécanisme de libération de l'ADNcir le plus pertinent puisque de nombreuses études ont montré que l'ADNcir a un profil de taille aux alentours de 150-180 bp (et des multiples de cette taille). Nous montrons qu'une fraction importante de l'ADNcir retrouvée chez les patients CCRm proviendrait du phénomène de NETose. Ces travaux redéfinissent les paradigmes existants sur les mécanismes de libération de l'ADNcir. Ce travail est en lien étroit avec les détections de mutations chez les patients CCRm puisque la dégradation des NETs pourraient expliquer que nous retrouvons une grande amplitude de la fréquence allélique dans le sang des patients atteints de CRCm. Cependant, il reste encore à démontrer l'ensemble des acteurs conduisant à la production des ADNcir par la dégradation des Nets *in vivo*. C'est un domaine dans lequel notre équipe de recherche travaille activement et des travaux sont en cours de publication.

3/ AUTRES CONTRIBUTIONS

J'ai également contribué à différents travaux recherches au sein de l'équipe, dont certains ont fait l'objet des publications suivantes :

A/ Progrès récents dans les applications cliniques des acides nucléiques circulants en oncologie

Auteurs : A. Otandault, P. Anker, Z. Al Amir Dache, V. Guillaumon, R. Meddeb, **B. Pastor**, E. Pisareva, C. Sanchez, R. Tanos, G. Tousch, H. Schwarzenbach & A. R. Thierry

Cette revue a été publiée dans annal of Oncology en 2019

Résumé: L'ADN circulant (ADNcir) est l'un des domaines qui a connu la croissance la plus rapide et la plus passionnante en oncologie ces dernières années. Ses utilisations cliniques potentielles couvrent désormais chaque phase de la prise en charge des patients atteints de cancer (informations prédictives, détection de la maladie résiduelle minimale, détection précoce de la résistance, suivi du traitement, surveillance des récidives et détection précoce/dépistage du cancer). Cette revue relate les avancées récentes dans l'application de l'ADN ou de l'ARN circulant en oncologie en s'appuyant sur des résultats/travaux inédits ou initiaux présentés lors du 10ème symposium international sur les acides nucléiques circulants dans le plasma et le sérum qui s'est tenu à Montpellier du 20 au 22 septembre 2017. Cette année, les présentateurs ont dévoilé leurs dernières données et observations cruciales notamment en ce qui concerne (i) la structure de l'ADN circulant libre de cellules (ADNcir) et les implications concernant leur détection optimale ; (ii) leur rôle dans les processus métastatiques ou immunologiques ; (iii) l'évaluation de panels de miRNA pour le suivi des patients atteints de cancer ; (iv) la détection de la maladie résiduelle minimale ; (v) l'évaluation d'un test de dépistage du cancer utilisant l'analyse de l'ADNcir ; et (vi) les éléments des directives pré-analytiques. Cet ouvrage passe en revue les progrès récents dans le domaine mis en lumière lors de la réunion, ainsi que dans les rapports les plus importants de la littérature, passés et présents. Il propose une image plus large de la recherche fondamentale et de son potentiel, ainsi que de la mise en œuvre et des défis actuels de l'utilisation des acides nucléiques circulants en oncologie.

Contribution: J'ai participé à l'organisation du 10^{ième} symposium international (Montpellier, 2017) sur les acides nucléiques circulants dans le plasma et le sérum (CNAPS), et j'ai participé à l'écriture de la revue surtout dans la rédaction des parties « Theragnostics/companion test » et «Treatment and résistance monitoring ».

Annals of Oncology 30: 374–384, 2019
doi:10.1093/annonc/mdz031
Published online 7 February 2019

REVIEW

Recent advances in circulating nucleic acids in oncology

A. Otandault[1,2,3,4], P. Anker[1,2,3,4], Z. Al Amir Dache[1,2,3,4], V. Guillaumon[4,5], R. Meddeb[1,2,3,4], B. Pastor[1,2,3,4], E. Pisareva[1,2,3,4], C. Sanchez[1,2,3,4], R. Tanos[1,2,3,4], G. Tousch[1,2,3,4], H. Schwarzenbach[6] & A. R. Thierry[1,2,3,4]*

[1]IRCM, Institute of Research in Oncology of Montpellier, Montpellier; [2]INSERM, U1194, Montpellier; [3]Department of Oncology, Montpellier University, Montpellier; [4]Regional Institute of Cancer of Montpellier, Montpellier; [5]SIRIC, Integrated Cancer Research Site, Montpellier, France; [6]Department of Tumor Biology, University Medical Center Hamburg-Eppendorf, Hamburg, Germany

*Correspondence to: Dr Alain R. Thierry, INSERM, U1194, IRCM, 208 rue des Apothicaires, 34298 Montpellier cedex 5, France. Tel: +33-6-63-82-19-94; E-mail: alain.thierry@inserm.fr

Circulating cell-free DNA (cfDNA) is one of the fastest growing and most exciting areas in oncology in recent years. Its potential clinical uses cover now each phase of cancer patient management care (predictive information, detection of the minimal residual disease, early detection of resistance, treatment monitoring, recurrence surveillance, and cancer early detection/screening). This review relates the recent advances in the application of circulating DNA or RNA in oncology building on unpublished or initial findings/work presented at the 10th international symposium on circulating nucleic acids in plasma and serum held in Montpellier from the 20th to the 22nd of September 2017. This year, presenters revealed their latest data and crucial observations notably in relation to (i) the circulating cell-free (cfDNA) structure and implications regarding their optimal detection; (ii) their role in the metastatic or immunological processes; (iii) evaluation of miRNA panels for cancer patient follow up; (iv) the detection of the minimal residual disease; (v) the evaluation of a screening tests for cancer using cfDNA analysis; and (vi) elements of preanalytical guidelines. This work reviews the recent progresses in the field brought to light in the meeting, as well as in the most important reports from the literature, past and present. It proposes a broader picture of the basic research and its potential, and of the implementation and current challenges in the use of circulating nucleic acids in oncology.

Key words: cancer, circulating DNA, diagnostic, treatment, resistance, screening

Introduction

Use of circulating DNA (Figure 1) or RNA (Figure 2) received high scrutiny (Figure 3), especially during the last decade in various oncology fields (Figure 4). Circulating nucleic acids in plasma and serum (CNAPS) meetings (supplementary data S1, available at *Annals of Oncology* online) are unique in that they focus on and link together basic and applied research in various pathologies for nearly 20 years. Held once every 2 years, they are typically the occasion for the early presentation of new observations, and gave us the opportunity to relate these to previous milestone reports and recent literature, and to review the potential of these new avenues of research, as well as the challenges, which exist in developing the use of circulating nucleic acids in oncology.

Structures and tissue origins

Circulating cell-free DNA (cfDNA) can be present in the form of protein-associated DNA fragments or extracellular vesicles (EV), in the physiological circulating fluids of healthy and diseased individuals as recently reviewed [1, 2]. cfDNA is derived not only from genomic DNA but also from extrachromosomal mitochondrial DNA. While various clinical applications of cfDNA are currently progressing [3, 4], the identification of structural characteristics remains under investigation.

Confirming pioneering work on size profiling [5, 6], a higher fragmentation of cfDNA in metastatic colorectal and non-small-cell lung cancer (NSCLC) patients compared with healthy donors, and a significant difference in size profile between mutated and wild type DNA in cancer patients were

Figure 1. Publication number reporting use of circulating DNA in cancer upon research areas in 2017 and 2018. Web of science citation reports showing 2113 records for TOPIC: (cancer circulating DNA) in 2017 and 2018. This citation level corresponds to 36% to the total number of records up to 2018 (5800 records). A 51% of the publications concerned use in clinical oncology.

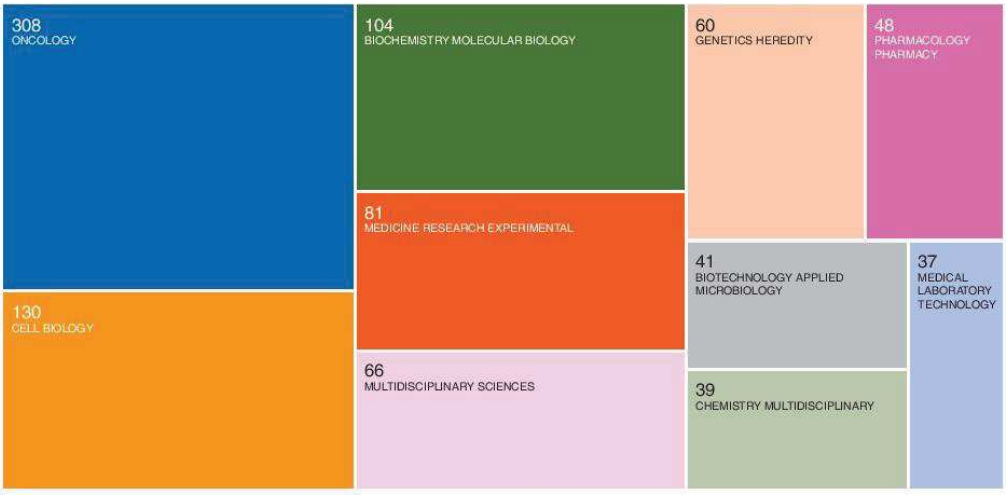

Figure 2. Publication number reporting use of circulating RNA in cancer upon research areas in 2017 and 2018. Web of Science citation reports showing 912 records for TOPIC: (cancer circulating RNA). This citation level corresponds to 24% to the total number up to 2018 (3751 records). A 34% of publications concerned use in clinical oncology. Number of records during that period of time was more than twofold less than records reporting circulating DNA in cancer (2113). The number of reports on the use of microRNA was nearly threefold higher than those on mRNA.

demonstrated, during the CNAPS, by Garlan et al., using the BIABooster system [7]. Similarly, Piskorz et al. presented their previous work which showed that in an ovarian cancer mouse, circulating tumor DNA fragments are shorter than nontumor cell-free DNA in plasma, and that the selection of fragments between 90 and 150 bp, using targeted and whole-genome sequencing (WGS) approaches, could enrich the tumor DNA up to 11-fold [8].

During the meeting, a blinded study by Sanchez et al. [9] demonstrated that circulating tumor DNA from cancer patients showed a similar size profile using either whole genome deep sequencing from single strand library preparation or using a q-PCR based method, revealing a higher proportion of shorter cfDNA fragments (below 80 bp) not readily detectable by standard double-stranded DNA library preparation protocols (as previously shown by Underhill et al.). This showed the higher capacity of single strand DNA template analysis to detect cfDNA fragments, and revealed that cfDNA molecules, which are initially packed in chromatin, are released from cells and then dynamically degraded in blood, both within and between nucleosomes or transcription factor-associated subcomplexes. In addition, this study revealed that cfDNA size distribution obtained from the

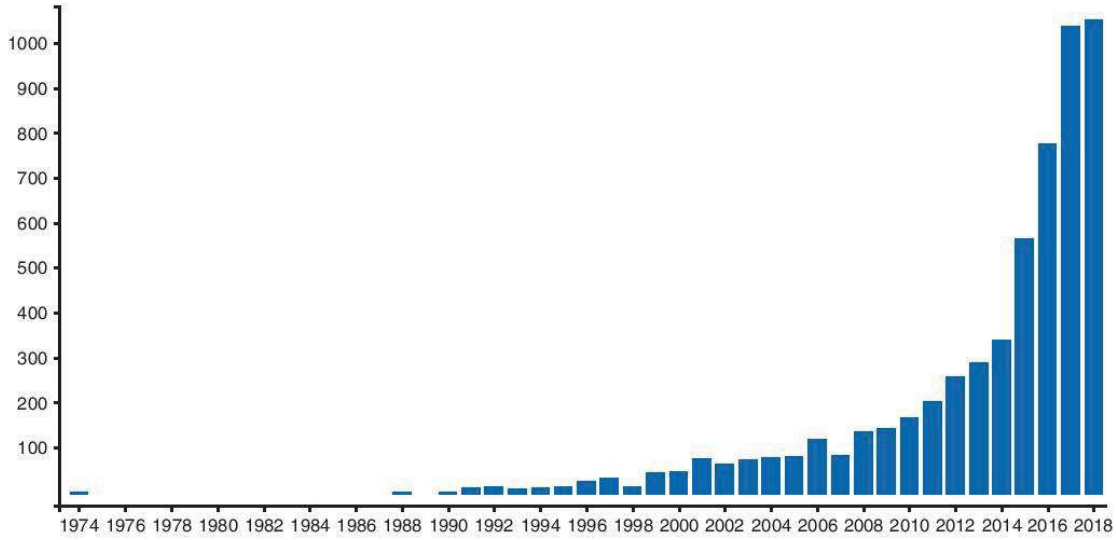

Figure 3. Publication record. Web of science publication records per year reached up to 1050 in 2018 for TOPIC: (cancer circulating DNA). The sum of publication records up to now is 5800. The sum of times cited per year was in exponential phase in the last decade up to 28 000 in 2018.

conventional WGS from a double-stranded DNA library should be distinguished from that obtained with q-PCR or WGS from a single-stranded DNA library which use single-strand DNA as a first template. Using standard WGS, Markus et al. showed that, in contrast to plasma where cfDNA fragments of mononucleosome length are predominant, the length of the most abundant fragments in urine is short (80–81 bp), which is consistent with DNA wrapped in a subnucleosomal structure and undergoing DNA digestion.

Bronkhorst et al. had previously demonstrated that 143B cancer cell line is able to actively release 2000–3000 bp sized segments of heterochromatin [10]. In their new work, they found that these fragments are of a repetitive nature, including alpha satellite, mini satellite and active transposons originating from the centromeric and the pericentromeric regions of chromosomes 1, 9 and 16. They suggest that this secretion into the extracellular environment can induce a wide range of detrimental biological effects.

Following initial observations from Lehmann-Werman et al. [11], Lo et al. [12] and Snyder et al. [13], the tissue origin of cfDNA has become of great interest especially in determining a particular biological state leading to a higher diagnostic value. These studies, among others, revealed the high proportion of cfDNA released by hematopoietic cells. Moss et al. had previously proposed a novel strategy for the identification of tissue origin of cfDNA, based on the discovery of the DNA methylation profile by Illumic Epic array [11]. Using this approach, the team was recently able to detect and monitor breast cancer. Moreover, in the CNAPS meeting they confirmed that this strategy is useful for the simultaneous identification of multiple tissue contributors of cfDNA in healthy individuals, transplant recipients and cancer patients [14]. This report followed the previous demonstration of the noninvasive monitoring of infection and rejection after lung transplantation [15] using the same approach. Lam et al. presented their published data demonstrating that erythroid DNA represents a median of 30.1% of plasma DNA in healthy subjects [16]. Simon et al. had earlier found that cfDNA is predominantly released as pro-inflammatory chromatin from cells of the hematopoietic lineage in response to acute exercise [17].

Specific cfDNA structure, as observed by size profile analysis [9, 18, 19], methylation [14, 20] or nucleosome positioning [11, 13] may benefit to higher capacity in diagnostics or cancer screening.

Biology

A number of previous studies had supported the concept that cfDNA can penetrate host cells and modify the biology of those cells. In their prior studies, Mittra et al. considered that DNA which exists in the extracellular compartment, including the circulation, had local and systemic biological functions that could form the basis of some human diseases. His team had demonstrated previously that DNA molecules which originate from dying cells due to chemotherapy and radiotherapy have the ability to integrate into genomes of bystander healthy cells in order to induce DNA damage and trigger apoptotic and inflammatory responses. They have shown that this patho-physiological effect can be prevented by using DNA-neutralizing and degrading agents [21]. Their preliminary data showed that circulating DNA released from hypoxic cells is directly involved in the activation of paracrine factors that modulate cells of the tumor microenvironment. In addition, Glebova et al. suggested that oxidized DNA can act as genetic elements involved in horizontal gene transfer, as shown in experiments with MCF-7 cells able to uptake and transcript previously oxidized cfDNA. In addition, Raghuram et al. have already confirmed that this phenomenon of horizontal gene transfer with cfDNA is a function of cfDNA size [22]. Their study showed that high molecular weight DNA is not able to enter cells, while sonicated DNA from different sources with sizes ranging from 300 to 3000 bp is able to do so, regardless of species or kingdom boundaries. They also proved that sonicated DNA has a

biological effect, such as the activation of the proinflammatory transcription factor. Here, Neuberger et al. have demonstrated the immunological effects of cfDNA. A higher gene expression of *IL1B*, *TNF* and *IL8* in THP1 cell line was observed after their stimulation with nucleosomal DNA released by netosis, compared with stimulation with purified genomic DNA. Netosis is a very recently discovered pathogen-killing mechanism in which neutrophils produce and release neutrophil extracellular traps that are composed of DNA and granular proteins [23]. Furthermore, using whole-transcriptome sequencing, Semenov et al. have recently reported that the incubation of A549 cell line with exosomes purified from human blood plasma induced the upregulation of innate immunity genes and the activation of toll-like receptors (TLR) and p53 signaling pathway.

Additionally, Rykova et al. discussed data published in the literature that encourages the development of immunomodulatory DNA-based therapeutics. The consequence of nucleic acids and their metabolites accumulation in the bloodstream due to obstruction of clearance functions, to specifically activate immune receptors is significant. For example, TLR9 is activated by unmethylated CpG motif [24], and TBK1 receptor is activated by cytoplasmic double stranded DNA [25]. Rykova also showed results proving that synthetic immunomodulatory CpG ODNs (oligodeoxynucleotides) can be used as vaccine adjuvants against different types of cancer and many other diseases [26, 27]. Taking into consideration all these supporting results, further studies should be carried out to develop potential specifically targeted nontoxic immunomodulatory DNA-based therapeutics.

It has previously been shown that telomeric sequences in the pool of cfDNA are able to block TLR9 and inhibit the abovementioned immune response [28]. Korabecna et al. studied the stimulatory effects on monocytic THP1 cells of telomeric cfDNA present in plasma and serum, before and after treatment with DNases [29]. TNF-α messenger RNA (mRNA) expression in stimulated THP1 cells increased significantly after DNase treatment. Thus, they confirmed the involvement of cell-free telomeric sequences in the regulation of immune functions.

Mittra hypothesized that cfDNA could integrate into genomes of healthy cells to trigger inflammatory effects. Finally, because the circulatory system is crucial for cancer propagation, many researchers are now working on genomestasis theory, which considers nucleic acids in the circulation as a driver of metastasis [30, 31].

Additional work should be done to elucidate more completely the biological properties of cfDNA, in order to extend our knowledge of the subject with a mind toward clinical implementation of cfDNA analysis. New data combining structural and biological features of cfDNA have promising possibilities for the diagnosis and treatment of cancer and other diseases.

Theragnostics/companion test

The utility of circulating tumoral DNA (mutant cfDNA) as a predictive biomarker for the therapeutic adaptation/response of patients suffering from various types of cancers, as foreseen by Stroun et al. [32, 33], Leon et al. [34], and first clinically evaluated by Diehl et al. [35], is now widely described in the literature [3, 36]. Recently, Thierry et al. demonstrated the clinical utility of using cfDNA analysis by rapidly detecting *RAS* and *BRAF* mutations in metastatic colorectal cancer (mCRC) patient plasma showing a median data turnaround-time of 2 and 16 days for mutant cfDNA and tumor-tissue analysis, respectively [37]. In addition, the authors found a higher presence of mutations (24% of WT scored patients for both genes, instead of 45% by tumor-tissue analysis). It should be noted that the mutation profile, as determined from cfDNA analysis using various detection thresholds, highlights the importance of the test sensitivity. Kopetz et al. and Laurent-Puig et al. showed results of a clinical study named AGEO RASANC, already presented by Bachet at ASCO 2017 and published after the CNAPS meeting. This focused on the concordance between mutant cfDNA- and tissue-analysis in mCRC using next-generation sequencing (NGS) [38]. For instance, Laurent-Puig et al. obtained 92% of sensitivity, 94% of specificity and 93% of concordance between plasma and tissue analysis.

Lyskjær et al. presented unpublished results of a proof-of-concept phase II study about the prediction of Irinotecan efficacy in a cohort of 18 mCRC patients using mutant cfDNA assessed by droplet digital PCR (ddPCR). The aim of this study was to test if early alterations in plasma mutant cfDNA can be used as a marker for therapeutic effectiveness in mCRC patients treated with first line Irinotecan. The authors showed that mutant cfDNA levels decreased during the first 40 days of treatment, in accordance with the fact that none of the 18 patients had relapsed by the time of the first scan. Patients with a high baseline level of ctDNA (>median) were associated with an earlier progression. In addition, authors found an approximatively fivefold increase in the relative risk of progression in patients with <10-fold reduction in mutant cfDNA levels at day 40 post-treatment start. In sum, mutant cfDNA is a promising marker for early prediction of Irinotecan response in mCRC patients.

Keller et al. also presented results which were published after the CNAPS meeting which focused on the correlation between the results of medical imaging and the variation of cfDNA assessed using ddPCR [39] in a cohort of melanoma patients treated by immunotherapy, and found statically significant results (Fisher's exact test: $P = 0.034$). They also conducted an analysis of 13 patients with blood samples taken at baseline (BL) and during the early course of treatment (cycle C2 or C3). The results showed significantly lower progression-free survival (PFS) in patients with increased mutant cfDNA levels between BL and C3, compared with patients with decreased mutant cfDNA (21 versus 145 days, respectively). From these results, they suggested early mutant cfDNA variation as a predictor of tumor response to immunotherapy in melanoma patients.

The presentation of Rosenfeld et al. pointed out the recent approval for use by the European Medicines Agency (EMA) and the Food and Drug Administration (FDA) of cobas *EGFR* Mutation real-time PCR Test v2, using plasma specimens as a companion test for the detection of exon 19 deletions or exon 21 substitution (*L858R*) mutations in the epidermal growth factor receptor (*EGFR*) gene, necessary for identifying patients with metastatic NSCLC eligible for treatment with Tarceva® (erlotinib). Rosenfeld et al. also presented the published results of Remon about the Tagrisso® (Osimertinib) benefit in *EGFR*-mutant NSCLC patients with *T790M*-mutation detected by mutant cfDNA [40]. In this study, the authors showed that among assessable patients Osimertinib gave a partial response rate of 62.5%

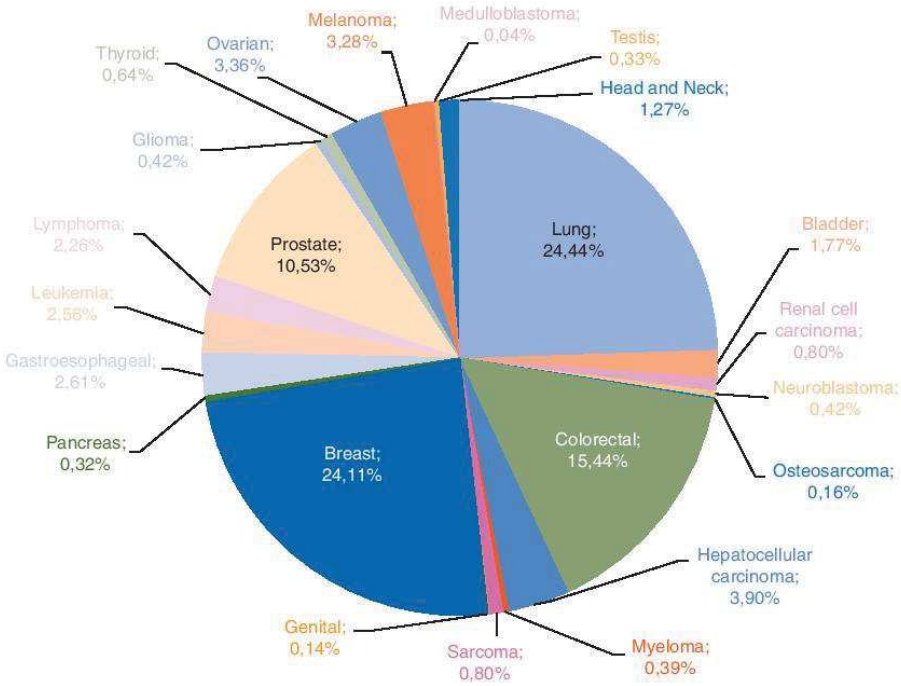

Figure 4. Proportion of the publication number reporting use of circulating DNA in cancer upon cancer types. Web of science citation reports showing 5800 records for TOPIC: (cancer circulating DNA) in up to end 2018.

and a stable disease rate of 37.5%, and they concluded that mutant cfDNA can be used as a substitute marker for *T790M* detection. In sum, cfDNA qualitative (mutation testing) and/or quantitative analysis shows considerable promise in the prediction of therapeutic tumor response in various types of cancer.

Data as regards the theragnostic/companion test field is also very encouraging. The recently approved use of cobas *EGFR* Mutation real-time PCR Test v2 using plasma samples in metastatic NSCLC should open the door for the approval of other tests for the prediction of therapeutic response. However, prospective randomized clinical trials to test the clinical utility of cfDNA as a stand-alone diagnostic test are still needed.

Minimal residual disease and recurrence

CfDNA analysis presents the opportunity to detect minimal residual disease and monitor recurrence, which might help improve patients' management and outcomes. However, the sensitivity of the analysis is often limited by the small amount of mutant DNA. This topic was widely discussed in the meeting and was the subject of numerous publications briefly before or after the conference. Tie et al. reported that cfDNA analysis may help in detecting the minimal residual disease, suggesting the capacity to select cancer patients for adjuvant therapy based on the detection of mutant cfDNA [41]. Rosenfeld suggested that massively multiplexed assays are needed to detect low levels of mutant cfDNA, hence the TAilored PAnel Sequencing (TAPAS) method that analyses 100s–1000s of mutant loci. Wan et al. demonstrated that this method's sensitivity allows the detection of residual levels of tumor DNA in the plasma and urine samples of melanoma patients receiving therapy [3]. Mutant cfDNA's ability to track tumor progression and provide evidence of minimal residual disease was investigated by Openshaw et al. [42], by tracking *TP53* mutation frequency in tumor tissues and corresponding plasma samples from patients with gastroesophageal adenocarcinoma. A different study by Phallen et al. used massively parallel sequencing to identify somatic mutations to be used as mutant cfDNA markers in CRC patients for the detection of minimal residual disease and to monitor changes in tumor burden during a 3-year follow-up period. Mutant cfDNA was detected in all relapsing patients but not in nonrelapsing patients [43]. Lin et al. evaluated the utility of a sensitive 54-cancer gene digital NGS assay, which covers all major melanoma driver genes, in melanoma patients with regional metastasis following curative surgical resection [44]. They showed that cfDNA mutation levels correlated with tumor burden ($P = 0.019$) and that monitoring these enabled earlier detection of recurrence than by monitoring serum LDH levels ($P = 0.01$). In the plasma of gastric cancer (GC) patients, Ogino et al. showed that the *HER2* ratio determined by ddPCR is a repeatable noninvasive approach for the detection of recurrence and for real-time evaluations of the *HER2* status to monitor the effects of treatments for patients with *HER2*-positive GC [45]. A copy-number aberration score was calculated by Silva et al. for melanoma patients with active disease and patients with recently excised disease [46]. cfDNA was higher in the first group and was

considered a good predictor of the presence of active disease with an AUC of 0.89.

Another group, Ehlert et al. developed a specific q-PCR approach, which was presented in the meeting, employing a first round blocking primer, *KRAS* mutation-specific ARMS primers and short LNA-probes to quantify minute amounts of mutant cfDNA. Martinson examined variant frequencies by using single-strand library preparation technology, an approach developed by Abbosh et al. [47], to study extremely fragmented DNA in baseline and postsurgical NSCLC samples. He showed in the conference that the fraction of variant-positive cases decreased in postsurgical samples. In another study, Kothari et al. evaluated the feasibility of detecting cfDNA and using it to noninvasively characterize genetic profiles of high-risk relapsed neuroblastoma.

In sum, the ability of mutant cfDNA detection to provide evidence of residual disease and identify patients at very high risk of relapse was validated in different studies, and work on the implementation of this analysis in clinical practice is ongoing.

Treatment and resistance monitoring

Drug resistance is clearly a challenge in oncology. Since previous pioneering works from L. Diaz and Bardelli's group [4, 48–50] demonstrating that resistant clones emerge in the tumor causing resistance to targeted therapy, the use of cfDNA analysis has emerged as a potential tool in detecting early resistance in the course of treatment. Works presented at the CNAPS 2017 showed advances in the identification of *de novo* or acquired methylations and point mutations leading to drug resistance [48]. In this context, a previous study by Thierry et al. showed the need for an ultrasensitive method of detecting *RAS* and *BRAF* point mutations in cfDNA before treatments, or when tracking secondary resistance in mCRC patients treated with chemotherapy and cetuximab [51]. Results revealed that 64% and 21% of point mutations detected in cfDNA would be missed if the limit of detection was below 1% or 0.1%, respectively [51]. Bardelli's team also showed in 2016 that, in mCRC patients, EGFR extracellular domain (ECD) point mutations can emerge during anti-EGFR therapy, leading to secondary resistance [49]. EGFR ECD point mutations induce a change in the EGFR structure, leading to nonrecognition by anti-*EGFR* monoclonal antibodies (cetuximab or panitumumab). To override this problem, Bardelli prepared a murine avatar from a G465E *EGFR*-mutant tumor derived from an mCRC patient. The resulting 2D cell culture was treated with a combination of anti-*EGFR* antibodies (MM-151), showing a dramatic reduction in cell viability compared with cetuximab or panitumumab alone [52]. Kopetz's team showed in the CNAPS meeting one of the first examples of cfDNA genomic landscape, in 1397 patients with CRC. Firstly, data showed that the mutational prevalence of the 20 most commonly mutated genes in cfDNA was strongly associated with the mutational prevalence in tumor tissue ($R^2 = 0.95$; $P < 0.0001$). Secondly, data revealed that 91% of patients with *EGFR* ECD mutations also harboring multiple alterations including *RAS* and *BRAF* point mutations, leading to resistance [53]. The emergence of point mutations is not the only way to monitor treatment. The modulation of mutant cfDNA concentration could also predict the efficacy of various treatments. Laurent-Puig's team suggested that in their published data [54] early decreases in mutant cfDNA concentration (*KRAS* point mutation or *WIF1* and *NPY* hypermethylation) was a marker of therapeutic efficacy in mCRC patients. Moreover, Mouliere et al. designed a patient-TAPAS approach to track mutation levels and fragmentation patterns in cfDNA. They observed changes in mutant cfDNA levels in the first 2 days following treatment initiation, including the emergence of subclonal mutations. In the same way, Reinert et al. showed earlier in CRC patients after local or systemic interventions that changes in mutant cfDNA level showed a good agreement with changes in tumor volume ($\kappa = 0.41$, Spearman's $\rho = 0.4$) [55]. Heitzer et al. developed the mFAST SeqS, an untargeted assessment of tumor DNA fraction, to monitor treatment response in metastatic breast cancer patients. They showed before the meeting that changing in levels of mutant cfDNA (z-score FAST-Seq) correlate with treatment response [56].

As the development of cfDNA analysis continues, more and more work is now focused on its implementation in nonmetastatic stage cancer [57, 58], and in investigating predictive response to chemotherapy [59]. It should be noted that, in addition to mutation analysis, methylation was found to be a great surrogate marker for following up metastatic cancer patients [60]. cfDNA analysis in oncology is a promising tool in the identification of early drug sensitivity or resistance, and in doing so guide the clinician for adapting therapies to tumor evolution. The next step in its development will be to use interventional clinical studies to investigate whether cfDNA analysis can increase patient survival (PFS and OS) by adapting therapies in real time.

Circulating RNA in oncology

In the session on cfRNA in oncology, the speakers presented their data on cfRNA, which is also a highly important research area in the field of liquid biopsy (Figure 2). In the bloodstream, cfRNA consists of diverse RNA subpopulations that are protected from degradation by association with lipids/proteins or by incorporation into EV such as exosomes.

Tewari et al. presented his data on RNA-seq, which are increasingly being used for profiling of cfRNA present in plasma and other biofluids. Many different methods for performing RNA-seq have been described to date. Tewari et al. improved the protocol- and sequence-specific bias of RNA-seq by using adapters for ligation with randomized end-nucleotides and computational correction factors. They detected that EV populations exhibit a common mRNA signature, carry tumor-specific alterations and can be interrogated as a source of cancer-derived cargo [61]. Garcia-Olmo showed the clinical relevance of perioperative detection of mRNA encoding *hTERT* and *GAPDH* in plasma from laryngeal and hypopharyngeal cancer patients by real-time PCR. Detection of *hTERT* mRNA before surgery had diagnostic value and was related to subsequent recurrence. Mean levels of plasma *GAPDH* mRNA in untreated patients were significantly higher than in healthy subjects [62]. Epigenetic biomarkers are increasingly recognized as promising diagnostic and prognostic tools in CRC. Using an ELISA-based assay, Gezer demonstrated that the levels of trimethylation of histone H4 lysine 20 (H4K20me3), a repressive histone methylation mark usually enriched in pericentromeric heterochromatin, decrease in circulating nucleosomes in blood of CRC patients [20].

Several studies in recent years have focused on circulating miRNAs, short single-stranded noncoding RNA that inhibits mRNA expression. In this area, Laktionov presented his screening of miRNAs in urine from prostate cancer patients. Expression of four pairs of miR-15a/miR-26b, miR-19b/miR-26b, miR-22-3p/miR-26b, miR-26b/miR-378a differentiated 80% of these patients with absolute specificity [63]. Using TaqMan real-time PCR and microarrays, Schwarzenbach's laboratory revealed that a network of deregulated cell-free and exosomal miRNAs involved in the regulation of cancer-associated signaling pathways, such as the phosphatidylinositol 3-kinase/AKT way, are associated with a particular biology of breast and ovarian carcinomas. Furthermore, they found an excessive secretion of exosomes in these patients, something associated with the prevalence of miRNAs in exosomes, when compared with cell-free miRNAs [64, 65].

Overall, the recent advances in cfRNA highlight the significant potential of cfRNAs as future tumor markers and their therapeutic value.

Cancer screening

Early cancer detection can improve survival and decrease mortality by increasing the chances of successful treatment. Papadopoulos' team managed to increase the sensitivity of cancer detection by combining mutation detection in more than one bodily fluid (saliva and blood) from the same individual, or by associating mutation detection with other markers or other clinical information. In a study called CancerSeek, published in January 2018 and including more than 1000 patients with 8 different cancer types (pancreas, colon, breast, liver, lung, ovarian, stomach and esophagus) and healthy individuals, they also showed an increased sensitivity in cancer detection while preserving specificity by combining mutation detection in the plasma of 16 genes commonly mutated in cancer and 41 protein markers [66]. While the CancerSeek test showed unrivaled performance, it nonetheless presents certain limitations in the context of universal cancer screening; for instance, it is principally used to confirm a previous diagnosis, with a low median sensitivity of only 43% for stage I cancers, whereas universal cancer screening should be carried out on an ostensibly healthy population [67].

Dennis Lo's group developed a test for nasopharyngeal cancer (NPC) by detecting the Epstein–Barr virus (EBV) involved in most NPC cases. Among the 20 174 male subjects recruited and screened, 5.5% showed a positive first test for EBV DNA, 1.5% had 2 consecutive positive plasma EBV DNA tests and 34 cases of NPC were identified [68]. Volition, a multi-national life sciences company, developed an age-adjusted algorithm of four normalized assays, each of which captures intact cell-free nucleosomes and labels a specific structural feature by double antibody ELISA. This algorithm improved precancerous polyp/adenoma detection and early stage CRC detection [69].

A study conducted by Rykova et al. [70] assessed the diagnostic potential of combinations of circulating aberrant methylated DNA and microRNAs (miRNAs) markers for lung cancer. Adleff et al. [43] proposed an approach called Targeted Error Correction Sequencing (TEC-Seq) that was able to detect mutant cfDNA in over half of early stage patients (I and II) and over three quarters of late stage patients (III and IV) with breast, lung, colorectal and ovarian cancers ($n = 200$), while no mutations were identified in the control population ($n = 44$). The authors suggest that this technique could be applicable for noninvasive early cancer detection, screening and cancer patient management. Tanos et al. developed a multiparametric cfDNA screening test using a specific q-PCR-based method and targeting nuclear and mitochondrial sequences in the plasma of healthy individuals and CRC patients. This study showed a significant difference between these two groups, and gave a strong indication of the test's capacity to discriminate healthy and cancer patients [71].

Cancer screening and early detection by using cfDNA analysis start to be evaluated. Moore et al., who used targeted sequencing for *TP53* on plasma samples of 130 women with high-grade serous ovarian cancer (HGSOC). The technique was able to detect mutant cfDNA in patients with stage I HGSOC, as well as 50% of all cancer cases, although optimization is necessary to improve sensitivity and increase detection. In the LUCID study, Heider et al. developed a technique for early stage mutant cfDNA detection based on patient-specific panels, using a parallel analysis of large numbers of mutations to assess mutant cfDNA levels at diagnosis. Several other studies were based on the detection of methylated markers, such as that of Mijnes et al., who examined the tumor-specific hypermethylation of *SPAG6*, *NKX2* and *PER1* promoters, which appears to be a promising tool for blood-based breast cancer detection. Indeed, it showed a 70% sensitivity and a 80% specificity for ductal carcinoma in situ detection. Fleischhacker et al. presented preliminary data suggesting the ability of a panel combining the methylation markers *mSHOX2* and *mSEPT9* to discriminate between patients with hepatocellular carcinoma from patients with alcohol-induced liver cirrhosis.

All of these studies encourage the opinion that cfDNA analysis presents a promising avenue for cancer screening and early detection. That said, further investigation of these emerging biomarkers is vital, since most studies underline the necessity of combining different parameters and markers in order to increase sensitivity and specificity for a better discrimination between early stage cancer patients and healthy individuals.

Preanalytics

Dana Tsui (New York, USA) and Michael Fleischhacker (Halle/Saale, Germany) organized a workshop dedicated to preanalytical procedures for the analysis of circulating nucleic acids. This session consisted of two parts. The first involved the oral presentations of Markus Havell and Ørntoft Mai-britt Worm on the evaluation of preanalytical factors affecting plasma DNA analysis, and the establishment of a standard operating procedure for cell-free DNA purification. The second part was an interactive workshop involving the contribution of all participants.

The lack of standardization of the preanalytical conditions hinders the use of cfDNA as a clinically robust biomarker in oncology [72, 73]. The main long-term objective of this workshop was to reach an agreement on the optimal handling of blood samples for cfDNA analysis, by presenting the importance of preanalytical factors, by exchanging on current practices in different laboratories, and efforts to standardize these procedures.

The discussion focused on time collection, collection tubes, sample processing delay, DNA extraction methods, methods of

Figure 5. Comparison of the number of publications reporting use of NGS- and PCR-based methods upon research areas in 2017 and 2018. (A) Web of science citation reports showing 146 records for TOPIC: (cancer circulating DNA NGS) in 2017 and 2018. This citation level corresponds to 67% to the total number up to 2018 (219 records). (B) Web of science citation reports showing 278 records for TOPIC: (cancer circulating DNA PCR-based) in 2017 and 2018. This citation level corresponds to 28% to the total number up to 2018 (988). PCR-based methods are still twice as much used when compared with NGS-based methods. However, increase of using NGS-based methods in the last 2 years is about twofold higher than the increase of using of PCR-based methods. A 62% of publication reporting NGS-based methods concern use in clinical oncology, while 30% of publication reporting PCR-based methods concerned use in clinical oncology. The numbers of publications reporting use of NGS- and PCR-based methods in clinical oncology were similar in the 2017–2018 period.

DNA quantification, and the storage of plasma and DNA samples. Preanalytical procedures still appear to vary from one laboratory to another. In addition, NGS- or PCR-based methods are among others the most used methods for analyzing cfDNA (Figure 5A and B). Nevertheless, with regard to sample processing, there is a general consensus in the scientific community on double centrifugation and a maximum delay in sample processing of 4 h in order to avoid genomic DNA contamination. The use of different extraction kits and quantification techniques in different laboratories were seen to influence the quality and quantity of extracted cfDNA.

Other comments on the origin of circulating DNA have emphasized the need not to quantify the mitochondrial DNA as nuclear DNA, but to calculate the copy number in DNA samples.

Method reproducibility and cost of the analysis are additional important factors to be taken into account in considering the use of circulating nucleic acids in clinical practice.

Despite routine analysis in clinical areas such as prenatal testing or oncology, and active investigation toward applying cfDNA analysis, the significance of preanalytics and demographic variables is not widely known. Consequently, the lack of standard operating procedures impedes the maturing of this new and promising diagnostic tool. Recent efforts from Meddeb et al. [74] to characterize and optimize cfDNA quantification in humans will help to address this.

Nomenclature

Historically, since the discovery of circulating DNA, no homogeneous nomenclature has been given to total circulating DNA in the bloodstream, unlike circulating DNA from tumor cells named ctDNA. For this purpose, during the CNAPS symposium a survey was taken to determine a common consensus on the matter. The three terms most widely used in the literature (cfDNA for cell-free DNA, ccfDNA for circulating cell-free DNA and cfDNA for circulating DNA) were proposed to the scientific community, who were also allowed to suggest other denominations. Sixty-three people participated in this vote. A 76% of the participants chose cfDNA, 16% ccfDNA, 5% cirDNA and 3% suggested another denomination. The results of this survey confirm 'cfDNA' as a term that can be used to commonly designate all extracellular circulating DNA in the blood.

In the oncology field, most reports use the term ctDNA (circulating tumor DNA), as illustrated by this small survey. One can discriminate among cfDNA origins three constituents in the blood of a cancer patient: malignant tumor cell-derived DNA, nonmalignant tumor cell-derived DNA and normal cells germline DNA [67]. However, ctDNA is employed in the literature to mean cfDNA bearing genetic or epigenetic alterations. Alternatively, ctDNA would word-by-word mean circulating DNA deriving from the tumor which is constituted of malignant and nonmalignant cells (stromal, endothelial and hematopoietic cells). Since the concentration of wild type cfDNA deriving from the microenvironment cells increases with the progression of the tumor, part of cfDNA is specific to the tumor growth. Readers could also be confused by the fact that ctDNA concentration values are biased in the literature, since in most cases ctDNA is determined from mutations of a few or a panel of genes, which inevitably leads to a bias in considering the total amount of cfDNA deriving from all the malignant cells. Because of these considerations, instead of the term ctDNA we used the term mutant cfDNA in this review.

This survey also addressed a second issue. The term 'biopsy' was first introduced by Besnier in 1879 [75] to designate the technique used to collect an organ or tissue fragment (cell samples) in order to establish an accurate diagnosis. According to the definition established by the National Cancer Institute (NCI Dictionary of Cancer Terms; available at https://www.kucancercenter.org/cancer-information/cancer-terms-dictionary), a liquid biopsy is a test done on a blood sample to look for cancer cells or pieces of tumor DNA found in the bloodstream. Given that cfDNA has nothing in common with DNA released from circulating tumor cells, and that cfDNA can also derive from nontumor cells, the question might be raised as to whether or not circulating DNA and RNA analysis ought to be considered as a 'liquid biopsy' properly speaking? A 80% of the voters supported this opinion, 10% disapproved and 10% had no opinion regarding the issue. F. Diehl (Hamburg, Germany) who organized the workshop session acknowledged the vote showing the need from the researchers from the field to unify the nomenclature despite inconstancies.

In conclusion, cfDNA with PD-1 and cfDNA with PD-L1 checkpoint pathway immunotherapies are the two fastest growing and most exciting areas in oncology in recent years. Following their first clinical evaluation in predictive medicine, all six potentials of cfDNA analysis in oncology (predictive information, detection of the minimal residual disease, early detection of resistance, treatment monitoring, recurrence surveillance and cancer early detection/screening) are now well covered by a comprehensive literature on each phase of cancer patient management care. A new and exciting therapeutic challenge now faces the scientific/clinical community: the use of cfDNA analysis to guide immunotherapy. Meanwhile, broadening our knowledge of the structural and biological features of cfDNA, as well as standardizing the preanalytical conditions, remain key steps to be taken toward the clinical implementation of cfDNA analysis, and may provide new avenues of research in tumor biology.

Acknowledgements

A special thanks and tribute to Maurice Stroun who past away just before the CNAPS Xth meeting. Maurice Stroun was remembered as one of the 'founding parents' of the circulating nucleic acids community. In particular, he founded the CNAPS conference series together with Anker [76]. Maurice was able to see his lifelong pursuit of circulating nucleic acids become an important part of scientific research and medical diagnostics. The field will continue to grow, and while those working in it will miss Maurice's physical presence, his indomitable pioneering spirit and his remarkable contributions will remain with the CNAPS community even as it reaches new frontiers.

The authors would like to thank all of the CNAPS scientific committee: P. Anker (Geneva, Switzerland), F. Diehl (Baltimore, USA), L. Diaz (New York, USA), M. Fleischhacker (Halle/Saale, Germany), P. Gahan (Montpellier, France), D. Lo (Hong Kong, China), N. Rosenfeld (Cambridge, UK), H. Schwarzenbach (Hamburg, Germany), M. Stroun (Geneva, Switzerland), and A. R. Thierry (Montpellier, France). We thank to Safia El Messaoudi who co-organized with A. R. Thierry the Xth CNAPS meeting with the critical contribution of the French Society of Nucleic Acids (SFAC) and Sabine Dejasse, SFAC President. Authors thank Marc Ychou, Karine Saget and Aurore Marquis from the SIRIC Montpellier. The authors would also like to thank Stefan Holdenrieder, Barbara Ottolini, Jean-Yves Cance, Serge Thierry and Philippe Grandjean.

Funding

This work was supported by the SFAC (Société Française des Acides Nucléiques Circulants/French Society of Circulating Nucleic Acids), the University of Montpellier (France), the GSO canceropole (France), the Languedoc-Roussillon region (France), Lilly (France) and the SIRIC Montpellier Grant

(INCa-DGOS Inserm 6045), France. This project has received funding from the European Union's Horizon 2020 research and innovation program under grant agreement No. 755333 (LIMA). ART is supported by the INSERM (Institut National de la Santé et de la Recherche Médicale, France).

Disclosure

ART is cofounder, shareholder of DiaDx SAS and co-inventor of patent applications on cfDNA analytical methods. PA, CS and HS are co-inventors of patent applications on cfDNA analytical methods. All remaining authors have declared no conflicts of interest.

References

1. Thierry AR, El Messaoudi S, Gahan PB et al. Origins, structures, and functions of circulating DNA in oncology. Cancer Metastasis Rev 2016; 35(3): 347–376.
2. Pös O, Biró O, Szemes T, Nagy B. Circulating cell-free nucleic acids: characteristics and applications. Eur J Hum Genet 2018; 26(7): 937–945.
3. Wan JCM, Massie C, Garcia-Corbacho J et al. Liquid biopsies come of age: towards implementation of circulating tumour DNA. Nat Rev Cancer 2017; 17(4): 223–238.
4. Diaz LA, Bardelli A. Liquid biopsies: genotyping circulating tumor DNA. J Clin Oncol 2014; 32(6): 579–586.
5. Mouliere F, Robert B, Peyrotte EA et al. High fragmentation characterizes tumour-derived circulating DNA. PLoS One 2011; 6(9): e23418.
6. Mouliere F, Messaoudi SE, Gongora C et al. Circulating cell-free DNA from colorectal cancer patients may reveal high *KRAS* or *BRAF* mutation load. Transl Oncol 2013; 6(3): 319.
7. Andriamanampisoa C-L, Bancaud A, Boutonnet-Rodat A et al. BIABooster: online DNA concentration and size profiling with a limit of detection of 10 fg/μL and application to high-sensitivity characterization of circulating cell-free DNA. Anal Chem 2018; 90(6): 3766–3774.
8. Mouliere F, Piskorz AM, Chandrananda D et al. Selecting short DNA fragments in plasma improves detection of circulating tumour DNA. Sci Transl Med 2018; 10(466). doi: https://doi.org/10.1101/134437.
9. Sanchez C, Snyder MW, Tanos R et al. New insights into structural features and optimal detection of circulating tumor DNA determined by single-strand DNA analysis. NPJ Genomic Med 2018; 3(1): 31.
10. Bronkhorst AJ, Wentzel JF, Aucamp J et al. Characterization of the cell-free DNA released by cultured cancer cells. Biochim Biophys Acta 2016; 1863(1): 157–165.
11. Lehmann-Werman R, Neiman D, Zemmour H et al. Identification of tissue-specific cell death using methylation patterns of circulating DNA. Proc Natl Acad Sci USA 2016; 113(13): E1826–E1834.
12. Sun K, Jiang P, Chan KCA et al. Plasma DNA tissue mapping by genome-wide methylation sequencing for noninvasive prenatal, cancer, and transplantation assessments. Proc Natl Acad Sci USA 2015; 112(40): E5503–E5512.
13. Snyder MW, Kircher M, Hill AJ et al. Cell-free DNA comprises an in vivo nucleosome footprint that informs its tissues-of-origin. Cell 2016; 164(1–2): 57.
14. Moss J, Magenheim J, Neiman D et al. Comprehensive human cell-type methylation atlas reveals origins of circulating cell-free DNA in health and disease. Nat Commun 2018; 448142.
15. De Vlaminck I, Martin L, Kertesz M et al. Noninvasive monitoring of infection and rejection after lung transplantation. Proc Natl Acad Sci USA 2015; 112(43): 13336–13341.
16. Lam WKJ, Gai W, Sun K et al. DNA of erythroid origin is present in human plasma and informs the types of anemia. Clin Chem 2017; 63(10): 1614–1623.
17. Tug S, Helmig S, Deichmann ER et al. Exercise-induced increases in cell free DNA in human plasma originate predominantly from cells of the haematopoietic lineage. Exerc Immunol Rev 2015; 21: 164–173.
18. Chandrananda D, Thorne NP, Bahlo M. High-resolution characterization of sequence signatures due to non-random cleavage of cell-free DNA. BMC Med Genomics 2015; 8: 29.
19. Underhill HR, Kitzman JO, Hellwig S et al. Fragment length of circulating tumor DNA. PLoS Genet 2016; 12(7): e1006162.
20. Gezer U, Yörüker EE, Keskin M et al. Histone methylation marks on circulating nucleosomes as novel blood-based biomarker in colorectal cancer. IJMS 2015; 16(12): 29654–29662.
21. Mittra I, Pal K, Pancholi N et al. Prevention of chemotherapy toxicity by agents that neutralize or degrade cell-free chromatin. Ann Oncol 2017; 28(9): 2119–2127.
22. Raghuram GV, Gupta D, Subramaniam S et al. Physical shearing imparts biological activity to DNA and ability to transmit itself horizontally across species and kingdom boundaries. BMC Mol Biol 2017; 18(1): 21.
23. Bonaventura A, Liberale L, Carbone F et al. The pathophysiological role of neutrophil extracellular traps in inflammatory diseases. Thromb Haemost 2018; 118(1): 6–27.
24. Roers A, Hiller B, Hornung V. Recognition of endogenous nucleic acids by the innate immune system. Immunity 2016; 44(4): 739–754.
25. Corrales L, McWhirter SM, Dubensky TW, Gajewski TF. The host STING pathway at the interface of cancer and immunity. J Clin Invest 2016; 126(7): 2404–2411.
26. Scheiermann J, Klinman DM. Clinical evaluation of CpG oligonucleotides as adjuvants for vaccines targeting infectious diseases and cancer. Vaccine 2014; 32(48): 6377–6389.
27. Wittig B, Schmidt M, Scheithauer W, Schmoll H-J. MGN1703, an immunomodulator and toll-like receptor 9 (TLR-9) agonist: from bench to bedside. Crit Rev Oncol Hematol 2015; 94(1): 31–44.
28. Gursel I, Gursel M, Yamada H et al. Repetitive elements in mammalian telomeres suppress bacterial DNA-induced immune activation. J. Immunol 2003; 171(3): 1393–1400.
29. Zinkova A, Brynychova I, Svacina A et al. Cell-free DNA from human plasma and serum differs in content of telomeric sequences and its ability to promote immune response. Sci Rep 2017; 7(1): 2591.
30. Chaudhary S, Raghuram GV, Mittra I. Is inflammation a direct response to dsDNA breaks? Mutat Res 2018; 808: 48–52.
31. Olmedillas-López S, García-Olmo DC, García-Arranz M et al. Liquid biopsy by NGS: differential presence of exons (DPE) in cell-free DNA reveals different patterns in metastatic and nonmetastatic colorectal cancer. Cancer Med 2018; 7(5): 1706–1716.
32. Stroun M, Anker P, Maurice P et al. Neoplastic characteristics of the DNA found in the plasma of cancer patients. Oncology 1989; 46(5): 318–322.
33. Stroun M, Anker P, Maurice P, Gahan PB. Circulating nucleic acids in higher organisms. Int Rev Cytol 1977; 51: 1–48.
34. Leon SA, Shapiro B, Sklaroff DM, Yaros MJ. Free DNA in the serum of cancer patients and the effect of therapy. Cancer Res 1977; 37(3): 646–650.
35. Diehl F, Li M, Dressman D et al. Detection and quantification of mutations in the plasma of patients with colorectal tumors. Proc Natl Acad Sci USA 2005; 102(45): 16368–16373.
36. Moati E, Taly V, Didelot A et al. Role of circulating tumor DNA in the management of patients with colorectal cancer. Clin Res Hepatol Gastroenterol 2018; 42(5): 396–402.
37. Thierry AR, El Messaoudi S, Mollevi C et al. Clinical utility of circulating DNA analysis for rapid detection of actionable mutations to select metastatic colorectal patients for anti-EGFR treatment. Ann Oncol 2017; 28(9): 2149–2159.
38. Bachet JB, Bouché O, Taieb J et al. *RAS* mutation analysis in circulating tumor DNA from patients with metastatic colorectal cancer: the AGEO RASANC prospective multicenter study. Ann Oncol 2018; 29(5): 1211–1219.
39. Keller L, Guibert N, Casanova A et al. Early circulating tumour DNA variations predict tumour response in melanoma patients treated with immunotherapy. Acta Derm Venerol 2019; 99(2): 206–210.
40. Remon J, Caramella C, Jovelet C et al. Osimertinib benefit in EGFR-mutant NSCLC patients with T790M-mutation detected by circulating tumour DNA. Ann Oncol 2017; 28(4): 784–790.

41. Tie J, Wang Y, Tomasetti C et al. Circulating tumor DNA analysis detects minimal residual disease and predicts recurrence in patients with stage II colon cancer. Sci Transl Med 2016; 8(346): 346ra92.
42. Openshaw MR, Richards CJ, Guttery DS et al. The genetics of gastroesophageal adenocarcinoma and the use of circulating cell free DNA for disease detection and monitoring. Expert Rev Mol Diagn 2017; 17(5): 459–470.
43. Phallen J, Sausen M, Adleff V et al. Direct detection of early-stage cancers using circulating tumor DNA. Sci Transl Med 2017; 9(403). doi: 10.1126/scitranslmed.aan2415
44. Lin SY, Huang SK, Huynh KT et al. Multiplex gene profiling of cell-free DNA in patients with metastatic melanoma for monitoring disease. JCO Precision Oncol 2018; (2): 1–30.
45. Ogino S, Konishi H, Ichikawa D et al. Detection of fusion gene in cell-free DNA of a gastric synovial sarcoma. World J Gastroenterol 2018; 24(8): 949–956.
46. Silva S, Danson S, Teare D et al. Genome-wide analysis of circulating cell-free DNA copy number detects active melanoma and predicts survival. Clin Chem 2018; 64(9): 1338–1346.
47. Abbosh C, Birkbak NJ, Wilson GA et al. Phylogenetic ctDNA analysis depicts early-stage lung cancer evolution. Nature 2017; 545(7655): 446–451.
48. Misale S, Yaeger R, Hobor S et al. Emergence of *KRAS* mutations and acquired resistance to anti-EGFR therapy in colorectal cancer. Nature 2012; 486(7404): 532–536.
49. Van Emburgh BO, Arena S, Siravegna G et al. Acquired *RAS* or *EGFR* mutations and duration of response to EGFR blockade in colorectal cancer. Nat Commun 2016; 7: 13665.
50. Diaz LA, Williams R, Wu J et al. The molecular evolution of acquired resistance to targeted EGFR blockade in colorectal cancers. Nature 2012; 486(7404): 537–540.
51. Thierry AR, Pastor B, Jiang Z-Q et al. Circulating DNA demonstrates convergent evolution and common resistance mechanisms during treatment of colorectal cancer. Clin Cancer Res 2017; 23(16): 4578–4591.
52. Arena S, Siravegna G, Mussolin B et al. MM-151 overcomes acquired resistance to cetuximab and panitumumab in colorectal cancers harboring EGFR extracellular domain mutations. Sci Transl Med 2016; 8(324): 324ra14.
53. Strickler JH, Loree JM, Ahronian LG et al. Genomic landscape of cell-free DNA in patients with colorectal cancer. Cancer Discov 2018; 8(2): 164–173.
54. Garlan F, Laurent-Puig P, Sefrioui D et al. Early evaluation of circulating tumor DNA as marker of therapeutic efficacy in metastatic colorectal cancer patients (PLACOL study). Clin Cancer Res 2017; 23(18): 5416–5425.
55. Schøler LV, Reinert T, Ørntoft M-BW et al. Clinical implications of monitoring circulating tumor DNA in patients with colorectal cancer. Clin Cancer Res 2017; 23(18): 5437–5445.
56. Belic J, Koch M, Ulz P et al. mFast-SeqS as a monitoring and prescreening tool for tumor-specific aneuploidy in plasma DNA. Adv Exp Med Biol 2016; 924: 147–155.
57. Tie J, Cohen JD, Wang Y et al. Serial circulating tumour DNA analysis during multimodality treatment of locally advanced rectal cancer: a prospective biomarker study. Gut 2018; doi:10.1136/gutjnl-2017-315852.
58. Schou JV, Larsen FO, Sørensen BS et al. Circulating cell-free DNA as predictor of treatment failure after neoadjuvant chemo-radiotherapy before surgery in patients with locally advanced rectal cancer. Ann Oncol 2018; 29(3): 610–615.
59. Yao J, Zang W, Ge Y et al. *RAS/BRAF* circulating tumor DNA mutations as a predictor of response to first-line chemotherapy in metastatic colorectal cancer patients. Can J Gastroenterol Hepatol 2018; 2018: 4248971.
60. Boeckx N, Op de Beeck K, Beyens M et al. Mutation and methylation analysis of circulating tumor DNA can be used for follow-up of metastatic colorectal cancer patients. Clin Colorectal Cancer 2018; 17(2): e369–e379.
61. Conley A, Minciacchi VR, Lee DH et al. High-throughput sequencing of two populations of extracellular vesicles provides an mRNA signature that can be detected in the circulation of breast cancer patients. RNA Biol 2017; 14(3): 305–316.
62. García–Olmo DC, Contreras JD, Picazo MG et al. Potential clinical significance of perioperative levels of mRNA in plasma from patients with cancer of the larynx or hypopharynx. Head Neck 2017; 39(4): 647–655.
63. Bryzgunova OE, Konoshenko MY, Laktionov PP. MicroRNA-guided gene expression in prostate cancer: literature and database overview. J Gene Med 2018; 20(5): e3016.
64. Meng X, Müller V, Milde-Langosch K et al. Diagnostic and prognostic relevance of circulating exosomal miR-373, miR-200a, miR-200b and miR-200c in patients with epithelial ovarian cancer. Oncotarget 2016; 7(13): 16923–16935.
65. Eichelser C, Stückrath I, Müller V et al. Increased serum levels of circulating exosomal microRNA-373 in receptor-negative breast cancer patients. Oncotarget 2014; 5(20): 9650–9663.
66. Cohen JD, Li L, Wang Y et al. Detection and localization of surgically resectable cancers with a multi-analyte blood test. Science 2018; 359(6378): 926–930.
67. Thierry AR. A step closer to cancer screening by blood test. Clin Chem 2018; 64(10):1420–1422.
68. Lam WKJ, Jiang P, Chan KCA et al. Sequencing-based counting and size profiling of plasma Epstein–Barr virus DNA enhance population screening of nasopharyngeal carcinoma. Proc Natl Acad Sci USA 2018; 115(22): E5115–E5124.
69. Rahier J-F, Druez A, Faugeras L et al. Circulating nucleosomes as new blood-based biomarkers for detection of colorectal cancer. Clin Epigenetics 2017; 9: 53.
70. Zaporozhchenko IA, Ponomaryova AA, Rykova EY, Laktionov PP. The potential of circulating cell-free RNA as a cancer biomarker: challenges and opportunities. Expert Rev Mol Diagn 2018; 18(2): 133–145.
71. Tanos R, Thierry AR. Clinical relevance of liquid biopsy for cancer screening. Transl Cancer Res 2018; 7(S2): S105–S129.
72. Schmidt B, Reinicke D, Reindl I et al. Liquid biopsy - performance of the PAXgene® blood ccfDNA tubes for the isolation and characterization of cell-free plasma DNA from tumor patients. Clin Chim Acta 2017; 469: 94–98.
73. Schmidt B, Fleischhacker M. Is liquid biopsy ready for the litmus test and what has been achieved so far to deal with pre-analytical issues? Transl Cancer Res 2018; 7(S2): S130–S139.
74. Meddeb R, Al Amir Dache Z, Thezenas S et al. Quantifying circulating cell-free DNA in humans. Sci Rep 2018.
75. Nezelof C, Guinebretière J-M. [1879, Ernest Besnier inventor of the word "biopsy"]. Rev Prat 2006; 56(18): 2081–2085.
76. Anker P, Stroun M (eds). Circulating Nucleic Acids in Plasma or Serum, Vol. 906. New York, NY: New York Academy of Sciences 2000; 1–188.

B/ Quantification de l'ADN circulant chez l'homme

Auteurs : Romain Meddeb, Zahra Al Amir Dache, Simon thezenas, Amaëlle otandault, Rita tanos, **Brice pastor**, Cynthia sanchez, Joelle Azzi, Geoffroy tousch, Simon Azan, Caroline Mollevi Antoine Adenis, Safia el Messaoudi, Philippe Blache & Alain R. thierry

Cette publication a été publiée dans Scientific Reports en 2019

Résumé: À notre connaissance, il s'agit de la première étude complète sur l'influence de plusieurs paramètres pré-analytiques et démographiques qui pourraient être une source de variabilité dans la quantification de l'ADN circulant nucléaire et mitochondrial (ADNcirN et ADNcirM). Nous rapportons les données d'un total de 222 sujets, 104 individus sains et 118 patients atteints de cancer colorectal métastatique (mCRC). Environ 50 000 et 3 000 fois plus de copies du génome mitochondrial que du génome nucléaire ont été trouvées dans le plasma des individus sains et des patients atteints de cancer colorectal métastatique, respectivement. Chez les individus sains, la concentration de ADNcirN était influencée par l'âge ($p = 0,009$) et le sexe ($p = 0,048$). L'analyse multivariée avec régression logistique a spécifié que l'âge de plus de 47 ans était prédictif d'une concentration plus élevée de ADNcirN ($oR = 2,41$; $p = 0,033$). La concentration de ADNcirM était indépendante de l'âge et du sexe chez les individus sains. Chez les patients atteints de mCRC, les concentrations de ADNcirN et de ADNcirM étaient indépendantes de l'âge, du sexe, du délai entre la prise alimentaire et le prélèvement sanguin, et de l'aspect du plasma, que ce soit en analyse univariée ou multivariée. Néanmoins, une étude *ad hoc* a suggéré que la ménopause et le moment du prélèvement sanguin pourraient avoir tendance à influencer la quantification de l'ADNcir. En outre, des différences statistiques très significatives ont été trouvées entre les patients atteints de mCRC et les individus sains pour le ADNcirN ($p < 0,0001$), le ADNcirM ($p < 0,0001$) et le rapport ADNcirM/ADNcirN($p < 0,0001$). Les niveaux de ADNcirN et de ADNcirM ne varient pas de la même manière en fonction du statut de cancer ou de santé, des facteurs pré-analytiques et démographiques.

Contribution: J'ai participé à la quantification des ADNcir nucléaire de la cohorte de patients atteints de cancer colorectal métastatique, j'ai aussi contribué à la discussion des résultats.

SCIENTIFIC REPORTS

OPEN

Quantifying circulating cell-free DNA in humans

Romain Meddeb[1,2,3,4], Zahra Al Amir Dache[1,2,3,4], Simon Thezenas[1,2,3,4,5], Amaëlle Otandault[1,2,3,4], Rita Tanos[1,2,3,4], Brice Pastor[1,2,3,4], Cynthia Sanchez[1,2,3,4], Joelle Azzi[1,2,3,4], Geoffroy Tousch[1,2,3,4], Simon Azan[1,2,3,4], Caroline Mollevi[1,2,3,4,5], Antoine Adenis[1,2,3,4,6], Safia El Messaoudi[1,2,3,4], Philippe Blache[1,2,3,4] & Alain R. Thierry[1,2,3,4]

Received: 6 September 2018
Accepted: 9 January 2019
Published online: 26 March 2019

To our knowledge, this is the first comprehensive study on the influence of several pre-analytical and demographic parameters that could be a source of variability in the quantification of nuclear and mitochondrial circulating DNA (NcirDNA and McirDNA). We report data from a total of 222 subjects, 104 healthy individuals and 118 metastatic colorectal cancer (mCRC) patients. Approximately 50,000 and 3,000-fold more mitochondrial than nuclear genome copies were found in the plasma of healthy individuals and mCRC patients, respectively. In healthy individuals, NcirDNA concentration was statistically influenced by age ($p = 0.009$) and gender ($p = 0.048$). Multivariate analysis with logistic regression specified that age over 47 years-old was predictive to have higher NcirDNA concentration (OR = 2.41; $p = 0.033$). McirDNA concentration was independent of age and gender in healthy individuals. In mCRC patients, NcirDNA and McirDNA levels were independent of age, gender, delay between food intake and blood collection, and plasma aspect, either with univariate or multivariate analysis. Nonetheless, ad hoc study suggested that menopause and blood collection time might have tendency to influence cirDNA quantification. In addition, high significant statistical differences were found between mCRC patients and healthy individuals for NcirDNA ($p < 0.0001$), McirDNA ($p < 0.0001$) and McirDNA/NcirDNA ratio ($p < 0.0001$). NcirDNA and McirDNA levels do not vary in the same way with regards to cancer vs healthy status, pre-analytical and demographic factors.

Since Mandel and Metais discovered the presence of nucleic acids in serum in the 1940s[1], different studies have reported elevated levels of circulating DNA (cirDNA) in the blood of patients suffering from various diseases[2–6], especially cancer[7–10]. Despite scant early consideration, interest in the feasibility of cirDNA analysis has increased exponentially, over the last decade, among researchers working on a large range of disorders. CirDNA was first clinically implemented in prenatal diagnosis of sex-determination and pregnancy-associated disorders by assaying fetal DNA in maternal plasma[11–13]. The main sources of cirDNA are cell death, either by necrosis or apoptosis, and active release by viable cells, including exocytosis and NETosis[14,15]. Note, cirDNA may derive from either nuclear (NcirDNA) or mitochondrial DNA (McirDNA). To date, research and development of cirDNA analysis has focused on the qualitative rather than the quantitative information provided. For example, cirDNA analysis is now clinically validated for detecting specific sequences or mutations to guide the oncologist toward the most appropriate treatment. CirDNA analysis is also performed for prenatal and embryo-culture genetic testing. There have been several years of intensive studies validating cirDNA quantitation in different clinical scenarios, including sepsis, transplant recipients and immune disorders. CirDNA quantification is also now taken into consideration in oncology as, it was recently shown that, the level of mutant cirDNA is useful for following-up cancer patients to detect minimal residual disease and to monitor response to therapy and disease recurrence. Although total cirDNA levels were first examined in the early phase of cirDNA research and development, it is now not considered as a single biomarker because of its lack of specificity. Nevertheless, all cirDNA analysis relies on the optimal quantification of total amount of cirDNA. Biological biomarkers should be highly dynamic, and their diagnostic performance may vary depending on internal and external changes. The clinical efficacy of cirDNA will require the identification and the control of various patient-related confounders that may

[1]IRCM, Institute of Research in Oncology of Montpellier, Montpellier, France. [2]INSERM, U1194, Montpellier, France. [3]University of Montpellier, Montpellier, France. [4]Regional Institute of Cancer of Montpellier, Montpellier, France. [5]Biometry Unit, Regional Institute of Cancer of Montpellier, Montpellier, France. [6]Digestive Oncology Department, Regional Institute of Cancer of Montpellier, Montpellier, France. Correspondence and requests for materials should be addressed to A.R.T. (email: alain.thierry@inserm.fr)

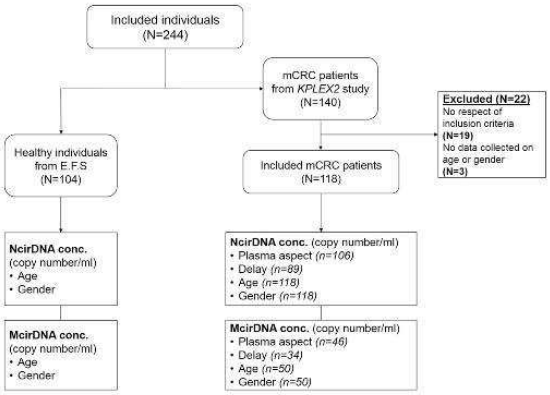

Figure 1. Flow chart of the study.

affect its measurement[16]. Human cellular aging is usually marked by senescence and cell death. Similarly, it often features a phenomenon, originally called "Inflamm-aging", that induces a chronic or low-grade inflammatory state[17–20]. Indeed, it was demonstrated that tissue damage and a pro-inflammatory environment increase release of cirDNA into the blood stream[14]. Additionally, we may speculate that sex-based differences, such as genetic dissimilarity and steroid hormones levels, could cause differences in cirDNA concentration between men and women. Likewise, blood component concentrations may vary with the circadian clock and upon food intake and potentially influencing cirDNA concentration[21]. Despite outstanding research in the field of cirDNA, relatively few studies have examined the effect of pre-analytical and demographic parameters as sources of intra- and inter-individual variability in cirDNA levels. There is currently no single operating procedure and there are relatively few clinical guidelines in the literature[22–25]. This study aims first at defining a framework for cirDNA analysis, to harmonize NcirDNA and McirDNA quantification and to explore potential sources of variability that could cause interpretation errors. Previous studies already documented various pre-analytical limitations and specified conditions for cirDNA analysis, including specific collection tubes, and specific plasma isolation and extraction protocols, including storage condition variables and limits on the number of freeze-thaw cycles[22–24,26]. Here, we study the influence of various pre-analytical (plasma aspect, delay between blood collection and last food intake) and demographic variables such age and gender in NcirDNA and McirDNA concentration determination, from plasma of 104 healthy donors and 118 mCRC patients (Fig. 1). In addition, we compared McirDNA and NcirDNA levels in healthy individuals and mCRC patients. Some others pre-analytical conditions such as blood collection tubes, blood collection time and blood stability were examined *ad hoc* study on healthy volunteers.

Results

Simultaneous quantification of NcirDNA and McirDNA. We used serial dilutions of genomic DNA and of mitochondrial plasmid DNA to validate a reproducible, linear and sensitive assay to quantify, both nuclear and mitochondrial, circulating DNA (NcirDNA and McirDNA). The NcirDNA assay is based upon the qPCR detection of a sequence of the *KRAS* gene and it can detect one copy of nuclear *KRAS* gene per 6 microliters of plasma (1 nuclear Genome Equivalent per 12 µL). The McirDNA assay can detect down to one copy of the mitochondrial *MT-CO3* gene per 1.7 microliter of plasma (1 mitochondrial Genome Equivalent per 1.7 µL). Note, the targeted MT-CO3 gene sequence was selected as being not mutated in the mitochondrial genome of cancer patients. Copy number calculation is performed by using a specific equation that eliminates bias in the nuclear or mitochondrial DNA calibration curves to allow simultaneous calculation of their real relative proportions. For example, in the cohort of 104 healthy individuals, we found a median NcirDNA and McirDNA plasma concentration of 1.64×10^3 and 8.32×10^7 copies/mL, respectively, corresponding to 5.43 and 1.36 ng/mL of plasma.

Comparison between NcirDNA and McirDNA levels. We compared NcirDNA and McirDNA concentration, in healthy individuals and mCRC patients groups, expressed either in copy number/ml and ng/ml of plasma. A supplementary table summarizes all quantification data and comparative tests in detail (Supplementary Table S1). There was a highly statistical difference between NcirDNA and McirDNA concentration expressed in copy number/ml, in healthy individuals (Fig. 2A; *Mann-Whitney U test, P value* < 0.0001) and equally in mCRC patients (Fig. 2B; *Mann-Whitney U test, P value* < 0.0001). We next compared McirDNA and NcirDNA concentration expressed in ng/ml, in healthy individuals and mCRC patients groups. Here, also, we observed a considerable statistical difference between NcirDNA and McirDNA concentrations in healthy individuals (Fig. 2C; *Mann-Whitney U test, P value* < 0.0001) and mCRC patients (Fig. 2D; *Mann-Whitney U test, P value* < 0.0001). McirDNA concentration is significantly higher than NcirDNA concentration when measured in units of copy number/ml, and conversely, the NcirDNA concentration was significantly higher than the McirDNA concentration when measured in ng/ml, either in healthy individuals and mCRC patients.

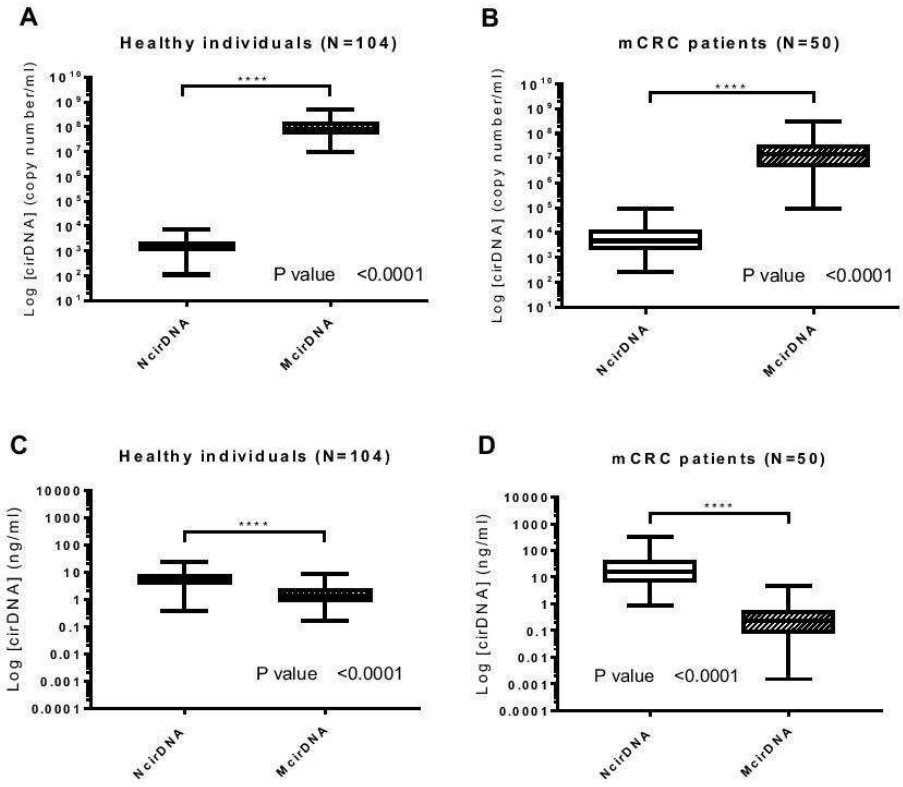

Figure 2. Respective values of NcirDNA and McirDNA plasma concentration. Boxplot analysis of cirDNA concentrations from healthy individuals (N = 104) (**A**,**C**) and mCRC patients (N = 50) (**B**,**D**). Values are expressed either as copy number/ml (**A**,**B**) or as ng/ml (**C**,**D**). CirDNA concentration was determined as described in Materials and Methods. Boxplot represent median with min to max of values and Mann-Whitney U test was performed for comparison. A probability of ≤ 0.05 was considered to be statistically significant; *$P \leq 0.05$, **$p \leq 0.01$, ***$p \leq 0.001$, ****$p \leq 0.0001$.

Effect of age and gender on cirDNA concentrations in healthy individuals. *NcirDNA.* **Age (n = 104):** We dichotomized the healthy individuals cohort in two groups around the median age, which was 47 (Table 1). The median NcirDNA copy number in the <47 years-old group (n = 52) and in the ≥47 years-old group (n = 52) were 1.36×10^3 and 1.73×10^3 copies/ml, respectively. A statistical difference was found between young and older healthy individuals groups (Fig. 3A; *Mann-Whitney U test, P value = 0.009*).

Gender (n = 104): The median NcirDNA copy number in the healthy male group (n = 62) and in the group of healthy females (n = 42) were 1.69×10^3 and 1.48×10^3 copies/ml, respectively. This difference in the NcirDNA copy number between healthy males and females was statistically significant (Fig. 3B; *Mann-Whitney U test, P value = 0.048*).

Multivariate analysis: Logistic regression analysis including age and gender specified that age over 47 years-old was predictive to have higher NcirDNA concentration (Fig. 3C; OR = 2.41, *P = 0.033*). Results of multivariate analysis and Odds ratios (OR) with 95% confidence intervals (CIs) are summarized in Supplementary Table S2A.

McirDNA. **Age (n = 104):** The median McirDNA copy number in the <47 (n = 52) and in the ≥47 year-old group (n = 52) were 7.77×10^7 and 8.40×10^7 copies/ml, respectively. There was no statistical difference in the McirDNA copy number between these groups (Fig. 3D; *Mann-Whitney U test, P value = 0.489*).

Gender (n = 104): The median McirDNA copy number in the healthy male group (n = 62) and in the group of healthy women (n = 42) were 8.03×10^7 and 9.39×10^7 copies/ml, respectively. No statistical difference in McirDNA copy number was observed between healthy males and females (Fig. 3E; *Mann-Whitney U test, P value = 0.485*).

Multivariate analysis: Logistic regression analysis including age and gender confirmed no statistically significant difference between studied groups (Fig. 3F). Results of multivariate analysis and Odds ratios (OR) with 95% confidence intervals (CIs) are summarized in Supplementary Table S2B.

Patient's characteristics					
Healthy individuals (N = 104)			**mCRC patients (N = 118)**		
Age (years)					
Mean	45		Mean	65	
Median	47		Median	65	
(min-max)	(18–69)		(min-max)	(22–91)	
Gender					
Males	62	59,6%	Males	68	57,6%
Females	42	40,4%	Females	50	42,4%
TOTAL	99		TOTAL	118	
Males (N)					
Mean age	45		Mean age	65	
Median age	47		Median age	65	
(min-max)	(19–69)		(min-max)	(34–88)	
Females (N)					
Mean age	44		Mean age	65	
Median age	45		Median age	67	
(min-max)	(18–63)		(min-max)	(22–91)	

Table 1. Characteristics of healthy individuals (N = 104) and mCRC patients (N = 118).

Effect of various parameters on cirDNA concentrations in mCRC patients. *NcirDNA*. **Plasma aspect (n = 106):** We first compared two groups, 27 abnormal plasmas (icteric and/or opaque plasmas) and 79 normal plasmas. There was no statistical difference in NcirDNA levels between abnormal plasmas and normal plasmas groups (Fig. 4A; *Mann-Whitney U test; P value = 0.266*). However, the median NcirDNA amount determined in abnormal plasmas group was slightly lower than in normal plasmas (3.62×10^3 vs 5.22×10^3 copies/ml).

Delay between blood collection time and last food intake (n = 89): We then compared two groups, "1 h < delay < 5 h" (n = 69) and "other delays" (n = 20). There was no statistical difference in NcirDNA levels between "1 h < delay < 5 h" and "other delays" (Fig. 4B; *Mann-Whitney U test; P value = 0.220*). Nonetheless, the "1 h < delay < 5 h" group showed lower median NcirDNA amount than the group "other delays" (3.68×10^3 vs 5.72×10^3 copies/ml).

Age (n = 118): We also dichotomized the mCRC cohort into two groups around the median age of 65 (Table 1). The median NcirDNA copy number in the <65 year-old group (n = 52) and in the ≥65 year-old group (n = 66) were 4.73×10^3 and 4.94×10^3 copies/ml, respectively. No statistical difference was found (Fig. 4C; *Mann-Whitney U test, P value = 0.757*). A comparative study using the same cut-off for both healthy and mCRC cohorts as the median age of all individuals tested here (N = 222, median age = 56 years) confirmed the statistical difference between young (N = 79) and older (N = 25) healthy individuals groups (*Mann-Whitney U test, P value = 0.0026)*, and also the no statistical difference between young (N = 25) and older (N = 93) mCRC groups (*Mann-Whitney U test, P value = 0.913*) (Supplementary Fig. S1A,B).

Gender (n = 118): The median NcirDNA copy number in the mCRC males (n = 68) and in and females (n = 50) mCRC patients were 4.65×10^3 and 5.40×10^3 copies/ml, respectively. No statistical difference was found (Fig. 4D; *Mann-Whitney U test, P value = 0.971*).

Multivariate analysis: Logistic regression analysis including all the parameters (plasma aspect, delay, age and gender) confirmed no statistical significant results (Fig. 4E). Results of multivariate analysis and Odds ratios (OR) with 95% confidence intervals (CIs) are summarized in Supplementary Table S2C.

McirDNA. **Plasma aspect (n = 46):** We next compared the abnormal plasmas (n = 11) and normal plasmas (n = 35) groups. There was no statistical difference in NcirDNA levels between abnormal and normal plasmas groups (Fig. 5A; *Mann-Whitney U test; P value = 0.263*). However, the median McirDNA amount determined in abnormal plasmas was slightly lower than in normal plasmas (6.64×10^6 vs 1.19×10^7 copies/ml).

Delay between day-time of blood draw and the last food intake (n = 34): There was no statistical difference in McirDNA copy number between the "1 h < delay < 5 h" group (n = 25) and the "other delay" group (n = 9) (Fig. 5B; *Mann-Whitney U test; P value = 0.509*). The "1 h < delay < 5 h" group showed higher median NcirDNA amount than the group "other delay" (1.68×10^7 vs 1.19×10^7 copies/ml).

Age (n = 50): The median McirDNA copy number in the < 65 year-old (n = 23) and ≥ 65 year-old (n = 27) groups were 1.12×10^7 and 1.84×10^7 copies/ml, respectively. There was no statistical difference in the McirDNA copy number between the groups (Fig. 5C; *Mann-Whitney U test, P value = 0.240*).

Gender (n = 50): The median McirDNA copy number in the mCRC males group (n = 25) and in the group of mCRC women (n = 25) were 1.19×10^7 and 1.68×10^7 copies/ml, respectively. We did not found any statistical difference in the McirDNA copy number between mCRC males and females (Fig. 5D; *Mann-Whitney U test, P value = 0.261*).

Multivariate analysis: Logistic regression analysis including all the parameters (plasma aspect, delay, age and gender) confirmed no statistically significant results (Fig. 5E). Results of multivariate analysis and Odds ratios (OR) with 95% confidence intervals (CIs) are summarized in Supplementary Table S2D.

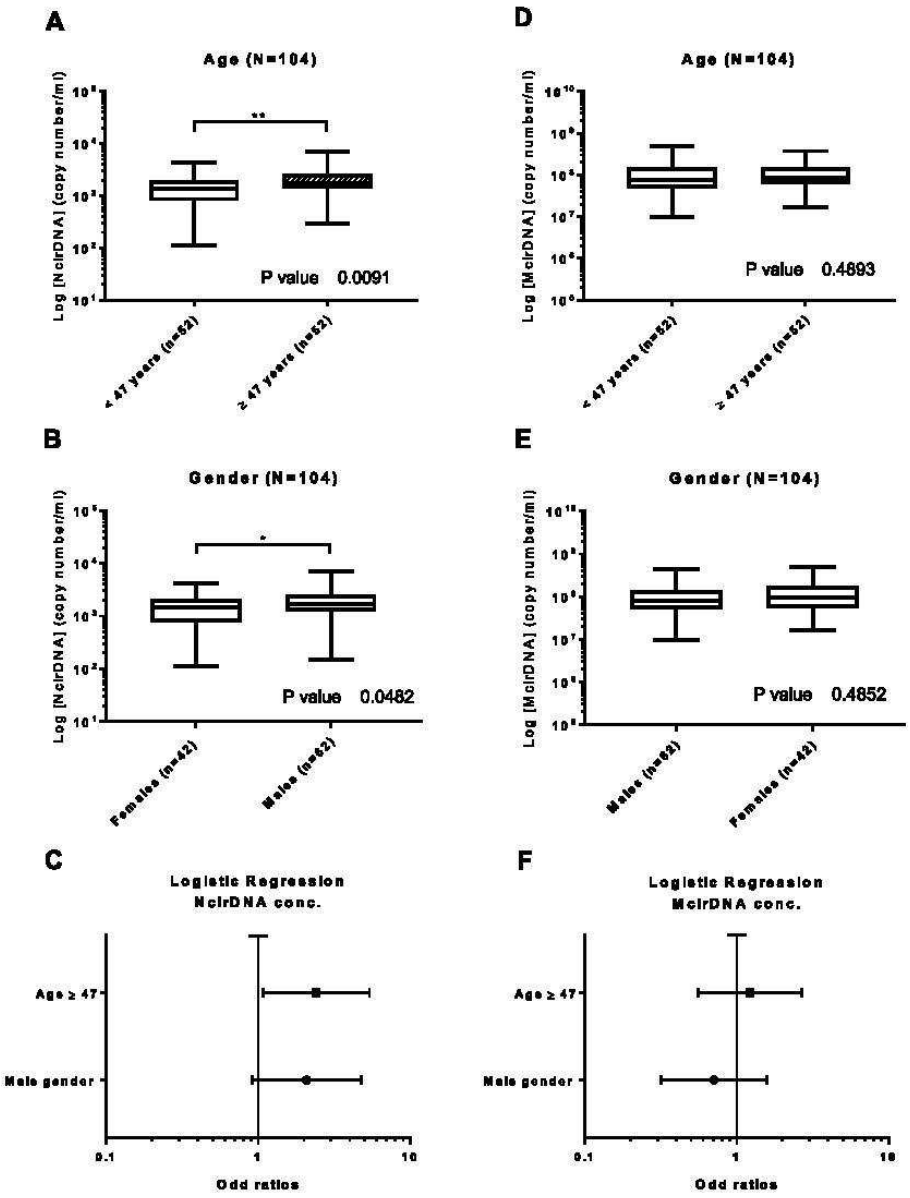

Figure 3. Influence of age and gender on cirDNA concentration in healthy individuals. Boxplot analysis of cirDNA concentration extracted from healthy individuals (N = 104), with regards to age (**A**,**D**) and gender (**B**,**E**). (**C**,**F**) Multivariate analysis representations. NcirDNA (**A**–**C**) and McirDNA (**D**–**F**) concentrations are expressed in copy number/ml of plasma. Boxplot represent median with min to max of values. Mann-Whitney U test was performed for univariate analysis and logistic regression was performed for multivariate analysis. Odds ratio (OR) with 95% confidence intervals (CIs) are represented. A probability of ≤ 0.05 was considered to be statistically significant; *$p \leq 0.05$, **$p \leq 0.01$, ***$p \leq 0.001$, ****$p \leq 0.0001$.

Comparing cirDNA levels between mCRC patients and healthy individuals. *NcirDNA.* We compared the median NcirDNA amount between healthy individuals (n = 104) and mCRC patients (n = 118). The median NcirDNA concentration in healthy individuals and mCRC patients was 1.64×10^3 and 4.73×10^3 copies/ml, respectively, revealing a significant difference between healthy individuals and mCRC patients (Fig. 6A; *Mann-Whitney U test, P value < 0.0001*).

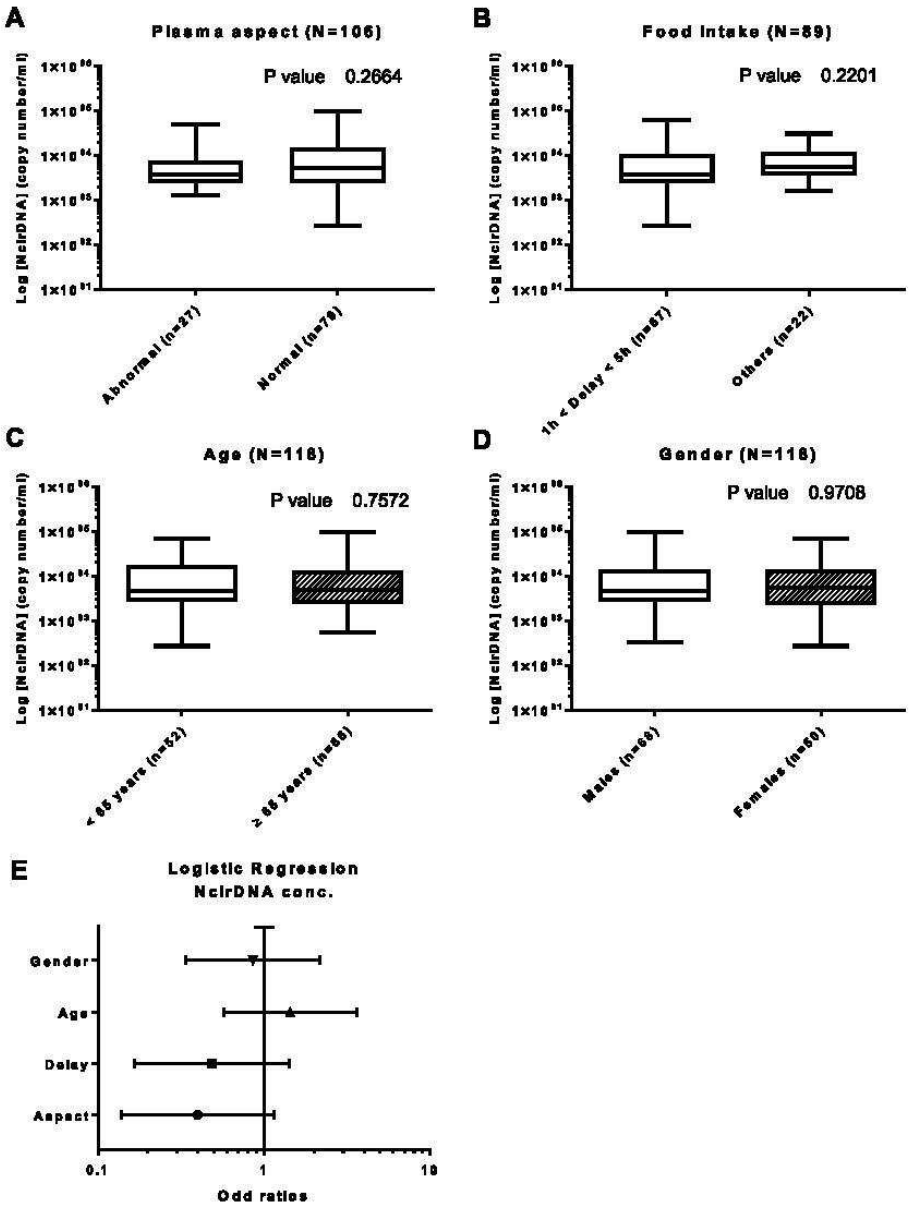

Figure 4. Influence of various factors on NcirDNA concentration in mCRC patients. Boxplot analysis of NcirDNA concentration extracted from mCRC patients (N = 118), with regards to plasma aspect (**A**); delay between blood collection and last food intake (**B**); age (**C**) and gender (**D**). (**E**) Multivariate analysis representation. Boxplot represent median with min to max of values. Mann-Whitney U test was performed for univariate analysis and logistic regression was performed for multivariate analysis. Odds ratio (OR) with 95% confidence intervals (CIs) are presented. A probability of ≤ 0.05 was considered to be statistically significant; $^{*}p \leq 0.05$, $^{**}p \leq 0.01$, $^{***}p \leq 0.001$, $^{****}p \leq 0.0001$.

McirDNA. Next we compared the median McirDNA amount between healthy individuals (n = 104) and mCRC group (n = 50). The median McirDNA concentration in healthy individuals and mCRC patients was statistically different at 8.32×10^7 and 1.44×10^7 copies/ml, respectively (Fig. 6B; *Mann-Whitney U test, P value < 0.0001*).

McirDNA/NcirDNA ratio. Finally we compared the median McirDNA/NcirDNA ratio between healthy individuals (n = 104) and mCRC patients (n = 50). The median McirDNA/NcirDNA ratio in healthy individuals

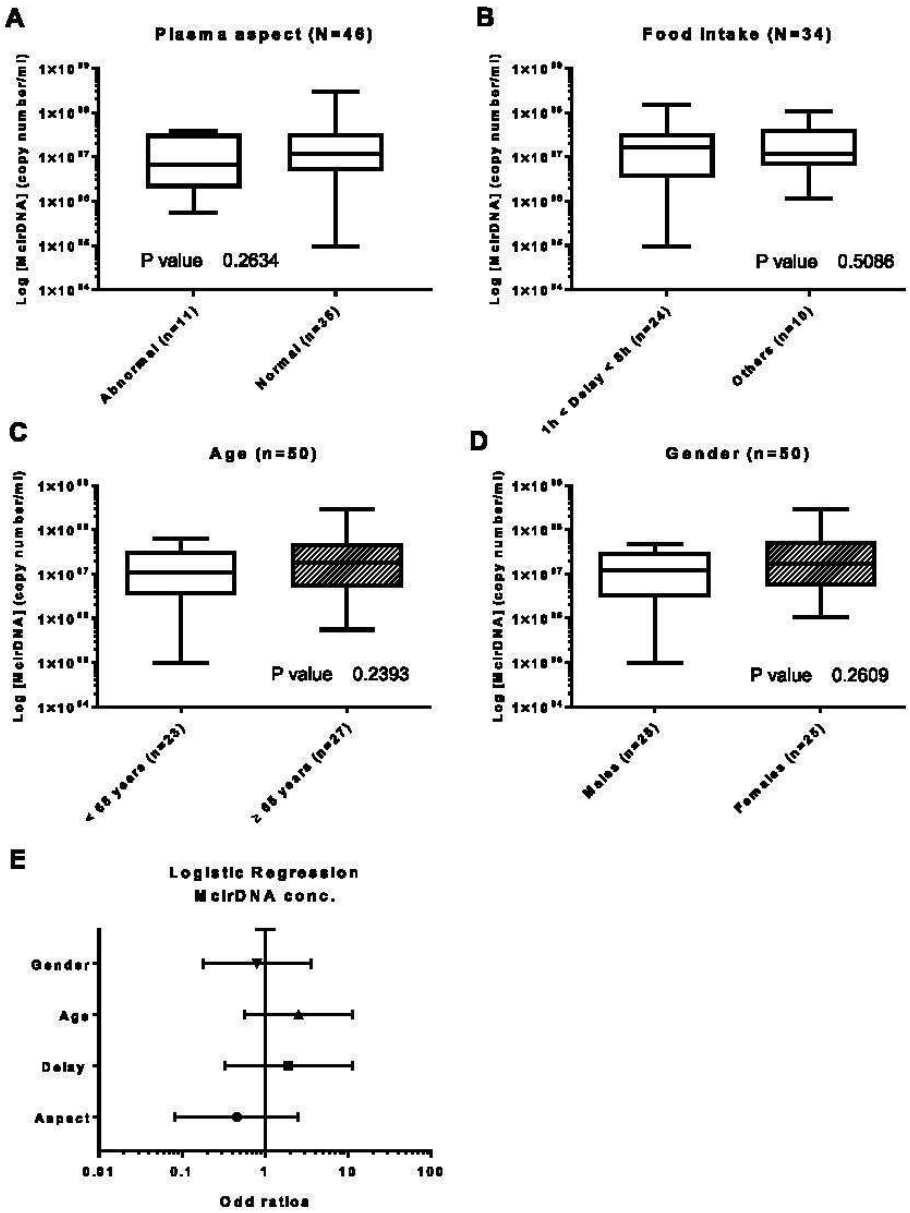

Figure 5. Influence of various factors on McirDNA concentration in mCRC patients. Boxplot analysis of McirDNA concentration extracted from mCRC patients (N = 50), with regards to plasma aspect (**A**); delay between blood collection and last food intake (**B**); age (**C**) and gender (**D**). (**E**) Multivariate analysis representation. Boxplot represent median with min to max of values. Mann-Whitney U test was performed for univariate analysis and logistic regression was performed for multivariate analysis. Odds ratio (OR) with 95% confidence intervals (CIs) are presented. A probability of ≤ 0.05 was considered to be statistically significant; *$p \leq 0.05$, **$p \leq 0.01$, ***$p \leq 0.001$, ****$p \leq 0.0001$.

and mCRC patients were statistically different at 5.41×10^4 and 2.70×10^3 copies/ml, respectively (Fig. 6C; *Mann-Whitney U test, P value < 0.0001*). The median McirDNA/NcirDNA ratio was 20-fold higher in the healthy individuals group than in the mCRC patients group. We did the same comparison using McirDNA and NcirDNA concentrations expressed in ng/ml and we obtained the same results (Supplementary Fig. S2, *Mann-Whitney U test, P value < 0.0001).*

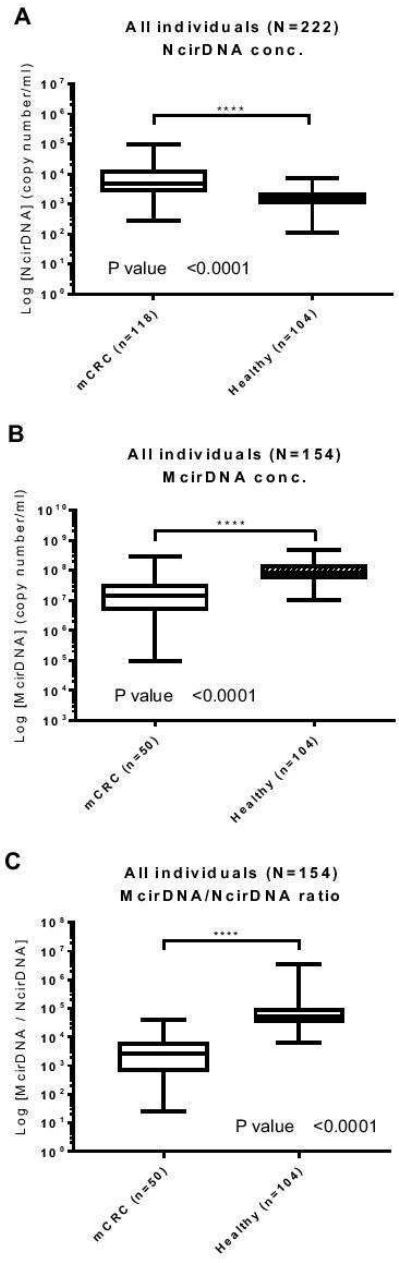

Figure 6. Biomarker capacity of respective NcirDNA and McirDNA concentration for discriminating healthy individuals and mCRC patients. The cohort was dichotomized in two populations (mCRC patients and healthy individuals). Boxplot analysis of the amount of NcirDNA (**A**) and McirDNA (**B**) extracted from plasma of all individuals (N = 222 and N = 154, respectively). (**C**) Boxplot analysis of the McirDNA/NcirDNA ratio of all individuals (N = 154). The boxplots represent medians with min to max of values and Mann-Whitney U test was performed for comparison. A probability of ≤ 0.05 was considered to be statistically significant; *$p \leq 0.05$, **$p \leq 0.01$, ***$p \leq 0.001$, ****$p \leq 0.0001$.

CirDNA stability in whole blood samples of healthy volunteers. NcirDNA concentration in blood collected in EDTA tubes increased by more than two-fold and three-fold respectively, at days 2 and 5 after blood collection (Supplementary Fig. S3A). In contrast, there was no difference between days 0, 2, 5 and 7 following

blood collection in Cell-Free DNA BCT® STRECK (BCT) tubes (Supplementary Fig. S3B). Note, median values at day 0 are similar in plasma from blood collected in EDTA or BCT tubes. In addition, The McirDNA concentration in blood collected in EDTA tubes approximately increased more than 12-fold and 27-fold respectively, at days 2 and 5 after blood collection (Supplementary Fig. S3C).

Effect of the blood collection time on cirDNA levels in healthy volunteers. *NcirDNA.* In EDTA tubes at 9.00 AM (fasted state), 12.00 PM (2 hours after breakfast), 3.00 PM (2 hours after lunch) and 6.00 PM, the median NcirDNA copy numbers were 1500, 480, 715 and 709 copies/ml respectively. An additional figure shows this in more detail (Supplementary Fig. S4A,E). Taking the four healthy individuals together, the median NcirDNA concentration strongly changed from the fasted state to three hours after breakfast. Median NcirDNA concentration was slightly higher at the earliest collection time in BCT tubes, over the same time-course of the day, at 874, 562, 728 and 313 copies/ml, respectively. An additional figure shows this in more detail (Supplementary Fig. S4B,F). Altogether our data from both collection methods showed that NcirDNA content in healthy individuals declined from 9.00 AM to 12.00 PM then plateaued up to the 6.00 PM collection time. An additional figure shows this in more detail (Supplementary Fig. S4C,D,G,H).

McirDNA. In EDTA tubes from healthy individuals, the median NcirDNA copy numbers were unchanged over the time course at 1.05, 1.25, 1.17 and 1.26 million copies/ml. An additional figure shows this in more detail (Supplementary Fig. S5A,B). No clear difference was found when comparing McirDNA amounts collected at the various collection time points. Note, plasma appearance become opaque at 6.00 PM. An additional picture illustrates this observation (Supplementary Fig. S6).

Discussion

Here, we present a comprehensive study on the quantification of nuclear and mitochondrial cirDNA in the plasma of healthy individuals and a homogenous cohort of mCRC patients. To our knowledge, this work is the first to address altogether the influence of various preanalytical, analytical and demographical factors on NcirDNA and McirDNA levels in a large set of individuals ($n > 200$). Solid tumor mass is composed of a variety of cells, mostly consisting of malignant/cancer, stromal, endothelial and immunological cells. In order to avoid any confusion in nomenclature, we define as 'tumor cells' all the cells composing the tumor mass. The concentration values presented in this study correspond to total cell-free DNA in plasma, either of nuclear or mitochondrial origin. Our observations are summarized in Table 2 and Supplementary Table S3.

Total cirDNA levels. This study design relies on the analytical performance of the assay. We used here a qPCR-based method with an unmatched combination, of reproducibility, sensitivity and specificity for quantifying plasma cirDNA (see Methods section). Furthermore, our assay benefits from a clinically-validated optimal pre-analytic process that we previously set up for plasma preparation[22]; and adapted from Chiu *et al.*, DNA extraction and sample handling[27]. The accuracy of the cirDNA concentration measurement in this study is supported by two assessments: (i) total cirDNA concentration by targeting a *KRAS* sequence was routinely controlled by quantifying a *BRAF* sequence. In addition, this control quality enable to detect and exclude sample with loss of heterozygosity (LOH) or gene amplification which have been reported in CRC patients[28]. Moreover, since *KRAS* amplification is an infrequent event in CRC (0.67%)[28], this level will not modify our observations or the values described in our manuscript; and (ii) the study of cirDNA measurement under Poisson law distribution revealed single copy detection of nuclear cirDNA.

Respective NcirDNA and McirDNA proportions inverted when the plasma cirDNA concentrations were calculated according to copy number or mass (Fig. 2A,C). For example, data obtained from 104 healthy individuals revealed that median McirDNA plasma concentration was approximately 50,000-fold higher than median NcirDNA plasma concentration in terms of copy number/mL (99.998% McirDNA and 0.002% NcirDNA), corresponding to approximately 4-fold lower in terms of ng/ml (25.0% McirDNA and 75.0% NcirDNA). This highlights the much lower size of the mitochondrial genome (16569 bp) than the nuclear genome (about 3×10^9 bp), and also the high number of mitochondrial genome copies within a cell. Each human cell, depending on its type, contains a number of mitochondria ranging from 500 to 2,000 and each mitochondria holds between 2 and 10 mitochondrial DNA molecules. Therefore, each cell may contain approximatively 1,000 to 20,000 mitochondrial DNA molecules and only one nuclear genome equivalent, which is consistent with our results. Our method of calculation, described here, appears as the most rigorous means to simultaneously quantify mitochondrial and nuclear DNA concentrations. A higher coefficient of variation was routinely observed for mitochondrial than for nuclear DNA, despite the higher analytical signal for McirDNA copy number. The median concentration levels we found here appear to be similar to the average values observed in several studies[27,29]. In addition, performance of our assay support the accuracy of the values presented throughout this study such as 5.43 and 1.36 ng/mL in healthy subject plasma of N- and McirDNA, respectively. Considering the significant percentage of McirDNA (i.e.: 25% in healthy subjects) among total cirDNA mass existing in plasma, we propose to always specify the origin of cirDNA when examining total circulating WT DNA.

Influence of age and gender on NcirDNA levels in healthy individual plasma. Most studies found no relationship between NcirDNA levels and any demographic parameters, such as age and gender, in healthy individuals[30–32]. A few studies showed opposite observations[33–35]. Here, we observed an influence of age on NcirDNA plasma concentration in the healthy individual cohort as a whole ($p = 0.009$). Our data also revealed a statistical difference in NcirDNA amount between healthy males and females ($p = 0.048$). We performed logistic regression for multivariate analysis including age and gender and showed that age ≥ 47 was predictive of a high NcirDNA concentration (OR = 2.41, $p = 0.033$). This observation is in accordance with a study by Jylhävä *et al.*

Demographical considerations	Group	N	In accordance with previous works
NcirDNA concentration			
A statistical difference between males and females	Healthy	104	Catarino R, *et al.*[63]
No statistical difference between males and females	mCRC	118	Hao TB, *et al.*[31]
A statistical difference with regard to age	Healthy	104	Jylhävä J, *et al.*[35]
No statistical difference with regard to age	mCRC	118	Van der Drift MA, *et al.*[30]
Statistical increase in mCRC patients as compared to healthy individuals	Healthy mCRC	104 118	Bedin C, *et al.*[64]
McirDNA concentration			
No statistical difference between males and females	Healthy mCRC	104 50	New observation
No statistical difference with regard to age	Healthy mCRC	104 50	Jylhävä J, *et al.*[35] New observation
Statistical decrease in mCRC patients as compared to healthy individuals	Healthy mCRC	104 50	New observation
McirDNA vs NcirDNA concentration			
Necessity of independently quantifying NcirDNA and McirDNA			
About 50,000-fold more McirDNA copy number as compared to NcirDNA in healthy individuals	Healthy	104	New observation
About 3,000-fold more McirDNA copy number as compared to NcirDNA in cancer patients	mCRC	50	New observation
About 20-fold more McirDNA/NcirDNA ratio in healthy individuals as compared to mCRC patients	Healthy mCRC	104 50	New observation

Table 2. Summary of the observations made on the influence of demographical factors.

that consisted of 12 nonagenarian women (age > 90 years) and 11 healthy control female (22 < age < 37 years) that showed a higher concentration of NcirDNA in nonagenarians than in control women[33]. The authors explained this increase in the amount of cirDNA with age, as the accentuation of a senescence phenomenon and cell death, caused by an inflammation associated with age and even by decreased clearance and phagocytic capacity. Zhong *et al.* showed a significant increase in total plasma cirDNA concentration in women over 60, compared to younger women, which appears to be consistent with Jylhävä's study. We may speculate that menopause could be an explanation of the statistically higher NcirDNA concentration in healthy males as compared to healthy females ($p = 0.048$), whereas no difference between mCRC males and females was observed ($p = 0.971$). This speculation is based on two observations: (i) Median menopausal age in the European population is 51 years-old; 10–15% of women go into menopause before the age of 45, and globally 90–95% reach menopause by 55 years of age. By applying these categories of age to our women cohorts, we observed no statistical difference and no tendency between mCRC women <45, 45–54 and ≥55 year-old (*Kruskal-Wallis rank test, P value = 0.592*) while we showed a statistical difference between healthy women <45, 45–54 and ≥55 year-old, with a concentration gradient: 1275, 1440 and 2610 median copy number, respectively (*Kruskal-Wallis rank test, P value = 0.026*); and (ii) CRC females are at a high risk of chemotherapy-induced menopause or menstrual disorders like amenorrhea or a decrease of steroid hormone levels[36,37], and metachronous mCRC patients may attain a menopausal state earlier. An additional figure shows these results in more detail (Supplementary Fig. S7).

Influence of various parameters on NcirDNA levels in mCRC patients plasma. Despite the large number of studies that aimed at determining if age and gender might influence NcirDNA levels, no clear results have been demonstrated[30–32,38]. There are discrepancies in the literature with regards to the influence of age and gender in patient populations suffering from various types of cancers. These discrepancies could result from use of serum, or pre-analytical or analytical factors. Note, a study by Hohaus *et al.* showed that patients with Hodgkin and non-Hodgkin's lymphoma over 60 year-old (n = 142) had higher levels of cirDNA in plasma than younger patients ($p = 0.018$)[38]. Conversely, our data showed no statistical influence of age ($p = 0.757$) and gender ($p = 0.971$) on NcirDNA concentration in mCRC patients and these results was confirmed with a multivariate analysis using logistic regression. We also demonstrated no influence of pre-analytical factors like plasma aspect ($p = 0.266$) or delay between last food intake and blood collection ($p = 0.220$). On the other hand, our results also confirm those previously published by our laboratory[25] and by many teams[39,40], namely that NcirDNA concentration is significantly higher cancer patients than in healthy individuals ($p < 0.0001$), whether male or female. For more than a decade it was suggested that total NcirDNA could be a cancer biomarker[25,41,42]. However, previous attempts to apply total cirDNA quantity as a screening test for cancer lacked a strong statistical demonstration[43]. High standards, with regard to pre-analytical factors and quantification, could lead to its use as one marker, among other, for tumor burden.

McirDNA levels in plasma. Relatively few reports have quantitatively analyzed McirDNA and there are discrepancies among them. In one study there was no significant difference between young and aged healthy subjects[35]. For Pinti *et al.* however, McirDNA concentration would increase with age[18]. In this study, McirDNA content was analyzed in 831 plasma samples from subjects with different healthy status, aged from 1 to 104 years; McirDNA content significantly increased after fifty years-of-age and it peaked in nonagenarians. Elevated McirDNA levels might

help maintain the low-grade chronic inflammation that is common in elderly individuals. With regards to McirDNA level in cancer patients, Mengel-From *et al*. measured McirDNA copy number in blood cells from 1,067 subjects aged 18 to 93 and conversely, observed a tendency for lower mitochondrial DNA copy number with advanced age[44]. These findings are consistent with other studies, performed on different types of tissue, such as skeletal muscle and pancreatic islets[45,46]. This age-related tissue-specific depletion of cellular mitochondrial DNA could lead to a proportional reduction of McirDNA copy-number in plasma. Inversely, there was no association between serum McirDNA levels and demographic parameters (age/gender) in urological malignancies[47,48]. Likewise, in breast cancer, there was no significant difference in McirDNA content in blood samples of stage I patients with respect to their age[49]. Our data revealed no influence of age and gender on McirDNA concentration, either in plasma of healthy individuals or mCRC patients. These results were confirmed in multivariate analysis. We also reported no significant influence of plasma aspect ($p = 0.263$) and delay between last food intake and blood collection ($p = 0.509$). Nonetheless, our data revealed a significant higher McirDNA than NcirDNA concentration in plasma, whether for mCRC patients, healthy individuals, male or female, and regardless of the age of the subject. Note, while median NcirDNA concentration is much higher in mCRC patients than in healthy individuals, median McirDNA concentration is conversely lower in mCRC patients, revealing a proportionally lower McirDNA release from cancer cells. This might be explained by the fact that cancer cells, in comparison to healthy cells, may have, among other differences, fewer mitochondria per cell and less DNA within their mitochondria[34,50]. However, this is still controversial and explanation of our striking observation is under active investigation in our team. Nevertheless, we may speculate that the McirDNA/NcirDNA ratio might have some power in discriminating healthy individuals from cancer patients. McirDNA/NcirDNA ratio is undergoing clinical validation as potential biomarker for tumor burden or diagnosis in a large study involving broader scope of cancer patients with various malignancies and stages. In light of the high copy number of McirDNA and its tendency to be mutated in cancer[51], our observations confirm the gradual acceptance of McirDNA as a new potent diagnostic and prognostic biomarker for many solid tumors[52].

Blood stability for cirDNA plasma assessment. As previously reported[23,53], NcirDNA concentration determined from blood collected in EDTA tubes increased with time highlighting release of genomic DNA resulting from blood cell lysis when stored at room temperature or +4 °C and consequently to contamination of cell-derived DNA. Note, whole blood stored in EDTA tubes at +4 C° showed no change in cirDNA concentration for up to one day suggesting their potential use within this time period (data not shown)[23,53]. We propose routine clinical analyses use plasma stored in EDTA tubes for up to 6 hours, given the uncertainty of maintaining the temperature of samples in the course of blood processing, as we earlier described[54]. Conversely, BCT tubes appeared to conserve blood cell integrity, since no DNA concentration increase was observed up to 7 days following blood collection[23,55]. Thus, BCT tubes maintain the true cirDNA concentration and are good tools to conserve/stabilize blood for optimal quantification of NcirDNA for up to 7 days following collection. Cell-preserving tubes greatly allows postal shipment of whole-blood within this time period and it allows interventional analysis as well as enabling clinical centers that lack lab facilities to immediately prepare plasma. While being cheaper by themselves, use of EDTA tubes necessitates plasma preparation within a short time frame and immediate subsequent storage under frozen conditions until analysis requiring costly shipment when plasma originate from a single patient. We first reported that McirDNA concentration determined from blood collected in EDTA tubes strongly increased with time. We may assume that this results as well blood cell lysis and blood cell-derived mitochondrial DNA contamination.

Effect of blood collection time on cirDNA plasma concentration. There is currently no indication in the literature on the optimal time for blood collection when analyzing cirDNA. Our data seem to indicate that NcirDNA median levels are 2- to 3-fold higher at 9.00 AM, which is the earliest time-point examined, compared to later blood-collection time-points (12.00, 3.00 and 6.00 PM) when the NcirDNA level stabilizes. Decrease from 9.00 AM to 12.00 PM might be explained by the postprandial effect of the breakfast being taken at 10.00 AM. This hypothesis is supported by several observations. First, we reported that NcirDNA plasma levels in blood collected between one and five hours after food intake were lower than in blood collected on patients under fasting conditions. It was previously showed that plasma triglyceride increased one hour after food intake, peaked ≈3 hours after intake of a test meal and baseline values were restored back to initial values after 5 hours[56]. Second, NcirDNA concentration was lower in opaque than in non-opaque plasmas. Multivariate analysis including age, gender, plasma aspect and delay between food intake and blood collection revealed no statistical influence but abnormal plasma aspect showed a clear tendency to have lower NcirDNA concentration (OR = 0.399; $p = 0.089$). These observations are all consistent with postprandial effects. Food intake with high lipid content may result in hyperlipidemia which can be characterized by opaque plasma and high triglyceride concentrations. However, despite the large examined cohort data, we cannot state that postprandial is the explanation since no statistical difference was found. This may be due to various factors: (i) blood triglyceride levels largely depend on fat distribution and body weight, lifestyle choices, and also genetic factors[57]; (ii) there were considerable within- and between-subject variations in non-fasting plasma triglycerides[58]; and (iii) the subjects had a chronic illness, mCRC. We speculate that the postprandial effect could occur because the presence of lipids or proteins may interfere with DNA extraction yield from plasma. We cannot exclude the possibility that NcirDNA levels depend on circadian clocks and metabolism, resulting in more elevated concentration in the morning. Moreover, we cannot exclude the possibility that other metabolic changes during fasting/feeding alter cirDNA yield. Nevertheless, our data suggest that fasting blood samples should be included when studying or clinically examining cirDNA to improve its diagnostic performance, especially when low mutation frequency in cancer patients or prenatal testing is considered. Note, in addition to opaque plasma, we remarked on various occasions that, icteric plasma had aberrant cirDNA concentration when qPCR was the analytical method. Therefore, we propose observation of icteric, hemolytic and opaque plasma as criteria of blood sample exclusion.

Limitations of the study. While the study was carried out with statistically sufficient number of subjects to support the observations, the *ad hoc* study is limited by the low number of tested individuals since *ad hoc* study experiments are cumbersome and time-consuming. Thus, blood stability and blood collection time was only carried out on a few number of healthy volunteers (n = 5) and not on mCRC patients. This not allowed us to provide statistical analysis while the results showed clear tendencies. A specific study should be performed to statistically confirm these results on a larger cohort of healthy volunteers as well as mCRC patients. Although we routinely experienced that abnormal plasmas resulted in lowering cirDNA concentration values, we cannot fully discriminate the implication of postprandial effects like triglycerides serum level, to the possible involvement of biological changes dues to the circadian rhythm. In order to definitively address this issue, it would be interesting to compare NcirDNA levels at 9.00 AM and 12.00 AM, with and without breakfast, in order to determine the impact of food intake and circadian rhythm, respectively. In addition, the influence of the menopause on cirDNA concentration with regard to our observations of gender, age and pathological status is only speculative. A specific study on the difference of NcirDNA concentration between postmenopausal and premenopausal healthy females, as well as the difference between premenstrual and postmenstrual young women, should be performed to definitively address this issue. Conclusions drawn here in respect to cancer plasma samples should be restricted to mCRC patients and extension to other malignancies or even to localized disease is speculative.

In conclusion, the levels of mitochondrial and nuclear circulating DNA differently vary with regards to pre-analytical and demographic factors. Those variables should be taken into consideration when evaluating cirDNA analysis in clinical setting and perhaps in the future clinical practice when cirDNA quantification is directly or indirectly used as a biomarker. In addition, our study highlights the potential for combining the analysis of NcirDNA and McirDNA since examining their respective levels may have diagnostic value.

Methods

Patients. Blood samples collected from 104 healthy donors were provided by the Etablissement Français du Sang (E.F.S), the blood transfusion center of Montpellier (Convention EFS-PM N° 21PLER2015-0013). Blood samples collected by the E.F.S were analyzed (virology, serology, immunology, blood numeration). If an anomaly is detected, the sample is ruled out and the donor is warned then by mail. NcirDNA concentration and McirDNA copy number were determined for all healthy individuals. Data on age and gender were collected for all healthy individuals. mCRC patients data are taken from a study comparing the detection of *KRAS* exon 2 and *BRAF V600E* mutations by circulating DNA (cirDNA) analysis to conventional detection by tumor tissue analysis[59]. This study (KPLEX2) was performed and presented under the STARD criteria. 140 patients have been included in 11 clinical centers in France, over a period of 12 months. Eligible patients were male or female, aged ≥18 years, with a proven histologically mCRC, a measurable disease as defined by response evaluation criteria in solid tumors (RECIST v1.1) and untreated by radiotherapy or chemotherapy in the last 4 weeks before inclusion. There is no possibility that cirDNA from mCRC patients can be affected by therapy since eligible patients were untreated by radiotherapy or chemotherapy in the last 4 weeks before blood collection (inclusion criteria). Written consent was obtained from the part of all patients. Inclusion criteria were described previously[59]. 19 were excluded from analysis for no respect of the inclusion criteria (due to various inclusion criteria) and 3 were excluded due to lack of data collected on age or gender. NcirDNA analysis was performed on 118 patients and McirDNA analysis on 50/118 mCRC patients. While study on age and gender effect were carried out on all the included mCRC patients for NcirDNA (N = 118), cohort patient number varied when studying plasma aspect and delay for NcirDNA, or age and gender for McirDNA because of two main reasons: non-reported information for delay and plasma aspect for to NcirDNA and insufficient plasma volume needed to carry out supplementary analysis for McirDNA. All data on age and gender were collected. Plasma aspect (normal, abnormal: opaque or/and icteric) was noted for 106/118 mCRC patients and delay between time of blood draw and the last food intake was informed for 89/118 mCRC patients.

Ethics approval and consent to participate. Blood samples collected from 104 healthy donors were provided by the Etablissement Français du Sang (E.F.S), the blood transfusion center of Montpellier (Convention EFS-PM N° 21PLER2015-0013). Plasma samples from mCRC patients were obtained from the Kplex2 study registration number EUDRACT 2016-001490-33 with ethic committee approval ("Comité de Protection des Personnes", Nimes, France). All methods were performed in accordance with the relevant guidelines and regulations. The study obtained informed consent from all participants for the study.

Blood stability. 7 samples for each healthy donor were collected at 9.00 a.m. on Day 0 (fasted state): 3 with EDTA K2 tubes and 4 with Cell-Free DNA BCT® STRECK tubes. Each tube was processed as we early described, at day 0, 2 and 5 for EDTA tubes and day 0, 2, 5 and 7 for BCT tubes. EDTA tubes were stored at +4 °C and BCT tubes were conserved at room temperature before isolation. Healthy individual N°1 (HI1) and N°2 (HI2) are 57 year-old and 29 year-old men, respectively, both with no known disease. Healthy individual N°3 (HI3), N°4 (HI4) and N°5 (HI5) are 25 year-old, 24 year-old and 28 year-old women, respectively, both with no known diseases. NcirDNA analysis for HI1 was not performed due to clotting in BCT tubes.

Blood collection time. 4 blood collection times were defined 9.00 a.m. (fasted state), 12.00 p.m. (2 hours after breakfast), 3.00 p.m. (2 hours after lunch) and 6.00 p.m. (4 hours after lunch). One EDTA K2 and one Cell-Free DNA BCT® STRECK tube per day-time were collected for each donor. Healthy individual N°6 (HI6) and N°7 (HI7) are 29 year-old and 27 year-old men, respectively, both with no known diseases. Healthy individual N°8 (HI8) and N°9 (HI9) are 28 year-old and 30 year-old women respectively, both with no known diseases. Each donors took the same meal during breakfast: one butter croissant, one chocolate croissant and one coffee with sugar; and for the lunch: a dish of tomato rice with sausage, bread and one coffee with sugar.

Sample characteristics and preparation. Samples were collected and treated in accordance with a pre-analytical guideline previously established by our group[22]. In summary, blood was collected in EDTA K3 tubes and plasma was isolated within 2 hours. The isolation technique consist of a double centrifugation. Initially, tubes were centrifuged for 10 minutes at 4 °C and 1,200 g in a Heraeus Multifuge LR centrifuge. The supernatant was collected while carefully avoiding the buffy-coat. The second centrifugation was conducted for 10 minutes at 4 °C and 16,000 g. The supernatant was transferred to 1.5 ml tubes before performing the extraction of cirDNA or being stored at −20 °C. CirDNA extraction was performed with the Qiagen Blood Mini kit, following all steps of the protocol. In all, 0.2 to 1 ml of plasma was extracted in several successive passes on a column. The final elution volume was 80 to 130 µl and eluates were frozen at −20 °C prior to analysis by qPCR. Freeze-thaw cycles should be avoided to reduce the phenomenon of cirDNA fragmentation and the extracts are not kept longer than 3 months at −20 °C.

Q-PCR analysis. CirDNA analysis was performed by a qPCR technique developed in our laboratory, and clinically validated previously[60]. The method is based on an innovative design of short amplicons (60–100 bp ± 10 bp) targeting a wild-type sequence of the gene, (here the *KRAS* nuclear gene and the mitochondrial Cytochrome oxidase III gene, *MT-CO3).* Quantification of this amplicon gives an estimation of the total NcirDNA and McirDNA concentration, respectively. For the quantification of NcirDNA, we amplified of a 67 bp-length sequence of the KRAS gene with the following primers: forward (5′ CCTTGGGTTTCAAGTTATATG 3′) and reverse (5′ CCCTGACATACTCCCAAGGA 3′). For McirDNA, we amplified a 67 bp-length sequence of the cytochrome oxidase sub-unit 3 mitochondrial gene with the following primers: forward (5′ GACCCACCAATCACATGC 3′) and reverse (5′ TGAGAGGGCCCCTGTTAG 3′). These primers were designed using the Primer 3 software according to the following requirements: (i) T_m ranging from 50 to 64 °C; (ii) GC-content between 40 and 60%; (iii) size from 18 to 23 NT; (iv) amplicon size ranging from 60 to 100 bp. We performed local-alignment analyses with the BLAST program to confirm the specificity of the designed primers. All sequences were checked for self- or inter-molecular annealing with nucleic-acid-folding software (Mfold and oligoAnalyzer 1.2). Oligonucleotides were synthesized and HPLC-purified by Eurofins (Ebersberg, Germany) and quality control of the oligonucleotides was performed by MALDI-TOF. For all analyses, negative controls and standard curves were used. All tests are performed in triplicate with 5 µl of DNA extract in a 25 µl reaction volume, on a CFX96 instrument using CFX manager software (Bio-Rad). This method (qPCR, primer design, program) and technical validation have been described previously[25]. The mCRC patient's blood samples were excluded if the total cirDNA concentration, due to a problem of pre-analytic treatment or even for unknown reasons, was below a quality threshold.

The DNA concentration quality threshold was 3 ng/mL (about 900 copies/mL) for cancer patients. Note, this value corresponds to about the half of the median concentration found for healthy individuals (N = 104, median NcirDNA concentration = 5.43 ng/mL of plasma corresponding to 1645 copies/mL). In addition to quantifying cirDNA by targeting two different sequences on two different chromosomes, an experiment based on Poisson law distribution showed the accuracy of our cirDNA amount measurement (Supplementary Fig. S8). It should be noted that our Q-PCR systems enable the detection of a single genome copy (Supplementary Table S4), and that we have previously shown that targeting a DNA sequence of the same size or longer than the input DNA fragment produced a similar PCR yield[61]. The measurement of the total cirDNA concentration by targeting a *KRAS* sequence was routinely controlled by quantifying a *BRAF* sequence. Control quality is acceptable when the *KRAS*-based value is 1.3 to 1.8-fold higher than that of the *BRAF*-based value when using the reported Q-PCR primer systems; otherwise, a second analysis is performed. Note, *BRAF* analysis data from 33 healthy individuals were not available. In addition, we excluded 26 patient plasmas (17 mCRC and 9 healthy) in which the *KRAS*/*BRAF* ratio was over 3 or below 0.5. Data revealed that the *KRAS*-based concentration value was positively correlated with the *BRAF*-based concentration values in the 62 healthy individuals (Spearman analysis; r = 0.762, *P value* < *0.0001*) and in the 101 mCRC patients (Spearman analysis; r = 0.882, *P value* < *0.0001*) (Supplementary Fig. S9). We already addressed this issue in our previous report (Spearman analysis; r = 0.966, *P value* < *0.001*)[25].The *KRAS* and *BRAF* genes are monogenic and poorly amplified in both healthy and cancer individuals[62]. Supplementary section figures present NcirDNA concentration determined from targeting *BRAF* with using a primer set of similar size. Data revealed that the same observations could be made: the NcirDNA amount, as determined using *BRAF* sequence targeting, is statistically different in healthy (N = 62) and mCRC individuals (N = 101) (Supplementary Fig. S10; Mann-Whitney U test, *P value* < *0.0001*), and fully correlates with our observation based on *KRAS* sequence targeting. We may therefore indicate that amplification of the *KRAS* gene will not have any influence on the observations and conclusions made in this study. Valtorta *et al.* detected *KRAS* amplification in 7/1,039 (0.67%) evaluable CRC specimens, demonstrating that *KRAS* amplification is an infrequent event in CRC[28]. Thus this level will not modify significantly the observations or values described in our manuscript.

CirDNA calibration assay. *NcirDNA.* A genomic DNA extract from human wild-type *KRAS* colorectal cells was used for the NcirDNA calibration assay. Initial genomic DNA solution concentration and purity were determined by measuring optic density at λ = 260 nm, 230 nm and 280 nm, with an Eppendorf BioPhotometer® D30. Starting genomic DNA concentration was adjusted to 1800 pg/µl for the first dilution point, according to optic density measurement at λ = 260 nm. A qPCR standard curve was obtained by 6 successive dilutions of the vector solution (1800, 180, 45, 20, 10 and 5 pg/µl). The standard curve was used to determine the NcirDNA concentration of the mCRC patients and healthy individuals and calculate the NcirDNA copy number per milliliter of plasma.

McirDNA. A 3382-pb human ORF vector with a 786-pb *MT-CO3* insert was obtained from ABM good® (accession no.YP_003024032) and used for the McirDNA calibration assay. Initial vector solution concentration

and purity were determined by measuring optic density at λ = 260 nm, 230 nm and 280 nm, with an Eppendorf BioPhotometer® D30. Starting vector concentration was adjusted at 1800 pg/µl for the first dilution point, according to optic density measurement at λ = 260 nm. A qPCR standard curve was obtained by 6 successive dilutions of the vector solution (1800, 180, 45, 20, 10 and 5 pg/µl). The standard curve was used to determine the McirDNA concentration of the mCRC patients and healthy individuals and calculate the McirDNA copy number per milliliter of plasma.

CirDNA copy number calculation. *NcirDNA.* NcirDNA copy number per milliliter of plasma, in all analyses, was determined with the following calculation:

$$Qnuclear = \left(\frac{c}{3,3}\right) * \left(\frac{Vélution}{Vplasma}\right)$$

$Q_{nuclear}$ is the NcirDNA copy number per milliliter, c is the NcirDNA concentration (pg/µl) determined by qPCR targeting the nuclear *KRAS* gene sequence and 3.3 pg is the human haploid genome mass. $V_{elution}$ is the volume of cirDNA extract (µl) and V_{plasma} is the volume of plasma used for the extraction (ml).

McirDNA. McirDNA copy number per milliliter of plasma, in all analyses, was determined with the following calculation:

$$Qmito = \left(\frac{c * Na}{2 * MW * Lvector}\right) * \left(\frac{Vélution}{Vplasma}\right)$$

$Q_{mitochondrial}$ is the McirDNA copy number per milliliter, 'c' is the McirDNA mass concentration (g/µl) determined by a qPCR targeting the mitochondrial *MT-CO3* gene. N_A is Avogadro's number ($6.02 * 10^{23}$ molecules per mole), L_{vector} is the plasmid length (nucleotides) and MW is the molecular weight of one nucleotide (g/mol). $V_{elution}$ is the elution volume of cirDNA extract (µl) and V_{plasma} is the volume of plasma used for the extraction (ml).

Statistical analysis. For continuous variables, median and range were computed. To investigate their associations with the biologic parameters, univariate statistical analyses were performed using Mann-Whitney U test or Kruskal-Wallis rank test for continuous variables. Moreover, multivariate analyses were carried out using logistic regressions, with a stepwise selection procedure, to investigate known predictive. Odds ratio (OR) with 95% confidence intervals (CIs) are presented. The power of analysis was reduced due to all patients did not have measurements for all variables. All P values reported are two sided. A probability of ≤ 0.05 was considered to be statistically significant; $*p \leq 0.05$, $**p \leq 0.01$, $***p \leq 0.001$, $****p \leq 0.0001$. Statistical analysis was performed using the STATA 13.1 software (Stata Corporation, College Station, TX).

Data Availability

The datasets used and/or analyzed during the current study are available from the corresponding author on reasonable request.

References

1. Mandel, P. & Metais, P. [Not Available]. *C. R. Seances Soc. Biol. Fil.* **142**, 241–243 (1948).
2. Malik, A. N. *et al.* Altered circulating mitochondrial DNA and increased inflammation in patients with diabetic retinopathy. *Diabetes Res. Clin. Pract.* **110**, 257–265 (2015).
3. Dhondup, Y. *et al.* Low Circulating Levels of Mitochondrial and High Levels of Nuclear DNA Predict Mortality in Chronic Heart Failure. *J. Card. Fail.* **22**, 823–828 (2016).
4. Timmermans, K., Kox, M., Scheffer, G. J. & Pickkers, P. Plasma Nuclear and Mitochondrial DNA Levels, and Markers of Inflammation, Shock, and Organ Damage in Patients with Septic Shock. *Shock Augusta Ga* **45**, 607–612 (2016).
5. Zhang, S. *et al.* Elevated plasma cfDNA may be associated with active lupus nephritis and partially attributed to abnormal regulation of neutrophil extracellular traps (NETs) in patients with systemic lupus erythematosus. *Intern. Med. Tokyo Jpn.* **53**, 2763–2771 (2014).
6. Lam, N. Y. L., Rainer, T. H., Chan, L. Y. S., Joynt, G. M. & Lo, Y. M. D. Time course of early and late changes in plasma DNA in trauma patients. *Clin. Chem.* **49**, 1286–1291 (2003).
7. Yaros, M. J. S. A. L. Free DNA in the Serum of Cancer Patients and the Effect of Therapy. *Cancer Research* **37**, 647 (1977).
8. Zachariah, R. R. *et al.* Levels of circulating cell-free nuclear and mitochondrial DNA in benign and malignant ovarian tumors. *Obstet. Gynecol.* **112**, 843–850 (2008).
9. Mahmoud, E. H., Fawzy, A., Ahmad, O. K. & Ali, A. M. Plasma Circulating Cell-free Nuclear and Mitochondrial DNA as Potential Biomarkers in the Peripheral Blood of Breast Cancer Patients. *Asian Pac. J. Cancer Prev. APJCP* **16**, 8299–8305 (2015).
10. Gautschi, O. *et al.* Circulating deoxyribonucleic Acid as prognostic marker in non-small-cell lung cancer patients undergoing chemotherapy. *J. Clin. Oncol. Off. J. Am. Soc. Clin. Oncol.* **22**, 4157–4164 (2004).
11. Lo, Y. M. *et al.* Presence of fetal DNA in maternal plasma and serum. *Lancet Lond. Engl.* **350**, 485–487 (1997).
12. Lo, Y. M. *et al.* Quantitative analysis of fetal DNA in maternal plasma and serum: implications for noninvasive prenatal diagnosis. *Am. J. Hum. Genet.* **62**, 768–775 (1998).
13. Lo, Y. M. Fetal DNA in maternal plasma: biology and diagnostic applications. *Clin. Chem.* **46**, 1903–1906 (2000).
14. Thierry, A. R., Messaoudi, S. E., Gahan, P. B., Anker, P. & Stroun, M. Origins, structures, and functions of circulating DNA in oncology. *Cancer Metastasis Rev.* **35**, 347–376 (2016).
15. Stroun, M., Lyautey, J., Lederrey, C., Olson-Sand, A. & Anker, P. About the possible origin and mechanism of circulating DNA apoptosis and active DNA release. *Clin. Chim. Acta Int. J. Clin. Chem.* **313**, 139–142 (2001).
16. Aucamp, J. *et al.* Kinetic analysis, size profiling, and bioenergetic association of DNA released by selected cell lines in vitro. *Cell. Mol. Life Sci.* **74**, 2689–2707 (2017).
17. Franceschi, C. Inflammaging as a Major Characteristic of Old People: Can It Be Prevented or Cured? *Nutr. Rev.* **65**, S173–S176 (2007).

18. Pinti, M. *et al.* Circulating mitochondrial DNA increases with age and is a familiar trait: Implications for 'inflamm-aging'. *Eur. J. Immunol.* **44**, 1552–1562 (2014).
19. Hsu, F.-C. *et al.* Association between inflammatory components and physical function in the health, aging, and body composition study: a principal component analysis approach. *J. Gerontol. A. Biol. Sci. Med. Sci.* **64**, 581–589 (2009).
20. Franceschi, C. & Campisi, J. Chronic Inflammation (Inflammaging) and Its Potential Contribution to Age-Associated. *Diseases. J. Gerontol. Ser. A* **69**, S4–S9 (2014).
21. Tóth, K. *et al.* Circadian Rhythm of Methylated Septin 9, Cell-Free DNA Amount and Tumor Markers in Colorectal Cancer Patients. *Pathol. Oncol. Res.* **23**, 699–706 (2017).
22. El Messaoudi, S., Rolet, F., Mouliere, F. & Thierry, A. R. Circulating cell free DNA: Preanalytical considerations. *Clin. Chim. Acta Int. J. Clin. Chem.* **424**, 222–230 (2013).
23. Parpart-Li, S. *et al.* The Effect of Preservative and Temperature on the Analysis of Circulating Tumor DNA. *Clin. Cancer Res.* **23**, 2471–2477 (2017).
24. Schmidt, B. & Fleischhacker, M. Is liquid biopsy ready for the litmus test and what has been achieved so far to deal with pre-analytical issues? *Transl. Cancer Res.* **7**, S130–S139 (2017).
25. Mouliere, F., El Messaoudi, S., Pang, D., Dritschilo, A. & Thierry, A. R. Multi-marker analysis of circulating cell-free DNA toward personalized medicine for colorectal cancer. *Mol. Oncol.* **8**, 927–941 (2014).
26. Kloten, V. *et al.* Liquid biopsy in colon cancer: comparison of different circulating DNA extraction systems following absolute quantification of KRAS mutations using Intplex allele-specific PCR. *Oncotarget* **8**, 86253–86263 (2017).
27. Chiu, R. W. K. *et al.* Quantitative analysis of circulating mitochondrial DNA in plasma. *Clin. Chem.* **49**, 719–726 (2003).
28. Valtorta, E. *et al.* KRAS gene amplification in colorectal cancer and impact on response to EGFR-targeted therapy. *Int. J. Cancer* **133**, 1259–1265 (2013).
29. Ye, W. *et al.* Accurate quantitation of circulating cell-free mitochondrial DNA in plasma by droplet digital PCR. *Anal. Bioanal. Chem.* **409**, 2727–2735 (2017).
30. van der Drift, M. A. *et al.* Circulating DNA is a non-invasive prognostic factor for survival in non-small cell lung cancer. *Lung Cancer Amst. Neth.* **68**, 283–287 (2010).
31. Hao, T. B. *et al.* Circulating cell-free DNA in serum as a biomarker for diagnosis and prognostic prediction of colorectal cancer. *Br. J. Cancer* **111**, 1482–1489 (2014).
32. Kim, K. *et al.* Circulating cell-free DNA as a promising biomarker in patients with gastric cancer: diagnostic validity and significant reduction of cfDNA after surgical resection. *Ann. Surg. Treat. Res.* **86**, 136–142 (2014).
33. Jylhävä, J. *et al.* Aging is associated with quantitative and qualitative changes in circulating cell-free DNA: the Vitality 90+ study. *Mech. Ageing Dev.* **132**, 20–26 (2011).
34. Zhong, X. Y., Hahn, S., Kiefer, V. & Holzgreve, W. Is the quantity of circulatory cell-free DNA in human plasma and serum samples associated with gender, age and frequency of blood donations? *Ann. Hematol.* **86**, 139–143 (2007).
35. Jylhävä, J. *et al.* Characterization of the role of distinct plasma cell-free DNA species in age-associated inflammation and frailty. *Aging Cell* **12**, 388–397 (2013).
36. Cercek, A., Siegel, C. L., Capanu, M., Reidy-Lagunes, D. & Saltz, L. B. Incidence of Chemotherapy-Induced Amenorrhea in Premenopausal Women Treated With Adjuvant FOLFOX for Colorectal Cancer. *Clin. Colorectal Cancer* **12**, 163–167 (2013).
37. Wan, J., Gai, Y., Li, G., Tao, Z. & Zhang, Z. Incidence of Chemotherapy- and Chemoradiotherapy-Induced Amenorrhea in Premenopausal Women With Stage II/III Colorectal Cancer. *Clin. Colorectal Cancer* **14**, 31–34 (2015).
38. Hohaus, S. *et al.* Cell-free circulating DNA in Hodgkin's and non-Hodgkin's lymphomas. *Ann. Oncol. Off. J. Eur. Soc. Med. Oncol. ESMO* **20**, 1408–1413 (2009).
39. Kohler, C. *et al.* Levels of plasma circulating cell free nuclear and mitochondrial DNA as potential biomarkers for breast tumors. *Mol. Cancer* **8**, 105 (2009).
40. Stroun, M., Anker, P., Lyautey, J., Lederrey, C. & Maurice, P. A. Isolation and characterization of DNA from the plasma of cancer patients. *Eur. J. Cancer Clin. Oncol.* **23**, 707–712 (1987).
41. Aucamp, J., Bronkhorst, A. J., Badenhorst, C. P. S. & Pretorius, P. J. A historical and evolutionary perspective on the biological significance of circulating DNA and extracellular vesicles. *Cell. Mol. Life Sci. CMLS* **73**, 4355–4381 (2016).
42. Rago, C. *et al.* Serial Assessment of Human Tumor Burdens in Mice by the Analysis of Circulating DNA. *Cancer Res.* **67**, 9364–9370 (2007).
43. Tanos, R. & Thierry, A. R. Clinical relevance of liquid biopsy for cancer screening. *Transl. Cancer Res.* **7**, S105–S129 (2018).
44. Mengel-From, J. *et al.* Mitochondrial DNA copy number in peripheral blood cells declines with age and is associated with general health among elderly. *Hum. Genet.* **133**, 1149–1159 (2014).
45. Nile, D. L. *et al.* Age-Related Mitochondrial DNA Depletion and the Impact on Pancreatic Beta Cell Function. *Plos One* **9** (2014).
46. Short, K. R. *et al.* Decline in skeletal muscle mitochondrial function with aging in humans. *Proc. Natl. Acad. Sci. USA* **102**, 5618–5623 (2005).
47. Ellinger, J., Müller, S. C., Wernert, N., von Ruecker, A. & Bastian, P. J. Mitochondrial DNA in serum of patients with prostate cancer: a predictor of biochemical recurrence after prostatectomy. *BJU Int.* **102**, 628–632 (2008).
48. Ellinger, J. *et al.* Circulating mitochondrial DNA in serum: a universal diagnostic biomarker for patients with urological malignancies. *Urol. Oncol.* **30**, 509–515 (2012).
49. Xia, P. *et al.* Decreased mitochondrial DNA content in blood samples of patients with stage I breast cancer. *BMC Cancer* **9**, 454 (2009).
50. Zhong, X. Y. *et al.* Elevated level of cell-free plasma DNA is associated with breast cancer. *Arch. Gynecol. Obstet.* **276**, 327–331 (2007).
51. Chatterjee, A., Mambo, E. & Sidransky, D. Mitochondrial DNA mutations in human cancer. *Oncogene* **25**, 4663–4674 (2006).
52. Yu, M. Generation, function and diagnostic value of mitochondrial DNA copy number alterations in human cancers. *Life Sci.* **89**, 65–71 (2011).
53. Kang, Q. *et al.* Comparative analysis of circulating tumor DNA stability In K3EDTA, Streck, and CellSave blood collection tubes. *Clin. Biochem.* **49**, 1354–1360 (2016).
54. El Messaoudi, S. *et al.* Circulating DNA as a Strong Multimarker Prognostic Tool for Metastatic Colorectal Cancer Patient Management Care. *Clin. Cancer Res.* **22**, 3067–3077 (2016).
55. Medina Diaz, I. *et al.* Performance of Streck cfDNA Blood Collection Tubes for Liquid Biopsy Testing. *PloS One* **11**, e0166354 (2016).
56. Boquist, S. *et al.* Alimentary Lipemia, Postprandial Triglyceride-Rich Lipoproteins, and Common Carotid Intima-Media Thickness in Healthy, Middle-Aged Men. *Circulation* **100**, 723–728 (1999).
57. Truong, V. *et al.* Blood triglyceride levels are associated with DNA methylation at the serine metabolism gene PHGDH. *Sci. Rep.* **7**, 11207 (2017).
58. Larsen, L. F., Bladbjerg, E.-M., Jespersen, J. & Marckmann, P. Effects of Dietary Fat Quality and Quantity on Postprandial Activation of Blood Coagulation Factor VII. *Arterioscler. Thromb. Vasc. Biol.* **17**, 2904–2909 (1997).
59. Thierry, A. R. *et al.* Clinical utility of circulating DNA analysis for rapid detection of actionable mutations to select metastatic colorectal patients for anti-EGFR treatment. *Ann. Oncol. Off. J. Eur. Soc. Med. Oncol.* **28**, 2149–2159 (2017).
60. Thierry, A. R. *et al.* Clinical validation of the detection of KRAS and BRAF mutations from circulating tumor DNA. *Nat. Med.* **20**, 430–435 (2014).

61. Sanchez, C., Snyder, M. W., Tanos, R., Shendure, J. & Thierry, A. R. New insights into structural features and optimal detection of circulating tumor DNA determined by single-strand DNA analysis. *Npj Genomic Med.* **3**, 31 (2018).
62. Corcoran, R. B. *et al.* BRAF Gene Amplification Can Promote Acquired Resistance to MEK Inhibitors in Cancer Cells Harboring the BRAF V600E Mutation. *Sci Signal* **3**, ra84–ra84 (2010).
63. Catarino, R. *et al.* Circulating DNA: diagnostic tool and predictive marker for overall survival of NSCLC patients. *PloS One* **7**, e38559 (2012).
64. Bedin, C. *et al.* Diagnostic and prognostic role of cell-free DNA testing for colorectal cancer patients. *Int. J. Cancer* **140**, 1888–1898 (2017).

Acknowledgements
We are grateful to A. Bauer and B. Ottolini for their help. We would like to thank the clinical investigators from the Kplex2 study: J.L. Raoul, R. Guimbaud, D. Pezet, P. Artru, E. Assenat, C. Borg, M. Mathonnet, C. De La Fouchardière, O. Bouché, and C. Gavoille for collecting the blood samples. The authors would like to thank Kevin Billings and Streck for providing the Cell-Free DNA BCT CE tubes. This work was supported by the INSERM (Institut National de la Santé et de la Recherche Médicale), Lilly (France), and the SIRIC Montpellier Grant (INCa-DGOS Inserm 6045), France.

Author Contributions
R.M. and A.R.T. designed the study, developed the methodology, analyzed the data and prepared the manuscript. R.M., Z.A.A.D., A.O., R.T., B.P., C.S., J.A., G.T., S.A. and S.E.M. realized the experiments. R.M., S.T. and C.M. performed the statistical analysis. All of the authors (R.M., Z.A.A.D., S.T., A.O., R.T., B.P., C.S., J.A., G.T., S.A., C.M., A.A., S.E.M., P.B. and A.R.T.) discussed the results and approved the manuscript.

Additional Information
Supplementary information accompanies this paper at https://doi.org/10.1038/s41598-019-41593-4.

Competing Interests: The authors declare no competing interests.

Publisher's note: Springer Nature remains neutral with regard to jurisdictional claims in published maps and institutional affiliations.

C/ Le sang contient des mitochondries libres circulantes

Auteurs : Zahra Al Amir Dache, Amaëlle Otandault, Rita Tanos, **Brice Pastor**, Romain Meddeb, Cynthia Sanchez, Giuseppe Arena, Laurence Lasorsa, Andrew Bennett, Thierry Grange, Safia El Messaoudi, Thibault Mazard, Corinne Prevostel, Alain R. Thierry

Cette publication a été publiée dans The Faseb Journal en 2019

Résumé: Les mitochondries sont considérées comme les unités de production d'énergie de la cellule en raison de leur rôle clé dans le métabolisme énergétique et la signalisation cellulaire. Cependant, les composants mitochondriaux peuvent être trouvés dans l'espace extracellulaire, sous forme de fragments ou encapsulés dans des vésicules. En outre, il a été récemment signalé que cet organite intact est libéré par les plaquettes exclusivement dans des conditions spécifiques. Ici, nous démontrons pour la première fois, que la préparation sanguine avec des plaquettes au repos, contient des mitochondries fonctionnelles entières dans un état physiologique normal. De même, nous montrons que des cellules normales et tumorales en culture sont capables de sécréter leurs mitochondries. En utilisant la centrifugation ou la filtration en série, suivie de méthodes basées sur la réaction en chaîne par polymérase, et le séquençage du génome entier, nous détectons l'ADN mitochondrial extracellulaire complet dans des particules de plus de 0,22 µm contenant des protéines spécifiques de la membrane mitochondriale. Nous identifions ces particules comme des mitochondries intactes exemptes de cellules en utilisant l'analyse de triage cellulaire activé par fluorescence, la microscopie à fluorescence et la microscopie électronique à transmission. L'analyse de la consommation d'oxygène a révélé que ces mitochondries sont compétentes sur le plan respiratoire. Compte tenu du potentiel des mitochondries dans le transfert intercellulaire décrit précédemment, cette découverte pourrait élargir considérablement le champ d'application de la biologie de la communication intercellulaire. D'autres étapes devraient être développées pour étudier le rôle potentiel des mitochondries en tant qu'organite de signalisation à l'extérieur de la cellule et pour déterminer si ces unités circulantes pourraient être utiles pour la détection précoce et le pronostic de diverses maladies.

Contribution: J’ai participé à la réalisation de certaines expériences ainsi qu’à la discussion des résultats.

Received: 29 July 2019 | Revised: 27 November 2019 | Accepted: 29 November 2019

DOI: 10.1096/fj.201901917RR

RESEARCH ARTICLE

THE FASEB JOURNAL

Blood contains circulating cell-free respiratory competent mitochondria

Zahra Al Amir Dache[1] | Amaëlle Otandault[1] | Rita Tanos[1] | Brice Pastor[1] | Romain Meddeb[1] | Cynthia Sanchez[1] | Giuseppe Arena[2] | Laurence Lasorsa[1] | Andrew Bennett[3] | Thierry Grange[3] | Safia El Messaoudi[1] | Thibault Mazard[1] | Corinne Prevostel[1] | Alain R. Thierry[1]

[1]IRCM, Institut de Recherche en Cancérologie de Montpellier, INSERM U1194, Université de Montpellier, Institut régional du Cancer de Montpellier, Montpellier, France

[2]Gustave Roussy Cancer Campus, INSERM U1030, Villejuif 94805, France

[3]Institut Jacques Monod, Université Paris Diderot, Paris, France

Correspondence
Alain R. Thierry, IRCM, INSERM, U1194, 208 rue des Apothicaires, Montpellier Cedex 5, 34298, France.
Email: alain.thierry@inserm.fr

Funding information
SIRIC Montpellier Grant, Grant/Award Number: INCa-DGOS-Inserm 6045; Institut National de la Santé et de la Recherche Médicale

Abstract

Mitochondria are considered as the power-generating units of the cell due to their key role in energy metabolism and cell signaling. However, mitochondrial components could be found in the extracellular space, as fragments or encapsulated in vesicles. In addition, this intact organelle has been recently reported to be released by platelets exclusively in specific conditions. Here, we demonstrate for the first time, that blood preparation with resting platelets, contains whole functional mitochondria in normal physiological state. Likewise, we show, that normal and tumor cultured cells are able to secrete their mitochondria. Using serial centrifugation or filtration followed by polymerase chain reaction-based methods, and Whole Genome Sequencing, we detect extracellular full-length mitochondrial DNA in particles over 0.22 μm holding specific mitochondrial membrane proteins. We identify these particles as intact cell-free mitochondria using fluorescence-activated cell sorting analysis, fluorescence microscopy, and transmission electron microscopy. Oxygen consumption analysis revealed that these mitochondria are respiratory competent. In view of previously described mitochondrial potential in intercellular transfer, this discovery could greatly widen the scope of cell-cell communication biology. Further steps should be developed to investigate the potential role of mitochondria as a signaling organelle outside the cell and to determine whether these circulating units could be relevant for early detection and prognosis of various diseases.

KEYWORDS

blood, circulating DNA, mitochondria, mitochondrial genome, respiratory competent

Abbreviations: 16gP, 16 000g pellet; ACD-A, anticoagulant citrate dextrose solution A; bp, base pair; BSA, bovine serum albumin; cfDNA, cell-free deoxyribonucleic acid; CCCM, centrifuged cell culture media; CTAD, citrate–theophylline–adenosine–dipyridamole; DAMPs, damage associated molecular patterns; DII, DNA integrity index; DNA, deoxyribonucleic acid; EDTA, ethylenediaminetetraacetic acid; EM, electron microscopy; F, filtrated; FACS, fluorescence-activated cell sorting (FACS); FCCP, carbonyl cyanide-4-(trifluoromethoxy) phenylhydrazone; FSC, forward scatter; HEPES, 2-[4-(2-hydroxyethyl) piperazin-1-yl] ethanesulfonic acid; HS, high speed; IM, isolated mitochondria; Kbp, kilo base pair; LR, long range; LS, low speed; MAS, mitochondrial assay solution; McfDNA, mitochondrial cell-free deoxyribonucleic acid; MIB, mitochondrial isolation buffer; NcfDNA, nuclear cell-free deoxyribonucleic acid; NF, non filtrated; OCR, oxygen consumption rate; PBS, phosphate-buffered saline; PCR, polymerase chain reaction; PPAP, protocol precluding activation of platelets; Q-PCR, quantitative polymerase chain reaction; ROS, reactive oxygen species; SSC, side scatter; TFAM, transcription factor A, mitochondrial; TIM 23, translocase of inner membrane 23; TMPD, N, N, N′, N′-tetramethyl-p-phenylenediamine; TOM 22, translocase of outer membrane 22; WGS, whole genome sequencing.

1 | INTRODUCTION

The presence of mitochondria in unicellular to mammalian organisms originates from an ancient symbiosis between primitive eukaryotic cells and free-living aerobic prokaryotes.[1,2] Mitochondria are crucial organelles for central cell functions,[3] and they are the principal nutrient-up-taking and energy-producing cell organelle; they also take part in calcium signaling, reactive oxygen species (ROS) production, cell death, and diverse cell signaling events.[4-7] Mitochondria have retained many of their ancestral bacterial features including length, proteome, double membrane, and circular genome.[8]

Cell-derived mitochondrial components, including mitochondrial DNA, have been found in the extracellular space.[9,10] Those deoxyribonucleic acid (DNA) fragments were found in the physiological circulating fluid of healthy subjects and patients with various diseases.[11] Lately, mitochondrial cell-free DNA (McfDNA) has emerged as an attractive circulating biomarker due to its potential role in diagnostic applications in multiple diseases (eg, Diabetes, acute myocardial infarction, cancer…),[12-14] and in physio-pathological conditions (eg, trauma).[15] Despite the promising future of McfDNA in clinical applications, knowledge regarding its origin, composition, and function is still lacking. In addition, the structure of McfDNA is currently unknown. In contrast, the structure of circulating DNA of nuclear origin is being characterized[16] and mono and di- nucleosomes and, to a lesser extent, transcription factors are found as stabilized cell-free DNA (cfDNA)-associated structures in the blood-stream.[17,18] It is expected that there are important configuration differences between nuclear and mitochondrial circulating DNA, since mitochondrial DNA is a small circular genome, without protective histones, and thus is more sensitive to degradation in the circulation. However, by revealing recently that there are approximately 50 000-fold more copies of the mitochondrial genome than the nuclear genome in the plasma of healthy individuals,[19] we confirmed that McfDNA is sufficiently stable to be detected and quantified,[12,20] implying the presence of stable structures protecting these DNA molecules.

The present study aims at identifying the structures containing mitochondrial DNA in peripheral blood. By examining McfDNA integrity, and associated structure size and density, we revealed the presence of stable particles with full-length mitochondrial genomes. We characterized the structures by fluorescence and electron microscopy (EM), flow cytometry, and we identified the presence of intact mitochondria in the circulation. Oxygen consumption assays suggested the functional viability of at least some of these extracellular mitochondria. Our work demonstrates for the first time the presence in blood of circulating cell-free respiratory competent mitochondria. Overall, in view of the potential roles of mitochondria in cell to cell communication, immune response, and inflammation, our discovery has broad implications in homeostasis and disease, and paves the way for new paths toward the treatment and prevention of diseases.

2 | MATERIALS AND METHODS

2.1 | Plasma isolation

Blood samples from healthy volunteers were provided by the "Etablissement Français du Sang (E.F.S)," the blood transfusion center of Montpellier, France (Convention EFS-PM N° 21PLER2015-0013). Blood samples from 50 mCRC patients were provided by a clinical study comparing the detection of *KRAS* exon 2 and *BRAF* V600E mutations by cfDNA analysis to conventional detection by tumor tissue analysis. All blood samples were processed within 4 hours after collection. Plasma was extracted by various protocols, depending on the experiments.

2.1.1 | For healthy individuals

Plasma isolation using Ficoll

Fresh blood was collected in EDTA tubes. Plasma was isolated by a Ficoll density-gradient centrifugation, performed at 400 *g* for 30 minutes at 18°C (Ficoll paque plus GE Healthcare, Fisher Scientific, Illkirch, France).

Plasma isolation by centrifugation

Fresh blood was collected in EDTA tubes. Plasma was isolated by a single centrifugation, performed at 1200 *g* for 10 minutes at 4°C.[21]

Plasma isolation without platelet activation

Fresh blood was collected in a BD Vacutainer citrate–theophylline–adenosine–dipyridamole (CTAD) tubes (Ozyme, Montigny-le-Bretonneux, France). Plasma was isolated via differential centrifugations, all performed for 10 minutes at room temperature without a break: two successive centrifugations were first performed at 200 *g* and were followed by a third centrifugation at 300 *g*. Preheated (37°C) anticoagulant Citrate Dextrose Solution A (ACD-A) buffer (0.1 M Trisodium citrate, 0.11 M Glucose and 0.08 M citric acid) and Prostaglandin E1 (1 μM) (Sigma-Aldrich, St. Quentin Fallavier Cedex) were then added to the plasma, which was further centrifuged at 1100 *g* and finally at 2500 *g*.

2.1.2 | For mCRC patients

Blood was collected in Ethylenediaminetetraacetic acid (EDTA) tubes, and plasma was isolated by a single centrifugation, performed at 1200 *g* for 10 minutes at 4°C.

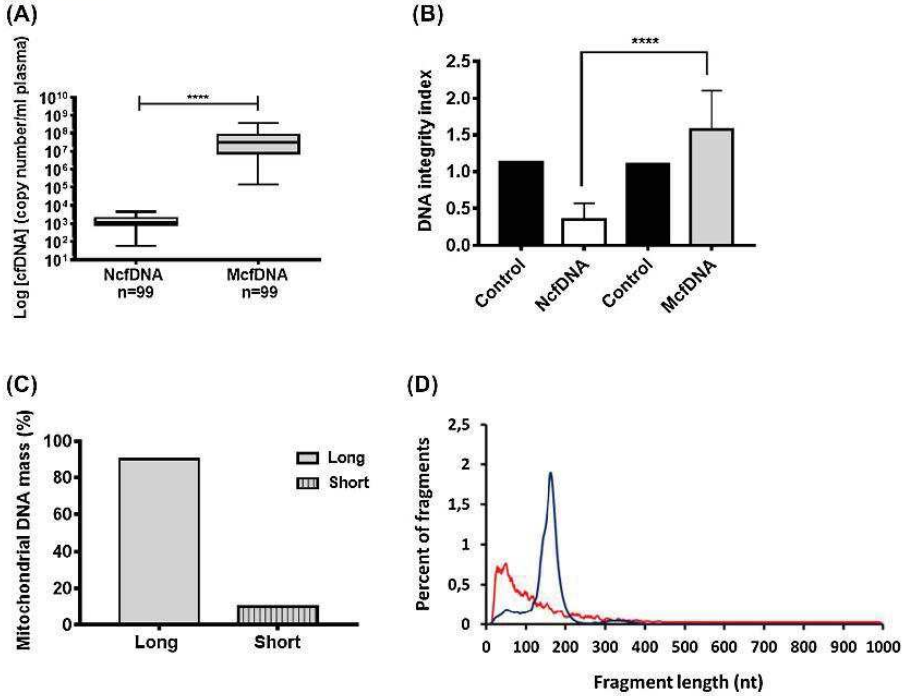

FIGURE 1 Plasma of healthy individuals contain a population of cell-free mitochondrial DNA that is well preserved and not fragmented. A, NcfDNA and McfDNA quantification in plasma samples of 99 healthy individuals. McfDNA copy number is significantly higher than that of NcfDNA ($P < .0001$). The lines inside the boxes and the upper and lower limits of the boxes indicate the median, 75th and 25th percentiles, respectively. The upper and lower horizontal bars indicate the maximum and minimum values, respectively. B, NcfDNA and McfDNA integrity index calculated for plasma samples of 13 healthy individuals, demonstrating that almost all the quantified McfDNA have a main size above 300 bp, and are less fragmented than NcfDNA ($P < .0001$). C, Size fractionation following agarose gel electrophoresis of a pool of cfDNA extracts obtained from 80 healthy individuals' plasma. McfDNA fragments were quantified by q-PCR from extracts of the excised agarose gel slices above (Long) and below (Short) 500 bp. D, DNA fragment size profile at single base resolution obtained by paired-end massively parallel WGS of cfDNA extracted from a healthy individual's plasma. (Blue for NcfDNA and red for McfDNA)

2.2 | Cell lines

Human colon cancer cell lines (DLD-1/SW620) were obtained from the American type culture collection (ATCC) and a normal immortalized cell line (CCD-18Co) was obtained from Andrei Turtoi's laboratory (IRCM, Montpellier, France). SW620 and CCD-18Co cells were grown in RPMI 1640 and DLD-1 cells in DMEM (Gibco, Fisher Scientific, Illkirch, France), both supplemented with 10% fetal bovine serum (Eurobio, les Ulis, France) and 1X streptomycin/penicillin (Gibco, Fisher Scientific, Illkirch, France). Cell culture, for all cell lines, was performed at 37°C in 5% CO_2.

1.5 million cells were seeded in a T-75 flask with 10 mL of appropriate supplemented medium. Cells were incubated for either 24 hours or 60 hours. Culture media were replaced with fresh medium 24 hours before experiments. Collected media from cultured cells were centrifuged at 600 *g* for 10 minutes at 4°C, to precipitate both floating cells and cells debris, and were further processed by various protocols, depending on the experiments.

2.3 | Quantification of nuclear cell-free DNA (NcfDNA) and mitochondrial cell free DNA (McfDNA) in healhy individuals and cancer patients

NcfDNA and McfDNA in healthy individuals (Figures 1A,B and S2A), and in mCRC patients (Figures S1 and S2B) were quantified from a plasma supernatant obtained following the first centrifugation step mentioned before at 1200 *g* for 10 minutes at 4°C and a second centrifugation step at 16 000 *g* for 10 minutes at 4°C. Following this centrifugation, total cfDNA was extracted from supernatant and analyzed with quantitative polymerase chain reaction (q-PCR).

2.4 | Kinetic study of cfDNA stability

First, SW620 and DLD-1 culture medium was removed after 24 hours of culture, centrifuged at 1200 *g*, and then at 16 000 *g* for 10 minutes, both at 4°C, and further incubated at 37°C in 5% CO_2 for 4 days. An aliquot of cell culture supernatant (400 µL) was withdrawn every day for DNA extraction. NcfDNA and McfDNA were quantified by q-PCR using specific primers (*KRAS* F2 and *KRAS* R1 for NcfDNA, MIT MT-CO3 F, and MIT MT-CO3 R2 for McfDNA) (Table S1).

2.5 | cfDNA extraction

Cell-free DNA was extracted with a Qiagen Blood Mini Kit (Qiagen, Courtaboeuf, France) according to the manufacturer's recommendations, except that extraction was performed with 1mL of plasma sequentially loaded on a single column and that the cfDNA was eluted with 130 µL of elution buffer. The cfDNA was stored at −20°C for further analysis. Freeze-thawing was avoided to reduce cfDNA fragmentation.

2.6 | Q-PCR analysis

Cell-free DNA was quantified by q-PCR according to an innovative design of short (60–100 bp ± 10 bp) and long (300 bp ± 10 bp) amplicons targeting the wild-type sequences of specific genes: the *KRAS* nuclear gene and the mitochondrial Cytochrome oxidase III gene, MT-CO3 (Table S1). Quantification of the short and long amplicons provides an estimation of the concentrations of the total NcfDNA and McfDNA. Q-PCR amplifications were performed in triplicate in a 25 µL final reaction volume controlled by the CFX manager software of a CFX96 touch Real-Time PCR detection system (Bio-Rad). Each polymerase chain reaction (PCR) reaction mixture was composed of 12.5 µL of SsoAdvanced Universal SYBR Green Supermix (Bio-Rad, Marnes-la-Coquette, France), 2.5 µL of nuclease-free water (Qiagen), 2.5 µL of forward and 2.5 µL reverse primers (3 pmoL/µL), and 5 µL of template. Thermal cycling conditions were as follows: 95°C (3:00) + [95°C (0:10) + 60°C (0:30)] × 40 cycles. Melting curves were investigated by increasing the temperature from 60°C to 90°C, reading the plate every 0.2°C. Each q-PCR run was performed with 1.8 ng/µL of genomic DNA extracted from the DiFi cell line (ATCC) for the standard curve and without DNA as the control condition. Q-PCR amplification was validated by melt curve differentiation.

2.7 | cfDNA calibration assay and copy number calculation

2.7.1 | NcfDNA quantification

A genomic DNA extract from human wild-type *KRAS* colorectal cells was used for the NcfDNA calibration assay. Initial genomic DNA solution concentration and purity were determined by measuring optic density at λ = 260, 230, and 280 nm, with an Eppendorf BioPhotometer D30. Starting genomic DNA concentration was adjusted to 1800 pg/µL for the first dilution point, according to optical density measurement at λ = 260 nm. A q-PCR standard curve was obtained by six successive dilutions of the vector solution (to 1800, 180, 45, 20, 10, and 5 pg/µL). The standard curve was used to determine the NcfDNA concentration per milliliter of plasma and cell media supernatant. The NcfDNA copy number was calculated as follows:

$$Q_{\text{nuclear}} = \left(\frac{c}{3.3}\right) \times \left(\frac{V_{\text{elution}}}{V_{\text{plasma}}}\right)$$

Q_{nuclear} is the NcfDNA copy number per milliliter; c is the NcfDNA mass concentration (pg/µL) determined by a q-PCR targeting the nuclear *KRAS* gene sequence and 3.3 pg is the human haploid genome mass. V_{elution} is the volume of cfDNA extract (µL) and V_{plasma} is the starting volume of plasma used for the extraction (mL).

2.7.2 | McfDNA quantification

A 3382-bp human ORF vector with a 786-bp MT-CO3 insert was obtained from ABM (accession no.YP_003024032) and used for the McfDNA calibration assay.

Initial vector solution testing, starting concentration adjustments and q-PCR standard curves were performed as for NcfDNA above.

The standard curve was used to determine the McfDNA concentration per milliliter of plasma and of cell media supernatant. The McfDNA copy number was calculated as follows:

$$Q_{\text{mito}} = \left(\frac{c \times \text{Na}}{2 \times \text{MW} \times Lvector}\right) \times \left(\frac{V_{\text{elution}}}{V_{\text{plasma}}}\right)$$

$Q_{\text{mitochondrial}}$ is the McfDNA copy number per milliliter, "c" is the McfDNA mass concentration (g/µL) determined by q-PCR targeting the mitochondrial *MT-CO3* gene sequence. N_A is Avogadro's number (6.02×10^{23} molecules per mol), L_{vector} is the plasmid length (nucleotides), and MW is the molecular weight of one nucleotide (g/moL); V_{elution} is the elution volume of cfDNA extract (µL) and

V_{plasma} is the starting volume of plasma used for the extraction (mL).

2.8 | DNA integrity index calculation

The degree of cfDNA fragmentation was assessed simultaneously by targeting *KRAS* and MT-CO3 sequences from each plasma DNA sample and calculating the DII (DNA integrity index). The DII was determined by calculating the ratio of the concentration determined using the primer set amplifying a large target (*KRAS* F2/R1 and MT-CO3 F/R2) to the concentration determined using the primer set amplifying a short target (*KRAS* F1/R1 and MT-CO3 F/R1) (Table S1).

2.9 | Examination of the percentage of McfDNA short and long fragments

Cell-free DNA was extracted from a pool of 80 healthy individual's plasma, with the Maxwell RSC ccfDNA plasma kit (Promega, Charbonnières-les-Bains, France). To obtain highly concentrated cfDNA, extracts were subjected to a second extraction with the same method followed by a Qiamp DNA blood Mini Kit extraction resulting in a final volume of 30 µL. The samples were then electrophoresed on a 2% agarose gel and DNA fractions of short (<500 bp) and long (>500 bp) fragments were extracted from the gel with a QIAquick Gel extraction Kit (Qiagen). The quantity of mitochondrial DNA fragments was then assessed with q-PCR by using mitochondrial specific primer (MT-CO3 F/R1) (Table S1).

2.10 | Library preparation for whole genome sequencing

Dual-indexed single-stranded libraries were prepared from 1 to 11 ng human DNA using TL137 as a linker oligo.[22] To allow sequencing with single-stranded libraries, custom double-stranded adapters were generated, identical to those used in the single-stranded method, by annealing a short oligo SLP4.[23] Ligations were performed with an NEBNext Quick Ligation Module kit (New England Biolabs) with 0.04 µM of each annealed adapter in a 50 µL total volume, incubated for 30 minutes at 20°C. Adapters were elongated by adding 50 µL OneTaq 1× Master Mix (New England Biolabs) to the ligation mixture and incubating for 20 minutes at 60°C. All oligos were purchased from Eurogentec (Kaneka Eurogentec, Seraing, Belgium). Single-stranded libraries were quantified via q-PCR, with a diluted fraction, in a LightCycler 2 (Roche Applied Science, Mannheim, Germany). Samples were then amplified using Taq polymerase and an optimal number of cycles for each sample to avoid plateau phase, as calculated from the Ct of the diluted q-PCR. Amplified samples were then purified by two rounds of Macherey-Nagel NGS beads at 1.3× volume, to retain shorter inserts, and eluted in 30 µL EBT. Purified libraries were then visualized on a Bioanalyzer 2100 (Agilent, Santa Clara, CA) and quantified via q-PCR, Qubit 2 Fluorometer (Life Technologies, Grand Island, NY), and Bioanalyzer 2100. Libraries were then pooled in equimolar amounts and sequenced on an Illumina MiSeq platform using two MiSeq v3 150 (2 × 75) kits, with sequencing primer CL72 replacing the first read sequencing primer.

2.11 | Sequence analysis

Adapter sequences were removed with cutadapt 1.3[24] and reads were aligned to the human genome reference (hg19) with BWA aln[25] using the default parameters and filtered for mapping quality 20 with SAMtools 1.5.[26] Duplicate removal and histogram generation was performed with MarkDuplicates and CollectInsertSizeMetrics, respectively, from Picard tools 1.88.

2.12 | Differential centrifugation and filtration of plasma and cell media

Schematic view and details are presented in Figure S6.

2.13 | Isolation of intracellular mitochondria

Mitochondria from cultured cells were isolated as a positive control. Cells were scraped from culture dishes, washed with phosphate-buffered saline (PBS) and centrifuged at 1300 rpm for 5 minutes at room temperature. Pelleted cells were resuspended in 1 mL of mitochondrial isolation buffer (MIB) (0.2 M sucrose, 0.01 M tris, 0.001 M EGTA, 1X protease inhibitor) and gently lysed using an IKA T18 Basic Dispersers Homogenizer (Ultraturrax) at speed 2 for 10 seconds until obtaining 80%-90% intact nuclei. Lysed cells were then centrifuged at 600 *g* at 4°C for 10 minutes to remove cell debris and nuclei, to recover supernatant containing both cytoplasm and mitochondria. Pelleted intact nuclei were washed twice in 1ml MIB and centrifuged again at 600 *g* for 10 minutes at 4°C, to be used as a negative control in experiments with flow cytometry, while the resulting supernatants were pooled together with the previous supernatants to further isolate mitochondria. For this, the 3 mL of supernatant were centrifuged at 600 *g* at 4°C for 10 minutes to eliminate contaminating nuclei and cell debris. The resulting supernatant was then further centrifuged at 8000 *g* for 10 minutes at 4°C to pellet mitochondria. The supernatant was collected again and

centrifuged again at 8000 *g* for 10 minutes at 4°C. These pellets were pooled together and gently resuspended in 500 µL MIB, transferred to 1.5 mL tubes and centrifuged again at 8000 *g* for 10 minutes at 4°C. The final supernatant was carefully discarded to collect the pelleted mitochondria.

2.14 | Isolation of extracellular mitochondria

Mitochondria in the plasma, extracted by Ficoll gradient, were isolated by sequential centrifugations at 600 *g*, then 1200 *g* and finally 2000 *g* for 10 minutes at 4°C to remove any contaminating blood cells or platelets. The resulting supernatant was centrifuged at 16 000 *g* to collect the extracellular mitochondria pellet.

Mitochondria in the plasma obtained without platelet activation were pelleted by a one-step centrifugation at 16 000 *g* for 10 minutes at 4°C.

Mitochondria in the cell media supernatant were isolated by sequential centrifugations at 600 *g*, then 1200 *g* for 10 minutes at 4°C to remove any contaminating cells. The pellet of extracellular mitochondria was collected from a subsequent centrifugation at 16 000 *g*.

Note that an extracellular mitochondrial pellet was also recovered from a centrifugation at 8000 *g* instead of 16 000 *g* to protect the mitochondrial membrane.

2.15 | Amplification of the mitochondrial genome

The DNA extracted from cell media pellets (40 flask T-75/cell line), and from two different plasma pools (without platelet activation) pellets was selectively amplified with the Repli-g mitochondrial DNA kit (Qiagen), according to the manufacturer's recommendations. The amplified mitochondrial genome was then amplified by long range (LR) PCR performed in a 50 µL total volume in a Mastercycle nexus eco thermal cycler (Eppendorf). Each PCR reaction mixture was composed of 30.5 µL of free water (Qiagen), 5 µL of 10× LA PCR Buffer II (Mg^{2+} plus), 8 µL of dNTPs (2.5 mM each), 5 µL of mixed forward and reverse primers (10 µM each), 1 µL of template (DNA mass between 10 and 100 ng, calculated with a Qubit broad range kit), and 0.5 µL of TAKARA LA Taq (5 U/µL) (Ozyme, Saint Quentin Yvelines, France). Thermal cycling conditions were as follows: 95°C (2:00) + [95°C (0:15) + 68°C (10:00)] × 30 cycles + 68°C (20:00) + 4°C (∞). PCR amplifications were performed with five pairs of overlapping primers (Mito1/Mito2/Mito3/hmt1/hmt2) (Integrated DNA Technologies, Leuven, Belgium). All PCR amplified products were loaded on a 0.8% agarose gel to check the size of amplicons with reference to the 1Kb plus DNA ladder (Thermo Fischer).

2.16 | Mitochondrion staining

The 16 000 *g* pellets (16gP) from both, the plasma without platelet activation (pool from 5 healthy individuals) and from the cell media (2 flask T-75/ cell line), were stained with 200 nM MitoTracker Green FM (Thermofisher) for 45 minutes, washed twice with PBS, and resuspended in 10 µL of PBS to be visualized by ApoTome microscopy (ZEISS Axio Imager 2). Images were edited with ZEN Software. In parallel, cell culture media pellets (8 T-75 flask/cell line), Ficoll-isolated plasma pellet and positive and negative controls were resuspended in 150 µL of PBS and analyzed by Gallios flow cytometry (Beckman Coulter). Mitochondria isolated from cultured cells were used as a positive control for the MitoTracker specificity and as a standard to delineate both the appropriate gate and voltages for the flow cytometry. All sample plots were collected according to size (Forward scatter FSC) and granularity (side scatter SSC) in logarithmic mode. Voltages were adjusted for submicron particles and the flow rate was set at "low." Doublets were excluded by plotting FSC-Area vs FSC-Height, both in logarithmic mode. Collected events in the newly created gate were gated as singlet. Following confirmation that all events recorded in this gate were MitoTracker Green positive, the gate was applied to all samples. Plot histograms were created for both unstained and stained samples. Results were analyzed with Kaluza analysis 1.5 software.

2.17 | Western blot

Pellets obtained at 8000 *g* from both the plasma (pool of 5 healthy individuals) and the cell media supernatant (100 flask T-75/cell line) were resuspended in 50 µL of 1X Laemli buffer, loaded on a 12% Acrylamide/Bis-Acrylamide gel and transferred onto nitrocellulose membranes (GE Healthcare). Membranes were blocked in 10% milk in 1X PBS-tween for 1h. Blotting was performed with either 1/500 diluted primary mouse anti-TOM22 (Sigma, St. Quentin Fallavier Cedex) or with 1/1000 diluted primary mouse anti-TIM23 (BD Transduction Laboratorie, France) antibodies over-night at 4°C and further with 1/10 000 diluted HRP-conjugated secondary Rabbit anti-mouse antibodies (Merck, Île-de-France, France) for 1h at room temperature. Immunoblots were visualized by ECL (Perkin Elmer, Villebon sur Yvette, France).

2.18 | Electron microscopy

The 8000 *g* pellets from either cell media (30 flask T-75/cell line) or plasma prepared without platelet activation (pool from 3 healthy individuals) were immersed in a solution of 2.5% glutaraldehyde in PHEM buffer (1X, pH 7.4) overnight at

4°C, washed in PHEM and post-fixed in 0.5% osmic acid for 2 hours in the dark at room temperature. Samples were then washed twice in PHEM buffer, dehydrated in a graded series from 30% to 100% ethanol solutions and finally embedded in EmBed 812 using an Automated Microwave Tissue Processor for Electronic Microscopy (Leica EM AMW). 70nm sections (Leica-Reichert Ultracut E), collected at different levels of each block, were counterstained, with 1.5% uranyl acetate in 70% Ethanol and lead citrate, and observed with a Tecnai F20 transmission electron microscope at 200 kV.

2.19 | Metabolic activity

Mitochondrial bioenergetics function was determined by oxygen consumption rate (OCR), with a Seahorse XF-96 extracellular flux analyzer (Agilent). We performed the electron flow assay that allows the functional assessment of selected mitochondrial complexes together in the same period. After isolation, 64 µg of freshly isolated DLD-1 mitochondria (positive control), and 64 µg of DLD-1 cell media pellet and plasma pool pellet prepared without platelets activation, were plated in each well in a volume of 25 µL containing MAS 1× (70 mM sucrose, 220 mM mannitol, 10 mM KH_2PO_4, 5 mM $MgCl_2$, 2 mM HEPES, 1 mM EGTA, and 0.2% fatty acid-free BSA, pH 7.2) supplemented with 10 mM pyruvate, 2 mM malate and 4 µM Carbonyl cyanide-4-(trifluoromethoxy) phenylhydrazone (FCCP). Note, pyruvate and malate drive respiration via complex I, and FCCP uncouples the mitochondrial function. The XF plate was then centrifuged for 20 minutes at 2000 *g* at 4°C. After centrifugation, 155 µL of electron flow substrate-containing 1×MAS was added to each well, and the plate was warmed up in a 37°C non-CO_2 incubator for 5-10 minutes. About 10-fold concentrated compounds were loaded in the ports of the cartridge, using the "loading helper" plate: port A, 20 µL of 20 µM rotenone, a complex I inhibitor (2 µM final); port B, 22 µL of 100 mM succinate, a complex II activator (10 mM final); port C, 24 µL of 40 µM Antimycin A, a complex III inhibitor (4 µM final); port D, 26 µL of 100 mM ascorbate plus 1 mM TMPD, complex IV activator (10 mM and 100 µM final, respectively). After calibration of the cartridge by the XF machine, the XF plate was introduced and the assay continued using Agilent's protocol for isolated mitochondria (IM).

2.20 | Statistical analysis

Statistical analysis was performed with GraphPad Prism software (version 7.01). A probability of ≤.05 was considered to be statistically significant by Student's *t* test: $*P \leq .05$, $**P \leq .01$, $***P \leq .001$, $****P \leq .0001$.

3 | RESULTS

3.1 | Mitochondrial cell-free DNA size distribution and stability

Mitochondrial cell-free DNA is sufficiently stable to be detected and quantified in plasma (Figures 1A, S1A, S2). However, mitochondrial DNA (16 kilo base pairs [kbp]) was thought to be more susceptible to degradation and less stable than nuclear DNA because of its lack of histones. In our initial investigation, we found, to our surprise, that McfDNA fragments over 300 base pairs (bp) are actually more stable than NcfDNA fragments (>300 bp), in fetal bovine serum supplemented culture medium (Figure 2). To establish mitochondrial genome cell-free DNA integrity, we determined the DNA integrity index (DII), we previously used for the study of NcfDNA fragmentation,[27] and data revealed that all

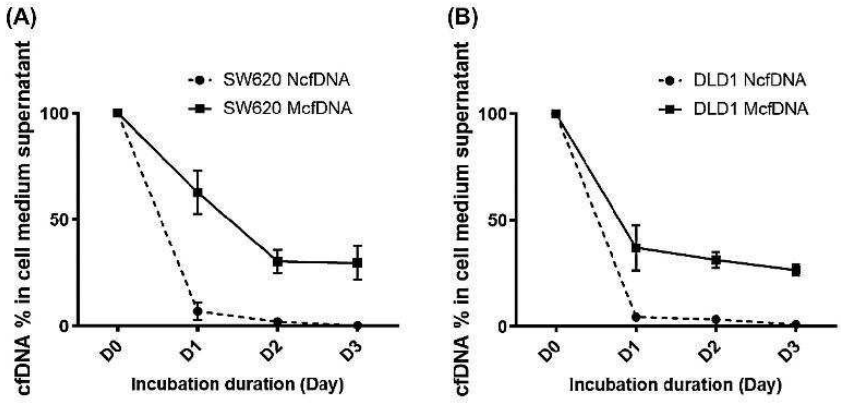

FIGURE 2 Kinetic study of NcfDNA and McfDNA stability in cell culture media. The evaluation of the stability of cfDNA (NcfDNA and McfDNA) derived from SW620 (A) and DLD-1 (B) cell culture media over time independently of the cells. NcfDNA and McfDNA concentration was measured using q-PCR, by amplifying an amplicon of 305 bp and 296 bp, respectively. (D: day)

or most McfDNA fragments are over 300 bp, in contrast to NcfDNA (Figures 1B and S1B). We next examined a plasma DNA extract pool, from 80 healthy humans, by agarose gel electrophoresis and q-PCR. Approximately 10% only of the McfDNA mass in healthy samples, were composed of fragments below 500 bp (Figure 1C).

Whole Genome Sequencing of healthy plasma revealed a wide-size ranging population of short mitochondrial DNA fragments mainly decreasing in abundance from 30 to 300 nucleotides. In contrast, NcfDNA had a more homogenous distribution, conventionally peaking at 167 bp, corresponding to mono-nucleosomes (Figure 1D).[17,28] Paired-end sequencing enables high-resolution measurement of DNA size but has a practical upper limit of readout at ~1000 bp. Since no McfDNA was detected between 500 bp and 1000 bp, Whole Genome Sequencing only detected the minor fraction formerly revealed by gel electrophoresis (Figure 1C).

Data suggest that McfDNA contain at least two populations: one minor composed of highly degraded fragments from 30 to 300 bp, and one major composed of DNA of length higher than 1000 bp. Intimate examination of the whole genome sequencing (WGS) resulting reads indicates that ≈ 63% of the McfDNA fragments below 300 bp ranged between 67 and 300 bp. When combining WGS data and Q-PCR based measurement of the fractionation assay, we could determine that only 5% of the total mass of McfDNA are below 67 bp. We therefore set out to characterize the structural elements that stabilize mitochondrial DNA over 1000 bp in the circulation.

3.2 | Plasma and cell culture media contain McfDNA in dense structures larger than 0.22 μm

We next used differential centrifugation of plasma to separate the different structures associated with cell-free nuclear and mitochondrial DNAs. First, we isolated the plasma from whole blood at 400 *g* on a ficoll gradient. This was followed by incremental centrifugations at 16, 40, and 200 000 *g* to remove the large organelles and remaining membrane debris, the micro-vesicles and finally the exosomes, respectively (Figure S6). Q-PCR of the resulting supernatant revealed, surprisingly, that McfDNA is packed in denser structures than NcfDNA (Figure 3A-C).

We therefore sought to further confirm our surprising result, that 16 000 *g* centrifugation precipitated large amounts of mitochondrial DNA but very little nuclear DNA, by performing a refined plasma isolation protocol that precludes platelet activation, based on sequential centrifugations at increasing strengths: 2 × 200 *g*, 300 *g*, 1100 *g*, 2500 *g*, and 16 000 *g*, each for 10 minutes at 20°C with no break in-between. Note, this protocol excludes blood cells from the final plasma preparation without activating or degrading them in the process[29,30] (Figure 3A) and this sequence (series) of centrifugations was used in all the following work described here. Notably, in the final plasma preparation, the nuclear DNA passed through a 0.22 μm filter whereas the mitochondrial DNA did not (Figures 3A,D,E and S3A-C). No statistically significant variation in NcfDNA content occurs, in contrast to McfDNA contents showing up to 7-fold difference when using these various procedures (Figure 3D,E); this demonstrated that mitochondrial DNA detected in plasma are included in cell-free structures and that plasma preparation is devoid of nucleated blood cells.

Next, we sought to completely eliminate the possibility that mitochondria or free mitochondrial DNA is actively released into the plasma by platelets, during handling of the blood samples. Therefore, we repeated all the above analysis on culture media supernatants from various cancer and normal cell lines, DLD-1, SW620, and CCD-18CO, and again here the McfDNA was sedimented at 16 000 *g* (Figures 3B and S4A-C), and was retained on 0.22 μm filters (Figure S3D,E). 73% ± 11% and 78% ± 15% of the McfDNA precipitated into the pellet from the cell culture supernatant and plasma, respectively (Figures 3C, S4C and Table S2). It has to be noted that mitochondria are between 0.4 and 1.5 microns in diameter and the conventional speed used for their sedimentation is between 7000 and 20 000 *g*. Mitochondrial DNA in the 16gP of cell culture media was not degraded by DNase I treatment, in contrast to nuclear DNA (Figure S4D). Overall, these experiments demonstrate that plasma and cell culture media contain McfDNA in dense and stable structures above 0.22 μm, excluding platelets as its source.

3.3 | Both plasma and cell culture media contain structures with full-length mitochondrial genomes

We next investigated the integrity of the mitochondrial DNA in the 16gP of two different plasma pools and in DLD-1 and SW620 culture media. After Highly Uniform Whole Mitochondrial Genome Amplification of the DNA extracts, we used long-range PCR with five mitochondria-specific primer sets (Figure 4A).[31] While no signal was detected in the negative controls, agarose gel electrophoresis sizing clearly revealed the expected mitochondrial amplicons from the cell media and plasma 16gP, thus demonstrating the presence of intact full-length mitochondrial DNA in cell culture media and in healthy individuals plasma (Figure 4B), consistent with the high integrity index of plasma mitochondrial DNA in Figure 1B.

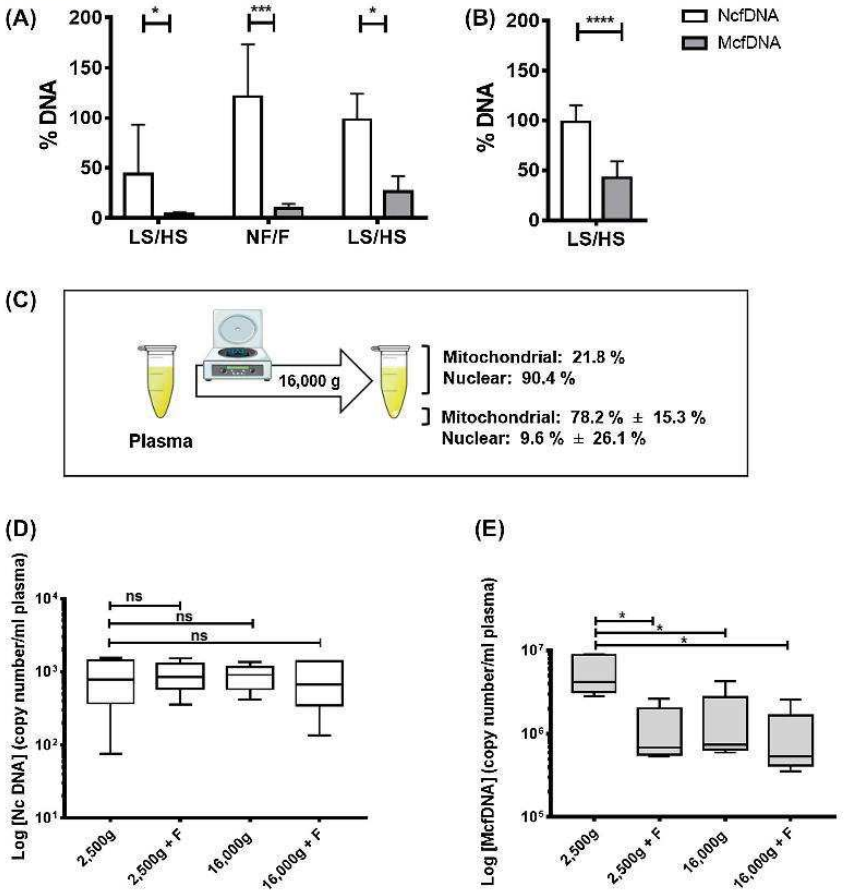

FIGURE 3 Plasma of healthy individuals and cell culture media contain structures enclosing mitochondrial cell-free DNA. A, cfDNA content following three different subsequent treatments of plasma: (i) by high-speed centrifugation, (ii) by filtration (0.22 μM) in Ficoll isolated plasma, and (iii) by high-speed centrifugation in plasma isolated by a protocol precluding activation of platelets (PPAP). LS and HS, low and high-speed centrifugation at 16 000 *g*; NF and F, nonfiltered and filtered plasma (Figure S4); n = 8 $P = .0630$, n = 7 $P = .0009$, and n = 4 $P = .0173$, respectively. B, Decrease of the cfDNA content in the DLD-1/SW620/CCD-18Co cell culture media after an initial low-speed (LS, 600 *g*) and a subsequent high-speed centrifugation (HS, 16 000 *g*). (Methods and Figure S4). n = 28. $P < .0001$. C, Proportion of NcfDNA and McfDNA plasma contents after treatment of PPAP plasma (Table S2). n = 4. D, NcfDNA copy number in healthy individuals' plasma prepared under PPAP and subsequently filtered and/or centrifuged at either 2500 or 16 000 *g* (n = 5). E, McfDNA copy number in healthy individuals' plasma prepared under PPAP and subsequently filtred and/or centrifuged at either 2500 or 16 000 *g*. n = 5, $P = .0111$, $P = .0114$, $P = .0115$, respectively

3.4 | Both plasma and cell culture media contain structurally intact mitochondria

To test for the presence of structurally intact mitochondria or material derived from mitochondria in plasma, we used the specific live mitochondrial marker, Mitotracker green, on the 16gP derived from cell cultures media and the plasma of five healthy individuals. Positively labeled mitochondria were specifically observed by Fluorescence microscopy in all biological sources (Figure 6A-C). In addition, Flow cytometry analysis was performed on the Mitotracker green-stained preparations. Nuclei (Figures 5B and S5B) and mitochondria (Figures 5A and S5A), purified from the DLD-1 and SW620 cells, were included as negative and positive control, respectively.

The 16gP from fresh cell media was also used as a negative control (Figures 5C and S5C). Similarly to the positive control, fluorescence signals were detected in the 16gP of both cell culture media (Figures 5D,E and S5D,E) and plasma (Figures 5F and S5F-I), indicating the presence of mitochondria. In addition, immunoblotting revealed the presence of the outer and inner membrane mitochondrial transport proteins, Translocase of outer membrane 22 (TOM 22) and Translocase of inner membrane 23 (TIM 23), in the 16gP from the DLD-1, SW620, and CCD-18Co cell culture media and the plasma supernatants (Figure 5G,H).

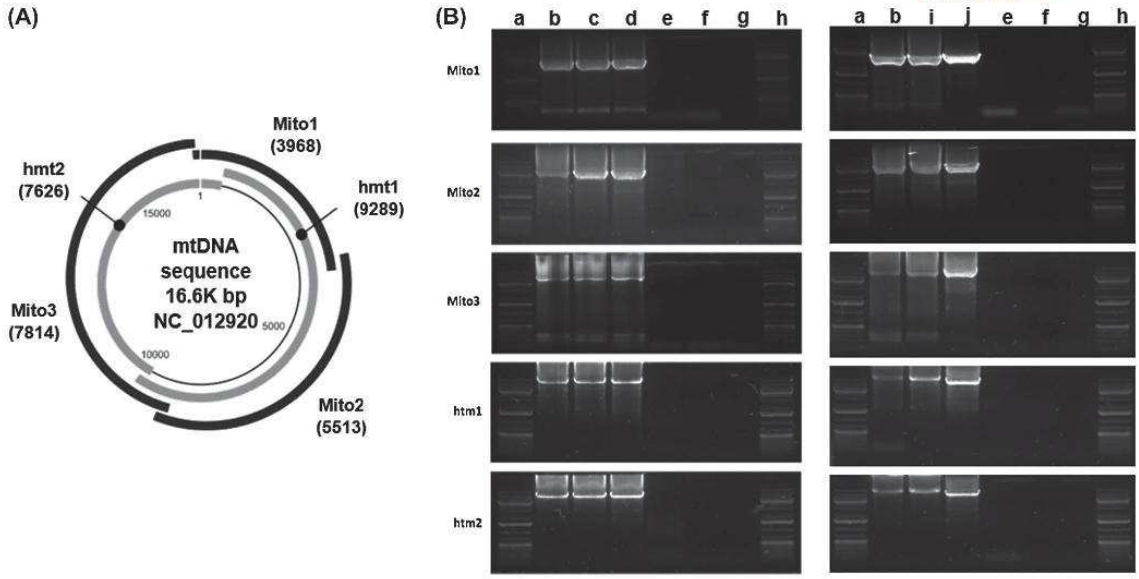

FIGURE 4 Plasma of healthy individuals and cell culture media contain structures enclosing whole intact mitochondrial genome. A, Adapted schematic view of the Long-range (LR) PCR amplification strategy for testing mitochondrial genome integrity. Overlapping amplicons amplify the whole mitochondrial genome by using the two htm1 and htm2 sequences or the three mito1, mito2, and mito3 sequences. B, Agarose gel analysis of LR-PCR amplified mitochondrial DNA demonstrating the presence of a preserved cell free mitochondrial genome in cell culture media and plasma pellet. Extracted DNA from isolated mitochondria from SW620 cells (lane b, positive control), the 16 000 *g* pellet (16gP) from the SW620 cells culture medium (lane c), the 16gP from the DLD-1 cells culture medium (lane d), a mouse genomic DNA (lane e, negative control), the Repli-g mitochondrial DNA kit's Water (lane f, negative control), the PCR water (lane g, negative control), the 16gP from two different plasma pools (lane i, j), were amplified using the repli-g mitochondrial DNA kit and the 5 sets of primers for the Mito1 (3968 bp), Mito2 (5513 bp), Mito3 (7814 bp) htm1 (9289 bp), and htm2 (7626 bp) amplicons. PCR-products analysis on a 0.8% agarose gel reveals the expected amplicons in the 16gP from cell culture media and from plasma, demonstrating the presence of a whole mitochondrial genome. No signal was detected in negative control. (Lanes a. Lane h, 1kbp DNA ladder)

To validate the presence of free intact mitochondria, we examined the pellet obtained from the cell culture media of DLD-1 and SW620, and from isolated plasma without platelet activation, by EM. Structures with a double membrane and a similar size to mitochondria were detected in all the samples (Figure 6D-F). The 16gP contained structures with all the morphological characteristics of mitochondria, including the inner and outer membranes and the corresponding intermembrane space and matrix. It has to be noted that not all these structures match perfectly the conventional morphology of mitochondria inside a cell. This is expected due to the various morphological alterations that mitochondria may undergo especially in different pathological conditions.[32]

3.5 | Both plasma and cell culture media contain respiratory competent mitochondria

To determine whether these mitochondria are functional, we evaluated the metabolic activity by measuring OCR with the Seahorse XF extracellular flux analyzer technology (Agilent). The electron flow assay clearly indicated that the pellets isolated from DLD-1 culture media, as well as from plasma pool of healthy individuals, consume oxygen and are sensitive to complex I inhibition by rotenone and to complex IV stimulation by ascorbate and N, N, N′, N′-tetramethyl-p-phenylenediamine (TMPD), suggesting that the extracellular mitochondria remain competent for respiration (Figure 7).

4 | DISCUSSION

To sum up, we report here that blood contains intact cell-free full-length mitochondrial DNA in dense and biologically stable structures over 0.22 μm in diameter and that these structures have specific mitochondrial proteins, double membranes and a morphology resembling that of mitochondria. We further demonstrate that these structurally intact cell-free mitochondria in the blood circulation are respiratory competent. We estimate that there are between 200 000 and 3.7 million cell-free intact mitochondria per mL

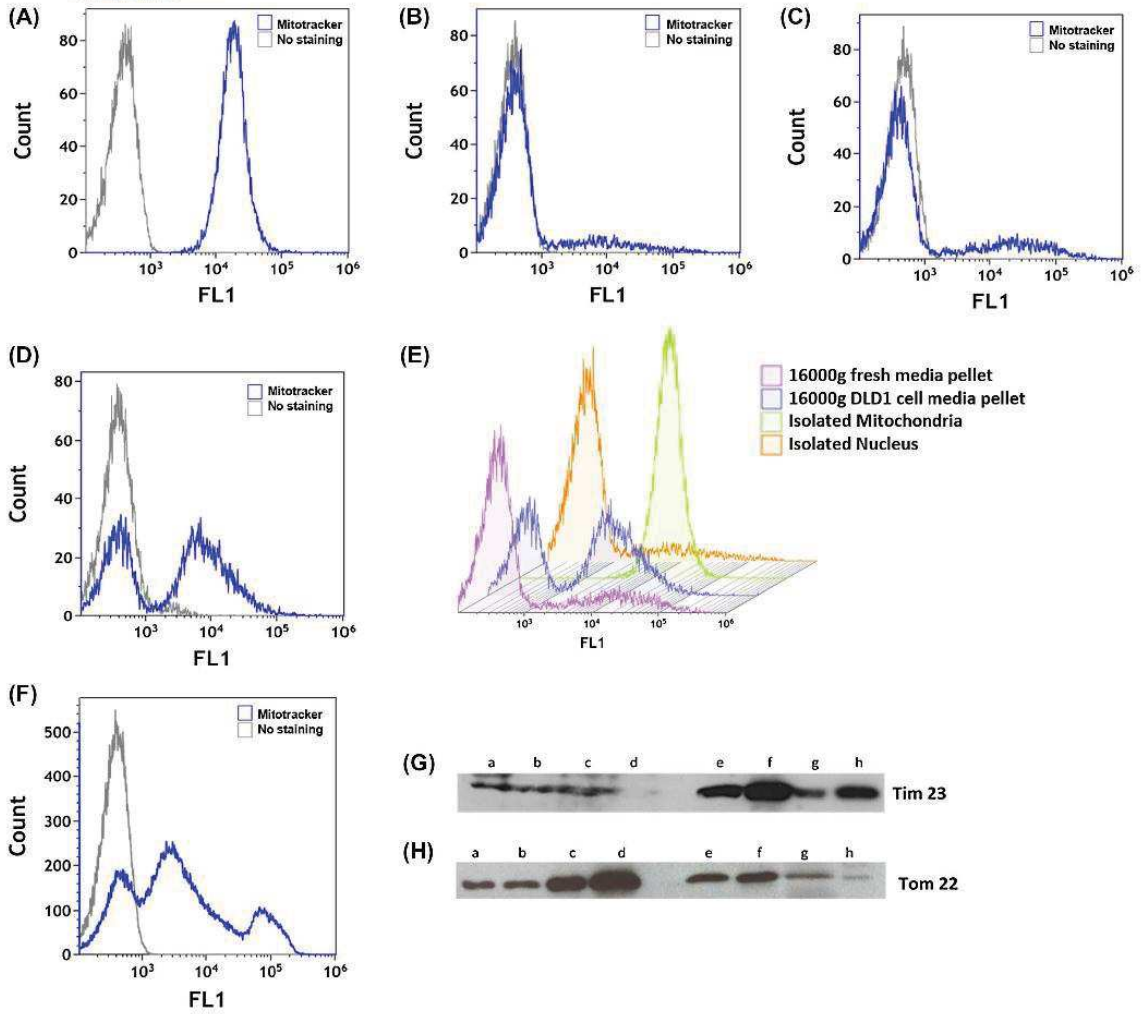

FIGURE 5 Both plasma of healthy individuals and cell culture media contain cell free mitochondrial material. Flow cytometry analysis of preparations stained with mitochondrial specific dye MitoTracker Green of A, Isolated mitochondria (IM) from DLD-1 cells (positive control); B and C, two negative controls: isolated nucleus and 16gP obtained from fresh cell media and; D, the 16gP isolated from DLD-1 centrifuged cell culture media (CCCM); E, the four previous samples; and F, the 16gP isolated from the plasma of an healthy donor. Results were analyzed with Kaluza analysis 1.5 software. Immunoblotting of membranes by labeling the inner (Tim 23) and outer (Tom 22) mitochondrial membrane proteins; G, Tim 23 (lane a: 16gP from PPAP plasma; lane b: 16gP from CCD-18Co CCCM; lane c: 16gP from SW620 CCCM; lane d: 16gP from DLD-1 CCCM; lane e: IM from CCD-18Co cells; lane f: IM from SW620 cells; lane g: IM from DLD-1 cells; lane h: IM from DLD-1 cells); H, Tom 22 (lane a: IM from DLD-1 cells; lane: IM from CCD-18Co cells; lane c: IM from SW620 cells; lane d: IM from SW620 cells; lane e: 16gP from DLD-1 CCCM; lane f: 16gP from CCD-18 Co CCCM; lane g: 16gP from SW620 CCCM; lane h: 16gP from PPAP plasma)

of plasma, based on the McfDNA copy number that was either pelleted at 16 000 *g* or filtered (Table S3). While several studies reported extracellular mitochondria in specific conditions resulting in platelet activation,[33] or encapsulated within microvesicles,[34] it is remarkable how the presence of intact cell-free mitochondria was unnoticed in normal physiological state. This could be explained by the high dilution of these organelles in the plasma and cell culture media. Note, our finding first corroborate previous collateral observations of plasma filtrates suggesting existence of particles containing mitochondrial DNA in the circulation.[10] Intact full mitochondrial genomes were also observed in the cell free DNA fraction of both healthy individuals and patients with mitochondrial disease. However, it was assumed that the circular

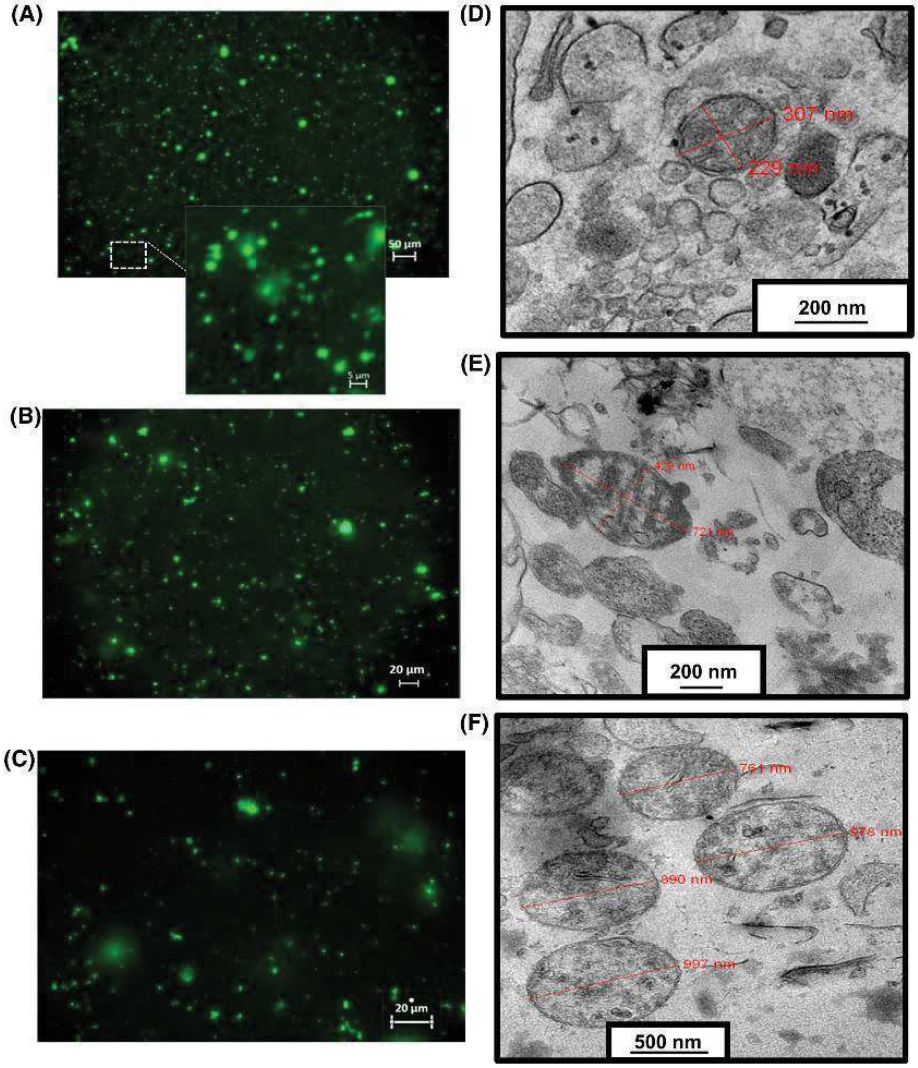

FIGURE 6 Both plasma of healthy individuals and cell culture media contain structurally intact mitochondria. Fluorescence microscopy images of the MitoTracker Green stained 16gP from PPAP plasma A, SW620 CCCM B, and DLD-1 CCCM C, Electron microscopy images of the 16gP from of a PPAP plasma D, SW620 CCCM E, and DLD-1 CCCM F.

nature of mitochondrial DNA delays its degradation by circulating nucleases, so the presence of intact mitochondria was not suspected and the structural characteristics associated with McfDNA were not investigated.[35]

In addition to observe by fractionation that a great part of mitochondrial DNA is associated to high size structures, we initially found striking differences between McfDNA and NcfDNA in respect to stability and size distribution. McfDNA is composed of, at least, two size-populations: one minor composed of fragments from 30 to 300 bp and one major composed of DNA of size higher than 1000 bp. We hypothesize, based on the exponential increase of McfDNA from 300 to 30 nucleotides, that the minor population represent DNA fragments in a dynamic degradation process.

All cell-free mitochondria in human plasma or cell culture media supernatant as observed by EM were not surrounded by a bi- or multi-layer phospholipid membrane. A few studies suggested that mitochondrial DNA could be encapsulated in extracellular vesicles such as exosomes and microvesicles, and act as efficient messengers in many biological systems.[34] One can speculate that the previously described biological effect of cell-free mitochondrial DNA enriched micro-particles could, as well, be performed by cell-free intact mitochondria as their presence in blood was not known before the study

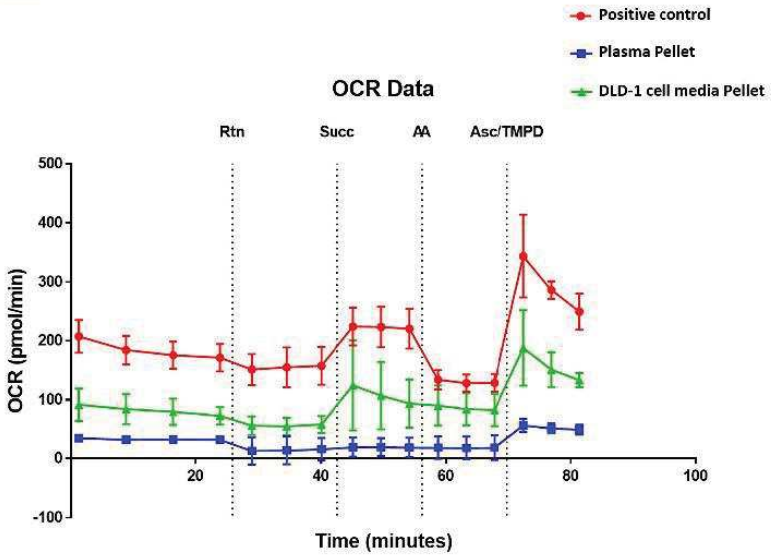

FIGURE 7 Both plasma of healthy individuals and cell culture media contain respiratory competent mitochondria. The electron flow experiment was performed using a seahorse XF96 instrument. Like the positive control (Isolated mitochondria from DLD-1), OCR was detectable in both 16gP from DLD-1 cell media and plasma pool, in the presence of pyruvate and malate that drive respiration via complex I. There was a decrease in OCR when rotenone was injected, indicating an inhibition of complex I-driven respiration. When complex II-driven respiration was initiated, by sequential addition of succinate, a slight increase in OCR was observed, indicating that complex II may be functional. The inhibition of complex III (antimycin A) and the stimulation of complex IV (ascorbate + TMPD), led to a detectable activity of cytochrome C/complex IV in all the samples. Each value shown was from a minimum of three replicates. The data are presented as mean (symbol) ± SD (line). The four injections are shown as dashed lines.

of Boudreau et al. and Puhm et al. on activated platelet and monocyte preparation.[33,36]

We believe that circulating cell-free intact mitochondria have crucial biological and physiological roles because mitochondria are already known as systemic messengers in cell-cell communication by transferring hereditary and nonhereditary constituents. Mitochondria were recently discovered to translocate from one cell to the other.[37] Indeed intercellular mitochondria trafficking was observed in vitro and in vivo, both in physiological and pathophysiological conditions including tissue injury and cancer.[38] In particular, the mitochondria transfer between differentiated and mesenchymal stem cells was observed in cardiomyocytes and endothelial cells as a means to rescue injured tissues.[39] Similarly, mitochondria are able to be internalized by different types of cells, by macro pinocytosis which is an endocytic pathway specific for large vesicles.[40] Clinical transplantation of mitochondria between cells is an active area of research but the specific mechanisms and critical factors involved in natural mitochondria transfer between the donor cells and recipient cells remain to be fully characterized.[41]

We speculate that mitochondrial clearance and degradation occurs principally by phagocytosis. This study is the first showing free structurally intact mitochondria in plasma, but it is not yet known how they are degraded there, in contrast to intracellular mitophagy, which is well described.[42] Presumably, mitochondria are degraded in plasma, and their content is released in the blood stream. Furthermore, it has been demonstrated that those organelles harbor many damage associated molecular patterns (DAMPs) including DNA, lipids, and metabolites, which are capable of activating immune cells and inducing an inflammatory response.[43,44] Our data demonstrate the presence of quintessential ancient symbiotic energy-providing component of all eukaryotic cells, the mitochondrion, as a previously unappreciated constituent of a critical organ, the blood. Further investigations are warranted to evaluate the impact and the potential implications of this discovery in the field of cell-cell communication, inflammation, and clinical applications.

ACKNOWLEDGMENTS

The authors would like to thank P. Blache, T. Salehzada, and C. Jay-Allemand for helpful comments. We are grateful to J. Venables (Science Sense) for help in editing the manuscript. We are grateful to the MRI platform (Montpellier Bio campus) for access to imaging facilities, and to METAMONTP platform for access to seahorse technology (M-L.Vignais). We thank B. Chabi (INRA, UMR 0866 DMEM Dynamique Musculaire et Métabolisme, Centre de recherche de Montpellier, Montpellier, France) for her contribution to the

oxygraph experiment. We thank A. Turtoi for providing us CCD-18Co cell line and reagents. ART is supported by the INSERM (Institut National de la Santé et de la Recherche Médicale).

CONFLICTS OF INTEREST

The authors declare no competing financial interests.

AUTHOR CONTRIBUTIONS

Z. Al Amir Dache, C. Prevostel, and A.R. Thierry designed the study, developed the methodology, analyzed the data and prepared the manuscript. Z. Al Amir Dache, A. Otandault, R. Tanos, B. Pastor, R. Meddeb, C. Sanchez, G. Arena, L. Lasorsa, A. Bennett, T. Grange, and S. El Messaoudi realized the experiments. All of the authors (Z. Al Amir Dache, A. Otandault, R. Tanos, B. Pastor, R. Meddeb, C. Sanchez, G. Arena, L. Lasorsa, A. Bennett, T. Grange, S. El Messaoudi, T. Mazard, C. Prevostel, and A.R. Thierry) discussed the results and approved the manuscript.

MATERIALS AND CORRESPONDENCE

The published article includes all data generated or analyzed during this study. Further information and requests for resources and reagents should be directed to and will be fulfilled by the Lead Contact: alain.thierry@inserm.fr.

REFERENCES

1. Roberts RG. Mitochondria—a billion years of cohabitation. *PLoS Biol*. 2017;15:e2002338.
2. Lane N, Martin W. The energetics of genome complexity. *Nature*. 2010;467:929-934.
3. Nunnari J, Suomalainen A. Mitochondria: in sickness and in health. *Cell*. 2012;148:1145-1159.
4. Rizzuto R, De Stefani D, Raffaello A, Mammucari C. Mitochondria as sensors and regulators of calcium signalling. *Nat Rev Mol Cell Biol*. 2012;13:566-578.
5. Wang C, Youle RJ. The role of mitochondria in apoptosis. *Annu Rev Genet*. 2009;43:95-118.
6. Tait SWG, Green DR. Mitochondria and cell signalling. *J Cell Sci*. 2012;125:807-815.
7. Murphy E, Ardehali H, Balaban RS, et al. Mitochondrial function, biology, and role in disease: a scientific statement from the american heart association. *Circ Res*. 2016;118:1960-1991.
8. Friedman JR, Nunnari J. Mitochondrial form and function. *Nature*. 2014;505:335-343.
9. Thierry AR, El Messaoudi S, Gahan PB, Anker P, Stroun M. Origins, structures, and functions of circulating DNA in oncology. *Cancer Metastasis Rev*. 2016;35:347-376.
10. Chiu RWK, Chan LYS, Lam NYL, et al. Quantitative analysis of circulating mitochondrial DNA in plasma. *Clin Chem*. 2003;49:719-726.
11. Yu M. Circulating cell-free mitochondrial DNA as a novel cancer biomarker: opportunities and challenges. *Mitochondrial DNA*. 2012;23:329-332.
12. Kohler C, Radpour R, Barekati Z, et al. Levels of plasma circulating cell free nuclear and mitochondrial DNA as potential biomarkers for breast tumors. *Mol Cancer*. 2009;8:105.
13. Malik AN, Parsade CK, Ajaz S, et al. Altered circulating mitochondrial DNA and increased inflammation in patients with diabetic retinopathy. *Diabetes Res Clin Pract*. 2015;110:257-265.
14. Sudakov NP, Popkova TP, Katyshev AI, et al. Level of blood cell-free circulating mitochondrial DNA as a novel biomarker of acute myocardial ischemia. *Biochemistry (Moscow)*. 2015;80:1387-1392.
15. Zhang Q, Itagaki K, Hauser CJ. Mitochondrial DNA is released by shock and activates neutrophils via p38 MAP kinase. *Shock*. 2010;34:55-59.
16. Otandault A, Anker P, Al Amir Dache Z, et al. Recent advances in circulating nucleic acids in oncology. *Ann Oncol*. 2019;30:374-384.
17. Sanchez C, Snyder MW, Tanos R, Shendure J, Thierry AR. New insights into structural features and optimal detection of circulating tumor DNA determined by single-strand DNA analysis. *npj Genomic Med*. 2018;3:31.
18. Snyder MW, Kircher M, Hill AJ, Daza RM, Shendure J. Cell-free DNA comprises an in vivo nucleosome footprint that informs its tissues-of-origin. *Cell*. 2016;164:57-68.
19. Meddeb R, Dache ZAA, Thezenas S, et al. Quantifying circulating cell-free DNA in humans. *Sci Rep*. 2019;9:5220.
20. Fliss MS. Facile detection of mitochondrial DNA mutations in tumors and bodily fluids. *Science*. 2000;287:2017-2019.
21. Meddeb R, Pisareva E, Thierry AR. Guidelines for the preanalytical conditions for analyzing circulating cell-free DNA. *Clin Chem*. 2019;65:623-633.
22. Gansauge M-T, Gerber T, Glocke I, et al. Single-stranded DNA library preparation from highly degraded DNA using *T4* DNA ligase. *Nucleic Acids Res*. 2017;45:e79.
23. Bennett EA, Massilani D, Lizzo G, Daligault J, Geigl E-M, Grange T. Library construction for ancient genomics: single strand or double strand? *Biotechniques*. 2014;56:289-290, 292-296, 298.
24. Martin M. Cutadapt removes adapter sequences from high-throughput sequencing reads. *EMBnet.J*. 2011;17:10-12.
25. Li H, Durbin R. Fast and accurate short read alignment with Burrows-Wheeler transform. *Bioinformatics*. 2009;25:1754-1760.
26. Li H, Handsaker B, Wysoker A, et al. The sequence alignment/map format and SAMtools. *Bioinformatics*. 2009;25:2078-2079.
27. Mouliere F, Robert B, Arnau Peyrotte E, et al. High fragmentation characterizes tumour-derived circulating DNA. *PLoS ONE*. 2011;6:e23418.
28. Zhang R, Nakahira K, Guo X, Choi AMK, Gu Z. Very short mitochondrial DNA fragments and heteroplasmy in human plasma. *Sci Rep*. 2016;6:36097.
29. Rigothier C, Daculsi R, Lepreux S, et al. CD154 induces matrix metalloproteinase-9 secretion in human podocytes. *J Cell Biochem*. 2016;117:2737-2747.
30. Coumans FAW, Brisson AR, Buzas EI, et al. Methodological guidelines to study extracellular vesicles. *Circ Res*. 2017;120:1632-1648.
31. Dames S, Eilbeck K, Mao R. A high-throughput next-generation sequencing assay for the mitochondrial genome. *Methods Mol Biol (Clifton, N.J.)*. 2015;1264:77-88.
32. Wiemerslage L, Ismael S, Lee D. Early alterations of mitochondrial morphology in dopaminergic neurons from Parkinson's disease-like pathology and time-dependent neuroprotection with D2 receptor activation. *Mitochondrion*. 2016;30:138-147.
33. Boudreau LH, Duchez A-C, Cloutier N, et al. Platelets release mitochondria serving as substrate for bactericidal group IIA-secreted phospholipase A2 to promote inflammation. *Blood*. 2014;124:2173-2183.
34. Sansone P, Savini C, Kurelac I, et al. Packaging and transfer of mitochondrial DNA via exosomes regulate escape from dormancy

in hormonal therapy-resistant breast cancer. *PNAS*. 2017;114: E9066-E9075.
35. Newell C, Hume S, Greenway SC, Podemski L, Shearer J, Khan A. Plasma-derived cell-free mitochondrial DNA: a novel non-invasive methodology to identify mitochondrial DNA haplogroups in humans. *Mol Genet Metab*. 2018;125:332-337.
36. Florian P, Taras A, Ulrike R, et al. Mitochondria are a subset of extracellular vesicles released by activated monocytes and induce type I IFN and TNF responses in endothelial cells. *Circ Res*. 2019;125:43-52.
37. Torralba D, Baixauli F, Sánchez-Madrid F. Mitochondria know no boundaries: mechanisms and functions of intercellular mitochondrial transfer. *Front Cell Dev Biol*. 2016;4:107.
38. Rodriguez A-M, Nakhle J, Griessinger E, Vignais M-L. Intercellular mitochondria trafficking highlighting the dual role of mesenchymal stem cells as both sensors and rescuers of tissue injury. *Cell Cycle*. 2018;17:712-721.
39. Mahrouf-Yorgov M, Augeul L, Da Silva CC, et al. Mesenchymal stem cells sense mitochondria released from damaged cells as danger signals to activate their rescue properties. *Cell Death Differ*. 2017;24:1224-1238.
40. Patel D, Rorbach J, Downes K, Szukszto MJ, Pekalski ML, Minczuk M. Macropinocytic entry of isolated mitochondria in epidermal growth factor-activated human osteosarcoma cells. *Sci Rep*. 2017;7:12886.
41. Wang J, Li H, Yao Y, et al. Stem cell-derived mitochondria transplantation: a novel strategy and the challenges for the treatment of tissue injury. *Stem Cell Res Ther*. 2018;9:106.
42. Pua HH, Guo J, Komatsu M, He Y-W. Autophagy is essential for mitochondrial clearance in mature T lymphocytes. *J Immunol*. 2009;182:4046-4055.
43. Grazioli S, Pugin J. Mitochondrial damage-associated molecular patterns: from inflammatory signaling to human diseases. *Front Immunol*. 2018;9:832.
44. Rodríguez-Nuevo A, Zorzano A. The sensing of mitochondrial DAMPs by non-immune cells. *Cell Stress*. 2019;3:195-207.

SUPPORTING INFORMATION

Additional supporting information may be found online in the Supporting Information section.

How to cite this article: Al Amir Dache Z, Otandault A, Tanos R, et al. Blood contains circulating cell free respiratory competent mitochondria. *The FASEB Journal*. 2020;34:3616–3630. https://doi.org/10.1096/fj.201901917RR

D/ Réponse aux commentaires sur la publication : « L'hypoxie module différemment la libération des ADN mitochondriaux et nucléaires »

Auteurs : Alain R. Thierry, **Brice Pastor** and Zahra Al Amir Dache

Ce commentaire a été a été publié dans British Journal of Cancer en 2021

Contribution: J'ai participé à la réalisation de certaines expériences supplémentaires et à l'écriture de la réponse.

BJC British Journal of Cancer

www.nature.com/bjc

CORRESPONDENCE

Reply to Comment on: 'Hypoxia differently modulates the release of mitochondrial and nuclear DNA'

British Journal of Cancer https://doi.org/10.1038/s41416-021-01288-y

We thank the Cox group for their comment on this relevant point. We would like to respond to it by adding a number of details and new observations, which we believe will help BJC readers to better appreciate our work[1] and provide additional perspective on it.

As indicated in their comments, a recent report by Cox et al.[2,3] (published after our own work appeared in BJC) showed a ninefold increase in circulating DNA of mitochondrial origin (cir-mtDNA[3]) when frozen storage is performed before high-speed centrifugation (i.e. 15,000×*g*, for 10 min), as compared with frozen storage only performed at the end of the two-step centrifugation process.[3]

We fully agree with this observation, having made it ourselves (subsequent to our BJC report) when accumulating data to demonstrate the circulation of intact cell-free mitochondria in blood.[4] As indicated in Table 1, our own data also shows that the use of frozen storage in the interval between low and high speed centrifugation led to a threefold increase of cir-mtDNA plasma concentration; by comparison, the same condition led to a slight decrease or similar level of cir-nDNA concentration.

We agree with Cox et al.[2] that the artefactual release of platelet mitochondrial DNA during sample processing may contaminate the plasma cirDNA extract. The low effect of storage conditions on cir-nDNA concentration which we observed (Table 1) is certainly due to the absence of a nucleus in platelets. This observation also confirms the involvement of platelets in cir-mtDNA release. Moreover, it might be remarked that the no or low effect of frozen storage following the first centrifugation was detected when analysing cell-free DNA (cfDNA) from cell culture supernatant where platelets are absent. Note, we are convinced that this extracellular release of mitochondria from platelets could arise in other specific conditions. This is probably the case during blood handling and plasma isolation, as the phenomenon can be caused by temperature variation or tube shaking.

For this reason, we applied a strict and standardised protocol during our work to demonstrate the presence of functional circulating cell-free mitochondria in blood.[4] That protocol enables plasma isolation with no (or minimal) platelet activation. It allowed us to demonstrate, for the first time, that blood preparation with resting platelets contains whole functional mitochondria in a normal physiological state. This is a breakthrough observation, since it had been previously reported that this this intact organelle is only released by platelets in specific conditions, such as those which result in platelet activation, or monocyte activation in vesicular or free forms.[5] Wishing to share this protocol with other researchers in this field, we have described it in a note at the end of this response. Note: Fresh blood was collected in a BD Vacutainer™ CTAD tubes. Plasma was isolated via incremental centrifugations, all performed for 10 min at room temperature without a break: two successive centrifugations were first

Table 1. Comparison of healthy individual plasma cirDNA concentration as determined following the fresh plasma and BJC protocols.

Target	Sample	Fresh plasma (ng/mL)	BJC protocol (ng/mL)	Fresh minus BJC protocol	BJC over fresh protocol ratio
mt testing	EFS 0653	0.03	0.08	0.05	2.7
	EFS 0661	0.04	0.08	0.04	2.0
	EFS 0688	0.01	0.03	0.02	3.0
	EFS 0696	0.01	0,03	0.02	3.0
	EFS 0709	0.03	0.14	0.11	4.7
	Median	0.03	0.08	0.04	3.0
nuc testing	EFS 0653	8.23	3.93	−4.3	0.5
	EFS 0661	6.34	9.78	3.44	1.5
	EFS 0688	8.96	6.63	−2.33	0.7
	EFS 0696	2.32	1.1	−1.22	0.5
	EFS 0709	9.07	2.4	−6.67	0.3
	Median	8	4	−2	0.5

Fresh plasma (protocol involving consecutive two step centrifugation); BJC protocol (frozen storage between the two centrifugation steps); mt testing (specific mitochondrial DNA sequence analysis); nuc testing (specific nuclear DNA sequence analysis); EFS, healthy individual.

Received: 20 January 2021 Revised: 22 January 2021 Accepted: 22 January 2021
Published online: 24 March 2021

performed at 200 *g* and were followed by a third centrifugation at 300 *g*. Preheated (37 °C) ACD-A buffer (0.1 M Trisodium citrate, 0.11 M Glucose and 0.08 citric acid) and Prostaglandin E1 (1 µM) were then added to the plasma, which was further centrifuged at 1100 *g* and finally at 2500 *g*.

With respect to the repercussions of the confounding factor pointed out by Wong et al., reservations must be kept in mind when using our in vivo data to compare cir-mtDNA and cir-nDNA, we nonetheless continue to believe that it does not influence the comparison between hypoxic and normal conditions; this is because plasma isolation is strictly standardised[6] and directly comparable. In addition, the highlighted confounding factor did not influence all of our observations made from the in vitro assays.[2]

We would again like to thank the Cox's group for their very pertinent comments, which we have addressed in our practice and protocols, in a manner we believe will be of interest to others working in the cirDNA field.

AUTHOR CONTRIBUTIONS

A.T.: drafted, approved the manuscript prior to submission and supervised the work. Z.A.D. and B.P.: drafted, approved the manuscript prior to submission.

ADDITIONAL INFORMATION

Ethical approval and consent to participate Not applicable.

Consent to publish This article does not contain any individual's identifiable data in any form. None of the material has been published or is under consideration elsewhere, including online journals. All authors have contributed to and agreed on the content of the 76 manuscript.

Data availability Not applicable.

Competing interests The authors declare no competing interests.

Funding information A.R. Thierry is supported by INSERM. This work was funded by the "SIRIC Montpellier Cancer Grant INCa_Inserm_DGOS_12553".

Alain R. Thierry[1], Brice Pastor[1] and Zahra Al Amir Dache[1]
[1]*IRCM, Institut de recherche en cancérologie de Montpellier, Inserm U1194, Université de Montpellier, ICM, Montpellier, France*
Correspondence: Alain R. Thierry (alain.thierry@inserm.fr)

REFERENCES

1. Otandault, A., Abraham, J. D., Al Amir Dache, Z., Khalyfa, A., Jariel-Encontre, I., Forné, T. et al. Hypoxia differently modulates the release of mitochondrial and nuclear DNA. *Br. J. Cancer* **122**, 715–725 (2020)..
2. Cox, D. R. A., Wong, B. K. L., Yang, L., Yoshino, O., Testro, A., Muralidharan, V. et al. High speed centrifugation before frozen storage of plasma is critical for quantitative analysis of mitochondrial-derived cell free DNA. *Clin. Chem.* **66**, 1111–1114 (2020).
3. Bronkhorst, A. J., Ungerer, V., Diehl, F., Anker, P., Dor, Y., Fleischhacker, M. et al. Towards systematic nomenclature for cell-free DNA. *Hum. Genet.* https://doi.org/10.1007/s00439-020-02227-2 (2020).
4. Al Amir Dache, Z., Otandault, A., Tanos, R., Pastor, B., Meddeb, R., Sanchez, C. et al. Blood contains circulating cell-free respiratory competent mitochondria. *FASEB J.* **34**, 3616–3630 (2020).
5. Boudreau, L., Duchez, A. C., Cloutier, N., Soulet, D., Martin, N., Bollinger, J. et al. Platelets 106 release mitochondria serving as substrate for bactericidal group IIA-secreted phospholipase A2 to promote inflammation. *Blood* **14**, 2173–2183 (2014).
6. Meddeb, R., Pisareva, E. & Thierry, A. R. Guidelines for the preanalytical conditions for analyzing circulating cell-free DNA. *Clin. Chem.* **5**, 623–633 (2019).

E/ Caractéristiques structurelles de l'ADN nucléaire circulant, origines et profil de taille complet révélés par la fragmentomics

Auteurs : Cynthia Sanchez, Benoit Roch, Thibault Mazard, Philippe Blache, Zahra Al Amir Dache, **Brice Pastor**, Ekaterina Pisareva, Rita Tanos,and Alain R. Thierry

Cette publication a été a été publiée dans Journal of Clinical Investigations Insight en 2021

Résumé: Afin d'aborder sans équivoque leurs structures intimes non résolues dans le sang, nous avons examiné la distribution de taille de l'ADN circulant sans cellules (cfDNA) en utilisant le séquençage du génome entier (WGS) à partir de préparations de bibliothèques d'ADN double et simple brin (DSP et SSP, n = 7) et en utilisant la PCR quantitative (Q-PCR, n = 116). Le profil de taille chez les individus sains était remarquablement homogène lors de l'utilisation du séquençage DSP ou du séquençage SSP. Le profil de taille du ADNcir présentait un schéma de fragmentation nucléosomique caractéristique. Dans l'ensemble, nos données indiquent que la proportion d'ADNcir inséré dans les mono-, di-nucléosomes et la chromatine de taille moléculaire plus élevée (>1000 pb) peut être estimée à 67,5% à 80%, 9,4% à 11,5% et 8,5% à 21,0%, respectivement. Nos données ont révélé que l'ADNcir est fortement associé (97%-98%) sur ces structures, qui semblent être soumises à une activité nucléasique continue dans la circulation sanguine. L'analyse des fragments permet de distinguer l'ADNcir de différentes origines : premièrement, l'analyse du profil de taille de l'ADNcir peut être utile pour le contrôle de la qualité des extraits d'ADNcir ; deuxièmement, des différences subtiles mais fiables entre les patients atteints de cancer colorectal métastatique et les individus sains varient en fonction de la proportion d'ADNcir provenant de cellules malignes dans les extraits de plasma, ce qui indique un degré plus élevé de fragmentation de l'ADNcir et d'activité nucléasique dans les échantillons à forte teneur en ADNcir de cellules malignes.

Contribution: J'ai participé à la réalisation de certaines analyses de l'ADN circulant nucléaire.

JCI insight

TECHNICAL ADVANCE

Circulating nuclear DNA structural features, origins, and complete size profile revealed by fragmentomics

Cynthia Sanchez,[1] Benoit Roch,[1,2] Thibault Mazard,[1] Philippe Blache,[1] Zahra Al Amir Dache,[1] Brice Pastor,[1] Ekaterina Pisareva,[1] Rita Tanos,[1] and Alain R. Thierry[1]

[1]IRCM, Institut de Recherche en Cancérologie de Montpellier, INSERM U1194, Université de Montpellier, Institut régional du Cancer de Montpellier, Montpellier, France. [2]Thoracic Oncology Unit, Arnaud de Villeneuve Hospital, University Hospital of Montpellier, Montpellier, France.

To unequivocally address their unresolved intimate structures in blood, we scrutinized the size distribution of circulating cell-free DNA (cfDNA) using whole-genome sequencing (WGS) from both double- and single-strand DNA library preparations (DSP and SSP, *n* = 7) and using quantitative PCR (Q-PCR, *n* = 116). The size profile in healthy individuals was remarkably homogenous when using DSP sequencing or SSP sequencing. CfDNA size profile had a characteristic nucleosome fragmentation pattern. Overall, our data indicate that the proportion of cfDNA inserted in mono-nucleosomes, di-nucleosomes, and chromatin of higher molecular size (>1000 bp) can be estimated as 67.5% to 80%, 9.4% to 11.5%, and 8.5% to 21.0%, respectively. Although DNA on single chromatosomes or mono-nucleosomes is detectable, our data revealed that cfDNA is highly nicked (97%–98%) on those structures, which appear to be subjected to continuous nuclease activity in the bloodstream. Fragments analysis allows the distinction of cfDNA of different origins: first, cfDNA size profile analysis may be useful in cfDNA extract quality control; second, subtle but reliable differences between metastatic colorectal cancer patients and healthy individuals vary with the proportion of malignant cell-derived cfDNA in plasma extracts, pointing to a higher degree of cfDNA fragmentation and nuclease activity in samples with high malignant cell cfDNA content.

Introduction

The analysis of circulating cell-free DNA (cfDNA) undoubtedly represents a breakthrough in the diagnostic field (1–4). The potential of this newly identified source of biological information has attracted the attention of researchers and clinicians in numerous fields (3–5). CfDNA sizing has emerged as a new strategy in the optimization of cfDNA analysis.

Because of the high nuclease sensitivity of the naked DNA molecule, the size of the extracted cfDNA is intimately associated with the biological particle structure transporting and stabilizing it. Consequently, in recent years these 2 features have been highly scrutinized, to improve knowledge of cfDNA release, to improve cfDNA detection, and to evaluate cfDNA potential to discriminate cfDNA tissue/cells of origin, with the aim of increasing cfDNA diagnostic power (6–10). CfDNA can exist as protein-associated DNA fragments, or can lie in extracellular vesicles, within the physiological circulating fluids of both healthy and diseased individuals (2, 3). CfDNA is derived not only from genomic DNA but also from extrachromosomal mitochondrial DNA (11). Even though cfDNA has presently an increasing number of clinical applications (1, 12), its structural characteristics have yet to be fully elucidated.

CfDNA was initially thought to be up to 40 kb in size, but principally 180 bp (or multiples of), corresponding to the size of the DNA packed in a mono-nucleosome (13, 14). Observations of mono- and oligo-nucleosomes led to the view that the major mechanism of cfDNA release is apoptosis (2, 14, 15). Using Q-PCR to examine fragment size, we initially demonstrated that (a) cfDNA is highly fragmented (16, 17); (b) cfDNA quantification is more efficient at lower amplicon sizes; and (c) cfDNA fragments can be as small as 45 bp (9, 18). Furthermore, we established that the lower the size of the detected cfDNA amplicon (down to 60–70 bp), the higher the quantified amount (16). Since that observation, all Q-PCR primer systems specifically designed for detecting cfDNA have now been designed to detect amplicons smaller than 100 bp, or, optimally, smaller than 80 bp (5, 6, 19–21).

Conflict of interest: TM discloses research funding from Roche and Amgen; honoraria from Amgen, Sanofi, Bristol Myers Squibb, Sandoz, and AAA; and travel, accommodations, and expenses paid by Amgen. ART is a shareholder of DiaDx SAS.

Submitted: September 22, 2020
Accepted: February 10, 2021
Published: March 22, 2021

Reference information: *JCI Insight*. 2021;6(6):e144561. https://doi.org/10.1172/jci.insight.144561.

However, cfDNA fragment size distribution obtained by Q-PCR was significantly different than that obtained by next-generation sequencing, showing a major population peaking at 166 to 167 bp. Q-PCR revealed high levels of fragmentation, with most of the fragments found below 145 bp in the plasma from both healthy and cancer patients (6, 8, 16, 18, 22, 23). Although no single current method for analyzing cfDNA size profile is optimal, previous reports have only used 1 method at a time. This has made it difficult to obtain a precise and unequivocal overall cfDNA size profile. In a blinded study, we previously observed that cfDNA from cancer patients has a similar size distribution, whether using Q-PCR or nonconventional whole-genome deep sequencing (WGS) from a single-strand DNA library preparation (SSP, ref. 6). In contrast to the standard WGS from double-strand DNA library preparation (DSP), SSP sequencing (SSP-S) revealed a significant proportion of short cfDNA fragments (below 80 bp); this was something not readily detectable by DSP sequencing (DSP-S), as previously shown by Underhill et al. (10). This provided new insights into cfDNA size profiles and harmonized sequencing and Q-PCR findings (16).

Previous deep sequencing examination of cfDNA fragmentation patterns revealed that they are specific signatures of tissue origins, that short cfDNA fragments harbor footprints of nucleosomes as well as transcription factors, and that cfDNA from healthy individuals derives from hematopoietic cells (8). Higher fragmentation has been found in the cfDNA of cancer patients (16), in tumor cells (9), and in the fetal fraction (24, 25). Efforts are ongoing to increase analytical sensitivity in this area, by focusing on a specific cfDNA fragment size range. CfDNA fragmentation analysis is also being pursued as a possible means of stratifying individuals (9, 26–30).

In our study, we used the synergistic analytical information provided by Q-PCR and by WGS of both double- and single-stranded DNA libraries in order to unequivocally observe cfDNA size distribution in healthy subjects. This enabled us to measure cfDNA size precisely over a wide range of lengths and thus obtain information about DNA strand degradation and detectable cfDNA structures. We also performed the following 2 comparisons, in a blinded fashion: first, using WGS (DSP-S and SSP-S), we precisely compared the size profile up to approximately 1000 bp of cfDNA obtained from 7 healthy individuals and 7 metastatic colorectal cancer patients; second, using Q-PCR, we compared the size fraction distribution of cfDNA in the wide range length in plasma obtained from 109 healthy individuals and 104 colorectal cancer (CRC) patients.

Results

Circulating plasma DNA size profiling by whole-genome sequencing. Sequencing libraries are prepared from either DSP or SSP. Both methods provide profiles from which variations can be detected and compared, with cfDNA sizes ranging from approximately 30 to approximately 1000 bp/nt (6, 31). Figure 1 shows size profiles of cfDNA from 7 healthy human individuals obtained by both DSP-S and SSP-S. For all the samples, we obtained a mean of 1,434,487 reads (1,079,717–1,611,205 reads) for DSP and 1,007,070 reads (963,701–1,299,291 reads) for SSP (Supplemental Figure 1; supplemental material available online with this article; https://doi.org/10.1172/jci.insight.144561DS1). Size profiling of cfDNA from the 7 plasma samples revealed very low variation, as all 7 curves superimposed, irrespective of the DSP-S or SSP-S libraries (Figure 1, A and B).

The DSP-S cfDNA profile of healthy subjects had a major monomodal population between 80 and 260 bp, peaking at 166 bp with approximately 2.5% of total fragments (Figure 1A). A smaller population was also detectable between 260 and 420 bp, ranging from 8.0% to 12.9% of the total fragments (Figure 1, A and B, and Supplemental Table 1A). Subpeaks of the 7 samples colocalized (Table 1 and Supplemental Table 1B). Reliable reads were detectable down to 40 bp in most of the samples.

The SSP-S cfDNA size profile of healthy subjects had a population between 45 and 260 bp, which peaked at 166 bp, corresponding to approximately 2.0% of the total fragments. Fragments plateaued between 70 and 120 bp at approximately 0.4% (Figure 1B). A very small population was observed between 250 and 400 nt that ranged from 2.7% to 4.5 % of the total fragment number (Supplemental Table 1). All subpeaks of the 7 samples colocalized (Table 1, Table 2, and Supplemental Table 1B). Reliable reads were detectable down to the limit of the sequencing detection, approximately 25 nt.

As determined by DSP-S and SSP-S, the cfDNA size profile showed clear discrepancies. Regarding the fraction ranging up to 90 bp, or from 90 to 240 bp, or from 240 to approximately 440 bp, the proportions of cfDNA averaged 0.1%, 87.2%, and 12.7%, respectively, as determined by DSP-S; and 8.0%, 87.2%, and 4.8%, respectively, as determined by SSP-S (Figure 1). Fragments shorter than 80 bp (nt) were only detectable by SSP-S (Figure 1C and Supplemental Table 2). Between 80 and 166 bp (nt), the proportion of cfDNA fragments determined by single-strand DNA sequencing was slightly higher than for double-strand DNA sequencing: 56.9% and 41.5%, respectively (Supplemental Table 2A). Conversely, SSP-S values were slightly lower in the 166 to 240 bp (nt)

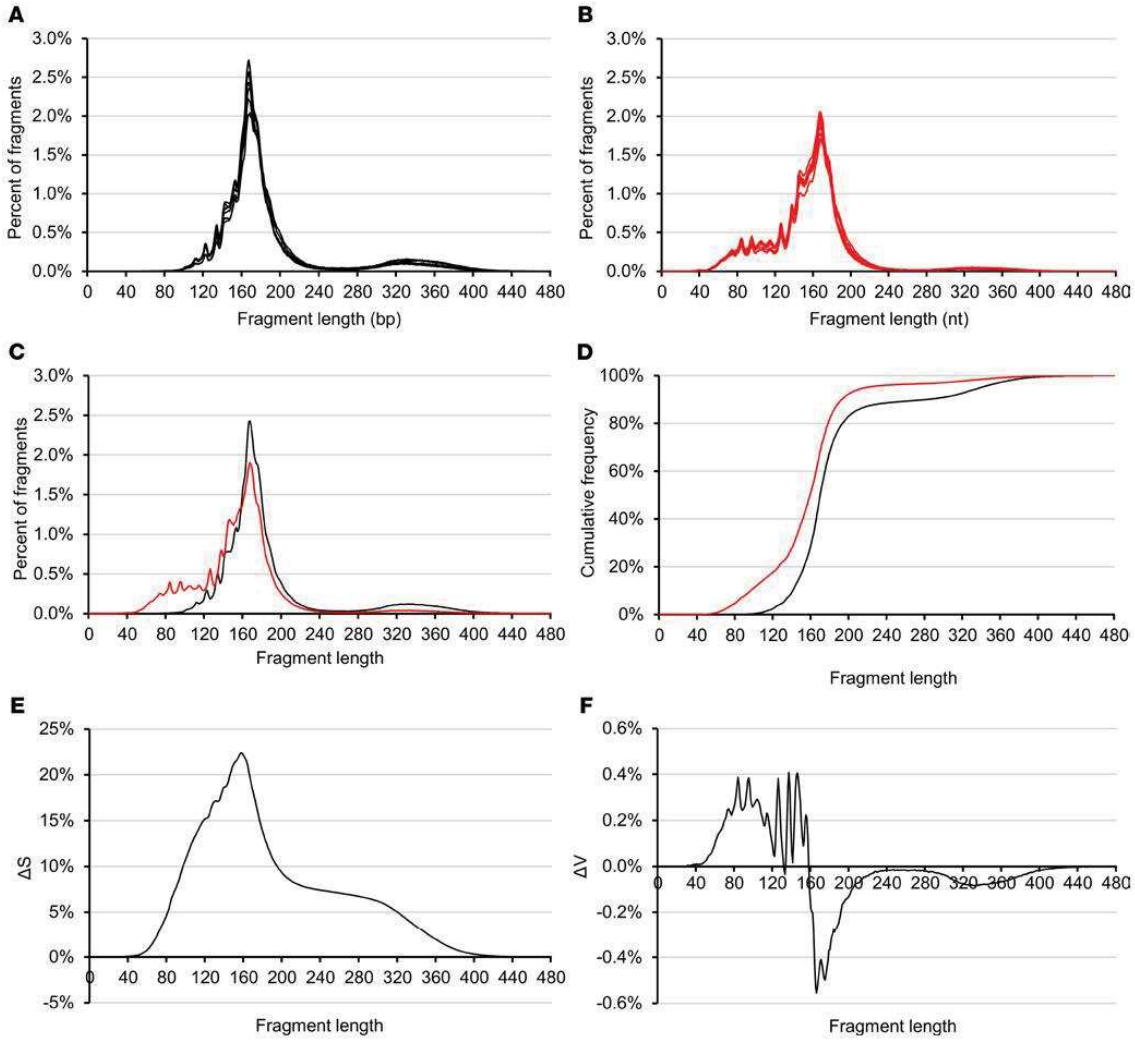

Figure 1. CfDNA size profile as determined from DSP-S and SSP-S. CfDNA size profiles of 7 healthy individuals, obtained by sequencing either from double- or single-strand DNA library preparations (**A** and **B**, respectively). Mean size profiles of the 7 individuals, as determined by DSP-S (black lines) and SSP-S (red lines) (**C**); curves of the cumulative frequencies between SSP-S and DSP-S (**D**); the difference in cumulative frequencies, denoted as ΔS, between SSP-S minus DSP-S (**E**); and the curve of the difference of % values, denoted as ΔV, between SSP-S minus DSP-S (**F**). The increasing part of the ΔS curve indicates the fragment size range, in which SSP-S detected fragment number is proportionally higher than DSP-S detected fragments; while the decreasing part of the ΔS curve indicates the fragment size range in which SSP-S–detected fragment number is proportionally lower than for DSP-S–detected fragments (**E**). Positive ΔV values for cfDNA size indicate where more fragments were detected by SSP-S than by DSP-S (**F**). Negative ΔV values for cfDNA size indicate where less fragments were detected by SSP-S than by DSP-S. More fragments are detected by SSP-S up to 158 bp (nt) as compared with DSP-S, and more fragments are detected by DSP-S over 158 bp (nt) (**F**).

range, constituting 33.1% of the total number of fragments, as compared with the DPS-S values, which constituted 45.5%. It is not possible to compare the number of reads in SSP-S and DSP-S size profiles, but the respective proportions within any size range is informative (Supplemental Figure 1).

We directly compared the performance of the 2 sequencing techniques by scrutinizing data obtained from difference in cumulative frequencies, denoted as ΔS, or the difference of fragment frequency, denoted ΔV (Supplemental Methods, Appendix 1). Altogether, data showed that SSP-S enabled the detection of a higher number of cfDNA fragments as compared with DSP-S and revealed a higher number of fragments in the 45 to 158 bp (nt) range and a lower number of fragments in ranges from 158 to 250 bp (nt) and, to a lesser extent, 280 to 440 bp (nt).

Table 1. Subpeak corresponding size

	HEALTHY													
	DSP-S (bp)							SSP-S (nt)						
Peak	1	2	3	4	5	6	7	1	2	3	4	5	6	7
1	-	-	-	-	-	-	-	53	54	-	53	-	52	53
2	-	-	-	-	-	-	-	63	-	-	62	-	63	61
3	-	-	-	-	-	-	-	72	72	74	73	73	73	73
4	-	-	-	-	-	-	-	83	83	83	83	83	83	83
5	-	-	-	-	-	-	-	94	94	94	94	94	94	94
6	101	-	-	104	102	102	-	103	101	105	104	102	103	104
7	111	111	111	112	112	111	111	114	113	113	113	114	113	113
8	121	121	121	121	121	121	121	125	125	125	125	125	125	125
9	133	133	133	133	133	133	133	136	136	137	136	136	136	136
10	144	145	144	142	144	142	141	145	145	145	144	145	145	144
11	152	152	152	151	152	152	152	-	-	-	-	-	-	-
12	166	166	167	166	165	167	166	166	166	166	167	166	167	166

Detailed characterization of the approximately 10 bp (nt) subpeaks, as observed from the size profile of the cfDNA of healthy individuals, as determined by DSP-S and SSP-S.

While a major cfDNA peak and a very minor peak were observable at approximately 166 bp and approximately 320 bp (Figure 1, A and B), there were also subpeaks every approximately 10 bp, due to the intimate structure of cfDNA and its association with histone octamers. Tables 1 and 2 summarize the detection of these subpeaks in healthy individual cfDNA, from either SSP or DSP. The different sequencing techniques produced differences in subpeaks at specific cfDNA sizes. The differences between the library preparations included subpeaks at 53, 63, 73, 83, and 94 bp that were only observed with SSP-S, and not with DSP-S; whereas a subpeak at 152 bp was only seen with DSP-S. No periodicity was detected between 145 and 167 bp when using SSP-S (Tables 1 and 2). Note also that the SSP-S–derived subpeaks are approximately 3 bp higher than those of DSP-S.

Size distribution analysis by Q-PCR. Next, we used nested Q-PCR primer systems to detect amplicons of 67, 145, and 320 bp, to estimate the proportion of the different cfDNA size fractions in the 7 samples (Figure 2A). (Note: cfDNA concentrations as reported here concern a *KRAS* DNA region, and are only indicative of the total cfDNA concentration, as indicated in the Methods section.) This technique could detect cfDNA down to 67 bp. The highly fragmented cfDNA fraction (HF, 67–145 bp) and the mononucleosome–derived cfDNA fragment fraction (MF, 145–320 bp) were detected in similar proportions (38% and 39%, mean, respectively), whereas the weakly fragmented fraction (WF, >320 bp) was found in a lower proportion (23%; Figure 2A). To corroborate our findings, we tested a panel of 109 healthy individuals (Figure 2B). The sample mean DNA Integrity Index (DII) was 0.134 ± 0.091 SD (Supplemental Figure 2), indicating that, for fragments over 67 bp, approximately 13.4% are over 320 bp; this confirms the WF fraction (19%) derived from the 7 samples mentioned above.

Comparison of the size profile of plasma cfDNA from healthy subjects and subjects with metastatic CRC. There was very little variation in the size profiles of cfDNA from the healthy individuals determined by each of the 2 sequencing methods (Figure 1A). Because of this, we used the mean size profile for healthy subjects as our reference in the remainder of this study, when comparing the fragmentation of cfDNA from cancer and healthy plasma.

There were subtle but reliable differences between the DSP-S size profiles of each of the 7 cancer patients and the mean of the 7 healthy individuals (Supplemental Figure 3). Although the cfDNA fragment populations of both cancer and healthy subjects peaked at 166 bp, cancer patient plasma had more cfDNA fragments between 40 and 150 bp and less between 150 and 260 bp. Also, the profile curve showed a shoulder between 145 and 166 bp in cancer patient plasma (Figure 3, A, C, E, G, and I; and Supplemental Figure 3).

The similar subtle but reliable differences were observed by SSP-S (Figure 3, B, D, F, H, and J; and Supplemental Figure 4); cancer patient plasma had more fragments between 30 and 145 nt and less between 145 and 260 nt, while both populations peaked at 166 nt (Figure 3). Note, the shoulder observed in cancer

Table 2. Subpeak periodicity

	HEALTHY													
	DSP-S (bp)							SSP-S (nt)						
Periodicity	1	2	3	4	5	6	7	1	2	3	4	5	6	7
(1–2)	-	-	-	-	-	-	-	10	-	-	9	-	11	8
(2–3)	-	-	-	-	-	-	-	9	-	-	11	-	10	12
(3–4)	-	-	-	-	-	-	-	11	11	9	10	10	10	10
(4–5)	-	-	-	-	-	-	-	11	11	11	11	11	11	11
(5–6)	-	-	-	-	-	-	-	9	7	11	10	8	9	10
(6–7)	10	-	-	8	10	9	-	11	12	8	9	12	10	9
(7–8)	10	10	10	9	9	10	10	11	12	12	12	11	12	12
(8–9)	12	12	12	12	12	12	12	11	11	12	11	11	11	11
(9–10)	11	12	11	9	11	9	8	9	9	8	8	9	9	8
(10–11)	8	7	8	9	8	10	11	-	-	-	-	-	-	-
(11–12)	14	14	15	15	13	15	14	-	-	-	-	-	-	-
(10–12)	22	21	23	24	21	25	25	21	21	21	23	21	22	22

Detailed characterization of the approximately 10 bp (nt) subpeak periodicity, as observed from the size profile of the cfDNA of healthy individuals, as determined by DSP-S and SSP-S.

patients (145–160 nt) was slightly more pronounced with SSP-S, as can be seen by comparing the size profile of the cfDNA with the highest mutant allele frequency (MAF) (Supplemental Figure 4).

CRC patient number 8 had the highest MAF (69%). Juxtaposing their DSP-S or SSP-S cfDNA size profile with the mean healthy line illustrated the overall differences in cfDNA fragmentation between healthy subjects and mCRC patients (Figure 4, A and B). Using DSP-S to make the same comparison, the respective size profile curves differed greatly. The curves of the DSP-S and SSP-S size profiles from cancer plasma appeared to be shifted to lower size, while peaking at the same size (166 bp) when compared with the curves from healthy individuals (Figure 4, A and B). As observed in Figure 4, A and B, as well as in ΔV curves (Figure 1F and Supplemental Figure 5), the difference in frequency between cancer and healthy subjects by DSP-S was positive in the 40 to 150 and 220 to 320 bp (nt) ranges and negative in the 150 to 220 bp range (Supplemental Figure 5); for SSP-S, it was positive in the 30 to 140 and 220 to 320 bp (nt) ranges and negative in the 140 to 220 bp (nt) range (Supplemental Figure 5).

Whether detected by DSP-S or SSP-S, the differences between healthy and cancer subjects increased with the MAF in all mCRC samples (Figure 3 and Supplemental Figures 2, 3, and 5). Note, the higher the MAF, the greater the number of shorter fragments and the smaller the peak at 166 bp. The mean fraction of cfDNA fragments whose size corresponded to that of cfDNA fragments packed in the di-nucleosome structure, was 8% to 12.9 % and 2.5% to 4.5% in healthy plasma, and 3.2% to 17.9% and 1.5% to 9.5% in cancer patients (Supplemental Table 1), with DSP-S and SSP-S, respectively. In contrast, the di-nucleosome–associated peak was significantly different in healthy and cancer patient plasma (~332 vs. approximately 300 bp, and approximately 327 vs. approximately 303 nt, as detected by DSP-S and SSP-S, respectively). As derived from DSP-S analysis, the 166 bp/145 bp fragment size frequency ratio showed discriminative power between the healthy samples (3.1 ± 0.33 SD) and the 7 mCRC samples (1.0 to 3.29; Supplemental Table 2A). Using SSP-S analysis, the 166 bp/145 bp fragment size frequency ratio was 1.58 ± 0.10, and ranged from 0.77 to 2.05 in the mean healthy samples and the 7 CRC samples, respectively (Supplemental Table 2A). Moreover, using DSP-S analysis, the fragment size frequency of the 30 to 145 bp range, as compared with the total fragment size in the 30 to 440 bp range (corresponding to DNA in mono- and di-nucleosomes), showed discriminative power between the healthy samples (13.40 ± 0.02 SD) and the 7 CRC samples (17.35 to 44.05). Using SSP-S analysis, the fragment size frequency of the 30 to 145 bp range was 33.08 ± 0.02 and ranged from 28.05 to 60.38 in the mean healthy samples and the 7 CRC samples, respectively (Supplemental Table 2A).

The observation of the size distribution plot of cumulative size frequencies, and the ΔS, or ΔV, between individual cancer samples and the healthy cfDNA mean, enabled us to refine the difference between mean healthy and each cancer patient (Figure 3, Supplemental Table 2, and Supplemental Figures 5–7). Note, this difference at the peak increased as MAF increased (0.9%, 3.2%, 14.3%, 23.3%, 47.3%, 54.6%, and 68.5%). Thus, ΔS peak value difference was smallest for the mCRC cases with the lowest MAF, using either

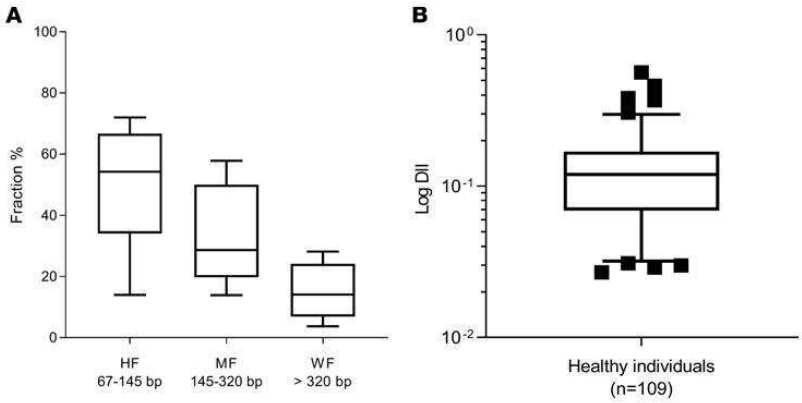

Figure 2. CfDNA size distribution as determined by Q-PCR. Fractional size distribution was performed using nested Q-PCR primer systems to detect amplicons of 67, 145, and 320 bp in the 7 healthy individuals (Supplemental Methods, Appendix 2). Note, fractional size distribution as presented here was obtained from cfDNA concentrations quantified by targeting the *KRAS* DNA region and is only indicative, as described in the Methods section. The cfDNA size distribution was summarized by presenting the levels (data represent mean ± SEM) in the highly fragmented cfDNA fraction (HF, 67–145 bp), the levels in the mono-nucleosome–derived fragmented cfDNA (MF, 145–320 bp), and a lower proportion (3%–20%) in the weakly fragmented cfDNA (WF, >320 bp). (**A**). The DNA Integrity Index (DII) was calculated based on the Q-PCR–based determination of the ratio of the number of fragments over 320 bp to those over 67 bp within a *KRAS* intron 3/exon 2 region in a panel of 109 healthy individuals (**B**). The sample median DII was 0.119. Bar, median; box, 25% to 75%; brackets, 5% to 95%; see *Statistics* section in Methods.

DSP-S (5%, 15%, 24%, and 34%) or SSP-S (0, 8, 18 and 26%; Figure 3 and Supplemental Figures 6 and 7). Nevertheless, the area under the ΔS curve appeared higher, when examining the size profile, in SSP-S than in DSP-S analysis (Figure 3 and Supplemental Figure 8). In addition, the ΔS at 155 bp (nt) varied from 3.9% to 31.80%, and from –5.70% to 24.9% (when using DSP-S and SSP-S, respectively), and appeared as a discriminatory factor when comparing cancer and healthy individuals (Supplemental Table 2B). Figure 5 illustrates that cfDNA fragment frequency at specific size ranges correlates with MAF. Fragment percentage of the 30–80 bp or 30–143 nt size range increased with elevated MAF as determined by DSP-S and SSP-S, respectively; fragment percentage of the 151–220 bp or 143–220 nt size range decreased with elevated MAF, as determined by DSP-S and SSP-S, respectively (Figure 5).

Similar observations can be made in relation to the calculation of ΔV. For both DSP-S and SSP-S analysis, the positive and negative ΔV curve peaks decreased with decreasing MAF, down to nearly no difference whatsoever (±0.2% at MAF = 0.9%, ΔV) (Supplemental Figure 5). Overall, data showed that the more MAF increased, the more observable differences there were in size profile and ΔS and ΔV curves (Supplemental Figure 5). When comparing cancer and healthy individual plasma, significant differences were observed in ΔS and ΔV data when DSP-S–derived values were subtracted from SSP-S–derived values (Supplemental Figures 5 and 8). In addition, the ΔV of the 40 to 160 bp (nt) size range varied from 3.32% to 29.96%, and from –6.13% to 22.05 %, when using DSP-S and SSP-S, respectively; ΔV also appeared as a discriminatory factor when comparing cancer and healthy individuals (Supplemental Figure 5 and Supplemental Table 2). Furthermore, ΔV calculated within the 40 to 160 bp (nt) range from the mean of 7 healthy plasma was 22.04 ± 0.68 SD %; and ΔV of the plasma from the 7 CRC patients varied from 12.27% to 16.68% (Supplemental Figure 5 and Supplemental Table 2B).

At specific cfDNA sizes, there were a number of differences in the presence of subpeaks between cancer and healthy individuals, depending on whether DSP-S or SSP-S analysis was used. These may be summed up as follows: DSP-S showed subpeaks at 71, 81, and 91 bp in cancer subjects (Supplemental Table 3) in contrast to healthy subjects (Table 1); SSP-S showed no subpeaks at approximately 150 nt in healthy subjects (Table 1), in contrast to cancer subjects (Supplemental Table 3).

The fractional size distribution determined by Q-PCR revealed that, in contrast to the plasma of healthy subjects, mCRC patient plasma samples showed a higher number of fragments in the HF than in the MF fraction and a very low level (~1%) in the WF fraction (Figure 4C). To corroborate our findings related to the DII, calculated for the 7 mCRC patients, we used a panel of 104 mCRC patients (Figure 4D and Supplemental

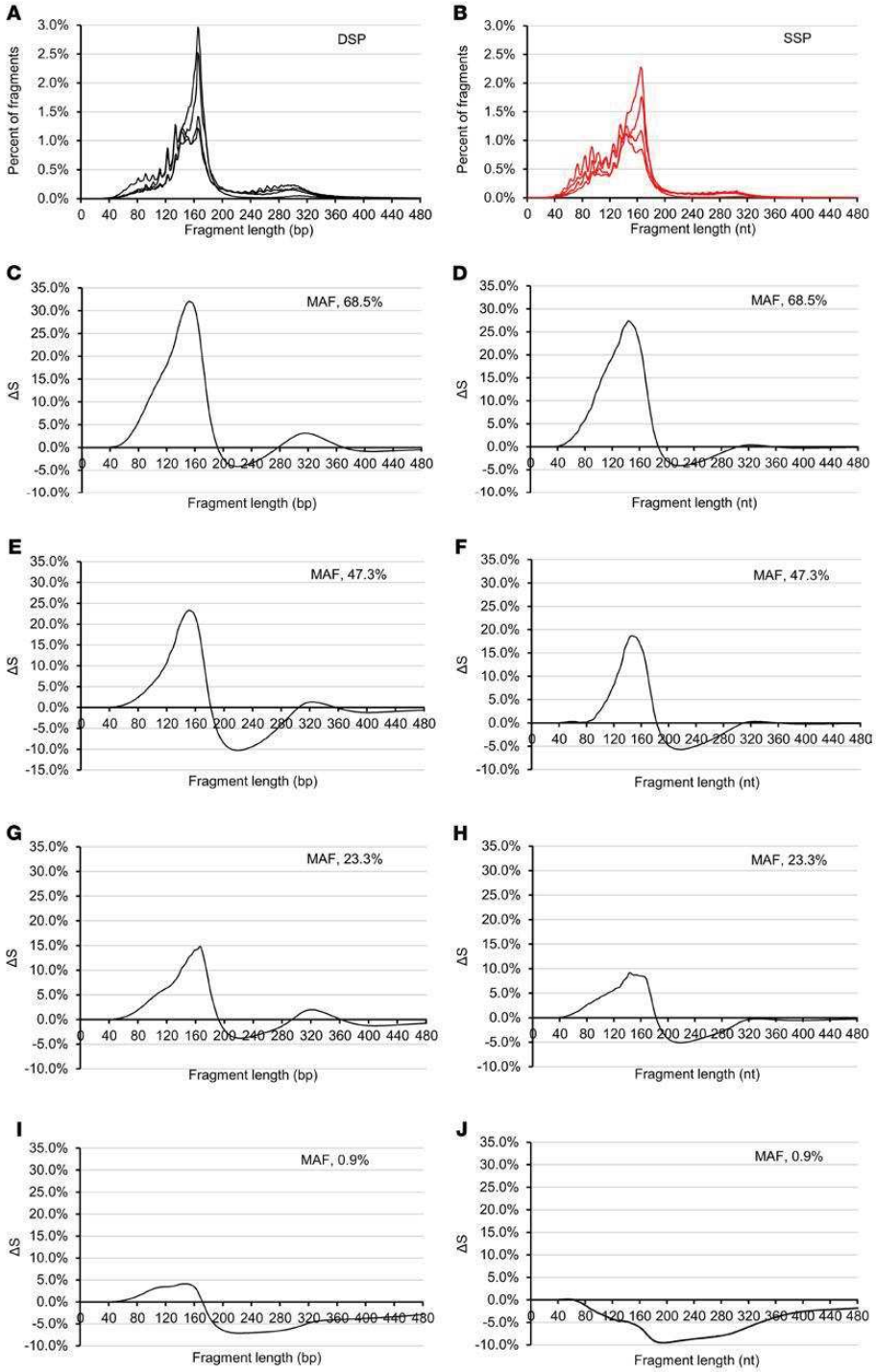

Figure 3. CfDNA size profile from 4 illustrative patients with metastatic CRC. Sequencing from double- or single-stranded DNA library preparations (**A** and **B**, respectively). The difference in cumulative size frequencies, denoted as ΔS, between individual cancer samples and healthy DNA mean as determined by DSP-S (**C**, **E**, **G**, and **I**) or SSP-S (**D**, **F**, **H**, and **J**). MAF of metastatic CRC (mCRC) patients: 68.5% (**C** and **D**), 47.3% (**E** and **F**), 23.3% (**G** and **H**), and 0.9% (**I** and **J**). The individual size profiles and cumulative size frequency curves from each mCRC patient are presented in Supplemental Figures 3, 4, 6, and 7.

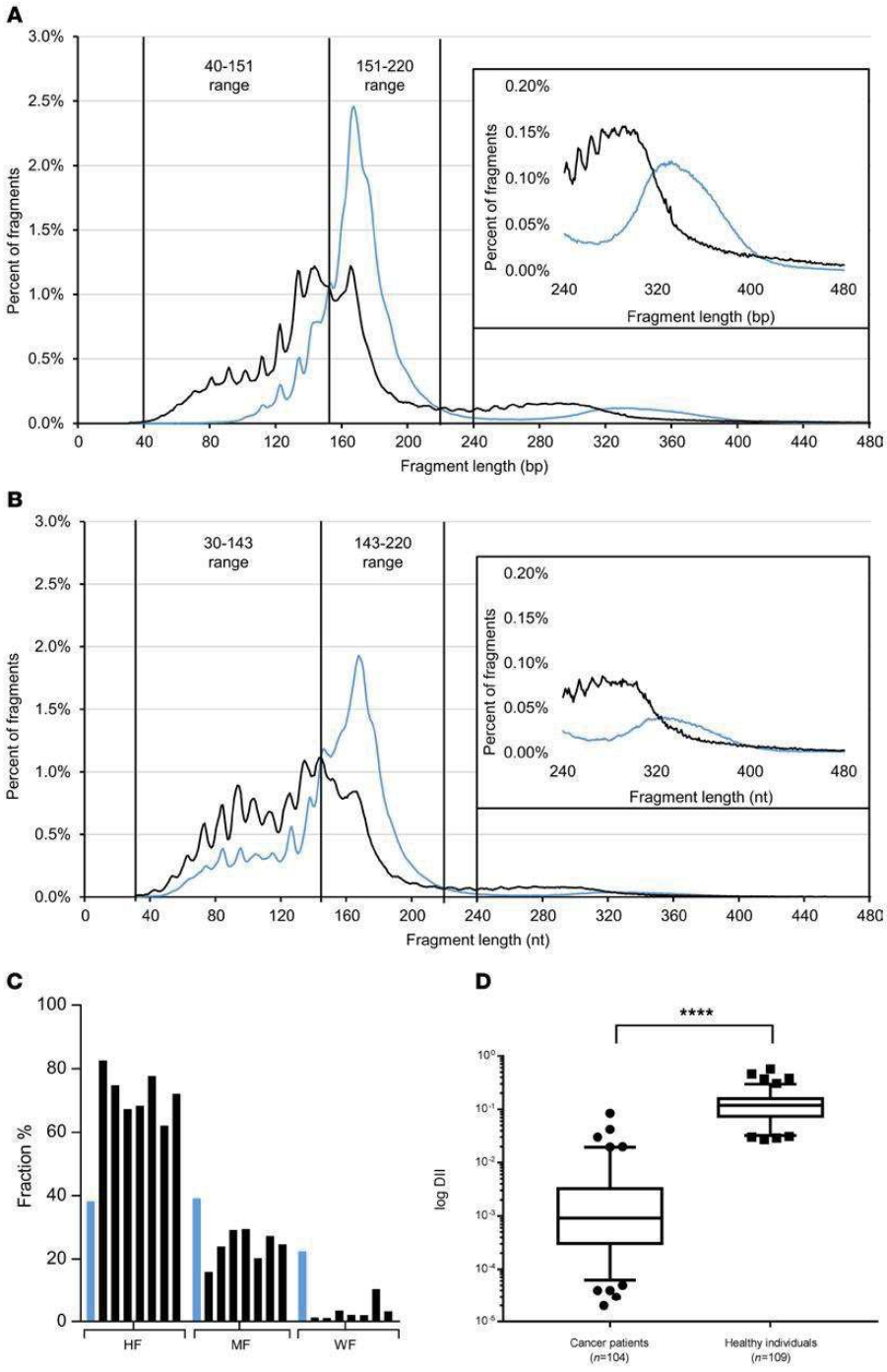

Figure 4. Comparison of the cfDNA size distribution of healthy individuals and mCRC patients. Comparison of the cfDNA size profile of the healthy individual mean (blue line) and a cancer patient with a MAF of 68.5% (black line), as determined by DSP-S (**A**) and SSP-S (**B**). Vertical lines indicate the fragment lengths, where the size profile curve of healthy mean cfDNA crosses that of cancer patient cfDNA. Insert, zoom on the 240–480 bp (nt) size range. Size distribution, as determined by Q-PCR analysis from mean of the 7 healthy individuals (blue) and 7 cancer (black), of the HF (67–145 bp), MF (145–320 bp), and WF (>320 bp) fractions (**C**). Note, fractional size distribution as presented here was obtained from cfDNA concentrations quantified by targeting the *KRAS* intron 3 region and is only indicative, as described in the Methods section. DII as determined by calculating the ratio of the WF fraction over total cfDNA concentration (>67 bp) within a *KRAS* intron 3 DNA region (**D**). Bar, median; box, 25% to 75%; brackets, 5% to 95%. The level of significance was assessed by Student's *t* test.

Figure 2). In the CRC patients, the mean DII was 0.004. This means that 0.4% were higher than 320 bp and, since no fragments over that size are detectable up to ~1000 bp by WGS, that 0.4% were over approximately 1000 bp. Thus, the DII from the healthy cohort (mean DII, 0.13) was significantly higher than the DII from CRC patients of all stages ($P < 0.0001$; Figure 2 and Supplemental Figure 2).

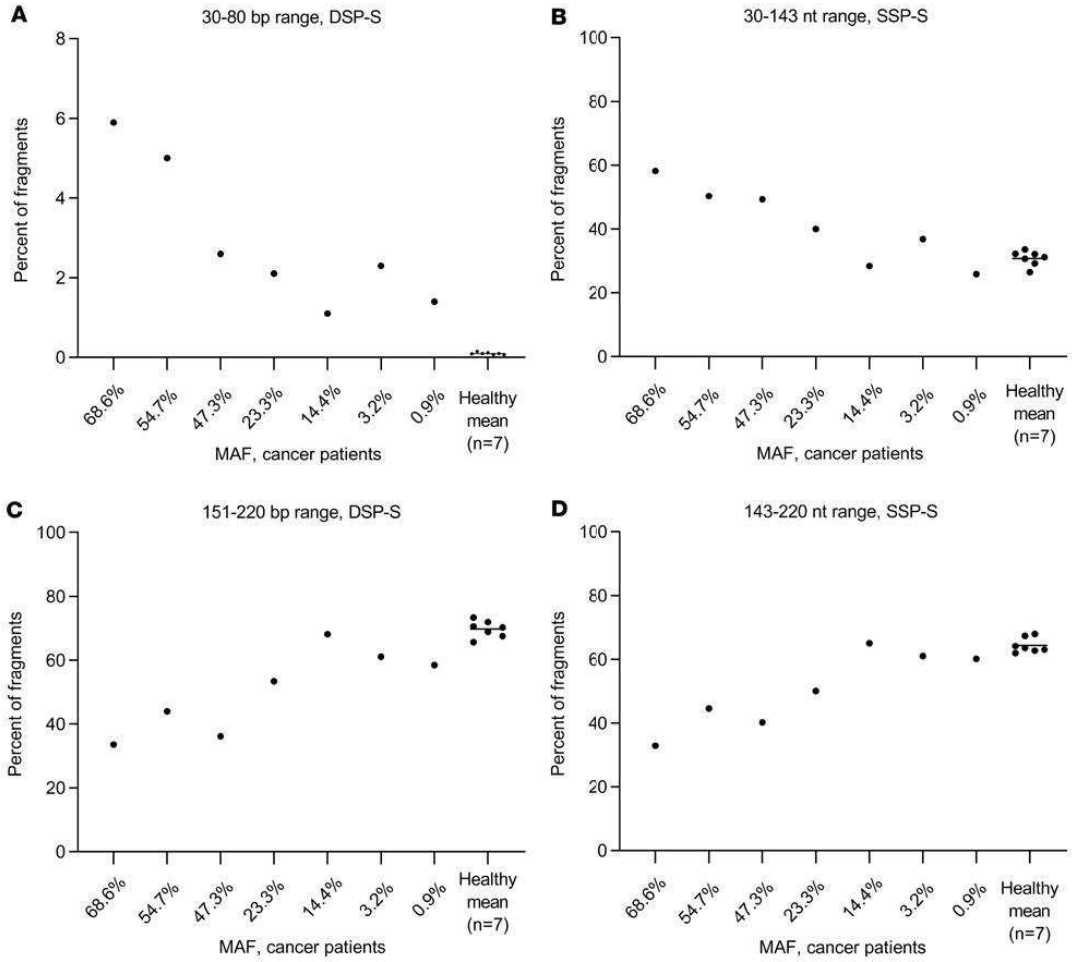

Figure 5. Illustration of the capacity of fragmentomics in distinguishing cfDNA released from healthy and malignant cells. Fragment percentage as determined by DSP-S (**A** and **C**) and SSP-S (**B** and **D**) in the 30–80 bp (**A**), 30–143 nt (**B**), 151–220 bp (**C**), and 143–220 nt (**D**) size ranges in the total cfDNA fragment population from healthy individual mean (n = 7) and from single cancer patients of various MAFs. The figure only presents the size range in which the cfDNA fragment proportion showed a the highest variation between the healthy mean and the patient with the highest MAF (68.6%).

Discussion

Sizing by WGS allows the precise measurement of cfDNA fragments below approximately 1000 bp. Conventional DSP-S–derived size distribution relies on double-strand breaks in the DNA molecule, whereas size profiling by SSP-S can also reveal the level of nicks on both strands and can artificially measure single-stranded cfDNA fragments. CfDNA size distribution obtained from the conventional whole-genome sequencing of a double-stranded DNA library should be distinguished from that obtained from a single-stranded DNA library, or from Q-PCR; both use single-strand DNA as a first template (6). Consequently, collecting the information from DSP-S and SSP-S sizing provides clues about the cfDNA molecule positioning on the biological constituents (complexes) that stabilize them in the blood circulation. Size profiling using Q-PCR, on the other hand, shows the fractional size distribution (16, 18, 23, 32) and relies on "denatured" cfDNA fragments just as SSP-S relies on single-strand fragments (6); also, in contrast to WGS, Q-PCR allows analysis to be extended to lengths over approximately 1000 bp.

Given all of the elements detailed above, it will be obvious that the originality and the significance of our work, both in purely scientific terms and in its potential for clinical application, are that it combines

Q-PCR, DSP-S, and SSP-S, and in doing so obtains an assessment of cfDNA size profile, fragmentation level, and associated structures that is simultaneously more complete and more precise.

Size distribution of healthy donor cfDNA

Our first, surprising observation was that the size profile curves of the 7 healthy subjects were equivalent with each other, as were the 7 curves superimposed with either DSP-S or SSP-S. Consequently, we postulate that (a) the dynamics of DNA degradation following cell release is the same in all healthy subjects or (b) the resulting stabilized cfDNAs all have the same structure. Detailed analysis of cfDNA sizing revealed an approximately 10 bp (nt) periodicity footprint, which is detected down to 101 bp and 53 nt within the 41 to 166 bp (nt) range, using DSP-S and SSP-S, respectively. This suggests that nucleosome-derived degradation occurs once nuclear DNA/chromatin is released in blood. Thus, this pattern was attributed to cleavage in nucleotides, which are accessible because they lie further from the surface of the histone core at each helical turn where DNA wraps around the core (33). Consequently, our data confirm that most of the detectable cfDNA in blood has a nucleosome footprint (6–8, 10, 30); this indicates that the stability of circulating DNA derives mostly from the nucleosome structure. Although the number of cfDNA fragments associated with di-nucleosomes is relatively low, the 10 bp periodicity footprint is detectable within the 280–400 bp (nt) size range (with both DSP-S and SSP-S); that range corresponds to the length of DNA wrapped around a di-nucleosome. Indeed, recent reports suggest that the 2 key DNA/protein complexes that protect DNA from blood nucleases are probably DNA-wrapped around a histone octamer, or DNA-bound to transcription factors (6, 8, 34, 35). By generating maps of genome-wide in vivo nucleosome occupancy, Snyder et al. (8) revealed the presence of shorter (35–80 bp) fragments associated with cleavage adjacent to transcription factor–binding sites, harboring footprints of transcription factors (8, 36). It is likely that such transcription factor–associated cfDNA exists and that it may be present in a hidden manner, without being characterized in the size profile within the population of short cfDNA fragments. Our current study was not designed to individualize transcription factor–associated structures. SSP-S clearly revealed a population of short fragments and a more pronounced shoulder at approximately 145 bp, further revealing nicks in both strands of the DNA packed in the mono-nucleosome– or transcription factor–associated cfDNA. CfDNA associated with di-nucleosomes would therefore represent a very small proportion of the total cfDNA of healthy individuals.

When using conventional Illumina Y adapters, we also assume that in the presence of double-stranded molecules with nick(s), only the strand without a nick will be recovered following DSP-S. In addition, DSP-S will reveal cfDNA fragments if there is 1 nick in both strands in the same vicinity. Furthermore, if there were 1 or 1+ nicks on each strand, and the double-stranded molecule still hung together, neither strand would be recovered by DSP-S; SSP-S, however, would detect as fragments n+1 number of single-stranded DNA pieces released from n nicks. Our data confirm that trimmed mono-nucleosome cfDNA-associated structures (theoretically condensing 165-bp length DNA) are predominant in the cfDNA size profile. Although WGS can only reveal the size profile from 30 to approximately 1000 bp, our data nevertheless distinctly demonstrate that the number and mass of cfDNAs within mono-nucleosomes is at least approximately 9 and approximately 4.5 times higher than the number and mass of cfDNAs associated with di-nucleosomes, respectively. Since both SSP-S and DSP-S gave the same peak at approximately 166 bp, we can hypothesize that a significant but low fraction (2–3%) of cfDNA fragments of this size are nick free, at least in 1 strand. This structure corresponded to the chromatosome, which consists of a histone octamer ($[H2A–H2B]_2$ $[H3\text{-}H4]_2$) plus the histone monomer linker H1 tightly associating 166 bp DNA (ref. 37 and Figure 6). Our data showed that the cfDNA molecule is highly nicked (97–98%) and that nuclease activity occurred in a continuous way on the nucleosomal structure. Thus, the nucleosome structure corresponding to the chromatosome devoid of the histone monomer linker H1 and then compacting only 147 bp DNA (the mono-nucleosome) was also highly represented among the cfDNA structural forms (Figure 6). DSP-S revealed nucleosomal footprints of cfDNA fragments smaller than 166 bp but did not reveal fragments smaller than 90 bp; this was in contrast to SSP-S analysis, which showed fragments as small as 45 nt. If fragments in the 45 to 90 nt range go undetected, this suggests that they are either degraded or no longer wrapped within the histone complex. Taken together, these observations imply that, in order to be protected, the cfDNA molecule needs to be surrounded by histones and as a result of this protection is detectable in blood samples. The 2 strands exposed to the surface of the nucleosome are shifted by 3 bp with a 3′ stagger. Indeed, our data showed a shift of 3 bp between the size of the molecules detected by DSP-S and SSP-S; in addition to the observation of the approximately 10 bp periodicity, this confirms that cfDNA are wrapped around the nucleosome (8).

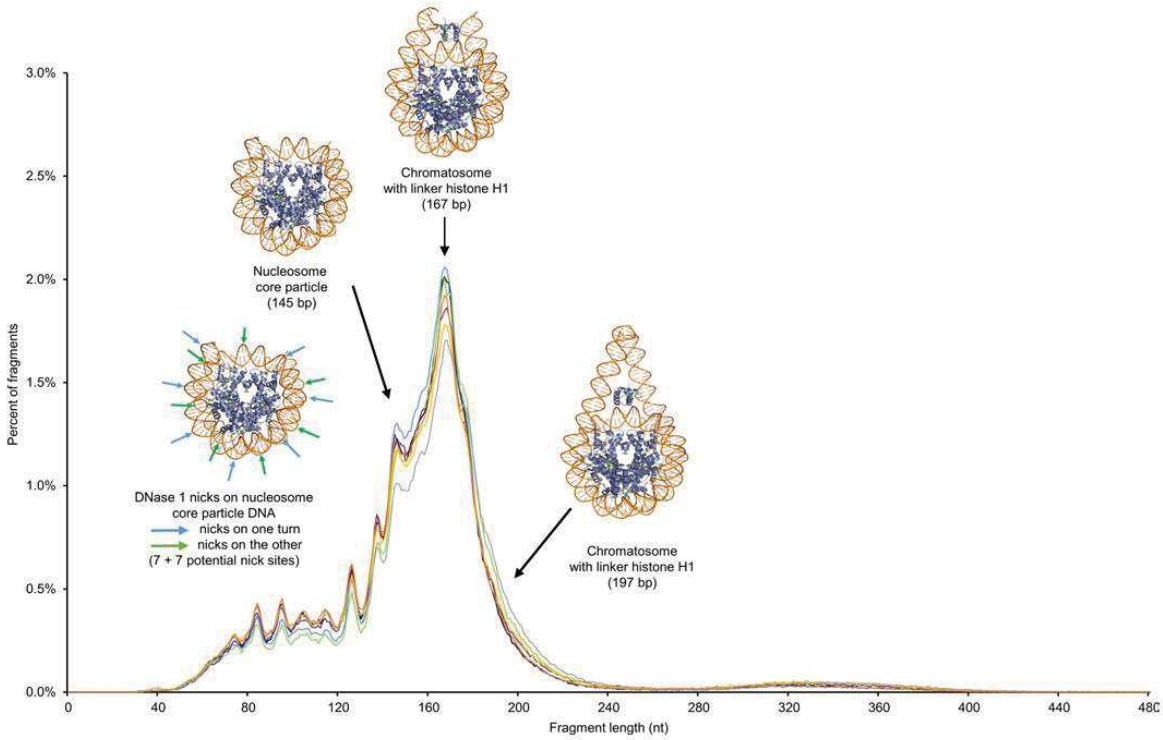

Figure 6. Representation of the crystal structure of the nucleosome core particle, chromatosome, and chromatosome with a flexible DNA chain, on the cfDNA fragment size profile of the 7 healthy subjects, as determined by SSP-S. The chromatosome with 167 bp DNA fragment is the most present cfDNA-associated structure, while being of low frequency (~2%). The nucleosome core particle devoid of H1 containing 147–160 bp is the second most present structure (1.1%–1.2%). Arrows on a nucleosome structure indicate the minor groove DNA sites subject to DNase attacks, explaining the ~10 bp periodic subpeaks in size profile revealing nicks on the nucleosome-associated DNA, and fragmentation down to 40 nt single-stranded DNA, when using SSP-S. Images of the crystal structure of chromatosome and nucleosome at 3.5 angstrom resolution, from the NIPDB data bank (4QLC and 5ONW, respectively). NIPDB, Nucleic Acid–Protein Interaction Database, https://npidb.belozersky.msu.ru.

Since the approximately 10 bp subpeaks were clearly observable within the 90 to 166 bp range, our data also suggest that most cfDNA molecules within that range derive from double-strand breaks occurring at the nucleosome extremity, as well as at 1 of the 14 positions on the DNA minor groove, where DNA is exposed at the nucleosome surface. It might be possible that rare double-strand breaks occur at 2 distinct positions at the nucleosome surface. Logically, double-strand breaks may occur at any one of the 14 positions (Figure 6). We should therefore have observed the same number of cfDNA fragments of each of the ~10, 20, 30, 40, 50, 60, 70, 80, 90, 100, 110, 120, 130, or 140 bp sizes. However, this was not the case; for instance, cfDNA fragments from 10 to 90 bp were not detected. The lower the DNA molecule size, the less tightly they are maintained on the nucleosome, as there are fewer binding forces. The disappearance of these fragments might result from their peeling off from the nucleosome and consequent rapid degradation. Reports have demonstrated that DNA may peel off from the edge of the nucleosome (37). This observation can therefore be taken as a convincing demonstration that the nucleosome is an essential element of cfDNA stability.

SSP-S revealed shorter cfDNA fragments, down to 45 nt, because the DNA molecule with only 1 nick on one of the 2 DNA molecule strands was still maintained and wrapped around the nucleosome and therefore did not peel off. The critical size of 70 bp corresponds to a full turn around the nucleosome. This suggests that if there is a DNA fragment associated with a less than full turn around the nucleosome, the probability of peeling off is high, as a consequence of its degradation. Figure 6 shows the position of the minor groove where nicks may occur and offers a schematic view of the nucleosome/chromatin structures associated with cfDNA, depending on cfDNA fragment length (Figure 6).

Table 3. Presumed main causes of fragmentation and resulting structures of healthy subject plasma cfDNA on the chromatin-derived particles

Presumed main causes of fragmentation of cfDNA within chromatin-derived particles				Structure of the DNA molecule hanging on the chromatin-derived particles
Size range	Predominant types of DNA breaks	Chromatin organization	Approximative fraction	CfDNA molecule integrity
40–83 bp	One or more SSBs or DSBs on both strands	Mono-nucleosome or chromatosome	~7%	Double-stranded DNA with nicks on both strands
83–165 bp	One DSB; 1 or more SSBs in only 1 strand	Mono-nucleosome or chromatosome	~38%	Double-stranded DNA with nicks on both strands; blunt intact double-stranded DNA; double-stranded DNA with nicks in 1 strand
121 bp	DSB	Mono-nucleosome or chromatosome	~0.4%	Blunt intact double-stranded DNA
133 bp	DSB	Mono-nucleosome or chromatosome	~0.7%	Blunt intact double-stranded DNA
144 bp	DSB	Mono-nucleosome or chromatosome	~1.2%	Blunt intact double-stranded DNA
166 bp	No break	Chromatosome	~2%	Blunt intact double-stranded DNA
160–240 bp	DSB; SSB in only 1 strand	Chromatosome	~49%	Double-stranded DNA with 1 or more nicks in 1 strand; blunt intact double-stranded DNA
280–440 bp	One or more SSB in only 1 or both strands; 1 or more DSBs	Di-nucleosome	~5%	Double-stranded DNA with 1 or more nicks in only 1 or both strands

Combined analysis of DSP-S– and SSP-S–based size profile (Figure 1) infers the predominant types of DNA breaks and resulting cfDNA molecule integrity hanging on mono-nucleosomes, chromatosomes, or di-nucleosomes, upon size ranges up to approximately 1000 bp. Note: intact double-strand DNA sizing 121, 133, and 144 bp were highlighted as they are predominant between approximately 116 and approximately 150 bp. DSB, double-stranded DNA break; SSB, single-stranded DNA break.

Theoretically, any fragment sizes detectable by DSP-S should also be detectable by SSP-S. In contrast to DSP-S analysis, no 152 bp subpeak was observable with SSP-S; however, this does not mean that this double-strand fragment was not present in the extract, rather that it was invisible because of its lower frequency, compared with that of the neighboring subpeaks, especially at 145 bp. Nevertheless, this highlights the fact that the 145 to 166 bp DNA region is more sensitive to nuclease degradation, suggesting higher exposure of DNA to nucleases between the mono-nucleosome and the chromatosome. Our data also highlight the predominance of double-stranded DNA of 121, 133, and 144 bp length resulting from double-strand breaks (Figure 1, A and B, and Table 3). Table 3 sums up the main causes of fragmentation and the resulting structures of cfDNA on the chromatin-derived particles, according to our WGS data.

Using WGS, we observed only 2 or 3 cfDNA size fragment populations; these corresponded to mono- or di-nucleosomes and traces of tri-nucleosomes, with the di-nucleosome–associated cfDNAs representing only a minor fraction of the total fragments. This confirmed the findings of a number of other studies that used either WGS or microcapillary electrophoresis (7, 38–44), performed in optimal preanalytical conditions (45). Note, some of those studies also revealed cfDNA of high molecular weight (2000 to 10,000 bp) at 10% to 20% (39, 41). When combining SSP-S and Q-PCR data concerning the 7 healthy individuals with the DII data concerning the 109 healthy individuals, we estimated the proportion of cfDNA inserted in mono-nucleosomes, di-nucleosomes, and chromatin of higher molecular size (>1000 bp) can be estimated as ranging 67.5% to 80.0%, 9.4% to 11.5%, and approximately 8.5% to 21.0%, respectively. Note, as indicated in Methods, these values are only indicative because of the inherent variation of cfDNA concentration as quantified when targeting a 320 bp amplicon.

These values correlated with the Chan et al. (23) data (15%–25%, and 10% in size fractions higher than approximately 300 bp and higher than ~500 bp, respectively) and with the values reported in several other studies (41). Bronkhorst et al. demonstrated that the 143B cancer cell line actively releases 2000 to 3000 bp sized segments of heterochromatin (46) and suggested that this secretion into the extracellular environment can induce a wide range of detrimental biological effects. Nevertheless, experiments with hemolytic plasma

samples or matching serum, or using cell preservative tubes (44) or longtime storage (44), have highlighted the contamination of cfDNA samples with white blood cell DNA in the 300 to 450 bp and the 2000 to 11,000 bp size ranges, as reported in several studies (5, 39, 40, 47). It is difficult to specifically distinguish cfDNA from contaminating DNA using current techniques. Numerous conclusions in the literature regarding fragment size distribution are biased by obvious hematopoietic cell–DNA contamination, caused by improper preanalytical conditions (13, 48–51). For instance, Li et al. (48) observed a high proportion of high–molecular weight DNA in normal individuals and proposed an erroneous conclusion regarding its cfDNA distribution; this in turn misled the noninvasive prenatal test (NIPT) field into incorrectly postulating that greater NIPT performance is obtained by cfDNA size separation using a cutoff point of 300 or 500 bp, whereas most cfDNA clearly displays sizes below 300 bp. In contrast, our work (which was performed under optimal stringent preanalytical conditions, ref. 45) indicates that only a minor fraction of cfDNA is larger than that existing in mono-nucleosomes or transcription factor complexes circulating in the blood of healthy individuals. This suggests that the cfDNA detectable in plasma is present predominantly within those structures. Consequently, our data can be seen as supporting the notion that cfDNA sizing quality control must be performed to overcome biased conclusions regarding cfDNA size profiles, and to better analyze cfDNA, particularly in the case of a rare fraction of a specific cfDNA population (i.e., mutant cfDNA in oncology or fetal cfDNA in NIPT). For instance, we postulate that the cfDNA extract of healthy individuals displaying a fraction of di-nucleosome–associated DNA fragments over 20% should only be taken into consideration with considerable reserve. Fragmentation should therefore be considered as a parameter that must be monitored in order to ensure quality control (11, 45).

Comparing cfDNA size profiles from healthy and cancer individuals

Because cancer is one of the most researched pathological conditions in the cfDNA field, our study sought to determine if fragmentation could provide a different perspective on the structure of cfDNA derived from cancer patients, as compared with that deriving from individuals of normal physiological condition, as described above. This exploratory study was based on the blinded examination of 7 plasma samples from healthy individuals and of plasma from 7 mCRC patients presenting a wide variation in MAF (0.9%, 3.2%, 14.4%, 23.3%, 47.3%, 54.7%, and 68.6%). Thus, it was possible to study the cancer cfDNA size profile across a wide range of malignant (mutant) cell-derived cfDNA. The cfDNA in cancer patients derives from the malignant cells, the tumor microenvironment cells (endothelial, stromal, immunological/lymphocytic cells), or the germinal cells. We and others have previously demonstrated that mutant cfDNA frequency varies widely in the plasma of cancer patients, independent of the stage of the disease and tumor size (19, 20). Nevertheless, we assume that the plasma DNA of mCRC patients exhibiting a high MAF (68.6%) displays characteristics very similar to cfDNA deriving from cancer/malignant cells (Table 4 and Table 5).

Overall, the plasma cfDNA of the cancer patients showed similar size profiles to those of healthy subjects and revealed the footprint of chromatin structures, in both DSP-S and SSP-S analysis. Our WGS study, however, clearly highlights differences in the plasma cfDNA fragment size range below 1000 bp, between cancer and healthy subjects: (a) cancer patients have more cfDNA fragments under 166 bp and less from 166 to 250 bp; (b) a size curve shoulder at 145 bp appears more pronounced in cancer individuals; and (c) these differences correlated directly with the proportion of tumor mutant (malignant) cfDNA.

As previously observed by Jiang et al. (22) in hepatocarcinoma cancer patients, the size profile obtained from conventional DSP-S showed a subtle but reliable difference between cancer and healthy subject–derived cfDNA. In our study, while DSP-S revealed a monomodal population of cfDNA peaking at 166 to 167 bp in both subject groups, we observed a moderate increase (10%–20%) of fragments between 90 and 166 bp, and a moderate decrease (<10%) between 166 and 250 bp in cancer patients, as compared with healthy individuals. As there is little or no variation in cfDNA size profiles among healthy subjects, as observed here and elsewhere (52–54), even subtle but reliable differences in size profile in the cancer cfDNA fragment population are potentially significant. Using either DSP-S or SSP-S analysis, the determination of the difference of cumulative frequencies demonstrated that, for cancer patient–derived cfDNA, the increase in fragment numbers was optimal around 160 bp. This indicates that cfDNA from tumor cells is more fragmented than that from healthy individuals. Note, the size profile of the cfDNA of the mCRC patient with the lowest MAF (0.9%) was not significantly different from that of the healthy individuals. Indeed, the fact that these differences increased with MAF tends to validate our observation of the differences between cancer and healthy cfDNA. Accordingly, the curve shoulder appearing at 145 to 155 bp in cancer patients would appear

Table 4. cfDNA size profile characteristics in healthy individuals

Three populations	80–240 bp	240–400 bp	>1000 bp
Aspect	Monomodal	Monomodal	Large range
Size at the highest frequency	166 bp	330 bp	
Approximate proportion	67.5%–80.0%	11.0%–11.5%	8.5%–21.3%

Characteristics of size profile of cfDNA from plasma of healthy subjects.

Table 5. Suggested size profile characteristics of cfDNA deriving from malignant cancer cells

Three populations	40–220 bp	220–400 bp	>1000 bp
Aspect	Monomodal with shoulder between 140 and 166 bp	Monomodal	Large range
Size at the highest frequency	166 bp	290 bp	
Approximate proportion	83%	16%	<1%

Characteristics of size profile of cfDNA from plasma of cancer subjects.

to be reliable. It will be remembered that 145 bp corresponds to DNA wrapped around a nucleosomal core unit (167 bp) minus a linker fragment of approximately 20 bp. We hypothesize that particles containing 145 and 166 bp DNA fragments are more stable than ones containing 153 bp fragments, due to the high nuclease sensitivity of the approximately 20 bp linker fragment. Consequently, our data showed that there are more cfDNA fragments in chromatosomes than in mono-nucleosomes, in healthy as compared with cancer subjects (Table 6 and Supplemental Table 2A). This in turn leads us to postulate that tumors have elevated or different DNase activity as recently postulated (7, 55).

The mean proportion of cfDNA over 320 bp in 104 all-stage CRC patients was estimated as approximately 0.4% by the *KRAS* intron 3 Q-PCR system. Because of the variation observed in the size profile of CRC patient–derived cfDNA relative to their MAF, the percentage range of the cfDNA fragment size populations cannot be estimated when combining data obtained by DSP-S, SSP-S, and Q-PCR analysis. Taken as a whole, however, the data reveal that the greater the MAF, the greater the number of fragments below 320 bp, and the fewer the number of fragments over approximately 1000 bp. Although these values are only indicative (Methods), they can be directly compared with those obtained in healthy individual plasma. As a consequence, in addition to the subtle difference in size profile within the 30 to 250 bp (nt) range, as previously observed in our study, the presence of a significant fraction (~8.5%–21%) of cfDNA with a fragment size over 1000 bp appears to be a landmark of healthy individual plasma (as compared with cancer patients), so long as the plasma cfDNA extracts are free of contaminating blood cell DNA. This finding confirmed the observation we previously made in xenograft mouse models and human plasma, that cfDNA from cancer patients is more fragmented than that of healthy individuals, when also considering fragment sizes over ~300 bp (16, 18, 29, 32). This has been convincingly established in the field, using various analytical methods (10, 18, 22, 56).

CfDNA fragmentation analysis or "fragmentomics" as a cognitive or diagnostic tool

Toward a cancer screening test. In addition to previously providing a proof-of-principle approach in using specific size fractions, size ratios, or size fraction ratios from cfDNA fragment size profile to distinguish cancer and healthy individual plasma (16, 29), our in-depth scrutiny of WGS size profiles offered another clear-cut assessment method for making such a distinction (Table 6 and ref. 57). Our initial observations (16, 29, 57) and the data presented here were confirmed using the Delfi cancer screening approach (28). The determination and evaluation of an algorithm combining different fragmentomics parameters is currently underway in our laboratory. Moreover, one of our recent reports (58) includes fragmentation indexes in a panel combined with other biomarkers, as a means of evaluating a machine-learning-assisted cancer screening test.

Diagnostics in oncology. We first demonstrated that cfDNA fragments less than 100 bp were more frequent in cancer patients than in healthy subjects (6, 9, 29) and that the size of mutant cfDNA fragments whose sequence contained a mutation is shorter than that of the corresponding WT sequence (17). This

Table 6. Suggested differences of the cancer patient cfDNA size profile from that of healthy individuals

Higher proportion in the 40–151 bp range	
Lower proportion in the 151–220 bp range	
Very poor proportion of fragments over 1000 bp	
Lower size at the highest frequency of the population corresponding to di-nucleosome–associated cfDNA	
Selected discriminative parameters:	Lower 166/145 bp ratio (<1% vs 3.1%)
	Presence of fragments in the 30–80 bp range
	Lower proportion of fragments in the 151–220 bp range (<33% vs. 70%)
	Higher proportion of fragments in the 30–145 bp range (>44% vs. 13%)
	ΔS at 155 bp > 32%
	ΔV within the 40–160 bp range > 30%
	ΔV (SSP-S minus DSP-S) within the 40–160 bp (nt) range (~14% vs. ~22%)

Differences between cfDNA extracted from cancer patient as compared with that of healthy individuals with highlighted most powerful parameters.

observation has been clearly confirmed by Jiang et al. (22) and recently by Garlan et al. (59). Snyder et al. (8) pointed out the value of examining cfDNA fragmentation as a means of determining their tissue of origin and thus providing potential clues as to individual physiological states as a diagnostic aid, particularly in cases of cancer. Selection of fragments between 90 to 150 bp, using targeted and whole-genome sequencing approaches, could enrich the tumor DNA up to 11-fold (26). Hence, isolation of short cfDNA fragments appears as a means of enriching tumor variants and improving the correction of PCR- and sequencing-associated errors, especially in theragnostic testing (60).

Fragmentomics in other clinical fields. Several reports have shown a clear, subtle, and reliable difference in size profile below 300 bp between fetal and maternal cfDNA (26). A parallel can be drawn between these cfDNA size profile differences and those that exist between cancer cfDNA and the cfDNA of healthy subjects. Remarkably, increases of fragment size within the 80 to 166 bp range and moderate decreases within the 166 to 220 bp range have also been observed.

CpG methylation, which is linked to an open chromatin structure and thus may be more accessible to native endonucleases (61), as well as difference of DNase activity and DNase species (7, 55), may contribute to the observed size difference. It is likely that some other physiological conditions may stimulate cells to produce cfDNA, and thus alter its size profile, i.e., lymphocytic cells during or after intense effort, or the immune cells after organ transplant.

CfDNA tissue of origin. We unveiled here differences in the intimate cfDNA size profile at nucleotide level, allowing the characterization of the malignant or healthy cell origin of cfDNA extracts from blood samples. By generating maps of genome-wide in vivo nucleosome occupancy, Snyder et al. (8) and Lehmann et al. (36) revealed that cfDNA harbors footprints of transcription factors and that the origin of cfDNA tissue or cell type can be inferred from the correlation of nucleosome spacing. These 2 pivotal works extend considerably the scope of fragmentomics so that it could now encompass noninvasive monitoring of numerous diseases and of normal physiological conditions.

Limitations and future directions

Our study has several limitations. Although we established the presence of cfDNA longer than 1000 bp in healthy individual plasma, we could not characterize the structure of this cfDNA population any further. Specific methods to do so are as yet unavailable. Furthermore, while sequencing analysis of the plasma of the 7 healthy individuals gave nearly identical size profiles, the number of plasma samples used for studying sizes below approximately 1000 bp is too low to consider our study anything more than exploratory. Confirmation performed on a large cohort remains necessary to demonstrate that all the discriminating factors revealed here have potential application in a screening test, as was convincingly but partially demonstrated by Cristiano et al. (28). Also, the WGS study on cfDNA from cancer patients was derived exclusively from mCRC patients. In addition, this study does not take into consideration mitochondria-derived cfDNA; similar investigation, therefore, should be performed that takes into account the growing interest of the clinical potential of mitochondrial cfDNA analysis (11). Finally, the different commercial DNA extraction kits

Table 7. Strongest differences of the size profile as determined by SSP-S as compared with that determined by DSP-S

Highest proportion of fragments in the 40–130 bp range
Presence of fragments in the 40–90 bp (nt) range
Lower proportion in the 160–420 bp (nt) range
Lower proportion of di-nucleosome–associated cfDNA
Lower 160/145 bp (nt) ratio
Fragments are globally shorter in the 40–1000 bp (nt) range (ΔS always positive)
Each fragment of size ranging from 160 to 420 bp (nt) is in lower proportion (ΔV always negative in that range)
Each fragment of size ranging from 40 to 160 bp (nt) is in higher proportion (ΔV always positive in that range)

Differences between cfDNA size profile obtained following DSP-S and SSP-S.

were found not all equally efficient at extracting DNA of specific sizes (45). This study used a single method to prepare cfDNA; while that method was validated under a stringent preanalytical guideline (45), we nonetheless further confirmed our data using a capillary electromobility assay, as well as the conventional phenol/chloroform extraction method (Supplemental Figure 9).

It has confirmed our earlier hypothesis that size profiling, or fragmentomics (62), is a valuable strategy for characterizing cancer individuals (ref. 16, Table 6, and Table 7); as such, it offers a possible alternative or synergistic supplement to the strategy of searching for cancer-associated mutations — a strategy that, it must be noted, has recently shown false positivity (63). For these reasons, we are convinced that specific cfDNA structures, as observed by fragmentomics (6, 10, 28, 34), methylation (64, 65) or nucleosome positioning (8, 35), possess significant potential to improve diagnostics and early cancer detection.

Methods

Clinical samples. The blood samples of healthy individuals (n = 7) were obtained from the Etablissement Français du sang (EFS, Supplemental Table 4). Blood samples from stage IV CRC patients (n = 7; Supplemental Table 4) were collected at the Montpellier Cancer Institute (Val d'Aurelle) and from the SIRIC Montpellier network. All individuals signed an informed consent form. Samples were handled according to a preanalytical guideline previously established by our group (45). In order to calculate a fragmentation index, a DII was generated in an ad hoc study using 109 control healthy subjects, sourced from the EFS, and 104 CRC patients of various stages (Supplemental Table 4), sourced via the SIRIC Montpellier network.

Plasma isolation and cfDNA extraction. All blood samples were collected in 4-milliliter EDTA tubes. The blood was then centrifuged at 1200*g* at 4°C for 10 minutes. The supernatants were isolated in sterile 1.55 mL Eppendorf tubes and centrifuged at 16,000*g* at 4°C for 10 minutes. Afterward, the plasma was either immediately used for DNA extraction or stored at –20°C. CfDNA was extracted from 1 mL of plasma using the QIAmp DNA Mini Blood kit (Qiagen) according to the "Blood and body fluid protocol." DNA extracts were kept at –20°C until used. The preanalytical conditions we followed are described (45).

Preparation of sequencing libraries and size profile analysis by deep sequencing. Preparation of sequencing libraries as well as WGS are detailed in Supplemental Methods, Appendix 1. Note, the lower and upper size limits of detection by sequencing carried out under these conditions are estimated to be 20 to 30 bp and approximately 1000 bp, respectively.

Fractional size distribution by Q-PCR. Fractional size distribution by Q-PCR was performed as previously described (6, 9, 18, 29). Specific Q-PCR systems, calculation, presentation of the results, and limitations of this study are detailed in Supplemental Methods, Appendix 2, and Supplemental Figure 10.

Determination of the cfDNA MAF. MAF corresponds to the proportion of cfDNA fragments within a plasma extract bearing a targeted mutation. MAF was determined using the IntPlex assay, which is clinically validated (19), by testing 28 mutations on *KRAS*, *BRAF*, and *NRAS* genes actionable in mCRC management care (20) (Supplemental Methods, Appendix 3).

Statistics. Statistical analysis was performed using the GraphPad Prism V6.01 software. Where appropriate data were log transformed prior to statistical analysis. The Student's t test, 1 tailed, was used to compare means. A P value of less than 0.05 was considered statistically significant; $^{*}P < 0.05$, $^{**}P < 0.01$; $^{***}P < 0.001$; $^{****}P < 0.0001$.

Study approval. We included mCRC patients from the screening procedure of the ongoing UCGI 28 PANIRINOX study (NCT02980510/EudraCT 2016-001490-33). Written informed consent was requested. Healthy individual blood samples were obtained from the EFS.

Author contributions

ART designed the study, developed the methodology, analyzed the data, and prepared the manuscript. CS, ZAAD, BP, EP, and RT performed the experiments. CS and BR prepared the manuscript. BR, TM, PB, CS, ZAAD, BP, EP, RT, and ART discussed the results and approved the manuscript.

Acknowledgments

The authors thank Charles Marcaillou and Steven Blanchard from Integragen, and Valerie Taly, Thierry Grange, Eva-Maria Geigl, Andrew Bennett, Nitzan Rosenfeld, and Denis Lo for their helpful discussions. The authors thank Cormac McCarthy, Marc Ychou, and Antoine Adenis for their support and helpful comments on the manuscript. We greatly acknowledge Emily Bottle, David Webb, and Sebastian Moore for helpful discussions. ART is supported by INSERM. This work was funded by the "SIRIC Montpellier Cancer Grant INCa_Inserm_DGOS_12553." This project has also received funding from the European Union's Horizon 2020 research 610 and innovation program under grant agreement 755333 (LIMA).

Address correspondence to: Alain R. Thierry, 208 rue des Apothicaires, F-34298 Montpellier Cedex 5, France. Phone: 33.6.63.82.19.94; Email: alain.thierry@inserm.fr.

1. Wan JCM et al. Liquid biopsies come of age: towards implementation of circulating tumour DNA. *Nat Rev Cancer*. 2017;17(4):223–238.
2. Thierry AR, et al. Origins, structures, and functions of circulating DNA in oncology. *Cancer Metastasis Rev*. 2016;35(3):347–376.
3. Wong FCK, Lo YMD. Prenatal diagnosis innovation: genome sequencing of maternal plasma. *Annu Rev Med*. 2016;67(1):419–432.
4. Pös O, et al. Circulating cell-free nucleic acids: characteristics and applications. *Eur J Hum Genet*. 2018;26(7):937–945.
5. Otandault A, et al. Recent advances in circulating nucleic acids in oncology. *Ann Oncol*. 2019;30(3):374–384.
6. Sanchez C, et al. New insights into structural features and optimal detection of circulating tumor DNA determined by single-strand DNA analysis. *NPJ Genom Med*. 2018;3(1):31.
7. Serpas L et al. *Dnase1l3* deletion causes aberrations in length and end-motif frequencies in plasma DNA. *Proc Natl Acad Sci U S A*. 2019;116(2):641–649.
8. Snyder MW, et al. Cell-free DNA comprises an in vivo nucleosome footprint that informs its tissues-of-origin. *Cell*. 2016;164(1–2):57–68.
9. Mouliere F, et al. Circulating cell-free DNA from colorectal cancer patients may reveal high KRAS or BRAF mutation load. *Transl Oncol*. 2013;6(3):319–328.
10. Underhill HR, et al. Fragment length of circulating tumor DNA. *PLoS Genet*. 2016;12(7):e1006162.
11. Meddeb R, et al. Quantifying circulating cell-free DNA in humans. *Sci Rep*. 2019;9(1):5220.
12. Diaz LA, Bardelli A. Liquid biopsies: genotyping circulating tumor DNA. *J Clin Oncol*. 2014;32(6):579–586.
13. Jahr S, et al. DNA fragments in the blood plasma of cancer patients: quantitations and evidence for their origin from apoptotic and necrotic cells. *Cancer Res*. 2001;61(4):1659–1665.
14. Holdenrieder S, et al. Stability of nucleosomal DNA fragments in serum. *Clin Chem*. 2005;51(6):1026–1029.
15. Deligezer U, et al. Circulating fragmented nucleosomal DNA and caspase-3 mRNA in patients with lymphoma and myeloma. *Exp Mol Pathol*. 2006;80(1):72–76.
16. Mouliere F, et al. High fragmentation characterizes tumour-derived circulating DNA. *PLoS One*. 2011;6(9):e23418.
17. Diehl F, et al. Detection and quantification of mutations in the plasma of patients with colorectal tumors. *Proc Natl Acad Sci U S A*. 2005;102(45):16368–16373.
18. Mouliere F, et al. Multi-marker analysis of circulating cell-free DNA toward personalized medicine for colorectal cancer. *Mol Oncol*. 2014;8(5):927–941.
19. Thierry AR, et al. Clinical validation of the detection of KRAS and BRAF mutations from circulating tumor DNA. *Nat Med*. 2014;20(4):430–435.
20. Thierry AR, et al. Clinical utility of circulating DNA analysis for rapid detection of actionable mutations to select metastatic colorectal patients for anti-EGFR treatment. *Ann Oncol*. 2017;28(9):2149–2159.
21. Andersen RF, et al. Improved sensitivity of circulating tumor DNA measurement using short PCR amplicons. *Clin Chim Acta*. 2015;439:97–101.
22. Jiang P, et al. Lengthening and shortening of plasma DNA in hepatocellular carcinoma patients. *Proc Natl Acad Sci U S A*. 2015;112(11):E1317–E1325.
23. Chan KCA, et al. Size distributions of maternal and fetal DNA in maternal plasma. *Clin Chem*. 2004;50(1):88–92.
24. Bianchi DW, Chiu RWK. Sequencing of circulating cell-free DNA during pregnancy. *N Engl J Med*. 2018;379(5):464–473.
25. Lo YM, et al. Quantitative analysis of fetal DNA in maternal plasma and serum: implications for noninvasive prenatal diagnosis. *Am J Hum Genet*. 1998;62(4):768–775.
26. Mouliere F, et al. Enhanced detection of circulating tumor DNA by fragment size analysis. *Sci Transl Med*. 2018;10(466):eaat4921.
27. Tanos R, Thierry AR. Clinical relevance of liquid biopsy for cancer screening. *Transl Cancer Res*. 2018;7(2):S105–S129.
28. Cristiano S, et al. Genome-wide cell-free DNA fragmentation in patients with cancer. *Nature*. 2019;570(7761):385–389.

29. Thierry A, Molina F, inventors. Centre National de la Recherche Scientifique (CNRS), assignee. Analytical methods for cell free nucleic acids and applications. International patent application WO2012028746A1. September 5, 2011.
30. Sun K, et al. Orientation-aware plasma cell-free DNA fragmentation analysis in open chromatin regions informs tissue of origin. *Genome Res*. 2019;29(3):418–427.
31. Burnham P, et al. Single-stranded DNA library preparation uncovers the origin and diversity of ultrashort cell-free DNA in plasma. *Sci Rep*. 2016;6:27859.
32. Thierry AR, et al. Origin and quantification of circulating DNA in mice with human colorectal cancer xenografts. *Nucleic Acids Res*. 2010;38(18):6159–6175.
33. Szerlong HJ, Hansen JC. Nucleosome distribution and linker DNA: connecting nuclear function to dynamic chromatin structure. *Biochem Cell Biol*. 2011;89(1):24–34.
34. Chandrananda D, et al. High-resolution characterization of sequence signatures due to non-random cleavage of cell-free DNA. *BMC Med Genomics*. 2015;8:29.
35. Lehmann-Werman R, et al. Identification of tissue-specific cell death using methylation patterns of circulating DNA. *Proc Natl Acad Sci U S A*. 2016;113(13):E1826–E1834.
36. Vierstra J, et al. Coupling transcription factor occupancy to nucleosome architecture with DNase-FLASH. *Nat Methods*. 2014;11(1):66–72.
37. Kassabov SR, et al. SWI/SNF unwraps, slides, and rewraps the nucleosome. *Mol Cell*. 2003;11(2):391–403.
38. Wu DC, Lambowitz AM. Facile single-stranded DNA sequencing of human plasma DNA via thermostable group II intron reverse transcriptase template switching. *Sci Rep*. 2017;7(1):8421.
39. Wolf A, et al. Purification of circulating cell-free DNA from plasma and urine using the automated large-volume extraction on the QIAsymphony SP instrument. In: Gahan PB, et al., eds. *Circulating Nucleic Acids in Serum and Plasma — CNAPS IX*. Springer; 2016:179–185.
40. Maggi EC, et al. Development of a method to implement whole-genome bisulfite sequencing of cfDNA from cancer patients and a mouse tumor model. *Front Genet*. 2018;9:6.
41. Fernando MR, et al. Analysis of human blood plasma cell-free DNA fragment size distribution using EvaGreen chemistry based droplet digital PCR assays. *Clin Chim Acta*. 2018;483:39–47.
42. Agilent. Automated Electrophoresis. https://www.agilent.com/en/product/automated-electrophoresis. Accessed May 27, 2019.
43. Tamkovich SN, et al. Features of circulating DNA fragmentation in blood of healthy females and breast cancer patients. In: Gahan PB, et al., eds. *Circulating Nucleic Acids in Serum and Plasma — CNAPS IX*. Springer; 2016:47–51.
44. Sato A, et al. Investigation of appropriate pre-analytical procedure for circulating free DNA from liquid biopsy. *Oncotarget*. 2018;9(61):31904–31914.
45. Meddeb R, et al. Guidelines for the preanalytical conditions for analyzing circulating cell-free DNA. *Clin Chem*. 2019;65(5):623–633.
46. Bronkhorst AJ, et al. Characterization of the cell-free DNA released by cultured cancer cells. *Biochim Biophys Acta*. 2016;1863(1):157–165.
47. Lin LH, et al. Increased plasma circulating cell-free DNA could be a potential marker for oral cancer. *Int J Mol Sci*. 2018;19(11):3303.
48. Li Y, et al. Size separation of circulatory DNA in maternal plasma permits ready detection of fetal DNA polymorphisms. *Clin Chem*. 2004;50(6):1002–1011.
49. Hromadnikova I, et al. Quantification of fetal and total circulatory DNA in maternal plasma samples before and after size fractionation by agarose gel electrophoresis. *DNA Cell Biol*. 2006;25(11):635–640.
50. Pérez-Barrios C, et al. Comparison of methods for circulating cell-free DNA isolation using blood from cancer patients: impact on biomarker testing. *Transl Lung Cancer Res*. 2016;5(6):665–672.
51. Azad AA et al. Androgen receptor gene aberrations in circulating cell-free DNA: biomarkers of therapeutic resistance in castration-resistant prostate cancer. *Clin Cancer Res*. 2015;21(10):2315–2324.
52. Fan HC, et al. Analysis of the size distributions of fetal and maternal cell-free DNA by paired-end sequencing. *Clin Chem*. 2010;56(8):1279–1286.
53. Heitzer E, et al. Establishment of tumor-specific copy number alterations from plasma DNA of patients with cancer. *Int J Cancer*. 2013;133(2):346.
54. Lo YMD. Fetal DNA in maternal plasma: biology and diagnostic applications. *Clin Chem*. 2000;46(12):1903–1906.
55. Han DSC, et al. The biology of cell-free DNA fragmentation and the roles of DNASE1, DNASE1L3, and DFFB. *Am J Hum Genet*. 2020;106(2):202–214.
56. Schwarzenbach H, et al. Loss of heterozygosity at tumor suppressor genes detectable on fractionated circulating cell-free tumor DNA as indicator of breast cancer progression. *Clin Cancer Res*. 2012;18(20):5719–5730.
57. Thierry AR. El Messaoudi S, inventors; Institut National de la Santé et la Recherche Médicale (INSERM), assignee. US Patent methods for screening a subject for a cancer. International patent application 15/518,392. August 24, 2017.
58. Tanos R, et al. Machine learning-assisted evaluation of circulating DNA quantitative analysis for cancer screening. *Adv Sci (Weinh)*. 2020;7(18):2000486.
59. Garlan F, et al. Circulating tumor DNA measurement by picoliter droplet-based digital pcr and vemurafenib plasma concentrations in patients with advanced BRAF-mutated melanoma. *Target Oncol*. 2017;12(3):365–371.
60. Hellwig S, et al. Automated size selection for short cell-free DNA fragments enriches for circulating tumor DNA and improves error correction during next generation sequencing. *PLoS One*. 2018;13(7):e0197333.
61. Jensen TJ, et al. Whole genome bisulfite sequencing of cell-free DNA and its cellular contributors uncovers placenta hypomethylated domains. *Genome Biol*. 2015;16(1):78.
62. Ivanov M, et al. Non-random fragmentation patterns in circulating cell-free DNA reflect epigenetic regulation. *BMC Genomics*. 2015;16(suppl 13):S1.
63. Salk JJ, et al. Ultra-sensitive TP53 sequencing for cancer detection reveals progressive clonal selection in normal tissue over a century of human lifespan. *Cell Rep*. 2019;28(1):132–144.
64. Moss J, et al. Comprehensive human cell-type methylation atlas reveals origins of circulating cell-free DNA in health and disease. *Nat Commun*. 2018;9(1):5068.
65. Gezer U, et al. Histone methylation marks on circulating nucleosomes as novel blood-based biomarker in colorectal cancer. *Int J Mol Sci*. 2015;16(12):29654–29662.

F/ Double inhibition de l'EGFR et de c-Src par le Cetuximab et le Dasatinib en association avec la chimiothérapie FOLFOX chez les patients atteints d'un cancer colorectal métastatique

Auteurs : Christine M. Parseghian, Nila U. Parikh, Ji Yuan Wu, Zhi-Qin Jiang, Laura Henderson, Feng Tian, **Brice Pastor**, Marc Ychou, Kanwal Raghav, Arvind Dasari, David R. Fogelman, Anastasia D. Katsiampoura, David G. Menter, Robert A. Wolff, Cathy Eng, Michael J. Overman, Alain R. Thierry, Gary E. Gallick, and Scott Kopetz

Cette publication a été a été publiée dans Clinical Cancer Reasearch en 2017

Résumé: L'activation aberrante de la tyrosine kinase intracellulaire Src a été impliquée comme mécanisme de résistance acquise à la chimiothérapie dans le cancer colorectal métastatique (CCRm). Le dasatinib, un inhibiteur oral de la tyrosine kinase Src, a été étudié en association avec FOLFOX et le cetuximab. **Conception expérimentale** : Nous avons réalisé une étude de phase IB/II sur 77 patients atteints de cancer colorectal métastatique déjà traités. Les objectifs principaux étaient de déterminer la dose maximale tolérée, les toxicités limitant la dose (TLD), la pharmacodynamique et l'efficacité. Selon un schéma 3 þ 3, les patients ont reçu FOLFOX6 avec cetuximab et des doses croissantes de dasatinib (100, 150, 200 mg par jour), suivi d'une cohorte d'expansion de 12 patients à 150 mg. Les études de phase II ont évalué FOLFOX plus dasatinib 100 mg chez les patients *KRAS* c12/13mut ou en association avec cetuximab si *KRAS* c12/13WT. FAK et paxilline ont été utilisés comme biomarqueurs sanguins de substitution de l'inhibition de Src, et des biopsies appariées de métastases hépatiques ont été obtenues chez les patients de la cohorte d'expansion. **Résultats** : Dans la phase IB, les DLT étaient une fatigue de grade 3/4 (20%) et une neutropénie (23%). En phase II, la fatigue de grade 3/4 (23%) et les épanchements pleuraux (11%) étaient présents. Les taux de réponse étaient de 20% (6 sur 30) dans la cohorte d'escalade et d'expansion de la phase IB et de 13% (3 sur 24) et 0% (0 sur 23) dans les cohortes *KRAS* c12/13WT et mutant de la phase II, respectivement. La survie médiane sans progression était de 4,6, 2,3 et 2,3 mois, respectivement. Il n'y avait aucune preuve d'inhibition de Src basée sur des biomarqueurs sanguins de substitution ou des biopsies tumorales appariées. **Conclusions** : L'association dasatinib plus FOLFOX avec ou sans cetuximab n'a montré qu'une activité clinique modeste dans le cancer colorectal réfractaire. Cela semble être principalement dû à l'incapacité d'inhiber complètement Src aux doses réalisables de dasatinib. L'association du dasatinib et de FOLFOX avec ou sans cetuximab n'a pas montré d'activité clinique significative dans le cancer colorectal réfractaire en raison de l'absence d'inhibition complète de Src.

Contribution: J'ai participé à la réalisation des analyses des ADNcir de cette étude. L'étude KPLEX R qui est présentée dans la partie résultats a été réalisée avec les échantillons plasmatiques des patients de cette étude. Les deux études ont été publiées ensemble dans Clinical Cancer Reaserch.

Published OnlineFirst March 9, 2017; DOI: 10.1158/1078-0432.CCR-16-3138

Cancer Therapy: Clinical

Clinical Cancer Research

Dual Inhibition of EGFR and c-Src by Cetuximab and Dasatinib Combined with FOLFOX Chemotherapy in Patients with Metastatic Colorectal Cancer

Christine M. Parseghian[1], Nila U. Parikh[1], Ji Yuan Wu[1], Zhi-Qin Jiang[1], Laura Henderson[1], Feng Tian[1], Brice Pastor[2], Marc Ychou[2], Kanwal Raghav[1], Arvind Dasari[1], David R. Fogelman[1], Anastasia D. Katsiampoura[1], David G. Menter[1], Robert A. Wolff[1], Cathy Eng[1], Michael J. Overman[1], Alain R. Thierry[2], Gary E. Gallick[1], and Scott Kopetz[1]

Abstract

Purpose: Aberrant activation of the intracellular tyrosine kinase Src has been implicated as a mechanism of acquired chemotherapy resistance in metastatic colorectal cancer (mCRC). Here, the oral tyrosine kinase Src inhibitor, dasatinib, was investigated in combination with FOLFOX and cetuximab.

Experimental Design: We performed a phase IB/II study of 77 patients with previously treated mCRC. Primary objectives were to determine the maximum tolerated dose, dose-limiting toxicities (DLT), pharmacodynamics, and efficacy. Using a 3 + 3 design, patients received FOLFOX6 with cetuximab and escalating doses of dasatinib (100, 150, 200 mg daily), followed by a 12-patient expansion cohort at 150 mg. Phase II studies evaluated FOLFOX plus dasatinib 100 mg in *KRAS* c12/13^{mut} patients or in combination with cetuximab if *KRAS* c12/13^{WT}. FAK and paxillin were utilized as surrogate blood biomarkers of Src inhibition, and paired biopsies of liver metastases were obtained in patients in the expansion cohort.

Results: In phase IB, the DLTs were grade 3/4 fatigue (20%) and neutropenia (23%). In phase II, grade 3/4 fatigue (23%) and pleural effusions (11%) were present. Response rates were 20% (6 of 30) in the phase IB escalation and expansion cohort and 13% (3 of 24) and 0% (0 of 23) in the *KRAS* c12/13^{WT} and mutant cohorts of phase II, respectively. Median progression-free survival was 4.6, 2.3, and 2.3 months, respectively. There was no evidence of Src inhibition based on surrogate blood biomarkers or paired tumor biopsies.

Conclusions: The combination of dasatinib plus FOLFOX with or without cetuximab showed only modest clinical activity in refractory colorectal cancer. This appears to be primarily due to a failure to fully inhibit Src at the achievable doses of dasatinib. The combination of dasatinib plus FOLFOX with or without cetuximab did not show meaningful clinical activity in refractory colorectal cancer due to failure to fully inhibit Src. *Clin Cancer Res; 23(15); 4146–54. ©2017 AACR.*

Introduction

Colorectal cancer remains one of the most common cancers worldwide and the second and third leading cause of death in men and women in the United States, respectively (1). For patients with surgically unresectable disease, the expected 5-year relative survival is less than 15% (2). Despite significant advances in treatment of metastatic colorectal cancer (mCRC) with currently available regimens, response rates for those that progress after first-line treatment are only 4% to 17% (3, 4).

Src family kinases have been implicated in drug resistance in mCRC. Cellular stimuli induce conformational changes that increase Src kinase activity via dephosphorylation of residue Y530 and autophosphorylation of residue Y418 (5). Src activation results in a variety of downstream signaling pathways involved in survival, angiogenesis, proliferation, and migration (6–9). Src can potentiate the effects of receptor tyrosine kinases as well as directly activate PI3K pathway that results in reduction of apoptosis signaling and increased cellular survival. Furthermore, signaling through the RAS/RAF/MAPK results in increased proliferation and numerous other proproliferation phenotypes. By additionally interacting with cytoskeletal components including focal adhesion kinase (FAK), paxillin, and E-cadherin, among others, Src is a key regulator of tumor cell adhesion, migration, and invasiveness (10). Src expression and activity have been shown to be higher in primary colon tumors compared with benign polyps and in metastatic compared with non-metastatic colon cancer, highlighting its role in colorectal progression (11–15).

Colon cancer cell lines with defective Src kinases are particularly sensitive to oxaliplatin-induced apoptosis (16). Patients with mCRC who received neoadjuvant oxaliplatin demonstrated

[1]Department of Gastrointestinal Medical Oncology, Division of Cancer Medicine, The University of Texas MD Anderson Cancer Center, Houston, Texas. [2]IRCM, Institut de Recherche en Cancérologie de Montpellier, Montpellier, France.

Note: Supplementary data for this article are available at Clinical Cancer Research Online (http://clincancerres.aacrjournals.org/).

Corresponding Author: Christine M. Parseghian, The University of Texas MD Anderson Cancer Center, 1400 Holcombe Boulevard, Unit 0463, Houston, TX 77030. Phone: 713-792-0051; Fax: 713-792-3708; E-mail: cparseghian@mdanderson.org

doi: 10.1158/1078-0432.CCR-16-3138

Published OnlineFirst March 9, 2017; DOI: 10.1158/1078-0432.CCR-16-3138

Translational Relevance

Our phase II study showed minimal benefit to the addition of dasatinib to the widely used regimen of FOLFOX plus cetuximab in metastatic colorectal cancer. This appears to be primarily due to a failure to fully inhibit Src at the achievable doses of dasatinib. It is unclear whether we may have seen some clinical activity if we were able to fully inhibit Src in this study, but given the requirement that enrolling patients have documented disease progression on cetuximab, acquired resistant *KRAS*-mutant clones may have been present, limiting future strategies to reverse EGFR resistance. Additional early-stage clinical trials are needed to further clarify the best approaches to targeting resistance to cetuximab and the role of Src tyrosine kinase inhibitors in metastatic colorectal cancer.

higher levels of Src pathway signaling in hepatic metastases, a finding associated with poorer relapse-free survival (17).

Dasatinib is an orally bioavailable, potent, multitargeted kinase inhibitor and an effective therapeutic agent for the treatment of several malignancies (18). Although relatively specific for the Src and Abl family kinases, dasatinib possesses broad-spectrum inhibition of kinases including Kit, PDGFR, EphA receptors, and many others (19). Several preclinical studies have demonstrated the ability of Src inhibitors like dasatinib to overcome chemoresistance as well as resistance to targeted agents, such as the EGFR monoclonal antibody cetuximab (20–23). Other preclinical studies suggest that the combination of dasatinib and oxaliplatin has additive and possibly synergistic activity. Colorectal cancer tumors treated with the combination of dasatinib and oxaliplatin demonstrate markedly decreased microvessel activity and increased oxidative stress (9, 24). In a mouse model of colorectal liver metastases, 28-day treatment with oxaliplatin resulted in chronic Src activation, and the combination of dasatinib plus oxaliplatin resulted in significantly smaller tumors compared with single-agent treatment with oxaliplatin alone, corresponding with reduced proliferation and angiogenesis (25).

We thus conducted a phase IB/II study combining the Src inhibitor dasatinib with a modified FOLFOX regimen with or without cetuximab in patients with previously treated mCRC to evaluate its efficacy as well as its toxicity profile in this patient population.

Patients and Methods

Eligibility criteria

Eligible patients were required to have histologically or cytologically confirmed colorectal adenocarcinoma with metastatic disease documented on diagnostic imaging studies, mass spectroscopy genotyping confirmed *KRAS* mutation status (exon 1, codon 12, 13), evaluable or measurable disease by Response Evaluation Guide for Solid Tumors (RECIST) version 1.0 and Eastern Cooperative Oncology Group (ECOG) Performance Status (PS) of 0 or 1. Patients also had to be $\geq$18 years of age with adequate hematopoietic, hepatic, and kidney function and a life expectancy $\geq$ 3 months. Each patient must have had previously progressed, either clinically or radiographically, on systemic therapy for mCRC, with no limit on the number of prior regimens. Patients in the phase II cohort must have progressed on fluorouracil (5-FU) or capecitabine and oxaliplatin if *KRAS*-mutant and either cetuximab or panitumumab if *KRAS* wild-type. Key exclusion criteria included recent (within 4 weeks of the first infusion of study drugs on this study) or planned participation in another experimental therapeutic drug study; systemic chemotherapy, radiotherapy, or major surgery within 21 days prior to the first infusion of study drugs; radiographic evidence of pleural effusions in the last 30 days prior to enrollment; known brain metastases; known dihydropyrimidine dehydrogenase deficiency; long QT syndrome; history of clinically significant ventricular arrhythmias; concurrent severe and/or uncontrolled medical conditions including uncontrolled high blood pressure ($\geq$140/90), unstable angina or stable angina markedly limiting ordinary physical activity, New York Heart Association (NYHA) $\geq$ grade 2 congestive heart failure, myocardial infarction within 6 months of study enrollment, history of stroke within 6 months of study enrollment, unstable symptomatic arrhythmia requiring medication, clinically significant peripheral vascular disease, uncontrolled diabetes, and serious active or uncontrolled infection. The trial was conducted in accordance with the Declaration of Helsinki. The protocol (ClinicalTrials.gov identifier: NCT00501410) was approved by the Institutional Review Board at UT MD Anderson Cancer Center (Houston, TX), and written informed consent was obtained for all patients before performing study-related procedures.

For the phase II cohort, patients were categorized as *KRAS* G12- and G13-mutant or wild-type on the basis of mass spectroscopy genotyping for all RAS mutations in tumor tissue.

Drug administration and study design

We conducted a single-institution, open-label, investigator-initiated phase IB/II study in patients with refractory mCRC treated with modified FOLFOX6, cetuximab, and dasatinib, with dasatinib dose escalation by cohort. The primary objectives of the phase IB portion of the study were to determine the maximum tolerated dose (MTD) and dose-limiting toxicity (DLT) of the combination of dasatinib, cetuximab, and modified FOLFOX6 in adult patients with mCRC and to determine whether biologic activity of the combination regimen on c-Src activity occurred at the MTD in the expansion cohort. The secondary objectives were to demonstrate the feasibility of peripheral blood biomarkers of Src inhibition, to determine the safety profile and tolerability of the regimen, and to document its antitumor effects.

The primary objective of the phase II arm was to determine the response rate distribution of dasatinib and FOLFOX with or without cetuximab. The secondary objectives were determination of time to treatment failure (TTF) and ratio of current TTF to TTF of immediate prior regimen, determination of overall survival (OS) on this regimen, and evaluation of its safety profile and tolerability.

A Bayesian design was utilized to assess efficacy, with a target response rate of interest of greater than 10%. Continuous reassessment was utilized for futility monitoring. The sample size ensured that the 95% confidence interval (CI) would have a width at most of 0.22 under the assumption of a 10% response rate. Operating characteristics can be found in Supplementary Materials and Supplementary Table S1.

Treatment

The regimen consisted of cetuximab (400 mg/m^2 week 1 followed by weekly doses of 250 mg/m^2), oxaliplatin (85 mg/m^2 q2weeks), bolus 5-FU (400 mg/m^2 q2weeks), and leucovorin

Published OnlineFirst March 9, 2017; DOI: 10.1158/1078-0432.CCR-16-3138

(400 mg/m^2 q2weeks), followed by a 46-hour infusion of 5-FU (2,400 mg/m^2 q2weeks). Dasatinib was dosed orally daily in cohorts of 100, 150, and 200 mg/d, administered without interruption. Dasatinib dose escalation was performed using a standard "3 + 3" design. Dose reductions were required for all grade 3 or 4 toxicities attributed to study medications. The symptom-specific dose adjustment table can be found in Supplementary Table S2. The dose reduction algorithm for all drugs can be found in Supplementary Table S3. Treatment was continued until disease progression, unacceptable toxicities, or withdrawal of consent. Adverse event (AE) grading was performed according to the National Cancer Institute Common Terminology Criteria for Adverse Events (CTCAE), version 3.0. Appropriate radiographic images were collected for all patients enrolled at baseline and at all post-baseline evaluations by the same radiological method to assess response. All radiologic tests that demonstrated tumor at baseline were repeated after every 4 cycles and at discontinuation of study treatment. For the phase II arm, mass spectroscopy genotyping for somatic gene mutations was performed on resected tumor tissue prior to any treatment with cetuximab. DNA extracted from formalin-fixed, paraffin-embedded resected tumor tissue was analyzed with Sequenom MassArray technology (Sequenom, Inc.) using the protocol developed in one of our institutional core facilities (26). Patients deemed to be *KRAS* c12/13 wild-type received the MTD from the phase I arm, whereas *KRAS*-mutant patients received the same, without cetuximab.

Correlative studies

Previous studies have demonstrated that peripheral blood mononuclear cells (PBMC) can provide information on Src activity (27). To demonstrate the feasibility of examining Src phosphorylation and phosphorylation of selected Src targets, PBMCs from normal subjects were treated *ex vivo* with dasatinib 300 nmol/L or a low dose of hydrogen peroxide as a positive control. The Src substrates, FAK and paxillin, were utilized for this study as they are expressed in detectable levels in mononuclear cells. Assay optimization demonstrated that protease and phosphatase inhibition were required to maintain signal. As shown in Supplementary Fig. S1, *ex-vivo* treatment with dasatinib significantly inhibited phosphorylation of FAK at tyrosine 861. Similarly, phosphorylation of FAK at tyrosine 118 on paxillin was reduced. Treatment with hydrogen peroxide led to a modest increase, as expected (Supplementary Fig. S1).

Furthermore, we sought to correlate peripheral blood mononuclear cell findings with pSrc levels in paired core liver biopsies obtained in the 12 patients in the expansion cohort. pFAK as categorized by standardized immunohistochemical grading on a scale of 0 to +4 was compared with baseline levels by the Wilcoxon matched-pairs signed-ranks test. Serum and PBMCs were collected at baseline, day 8 of the second and fourth cycles, and optionally at the time of study treatment discontinuation. Paired liver biopsies were obtained prior to therapy (within 4 weeks of initiation of therapy) and between day 8 and day 14 of cycles 2 or 3. See Supplementary Information for further details on methods.

Results

Safety and efficacy

Thirty patients were enrolled in the phase IB portion of the study. Eighteen patients were enrolled in the dose-escalation cohort and 12 patients in the expansion cohort. Baseline characteristics can be found in Table 1. Notable toxicities included grade 2 or 3 thrombocytopenia in 27% (representing platelet counts < 75,000), neutropenia (23% grade 3 or 4), and fatigue (20% grade 3 and 4; Table 2). Other toxicities such as diarrhea, nausea, vomiting, and mucositis were consistent with prior experience with the non-investigational components. Pleural effusions were commonly seen in this patient population. These pleural effusions appeared to be dose-related and were present predominantly in patients with pre-existing effusions or metastatic disease to the lung. These were not dose-limiting and rarely required intervention with thoracentesis.

Table 1. Baseline characteristics

Patient and disease characteristics	Phase IB ($N = 30$) Number of patients (%)	Phase II ($N = 47$) Number of patients (%)
Age, y		
Median (range)	54 (34–76)	58 (26–74)
Female	19 (63)	18 (38)
ECOG PS		
0	13 (43)	23 (49)
1	17 (57)	24 (51)
Location of tumor		
Liver	29 (97)	30 (64)
Lung	14 (47)	12 (26)
Peritoneum	10 (33)	10 (21)
Intact primary tumor	7 (23)	24 (51)
Nonregional lymph nodes	6 (20)	2 (4)
Omentum	0	4 (9)
Mesentery	0	2 (4)
Prior treatment[a]		
Median	4	3
Range	2–7	1–10
KRAS c12/13 mutation status		
WT		24 (51)
Mutant		23 (49)
Prior EGFR therapy		
Treatment	24 (80)	24 (51)
Documented refractory	23 (77)	24 (100)
Prior oxaliplatin therapy		
Treatment	29 (97)	47 (100)
Documented refractory	21 (70)	46 (97)

[a]Prior chemotherapy; immunotherapy; or hormonal, biologic, or small-molecule targeted therapy regimens.

No MTD was identified during the DLT period. A dasatinib dose of 200 mg was cleared on the basis of MTD criteria after 2-week assessment. However, because of high rates of dasatinib dose reduction after 2 weeks, 150 mg was utilized for the expansion cohort.

Of the 30 phase IB patients treated at all dose levels, including in the expansion cohort, 25 patients had measurable disease. The remaining 5 patients either had early toxicities that precluded assessment within the first 2 months or had disease that was not measurable by standard radiologic criteria. Of the 30 patients, 47% had their disease controlled after one restaging scan. Six of these 30 patients had a reduction in the size of their measurable tumors by >30%, representing a response rate of 20% (Fig. 1A). Of these 6 patients, 5 were previously refractory to oxaliplatin. One had received prior oxaliplatin but this was discontinued secondary to neuropathy. Four of the 6 patients had received prior EGFR-based therapy (3 with cetuximab and 1 with panitumumab), and all had failed to respond or subsequently progressed on this treatment. One of these responding patients was treated at the

Published OnlineFirst March 9, 2017; DOI: 10.1158/1078-0432.CCR-16-3138

Table 2. Summary of AEs while receiving treatment, irrespective of causality

	Phase IB ($N = 30$) Number of patients (%)		Phase II ($N = 47$) Number of patients (%)	
AE	All grades	Grade ≥ 3	All grades	Grade ≥ 3
Fatigue	19 (63)	6 (20)	17 (36)	11 (23)
Anemia	10 (33)	4 (13)	1 (2)	1 (2)
Nausea/vomiting	9 (30)	1 (3)	3 (6)	2 (4)
Thrombocytopenia	8 (26)	1 (3)	5 (11)	0
Neutropenia	7 (23)	7 (23)	6 (13)	3 (6)
Diarrhea	5 (17)	2 (7)	7 (15)	3 (6)
Pleural effusion	0	0	7 (9)	5 (11)
Peripheral neuropathy	0	0	5 (11)	0
Acute renal failure	0	0	4 (9)	0
Anorexia	0	0	3 (6)	2 (4)
Mucositis	0	0	3(6)	1 (2)
Dyspnea	0	0	1 (2)	1 (2)
Bleeding	0	0	1 (2)	1 (2)
Hypokalemia	0	0	1 (2)	1 (2)
Hemorrhagic shock (death)	0	0	1 (2)	1 (2)
Deep vein thrombosis	0	0	1 (2)	0
Rash	0	0	1 (2)	0
Cardiomyopathy	0	0	1 (2)	0

100-mg dose of dasatinib and 5 received a 150-mg dose. There were no responses in the 200-mg cohort. Dose reductions were eventually required in 4 of the 6 patients due to myelosuppression and/or fatigue. In addition to a dasatinib dose reduction in all 4 patients, one patient also had a 5-FU and oxaliplatin dose reduction and another patient had a cetuximab dose reduction.

Of the 6 responding patients, 5 had a wild-type *KRAS* oncogene, whereas the *KRAS* status was unknown for one patient. The median progression-free survival (PFS) for this cohort was 4.6 months and 23% of the patients were free of progression and continued on treatment at 6 months (Fig. 2A).

Twenty-four patients with *KRAS* c12/13 wild-type and 23 patients with *KRAS* c12/13 mutant colorectal cancer participated in the phase II portion of the study. Baseline characteristics of these patients can be found in Table 1. The most common toxicities of any grade while on treatment were fatigue (36%), diarrhea (15%), and neutropenia (13%). Overall, 21 of 47 patients experienced at least one grade 3 AE while on study. The most common grade 3 toxicities were fatigue and pleural effusions. There was one grade 4 episode of neutropenia and one grade 5 episode of hemorrhagic shock (Table 2). There was one toxicity-related death due to hemorrhagic shock. Sixteen patients (34%) had AEs leading to dose interruption across all cycles. The most common causes of dose interruption included pleural effusion ($n = 3$) and fatigue ($n = 3$).

Forty of the 47 patients in this trial had post-baseline scans. Fourteen of 47 patients (30%; 95% CI, 0.17–0.45) experienced an overall response. There were no complete responses. At the first restaging interval, 3 patients (6%; 95% CI, 0.1–0.18), all *KRAS* wild-type, and all who had been refractory to an oxaliplatin-based regimen and cetuximab previously, had a confirmed partial response, which was durable for a median of 5.2 months (range,

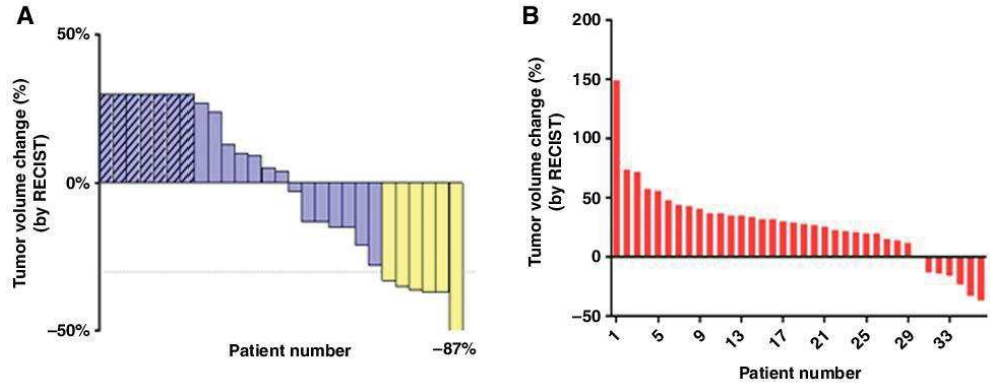

Figure 1.
Clinical efficacy of the FOLFOX + cetuximab + dasatinib treatment. **A,** Waterfall plot of best response for the regimen in the phase IB study demonstrates 6 patients with a RECIST response. An additional 7 patients had tumor regression that did not meet RECIST criteria for response. Patients with progressive disease noted by new lesions are listed as +30% growth. **B,** Waterfall plot of patients in the phase II study treated with dasatinib, FOLFOX, with or without cetuximab, measuring the maximum change from baseline in the sum of the longest diameter for target lesions.

Published OnlineFirst March 9, 2017; DOI: 10.1158/1078-0432.CCR-16-3138

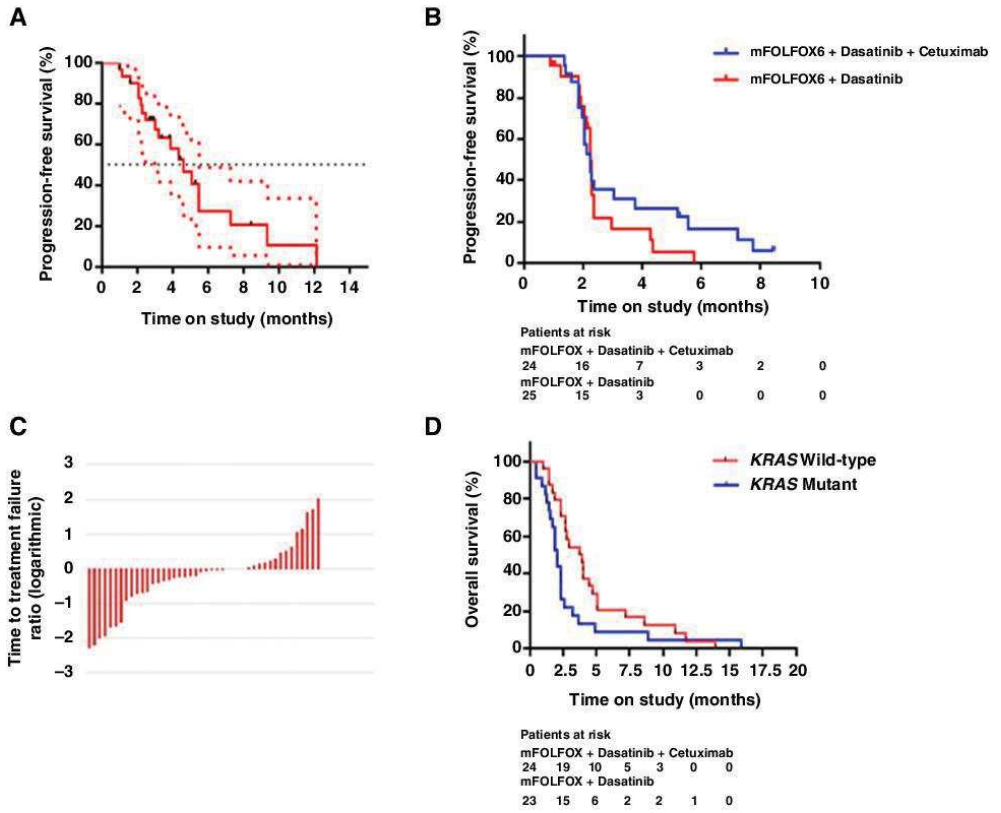

Figure 2.

A, PFS of patients treated on the FOLFOX, cetuximab, and dasatinib study, with 95% CIs shown. Median PFS was 4.6 months (95% CI, 3.0–5.5 months). **B,** TTF on study drugs. All censored patients in both treatment arms were assumed to have had an event at the date of censoring. **C,** Ratio of TTF on study regimen to TTF on prior regimen, assessed logarithmically in all patients. **D,** Kaplan–Meier curve of OS calculated as time from trial initiation to time of death, stratified by tumor *KRAS* mutational status.

1.6–8.5 months). Eleven patients (23%; 95% CI, 0.12–0.38) had stable disease; 6 of these patients were *KRAS* wild-type. Thirty-six patients (77%; 95% CI, 0.63–0.87) discontinued their regimen due to progressive disease after a median of 4 cycles of therapy (range, 1–16 cycles).

The median TTF on the immediate prior regimen to the study was 3.8 months in *KRAS* c12/13 wild-type patients (range, 0–14.0 months) and 2.0 months in *KRAS*-mutant patients (range, 0–16.0 months). The median TTF on our study regimen was 2.3 months in both the *KRAS* wild-type cohort (range, 1.4–8.5 months) and the *KRAS*-mutant cohort (range, 0.9–5.8 months; Fig. 2B). The median ratio of TTF on study regimen to TTF on prior regimen was 0.9 for all patients (range, 0.1–5.5), 0.8 in the *KRAS* wild-type patients (range, 0.1–7.6), and 1.0 in the *KRAS*-mutant patients (range, 0.1–5.5) , respectively (Fig. 2C). The median OS was 6.7 months (range, 1.0–28.4 months) in all patients, 7.7 months in *KRAS* wild-type patients (range, 2.0–22.6 months), and 5.9 months (range, 1.0–28.4 months) in *KRAS*-mutant patients (Fig. 2D).

PBMC pharmacodynamics

PBMC samples at baseline and cycle 2, day 8 were available for 29 of the 30 patients. These lysates were initially analyzed by Western blotting for both phospho-FAK(861) and phospho-paxillin(118). However, it became clear that phosphorylation of FAK was not maintained during processing, as there was no detectable phosphorylation band that was evident in baseline, nor cycle 2, day 8 samples. Conversely, paxillin maintained a phosphorylation signal on Western blotting and was used as the standard for effects of dasatinib in subsequent studies.

As shown in Fig. 3, there was a significant increase in phospho-paxillin in cycle 2, day 8 of therapy. When compared with baseline, an almost 4-fold increase was observed by densitometry ($P = 0.004$). There was no discernible correlation between the

Published OnlineFirst March 9, 2017; DOI: 10.1158/1078-0432.CCR-16-3138

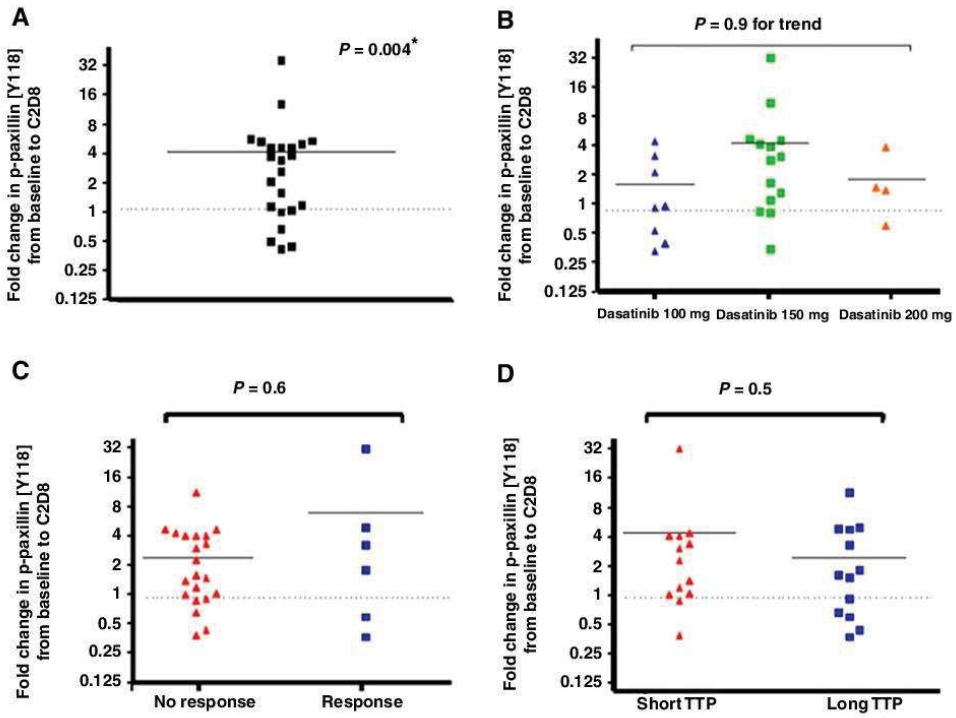

Figure 3.

Quantification of p-paxillin [Y118] from PBMCs of patients treated on the FOLFOX + cetuximab + dasatinib clinical trial. Samples were collected at baseline and after 3 weeks of therapy (at day 8 of cycle 2). **A,** p-Paxillin [Y118] was increased after 3 weeks on treatment. *, Paired *t* test for fold change by densitometry. **B,** No difference is seen in the induction of p-paxillin by cohort. **C,** There is no correlation between change in p-paxillin and response to therapy, nor time to progression (TTP). **D,** Short and long TTP were defined as less than 4 months and greater than or equal to 4 months, respectively (approximately the median TTP).

dose of dasatinib utilized and phospho-paxillin, although there were limited samples available from the patients remaining on the 200-mg dose. Likewise, there was not a correlation between phosphorylation and response to therapy or time on therapy (Fig. 3).

Pharmacodynamics in tumor tissue

Of the 12 patients in the expansion cohort, all consented for paired liver biopsies. These biopsies were obtained by interventional radiology as per phase IB methods. There were no complications noted for these 24 procedures. Adequate and viable tissue was available for all 24 patients. An average of 4 core biopsies was obtained from each patient with a range of 2 to 6 at each time point. A minimum of 4 biopsies was obtained in 22 of the 24 procedures. Frozen sections of the tumor tissue were stained for phospho-Src with tyrosine 418 and total Src. The results from viable sections as assessed from adjacent hematoxylin and eosin (H&E) slides were assessed qualitatively. The staining of these tumors was assessed semiquantitatively and the results are shown in Fig. 4. There was no change in phospho-Src [Y418] staining after 3 weeks of combination therapy ($P = 0.3$ by the Wilcoxon signed-rank test). However, there was a statistically significant increase in total Src after treatment ($P = 0.049$). As there were only 2 responders in this cohort, there was a limited ability to detect correlations between response and modulation. The second biopsy for one of the responders only contained acellular fibrosis without evidence of viable tumor in the region sampled and so could not be assessed for Src substrates.

As the second biopsy was obtained at cycle 2, day 8, the liver biopsy samples are correlated with PBMCs in Supplementary Fig. S2 in an attempt to evaluate the surrogacy of the peripheral mononuclear cell signal. This analysis is exploratory given the limited sample size in the biopsy cohort. There was no significant correlation of Src activity in the PBMCs (measured by fold change in phospho-paxillin) and increased Src or phospho-Src expression in the liver biopsy.

Discussion

Aberrant activation of the intracellular tyrosine kinase Src has been implicated as a mechanism of acquired chemotherapy resistance in mCRC. Preclinical studies have shown synergistic effects of Src inhibition with both oxaliplatin and cetuximab. On the basis of these results, we conducted a phase IB/II study of the

Published OnlineFirst March 9, 2017; DOI: 10.1158/1078-0432.CCR-16-3138

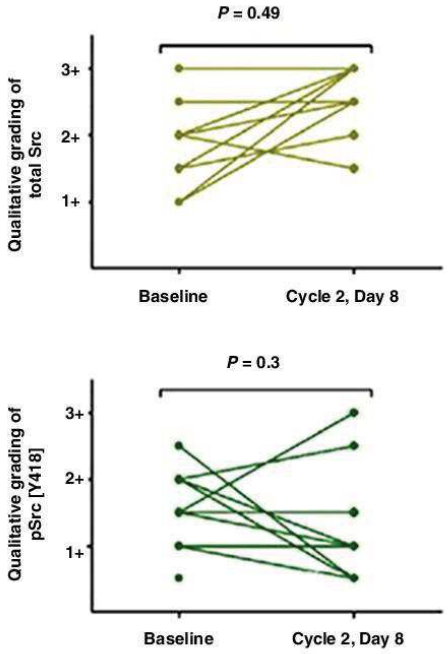

Figure 4.
In patients with evaluable paired biopsies in the expansion cohort, semiquantitative grading of total Src and phospho-Src [Y418] staining was performed. Each line represents an individual patient. There was a statistically significant increase in total Src staining after 3 weeks of treatment ($P = 0.049$). There was no change in phospho-Src staining ($P = 0.3$).

oral tyrosine kinase Src inhibitor, dasatinib, in combination with FOLFOX and cetuximab in patients with heavily pretreated mCRC.

The phase IB portion of our study determined a phase II dose of dasatinib that could be used safely in combination. Correlative studies were performed which included evaluation of peripheral mononuclear cells and paired liver biopsies from the expansion cohort. The enrolled population in the phase IB portion was heavily pretreated with a median of 4 prior lines of therapy. Ninety-seven percent of the patients had been exposed to prior oxaliplatin and 80% had been exposed to prior EGFR therapy. Response rate in this population was 20% in the evaluable subset. In patients who were previously refractory to oxaliplatin, there was a 25% response rate. Similarly, in patients who were refractory to EGFR-based therapy, the response rate was 20%. The median PFS of 4.6 months was better than would be expected in a similar cohort of patients treated with regorafenib (1.9 months) or TAS-102 (2.0 months; refs. 28, 29).

The toxicities associated with this regimen included fatigue and myelosuppression. The dose of 150-mg daily of dasatinib was chosen for further study based on the higher rates of myelosuppression seen with the 200-mg dose. Even at this reduced dose, there were no patients who were able to maintain a 150-mg dose beyond 3 months. The most common reason for dose reduction was myelosuppression and fatigue. The degree of fatigue was also greater than would be expected from this chemotherapy regimen alone in this patient population (30). However, a recent phase I study demonstrated that dasatinib 70 mg daily could be safely combined with capecitabine, oxaliplatin, and bevacizumab—a dose of dasatinib that was lower than anticipated (31). Thus, the intensity of this chemotherapy regimen in a heavily refractory population should not be discounted, and lower doses of dasatinib may be considered for further studies in this setting.

The pharmacodynamic studies incorporated in the phase IB portion of the study demonstrated that treatment with the dasatinib-containing regimen failed to inhibit Src and instead demonstrated a paradoxical increase in Src activation. This may, in part, be due to increased Src activity after oxaliplatin therapy, as shown in our tissue analysis after staining for phospho-Src. Murine studies have suggested that treatment with dasatinib at a higher dose is sufficient to inhibit Src activation after oxaliplatin (25). However, in our study, the analysis of the PBMCs demonstrated increased phosphorylation in the Src substrate of paxillin. This increase was robust and was statistically significant, suggesting that dasatinib was unable to inhibit Src activity in the presence of concurrent chemotherapy in this surrogate tissue. Similarly, paired biopsies failed to demonstrate phospho-Src inhibition. This is likely due to the robust activation of Src after oxaliplatin alone due to induction of reactive oxygen species, as we have previously described (25). If confirmed in further testing, this may impact how Src inhibitors are used in combination therapy with oxaliplatin.

In the phase II arm, we evaluated the role of *KRAS* mutation status on response to treatment and time to disease progression. There was a 30% overall response rate, which was restricted to the *KRAS* wild-type arm. Six patients who were refractory to an oxaliplatin-based regimen and cetuximab previously, had a confirmed partial response, which was durable for a median of 5.2 months. There was no meaningful activity in the *KRAS*-mutant arm. The median OS was 6.7 months in all patients and slightly better in *KRAS* wild-type patients.

There are several possible explanations for the response rates seen with this regimen. First, previous prospective, randomized phase II and III trials in advanced colorectal cancer have shown that intensified, repeated short courses of FOLFOX, including oxaliplatin reintroduction after progression, result in significantly improved response rates, PFS, and OS (32–37). In particular, these studies have shown a PFS of approximately 3 months (33, 34), a partial response rate of 33% (37), a stable disease rate ranging from 38% to 42.7% (33, 37), a median OS ranging from 9.9 to 22.1 months (34, 36), and an independent significant positive impact on OS (HR = 0.56, $P = 0.009$; ref. 35).

Similarly, the efficacy of cetuximab rechallenge is an area of active research and may provide a further explanation for the response rates seen with this regimen. Circulating tumor DNA profiles of patients with colorectal cancer that had acquired resistance to cetuximab has revealed that upon antibody withdrawal *KRAS* clones decay, whereas the population regains drug sensitivity (38, 39). The results from both the FOLFOX and cetuximab studies indicate that the colorectal cancer genome adapts dynamically to intermittent drug schedules and provide an explanation for the efficacy of rechallenge therapies.

Furthermore, it is well established that Src family kinases and the EGFR cooperate during tumorigenesis and cause resistance to cetuximab. This has prompted several preclinical studies that have

Published OnlineFirst March 9, 2017; DOI: 10.1158/1078-0432.CCR-16-3138

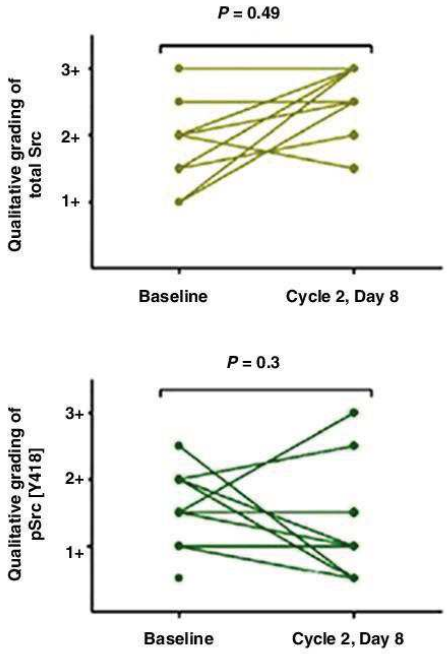

Figure 4.
In patients with evaluable paired biopsies in the expansion cohort, semiquantitative grading of total Src and phospho-Src [Y418] staining was performed. Each line represents an individual patient. There was a statistically significant increase in total Src staining after 3 weeks of treatment ($P = 0.049$). There was no change in phospho-Src staining ($P = 0.3$).

oral tyrosine kinase Src inhibitor, dasatinib, in combination with FOLFOX and cetuximab in patients with heavily pretreated mCRC.

The phase IB portion of our study determined a phase II dose of dasatinib that could be used safely in combination. Correlative studies were performed which included evaluation of peripheral mononuclear cells and paired liver biopsies from the expansion cohort. The enrolled population in the phase IB portion was heavily pretreated with a median of 4 prior lines of therapy. Ninety-seven percent of the patients had been exposed to prior oxaliplatin and 80% had been exposed to prior EGFR therapy. Response rate in this population was 20% in the evaluable subset. In patients who were previously refractory to oxaliplatin, there was a 25% response rate. Similarly, in patients who were refractory to EGFR-based therapy, the response rate was 20%. The median PFS of 4.6 months was better than would be expected in a similar cohort of patients treated with regorafenib (1.9 months) or TAS-102 (2.0 months; refs. 28, 29).

The toxicities associated with this regimen included fatigue and myelosuppression. The dose of 150-mg daily of dasatinib was chosen for further study based on the higher rates of myelosuppression seen with the 200-mg dose. Even at this reduced dose, there were no patients who were able to maintain a 150-mg dose beyond 3 months. The most common reason for dose reduction was myelosuppression and fatigue. The degree of fatigue was also greater than would be expected from this chemotherapy regimen alone in this patient population (30). However, a recent phase I study demonstrated that dasatinib 70 mg daily could be safely combined with capecitabine, oxaliplatin, and bevacizumab—a dose of dasatinib that was lower than anticipated (31). Thus, the intensity of this chemotherapy regimen in a heavily refractory population should not be discounted, and lower doses of dasatinib may be considered for further studies in this setting.

The pharmacodynamic studies incorporated in the phase IB portion of the study demonstrated that treatment with the dasatinib-containing regimen failed to inhibit Src and instead demonstrated a paradoxical increase in Src activation. This may, in part, be due to increased Src activity after oxaliplatin therapy, as shown in our tissue analysis after staining for phospho-Src. Murine studies have suggested that treatment with dasatinib at a higher dose is sufficient to inhibit Src activation after oxaliplatin (25). However, in our study, the analysis of the PBMCs demonstrated increased phosphorylation in the Src substrate of paxillin. This increase was robust and was statistically significant, suggesting that dasatinib was unable to inhibit Src activity in the presence of concurrent chemotherapy in this surrogate tissue. Similarly, paired biopsies failed to demonstrate phospho-Src inhibition. This is likely due to the robust activation of Src after oxaliplatin alone due to induction of reactive oxygen species, as we have previously described (25). If confirmed in further testing, this may impact how Src inhibitors are used in combination therapy with oxaliplatin.

In the phase II arm, we evaluated the role of *KRAS* mutation status on response to treatment and time to disease progression. There was a 30% overall response rate, which was restricted to the *KRAS* wild-type arm. Six patients who were refractory to an oxaliplatin-based regimen and cetuximab previously, had a confirmed partial response, which was durable for a median of 5.2 months. There was no meaningful activity in the *KRAS*-mutant arm. The median OS was 6.7 months in all patients and slightly better in *KRAS* wild-type patients.

There are several possible explanations for the response rates seen with this regimen. First, previous prospective, randomized phase II and III trials in advanced colorectal cancer have shown that intensified, repeated short courses of FOLFOX, including oxaliplatin reintroduction after progression, result in significantly improved response rates, PFS, and OS (32–37). In particular, these studies have shown a PFS of approximately 3 months (33, 34), a partial response rate of 33% (37), a stable disease rate ranging from 38% to 42.7% (33, 37), a median OS ranging from 9.9 to 22.1 months (34, 36), and an independent significant positive impact on OS (HR = 0.56, $P = 0.009$; ref. 35).

Similarly, the efficacy of cetuximab rechallenge is an area of active research and may provide a further explanation for the response rates seen with this regimen. Circulating tumor DNA profiles of patients with colorectal cancer that had acquired resistance to cetuximab has revealed that upon antibody withdrawal *KRAS* clones decay, whereas the population regains drug sensitivity (38, 39). The results from both the FOLFOX and cetuximab studies indicate that the colorectal cancer genome adapts dynamically to intermittent drug schedules and provide an explanation for the efficacy of rechallenge therapies.

Furthermore, it is well established that Src family kinases and the EGFR cooperate during tumorigenesis and cause resistance to cetuximab. This has prompted several preclinical studies that have

Published OnlineFirst March 9, 2017; DOI: 10.1158/1078-0432.CCR-16-3138

16. Griffiths GJ, Koh MY, Brunton VG, Cawthorne C, Reeves NA, Greaves M, et al. Expression of kinase-defective mutants of c-Src in human metastatic colon cancer cells decreases Bcl-xL and increases oxaliplatin- and Fas-induced apoptosis. J Biol Chem 2004;279:46113–21.
17. Kopetz S, Morris VK, Parikh N, Overman MJ, Jiang ZQ, Maru D, et al. Src activity is modulated by oxaliplatin and correlates with outcomes after hepatectomy for metastatic colorectal cancer. BMC Cancer 2014;14:660.
18. Kim LC, Song L, Haura EB. Src kinases as therapeutic targets for cancer. Nat Rev Clin Oncol 2009;6:587–95.
19. Hantschel O, Rix U, Superti-Furga G. Target spectrum of the BCR-ABL inhibitors imatinib, nilotinib and dasatinib. Leuk Lymphoma 2008; 49:615–9.
20. Lu Y, Li X, Liang K, Luwor R, Siddik ZH, Mills GB, et al. Epidermal growth factor receptor (EGFR) ubiquitination as a mechanism of acquired resistance escaping treatment by the anti-EGFR monoclonal antibody cetuximab. Cancer Res 2007;67:8240–7.
21. Duxbury MS, Ito H, Zinner MJ, Ashley SW, Whang EE. Inhibition of SRC tyrosine kinase impairs inherent and acquired gemcitabine resistance in human pancreatic adenocarcinoma cells. Clin Cancer Res 2004;10:2307–18.
22. Pengetnze Y, Steed M, Roby KF, Terranova PF, Taylor CC. Src tyrosine kinase promotes survival and resistance to chemotherapeutics in a mouse ovarian cancer cell line. Biochem Biophys Res Commun 2003;309:377–83.
23. George JA, Chen T, Taylor CC. SRC tyrosine kinase and multidrug resistance protein-1 inhibitions act independently but cooperatively to restore paclitaxel sensitivity to paclitaxel-resistant ovarian cancer cells. Cancer Res 2005;65:10381–8.
24. Kim YM, Kim YM, Lee YM, Kim HS, Kim JD, Choi Y, et al. TNF-related activation-induced cytokine (TRANCE) induces angiogenesis through the activation of Src and phospholipase C (PLC) in human endothelial cells. J Biol Chem 2002;277:6799–805.
25. Kopetz S, Lesslie DP, Dallas NA, Park SI, Johnson M, Parikh NU, et al. Synergistic activity of the SRC family kinase inhibitor dasatinib and oxaliplatin in colon carcinoma cells is mediated by oxidative stress. Cancer Res 2009;69:3842–9.
26. Stemke-Hale K, Gonzalez-Angulo AM, Lluch A, Neve RM, Kuo WL, Davies M, et al. An integrative genomic and proteomic analysis of PIK3CA, PTEN, and AKT mutations in breast cancer. Cancer Res 2008;68:6084–91.
27. Serrels A, Macpherson IR, Evans TR, Lee FY, Clark EA, Sansom OJ, et al. Identification of potential biomarkers for measuring inhibition of Src kinase activity in colon cancer cells following treatment with dasatinib. Mol Cancer Ther 2006;5:3014–22.
28. Grothey A, Van Cutsem E, Sobrero A, Siena S, Falcone A, Ychou M, et al. Regorafenib monotherapy for previously treated metastatic colorectal cancer (CORRECT): an international, multicentre, randomised, placebo-controlled, phase 3 trial. Lancet 2013;381:303–12.
29. Mayer RJ, Van Cutsem E, Falcone A, Yoshino T, Garcia-Carbonero R, Mizunuma N, et al. Randomized trial of TAS-102 for refractory metastatic colorectal cancer. N Engl J Med 2015;372:1909–19.
30. Giantonio BJ, Catalano PJ, Meropol NJ, O'Dwyer PJ, Mitchell EP, Alberts SR, et al. Bevacizumab in combination with oxaliplatin, fluorouracil, and leucovorin (FOLFOX4) for previously treated metastatic colorectal cancer: results from the Eastern Cooperative Oncology Group Study E3200. J Clin Oncol 2007;25:1539–44.
31. Strickler JH, McCall S, Nixon AB, Brady JC, Pang H, Rushing C, et al. Phase I study of dasatinib in combination with capecitabine, oxaliplatin and bevacizumab followed by an expanded cohort in previously untreated metastatic colorectal cancer. Invest New Drugs 2014; 32:330–9.
32. Maindrault-Goebel F, Tournigand C, Andre T, Carola E, Mabro M, Artru P, et al. Oxaliplatin reintroduction in patients previously treated with leucovorin, fluorouracil and oxaliplatin for metastatic colorectal cancer. Ann Oncol 2004;15:1210–4.
33. Tournigand C, Cervantes A, Figer A, Lledo G, Flesch M, Buyse M, et al. OPTIMOX1: a randomized study of FOLFOX4 or FOLFOX7 with oxaliplatin in a stop-and-Go fashion in advanced colorectal cancer–a GERCOR study. J Clin Oncol 2006;24:394–400.
34. Suenaga M, Mizunuma N, Matsusaka S, Shinozaki E, Ozaka M, Ogura M, et al. Phase II study of reintroduction of oxaliplatin for advanced colorectal cancer in patients previously treated with oxaliplatin and irinotecan: RE-OPEN study. Drug Des Devel Ther 2015;9:3099–108.
35. de Gramont A, Buyse M, Abrahantes JC, Burzykowski T, Quinaux E, Cervantes A, et al. Reintroduction of oxaliplatin is associated with improved survival in advanced colorectal cancer. J Clin Oncol 2007; 25:3224–9.
36. Andre T, Tournigand C, Mineur L, Fellague-Chebra R, Flesch M, Mabro M, et al. Phase II study of an optimized 5-fluorouracil-oxaliplatin strategy (OPTIMOX2) with celecoxib in metastatic colorectal cancer: a GERCOR study. Ann Oncol 2007;18:77–81.
37. Adams RA, Meade AM, Seymour MT, Wilson RH, Madi A, Fisher D, et al. Intermittent versus continuous oxaliplatin and fluoropyrimidine combination chemotherapy for first-line treatment of advanced colorectal cancer: results of the randomised phase 3 MRC COIN trial. Lancet Oncol 2011;12:642–53.
38. Siravegna G, Mussolin B, Buscarino M, Corti G, Cassingena A, Crisafulli G, et al. Clonal evolution and resistance to EGFR blockade in the blood of colorectal cancer patients. Nat Med 2015;21:827.
39. Morelli MP, Overman MJ, Dasari A, Kazmi SM, Mazard T, Vilar E, et al. Characterizing the patterns of clonal selection in circulating tumor DNA from patients with colorectal cancer refractory to anti-EGFR treatment. Ann Oncol 2015;26:731–6.
40. Li J, Rix U, Fang B, Bai Y, Edwards A, Colinge J, et al. A chemical and phosphoproteomic characterization of dasatinib action in lung cancer. Nat Chem Biol 2010;6:291–9.
41. Sos ML, Michel K, Zander T, Weiss J, Frommolt P, Peifer M, et al. Predicting drug susceptibility of non-small cell lung cancers based on genetic lesions. J Clin Invest 2009;119:1727–40.

F/ Association entre le confinement dû au COVID-19 et la charge tumorale chez les patients atteints d'un cancer colorectal métastatique nouvellement diagnostiqué

Auteurs : Alain R. Thierry, PhD; Brice Pastor, PhD; Ekaterina Pisareva, MD, PhD; Francois Ghiringhelli, MD, PhD; Olivier Bouché, MD, PhD; Christelle De La Fouchardière, MD, PhD; Julie Vanbockstael, MD, PhD; Denis Smith, MD, PhD; Eric François, MD, PhD; Mélanie Dos Santos, MD, PhD; Damien Botsen, MD, PhD; Stephen Ellis, MD; Marianne Fonck, MD, PhD; Thierry André, MD, PhD; Emmanuel Guardiola, MD, PhD; Faiza Khemissa, MD, PhD; Benjamin Linot, MD, PhD; J. Martin-Babau, MD; Yves Rinaldi, MD, PhD; Eric Assenat, MD, PhD; Lea Clavel, MD, PhD; Sophie Dominguez, MD, PhD; Celine Gavoille, MD, PhD; David Sefrioui, MD, PhD; Veronica Pezzella, MS; Caroline Mollevi, PhD; Marc Ychou, MD, PhD; Thibault Mazard, MD, PhD

Cette publication a été a été publiée dans JAMA Network Open en 2021

Résumé: MPORTANCE. La pandémie de COVID-19 a été associée à une réduction substantielle du dépistage, de l'identification des cas et de l'orientation vers les hôpitaux des patients atteints de cancer. Cependant, aucune étude n'a examiné quantitativement les implications de cette corrélation pour la prise en charge des patients atteints de cancer.

OBJECTIF. Évaluer l'association entre le verrouillage de la pandémie de COVID-19 et la charge tumorale des patients chez qui on a diagnostiqué un cancer colorectal métastatique (CCRm) avant et après le confinement

CONCEPTION, SITE ET PARTICIPANTS. Cette étude de cohorte a analysé les participants à la procédure de sélection de l'essai clinique randomisé de phase 2 PANIRINOX (Phase II Randomized Study Comparing FOLFIRINOX + Panitumumab vs FOLFOX + Panitumumab in Metastatic Colorectal Cancer Patients Stratified by RAS Status from Circulating DNA Analysis). Ces patients nouvellement diagnostiqués ont reçu des soins dans un des 18 centres cliniques différents en France et ont été recrutés avant ou après la mise en place du confinement en France au printemps 2020. Les patients ont subi une procédure de dépistage par prise de sang pour identifier leur statut tumoral *RAS* et *BRAF*.

EXPOSITIONS. mCRC.

PRINCIPAUX RÉSULTATS ET MESURES. L'analyse de l'ADN tumoral circulant (ADNcir) a été utilisée pour identifier le statut *RAS* et *BRAF*. La charge tumorale a été évaluée par la concentration plasmatique totale d'ADNc. La concentration médiane d'ADNcir a été comparée

chez les patients qui ont subi un dépistage avant (11 novembre 2019 au 9 mars 2020) vs après (14 mai au 3 septembre 2020) le confinement et chez les patients qui ont été inclus dès le début de l'étude PANIRINOX.

RÉSULTATS. Un total de 80 patients a été inclus, dont 40 ont subi un dépistage avant et 40 autres ont subi un dépistage après le premier confinement de COVID-19 en France. Ces patients comprenaient 48 hommes (60,0%) et 32 femmes (40,0%) et avaient un âge médian (fourchette) de 62 (37-77) ans. La concentration médiane d'ADNcir était statistiquement plus élevée chez les patients nouvellement diagnostiqués après le confinement que chez ceux diagnostiqués avant le confinement (119,2 ng/mL contre 17,3 ng/mL ; P < 0,001). Les patients atteints de cancer colorectal métastatique et présentant une concentration élevée d'ADNcir avaient une survie médiane inférieure à celle des patients présentant une concentration plus faible (14,7 [IC 95 %, 8,8-18,0] mois contre 20,0 [IC 95 %, 14,1-32,0] mois). Ce résultat met en évidence les conséquences négatives potentielles de la pandémie de COVID-19 et du confinement qui en découle.

CONCLUSIONS ET PERTINENCE. Cette étude de cohorte a révélé que la masse de la tumeur différait entre les patients ayant reçu un diagnostic de CCRm avant et après le premier confinement dû au COVID-19 en France. Les résultats de cette étude suggèrent que le CCR est un domaine majeur d'intervention pour minimiser les retards de dépistage, de diagnostic et de traitement liés à la pandémie.

Contribution: J’ai participé à la réalisation des analyses des ADNcir de cette étude et à l’écriture du manuscrit.

JAMA Network Open

Original Investigation | Oncology

Association of COVID-19 Lockdown With the Tumor Burden in Patients With Newly Diagnosed Metastatic Colorectal Cancer

Alain R. Thierry, PhD; Brice Pastor, PhD; Ekaterina Pisareva, MD, PhD; Francois Ghiringhelli, MD, PhD; Olivier Bouché, MD, PhD; Christelle De La Fouchardière, MD, PhD; Julie Vanbockstael, MD, PhD; Denis Smith, MD, PhD; Eric François, MD, PhD; Mélanie Dos Santos, MD, PhD; Damien Botsen, MD, PhD; Stephen Ellis, MD; Marianne Fonck, MD, PhD; Thierry André, MD, PhD; Emmanuel Guardiola, MD, PhD; Faiza Khemissa, MD, PhD; Benjamin Linot, MD, PhD; J. Martin-Babau, MD; Yves Rinaldi, MD, PhD; Eric Assenat, MD, PhD; Lea Clavel, MD, PhD; Sophie Dominguez, MD, PhD; Celine Gavoille, MD, PhD; David Sefrioui, MD, PhD; Veronica Pezzella, MS; Caroline Mollevi, PhD; Marc Ychou, MD, PhD; Thibault Mazard, MD, PhD

Abstract

IMPORTANCE The COVID-19 pandemic has been associated with substantial reduction in screening, case identification, and hospital referrals among patients with cancer. However, no study has quantitatively examined the implications of this correlation for cancer patient management.

OBJECTIVE To evaluate the association of the COVID-19 pandemic lockdown with the tumor burden of patients who were diagnosed with metastatic colorectal cancer (mCRC) before vs after lockdown.

DESIGN, SETTING, AND PARTICIPANTS This cohort study analyzed participants in the screening procedure of the PANIRINOX (Phase II Randomized Study Comparing FOLFIRINOX + Panitumumab vs FOLFOX + Panitumumab in Metastatic Colorectal Cancer Patients Stratified by *RAS* Status from Circulating DNA Analysis) phase 2 randomized clinical trial. These newly diagnosed patients received care at 1 of 18 different clinical centers in France and were recruited before or after the lockdown was enacted in France in the spring of 2020. Patients underwent a blood-sampling screening procedure to identify their *RAS* and *BRAF* tumor status.

EXPOSURES mCRC.

MAIN OUTCOMES AND MEASURES Circulating tumor DNA (ctDNA) analysis was used to identify *RAS* and *BRAF* status. Tumor burden was evaluated by the total plasma ctDNA concentration. The median ctDNA concentration was compared in patients who underwent screening before (November 11, 2019, to March 9, 2020) vs after (May 14 to September 3, 2020) lockdown and in patients who were included from the start of the PANIRINOX study.

RESULTS A total of 80 patients were included, of whom 40 underwent screening before and 40 others underwent screening after the first COVID-19 lockdown in France. These patients included 48 men (60.0%) and 32 women (40.0%) and had a median (range) age of 62 (37-77) years. The median ctDNA concentration was statistically higher in patients who were newly diagnosed after lockdown compared with those who were diagnosed before lockdown (119.2 ng/mL vs 17.3 ng/mL; $P < .001$). Patients with mCRC and high ctDNA concentration had lower median survival compared with those with lower concentration (14.7 [95% CI, 8.8-18.0] months vs 20.0 [95% CI, 14.1-32.0] months). This finding points to the potential adverse consequences of the COVID-19 pandemic and related lockdown.

CONCLUSIONS AND RELEVANCE This cohort study found that tumor burden differed between patients who received an mCRC diagnosis before vs after the first COVID-19 lockdown in France. The

(continued)

Key Points

Question What is the implication of the COVID-19 lockdown for the tumor burden of patients with a newly diagnosed metastatic colorectal cancer?

Findings In this cohort study of 80 patients with metastatic colorectal cancer, the tumor burden, which was evaluated using the circulating tumor DNA in plasma, appeared to be significantly higher in patients who received a diagnosis after lockdown compared with those who were diagnosed before lockdown (119.2 ng/mL vs 17.3 ng/mL). Patients with greater tumor burden had lower median survival than those with lower tumor burden.

Meaning In this study, the tumor burden of colorectal cancer varied and appeared to be associated with poor survival for those who received a postlockdown diagnosis, suggesting that this cancer is a major area for intervention to minimize COVID-19–associated diagnostic delay.

+ Supplemental content

Author affiliations and article information are listed at the end of this article.

Abstract (continued)

findings of this study suggest that CRC is a major area for intervention to minimize pandemic-associated delays in screening, diagnosis, and treatment.

JAMA Network Open. 2021;4(9):e2124483. doi:10.1001/jamanetworkopen.2021.24483

Introduction

The unprecedented burden placed on health systems worldwide by the COVID-19 crisis has had numerous and substantial implications for cancer care.[1,2] People have been more reluctant to come to health care facilities for services because of fear of infection, particularly those with cancer, given that cancer is considered a comorbidity. Reduction or suspension of screening programs and diagnostic services has been a factor in delays in diagnosis in many countries.[1,3-5] Access to treatment has been restricted to minimize the risk of SARS-CoV-2 exposure during therapy procedures for patients with cancer.[3] The reprioritization of human resources and equipment to COVID-19 pandemic management has also been associated with the provision of suboptimal or delayed care.[1,6]

These implications have been exacerbated by the COVID-19 containment measures implemented by different countries, which have tended to evolve from recommendations and restrictions to lockdowns at both the local and national levels.[1,2] Such measures were initially seen in the first few months of 2020 in Asia and Oceania and had spread to Europe and North and South America by March, depending mainly on the date of the first SARS-CoV-2 infection cases in those areas.[2] The sheer number of patients with COVID-19 infection necessitating hospitalization and critical care has continued to strain health services and already limited resources. Individual fears of contracting the virus as well as restrictions on movement imposed by local and national authorities have generated additional physical and psychological barriers for patients who need to access essential care.

We conducted a cohort study to evaluate the association of the COVID-19 pandemic lockdown with the tumor burden of patients who were newly diagnosed with metastatic colorectal cancer (mCRC) before vs after lockdown. To our knowledge, no such clinical evaluation has been performed thus far. Conventional circulating biomarkers, such as carcinoembryonic antigen (CEA) and carbohydrate antigen 19-9, do not fully satisfy the clinical requirements for monitoring colorectal cancer (CRC) tumor burden in clinical practice because of their moderate levels of sensitivity and specificity.[7] Therefore, we used circulating tumor DNA (ctDNA) analysis to assess the patients' tumor burden.

Circulating tumor DNA is a newly identified source of biological information that has attracted the attention of researchers and clinicians in numerous fields.[8] It has substantial clinical potential in oncology, including in molecular profiling, detection of residual disease, control of treatment efficacy, detection of clonal resistance, surveillance of recurrence, and screening.[9] It first showed its promise by contributing to companion tests as a liquid biopsy, and then it obtained European Medicines Agency approval for use in the detection of sensitizing and/or resistant somatic alterations in oncodrivers, such as those in lung cancer and melanoma, as a tool to guide clinicians in selecting targeted therapies.[9,10] Numerous studies have reported that tumors secrete DNA into the bloodstream in quantities that are proportional to their masses,[11-13] especially in the case of mCRC, according to several investigations[11,14-16] and work that illustrated the association of total ctDNA concentration with increasing hepatic tumor mass as identified by magnetic resonance imaging (eFigure 1 in the Supplement). Thus, ctDNA offers analytical and clinical advantages over conventional antigenic biomarkers, such as CEA, and may be considered as a surrogate marker of disease progression, at least in mCRC.[14,15,17-20]

Methods

This cohort study included patients from the screening procedure of the ongoing PANIRINOX study (Phase II Randomized Study Comparing FOLFIRINOX + Panitumumab vs FOLFOX + Panitumumab in Metastatic Colorectal Cancer Patients Stratified by *RAS* Status from Circulating DNA Analysis), who were recruited before and after the first COVID-19 lockdown was enacted in France in the spring of 2020. In the PANIRINOX trial, treatment (FOLFIRINOX [leucovorin, fluorouracil, irinotecan, and oxaliplatin] + panitumumab or mFOLFOX6 [modified fluorouracil, leucovorin, and oxaliplatin] + panitumumab) is allocated according to a randomization procedure. However, the present work was carried out on an ad hoc basis at the time of the screening procedure and before randomization. The PANIRINOX study was reviewed and approved by the human investigations committee Sud Méditerranée IV. All patients provided written informed consent before the screening procedure. This cohort study, along with other trial-related documents, received approval from Unicancer, the sponsor of the PANIRINOX study, which received authorization from the Agence Nationale de Sécurité du Médicament et des Produits de Santé and the Comités de Protection des Personnes, according to French national regulatory requirements. We followed the Strengthening the Reporting of Observational Studies in Epidemiology (STROBE) reporting guideline.[21]

The PANIRINOX study is a first-line, phase 2 randomized clinical trial that assesses the activity of a combination chemotherapy with fluorouracil, leucovorin, oxaliplatin, and panitumumab with or without irinotecan (FOLFOX + panitumumab vs FOLFIRINOX + panitumumab) in patients with unresectable mCRC, who were selected by their *RAS* (GenBank 6237) and *BRAF* (GenBank 673) tumor status, which was obtained from ctDNA analysis. To our knowledge, it is the first interventional study to use ctDNA as a companion test for selecting patients with mCRC for anti–estimated glomerular filtration rate targeted therapy (eAppendix in the Supplement). It involves 31 hospitals and cancer centers in France. Its primary end point is the complete response rate defined as the complete disappearance of metastatic lesions and CEA level normalization after a maximum of 12 treatment cycles. Among the major patient selection criteria are age 18 to 75 years, Eastern Cooperative Oncology Group Performance Status score of 0 or 1, no previous treatment for metastatic disease, and no previous use of oxaliplatin in an adjuvant setting (eAppendix in the Supplement).

In France, the first mandatory home lockdown of 2020 lasted 55 days, from March 17 to May 11. The PANIRINOX study screening was consequently interrupted for 53 days, starting on March 19 and ending on May 11. We compared the ctDNA concentration in all patients who underwent screening after the lockdown (from May 14, 2020, to September 3, 2020, a 110-day period) with the ctDNA concentration in all patients who underwent screening before the lockdown (from November 11, 2019, to March 9, 2020). These patients were newly diagnosed with mCRC and received care at 1 of 18 different clinical centers in France. We also compared the ctDNA concentration in the prelockdown and postlockdown groups and the fractional cohorts of those who were included from the start of the PANIRINOX study (June-September 2017, September 2017-January 2018, January-April 2018, April-August 2018, August-December 2018, December 2018-March 2019, March-July 2019, and July-November 2019). Preanalytical conditions of the ctDNA analysis followed strict guidelines and methodologies that have been previously validated.[22-25]

Patients were screened through a blood-sampling procedure to identify their *RAS* and *BRAF* tumor status according to plasma analysis of circulating cell-free DNA, using IntPlex technology (DiaDx SAS).[22,23] Those whose tumors were considered as *RAS* and *BRAF* wild type were subsequently included in the PANIRINOX study if they fulfilled all other inclusion criteria (eAppendix in the Supplement). The present study, therefore, benefited from the accuracy with which ctDNA can evaluate tumor burden and from the trial's rigorous inclusion procedure and reporting, all of which supported the accuracy of assessment needed to achieve the objective of this study.

We examined all patients who underwent screening before and after lockdown (N = 268), regardless of their *RAS* and *BRAF* sequence variation status, to preclude any potential bias associated

with sequence variation status. Given the interventional impact of ctDNA analysis in the PANIRINOX study, the analysis was completed within 5 days of receipt of the blood samples. In addition to ctDNA parameters analysis, we simultaneously collected demographic and clinicobiological parameters that are known to have prognostic value in this setting.[26,27]

Statistical Analysis

Statistical analysis of prelockdown and postlockdown data was performed with the GraphPad Prism, version 6.01 (GraphPad Software Inc) and survival analysis was conducted with Stata, version 16.0 (StataCorp LLC). Where appropriate, data were log transformed before statistical analysis. Continuous variables were compared using the Mann-Whitney test, and categorical variables were compared using the Pearson χ^2 test. Median follow-up was calculated with the reverse Kaplan-Meier method. Overall survival, defined as the time between the date of first metastatic diagnosis and the date of death from any cause, was estimated with the Kaplan-Meier method and compared using the log-rank test. Correlation analysis was performed using the Spearman test. Hazard ratios (HRs) are given with their 95% CIs. A 2-sided $P < .05$ was considered to be statistically significant.

Results

We analyzed the ctDNA concentration in 80 patients who underwent screening before (n = 40) or after (n = 40) the first COVID-19 lockdown in France in 2020. These patients included 48 men (60.0%) and 32 women (40.0%) and had a median (range) age of 62 (37-77) years.

As shown in **Figure 1**, the median (interquartile range [IQR]) ctDNA concentration was 17.3 (9.57-43.78) ng/mL before lockdown and 119.2 (43.38-315.8) ng/mL after lockdown (eTable 1 in the Supplement). This postlockdown ctDNA concentration represented a 6.9-fold increase. A statistically significant difference between the 2 cohorts was observed (17.3 [95% CI, 13.58-33.52] vs 119.2 [95% CI, 53.13-278.1]; $P < .001$) (Figure 1 and **Figure 2**). The values obtained from patients included before lockdown (n = 40) were similar to those obtained from all patients in the fractional cohorts (n = 188), who were included in the PANIRINOX study starting 30 months before lockdown, showing a median (IQR) ctDNA concentration in plasma of 13.0 (6.43-46.13) ng/mL (Figure 2). In addition, the median (IQR) ctDNA concentration in the fractional cohorts showed no statistical difference from the levels in the prelockdown cohort (June-September 2017: 29.94 [5.27-149.2] ng/mL, $P > .99$; September

Figure 1. Comparison of Circulating Tumor DNA (ctDNA) Concentration in Patients With Newly Diagnosed Metastatic Colorectal Cancer in the Prelockdown and Postlockdown Periods

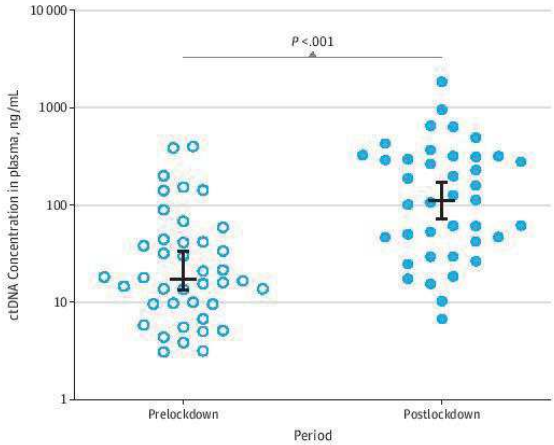

The long horizontal bars indicate the median; shorter bars, the 95% CIs; and each dot, the ctDNA concentration in a single patient. The Mann-Whitney test was performed to compare the patient distributions and revealed a significant difference between the prelockdown and postlockdown periods.

2017-January 2018: 9.13 [6.37-13.61] ng/mL, $P = .07$; January-April 2018: 18.36 [3-220.2] ng/mL, $P = .71$; April-August 2018: 18.51 [6.99-55.06] ng/mL, $P = .99$; August-December 2018: 13.38 [9.17-55.85] ng/mL, $P = .89$; December 2018-March 2019: 9.19 [4.72-40.91] ng/mL, $P = .27$; March-July 2019: 18.38 [5.11-49.25] ng/mL, $P = .54$; July-November 2019: 12.91 [7.05-49] ng/mL, $P = 40$), whereas they were statistically different from the levels in the postlockdown cohort (Figure 2).

Regarding patient characteristics, no difference was observed in the groups who received a diagnosis before vs after lockdown (**Table**; eFigures 2 and 3 in the Supplement). The delay of blood sample delivery was also similar, as was the alteration in ctDNA concentration and the alteration in allele frequency (eFigures 4 to 6; eTable 1 in the Supplement). For example, the median (IQR) alteration in allele frequency was 10.45% (0.88%-19.22%) in the prelockdown cohort and 6.18% (0.45%-21.96%) in the postlockdown cohort (eTable 1). The median white blood cell count, lactate dehydrogenase (LDH) level, and CEA level were slightly higher in the postlockdown vs prelockdown setting, but the differences were not statistically significant (Table; eFigures 7 to 9 in the Supplement). The ctDNA concentration was significantly associated with an increase in LDH level ($r = 0.72$; $P < .001$) and white blood cell count ($r = 0.73$; $P < .001$) in patients who underwent screening after lockdown. The CEA level was associated with an increase of ctDNA concentration in patients in the prelockdown ($r = 0.38$; $P = .04$) and postlockdown ($r = 0.22$; $P = .24$) groups (eFigures 10 to 14 in the Supplement). When dichotomizing this cohort by the median (IQR) ctDNA concentration (24.4 [2.3-1406] ng/mL), we found that patients who had higher ctDNA plasma concentration showed a statistically lower median survival (14.7 [95% CI, 8.8-18.0] months vs 20.0 [95% CI, 14.1-32.0] months; HR, 1.74 [95% CI, 1.2-2.6]; $P = .005$) (**Figure 3**B; eTable 2 in the Supplement).

Figure 2. Comparison of Patients at the Start of the PANIRINOX Study and the Prelockdown Period

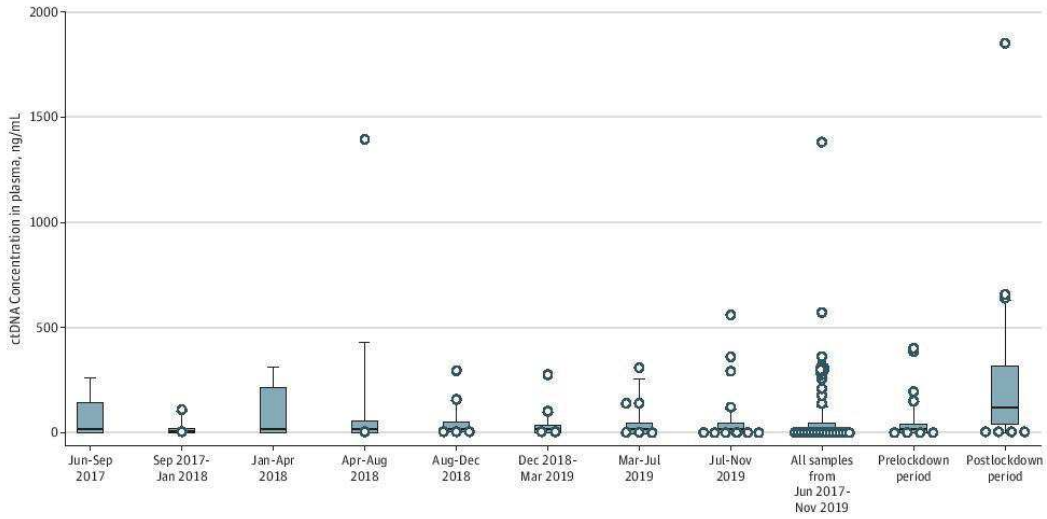

The box plot represents circulating tumor DNA (ctDNA) concentration in patients in the 110-day fractional cohorts vs patients in the prelockdown (n = 40) and postlockdown (n = 40) periods. The Mann-Whitney test was performed to compare patient distributions. The horizontal bars inside the boxes indicate the median; error bars, the 10th to 90th percentile; squares, the median between the 25% percentile and the 75% percentile; whiskers, the 10th to 90th percentile; and each dot, the ctDNA concentration of a single patient outside the 10th to 90th percentile.

Discussion

The differences in tumor burden between patients who were diagnosed before vs after lockdown and the resulting risk of reduced survival point to the association between the pandemic-related lockdown and unfavorable consequences for patients with newly diagnosed mCRC, who may have delayed their first visit to an oncologist. The lower number of mCRC diagnoses during the beginning of the COVID-19 pandemic[1,3] may be associated with patients' reluctance to visit a physician or health care facility. A possible reason for this reluctance was fear of COVID-19 infection or burdening the health system, as described by a quote from a patient with cancer[28] (eAppendix in the Supplement). In addition to patients' subjective anxieties and reticence, numerous reports observed the

Table. Patient Characteristics

Characteristic	No. (%)			*P* value
	Overall	Prelockdown group	Postlockdown group	
No. of patients	80 (100)	40 (50)	40 (50)	
Age, y				.86
Median (range)	62 (37-77)	63 (37-77)	61 (39-77)	
Missing data	1	0	1	
Sex				.65
Male	48 (60.0)	25 (62.5)	23 (57.5)	
Female	32 (40.0)	15 (37.5)	17 (42.5)	
Location of primary tumor				.84
Right colon	19 (24.0)	9 (23.1)	10 (25.0)	
Left colon	60 (76.0)	30 (76.9)	30 (75.0)	
Missing data	1	1	0	
Primary tumor in place				.81
Yes	57 (71.2)	28 (70.0)	29 (72.5)	
No	23 (28.8)	12 (30.0)	11 (27.5)	
No. of metastatic sites				
Median (range)	2 (1-4)	2 (1-3)	2 (1-4)	.30
1	28 (43.8)	15 (48.4)	13 (39.4)	.47
>1	36 (56.2)	16 (51.6)	20 (60.6)	
Missing data	16	9	7	
Liver involvement				.96
Yes	55 (84.6)	27 (84.4)	28 (84.9)	
No	10 (15.4)	5 (15.6)	5 (15.1)	
Missing data	15	8	7	
Limited liver disease				.81
Yes	23 (28.8)	12 (30.0)	11 (27.5)	
No	57 (71.2)	28 (70.0)	29 (72.5)	
LDH level, U/L				
Median (range)	345 (137-2690)	263 (148-2690)	410 (137-1256)	.46
<245	22 (39.3)	14 (48.3)	8 (29.6)	.18
≥245	34 (60.7)	15 (51.7)	19 (70.4)	
Missing data	24	11	13	
WBC count, G/L				
Median (range)	9.1 (4.4-27.3)	8.5 (4.8-22.4)	9.4 (4.4-27.3)	.31
<10	38 (62.3)	21 (67.7)	17 (56.7)	.37
≥10	23 (37.7)	10 (32.3)	13 (43.3)	
Missing data	19	9	10	
CEA level, ng/mL				
Median (range)	39.8 (0.7-13590)	34.0 (0.7-9902)	40.8 (1.4-13590)	.49
<5	9 (14.8)	4 (12.9)	5 (16.7)	.68
≥5	52 (85.2)	27 (87.1)	25 (83.3)	

Abbreviations: CEA, carcinoembryonic antigen; LDH, lactate dehydrogenase; WBC, white blood cell.

SI conversion factors: To convert CEA level to micrograms per liter, multiply by 1.0; LDH level to microkatal per liter, multiply by 0.0167; WBC count to $\times 10^9$/L, multiply by 0.001.

considerable delays in sending out millions of solicitations for bowel cancer screening and a backlog (in England alone) of thousands of individuals awaiting further investigation after receiving a positive screening result.[2,3]

Although the COVID-19 lockdown was a necessity, it led to unintended consequences in the diagnosis of various cancers. The pandemic has affected all aspects of the cancer care pathway, especially the areas of screening, diagnosis, and surgical treatment.[4,29,30] For instance, De Vincentiis et al[4] reported that the number of cancer diagnoses in Italy decreased by 39% in the first 6 months of 2020 compared with the mean number recorded in 2018 and 2019. The highest decreases in diagnosis rates were observed in prostate cancer (75%), bladder cancer (66%), and CRC (62%), when the number of new or first metastatic malignant diagnoses during lockdown (weeks 11-20 of 2020) was compared with the number in the same period in the previous 2 years.[4] Given that colonoscopy numbers are closely associated with initial CRC diagnoses, a 55% decrease in colon examinations was found between March and April 2020, as reported by Cancer Australia.[31]

In addition to the abrupt reduction (86%) in preventive CRC screenings in the US after the declaration of the COVID-19 national emergency (March 1, 2020), a 64% decrease (ie, 95 000) in the number of colonoscopies performed between March 15 and June 16, 2020, compared with previous years has been reported.[31] Furthermore, after June 16, 2020, weekly volumes remained 36% lower than the pre–COVID-19 levels.[31] Particularly relevant to the present study is the finding of an

Figure 3. Overall Survival Analysis of Patients With Newly Diagnosed Metastatic Colorectal Cancer (mCRC)

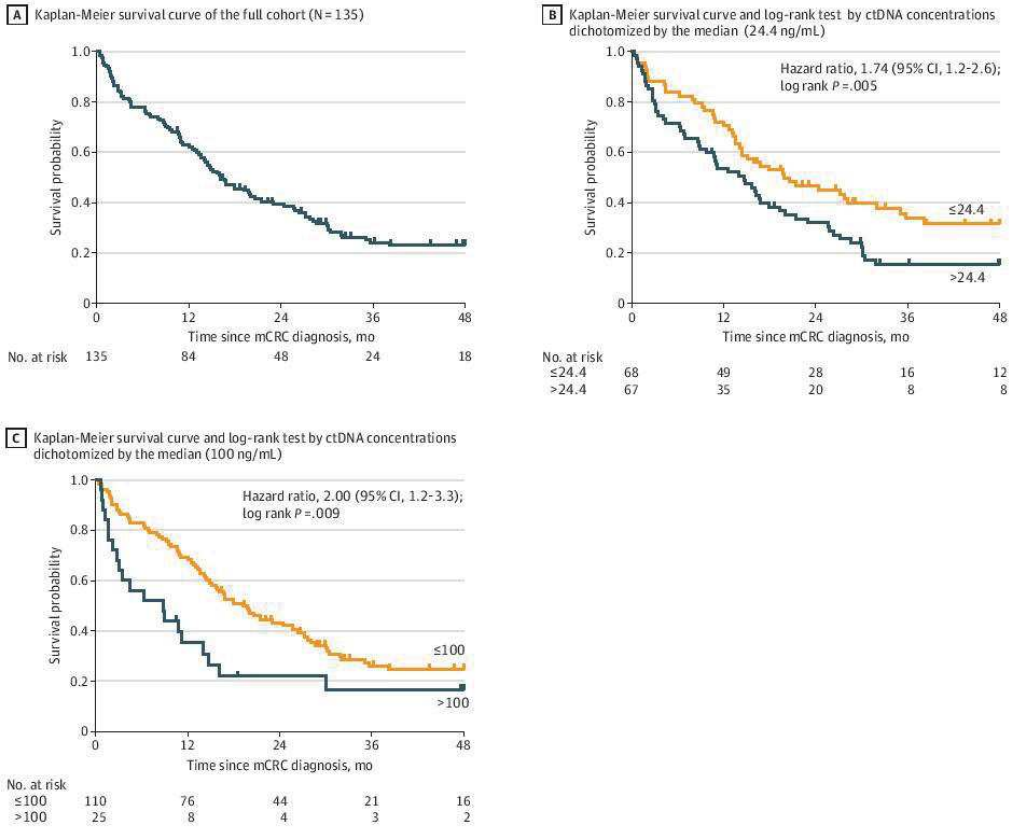

ctDNA indicates circulating tumor DNA.

observational Taiwanese cancer registry study based on 39 000 newly identified CRC cases that increases in the risk of death were significantly associated with the delay between diagnosis and treatment; the results for an interval of 31 to 150 days were an HR of 1.51 (95% CI, 1.43-1.59) and an HR of 1.64 (95% CI, 1.54-1.76) for 151 days or more.[32] The French ONCOCARE-COV study (Oncology Care Pathway's Modifications Impact During COVID-19 Pandemic) confirmed a reduction in CRC fecal immunochemical test screenings (−86%), CRC biomolecular somatic analyses (−59%), and the number of new patient files being discussed in multidisciplinary tumor board meetings (−39%) during the 3-month lockdown period in 2020 compared with the same trimester in 2019.[29] On a broader level, the ONCOCARE-COV study revealed the decreases in screening (−86% to −100%), diagnosis (−39%), and surgical treatment (−30%).[29]

Several studies have generated model-based estimates of the clinical consequences of delaying the first visit of patients who have been newly diagnosed with cancer.[33-35] In the UK, Sud et al[34] found that even a modest delay of 3 to 6 months in surgery for cancer may mitigate 19% to 43% of the life-years gained by hospitalization. Lai et al[36] estimated that approximately 18 000 excess cancer deaths over the next 12 months may be attributed to the COVID-19 crisis. In the US, in addition to the 1 million deaths from breast cancer that are expected to occur in the next decade, approximately 10 000 deaths have been estimated as the outcome of pandemic-related delays of less than 6 months in screening and cancer care.[37]

The health outcomes of COVID-19–associated lockdowns are particularly notable in oncology, and repeated or extended lockdowns may lead to decreased surveillance and advance care planning. To address this threat, regulatory institutions, such as the American Society of Clinical Oncology and the European Society for Medical Oncology, established recommendations and guidance for delivering care to patients with cancer during the pandemic and lockdowns.[1,2] To minimize risks to patients with gastrointestinal malignant neoplasms, for instance, the American College of Surgeons, Society of Surgical Oncology, French digestive oncology intergroup guideline (Thésaurus National de Cancérologie Digestive), and the European Society for Medical Oncology set new priorities, such as prioritizing surgery for colon cancer involving imminent obstruction or for locally advanced rectal cancer. Similarly, new priorities concerning CRC management were set by the Colorectal Cancer Alliance, Thésaurus National de Cancérologie Digestive, National Comprehensive Cancer Network, European Society for Medical Oncology, and the City of Hope National Medical Center.[1] Such recommendations were used to reclassify and reprioritize ongoing CRC care and management during the lockdown.

When CRC is diagnosed early, the treatment outcome is more favorable. In a large meta-analysis, Hanna et al[33] reported that even a 4-week delay in treatment was associated with increased mortality for 7 cancers, particularly CRC (HR, 1.04; 95% CI, 0.95-1.13). This quantitative observation, although focused on a small sample of a specific type of patient with cancer, showed that delays in diagnosis would unnecessarily cost lives and life-years. This increase in ctDNA concentration after lockdown is striking and points to the levels of tumor burden at diagnosis, which have been associated with patient survival.[33,38,39]

To estimate the association between tumor burden and survival, we retrospectively analyzed data from 2 previous clinical studies that examined ctDNA concentration in the same way.[22,23] Each of these studies used an identical, rigorous method to assess ctDNA before patients began first-line chemotherapy. All patients with newly diagnosed mCRC were identified from their data.[22,23] In the present study, patients who were diagnosed with higher ctDNA plasma concentration had a statistically lower median survival compared with those with lower ctDNA concentration. Such comparisons illustrate and anticipate the lockdown's unfavorable implications for patient survival. The full lockdown-related consequences for patient survival will be examined in a future 3-year survival study.

In response to the proliferation of the virus and its variants, many countries will likely implement further lockdowns. Thus, we believe that corrective action should be taken to minimize the clinical implications of delayed cancer diagnosis, including (1) reinforcing mass screening using the fecal

occult blood test, (2) improving the communication strategy to avoid late patient diagnosis, and (3) providing adequate resources and creating robust plans to deal with backlogs in diagnosis and treatment. Patient triage could be performed by a quick assessment of tumor burden and testing of biomarkers with predictive and prognostic value (such as immunohistochemistry for mismatch repair proteins; sequence variation analysis for *KRAS* [GenBank 3845], *NRAS* [GenBank 4893], and *BRAF*). For this purpose, we believe that ctDNA analysis that reveals qualitative (tumor molecular profiling) or quantitative information[9,14,22,23,40] may be an ideal tool, as previously reported.[17,20,41] The diagnostic power of ctDNA would be largely improved by using a multianalyte approach.[42,43] Such a strategy would include both qualitative (such as genetic or epigenetic alterations) and quantitative (such as tissue or cell of origin or structural characteristics) markers. Artificial intelligence may also help achieve this goal as highlighted in a recent report.[43]

Despite the growing number of reports about the magnitude of the burden that the pandemic has placed on health systems worldwide, no study has yet evaluated the increased tumor burden of patients who received a postlockdown cancer diagnosis. To our knowledge, this study was the first to assess the association between COVID-19 restrictions and delayed treatment and diagnostic services for a specific cancer. The findings suggest that CRC can benefit from interventions to minimize the adverse clinical outcomes of pandemic-associated delays.

Limitations

This study has some limitations. Although LDH level, white blood cell count, and to a lesser extent, CEA level were associated with an increase of ctDNA concentration, we could not provide tumor volume assessment by imaging in this study. Nonetheless, ctDNA concentration offers strong additional power to the routinely assessed serum markers. Although numerous studies found that lockdown was associated with delays in care and care seeking, we could not draw a direct association between our observation on tumor burden and the distinct delays in care for the newly diagnosed patients enrolled in the PANIRINOX study. It would be premature to evaluate the outcomes of the delays in screening, diagnosis, and treatment. This exploratory study instead offers a snapshot of a situation that continues to evolve.

Conclusions

This cohort study pointed out the differences in tumor burden for patients who were diagnosed before vs after COVID-19 lockdown, including risk of reduced survival for those with postlockdown diagnoses. The findings of this study suggest that CRC is a major area for intervention to minimize the clinical implications of a pandemic-associated diagnostic delay.

ARTICLE INFORMATION

Accepted for Publication: June 27, 2021.

Published: September 8, 2021. doi:10.1001/jamanetworkopen.2021.24483

Corresponding Author: Alain R. Thierry, PhD, IRCM, INSERM U1194, Université de Montpellier, Institut Régional du Cancer de Montpellier, Montpellier, F-34298, France (alain.thierry@inserm.fr).

Author Affiliations: Institut de Recherche en Cancérologie de Montpellier (IRCM), Institut National de la Santé et de la Recherche Médicale (INSERM) U1194, Université de Montpellier, Institut Régional du Cancer de Montpellier, Montpellier, France (Thierry, Pastor, Pisareva, Mollevi, Ychou, Mazard); Centre Georges François Leclerc, Dijon, France (Ghiringhelli); Hôpital Robert Debré, Reims, France (Bouché); Centre Léon Bérard, Lyon, France (De La Fouchardière); Institut de Cancérologie de l'Ouest, Angers, Saint-Herblain, France (Vanbockstael); Hôpital Haut-Lévêque, Centre Hospitalier Universitaire (CHU) de Bordeaux, Pessac, France (Smith); Centre Antoine Lacassagne, Nice, France (François); Centre François Baclesse, Caen, France (Dos Santos); Medical Oncology Department,

Godinot Institute, Reims, France (Botsen); Centre Catalan d'Oncologie, Perpignan, France (Ellis); Institut Bergonié, Bordeaux, France (Fonck); Hôpital Saint-Antoine, Paris, France (André); Centre de Cancérologie du grand Montpellier, Montpellier, France (Guardiola); Centre Hospitalier de Perpignan, Perpignan, France (Khemissa); Hôpital Privé du Confluent, Nantes, France (Linot); Centre Cario, Plerin, France (Martin-Babau); Hôpital Européen de Marseille, Marseille, France (Rinaldi); Department of Medical Oncology, St Eloi University Hospital, Montpellier, France (Assenat); Hôpital Privé Jean Mermoz, Lyon, France (Clavel); Hôpital Saint Vincent de Paul, Lille, France (Dominguez); Institue de Cancérologie de Lorraine, Vadoeuvre-les-Nancy, France (Gavoille); CHU de Rouen, Rouen, France (Sefrioui); Unicancer, Paris, France (Pezzella).

Author Contributions: Drs Thierry and Mazard had full access to all of the data in the study and take responsibility for the integrity of the data and the accuracy of the data analysis.

Concept and design: Thierry, Botsen, Ellis, Fonck, Ychou, Mazard.

Acquisition, analysis, or interpretation of data: Thierry, Pastor, Pisareva, Ghiringhelli, Bouché, De La Fouchardière, Vanbockstael, Smith, François, Dos Santos, André, Guardiola, Khemissa, Linot, Martin-Babau, Rinaldi, Assenat, Clavel, Dominguez, Gavoille, Sefrioui, Pezzella, Mollevi, Mazard.

Drafting of the manuscript: Thierry, Pastor, Ellis, Khemissa, Mollevi, Ychou, Mazard.

Critical revision of the manuscript for important intellectual content: Thierry, Pisareva, Ghiringhelli, Bouché, De La Fouchardière, Vanbockstael, Smith, François, Dos Santos, Botsen, Fonck, André, Guardiola, Linot, Martin-Babau, Rinaldi, Assenat, Clavel, Dominguez, Gavoille, Sefrioui, Pezzella, Mazard.

Statistical analysis: Thierry, Pastor, Pisareva, Assenat, Mollevi.

Obtained funding: Thierry, Smith, Fonck, Mazard.

Administrative, technical, or material support: Thierry, Pastor, Martin-Babau, Assenat, Clavel, Sefrioui, Pezzella, Ychou.

Supervision: Thierry, Rinaldi, Mazard.

Conflict of Interest Disclosures: Dr Bouché reported receiving personal fees from Amgen, Roche, Merck, Bayer, and Servier outside the submitted work. Dr De La Fouchardière reported receiving personal fees from Servier, Amgen, Bayer, Eisai, Ipsen, Lilly, Merck, MSD, Pierre Fabre, and Roche as well as nonfinancial support (travel for American Society of Clinical Oncology and European Society for Medical Oncology meetings) from Amgen, Roche, Sanofi-Aventis, and Servier. Dr Botsen reported receiving personal fees from Amgen, Chugai Pharmaceutical Co Ltd, Pierre Fabre, Sanofi, and Fresenius Kabi outside the submitted work. Dr André reported receiving personal fees from Amgen, Astra Zeneca, Astellas Pharma Inc, Bristol Myers Squibb, MSD, Gritstone Oncology, GlaxoSmithKline, Servier, Pierre Fabre, Roche, Ventana, Halliox, and Kaleido Biosciences outside the submitted work. Dr Khemissa reported receiving other (Congress fees) from Roche, Servier, Ipsen, and Fresenius Kabi as well as personal fees from Sanofi and Bayer outside the submitted work. Dr Sefrioui reported receiving personal fees from Ipsen, Roche, Servier, and Bayer outside the submitted work. Dr Thierry reported being a shareholder of DiaDx SAS. Dr Mazard reported receiving grants from Amgen SAS; nonfinancial support from Servier and MSD; and personal fees from Merck Serono, Bristol Myers Squibb, Sanofi Genzyme, AAA, Sandoz, and Bayer outside the submitted work. No other disclosures were reported.

Funding/Support: The PANIRINOX study was funded by Amgen and sponsored by Unicancer Research and Development (R&D). Dr Pastor was supported in part by grant INCa_Inserm_DGOS_12553 from SIRIC Montpellier Cancer. Dr Thierry was supported by INSERM.

Role of the Funder/Sponsor: The funder, Amgen, had no role in the design and conduct of the study; collection, management, analysis, and interpretation of the data; and preparation, review, or approval of the manuscript, but had a role in the decision to submit the manuscript for publication. The sponsor, Unicancer R&D, had a role in the collection, management, analysis, and interpretation of the data; preparation, review, or approval of the manuscript; and decision to submit the manuscript for publication.

Additional Contributions: We thank the patients and their families for their trust; all of the participating physicians and supporting staff; Unicancer Datacenter members (Institut Régional du Cancer de Montpellier); all clinician research associates and clinical co-investigators; and Marie Bergeaud, MsBS, Unicancer R&D. We thank Cynthia Sanchez, MS, and Andrei Kudriavtsev, MD, Institut Régional du Cancer de Montpellier, for providing excellent technical assistance. These individuals received no additional compensation, outside of their usual salary, for their contributions. We also thank Cormac McCarthy, MsLitt, McCarthy Consultant, for editing the English-language manuscript; Mr McCarthy received compensation for his services.

REFERENCES

1. Richards M, Anderson M, Carter P, Ebert BL, Mossialos E. The impact of the COVID-19 pandemic on cancer care. *Nat Cancer*. 2020;1(6):1-3. doi:10.1038/s43018-020-0074-y

2. Uzzo RG, Kutinov A, Geynisman DM. COVID-19: cancer screening, diagnosis, post-treatment surveillance in uninfected patients during the pandemic and issues related to COVID-19 vaccination in cancer patients. Accessed October 9, 2020. https://www.uptodate.com/contents/coronavirus-disease-2019-covid-19-cancer-screening-diagnosis-treatment-and-posttreatment-surveillance-in-uninfected-patients-during-the-pandemic

3. Greenwood E, Swanton C. Consequences of COVID-19 for cancer care—a CRUK perspective. *Nat Rev Clin Oncol*. 2021;18(1):3-4. doi:10.1038/s41571-020-00446-0

4. De Vincentiis L, Carr RA, Mariani MP, Ferrara G. Cancer diagnostic rates during the 2020 'lockdown', due to COVID-19 pandemic, compared with the 2018-2019: an audit study from cellular pathology. *J Clin Pathol*. 2021;74(3):187-189. doi:10.1136/jclinpath-2020-206833

5. Kaufman HW, Chen Z, Niles J, Fesko Y. Changes in the number of US patients with newly identified cancer before and during the coronavirus disease 2019 (COVID-19) pandemic. *JAMA Netw Open*. 2020;3(8):e2017267. doi:10.1001/jamanetworkopen.2020.17267

6. Vecchione L, Stintzing S, Pentheroudakis G, Douillard J-Y, Lordick F. ESMO management and treatment adapted recommendations in the COVID-19 era: colorectal cancer. *ESMO Open*. 2020;5(suppl 3):e000826. doi:10.1136/esmoopen-2020-000826

7. Ludwig JA, Weinstein JN. Biomarkers in cancer staging, prognosis and treatment selection. *Nat Rev Cancer*. 2005;5(11):845-856. doi:10.1038/nrc1739

8. Thierry AR, El Messaoudi S, Gahan PB, Anker P, Stroun M. Origins, structures, and functions of circulating DNA in oncology. *Cancer Metastasis Rev*. 2016;35(3):347-376. doi:10.1007/s10555-016-9629-x

9. Wan JCM, Massie C, Garcia-Corbacho J, et al. Liquid biopsies come of age: towards implementation of circulating tumour DNA. *Nat Rev Cancer*. 2017;17(4):223-238. doi:10.1038/nrc.2017.7

10. Diaz LA Jr, Bardelli A. Liquid biopsies: genotyping circulating tumor DNA. *J Clin Oncol*. 2014;32(6):579-586. doi:10.1200/JCO.2012.45.2011

11. Wei T, Zhang Q, Li X, et al. Monitoring tumor burden in response to FOLFIRINOX chemotherapy via profiling circulating cell-free DNA in pancreatic cancer. *Mol Cancer Ther*. 2019;18(1):196-203. doi:10.1158/1535-7163.MCT-17-1298

12. Fiala C, Diamandis EP. Utility of circulating tumor DNA in cancer diagnostics with emphasis on early detection. *BMC Med*. 2018;16(1):166. doi:10.1186/s12916-018-1157-9

13. Kananen L, Hurme M, Jylhä M, et al. Circulating cell-free DNA level predicts all-cause mortality independent of other predictors in the Health 2000 survey. *Sci Rep*. 2020;10(1):13809. doi:10.1038/s41598-020-70526-9

14. Thierry AR, Pastor B, Jiang Z-Q, et al. Circulating DNA demonstrates convergent evolution and common resistance mechanisms during treatment of colorectal cancer. *Clin Cancer Res*. 2017;23(16):4578-4591. doi:10.1158/1078-0432.CCR-17-0232

15. Saluja H, Karapetis CS, Pedersen SK, Young GP, Symonds EL. The use of circulating tumor DNA for prognosis of gastrointestinal cancers. *Front Oncol*. 2018;8:275. doi:10.3389/fonc.2018.00275

16. Xu X, Yu Y, Shen M, et al. Role of circulating free DNA in evaluating clinical tumor burden and predicting survival in Chinese metastatic colorectal cancer patients. *BMC Cancer*. 2020;20(1):1006. doi:10.1186/s12885-020-07516-7

17. El Messaoudi S, Mouliere F, Du Manoir S, et al. Circulating DNA as a strong multimarker prognostic tool for metastatic colorectal cancer patient management care. *Clin Cancer Res*. 2016;22(12):3067-3077. doi:10.1158/1078-0432.CCR-15-0297

18. Barault L, Amatu A, Siravegna G, et al. Discovery of methylated circulating DNA biomarkers for comprehensive non-invasive monitoring of treatment response in metastatic colorectal cancer. *Gut*. 2018;67(11):1995-2005. doi:10.1136/gutjnl-2016-313372

19. Spindler KG. Methodological, biological and clinical aspects of circulating free DNA in metastatic colorectal cancer. *Acta Oncol*. 2017;56(1):7-16. doi:10.1080/0284186X.2016.1253861

20. Hamfjord J, Guren TK, Dajani O, et al. Total circulating cell-free DNA as a prognostic biomarker in metastatic colorectal cancer before first-line oxaliplatin-based chemotherapy. *Ann Oncol*. 2019;30(7):1088-1095. doi:10.1093/annonc/mdz139

21. von Elm E, Altman DG, Egger M, Pocock SJ, Gøtzsche PC, Vandenbroucke JP, et al; STROBE Initiative. The Strengthening the Reporting of Observational Studies in Epidemiology (STROBE) Statement: guidelines for reporting observational studies. *Int J Surg*. 2014;12(12):1495-1499. doi:10.1016/j.ijsu.2014.07.013

22. Thierry AR, Mouliere F, El Messaoudi S, et al. Clinical validation of the detection of *KRAS* and *BRAF* mutations from circulating tumor DNA. *Nat Med*. 2014;20(4):430-435. doi:10.1038/nm.3511

23. Thierry AR, El Messaoudi S, Mollevi C, et al. Clinical utility of circulating DNA analysis for rapid detection of actionable mutations to select metastatic colorectal patients for anti-EGFR treatment. *Ann Oncol*. 2017;28(9):2149-2159. doi:10.1093/annonc/mdx330

24. Meddeb R, Pisareva E, Thierry AR. Guidelines for the preanalytical conditions for analyzing circulating cell-free DNA. *Clin Chem*. 2019;65(5):623-633. doi:10.1373/clinchem.2018.298323

25. Mouliere F, El Messaoudi S, Pang D, Dritschilo A, Thierry AR. Multi-marker analysis of circulating cell-free DNA toward personalized medicine for colorectal cancer. *Mol Oncol*. 2014;8(5):927-941. doi:10.1016/j.molonc.2014.02.005

26. Chibaudel B, Bonnetain F, Tournigand C, et al. Simplified prognostic model in patients with oxaliplatin-based or irinotecan-based first-line chemotherapy for metastatic colorectal cancer: a GERCOR study. *Oncologist*. 2011;16(9):1228-1238. doi:10.1634/theoncologist.2011-0039

27. Goey KKH, Mahmoud R, Sørbye H, et al. Reporting of patient characteristics and stratification factors in phase 3 trials investigating first-line systemic treatment of metastatic colorectal cancer: a systematic review. *Eur J Cancer*. 2018;96:115-124. doi:10.1016/j.ejca.2018.03.026

28. Daly N. Cancer tests and operations dropped up to 50 per cent during April lockdown, data shows. Accessed September 14, 2020. https://www.abc.net.au/news/2020-09-14/cancer-tests-operations-drop-up-to-50-per-cent-april-coronavirus/12622396

29. Brugel M, Carlier C, Essner C, et al. Dramatic changes in oncology care pathways during the COVID–19 pandemic: the French ONCOCARE-COV Study. *Oncologist*. 2021;26(2):e338-e341. doi:10.1002/onco.13578

30. Dinmohamed AG, Visser O, Verhoeven RHA, et al. Fewer cancer diagnoses during the COVID-19 epidemic in the Netherlands. *Lancet Oncol*. 2020;21(6):750-751. doi:10.1016/S1470-2045(20)30265-5

31. Desai A, Warner J, Kuderer N, et al. Crowdsourcing a crisis response for COVID-19 in oncology. *Nat Cancer*. 2020;1(5):1-4. doi:10.1038/s43018-020-0065-z

32. Lee SY, Lei B, Mallick B. Estimation of COVID-19 spread curves integrating global data and borrowing information. *PLoS One*. 2020;15(7):e0236860. doi:10.1371/journal.pone.0236860

33. Hanna TP, King WD, Thibodeau S, et al. Mortality due to cancer treatment delay: systematic review and meta-analysis. *BMJ*. 2020;371:m4087. doi:10.1136/bmj.m4087

34. Sud A, Torr B, Jones ME, et al. Effect of delays in the 2-week-wait cancer referral pathway during the COVID-19 pandemic on cancer survival in the UK: a modelling study. *Lancet Oncol*. 2020;21(8):1035-1044. doi:10.1016/S1470-2045(20)30392-2

35. Maringe C, Spicer J, Morris M, et al. The impact of the COVID-19 pandemic on cancer deaths due to delays in diagnosis in England, UK: a national, population-based, modelling study. *Lancet Oncol*. 2020;21(8):1023-1034. doi:10.1016/S1470-2045(20)30388-0

36. Lai AG, Pasea L, Banerjee A, et al. Estimated impact of the COVID-19 pandemic on cancer services and excess 1-year mortality in people with cancer and multimorbidity: near real-time data on cancer care, cancer deaths and a population-based cohort study. *BMJ Open*. 2020;10(11):e043828. doi:10.1136/bmjopen-2020-043828

37. Sharpless NE. COVID-19 and cancer. *Science*. 2020;368(6497):1290-1290. doi:10.1126/science.abd3377

38. Weitz J, Koch M, Debus J, Höhler T, Galle PR, Büchler MW. Colorectal cancer. *Lancet*. 2005;365(9454):153-165. doi:10.1016/S0140-6736(05)17706-X

39. Yan Q, Zhang K, Guo K, et al. Value of tumor size as a prognostic factor in metastatic colorectal cancer patients after chemotherapy: a population-based study. *Future Oncol*. 2019;15(15):1745-1758. doi:10.2217/fon-2018-0785

40. Meddeb R, Dache ZAA, Thezenas S, et al. Quantifying circulating cell-free DNA in humans. *Sci Rep*. 2019;9(1):5220. doi:10.1038/s41598-019-41593-4

41. Sundquist K, Sundquist J, Hedelius A, Memon AA. Diagnostic potential of circulating cell-free nuclear and mitochondrial DNA for several cancer types and nonmalignant diseases: a study on suspected cancer patients. *Mol Carcinog*. 2020;59(12):1362-1370. doi:10.1002/mc.23261

42. Bronkhorst AJ, Ungerer V, Holdenrieder S. Early detection of cancer using circulating tumor DNA: biological, physiological and analytical considerations. *Crit Rev Clin Lab Sci*. 2019;1-17. doi:10.1080/10408363.2019.1700902

43. Tanos R, Tosato G, Otandault A, et al. Machine learning-assisted evaluation of circulating DNA quantitative analysis for cancer screening. *Adv Sci (Weinh)*. 2020;7(18):2000486. doi:10.1002/advs.202000486

SUPPLEMENT.

eAppendix. Materials and Methods

eFigure 1. Illustration of the Correlation Between the Tumor Burden and Total cirDNA Level in Three Metachronous mCRC Patients (One Site) With Increasing Hepatic Tumor Mass as Determined by MRI

REFERENCES

1. Les cancers en France en 2018 - L'éssentiels des faits et chiffres (édition 2020).

2. Jooste V, Grosclaude P, Remontet L, Launoy G, Baldi I, Molinié F, Arveux P, Bossard N, Bouvier A-M, Colonna M, et al. Unbiased estimates of long-term net survival of solid cancers in France. Int J Cancer. 2013 May 15;132(10):2370–7.

3. Seppä K, Hakulinen T, Pokhrel A. Choosing the net survival method for cancer survival estimation. European Journal of Cancer. 2015 Jun;51(9):1123–9.

4. Bray F, Ferlay J, Soerjomataram I, Siegel RL, Torre LA, Jemal A. Global cancer statistics 2018: GLOBOCAN estimates of incidence and mortality worldwide for 36 cancers in 185 countries. CA: A Cancer Journal for Clinicians. 2018 Nov;68(6):394–424.

5. Dekker E, Tanis PJ, Vleugels JLA, Kasi PM, Wallace MB. Colorectal cancer. The Lancet. 2019 Oct;394(10207):1467–80.

6. Arnold M, Sierra MS, Laversanne M, Soerjomataram I, Jemal A, Bray F. Global patterns and trends in colorectal cancer incidence and mortality. Gut. 2017 Apr;66(4):683–91.

7. Henrikson NB, Webber EM, Goddard KA, Scrol A, Piper M, Williams MS, Zallen DT, Calonge N, Ganiats TG, Janssens ACJW, et al. Family history and the natural history of colorectal cancer: systematic review. Genet Med. 2015 Sep;17(9):702–12.

8. Schoen RE, Razzak A, Yu KJ, Berndt SI, Firl K, Riley TL, Pinsky PF. Incidence and mortality of colorectal cancer in individuals with a family history of colorectal cancer. Gastroenterology. 2015 Nov;149(6):1438-1445.e1.

9. Syngal S, Brand RE, Church JM, Giardiello FM, Hampel HL, Burt RW. ACG Clinical Guideline: Genetic Testing and Management of Hereditary Gastrointestinal Cancer Syndromes. American Journal of Gastroenterology. 2015 Feb;110(2):223–62.

10. Yurgelun MB, Hampel H. Recent Advances in Lynch Syndrome: Diagnosis, Treatment, and Cancer Prevention. American Society of Clinical Oncology Educational Book. 2018 May;(38):101–9.

11. Botteri E, Borroni E, Sloan EK, Bagnardi V, Bosetti C, Peveri G, Santucci C, Specchia C, van den Brandt P, Gallus S, et al. Smoking and Colorectal Cancer Risk, Overall and by Molecular Subtypes: A Meta-Analysis. Am J Gastroenterol. 2020 Dec;115(12):1940–9.

12. Cai S, Li Y, Ding Y, Chen K, Jin M. Alcohol drinking and the risk of colorectal cancer death: a meta-analysis. European Journal of Cancer Prevention. 2014 Nov;23(6):532–9.

13. Kyrgiou M, Kalliala I, Markozannes G, Gunter MJ, Paraskevaidis E, Gabra H, Martin-Hirsch P, Tsilidis KK. Adiposity and cancer at major anatomical sites: umbrella review of the literature. BMJ. 2017 Feb 28;j477.

14. Chan DSM, Lau R, Aune D, Vieira R, Greenwood DC, Kampman E, Norat T. Red and Processed Meat and Colorectal Cancer Incidence: Meta-Analysis of Prospective Studies. Tomé D, editor. PLoS ONE. 2011 Jun 6;6(6):e20456.

15. Amin MB, Greene FL, Edge SB, Compton CC, Gershenwald JE, Brookland RK, Meyer L, Gress DM, Byrd DR, Winchester DP. The Eighth Edition AJCC Cancer Staging Manual: Continuing to build a bridge from a population-based to a more "personalized" approach to cancer staging: The Eighth Edition AJCC Cancer Staging Manual. CA: A Cancer Journal for Clinicians. 2017 Mar;67(2):93–9.

16. Lecomte T, André T, Bibeau F, Blanc B, Cohen R, Lagasse JP, Laurent-Puig P, Lepage C, Lucidarme O, Martin-Babau J, et al. 'Cancer du côlon non métastatique' Thésaurus National de Cancérologie Digestive [Internet]. 2021. Available from: [https://www.snfge.org/tncd et http://www.tncd.org]

17. Manfredi S, Bouvier AM, Lepage C, Hatem C, Dancourt V, Faivre J. Incidence and patterns of recurrence after resection for cure of colonic cancer in a well defined population. British Journal of Surgery. 2006 Aug 17;93(9):1115–22.

18. Guyot F, Faivre J, Manfredi S, Meny B, Bonithon-Kopp C, Bouvier AM. Time trends in the treatment and survival of recurrences from colorectal cancer. Annals of Oncology. 2005 May;16(5):756–61.

19. Chau I, Allen MJ, Cunningham D, Norman AR, Brown G, Ford HER, Tebbutt N, Tait D, Hill M, Ross PJ, et al. The Value of Routine Serum Carcino-Embryonic Antigen Measurement and Computed Tomography in the Surveillance of Patients After Adjuvant Chemotherapy for Colorectal Cancer. JCO. 2004 Apr 15;22(8):1420–9.

20. Wong RKS, Berry S, Spithoff K, Simunovic M, Chan K, Agboola O, Dingle B. Preoperative or Postoperative Therapy for Stage II or III Rectal Cancer: An Updated Practice Guideline. Clinical Oncology. 2010 May;22(4):265–71.

21. Nordlinger B, Sorbye H, Glimelius B, Poston GJ, Schlag PM, Rougier P, Bechstein WO, Primrose JN, Walpole ET, Finch-Jones M, et al. Perioperative FOLFOX4 chemotherapy and surgery versus surgery alone for resectable liver metastases from colorectal cancer (EORTC 40983): long-term results of a randomised, controlled, phase 3 trial. The Lancet Oncology. 2013 Nov;14(12):1208–15.

22. Verwaal VJ, van Ruth S, de Bree E, van Slooten GW, van Tinteren H, Boot H, Zoetmulder FAN. Randomized Trial of Cytoreduction and Hyperthermic Intraperitoneal Chemotherapy Versus Systemic Chemotherapy and Palliative Surgery in Patients With Peritoneal Carcinomatosis of Colorectal Cancer. JCO. 2003 Oct 15;21(20):3737–43.

23. Zou X, Wang Q, Zhang J. Comparison of 5–FU-based and Capecitabine-based Neoadjuvant Chemoradiotherapy in Patients With Rectal Cancer: A Meta-analysis. Clinical Colorectal Cancer. 2017 Sep;16(3):e123–39.

24. Schmoll H-J, Twelves C, Sun W, O'Connell MJ, Cartwright T, McKenna E, Saif M, Lee S, Yothers G, Haller D. Effect of adjuvant capecitabine or fluorouracil, with or without oxaliplatin, on survival outcomes in stage III colon cancer and the effect of oxaliplatin on post-relapse survival: a pooled analysis of individual patient data from four randomised controlled trials. The Lancet Oncology. 2014 Dec;15(13):1481–92.

25. Sauer R, Liersch T, Merkel S, Fietkau R, Hohenberger W, Hess C, Becker H, Raab H-R, Villanueva M-T, Witzigmann H, et al. Preoperative Versus Postoperative Chemoradiotherapy for Locally Advanced Rectal Cancer: Results of the German CAO/ARO/AIO-94 Randomized Phase III Trial After a Median Follow-Up of 11 Years. JCO. 2012 Jun 1;30(16):1926–33.

26. Appelt AL, Pløen J, Harling H, Jensen FS, Jensen LH, Jørgensen JCR, Lindebjerg J, Rafaelsen SR, Jakobsen A. High-dose chemoradiotherapy and watchful waiting for distal rectal cancer: a prospective observational study. The Lancet Oncology. 2015 Aug;16(8):919–27.

27. Lièvre A, Bachet J-B, Le Corre D, Boige V, Landi B, Emile J-F, Côté J-F, Tomasic G, Penna C, Ducreux M, et al. KRAS mutation status is predictive of response to cetuximab therapy in colorectal cancer. Cancer Res. 2006 Apr 15;66(8):3992–5.

28. Douillard J-Y, Oliner KS, Siena S, Tabernero J, Burkes R, Barugel M, Humblet Y, Bodoky G, Cunningham D, Jassem J, et al. Panitumumab-FOLFOX4 treatment and RAS mutations in colorectal cancer. N Engl J Med. 2013 Sep 12;369(11):1023–34.

29. Douillard JY, Siena S, Cassidy J, Tabernero J, Burkes R, Barugel M, Humblet Y, Bodoky G, Cunningham D, Jassem J, et al. Final results from PRIME: randomized phase III study of panitumumab with FOLFOX4 for first-line treatment of metastatic colorectal cancer. Ann Oncol. 2014 Jul;25(7):1346–55.

30. Bokemeyer C, Köhne C-H, Ciardiello F, Lenz H-J, Heinemann V, Klinkhardt U, Beier F, Duecker K, van Krieken JH, Tejpar S. FOLFOX4 plus cetuximab treatment and RAS mutations in colorectal cancer. European Journal of Cancer. 2015 Jul;51(10):1243–52.

31. Bokemeyer C, Cutsem EV, Rougier P, Ciardiello F, Heeger S, Schlichting M, Celik I, Köhne C-H. Addition of cetuximab to chemotherapy as first-line treatment for KRAS wild-type metastatic colorectal cancer: Pooled analysis of the CRYSTAL and OPUS randomised clinical trials. European Journal of Cancer. 2012 Jul;48(10):1466–75.

32. Douillard J-Y, Siena S, Cassidy J, Tabernero J, Burkes R, Barugel M, Humblet Y, Bodoky G, Cunningham D, Jassem J, et al. Randomized, Phase III Trial of Panitumumab With Infusional Fluorouracil, Leucovorin, and Oxaliplatin (FOLFOX4) Versus FOLFOX4 Alone As First-Line Treatment in Patients With Previously Untreated Metastatic Colorectal Cancer: The PRIME Study. JCO. 2010 Nov 1;28(31):4697–705.

33. Heinemann V, von Weikersthal LF, Decker T, Kiani A, Vehling-Kaiser U, Al-Batran S-E, Heintges T, Lerchenmüller C, Kahl C, Seipelt G, et al. FOLFIRI plus cetuximab versus FOLFIRI plus bevacizumab as first-line treatment for patients with metastatic colorectal cancer (FIRE-3): a randomised, open-label, phase 3 trial. The Lancet Oncology. 2014 Sep;15(10):1065–75.

34. Arai H, Battaglin F, Wang J, Lo JH, Soni S, Zhang W, Lenz H-J. Molecular insight of regorafenib treatment for colorectal cancer. Cancer Treat Rev. 2019 Dec;81:101912.

35. Schmieder R, Hoffmann J, Becker M, Bhargava A, Müller T, Kahmann N, Ellinghaus P, Adams R, Rosenthal A, Thierauch K-H, et al. Regorafenib (BAY 73-4506): antitumor and antimetastatic activities in preclinical models of colorectal cancer. Int J Cancer. 2014 Sep 15;135(6):1487–96.

36. Grothey A, Van Cutsem E, Sobrero A, Siena S, Falcone A, Ychou M, Humblet Y, Bouché O, Mineur L, Barone C, et al. Regorafenib monotherapy for previously treated metastatic colorectal cancer (CORRECT): an international, multicentre, randomised, placebo-controlled, phase 3 trial. Lancet. 2013 Jan 26;381(9863):303–12.

37. Li J, Qin S, Xu R, Yau TCC, Ma B, Pan H, Xu J, Bai Y, Chi Y, Wang L, et al. Regorafenib plus best supportive care versus placebo plus best supportive care in Asian patients with previously treated metastatic colorectal cancer (CONCUR): a randomised, double-blind, placebo-controlled, phase 3 trial. Lancet Oncol. 2015 Jun;16(6):619–29.

38. Marcus L, Lemery SJ, Keegan P, Pazdur R. FDA Approval Summary: Pembrolizumab for the Treatment of Microsatellite Instability-High Solid Tumors. Clin Cancer Res. 2019 Jul 1;25(13):3753–8.

39. Le DT, Uram JN, Wang H, Bartlett BR, Kemberling H, Eyring AD, Skora AD, Luber BS, Azad NS, Laheru D, et al. PD-1 Blockade in Tumors with Mismatch-Repair Deficiency. N Engl J Med. 2015 Jun 25;372(26):2509–20.

40. Overman MJ, Lonardi S, Wong KYM, Lenz H-J, Gelsomino F, Aglietta M, Morse MA, Van Cutsem E, McDermott R, Hill A, et al. Durable Clinical Benefit With Nivolumab Plus Ipilimumab in DNA Mismatch Repair–Deficient/Microsatellite Instability–High Metastatic Colorectal Cancer. JCO. 2018 Mar 10;36(8):773–9.

41. Therasse P, Arbuck SG, Eisenhauer EA, Wanders J, Kaplan RS, Rubinstein L, Verweij J, Van Glabbeke M, van Oosterom AT, Christian MC, et al. New Guidelines to Evaluate the Response to Treatment in Solid Tumors. JNCI: Journal of the National Cancer Institute. 2000 Feb 2;92(3):205–16.

42. Eisenhauer EA, Therasse P, Bogaerts J, Schwartz LH, Sargent D, Ford R, Dancey J, Arbuck S, Gwyther S, Mooney M, et al. New response evaluation criteria in solid tumours: revised RECIST guideline (version 1.1). Eur J Cancer. 2009 Jan;45(2):228–47.

43. Thierry AR, El Messaoudi S, Mollevi C, Raoul JL, Guimbaud R, Pezet D, Artru P, Assenat E, Borg C, Mathonnet M, et al. Clinical utility of circulating DNA analysis for rapid detection of actionable mutations to select metastatic colorectal patients for anti-EGFR treatment. Ann Oncol. 2017 Sep 1;28(9):2149–59.

44. Nowell PC. The Clonal Evolution of Tumor Cell Populations: Acquired genetic lability permits stepwise selection of variant sublines and underlies tumor progression. Science. 1976 Oct;194(4260):23–8.

45. Pon JR, Marra MA. Driver and Passenger Mutations in Cancer. Annu Rev Pathol Mech Dis. 2015 Jan 24;10(1):25–50.

46. Kandoth C, McLellan MD, Vandin F, Ye K, Niu B, Lu C, Xie M, Zhang Q, McMichael JF, Wyczalkowski MA, et al. Mutational landscape and significance across 12 major cancer types. Nature. 2013 Oct 17;502(7471):333–9.

47. Lawrence MS, Stojanov P, Mermel CH, Robinson JT, Garraway LA, Golub TR, Meyerson M, Gabriel SB, Lander ES, Getz G. Discovery and saturation analysis of cancer genes across 21 tumour types. Nature. 2014 Jan;505(7484):495–501.

48. Swanton C. Intratumor heterogeneity: evolution through space and time. Cancer Res. 2012 Oct 1;72(19):4875–82.

49. Gerlinger M, Horswell S, Larkin J, Rowan AJ, Salm MP, Varela I, Fisher R, McGranahan N, Matthews N, Santos CR, et al. Genomic architecture and evolution of clear cell renal cell carcinomas defined by multiregion sequencing. Nat Genet. 2014 Mar;46(3):225–33.

50. Marusyk A, Almendro V, Polyak K. Intra-tumour heterogeneity: a looking glass for cancer? Nat Rev Cancer. 2012 May;12(5):323–34.

51. Gerlinger M, Rowan AJ, Horswell S, Larkin J, Endesfelder D, Gronroos E, Martinez P, Matthews N, Stewart A, Tarpey P, et al. Intratumor heterogeneity and branched evolution revealed by multiregion sequencing. N Engl J Med. 2012 Mar 8;366(10):883–92.

52. Paik PK, Shen R, Won H, Rekhtman N, Wang L, Sima CS, Arora A, Seshan V, Ladanyi M, Berger MF, et al. Next-Generation Sequencing of Stage IV Squamous Cell Lung Cancers Reveals an Association of PI3K Aberrations and Evidence of Clonal Heterogeneity in Patients with Brain Metastases. Cancer Discovery. 2015 Jun;5(6):610–21.

53. Zhang L-L, Kan M, Zhang M-M, Yu S-S, Xie H-J, Gu Z-H, Wang H-N, Zhao S-X, Zhou G-B, Song H-D, et al. Multiregion sequencing reveals the intratumor heterogeneity of driver mutations in TP53-driven non-small cell lung cancer: Intratumor heterogeneity in TP53-driven lung cancer. Int J Cancer. 2017 Jan 1;140(1):103–8.

54. Blighe K, Kenny L, Patel N, Guttery DS, Page K, Gronau JH, Golshani C, Stebbing J, Coombes RC, Shaw JA. Whole Genome Sequence Analysis Suggests Intratumoral Heterogeneity in Dissemination of Breast Cancer to Lymph Nodes. Gao J-X, editor. PLoS ONE. 2014 Dec 29;9(12):e115346.

55. Hiley C, de Bruin EC, McGranahan N, Swanton C. Deciphering intratumor heterogeneity and temporal acquisition of driver events to refine precision medicine. Genome Biol. 2014 Aug;15(8):453.

56. Hiley CT, Swanton C. Spatial and temporal cancer evolution: causes and consequences of tumour diversity. Clin Med. 2014 Dec;14(Suppl 6):s33–7.

57. Klein EA, Richards D, Cohn A, Tummala M, Lapham R, Cosgrove D, Chung G, Clement J, Gao J, Hunkapiller N, et al. Clinical validation of a targeted methylation-based multi-cancer early detection test using an independent validation set. Annals of Oncology. 2021 Sep;32(9):1167–77.

58. Shen SY, Singhania R, Fehringer G, Chakravarthy A, Roehrl MHA, Chadwick D, Zuzarte PC, Borgida A, Wang TT, Li T, et al. Sensitive tumour detection and classification using plasma cell-free DNA methylomes. Nature. 2018 Nov;563(7732):579–83.

59. Vermaat JS, Nijman IJ, Koudijs MJ, Gerritse FL, Scherer SJ, Mokry M, Roessingh WM, Lansu N, de Bruijn E, van Hillegersberg R, et al. Primary Colorectal Cancers and Their Subsequent Hepatic Metastases Are Genetically Different: Implications for Selection of Patients for Targeted Treatment. Clin Cancer Res. 2012 Feb 1;18(3):688–99.

60. Caldas C. Cancer sequencing unravels clonal evolution. Nat Biotechnol. 2012 May 7;30(5):408–10.

61. Rübben A, Araujo A. Cancer heterogeneity: converting a limitation into a source of biologic information. J Transl Med. 2017 Dec;15(1):190.

62. Negrini S, Gorgoulis VG, Halazonetis TD. Genomic instability — an evolving hallmark of cancer. Nat Rev Mol Cell Biol. 2010 Mar;11(3):220–8.

63. Murugaesu N, Wilson GA, Birkbak NJ, Watkins TBK, McGranahan N, Kumar S, Abbassi-Ghadi N, Salm M, Mitter R, Horswell S, et al. Tracking the Genomic Evolution of Esophageal Adenocarcinoma through Neoadjuvant Chemotherapy. Cancer Discovery. 2015 Aug;5(8):821–31.

64. Vandin F, Upfal E, Raphael BJ. De novo discovery of mutated driver pathways in cancer. Genome Res. 2012 Feb;22(2):375–85.

65. Win AK, Jenkins MA, Buchanan DD, Clendenning M, Young JP, Giles GG, Goldblatt J, Leggett BA, Hopper JL, Thibodeau SN, et al. Determining the frequency of de novo germline mutations in DNA mismatch repair genes. Journal of Medical Genetics. 2011 Aug 1;48(8):530–4.

66. Diaz LA, Williams RT, Wu J, Kinde I, Hecht JR, Berlin J, Allen B, Bozic I, Reiter JG, Nowak MA, et al. The molecular evolution of acquired resistance to targeted EGFR blockade in colorectal cancers. Nature. 2012 Jun 28;486(7404):537–40.

67. Misale S, Yaeger R, Hobor S, Scala E, Janakiraman M, Liska D, Valtorta E, Schiavo R, Buscarino M, Siravegna G, et al. Emergence of KRAS mutations and acquired resistance to anti-EGFR therapy in colorectal cancer. Nature. 2012 Jun 28;486(7404):532–6.

68. Arena S, Bellosillo B, Siravegna G, Martínez A, Cañadas I, Lazzari L, Ferruz N, Russo M, Misale S, González I, et al. Emergence of Multiple EGFR Extracellular Mutations during Cetuximab Treatment in Colorectal Cancer. Clin Cancer Res. 2015 May 1;21(9):2157–66.

69. Dagogo-Jack I, Shaw AT. Tumour heterogeneity and resistance to cancer therapies. Nat Rev Clin Oncol. 2018 Feb;15(2):81–94.

70. Mandel P, Metais P. Les acides nucléiques du plasma sanguin chez l'homme. C R Seances Soc Biol Fil. 1948 Feb;142(3–4):241–3.

71. Leon SA, Shapiro B, Sklaroff DM, Yaros MJ. Free DNA in the Serum of Cancer Patients and the Effect of Therapy. Cancer Res. 1977 Mar 1;37(3):646–50.

72. Stroun M, Anker P, Maurice P, Gahan PB. Circulating nucleic acids in higher organisms. Int Rev Cytol. 1977;51:1–48.

73. Stroun M, Anker P, Maurice P, Lyautey J, Lederrey C, Beljanski M. Neoplastic characteristics of the DNA found in the plasma of cancer patients. Oncology. 1989;46(5):318–22.

74. Vasioukhin V, Anker P, Maurice P, Lyautey J, Lederrey C, Stroun M. Point mutations of the N-ras gene in the blood plasma DNA of patients with myelodysplastic syndrome or acute myelogenous leukaemia. Br J Haematol. 1994 Apr;86(4):774–9.

75. Diehl F, Li M, Dressman D, He Y, Shen D, Szabo S, Diaz LA, Goodman SN, David KA, Juhl H, et al. Detection and quantification of mutations in the plasma of patients with colorectal tumors. PNAS. 2005 Aug 11;102(45):16368–73.

76. Thierry AR, Mouliere F, El Messaoudi S, Mollevi C, Lopez-Crapez E, Rolet F, Gillet B, Gongora C, Dechelotte P, Robert B, et al. Clinical validation of the detection of KRAS and BRAF mutations from circulating tumor DNA. Nat Med. 2014 Apr;20(4):430–5.

77. Thierry AR, El Messaoudi S, Gahan PB, Anker P, Stroun M. Origins, structures, and functions of circulating DNA in oncology. Cancer Metastasis Rev. 2016 Sep;35(3):347–76.

78. Lo YMD, Corbetta N, Chamberlain PF, Rai V, Sargent IL, Redman CW, Wainscoat JS. Presence of fetal DNA in maternal plasma and serum. The Lancet. 1997 Aug;350(9076):485–7.

79. Lo YM, Lau TK, Zhang J, Leung TN, Chang AM, Hjelm NM, Elmes RS, Bianchi DW. Increased fetal DNA concentrations in the plasma of pregnant women carrying fetuses with trisomy 21. Clin Chem. 1999 Oct;45(10):1747–51.

80. Dennis Lo YM, Chiu RWK. Prenatal diagnosis: progress through plasma nucleic acids. Nat Rev Genet. 2007 Jan;8(1):71–7.

81. Atamaniuk J, Hsiao Y-Y, Mustak M, Bernhard D, Erlacher L, Fodinger M, Tiran B, Stuhlmeier KM. Analysing cell-free plasma DNA and SLE disease activity: ANALYSING CELL-FREE PLASMA DNA AND DISEASE ACTIVITY. European Journal of Clinical Investigation. 2011 Jun;41(6):579–83.

82. Tug S, Helmig S, Deichmann ER, Schmeier-Jürchott A, Wagner E, Zimmermann T, Radsak M, Giacca M, Simon P. Exercise-induced increases in cell free DNA in human plasma originate predominantly from cells of the haematopoietic lineage. Exerc Immunol Rev. 2015;21:164–73.

83. Huang T, Yang Z, Chen S, Chen J. [Predictive value of plasma cell-free DNA for prognosis of sepsis]. Zhonghua Wei Zhong Bing Ji Jiu Yi Xue. 2018 Oct;30(10):925–8.

84. Glebova KV, Veiko NN, Nikonov AA, Porokhovnik LN, Kostuyk SV. Cell-free DNA as a biomarker in stroke: Current status, problems and perspectives. Crit Rev Clin Lab Sci. 2018 Jan;55(1):55–70.

85. Knight SR, Thorne A, Lo Faro ML. Donor-specific Cell-free DNA as a Biomarker in Solid Organ Transplantation. A Systematic Review. Transplantation. 2019 Feb;103(2):273–83.

86. Schütz E, Asendorf T, Beck J, Schauerte V, Mettenmeyer N, Shipkova M, Wieland E, Kabakchiev M, Walson PD, Schwenger V, et al. Time-Dependent Apparent Increase in dd-cfDNA Percentage in Clinically Stable Patients Between One and Five Years Following Kidney Transplantation. Clinical Chemistry. 2020 Oct 1;66(10):1290–9.

87. Sanchez C, Roch B, Mazard T, Blache P, Dache ZAA, Pastor B, Pisareva E, Tanos R, Thierry AR. Circulating nuclear DNA structural features, origins, and complete size profile revealed by fragmentomics. JCI Insight. 2021 Apr 8;6(7):e144561.

88. Bronkhorst AJ, Ungerer V, Holdenrieder S. The emerging role of cell-free DNA as a molecular marker for cancer management. Biomolecular Detection and Quantification. 2019 Mar;17:100087.

89. Snyder MW, Kircher M, Hill AJ, Daza RM, Shendure J. Cell-free DNA comprises an in vivo nucleosome footprint that informs its tissues-of-origin. Cell. 2016 Jan 14;164(0):57.

90. Moss J, Magenheim J, Neiman D, Zemmour H, Loyfer N, Korach A, Samet Y, Maoz M, Druid H, Arner P, et al. Comprehensive human cell-type methylation atlas reveals origins of circulating cell-free DNA in health and disease. Nature Communications. 2018 Oct 20;448142.

91. Elmore S. Apoptosis: A Review of Programmed Cell Death. Toxicol Pathol. 2007 Jun;35(4):495–516.

92. Singh R, Letai A, Sarosiek K. Regulation of apoptosis in health and disease: the balancing act of BCL-2 family proteins. Nat Rev Mol Cell Biol. 2019 Mar;20(3):175–93.

93. Jahr S, Hentze H, Englisch S, Hardt D, Fackelmayer FO, Hesch R-D, Knippers R. DNA Fragments in the Blood Plasma of Cancer Patients: Quantitations and Evidence for Their Origin from Apoptotic and Necrotic Cells. Cancer Res. 2001 Feb 2;61(4):1659–65.

94. Stroun M, Lyautey J, Lederrey C, Olson-Sand A, Anker P. About the possible origin and mechanism of circulating DNA apoptosis and active DNA release. Clin Chim Acta. 2001 Nov;313(1–2):139–42.

95. Nagata S. Apoptotic DNA Fragmentation. Experimental Cell Research. 2000 Apr;256(1):12–8.

96. van der Vaart M, Pretorius PJ. The Origin of Circulating Free DNA. Clinical Chemistry. 2007 Dec 1;53(12):2215–2215.

97. Rumore PM, Steinman CR. Endogenous circulating DNA in systemic lupus erythematosus. Occurrence as multimeric complexes bound to histone. J Clin Invest. 1990 Jul 1;86(1):69–74.

98. Vlassov VV, Laktionov PP, Rykova EY. Extracellular nucleic acids. Bioessays. 2007 Jul;29(7):654–67.

99. Holdenrieder S, Stieber P. Clinical use of circulating nucleosomes. Critical Reviews in Clinical Laboratory Sciences. 2009 Jan;46(1):1–24.

100. Leist M, Single B, Castoldi AF, Kühnle S, Nicotera P. Intracellular Adenosine Triphosphate (ATP) Concentration: A Switch in the Decision Between Apoptosis and Necrosis. Journal of Experimental Medicine. 1997 Apr 21;185(8):1481–6.

101. Syntichaki P, Tavernarakis N. Death by necrosis: Uncontrollable catastrophe, or is there order behind the chaos? EMBO Rep. 2002 Jul;3(7):604–9.

102. Frank D, Vince JE. Pyroptosis versus necroptosis: similarities, differences, and crosstalk. Cell Death Differ. 2019 Jan;26(1):99–114.

103. Youle RJ, Narendra DP. Mechanisms of mitophagy. Nat Rev Mol Cell Biol. 2011 Jan;12(1):9–14.

104. Thurairajah K, Briggs GD, Balogh ZJ. The source of cell-free mitochondrial DNA in trauma and potential therapeutic strategies. Eur J Trauma Emerg Surg. 2018 Jun;44(3):325–34.

105. Al Amir Dache Z, Otandault A, Tanos R, Pastor B, Meddeb R, Sanchez C, Arena G, Lasorsa L, Bennett A, Grange T, et al. Blood contains circulating cell-free respiratory competent mitochondria. FASEB J. 2020 Jan 19;

106. Jiang N, Reich CF, Pisetsky DS. Role of macrophages in the generation of circulating blood nucleosomes from dead and dying cells. Blood. 2003 Sep 15;102(6):2243–50.

107. Choi J-J, Reich CF, Pisetsky DS. The role of macrophages in the in vitro generation of extracellular DNA from apoptotic and necrotic cells. Immunology. 2005 May;115(1):55–62.

108. Aucamp J, Bronkhorst AJ, Badenhorst CPS, Pretorius PJ. A historical and evolutionary perspective on the biological significance of circulating DNA and extracellular vesicles. Cell Mol Life Sci. 2016 Dec 1;73(23):4355–81.

109. Brinkmann V, Reichard U, Goosmann C, Fauler B, Uhlemann Y, Weiss DS, Weinrauch Y, Zychlinsky A. Neutrophil extracellular traps kill bacteria. Science. 2004 Mar 5;303(5663):1532–5.

110. Brinkmann V. Neutrophil Extracellular Traps in the Second Decade. J Innate Immun. 2018;10(5–6):414–21.

111. Jorch SK, Kubes P. An emerging role for neutrophil extracellular traps in noninfectious disease. Nat Med. 2017 Mar 7;23(3):279–87.

112. Fuchs TA, Kremer Hovinga JA, Schatzberg D, Wagner DD, Lämmle B. Circulating DNA and myeloperoxidase indicate disease activity in patients with thrombotic microangiopathies. Blood. 2012 Aug 9;120(6):1157–64.

113. Yipp BG, Kubes P. NETosis: how vital is it? Blood. 2013 Oct 17;122(16):2784–94.

114. Papayannopoulos V. Neutrophil extracellular traps in immunity and disease. Nat Rev Immunol. 2018 Feb;18(2):134–47.

115. Yousefi S, Stojkov D, Germic N, Simon D, Wang X, Benarafa C, Simon H. Untangling “NETosis” from NETs. Eur J Immunol. 2019 Feb;49(2):221–7.

116. Cools-Lartigue J, Spicer J, McDonald B, Gowing S, Chow S, Giannias B, Bourdeau F, Kubes P, Ferri L. Neutrophil extracellular traps sequester circulating tumor cells and promote metastasis. J Clin Invest. 2013 Aug 1;123(8):3446–58.

117. Luo L, Zhang S, Wang Y, Rahman M, Syk I, Zhang E, Thorlacius H. Proinflammatory role of neutrophil extracellular traps in abdominal sepsis. American Journal of Physiology-Lung Cellular and Molecular Physiology. 2014 Oct 1;307(7):L586–96.

118. Brinkmann V, Zychlinsky A. Neutrophil extracellular traps: Is immunity the second function of chromatin? Journal of Cell Biology. 2012 Sep 3;198(5):773–83.

119. Fuchs TA, Brill A, Duerschmied D, Schatzberg D, Monestier M, Myers DD, Wrobleski SK, Wakefield TW, Hartwig JH, Wagner DD. Extracellular DNA traps promote thrombosis. Proceedings of the National Academy of Sciences. 2010 Sep 7;107(36):15880–5.

120. Kaplan MJ, Radic M. Neutrophil Extracellular Traps: Double-Edged Swords of Innate Immunity. JI. 2012 Sep 15;189(6):2689–95.

121. Wartha F, Henriques-Normark B. ETosis: A Novel Cell Death Pathway. Sci Signal [Internet]. 2008 May 27 [cited 2022 Jan 21];1(21). Available from: https://www.science.org/doi/10.1126/stke.121pe25

122. Yousefi S, Simon D, Simon H-U. Eosinophil extracellular DNA traps: molecular mechanisms and potential roles in disease. Current Opinion in Immunology. 2012 Dec;24(6):736–9.

123. Yousefi S, Gold JA, Andina N, Lee JJ, Kelly AM, Kozlowski E, Schmid I, Straumann A, Reichenbach J, Gleich GJ, et al. Catapult-like release of mitochondrial DNA by eosinophils contributes to antibacterial defense. Nat Med. 2008 Sep;14(9):949–53.

124. Boe DM, Curtis BJ, Chen MM, Ippolito JA, Kovacs EJ. Extracellular traps and macrophages: new roles for the versatile phagocyte. Journal of Leukocyte Biology. 2015 Jun;97(6):1023–35.

125. Rogers JC, Boldt D, Kornfeld S, Skinner SA, Valeri CR. Excretion of Deoxyribonucleic Acid by Lymphocytes Stimulated with Phytohemagglutinin or Antigen. Proceedings of the National Academy of Sciences. 1972 Jul 1;69(7):1685–9.

126. Anker P, Stroun M, Maurice PA. Spontaneous extracellular synthesis of DNA released by human blood lymphocytes. Cancer Res. 1976 Aug;36(8):2832–9.

127. Fernando MR, Jiang C, Krzyzanowski GD, Ryan WL. New evidence that a large proportion of human blood plasma cell-free DNA is localized in exosomes. Camussi G, editor. PLoS ONE. 2017 Aug 29;12(8):e0183915.

128. van Niel G, D'Angelo G, Raposo G. Shedding light on the cell biology of extracellular vesicles. Nat Rev Mol Cell Biol. 2018 Apr;19(4):213–28.

129. Minciacchi VR, Freeman MR, Di Vizio D. Extracellular Vesicles in Cancer: Exosomes, Microvesicles and the Emerging Role of Large Oncosomes. Seminars in Cell & Developmental Biology. 2015 Apr;40:41–51.

130. Zaborowski MP, Balaj L, Breakefield XO, Lai CP. Extracellular Vesicles: Composition, Biological Relevance, and Methods of Study. BioScience. 2015 Aug 1;65(8):783–97.

131. Mouliere F, El Messaoudi S, Gongora C, Guedj A-S, Robert B, Del Rio M, Molina F, Lamy P-J, Lopez-Crapez E, Mathonnet M, et al. Circulating Cell-Free DNA from Colorectal Cancer Patients May Reveal High KRAS or BRAF Mutation Load. Transl Oncol. 2013 Jun;6(3):319–28.

132. Mouliere F, Robert B, Arnau Peyrotte E, Del Rio M, Ychou M, Molina F, Gongora C, Thierry AR. High fragmentation characterizes tumour-derived circulating DNA. PLoS ONE. 2011;6(9):e23418.

133. Jiang P, Chan CWM, Chan KCA, Cheng SH, Wong J, Wong VW-S, Wong GLH, Chan SL, Mok TSK, Chan HLY, et al. Lengthening and shortening of plasma DNA in hepatocellular carcinoma patients. PNAS. 2015 Mar 17;112(11):E1317–25.

134. Thierry AR, Mouliere F, Gongora C, Ollier J, Robert B, Ychou M, Del Rio M, Molina F. Origin and quantification of circulating DNA in mice with human colorectal cancer xenografts. Nucleic Acids Res. 2010 Oct;38(18):6159–75.

135. Mouliere F, El Messaoudi S, Pang D, Dritschilo A, Thierry AR. Multi-marker analysis of circulating cell-free DNA toward personalized medicine for colorectal cancer. Mol Oncol. 2014 Jul;8(5):927–41.

136. Underhill HR, Kitzman JO, Hellwig S, Welker NC, Daza R, Baker DN, Gligorich KM, Rostomily RC, Bronner MP, Shendure J. Fragment Length of Circulating Tumor DNA. PLoS Genetics [Internet]. 2016 Jul [cited 2017 Aug 31];12(7). Available from: https://www-ncbi-nlm-nih-gov.gate2.inist.fr/pmc/articles/PMC4948782/

137. Sanchez C, Snyder MW, Tanos R, Shendure J, Thierry AR. New insights into structural features and optimal detection of circulating tumor DNA determined by single-strand DNA analysis. NPJ Genom Med. 2018;3:31.

138. Mittra I, Khare NK, Raghuram GV, Chaubal R, Khambatti F, Gupta D, Gaikwad A, Prasannan P, Singh A, Iyer A, et al. Circulating nucleic acids damage DNA of healthy cells by integrating into their genomes. J Biosci. 2015 Mar;40(1):91–111.

139. Maas SLN, Breakefield XO, Weaver AM. Extracellular Vesicles: Unique Intercellular Delivery Vehicles. Trends in Cell Biology. 2017 Mar;27(3):172–88.

140. Yáñez-Mó M, Siljander PR-M, Andreu Z, Bedina Zavec A, Borràs FE, Buzas EI, Buzas K, Casal E, Cappello F, Carvalho J, et al. Biological properties of extracellular vesicles and their physiological functions. Journal of Extracellular Vesicles. 2015 Jan 1;4(1):27066.

141. Bendich A, Wilczok T, Borenfreund E. Circulating DNA as a Possible Factor in Oncogenesis. Science. 1965 Apr 16;148(3668):374–6.

142. Anker P, Lyautey J, Lefort F, Lederrey C, Stroun M. [Transformation of NIH/3T3 cells and SW 480 cells displaying K-ras mutation]. C R Acad Sci III. 1994 Oct;317(10):869–74.

143. García-Olmo DC, Domínguez C, García-Arranz M, Anker P, Stroun M, García-Verdugo JM, García-Olmo D. Cell-Free Nucleic Acids Circulating in the Plasma of Colorectal Cancer Patients Induce the Oncogenic Transformation of Susceptible Cultured Cells. Cancer Res. 2010 Jan 15;70(2):560–7.

144. Erpenbeck L, Schön MP. Neutrophil extracellular traps: protagonists of cancer progression? Oncogene. 2017 May;36(18):2483–90.

145. Demers M, Wong SL, Martinod K, Gallant M, Cabral JE, Wang Y, Wagner DD. Priming of neutrophils toward NETosis promotes tumor growth. OncoImmunology. 2016 May 3;5(5):e1134073.

146. Picca A, Lezza AMS, Leeuwenburgh C, Pesce V, Calvani R, Bossola M, Manes-Gravina E, Landi F, Bernabei R, Marzetti E. Circulating Mitochondrial DNA at the Crossroads of Mitochondrial Dysfunction and Inflammation During Aging and Muscle Wasting Disorders. Rejuvenation Research. 2018 Aug;21(4):350–9.

147. West AP. Mitochondrial dysfunction as a trigger of innate immune responses and inflammation. Toxicology. 2017 Nov;391:54–63.

148. Pisetsky DS. The origin and properties of extracellular DNA: From PAMP to DAMP. Clinical Immunology. 2012 Jul;144(1):32–40.

149. Napirei M, Karsunky H, Zevnik B, Stephan H, Mannherz HG, Möröy T. Features of systemic lupus erythematosus in Dnase1-deficient mice. Nat Genet. 2000 Jun;25(2):177–81.

150. Martinez-Valle F, Balada E, Ordi-Ros J, Bujan-Rivas S, Sellas-Fernandez A, Vilardell-Tarres M. DNase 1 activity in patients with systemic lupus erythematosus: relationship with epidemiological, clinical, immunological and therapeutical features. Lupus. 2009 Apr;18(5):418–23.

151. Mehrotra M, Singh RR, Chen W, Huang RSP, Almohammedsalim AA, Barkoh BA, Simien CM, Hernandez M, Behrens C, Patel KP, et al. Study of Preanalytic and Analytic Variables for Clinical Next-Generation Sequencing of Circulating Cell-Free Nucleic Acid. J Mol Diagn. 2017 Jul;19(4):514–24.

152. Wagner J. Free DNA – new potential analyte in clinical laboratory diagnostics? Biochem Med. 2012;24–38.

153. El Messaoudi S, Rolet F, Mouliere F, Thierry AR. Circulating cell free DNA: Preanalytical considerations. Clin Chim Acta. 2013 Sep 23;424:222–30.

154. Meddeb R, Dache ZAA, Thezenas S, Otandault A, Tanos R, Pastor B, Sanchez C, Azzi J, Tousch G, Azan S, et al. Quantifying circulating cell-free DNA in humans. Sci Rep. 2019 Mar 26;9(1):5220.

155. Meddeb R, Pisareva E, Thierry AR. Guidelines for the Preanalytical Conditions for Analyzing Circulating Cell-Free DNA. Clin Chem. 2019 May;65(5):623–33.

156. Wilkening S, Hemminki K, Kumar Thirumaran R, Lorenzo Bermejo J, Bonn S, Försti A, Kumar R. Determination of allele frequency in pooled DNA: comparison of three PCR-based methods. BioTechniques. 2005 Dec;39(6):853–8.

157. Santis G, Angell R, Nickless G, Quinn A, Herbert A, Cane P, Spicer J, Breen R, McLean E, Tobal K. Screening for EGFR and KRAS Mutations in Endobronchial Ultrasound Derived Transbronchial Needle Aspirates in Non-Small Cell Lung Cancer Using COLD-PCR. Königshoff M, editor. PLoS ONE. 2011 Sep 19;6(9):e25191.

158. Castellanos-Rizaldos E, Liu P, Milbury CA, Guha M, Brisci A, Cremonesi L, Ferrari M, Mamon H, Makrigiorgos GM. Temperature-Tolerant COLD-PCR Reduces Temperature Stringency and Enables Robust Mutation Enrichment. Clinical Chemistry. 2012 Jul 1;58(7):1130–8.

159. Taly -->Valerie, Huggett J. Digital PCR, a technique for the future. Biomolecular Detection and Quantification. 2016 Dec;10:1.

160. Didelot A, Kotsopoulos SK, Lupo A, Pekin D, Li X, Atochin I, Srinivasan P, Zhong Q, Olson J, Link DR, et al. Multiplex Picoliter-Droplet Digital PCR for Quantitative Assessment of DNA Integrity in Clinical Samples. Clinical Chemistry. 2013 May 1;59(5):815–23.

161. Taly V, Pekin D, Benhaim L, Kotsopoulos SK, Le Corre D, Li X, Atochin I, Link DR, Griffiths AD, Pallier K, et al. Multiplex picodroplet digital PCR to detect KRAS mutations in circulating DNA from the plasma of colorectal cancer patients. Clin Chem. 2013 Dec;59(12):1722–31.

162. Frattini M, Gallino G, Signoroni S, Balestra D, Lusa L, Battaglia L, Sozzi G, Bertario L, Leo E, Pilotti S, et al. Quantitative and qualitative characterization of plasma DNA identifies primary and recurrent colorectal cancer. Cancer Letters. 2008 May;263(2):170–81.

163. Pérez-Callejo D, Romero A, Provencio M, Torrente M. Liquid biopsy based biomarkers in non-small cell lung cancer for diagnosis and treatment monitoring. Transl Lung Cancer Res. 2016 Oct;5(5):455–65.

164. Huerta M, Roselló S, Sabater L, Ferrer A, Tarazona N, Roda D, Gambardella V, Alfaro-Cervelló C, Garcés-Albir M, Cervantes A, et al. Circulating Tumor DNA Detection by Digital-Droplet PCR in Pancreatic Ductal Adenocarcinoma: A Systematic Review. Cancers. 2021 Feb 27;13(5):994.

165. The dMIQE Group, Whale AS, De Spiegelaere W, Trypsteen W, Nour AA, Bae Y-K, Benes V, Burke D, Cleveland M, Corbisier P, et al. The Digital MIQE Guidelines Update: Minimum Information for Publication of Quantitative Digital PCR Experiments for 2020. Clinical Chemistry. 2020 Aug 1;66(8):1012–29.

166. Diehl F, Li M, He Y, Kinzler KW, Vogelstein B, Dressman D. BEAMing: single-molecule PCR on microparticles in water-in-oil emulsions. Nat Methods. 2006 Jul;3(7):551–9.

167. Li M, Diehl F, Dressman D, Vogelstein B, Kinzler KW. BEAMing up for detection and quantification of rare sequence variants. Nature Methods. 2006 Feb;3(2):95–7.

168. Caen O, Nizard P, Garrigou S, Perez-Toralla K, Zonta E, Laurent-Puig P, Taly V. PCR digitale en micro-compartiments: II. Apport pour la détection quantitative d'ADN tumoral circulant. Med Sci (Paris). 2015 Feb;31(2):180–6.

169. Baer C, Kern W, Koch S, Nadarajah N, Schindela S, Meggendorfer M, Haferlach C, Haferlach T. Ultra-deep sequencing leads to earlier and more sensitive detection of the tyrosine kinase inhibitor resistance mutation T315I in chronic myeloid leukemia. Haematologica. 2016 Jul 1;101(7):830–8.

170. Gale D, Lawson ARJ, Howarth K, Madi M, Durham B, Smalley S, Calaway J, Blais S, Jones G, Clark J, et al. Development of a highly sensitive liquid biopsy platform to detect clinically-relevant cancer mutations at low allele fractions in cell-free DNA. Galli A, editor. PLoS ONE. 2018 Mar 16;13(3):e0194630.

171. Kinde I, Wu J, Papadopoulos N, Kinzler KW, Vogelstein B. Detection and quantification of rare mutations with massively parallel sequencing. Proceedings of the National Academy of Sciences. 2011 Jun 7;108(23):9530–5.

172. Oliveira KCS, Ramos IB, Silva JMC, Barra WF, Riggins GJ, Palande V, Pinho CT, Frenkel-Morgenstern M, Santos SEB, Assumpcao PP, et al. Current Perspectives on Circulating Tumor DNA, Precision Medicine, and Personalized Clinical Management of Cancer. Mol Cancer Res. 2020 Apr;18(4):517–28.

173. Thierry AR, Pastor B, Jiang Z-Q, Katsiampoura AD, Parseghian C, Loree JM, Overman MJ, Sanchez C, Messaoudi SE, Ychou M, et al. Circulating DNA Demonstrates Convergent Evolution and Common Resistance Mechanisms during Treatment of Colorectal Cancer. Clin Cancer Res. 2017 Aug 15;23(16):4578–91.

174. Moati E, Taly V, Garinet S, Didelot A, Taieb J, Laurent-Puig P, Zaanan A. Role of Circulating Tumor DNA in Gastrointestinal Cancers: Current Knowledge and Perspectives. Cancers. 2021 Sep 22;13(19):4743.

175. Otandault A, Anker P, Al Amir Dache Z, Guillaumon V, Meddeb R, Pastor B, Pisareva E, Sanchez C, Tanos R, Tousch G, et al. Recent advances in circulating nucleic acids in oncology. Ann Oncol. 2019 01;30(3):374–84.

176. Heitzer E, Ulz P, Geigl JB. Circulating Tumor DNA as a Liquid Biopsy for Cancer. Clinical Chemistry. 2015 Jan 1;61(1):112–23.

177. Lamb YN, Dhillon S. Epi proColon® 2.0 CE: A Blood-Based Screening Test for Colorectal Cancer. Mol Diagn Ther. 2017 Apr;21(2):225–32.

178. Shirley M. Epi proColon® for Colorectal Cancer Screening: A Profile of Its Use in the USA. Mol Diagn Ther. 2020 Aug;24(4):497–503.

179. Chen X, Gole J, Gore A, He Q, Lu M, Min J, Yuan Z, Yang X, Jiang Y, Zhang T, et al. Non-invasive early detection of cancer four years before conventional diagnosis using a blood test. Nat Commun. 2020 Dec;11(1):3475.

180. Tanos R, Thierry AR. Clinical relevance of liquid biopsy for cancer screening. Translational Cancer Research. 2018 Mar 19;7(2):S105–29.

181. Tanos R, Tosato G, Otandault A, Al Amir Dache Z, Pique Lasorsa L, Tousch G, El Messaoudi S, Meddeb R, Diab Assaf M, Ychou M, et al. Machine Learning-Assisted Evaluation of Circulating DNA Quantitative Analysis for Cancer Screening. Adv Sci (Weinh). 2020 Sep;7(18):2000486.

182. Bettegowda C, Sausen M, Leary RJ, Kinde I, Wang Y, Agrawal N, Bartlett BR, Wang H, Luber B, Alani RM, et al. Detection of circulating tumor DNA in early- and late-stage human malignancies. Sci Transl Med. 2014 Feb 19;6(224):224ra24.

183. Nygaard AD, Holdgaard PC, Spindler K-LG, Pallisgaard N, Jakobsen A. The correlation between cell-free DNA and tumour burden was estimated by PET/CT in patients with advanced NSCLC. Br J Cancer. 2014 Jan;110(2):363–8.

184. El Messaoudi S, Mouliere F, Du Manoir S, Bascoul-Mollevi C, Gillet B, Nouaille M, Fiess C, Crapez E, Bibeau F, Theillet C, et al. Circulating DNA as a Strong Multimarker Prognostic Tool for Metastatic Colorectal Cancer Patient Management Care. Clin Cancer Res. 2016 Jun 15;22(12):3067–77.

185. Sirera R, Bremnes RM, Cabrera A, Jantus-Lewintre E, Sanmartín E, Blasco A, del Pozo N, Rosell R, Guijarro R, Galbis J, et al. Circulating DNA is a Useful Prognostic Factor in Patients with Advanced Non-small Cell Lung Cancer. Journal of Thoracic Oncology. 2011 Feb;6(2):286–90.

186. Sunami E, Shinozaki M, Higano CS, Wollman R, Dorff TB, Tucker SJ, Martinez SR, Singer FR, Hoon DSB. Multimarker Circulating DNA Assay for Assessing Blood of Prostate Cancer Patients. Clinical Chemistry. 2009 Mar 1;55(3):559–67.

187. Lecomte T, Berger A, Zinzindohoué F, Micard S, Landi B, Blons H, Beaune P, Cugnenc P-H, Laurent-Puig P. Detection of free-circulating tumor-associated DNA in plasma of colorectal cancer patients and its association with prognosis: Plasma DNA in Colorectal Cancer Patients. Int J Cancer. 2002 Aug 10;100(5):542–8.

188. Siegel RL, Miller KD, Goding Sauer A, Fedewa SA, Butterly LF, Anderson JC, Cercek A, Smith RA, Jemal A. Colorectal cancer statistics, 2020. CA A Cancer J Clin. 2020 May;70(3):145–64.

189. André T, de Gramont A, Vernerey D, Chibaudel B, Bonnetain F, Tijeras-Raballand A, Scriva A, Hickish T, Tabernero J, Van Laethem JL, et al. Adjuvant Fluorouracil, Leucovorin, and Oxaliplatin in Stage II to III Colon Cancer: Updated 10-Year Survival and Outcomes According to *BRAF* Mutation and Mismatch Repair Status of the MOSAIC Study. JCO. 2015 Dec 10;33(35):4176–87.

190. Tie J, Cohen JD, Wang Y, Li L, Christie M, Simons K, Elsaleh H, Kosmider S, Wong R, Yip D, et al. Serial circulating tumour DNA analysis during multimodality treatment of locally advanced rectal cancer: a prospective biomarker study. Gut. 2018 Feb 2;

191. Taieb J, Taly V, Henriques J, Bourreau C, Mineur L, Bennouna J, Desrame J, Louvet C, Lepere C, Mabro M, et al. Prognostic Value and Relation with Adjuvant Treatment Duration of ctDNA in Stage III Colon Cancer: a *Post Hoc* Analysis of the PRODIGE-GERCOR IDEA-France Trial. Clin Cancer Res. 2021 Oct 15;27(20):5638–46.

192. Tie J, Wang Y, Tomasetti C, Li L, Springer S, Kinde I, Silliman N, Tacey M, Wong H-L, Christie M, et al. Circulating tumor DNA analysis detects minimal residual disease and predicts recurrence

in patients with stage II colon cancer. Sci Transl Med [Internet]. 2016 Jul 6 [cited 2022 Jan 21];8(346). Available from: https://www.science.org/doi/10.1126/scitranslmed.aaf6219

193. Reinert T, Henriksen TV, Christensen E, Sharma S, Salari R, Sethi H, Knudsen M, Nordentoft I, Wu H-T, Tin AS, et al. Analysis of Plasma Cell-Free DNA by Ultradeep Sequencing in Patients With Stages I to III Colorectal Cancer. JAMA Oncol. 2019 Aug 1;5(8):1124.

194. Belic J, Graf R, Bauernhofer T, Cherkas Y, Ulz P, Waldispuehl-Geigl J, Perakis S, Gormley M, Patel J, Li W, et al. Genomic alterations in plasma DNA from patients with metastasized prostate cancer receiving abiraterone or enzalutamide: Prostate cancer and plasma DNA analyses. Int J Cancer. 2018 Sep 1;143(5):1236–48.

195. Tanaka K, Nosaki K, Otsubo K, Azuma K, Sakata S, Ouchi H, Morinaga R, Wataya H, Fujii A, Nakagaki N, et al. Acquisition of the T790M resistance mutation during afatinib treatment in EGFR tyrosine kinase inhibitor-naïve patients with non–small cell lung cancer harboring *EGFR* mutations. Oncotarget. 2017 Sep 15;8(40):68123–30.

196. Chandarlapaty S, Chen D, He W, Sung P, Samoila A, You D, Bhatt T, Patel P, Voi M, Gnant M, et al. Prevalence of *ESR1* Mutations in Cell-Free DNA and Outcomes in Metastatic Breast Cancer: A Secondary Analysis of the BOLERO-2 Clinical Trial. JAMA Oncol. 2016 Oct 1;2(10):1310.

197. Kulkarni A, Al-Hraishawi H, Simhadri S, Hirshfield KM, Chen S, Pine S, Jeyamohan C, Sokol L, Ali S, Teo ML, et al. *BRAF* Fusion as a Novel Mechanism of Acquired Resistance to Vemurafenib in *BRAF* ^{V600E} Mutant Melanoma. Clin Cancer Res. 2017 Sep 15;23(18):5631–8.

198. Siravegna G, Mussolin B, Buscarino M, Corti G, Cassingena A, Crisafulli G, Ponzetti A, Cremolini C, Amatu A, Lauricella C, et al. Clonal evolution and resistance to EGFR blockade in the blood of colorectal cancer patients. Nat Med. 2015 Jul;21(7):827.

199. Cremolini C, Rossini D, Dell'Aquila E, Lonardi S, Conca E, Del Re M, Busico A, Pietrantonio F, Danesi R, Aprile G, et al. Rechallenge for Patients With *RAS* and *BRAF* Wild-Type Metastatic Colorectal Cancer With Acquired Resistance to First-line Cetuximab and Irinotecan: A Phase 2 Single-Arm Clinical Trial. JAMA Oncol. 2019 Mar 1;5(3):343.

200. Nakajima H, Kotani D, Bando H, Kato T, Oki E, Shinozaki E, Sunakawa Y, Yamazaki K, Yuki S, Nakamura Y, et al. REMARRY and PURSUIT trials: liquid biopsy-guided rechallenge with anti-epidermal growth factor receptor (EGFR) therapy with panitumumab plus irinotecan for patients with plasma RAS wild-type metastatic colorectal cancer. BMC Cancer. 2021 Dec;21(1):674.

201. Parseghian CM, Napolitano S, Loree JM, Kopetz S. Mechanisms of Innate and Acquired Resistance to Anti-EGFR Therapy: A Review of Current Knowledge with a Focus on Rechallenge Therapies. Clin Cancer Res. 2019 Dec 1;25(23):6899–908.

202. Van Cutsem E, Cervantes A, Adam R, Sobrero A, Van Krieken JH, Aderka D, Aranda Aguilar E, Bardelli A, Benson A, Bodoky G, et al. ESMO consensus guidelines for the management of patients with metastatic colorectal cancer. Ann Oncol. 2016;27(8):1386–422.

203. Allegra CJ, Rumble RB, Hamilton SR, Mangu PB, Roach N, Hantel A, Schilsky RL. Extended RAS Gene Mutation Testing in Metastatic Colorectal Carcinoma to Predict Response to Anti-Epidermal Growth Factor Receptor Monoclonal Antibody Therapy: American Society of Clinical Oncology Provisional Clinical Opinion Update 2015. J Clin Oncol. 2016 Jan 10;34(2):179–85.

204. De Roock W, Claes B, Bernasconi D, De Schutter J, Biesmans B, Fountzilas G, Kalogeras KT, Kotoula V, Papamichael D, Laurent-Puig P, et al. Effects of KRAS, BRAF, NRAS, and PIK3CA mutations on the efficacy of cetuximab plus chemotherapy in chemotherapy-refractory metastatic colorectal cancer: a retrospective consortium analysis. Lancet Oncol. 2010 Aug;11(8):753–62.

205. Amado RG, Wolf M, Peeters M, Van Cutsem E, Siena S, Freeman DJ, Juan T, Sikorski R, Suggs S, Radinsky R, et al. Wild-type KRAS is required for panitumumab efficacy in patients with metastatic colorectal cancer. J Clin Oncol. 2008 Apr 1;26(10):1626–34.

206. Van Cutsem E, Lenz H-J, Köhne C-H, Heinemann V, Tejpar S, Melezínek I, Beier F, Stroh C, Rougier P, van Krieken JH, et al. Fluorouracil, leucovorin, and irinotecan plus cetuximab treatment and RAS mutations in colorectal cancer. J Clin Oncol. 2015 Mar 1;33(7):692–700.

207. Waring P, Tie J, Maru D, Karapetis CS. RAS Mutations as Predictive Biomarkers in Clinical Management of Metastatic Colorectal Cancer. Clin Colorectal Cancer. 2016 Jun;15(2):95–103.

208. Schwarzenbach H, Hoon DSB, Pantel K. Cell-free nucleic acids as biomarkers in cancer patients. Nat Rev Cancer. 2011 Jun;11(6):426–37.

209. Diaz LA, Bardelli A. Liquid biopsies: genotyping circulating tumor DNA. J Clin Oncol. 2014 Feb 20;32(6):579–86.

210. Murtaza M, Dawson S-J, Tsui DWY, Gale D, Forshew T, Piskorz AM, Parkinson C, Chin S-F, Kingsbury Z, Wong ASC, et al. Non-invasive analysis of acquired resistance to cancer therapy by sequencing of plasma DNA. Nature. 2013 May 2;497(7447):108–12.

211. Diehl F, Schmidt K, Choti MA, Romans K, Goodman S, Li M, Thornton K, Agrawal N, Sokoll L, Szabo SA, et al. Circulating mutant DNA to assess tumor dynamics. Nat Med. 2008 Sep;14(9):985–90.

212. Perkins G, Yap TA, Pope L, Cassidy AM, Dukes JP, Riisnaes R, Massard C, Cassier PA, Miranda S, Clark J, et al. Multi-purpose utility of circulating plasma DNA testing in patients with advanced cancers. PLoS ONE. 2012;7(11):e47020.

213. Fu Y, Jovelet C, Filleron T, Pedrero M, Motté N, Boursin Y, Luo Y, Massard C, Campone M, Levy C, et al. Improving the Performance of Somatic Mutation Identification by Recovering Circulating Tumor DNA Mutations. Cancer Res. 2016 Oct 15;76(20):5954–61.

214. Sorich MJ, Wiese MD, Rowland A, Kichenadasse G, McKinnon RA, Karapetis CS. Extended RAS mutations and anti-EGFR monoclonal antibody survival benefit in metastatic colorectal cancer: a meta-analysis of randomized, controlled trials. Ann Oncol. 2015 Jan;26(1):13–21.

215. Fakih M. Biologic therapies in colorectal cancer: indications and contraindications. Am Soc Clin Oncol Educ Book. 2015;e197-206.

216. Li Z-Z, Wang F, Zhang Z-C, Wang F, Zhao Q, Zhang D-S, Wang F-H, Wang Z-Q, Luo H-Y, He M-M, et al. Mutation profiling in chinese patients with metastatic colorectal cancer and its correlation with clinicopathological features and anti-EGFR treatment response. Oncotarget. 2016 May 10;7(19):28356–68.

217. Garcia-Murillas I, Schiavon G, Weigelt B, Ng C, Hrebien S, Cutts RJ, Cheang M, Osin P, Nerurkar A, Kozarewa I, et al. Mutation tracking in circulating tumor DNA predicts relapse in early breast cancer. Sci Transl Med. 2015 Aug 26;7(302):302ra133.

218. Kim M-J, Lee HS, Kim JH, Kim YJ, Kwon JH, Lee J-O, Bang S-M, Park KU, Kim D-W, Kang S-B, et al. Different metastatic pattern according to the KRAS mutational status and site-specific discordance of KRAS status in patients with colorectal cancer. BMC Cancer. 2012 Aug 9;12:347.

219. Newman AM, Bratman SV, To J, Wynne JF, Eclov NCW, Modlin LA, Liu CL, Neal JW, Wakelee HA, Merritt RE, et al. An ultrasensitive method for quantitating circulating tumor DNA with broad patient coverage. Nat Med. 2014 May;20(5):548–54.

220. Knijn N, Mekenkamp LJM, Klomp M, Vink-Börger ME, Tol J, Teerenstra S, Meijer JWR, Tebar M, Riemersma S, van Krieken JHJM, et al. KRAS mutation analysis: a comparison between primary tumours and matched liver metastases in 305 colorectal cancer patients. Br J Cancer. 2011 Mar;104(6):1020–6.

221. Oltedal S, Aasprong OG, Møller JH, Kørner H, Gilje B, Tjensvoll K, Birkemeyer EM, Heikkilä R, Smaaland R, Nordgård O. Heterogeneous distribution of K-ras mutations in primary colon carcinomas: implications for EGFR-directed therapy. Int J Colorectal Dis. 2011 Oct;26(10):1271–7.

222. Kuo Y-B, Chen J-S, Fan C-W, Li Y-S, Chan E-C. Comparison of KRAS mutation analysis of primary tumors and matched circulating cell-free DNA in plasmas of patients with colorectal cancer. Clin Chim Acta. 2014 Jun 10;433:284–9.

223. Lee KH, Kim JS, Lee CS, Kim JY. KRAS discordance between primary and recurrent tumors after radical resection of colorectal cancers: KRAS Discordance of Colorectal Cancers. J Surg Oncol. 2015 Jun;111(8):1059–64.

224. Cejas P, Lopez-Gomez M, Aguayo C, Madero R, Moreno-Rubio J, de Castro Carpeno J, Belda-Iniesta C, Barriuso J, Moreno Garcia V, Diaz E, et al. Analysis of the Concordance in the EGFR Pathway Status Between Primary Tumors and Related Metastases of Colorectal Cancer Patients:Implications for Cancer Therapy. CCDT. 2012 Feb 1;12(2):124–31.

225. de Macedo MP, de Melo FM, da Silva Ribeiro J, Lopes de Mello CA, de Souza Begnami MDF, Soares FA, Carraro DM, da Cunha IW. RAS mutations vary between lesions in synchronous primary Colorectal Cancer: Testing only one lesion is not sufficient to guide anti-EGFR treatment decisions. Oncoscience. 2015 Feb 9;2(2):125–30.

226. Laurent-Puig P, Pekin D, Normand C, Kotsopoulos SK, Nizard P, Perez-Toralla K, Rowell R, Olson J, Srinivasan P, Le Corre D, et al. Clinical relevance of KRAS-mutated subclones detected with picodroplet digital PCR in advanced colorectal cancer treated with anti-EGFR therapy. Clin Cancer Res. 2015 Mar 1;21(5):1087–97.

227. Tougeron D, Lecomte T, Pagès JC, Villalva C, Collin C, Ferru A, Tourani JM, Silvain C, Levillain P, Karayan-Tapon L. Effect of low-frequency KRAS mutations on the response to anti-EGFR therapy in metastatic colorectal cancer. Ann Oncol. 2013 May;24(5):1267–73.

228. Bertotti A, Papp E, Jones S, Adleff V, Anagnostou V, Lupo B, Sausen M, Phallen J, Hruban CA, Tokheim C, et al. The genomic landscape of response to EGFR blockade in colorectal cancer. Nature. 2015 Oct 8;526(7572):263–7.

229. Assenat E, Desseigne F, Thezenas S, Viret F, Mineur L, Kramar A, Samalin E, Portales F, Bibeau F, Crapez-Lopez E, et al. Cetuximab plus FOLFIRINOX (ERBIRINOX) as first-line treatment for unresectable metastatic colorectal cancer: a phase II trial. Oncologist. 2011;16(11):1557–64.

230. Fornaro L, Lonardi S, Masi G, Loupakis F, Bergamo F, Salvatore L, Cremolini C, Schirripa M, Vivaldi C, Aprile G, et al. FOLFOXIRI in combination with panitumumab as first-line treatment in quadruple wild-type (KRAS, NRAS, HRAS, BRAF) metastatic colorectal cancer patients: a phase II trial by the Gruppo Oncologico Nord Ovest (GONO). Annals of Oncology. 2013 Aug;24(8):2062–7.

231. Cremolini C, Antoniotti C, Lonardi S, Aprile G, Bergamo F, Masi G, Grande R, Tonini G, Mescoli C, Cardellino GG, et al. Activity and Safety of Cetuximab Plus Modified FOLFOXIRI Followed by Maintenance With Cetuximab or Bevacizumab for *RAS* and *BRAF* Wild-type Metastatic Colorectal Cancer: A Randomized Phase 2 Clinical Trial. JAMA Oncol. 2018 Apr 1;4(4):529.

232. Bekaii-Saab TS, Ou F-S, Ahn DH, Boland PM, Ciombor KK, Heying EN, Dockter TJ, Jacobs NL, Pasche BC, Cleary JM, et al. Regorafenib dose-optimisation in patients with refractory metastatic colorectal cancer (ReDOS): a randomised, multicentre, open-label, phase 2 study. The Lancet Oncology. 2019 Aug;20(8):1070–82.

233. Tabernero J, Lenz H-J, Siena S, Sobrero A, Falcone A, Ychou M, Humblet Y, Bouché O, Mineur L, Barone C, et al. Analysis of circulating DNA and protein biomarkers to predict the clinical activity of regorafenib and assess prognosis in patients with metastatic colorectal cancer: a retrospective, exploratory analysis of the CORRECT trial. Lancet Oncol. 2015 Aug;16(8):937–48.

234. Adenis A, de la Fouchardiere C, Paule B, Burtin P, Tougeron D, Wallet J, Dourthe L-M, Etienne P-L, Mineur L, Clisant S, et al. Survival, safety, and prognostic factors for outcome with Regorafenib in patients with metastatic colorectal cancer refractory to standard therapies: results from a multicenter study (REBECCA) nested within a compassionate use program. BMC Cancer. 2016 07;16:412.

235. Vitiello PP, De Falco V, Giunta EF, Ciardiello D, Cardone C, Vitale P, Zanaletti N, Borrelli C, Poliero L, Terminiello M, et al. Clinical Practice Use of Liquid Biopsy to Identify RAS/BRAF Mutations in Patients with Metastatic Colorectal Cancer (mCRC): A Single Institution Experience. Cancers (Basel). 2019 Oct 8;11(10).

236. Yao J, Zang W, Ge Y, Weygant N, Yu P, Li L, Rao G, Jiang Z, Yan R, He L, et al. RAS/BRAF Circulating Tumor DNA Mutations as a Predictor of Response to First-Line Chemotherapy in Metastatic Colorectal Cancer Patients. Can J Gastroenterol Hepatol. 2018;2018:4248971.

237. van Helden EJ, Angus L, Menke-van der Houven van Oordt CW, Heideman DAM, Boon E, van Es SC, Radema SA, van Herpen CML, de Groot DJA, de Vries EGE, et al. RAS and BRAF mutations in cell-free DNA are predictive for outcome of cetuximab monotherapy in patients with tissue-tested RAS wild-type advanced colorectal cancer. Mol Oncol. 2019;13(11):2361–74.

238. Danese E, Minicozzi AM, Benati M, Montagnana M, Paviati E, Salvagno GL, Lima-Oliveira G, Gusella M, Pasini F, Lippi G, et al. Comparison of genetic and epigenetic alterations of primary tumors and matched plasma samples in patients with colorectal cancer. PLoS ONE. 2015;10(5):e0126417.

239. Gao J, Wang H, Zang W, Li B, Rao G, Li L, Yu Y, Li Z, Dong B, Lu Z, et al. Circulating tumor DNA functions as an alternative for tissue to overcome tumor heterogeneity in advanced gastric cancer. Cancer Sci. 2017 Sep;108(9):1881–7.

240. Lucidarme O, Wagner M, Gillard P, Kim S, Bachet J-B, Rousseau B, Mazard T, Louvet C, Chibaudel B, Cohen R, et al. RECIST and CHOI criteria in the evaluation of tumor response in patients with metastatic colorectal cancer treated with regorafenib, a prospective multicenter study. Cancer Imaging. 2019 Dec 9;19(1):85.

241. Falcone A, Ricci S, Brunetti I, Pfanner E, Allegrini G, Barbara C, Crinò L, Benedetti G, Evangelista W, Fanchini L, et al. Phase III Trial of Infusional Fluorouracil, Leucovorin, Oxaliplatin, and Irinotecan (FOLFOXIRI) Compared With Infusional Fluorouracil, Leucovorin, and Irinotecan (FOLFIRI) As First-Line Treatment for Metastatic Colorectal Cancer: The Gruppo Oncologico Nord Ovest. JCO. 2007 May 1;25(13):1670–6.

242. Ychou M, Rivoire M, Thezenas S, Quenet F, Delpero J-R, Rebischung C, Letoublon C, Guimbaud R, Francois E, Ducreux M, et al. A Randomized Phase II Trial of Three Intensified Chemotherapy Regimens in First-Line Treatment of Colorectal Cancer Patients with Initially Unresectable or Not Optimally Resectable Liver Metastases. The METHEP Trial. Ann Surg Oncol. 2013 Dec;20(13):4289–97.

243. Modest DP, Heinemann V, Folprecht G, Denecke T, Pratschke J, Lang H, Bemelmans M, Becker T, Rentsch M, Seehofer D, et al. Factors That Influence Conversion to Resectability and Survival After Resection of Metastases in RAS WT Metastatic Colorectal Cancer (mCRC): Analysis of FIRE-3- AIOKRK0306. Ann Surg Oncol. 2020 Jul;27(7):2389–401.

244. Loupakis F, Cremolini C, Masi G, Lonardi S, Zagonel V, Salvatore L, Cortesi E, Tomasello G, Ronzoni M, Spadi R, et al. Initial Therapy with FOLFOXIRI and Bevacizumab for Metastatic Colorectal Cancer. N Engl J Med. 2014 Oct 23;371(17):1609–18.

245. Cremolini C, Loupakis F, Antoniotti C, Lupi C, Sensi E, Lonardi S, Mezi S, Tomasello G, Ronzoni M, Zaniboni A, et al. FOLFOXIRI plus bevacizumab versus FOLFIRI plus bevacizumab as first-line treatment of patients with metastatic colorectal cancer: updated overall survival and molecular subgroup analyses of the open-label, phase 3 TRIBE study. The Lancet Oncology. 2015 Oct;16(13):1306–15.

246. Schultheis B, Folprecht G, Kuhlmann J, Ehrenberg R, Hacker UT, Köhne CH, Kornacker M, Boix O, Lettieri J, Krauss J, et al. Regorafenib in combination with FOLFOX or FOLFIRI as first- or second-line treatment of colorectal cancer: results of a multicenter, phase Ib study. Annals of Oncology. 2013 Jun;24(6):1560–7.

247. Sanoff HK, Goldberg RM, Ivanova A, O'Reilly S, Kasbari SS, Kim RD, McDermott R, Moore DT, Zamboni W, Grogan W, et al. Multicenter, randomized, double-blind phase 2 trial of FOLFIRI with regorafenib or placebo as second-line therapy for metastatic colorectal cancer. Cancer. 2018 Aug;124(15):3118–26.

248. Vandeputte C, Kehagias P, El Housni H, Ameye L, Laes J-F, Desmedt C, Sotiriou C, Deleporte A, Puleo F, Geboes K, et al. Circulating tumor DNA in early response assessment and monitoring of advanced colorectal cancer treated with a multi-kinase inhibitor. Oncotarget. 2018 Apr 3;9(25):17756–69.

249. Amatu A, Schirripa M, Tosi F, Lonardi S, Bencardino K, Bonazzina E, Palmeri L, Patanè DA, Pizzutilo EG, Mussolin B, et al. High Circulating Methylated DNA Is a Negative Predictive and

Prognostic Marker in Metastatic Colorectal Cancer Patients Treated With Regorafenib. Front Oncol. 2019;9:622.

250. Adenis A, Mazard T, Fraisse J, Chalbos P, Pastor B, Evesque L, Ghiringhelli F, Mollevi C, Delaine S, Ychou M. FOLFIRINOX-R study design: a phase I/II trial of FOLFIRINOX plus regorafenib as first line therapy in patients with unresectable RAS-mutated metastatic colorectal cancer. BMC Cancer. 2021 Dec;21(1):564.

251. Rostami A, Lambie M, Yu CW, Stambolic V, Waldron JN, Bratman SV. Senescence, Necrosis, and Apoptosis Govern Circulating Cell-free DNA Release Kinetics. Cell Reports. 2020 Jun;31(13):107830.

252. Metzler KD, Goosmann C, Lubojemska A, Zychlinsky A, Papayannopoulos V. A Myeloperoxidase-Containing Complex Regulates Neutrophil Elastase Release and Actin Dynamics during NETosis. Cell Reports. 2014 Aug;8(3):883–96.

253. Wolach O, Sellar RS, Martinod K, Cherpokova D, McConkey M, Chappell RJ, Silver AJ, Adams D, Castellano CA, Schneider RK, et al. Increased neutrophil extracellular trap formation promotes thrombosis in myeloproliferative neoplasms. Sci Transl Med. 2018 Apr 11;10(436):eaan8292.

254. Abdel-Wahab N, Tayar JH, Fa'ak F, Sharma G, Lopez-Olivo MA, Yousif A, Shagroni T, Al-Hawamdeh S, Rojas-Hernandez CM, Suarez-Almazor ME. Systematic review of observational studies reporting antiphospholipid antibodies in patients with solid tumors. Blood Advances. 2020 Apr 28;4(8):1746–55.

255. Leal Rato M, Bandeira M, Romão VC, Aguiar de Sousa D. Neurologic Manifestations of the Antiphospholipid Syndrome — an Update. Curr Neurol Neurosci Rep. 2021 Aug;21(8):41.

256. Gómez-Puerta JA, Cervera R, Espinosa G, Aguiló S, Bucciarelli S, Ramos-Casals M, Ingelmo M, Asherson RA, Font J. Antiphospholipid Antibodies Associated with Malignancies: Clinical and Pathological Characteristics of 120 Patients. Seminars in Arthritis and Rheumatism. 2006 Apr;35(5):322–32.

257. Islam MdA. Antiphospholipid antibodies and antiphospholipid syndrome in cancer: Uninvited guests in troubled times. Seminars in Cancer Biology. 2020 Aug;64:108–13.

258. Vagner T, Spinelli C, Minciacchi VR, Balaj L, Zandian M, Conley A, Zijlstra A, Freeman MR, Demichelis F, De S, et al. Large extracellular vesicles carry most of the tumour DNA circulating in prostate cancer patient plasma. Journal of Extracellular Vesicles. 2018 Dec;7(1):1505403.

259. Thakur BK, Zhang H, Becker A, Matei I, Huang Y, Costa-Silva B, Zheng Y, Hoshino A, Brazier H, Xiang J, et al. Double-stranded DNA in exosomes: a novel biomarker in cancer detection. Cell Res. 2014 Jun;24(6):766–9.

260. Al-Khafaji AB, Tohme S, Yazdani HO, Miller D, Huang H, Tsung A. Superoxide induces Neutrophil Extracellular Trap Formation in a TLR-4 and NOX-Dependent Mechanism. Mol Med. 2016 Jan;22(1):621–31.

261. Bhangu JS, Taghizadeh H, Braunschmid T, Bachleitner-Hofmann T, Mannhalter C. Circulating cell-free DNA in plasma of colorectal cancer patients - A potential biomarker for tumor burden. Surgical Oncology. 2017 Dec;26(4):395–401.

262. Wang X, Wang L, Su Y, Yue Z, Xing T, Zhao W, Zhao Q, Duan C, Huang C, Zhang D, et al. Plasma cell-free DNA quantification is highly correlated to tumor burden in children with neuroblastoma. Cancer Med. 2018 Jul;7(7):3022–30.

263. Wei T, Zhang Q, Li X, Su W, Li G, Ma T, Gao S, Lou J, Que R, Zheng L, et al. Monitoring Tumor Burden in Response to FOLFIRINOX Chemotherapy Via Profiling Circulating Cell-Free DNA in Pancreatic Cancer. Mol Cancer Ther. 2019 Jan;18(1):196–203.

264. Xu X, Yu Y, Shen M, Liu M, Wu S, Liang L, Huang F, Zhang C, Guo W, Liu T. Role of circulating free DNA in evaluating clinical tumor burden and predicting survival in Chinese metastatic colorectal cancer patients. BMC Cancer. 2020 Dec;20(1):1006.

265. Syrigos KN, Charalampopoulos A, Konstantoulakis MM, Karayiannakis A, Tsibloulis V, Peveretos P. Autoantibodies against Cardiolipin in the Serum of Patients with Colorectal Adenocarcinoma:Their Prognostic Significance. Eur Surg Res. 1998;30(1):55–60.

266. Wichmann D, Sperhake J-P, Lütgehetmann M, Steurer S, Edler C, Heinemann A, Heinrich F, Mushumba H, Kniep I, Schröder AS, et al. Autopsy Findings and Venous Thromboembolism in Patients With COVID-19: A Prospective Cohort Study. Annals of Internal Medicine. 2020 Aug 18;173(4):268–77.

267. Tambralli A, Gockman K, Knight JS. NETs in APS: Current Knowledge and Future Perspectives. Curr Rheumatol Rep. 2020 Oct;22(10):67.

268. Thierry AR, Roch B. Neutrophil Extracellular Traps and By-Products Play a Key Role in COVID-19: Pathogenesis, Risk Factors, and Therapy. JCM. 2020 Sep 11;9(9):2942.

269. Strickler JH, Loree JM, Ahronian LG, Parikh AR, Niedzwiecki D, Pereira AAL, McKinney M, Korn WM, Atreya CE, Banks KC, et al. Genomic Landscape of Cell-Free DNA in Patients with Colorectal Cancer. Cancer Discov. 2018 Feb;8(2):164–73.

270. Chen M, Zhao H. Next-generation sequencing in liquid biopsy: cancer screening and early detection. Hum Genomics. 2019 Dec;13(1):34.

271. Lai E, Pretta A, Impera V, Mariani S, Giampieri R, Casula L, Pusceddu V, Coni P, Fanni D, Puzzoni M, et al. BRAF-mutant colorectal cancer, a different breed evolving. Expert Review of Molecular Diagnostics. 2018 Jun 3;18(6):499–512.

272. Cortiula F, Pasello G, Follador A, Nardo G, Polo V, Scquizzato E, Del Conte A, Miorin M, Giovanis P, D'Urso A, et al. A Multi-Center, Real-Life Experience on Liquid Biopsy Practice for EGFR Testing in Non-Small Cell Lung Cancer (NSCLC) Patients. Diagnostics. 2020 Sep 28;10(10):765.

273. Ulz P, Auer M, Heitzer E. Detection of Circulating Tumor DNA in the Blood of Cancer Patients: An Important Tool in Cancer Chemoprevention. Methods Mol Biol. 2016;1379:45–68.

274. Van Emburgh BO, Arena S, Siravegna G, Lazzari L, Crisafulli G, Corti G, Mussolin B, Baldi F, Buscarino M, Bartolini A, et al. Acquired RAS or EGFR mutations and duration of response to EGFR blockade in colorectal cancer. Nat Commun. 2016 Dec 8;7:13665.

275. Pastor B, André T, Henriques J, Trouilloud I, Tournigand C, Jary M, Mazard T, Louvet C, Azan S, Bauer A, et al. Monitoring levels of circulating cell-free DNA in patients with metastatic

colorectal cancer as a potential biomarker of responses to regorafenib treatment. Mol Oncol. 2021 Sep;15(9):2401–11.

276. Jensen LH, Olesen R, Petersen LN, Boysen AK, Andersen RF, Lindebjerg J, Nottelmann L, Thomsen CEB, Havelund BM, Jakobsen A, et al. NPY Gene Methylation as a Universal, Longitudinal Plasma Marker for Evaluating the Clinical Benefit from Last-Line Treatment with Regorafenib in Metastatic Colorectal Cancer. Cancers (Basel) [Internet]. 2019 Oct 25 [cited 2020 Dec 14];11(11). Available from: https://www.ncbi.nlm.nih.gov/pmc/articles/PMC6896074/

277. Thierry AR, Pastor B, Pisareva E, Ghiringhelli F, Bouché O, De La Fouchardière C, Vanbockstael J, Smith D, François E, Dos Santos M, et al. Association of COVID-19 Lockdown With the Tumor Burden in Patients With Newly Diagnosed Metastatic Colorectal Cancer. JAMA Netw Open. 2021 Sep 8;4(9):e2124483.

278. Wong ALA, Lim JSJ, Sinha A, Gopinathan A, Lim R, Tan C-S, Soh T, Venkatesh S, Titin C, Sapari NS, et al. Tumour pharmacodynamics and circulating cell free DNA in patients with refractory colorectal carcinoma treated with regorafenib. Journal of Translational Medicine. 2015 Feb 12;13(1):57.

279. Martinelli E, Ciardiello D, Martini G, Troiani T, Cardone C, Vitiello PP, Normanno N, Rachiglio AM, Maiello E, Latiano T, et al. Implementing anti-epidermal growth factor receptor (EGFR) therapy in metastatic colorectal cancer: challenges and future perspectives. Annals of Oncology. 2020 Jan;31(1):30–40.

280. Daniel C, Leppkes M, Muñoz LE, Schley G, Schett G, Herrmann M. Extracellular DNA traps in inflammation, injury and healing. Nat Rev Nephrol. 2019 Sep;15(9):559–75.

281. Kos K, de Visser KE. Neutrophils create a fertile soil for metastasis. Cancer Cell. 2021 Mar;39(3):301–3.

282. Nolan E, Malanchi I. Neutrophil 'safety net' causes cancer cells to metastasize and proliferate. Nature. 2020 Jul 2;583(7814):32–3.

283. Yang L-Y, Luo Q, Lu L, Zhu W-W, Sun H-T, Wei R, Lin Z-F, Wang X-Y, Wang C-Q, Lu M, et al. Increased neutrophil extracellular traps promote metastasis potential of hepatocellular carcinoma via provoking tumorous inflammatory response. J Hematol Oncol. 2020 Dec;13(1):3.

284. Koyama R, Arai T, Kijima M, Sato S, Miura S, Yuasa M, Kitamura D, Mizuta R. DNase γ, DNase I and caspase-activated DNase cooperate to degrade dead cells. Genes Cells. 2016 Nov;21(11):1150–63.

285. Jiménez-Alcázar M, Rangaswamy C, Panda R, Bitterling J, Simsek YJ, Long AT, Bilyy R, Krenn V, Renné C, Renné T, et al. Host DNases prevent vascular occlusion by neutrophil extracellular traps. Science. 2017 Dec;358(6367):1202–6.

286. Serpas L, Chan RWY, Jiang P, Ni M, Sun K, Rashidfarrokhi A, Soni C, Sisirak V, Lee W-S, Cheng SH, et al. Dnase1l3 deletion causes aberrations in length and end-motif frequencies in plasma DNA. Proc Natl Acad Sci USA. 2019 08;116(2):641–9.

287. Waisberg M, Molina-Cruz A, Mizurini DM, Gera N, Sousa BC, Ma D, Leal AC, Gomes T, Kotsyfakis M, Ribeiro JMC, et al. Plasmodium falciparum Infection Induces Expression of a

Mosquito Salivary Protein (Agaphelin) That Targets Neutrophil Function and Inhibits Thrombosis without Impairing Hemostasis. Vernick KD, editor. PLoS Pathog. 2014 Sep 11;10(9):e1004338.

288. Paunel-Görgülü A, Wacker M, El Aita M, Hassan S, Schlachtenberger G, Deppe A, Choi Y-H, Kuhn E, Mehler TO, Wahlers T. cfDNA correlates with endothelial damage after cardiac surgery with prolonged cardiopulmonary bypass and amplifies NETosis in an intracellular TLR9-independent manner. Sci Rep. 2017 Dec;7(1):17421.

289. Wan JCM, Heider K, Gale D, Murphy S, Fisher E, Mouliere F, Ruiz-Valdepenas A, Santonja A, Morris J, Chandrananda D, et al. ctDNA monitoring using patient-specific sequencing and integration of variant reads. Sci Transl Med. 2020 Jun 17;12(548):eaaz8084.